Woodhead Publishing in Mechanical Engineering

Condition assessment of aged structures

Edited by J. K. Paik and R. E. Melchers



CRC

WP

Condition assessment of aged structures

© 2008 Woodhead Publishing Limited

Related titles:

Fatigue assessment of welded joints by local approaches Second edition
(ISBN 978-1-85573-948-2)
Local approaches to fatigue assessment are used to predict the structural durability of welded joints, to optimise their design and to evaluate unforeseen joint failures. This completely reworked second edition of a standard work provides a systematic survey of the principles and practical applications of the various methods. It covers the hot spot structural stress approach to fatigue in general, the notch stress and notch strain approach to crack initiation and the fracture mechanics approach to crack propagation. Seam-welded and spot-welded joints in structural steels and aluminium alloys are also considered.

Weld cracking in ferrous alloys
(ISBN 978-1-84569-300-8)
Weld cracks are unacceptable defects that can compromise the integrity of welded structures. Weld cracking can lead to structural failures which at best will require remedial action and at worst can lead to loss of life. All industries that utilise welding can be affected, including nuclear, aerospace, automotive, shipbuilding and civil engineering. This book covers the processes of weld cracking in different ferrous alloys and for different welding technologies. It also covers methods of testing for weld cracks, avoidance and repair.

Techniques for corrosion monitoring
(ISBN 978-1-84569-187-5)
Corrosion monitoring technologies are a vital step in efforts to combat corrosion, which can have major economic and safety implications. Part I reviews electrochemical techniques for corrosion monitoring. Part II analyses other physical or chemical methods of corrosion monitoring. Part III examines corrosion monitoring in special environments and conditions. Part IV covers the selection of monitoring techniques and probes, and Part V discusses applications and case studies.

Details of these and other Woodhead Publishing books can be obtained by:

- visiting our web site at www.woodheadpublishing.com
- contacting Customer Services (e-mail: sales@woodhead-publishing.com; fax: +44 (0) 1223 893694; tel.: +44 (0) 1223 891358 ext. 130; address: Woodhead Publishing Limited, Abington Hall, Granta Park, Great Abington, Cambridge CB21 6AH, England)

If you would like to receive information on forthcoming titles, please send your address details to: Francis Dodds (address, tel. and fax as above; email: francisd@woodhead-publishing.com). Please confirm which subject areas you are interested in.

© 2008 Woodhead Publishing Limited

Condition assessment of aged structures

Edited by
J. K. Paik
and
R. E. Melchers

WPTF2005



CRC Press
Boca Raton Boston New York Washington, DC

WOODHEAD PUBLISHING LIMITED
Cambridge England

© 2008 Woodhead Publishing Limited

Published by Woodhead Publishing Limited, Abington Hall, Granta Park
Great Abington, Cambridge CB21 6AH, England
www.woodheadpublishing.com

Published in North America by CRC Press LLC, 6000 Broken Sound Parkway, NW,
Suite 300, Boca Raton, FL 33487, USA

First published 2008, Woodhead Publishing Limited and CRC Press LLC
© 2008 Woodhead Publishing Limited
The authors have asserted their moral rights.

This book contains information obtained from authentic and highly regarded sources. Reprinted material is quoted with permission, and sources are indicated. Reasonable efforts have been made to publish reliable data and information, but the authors and the publishers cannot assume responsibility for the validity of all materials. Neither the authors nor the publishers, nor anyone else associated with this publication, shall be liable for any loss, damage or liability directly or indirectly caused or alleged to be caused by this book.

Neither this book nor any part may be reproduced or transmitted in any form or by any means, electronic or mechanical, including photocopying, microfilming and recording, or by any information storage or retrieval system, without permission in writing from Woodhead Publishing Limited.

The consent of Woodhead Publishing Limited does not extend to copying for general distribution, for promotion, for creating new works, or for resale. Specific permission must be obtained in writing from Woodhead Publishing Limited for such copying.

Trademark notice: Product or corporate names may be trademarks or registered trademarks, and are used only for identification and explanation, without intent to infringe.

British Library Cataloguing in Publication Data
A catalogue record for this book is available from the British Library.

Library of Congress Cataloging in Publication Data
A catalog record for this book is available from the Library of Congress.

Woodhead Publishing Limited ISBN 978-1-84569-334-3 (book)
Woodhead Publishing Limited ISBN 978-1-84569-521-7 (e-book)
CRC Press ISBN 978-1-4200-9304-9
CRC Press order number: WP9304

The publishers' policy is to use permanent paper from mills that operate a sustainable forestry policy, and which has been manufactured from pulp which is processed using acid-free and elementary chlorine-free practices. Furthermore, the publishers ensure that the text paper and cover board used have met acceptable environmental accreditation standards.

Typeset by Godiva Publishing Services Limited, Coventry, West Midlands, England
Printed by TJ International Limited, Padstow, Cornwall, England

© 2008 Woodhead Publishing Limited

Contents

Contributor contact details xi

Preface xv

Part I Current practices

1 Current practices in condition assessment of aged ships and floating offshore structures 3
G WANG, C SERRATELLA and S KALGHATGI, American Bureau of Shipping (ABS), USA

1.1 Introduction 3
1.2 International Association of Classification Societies (IACS) and vessel inspections by classification societies 5
1.3 International Maritime Organization (IMO), flag states and port states 10
1.4 Industry self-regulation and voluntary inspections 13
1.5 Design, maintenance, inspection and repair of ship structures 14
1.6 Design, maintenance, inspection and repair of floating offshore structures 22
1.7 Nondestructive examination and monitoring 28
1.8 Challenges and future trends 30
1.9 Sources of further information and advice 31
1.10 Acknowledgments 31
1.11 References 31
1.12 Appendix: abbreviations used in this chapter 34

2 Current practices in condition assessment of aged fixed-type offshore structures 36
I LOTSBERG, Det Norske Veritas (DNV), Norway

2.1 Introduction 36
2.2 Design standards and acceptance criteria for assessment 38

© 2008 Woodhead Publishing Limited

2.3 Process for structural assessment 41
2.4 Collection of data from design, fabrication, transportation, installation and in-service life 43
2.5 Assessment of data and structural analyses 52
2.6 Mitigation 59
2.7 Future trends 60
2.8 Sources of further information and advice 61
2.9 References 62

3 Definition and assessment of deficiencies in building construction 65
A VAN GRIEKEN, Connell Wagner Pty Ltd, Australia

3.1 Historical perspective 65
3.2 History of global construction developments 66
3.3 The Australian experience 67
3.4 The benefit of the historical perspective 70
3.5 General causes of deficiencies 70
3.6 The three types of deficiencies: deterioration, defect and damage 71
3.7 Assessment of deficiencies 73
3.8 References 73

Part II Mechanisms, mathematical models and preventive measures for age-related deterioration

4 Corrosion wastage in aged structures 77
R E MELCHERS, The University of Newcastle, Australia

4.1 Introduction 77
4.2 Some fundamental corrosion principles 81
4.3 A model based on fundamentals 85
4.4 Environmental and other influences 91
4.5 Variability and probabilistic models 92
4.6 Some other corrosion loss models 93
4.7 Coastal atmospheric corrosion 96
4.8 Inland atmospheric corrosion 98
4.9 Pitting corrosion 98
4.10 Discussion 102
4.11 Conclusions 103
4.12 Acknowledgement 103
4.13 References 103

© 2008 Woodhead Publishing Limited

5 Fatigue cracking in aged structures 107
W C CUI, China Ship Scientific Research Center, China

5.1 Introduction 107
5.2 Historical overview of metal fatigue 107
5.3 Current understanding of fatigue mechanisms 110
5.4 Fatigue life prediction methods 111
5.5 Preventive measures for fatigue cracking 132
5.6 Conclusions 140
5.7 References 141

6 Local denting and other deterioration in aged structures 149
N YAMAMOTO, Research Institute of Nippon Kaiji Kyokai, Japan

6.1 Introduction 149
6.2 Local deformation damage caused by mechanical external cause 150
6.3 Local deformation damage caused by corrosion 156
6.4 Conclusions 161
6.5 References 161

Part III Residual strength of aged structures

7 Corroded structures and residual strength 165
T NAKAI, Nippon Steel Corporation, Japan and
N YAMAMOTO, Research Institute of Nippon Kaiji Kyokai, Japan

7.1 Introduction 165
7.2 Probabilistic modeling of corrosion 165
7.3 Degradation of hull girder strength 167
7.4 Pitting corrosion 168
7.5 Equivalent thickness of plates with pitting corrosion 174
7.6 Conclusions 183
7.7 References 183

8 Cracked structures and residual strength 186
F WANG and W C CUI, China Ship Scientific Research Center, China

8.1 Fundamentals of residual strength of cracked structures 186
8.2 Residual ultimate strength of cracked plates 189
8.3 Plates with a single crack under ultimate tensile loads 189

© 2008 Woodhead Publishing Limited

8.4 Plates with a single crack under ultimate compressive loads 201
8.5 Residual strength of plates with multiple collinear cracks 211
8.6 Random cracks 215
8.7 Ultimate strength of cracked stiffened panels 216
8.8 Ultimate strength of cracked ship hull girder 222
8.9 Conclusions 228
8.10 References 228

9 Dented structures and residual strength 231
J K PAIK, Pusan National University, Korea

9.1 Introduction 231
9.2 Mechanism of local denting damage 232
9.3 Residual ultimate strength characteristics of dented plates 239
9.4 Methods of damage detection and their uncertainties 247
9.5 Conclusions 248
9.6 References 249

Part IV Reliability of aged structures

10 Reliability of aged ship structures 253
Y GARBATOV and C GUEDES SOARES, Technical University of Lisbon, Portugal

10.1 Introduction 253
10.2 Time-dependent hull section modulus subject to crack growth 261
10.3 Effect of corrosion on the hull section modulus 265
10.4 Time-dependent section modulus of a hull with cracks and corrosion 266
10.5 Time-dependent reliability of the ship hull girder 267
10.6 Modelling crack inspections and reliability 270
10.7 Modelling corrosion inspection and reliability 274
10.8 Time-dependent reliability of ship hull subjected to fatigue and corrosion failure 275
10.9 Numerical example 277
10.10 Discussion and conclusions 282
10.11 Acknowledgements 283
10.12 References 284

11 Reliability of aged offshore structures 287
T MOAN, Norwegian University of Science and Technology (NTNU), Norway

11.1 Introduction 287
11.2 Current design practice for offshore structures: limit states 291

© 2008 Woodhead Publishing Limited

11.3 Inspection and maintenance of offshore structures 299
11.4 Concluding remarks on component design criteria 301
11.5 System failure criteria for offshore structures 301
11.6 Uncertainty measures used in reliability analysis 302
11.7 Load effects on offshore structures 304
11.8 Structural reliability analysis: elementary case 310
11.9 Fatigue reliability 318
11.10 Systems reliability 322
11.11 Updating of variables in reliability analysis 326
11.12 Decision making during design of offshore structures and in service 335
11.13 Target safety levels in reliability analysis 337
11.14 Improving the reliability of offshore structures 342
11.15 Conclusions 346
11.16 References 347

12 Reliability of aged land-based structures 352
R E MELCHERS, The University of Newcastle, Australia

12.1 Introduction 352
12.2 Components in structural reliability 353
12.3 Outline of structural reliability theory 355
12.4 Structural systems reliability 357
12.5 General approach 360
12.6 Deteriorating structures 362
12.7 Conclusion 362
12.8 References 362

Part V Inspection and maintenance

13 Inspection of aged ships and offshore structures 367
C M RIZZO, University of Genova, Italy

13.1 Reasons for inspections 367
13.2 The inspection event 368
13.3 Current inspection practices 375
13.4 Detection and sizing methods 382
13.5 Structural monitoring 401
13.6 Acknowledgements 403
13.7 References 404

14 Inspection of aged land-based structures 407
A VAN GRIEKEN, Connell Wagner Pty Ltd, Australia

14.1 Introduction 407

© 2008 Woodhead Publishing Limited

14.2 Six reasons for assessment 408
14.3 Assessment outcome and sequence 410
14.4 Concrete structures 410
14.5 Masonry structures 416
14.6 Steel structures 424
14.7 References 429

15 Maintenance of aged ships and offshore structures 430
C M RIZZO, University of Genova, Italy

15.1 Maintenance strategies 430
15.2 Current maintenance and repair practices 439
15.3 Temporary repairs 442
15.4 Permanent repairs 448
15.5 Examination and testing of repairs 455
15.6 Acknowledgements 457
15.7 References 457

16 Maintenance of aged land-based structures 459
A VAN GRIEKEN, Connell Wagner Pty Ltd, Australia

16.1 A structured approach 459
16.2 Key considerations 460
16.3 Documentation 462
16.4 Site phase of the works 464
16.5 Repair and protection of concrete structures 464
16.6 Brick growth repairs 483
16.7 Repair of metal structures 484
16.8 References 485

17 Risk-based inspection and maintenance of aged structures 487
C SERRATELLA, G WANG and K TIKKA, American Bureau of Shipping (ABS), USA

17.1 Introduction 487
17.2 Risk-based approaches 489
17.3 Fundamentals of risk-based approaches 495
17.4 Risk-based inspection (RBI) 502
17.5 Risk-based maintenance (RBM) 514
17.6 Risk-based repairs (RBR) 515
17.7 Future trends 516
17.8 References and bibliography 517

© 2008 Woodhead Publishing Limited

Contributor contact details

(* = main contact)

Editors

Professor Jeom Kee Paik
LRET Research Centre of Excellence
Department of Naval Architecture and Ocean Engineering
Pusan National University
30 Jangjeon-Dong
Gumjeong-Gu
Busan 609-735
Korea
E-mail: jeompaik@pusan.ac.kr

Professor Robert E. Melchers
Centre for Infrastructure Performance and Reliability
The University of Newcastle
Callaghan 2308
NSW
Australia
E-mail: rob.melchers@newcastle.edu.au

Chapter 1

Ge Wang,* Chris Serratella, Sameer Kalghatgi
American Bureau of Shipping (ABS)
ABS Plaza
16855 Northchase Drive
Houston, TX 77060-6008
USA
E-mail: gwang@eagle.org
CSerratella@eagle.org

Chapter 2

Dr Inge Lotsberg
Department for Offshore Structures
Det Norske Veritas (DNV)
Veritasveien 1
N 1322 Høvik
Norway
E-mail: Inge.Lotsberg@dnv.com

Chapters 3, 14 and 16

Albert N. van Grieken
Connell Wagner Pty Ltd
PO Box 321
South Melbourne
Victoria
Australia
E-mail: vangriekena@conwag.com

© 2008 Woodhead Publishing Limited

Chapters 4 and 12
Professor Robert E. Melchers
Centre for Infrastructure Performance and Reliability
The University of Newcastle
Callaghan 2308
NSW
Australia
E-mail: rob.melchers@newcastle.edu.au

Chapter 5
Professor Cui Weicheng
China Ship Scientific Research Center
Wuxi 214082
China
E-mail: wccui@cssrc.com.cn

Chapter 6
Norio Yamamoto
Research Institute of Nippon Kaiji Kyokai (ClassNK)
1-8-3 Ohnodai, Midori-Ku
Chiba 267-0056
Japan
E-mail: yamamoto@classnk.or.jp

Chapter 7
Tatsuro Nakai
Steel Products Research Lab I
Steel Research Laboratories
Nippon Steel Corporation
20-1 Shintomi, Futtsu-city
Chiba 293-8511
Japan
E-mail: nakai.tatsuroh@nsc.co.jp

Norio Yamamoto*
Research Institute of Nippon Kaiji Kyokai (ClassNK)
1-8-3 Ohnodai, Midori-Ku
Chiba 267-0056
Japan
E-mail: yamamoto@classnk.or.jp

Chapter 8
F. Wang and Professor Cui Weicheng*
China Ship Scientific Research Center
Wuxi 214082
China
E-mail: wccui@cssrc.com.cn

Chapter 9
Professor Jeom Kee Paik
LRET Research Centre of Excellence
Department of Naval Architecture and Ocean Engineering
Pusan National University
30 Jangjeon-Dong
Gumjeong-Gu
Busan 609-735
Korea
E-mail: jeompaik@pusan.ac.kr

Chapter 10
Professor Yordan Garbatov* and Professor C. Guedes Soares
Centre for Marine Technology and Engineering
Technical University of Lisbon
Instituto Superior Tecnico
Pavilho Central
Av. Rovisco Pais
1049-001 Lisboa
Portugal
E-mail:
yordan.garbatov@mar.ist.utl.pt
guedess@mar.ist.utl.pt

Chapter 11
Professor Torgeir Moan
Norwegian University of Science and Technology (NTNU)
7491 Trondheim
Norway
E-mail: Torgeir.Moan@ntnu.no

© 2008 Woodhead Publishing Limited

Chapters 13 and 15
Dr Cesare Mario Rizzo
University of Genova
Dept. of Naval Architecture and
Marine Technologies (DINAV)
Via Montallegro 1
I-16145 Genova
Italy
E-mail: cesare.rizzo@unige.it

Chapter 17
Chris Serratella,* Ge Wang, K. Tikka
American Bureau of Shipping (ABS)
ABS Plaza
16855 Northchase Drive
Houston, TX 77060-6008
USA
E-mail: gwang@eagle.org
CSerratella@eagle.org

© 2008 Woodhead Publishing Limited

Preface

Infrastructure, including ships, offshore and land-based structures, increasingly is required to perform for longer, at higher levels of intensity and with lower operational costs. It is also subject to age-related deterioration. Together these potentially conflicting requirements may raise significant issues in terms of safety, health, the environment, and financial expenditure. Indeed, deterioration appears to have been involved in many structural failures, contributing to the safety or performance failure of individual structural components or entire infrastructure systems.

Optimal management of infrastructure assets and their continued integrity is increasingly of interest, world-wide. High-quality asset integrity management requires refined strategies: for condition assessment; for appropriate, timely and sufficiently accurate assessment and inspection; and for suitable maintenance technology, techniques and approaches. These activities are required throughout the service life of the infrastructure system to assure that the infrastructure remains fit for service, with the involvement of repairs, replacements, adjustments and modifications as necessary.

This book is a single source of information on structural condition assessment for marine and land-based structures such as ships, offshore installations, industrial plant and buildings. Topics covered include current practices and standards for structural condition assessment, fundamental mechanisms and advanced mathematical methods for predicting structural deterioration, residual strength assessment of deteriorated structures, inspection and maintenance of aged structures, and reliability and risk assessment of aged structures.

The book is composed of five parts. Part I describes current practices in condition assessment of ageing structures such as ships, floating offshore structures, fixed-type offshore structures and land-based structures. Part II presents mechanisms, mathematical models and preventive/corrective measures for age-related deterioration. Part III describes residual strength of structures with age-related damage such as corrosion wastage, cracking damage and denting. Part IV describes reliability of ship structures, offshore structures and land-based structures with age-related deterioration. Part V presents

© 2008 Woodhead Publishing Limited

methodologies for inspection and maintenance of marine and land-based structures. Methods for risk-based inspection and maintenance of aged structures are also presented.

We believe and hope that this book will be useful for practising engineers involved in condition assessment or health monitoring of ageing structures. Coverage of the fundamentals as well as practices will mean that the book will also be useful for engineers-in-training and university students approaching both initial and more advanced studies of condition assessment.

The editors are pleased to acknowledge all the chapter authors for their unfailing efforts and contributions during the compilation of the book. Our heartfelt thanks are also due to all the staff at Woodhead Publishing Limited, for their extraordinary efforts and assistance to make this book possible.

Finally, the views and insights presented in the book are those of the chapter authors and not necessarily those of the institutions with which the chapter authors are affiliated. Also, the editors are not responsible for any consequences arising from the use of any guidance provided by the chapter authors.

Jeom Kee Paik, Pusan National University, Korea
Robert E. Melchers, University of Newcastle, Australia

© 2008 Woodhead Publishing Limited

Part I

Current practices

© 2008 Woodhead Publishing Limited

1

Current practices in condition assessment of aged ships and floating offshore structures

G WANG, C SERRATELLA and S KALGHATGI,
American Bureau of Shipping (ABS), USA

Abstract: This chapter introduces the background of the inspection regime, including inspections by classification societies, regulatory requirements, and industry voluntary inspections. It also explains the practice of designing and maintaining marine structures, typically ships and offshore floating structures, and nondestructive examination and monitoring techniques. The chapter concludes with challenges and future trends that serve as the starting point for the entire book.

Key words: inspection, corrosion, crack, nondestructive testing, coating.

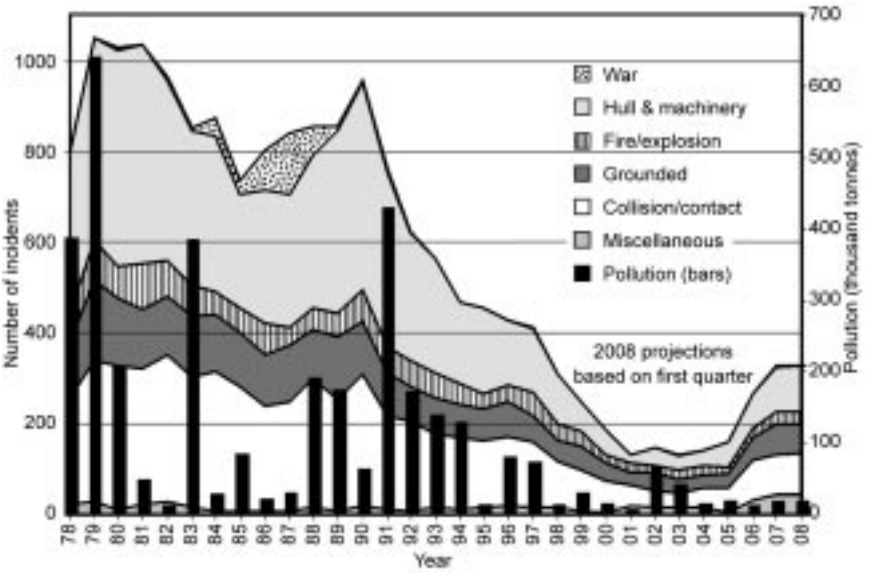
1.1 Introduction

The economic boom that started in Asia created the demands for the shipping of more energy, materials and products. This boom has been driving the shipping industry to build larger and more sophisticated vessels. Oil prices are at a historically high level, which in turn have made development of the oil fields in remote and less accessible locations economically feasible. The shipping and offshore industries are taking a more proactive approach and are embracing innovative and novel concepts. A foreseeable result of these actions is the need for more proactive and intelligent maintenance as well.

In response to ever-heightening public concerns over safety at sea, the regulatory agencies are increasingly involved in the design, operation and maintenance of marine structures. The European Union has decided to accelerate phasing out of single-hull tankers. The International Maritime Organization (IMO) has embarked on developing regulations for design and maintenance of ship structures. This goal-based standards (GBS) initiative reflects the demand of the public for explicitly defined safety or risk levels for the marine industry. One of the keys to maintaining and improving safety levels is to more effectively and efficiently manage the structural integrity of ships and offshore installations.

The network of maritime safety partners includes the shipowner and shipbuilder, the classification society, the IMO, the flag state, port state, underwriter, financier, marine insurance company, and charterer, among others.

© 2008 Woodhead Publishing Limited



1.1 Number of reported tanker incidents during 1978–2007 and extent of accidental pollution (INTERTANKO 2006).

Responsible parties are committed to continuous improvement in overall safety and in the reduction of pollution, 'striving for zero' – zero fatalities, zero pollution and zero detentions! To achieve these goals, the industry has developed and implemented a series of initiatives and is embarking on others. The accumulated efforts of these partners have led to an improved level of safety. The number of marine incidents clearly demonstrates a declining trend, as illustrated by the tanker industry information shown in Fig. 1.1.

The industry has established a practice of maintaining the life-cycle integrity of hull structures through design, corrosion protection, inspection, monitoring and repair. Periodic inspection and survey play a key role in maintaining life-cycle structural integrity. The primary purpose of hull inspections is to identify the condition of the structures in order for the risks of potential structural failures to be assessed so that appropriate actions can be taken.

This chapter introduces the background of the inspection regime, including inspections by classification societies, regulatory requirements, and industry voluntary inspections. It also explains the practice of designing and maintaining marine structures, typically ships and offshore floating structures, and non-destructive examination (NDE) and monitoring techniques. The chapter concludes with challenges and future trends that serve as the starting point for the entire book.

© 2008 Woodhead Publishing Limited

1.2 International Association of Classification Societies (IACS) and vessel inspections by classification societies

1.2.1 Classification societies and the International Association of Classification Societies

Classification societies were established to act as neutral third parties, undertaking ship surveys in support of insurers. Classification societies establish standards, usually called classification rules, regulating design and maintenance of ships, and conduct periodic surveys to implement these standards (IACS 2004a). Classification societies have their own individual histories, some having been in business for more than 100 years. Their primary purpose is to perform inspections and surveys of vessels to verify that they are maintained to the requirements of classification societies' rules and standards. These inspections and surveys are performed at periodic intervals to ensure compliance with the respective rules.

The *International Association of Classification Societies* (IACS) was formed by seven leading societies on 11 September 1968. IACS presently consists of 10 member societies and one associate member. With 90% of world cargo-carrying tonnage covered by the rules of IACS members, IACS plays a vital role in improving the standards of the maritime industry. The value of their combined and unique levels of knowledge and experience has been widely recognized. In 1969, IACS was given consultative status with the IMO with the first permanent representative appointed in 1976.

1.2.2 Hull inspections by classification societies

Fundamentally, there are three reasons for ships to be inspected – to verify the condition of the vessel, to check for compliance with statutory requirements for the ship and its manning, and to confirm the suitability of the ship for its intended commercial operation. It has been a challenge to inspect hull structures due to the sheer size of ships and offshore structures (see Fig. 1.2). Classification societies carry out hull classification surveys to confirm the condition of a vessel through a process of overall visual examinations, close-up visual examinations, NDE and thickness measurements. Surveys are typically made up of Annual Surveys, Intermediate Surveys and Special Surveys (ABS 2007).

Annual Surveys (AS) are carried out each year to ensure that the hull structure and piping are maintained in satisfactory condition. An Annual Survey typically takes one to two days. Usually, the survey includes the externally accessible hull and piping surfaces.

Intermediate Surveys (IS) are carried out at the mid-point of the five-year special survey/certificate cycle. The Intermediate Survey is comprised of the same inspection of external hull and piping surfaces as in the Annual Surveys

© 2008 Woodhead Publishing Limited



1.2 Inspection of marine structures is very challenging because of their sheer size – the two diagrams are to the same scale (EMSA 2005).

plus an examination of ballast tanks and cargo tanks. The aim of the Intermediate Survey is to verify that conditions have not deteriorated at a rate greater than that assumed during the preceding Special Survey (see below). For vessels that are older than 10 years, the extent of the survey is increased. More extensive thickness measurements may be required. Intermediate Surveys take approximately three to four days for completion.

© 2008 Woodhead Publishing Limited

Special Surveys (SS) are carried out every five years in order to provide an in-depth examination of the structural condition of the vessel. All compartments are subjected to survey while the vessel is dry-docked. Special Surveys take about one to two weeks, and the extent of time increases with the age of the ship.

General Visual Inspection (GVI) is carried out as part of an SS. GVI is an overall visual examination of the structure to decide upon its general condition and to narrow down the areas that need to be examined in close proximity.

Close Visual Inspection (CVI) is the visual examination in close proximity. CVI provides the best representative samplings of areas likely to be most exposed to the effects of corrosion, sloshing and stress concentration. The special value of CVI is that it provides the best representative samplings of those areas most likely experiencing the greatest exposure from the effects of corrosion, sloshing and stress concentration. The close proximity of the inspection is usually considered to be within hands' reach or less than three feet of distance between the structure and the inspector's eyes. CVI provides an assessment to the inspector as to the quality of coating protection, the rate of material degradation, and the ability of the structure to serve its intended or design purpose.

Both GVI and CVI may be supplemented by thickness measurement, with requirements based on age and type of vessel.

1.2.3 Thickness measurement

Thickness measurement is also called gauging. Its purpose is to establish, in conjunction with a visual examination, that the condition of the existing structure is fit for continued service during the subsequent survey interval, assuming that the vessel is properly operated and maintained. Thickness measurements are a confirmation of conditions sighted by the attending surveyor and function as a tool used to assess structures, not a stand-alone method of inspection. Guidelines for ultrasonic thickness measurements are given by the IACS in general terms and by the individual classification societies at a detailed level.

Thickness measurement is usually done by ultrasound equipment to determine the remaining thickness of the steel plating. This procedure indicates the diminution of the plate thickness compared to the design and as-built thickness. The thickness measurement requirements and locations for AS and IS are based on the conditions found at the time of that survey as well as conditions documented at the previous SS. The specified thickness measurements for SS are based on age and type of vessel.

The transverse sections for thickness measurements are normally selected by locating the areas where the largest reductions are suspected to have occurred. The attending surveyor indicates the locations to be measured, preferably after carrying out an overall examination of all tanks. The surveyor will specify additional thickness measurements in areas of known or suspected wastage.

© 2008 Woodhead Publishing Limited

During the thickness measurement process, the surveyor will also advise if any additional readings are to be taken to confirm questionable readings or marginal conditions.

1.2.4 Coating and coating inspection

The application of coatings to water ballast tanks and cargo tanks is the primary means of corrosion protection for ships and is recognized as one of the most important factors affecting integrity, maintenance cost and service life. Coatings serve mainly to minimize the corrosion rate, thereby potentially delaying the utilization of the built-in corrosion margins included in a vessel's structural scantlings.

In recent years, there has been an increased industry focus on the consequences of corrosion and an increased demand for better performance from the coatings used for corrosion control. The recently introduced IMO Performance Standards for Protective Coatings (IMO 2006), or IMO PSPC, specify requirements for coating certification, surface preparation, coating application, inspection and measurements and the creation of a coating technical file to document each step of the process.

IACS has developed Unified Requirements and Recommendations for the assessment of surface coating systems. IACS requires that the protective coating system in ballast tanks for all types of ships, except oil carriers, be maintained in at least a *Fair* coating condition in order to avoid annual re-examination of the ballast tank. The definition of each grade is shown in Table 1.1 (ABS 2007, IMO Resolution A.744(18)).

For oil carriers, chemical carriers and double-hull oil carriers, IACS requires that the protective coating system in ballast tanks be maintained in a *Good* coating condition in order to avoid annual re-examination of the ballast tank (IACS 2004c). Table 1.2 shows the IACS definition of each grade of coating condition.

The coating condition is assessed based on scattered coating failure, localized coating failure and linear coating failure on edges. A combination of these diagrams, shown in Fig. 1.3 as an example, which is excerpted from ABS 2007,

Table 1.1 Rating of coating conditions of vessels other than tankers

Rating/condition	Good	Fair	Poor
Spot rust, light rust	Minor	>20%	
Edges and welds		Local breakdown	
Hard scale			>10%
General breakdown			>20%

© 2008 Woodhead Publishing Limited

Table 1.2 IACS rating of coating conditions of tankers

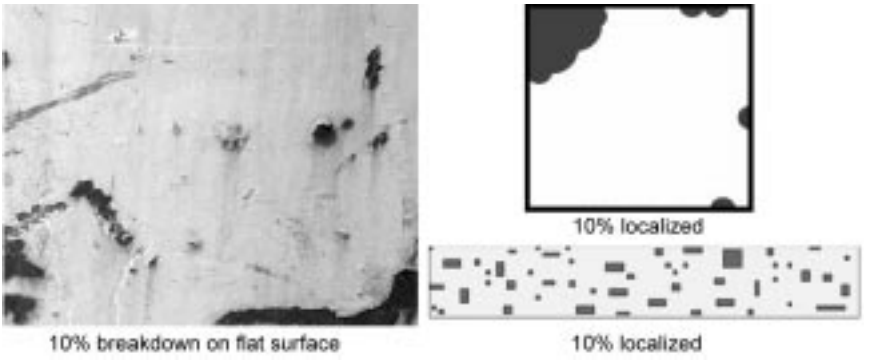
Rating/condition	Good	Fair	Poor
Breakdown of coating or area rusted	<3%	3–20%	>20%
Area of hard rust scale	–	<10%	≥10%
Local breakdown of coating or rust on edge of weld lines	<20%	20–50%	>50%

helps to assess the coating condition. This flat area shows 10% breakdown and is assessed as *Fair* by both IMO PSPC and IACS Recommendation 87.

For recognizing the conditions in the different areas of the tank, such as different coating breakdown and corrosion patterns, the IACS recommends dividing a ballast tank into logical areas in order to grade each area separately. Therefore, the area with the lowest rating shall govern the final rating of the ballast tank under consideration.

The positive impact of an effective coating system in tanks and holds has been understood. The selected use of high-tensile steel may impose increased stress on both steel and coatings, placing greater emphasis on the performance of coatings. The adoption of ballast water exchange practices may potentially place further stress on the hull structure. The process of reintroducing oxygen-enriched ballast water within tanks may also affect the longevity of coatings (ABS 2007). The IMO, IACS and other industry organizations are continuing to work on improving coating-related standards.

The impact of coating performance standards on the shipbuilding process remains to be seen. While some tanker owners have had detailed painting specifications similar to the Tanker Structure Cooperative Forum (TSCF) standards in their building contracts for some time now, others have not. With all tankers now having to apply the PSPC, initial feedback from shipbuilders



1.3 Example of 10% breakdown on flat area assessed as *Fair* by IMO and IACS Rec. 87 (ABS 2007).

© 2008 Woodhead Publishing Limited

indicates further concerns to be addressed, such as the potential for weather conditions affecting building schedules, a new step for coatings to be certified, a high demand for certified coating inspectors, a large amount of increased documentation, and possibly a new source of conflict between parties regarding compliance issues when delivering the vessel.

1.3 International Maritime Organization (IMO), flag states and port states

In addition to the classification rules, government administrations and international agencies codify safety standards for ships on the basis of international conventions or laws enacted by their own authority. Because of the international nature of the shipping industry, it has long been recognized that actions to improve safety in maritime operations would be more effective if carried out at an international level rather than by individual countries acting unilaterally and without coordination with others.

The classification societies undertake statutory surveys on behalf of flag administrations. The reason for this is that the classification societies have the technical capability and expertise and play an independent role internationally. Classification societies, however, are private entities, and class surveyors are not a substitute for government officials who have enforcement powers.

1.3.1 International Maritime Organization (IMO)

The International Maritime Organization was established by the United Nations in 1948 as the first international body devoted exclusively to maritime matters. The objective of the organization is 'to provide machinery for cooperation among governments in the field of governmental regulation and practices relating to technical matters of all kinds affecting shipping engaged in international trade; to encourage and facilitate the general adoption of the highest practicable standards in matters concerning maritime safety, efficiency of navigation and prevention and control of marine pollution from ships'.

The IMO is a technical organization and most of its work is carried out in a number of committees and subcommittees. The IMO has promoted the adoption of some 40 conventions and protocols and has adopted well over 800 codes and recommendations concerning maritime safety, the prevention of pollution and related matters. The most important IMO regulations are the International Convention on Load Lines, 1966, and Amendments 1971, 1975, 1979, 1983, 1995 and 2003; the International Convention for the Prevention of Pollution from Ships, 1973, as modified by the Protocol of 1978 (often called MARPOL 73/78); and the International Convention for the Safety of Life at Sea 1974 (often called SOLAS).

© 2008 Woodhead Publishing Limited

1.3.2 Enhanced Survey Program (ESP)

The Enhanced Survey Program of inspections during surveys of bulk carriers and oil tankers, called the ESP, was adopted by the IMO by resolution A.744 (18). The ESP is a set of guidelines on the enhanced program of inspections during surveys of bulk carriers and oil tankers incorporated into SOLAS Reg XI/2 and MARPOL Reg I/13F and 13G. These guidelines have currently been adopted by classification societies into their respective rules and are implemented during the classification and statutory surveys.

The ESP was developed on the basis of a critical evaluation of ship structures together with an appreciation of current experience with corrosion and cracking, as well as the need to make clear, specific procedures to avoid loopholes that could lead to insufficient follow-up and, consequently, substandard ships (IACS 2005). To ensure a consistent quality of hull surveys, the ESP provides detailed and prescriptive requirements for the actual surveys. The scope and scheduling were developed based on a generic risk assessment of critical structures with detailed and comprehensive requirements for reporting, utilizing what had been previously surveyed and found.

The ESP survey schedules and the extent of surveys are based on the understanding that, with the sheer size of the vessels, their real condition can only be revealed with detailed close-up inspections and extensive thickness measurements, and that the deterioration process happens slowly over time. It is therefore considered more effective to have fewer thorough surveys rather than more frequent but less extensive ones. The cornerstone of the inspection process has therefore become the Special Survey requiring close-up access to critical structure and components. This survey may sometimes take weeks to complete.

For older ships, it was considered that five years would be too long a time interval between such detailed surveys. As a result, the Intermediate Survey was also tightened up with similar, though less extensive, procedures to the Special Survey. After the *Erika* and *Prestige* accidents, these IS surveys were further tightened and made identical to the SS for ships of 17.5 years of age and older.

Furthermore, ballast tanks will be subjected to an Annual Survey when, during an SS or IS, a protective coating in less than 'good' condition or with 'substantial corrosion' (see Section 1.2.4) is found with, for example, a condition of no protective coating from the time of construction.

As the quality of the close-up survey is very dependent upon the trustworthiness of the thickness measurements, a special certification scheme was implemented as part of the ESP for thickness measurement companies.

1.3.3 Condition Assessment Scheme (CAS)

The IMO initiated the Condition Assessment Scheme (CAS) for single-hull oil tankers which was developed in line with the Enhanced Survey Program. As a

© 2008 Woodhead Publishing Limited

consequence of some high-profile marine incidents, the phasing out of single-hull tankers was accelerated in amendments to IMO Regulation 13G of MARPOL Annex I. The amended Regulation 13G allows for a certain extent of continued trading provided that a CAS is carried out with a satisfactory result. In short, the CAS is an enhanced scheme to the survey scope at the third renewal survey defined by the ESP – IACS UR Z 10.1 and IMO Res A.744(18). The main differences between CAS and ESP are related to survey planning, survey reporting, flag state involvement and the strict timeline that needs to be followed.

1.3.4 Flag states

The flag state is the country under which a vessel is registered. The flag state is responsible for carrying out surveys and issuing the statutory certificates to the vessel in accordance with IMO regulations (SOLAS, MARPOL, ITC, LL, etc.). Flag states generally delegate the authority to carry out statutory surveys and issue statutory certificates to classification societies. Some flag states may give full, partial or no authorization to classification societies. The flag states may carry out unscheduled inspections on the vessel. This action is regulated in SOLAS Ch. 1 Reg. 10. The class certificate, including the already defined ESP for tankers and bulk carriers, therefore becomes the cornerstone of the quality system for aging ships (IACS 2002, 2004b, 2004c, 2005).

Certain flag states have regional requirements that go beyond the international requirements of IMO. For example, the United States has implemented the Oil Pollution Act of 1990, often referred to as OPA90, to enforce special quality requirements for tankers and their operation before they are allowed entry into US waters.

The Critical Area Inspection Plan (CAIP) was an outcome of the United States Coast Guard (USCG) initiative for carrying out inspections on single-hull tankers and tank barges which do not meet double-hull criteria. The CAIP was a result of the US Oil Pollution Act (OPA) 1990, which was aimed towards reduction of oil spills from single-hull tankers. CAIP is a plan which focuses periodic structural inspections of historically identified problem areas, based on repair history, engineering analysis and service history.

1.3.5 Port states

Port states are coastal states with ships passing their territorial waters and entering their ports. The port state authorities are authorized by the statutory regulations to perform statutory inspections on vessels entering their ports to check for compliance with IMO regulations. These states have special concerns for the safety of ships and people, either on the ships or on land, as well as for the protection of the environment. The flag and port state responsibilities are often exercised by the same national maritime administration. Most port states

© 2008 Woodhead Publishing Limited

have agreed on common procedures for port state controls (PSCs) and sharing of information on quality issues. Port state controls are the inspections carried out by countries on the vessels visiting their ports and serve as spot checks to gain a general impression of a ship's condition.

1.4 Industry self-regulation and voluntary inspections

In addition to the mandatory inspection and survey required by the IACS, the IMO, flag and port states, the industry has also established recommended practices or standards to better manage its vessels. While class surveys previously were often the only thorough evaluation of the hull structure, a basic element of the safety network today is that owners have implemented a proper maintenance system whereby all damages and defects should be reported to class to identify critical areas. Furthermore, the owner is responsible for proper planning of class surveys including, for example, proper cleaning and descaling and safe access facilities for the surveys.

1.4.1 Tanker Structure Cooperative Forum (TSCF)

The Tanker Structure Cooperative Forum was established to implement industry guidelines for maintenance and inspection of tankers. The TSCF members are classification societies, ship owners and charterers. The TSCF has issued a series of guidance manuals for inspecting and maintaining tanker structures (TSCF 1992, 1995, 1997, 2000). These guidelines and the procedures for ESP have largely been harmonized, and the TSCF gives valuable guidance for maintenance and repair of ship structures. Such guidelines have been issued by the IACS for general cargo ships and bulk carriers. The guidelines follow the same format as the guidelines for tankers issued by the TSCF (1997).

1.4.2 Ship Inspection Report Program (SIRE)

Charterers of tanker tonnage have implemented 'vetting' survey schemes with inspection of ships and requirements on ship owners. An overview of these is described by INTERTANKO (2003) in *A Guide to the Vetting Process*. The system was introduced by the Oil Companies International Marine Forum (OCIMF), which was established in 1970 to increase public awareness of marine pollution as a response to the *Torrey Canyon* accident in 1970. A cornerstone of the vetting system is the Ship Inspection Report Program (SIRE) launched in 1993 as a ship condition-vetting program with a transparent database for the ship stakeholders. The aim of the system is to reveal the general condition related to all quality and safety systems on board. For the hull condition, it addresses the general condition and the repair history and refers to the class (ESP) certificates and its status.

© 2008 Woodhead Publishing Limited

1.4.3 Insurance inspection

Insurance companies normally base their assessment on a number of issues such as their past experience with the particular ship or ship owners and the status of the class certificate. During the late 1980s and early 1990s, however, they also extended their involvement. They decided to follow up annually on a certain number of the insured fleet, say 5%, with their own inspections, typically a one-day inspection, looking for special critical areas and the general appearance of the ships to identify ships suspected to be substandard.

1.4.4 Condition Assessment Program (CAP)

During the late 1980s and 1990s, a number of financial institutions started to question the value of aged tankers, and some charterers started to restrict the use of aged vessels (beyond 15 to 20 years of age) without special inspections beyond the minimum requirements of IACS. The classification societies met these demands by offering a special, voluntary Condition Assessment Program (CAP) with extended inspection, thickness measurements, and an evaluation of hull structures, recognizing the effects of corrosion with respect to yielding, buckling and fatigue failures. The program resulted in a rating of the ships from excellent to poor. As of today, this program is requested by a number of oil companies as a basis for chartering tankers 15 years old and beyond.

1.5 Design, maintenance, inspection and repair of ship structures

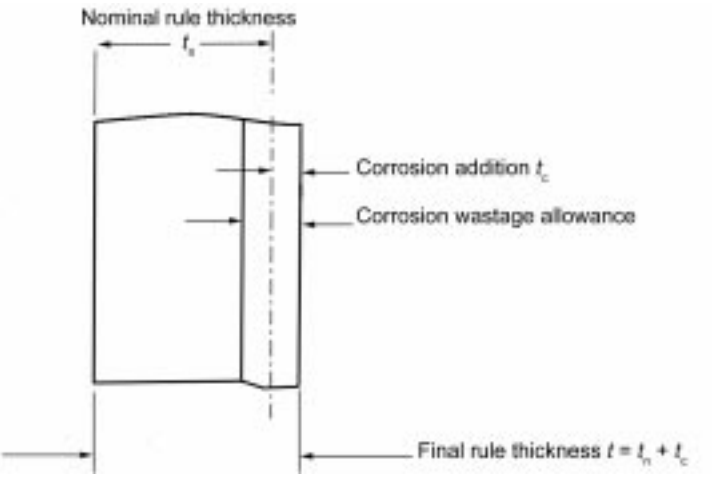
The shipping industry has established a practice that addresses the life-cycle structural integrity management:

- *Designing* by considering expected loads, structural failures (yielding, buckling and fatigue), and corrosion addition
- *Maintaining* the steel by using coatings and anodes
- *Inspecting* to monitor the conditions of structures and corrosion system
- *Repairing* when structural components are viewed as not suitable for the intended services.

1.5.1 Corrosion addition, wastage allowance, and substantial corrosion

Classification societies have established standards requiring that structural scantlings of ships be designed with a certain allowance for corrosion wastage. This design allowance is normally known as ‘corrosion addition’ (Fig. 1.4). Corrosion additions provide a safety margin for avoiding an undue increase of working stresses and a means for avoiding unnecessary frequent steel renewals.

© 2008 Woodhead Publishing Limited



1.4 Corrosion addition and wastage allowance (TSCF 1992).

In the early 1990s, the first-principle approaches were introduced in design rules (ABS 2007). Associated with this advance, the concept of 'nominal design corrosion values' (NDCV) was developed for structural design. The rules are formulated using a net thickness approach. This approach assumes that various degrees of corrosion will occur to the structural members during the life of the vessel. Generally, an additional thickness, which is NDCV, is added to the net plate thickness that is determined according to the expected loads and permissible resultant stresses.

Ships in service are periodically surveyed and inspected. While deemed necessary according to defined criteria, i.e., the *wastage allowances* (Fig. 1.4), wasted plates have to be replaced. Classification societies advise their surveyors and vessel owners of the maximum corrosion wastage allowance. The values of wastage allowance are dependent on vessel type, compartment and location of the structure.

Corrosion wastage allowances are generally given as a percentage of as-built scantlings. Criteria about whether or not a structure has to be replaced or may remain in place are established based on judgments about possible consequences of failures, the materials, corrosion types (pitting or general corrosion), and many other factors. Plate renewal is decided upon by considering the local wastage limit and the potential of buckling failure of the structure. Under some circumstances, the hull girder strength has to be assessed before steel renewals are requested. The values of wastage allowance of trading ships are normally in the range of 15–25% for local structural members, and 10% for the global hull girder strength.

Substantial corrosion is an extent of corrosion such that the wastage is in excess of 75% of the allowable margins. Structures found to be subject to

© 2008 Woodhead Publishing Limited

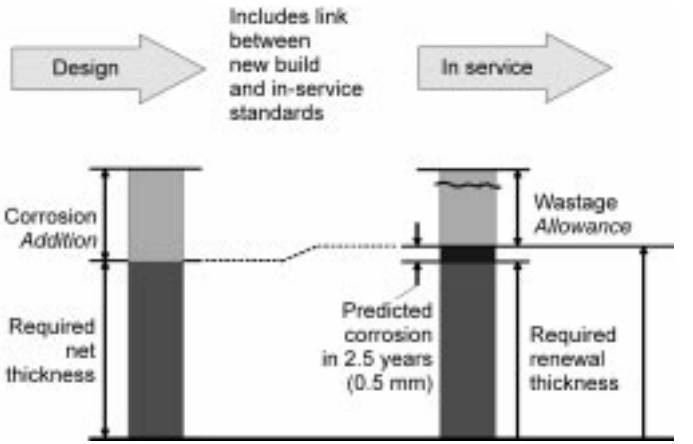
substantial corrosion are generally viewed as more likely to fail, and warrant more stringent inspection. A record of substantial corrosion will be made even if the owner selects to coat the area and arrest further corrosion. This practice by the classification societies has a large influence on the actual repair and maintenance performed by the owners. Most major oil companies do not charter ships with a record of substantial corrosion.

1.5.2 The concept of IACS Common Structural Rules (CSR) for tankers and bulk carriers

The *Common Structural Rules* have adopted a concept that explicitly links the potential lifetime corrosion wastage with the design allowance (Horn and Baumans 2007) for tankers and bulk carriers. The net scantling approach sets out to determine and verify the minimum hull scantlings that are to be maintained from the new building stage throughout the ship's design life. The CSR concept is illustrated in Fig. 1.5, and the values used for tankers are in Fig. 1.6.

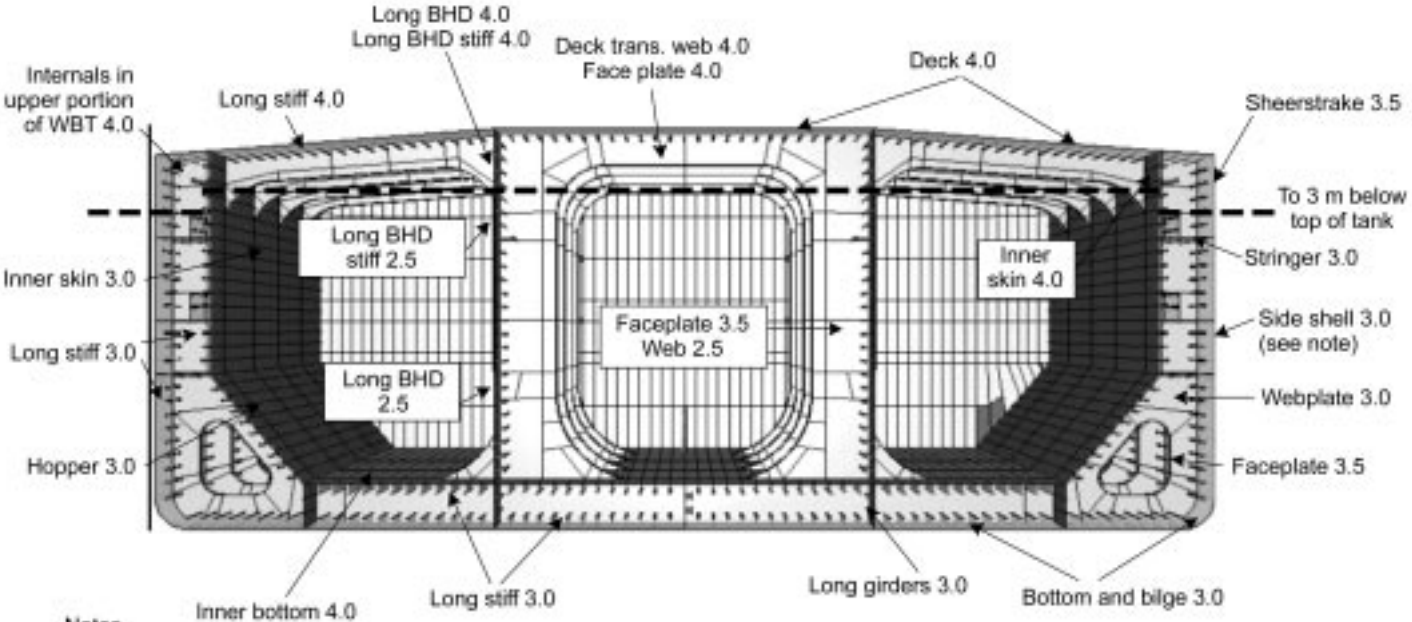
The strength of local structural members is assessed using the structural scantlings in the wasted condition, or net thickness, while applying the expected extreme loads. This will ensure that the vessel will meet the minimum strength requirements even while in the defined extreme wasted condition.

Lower values of the corrosion margin are used for evaluating the strength of large structural members such as hull girders and main supporting members. These values reflect the average condition of these large structural members that are composed of many local members. Each local member can be in different degrees of wastage at the end of the ship's service life. At the hull girder level, the average condition of all the members will determine the global strength.



1.5 IACS CSR net scantling concept for local structural members (Horn and Baumans 2007).

© 2008 Woodhead Publishing Limited



1.6 Corrosion addition, t_{corr}, for typical structural elements within the cargo tank of CSR tankers (see IACS CSR).

© 2008 Woodhead Publishing Limited

Therefore, the CSR assume half of the corrosion margins of local members when assessing the hull girder strength.

Fatigue is a cumulative mode of failure that starts from the first day of service until the last day of service. Therefore, the net thickness associated with fatigue failure assessment is averaged and is taken as half of the full margin.

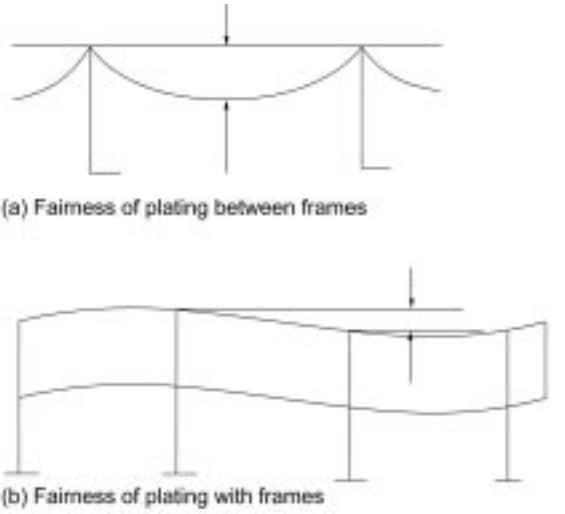
The CSR corrosion additions have been established based on the extensive work of the IACS working party, member societies (e.g., Horn and Baumans 2007, Yoneya *et al.* 2004, Harada *et al.* 2001, Wang *et al.* 2003a, 2003b, 2005a, 2008, Yamamoto and Ikegami 1998), and other resources (e.g., Paik *et al.* 2003, Paik and Thayamballi 2007, Melchers 2001). Corrosion processes from initial occurrence through propagation were investigated on extensive thickness measurement data. A corrosion process model was developed based on probabilistic theory to estimate the thickness diminution of structural members. The corrosion addition values are generally associated with the 95% percentile of the database for 25 years. The effects of coatings are not directly included in the application of corrosion additions used for design. The main reason for this is that coatings will eventually break down. Some statistical studies show that coating breakdown can take place after 2 to 10 years (Contraros 2004, Serratella and Spong 2007, Wang *et al.* 2008). The other consideration is that it is not always possible to recoat the structure while the vessel is in service and exposed to adverse environmental conditions. On the other hand, the efficiency of the coating during the ship's life depends on the conditions of application and the owner maintenance policy. See also Section 1.2.4 for coating inspection.

1.5.3 Structural deformations

Structural deformations are measured between stiffeners (plating) or between transverse main supporting members (stiffening members). IACS has established standards for acceptable fairness of plates during new construction of conventional design (IACS 2006), which are acceptable deformations of plating between frames and with frames, respectively. Taking shell plating as an example, the fairness of plating between frames is 4 mm as standard and 8 mm as the limit, while the fairness of plating with frames is 2–3/1000 mm as standard and 3–4/1000 mm as the limit (see Fig. 1.7).

Often, deformations measuring up to about three inches (75 mm) are not considered a major threat to structural integrity. Decisions on whether a deformed structural member needs to be repaired depend on the degree of deformation, the location of the structure, and conditions of the surrounding structures, among other considerations. Permanent structural deformations are associated with plastic deformation of material. Dents can be seen in areas subject to impact loads of wave slamming (side shell of ship bow), sloshing (boundary of tanks partially filled) and green water (deck), side structures in the

© 2008 Woodhead Publishing Limited



1.7 Fairness of plating between or with frames (IACS 2006).

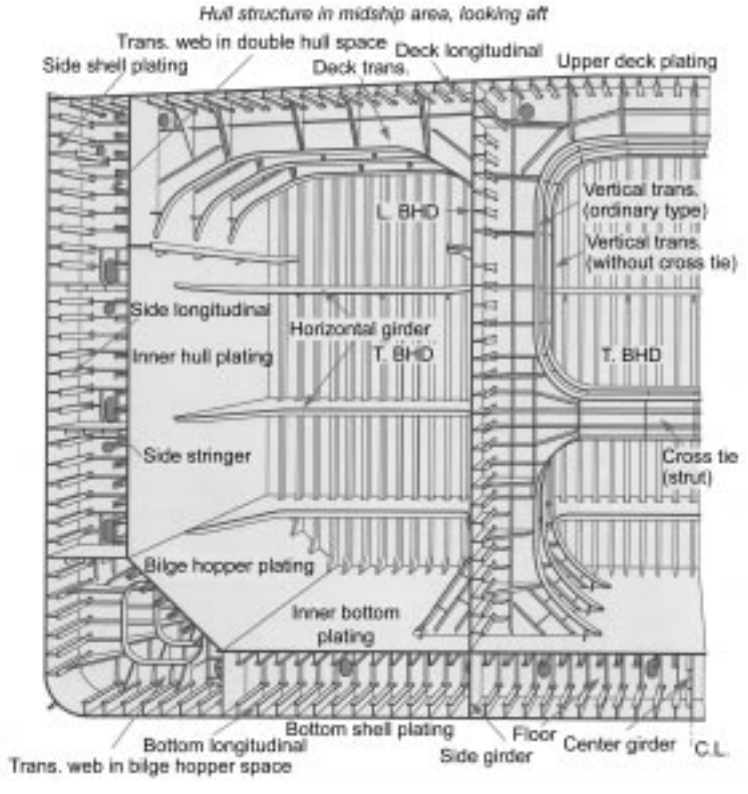
ice belt (at waterline) and side shell exposed to contact with pier or tug boat. For these areas, permanent deformations of less than the plate thickness are often considered acceptable (e.g., Jones 1989, Paik *et al.* 2004, Wang *et al.* 2002, 2005b, 2006).

IACS has also established standards of workmanship for repairing deformed primary and secondary structures (IACS 2006). Restoration of a structure to the original standard (flatness) may not constitute durable repairs of damages originating from insufficient strength or inadequate detail design. In general, when the hull structure covered by classification is to be subjected to repairs, the work is to be carried out under the supervision of the surveyor to the classification society. Such repairs are to be agreed upon prior to the commencement of the work.

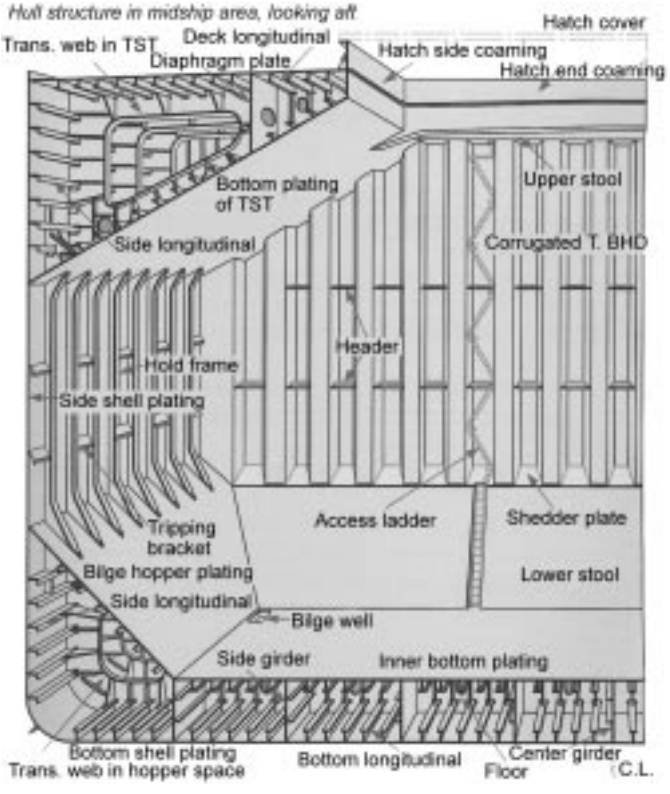
1.5.4 Operational experiences of ships

Oil tankers were single-hull structures until the early 1990s. Since then, they have been of double-hull construction (see Fig. 1.8a). Structures in the ballast tanks are prone to corrosion wastage (TSCF 1997, EMSA 2005), and it is currently required that the ballast spaces are to be fully coated. The underdeck areas in cargo oil tanks are also prone to corrosion attack. The inner bottom, which is the bottom of cargo tanks, is susceptible to pitting corrosion and to microbially-induced corrosion (MIC) under some circumstances. Though it is not required to coat cargo oil tanks, some owners have the under-deck area and inner bottom of cargo oil tanks coated. The connections of longitudinal stiffeners with transverse structures are known to be prone to fatigue damage.

© 2008 Woodhead Publishing Limited

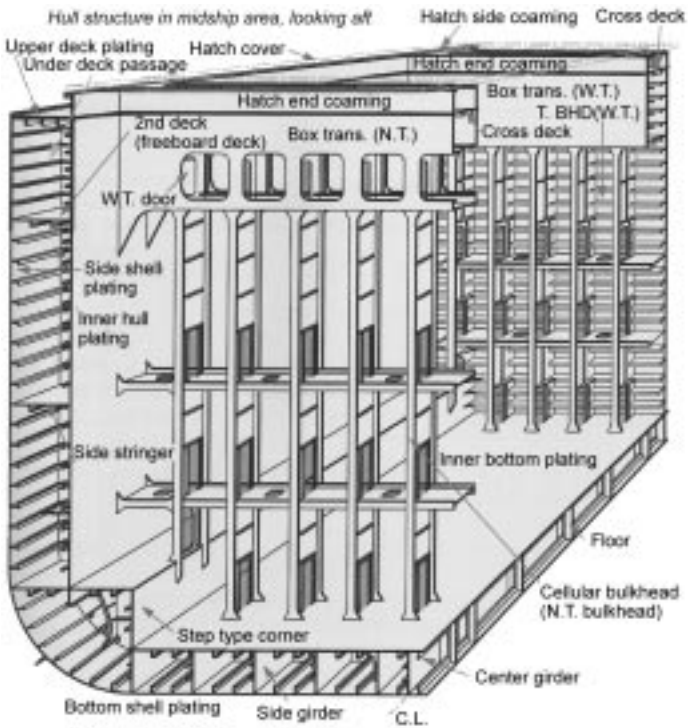


(a) Double-hull tanker structures

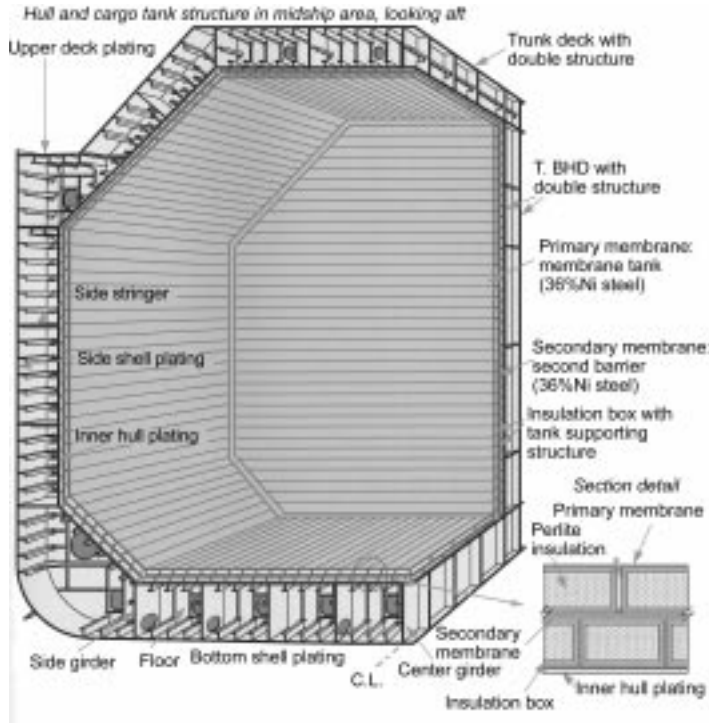


(b) Bulk carrier structures

© 2008 Woodhead Publishing Limited



(c) Container carrier structures



(d) LNG carrier structures (membrane containment system)

1.8 Complex ship structures (Emi 2006).

© 2008 Woodhead Publishing Limited

Significant failure problems were reported in side longitudinals of young very large crude carriers (VLCCs) in the Alaska–West Coast trade.

Bulk carriers have upper and lower wing tanks and a double bottom structure. The side shell in the way of the cargo hold is usually single skin (Fig. 1.8b). In addition to the corrosion problems typical of ballast tanks, some areas of the cargo holds also suffer from corrosion wastage. The hold frames between the upper and lower ballast tanks experience both severe corrosion wastage and cracking. As grab handling is commonly used in bulk carriers, their inner bottom is prone to mechanical damage as a result of contact of the cargo and/or cargo gear with the structure.

Container carriers are built to have large open spaces to allow for carrying containers and for handling containers at berth (see Fig. 1.8c). This type of vessel usually has fracture problems in the way of the hatch corners, box girder attachments, and longitudinal bulkhead associated with container cell guides. Some container carriers have experienced fatigue cracks in longitudinal connections due to the large slamming pressure and whipping response of hull girders.

Gas carriers transport liquefied natural gas (LNG), liquefied petroleum gas (LPG) or compressed natural gas (CNG). The liquefied gas is stored in the containment systems, which are membrane tanks (see Fig. 1.8d), self-supporting prismatic membrane tanks, spherical tanks, or pressure vessel-shaped independent deck tanks. This vessel category has been developing rapidly in recent years, with more design variations likely to be presented in the near future with novel concepts to increase the capacity. The maintenance and inspection of the containment system has been important in maintaining the integrity of gas carriers.

1.6 Design, maintenance, inspection and repair of floating offshore structures

Various kinds of offshore installations are used to support drilling and production of oil and gas. Their primary function is to provide support of facilities for the drilling operation (mobile offshore drilling unit, or MODU) or for oil and gas production (floating production installation, or FPI). Their hull structures can be a converted oil tanker, tank barge, tension leg platform, spar, column-stabilized unit, new-build floating production, storage and offloading units (FPSOs), etc. While drilling units are designed to be mobile, floating production platforms are normally permanently located on a site by a mooring system which may consist of several mooring lines and anchors. Some FPIs allow for disconnection in typhoons.

Design, operation, maintenance and repair of MODUs and FPIs are to comply with regulations of the flag state, the coastal state (the government where the structures are stationed), the recommended practice of industrial organizations, and the rules of classification societies. Current design and inspection approaches for offshore structures are implemented in the latest codes (e.g., API

© 2008 Woodhead Publishing Limited

2002, ISO 2002, NORSOK 2004, UK DOE 1990, UKOOA 2003, ABS 2006). Because of the inherently innovative nature of offshore oil and gas exploration and production, newer types of structures often draw upon the experiences of existing types.

1.6.1 Regulations

Offshore structures are subject to the regulations of the nation in the waters in which they operate. Some flag administrations have developed their own rules. The majority of flags refer to the IMO Code for the construction and equipment of mobile offshore drilling units (IMO 1989), often referred to as the IMO MODU Code, as the applicable standard for mobile drilling units.

Operations of offshore structures in the Gulf of Mexico outer continental shelf of the USA need regulatory approval from the United States Coast Guard and the Minerals Management Service (MMS) (Parker and Grove 2002). In the UK sector of the North Sea, the Offshore Installations (Safety Case) Regulations 2005 (SCR05) require all offshore installations to have a safety case accepted in writing by the Health and Safety Executive (HSE) before they start operating in UK waters. Those parts of an installation that are identified as critical for the safety of the installation must be verified as suitable by independent and competent people. In the Norwegian sector of the North Sea, the Petroleum Safety Authority (PSA) has responsibility for the safety, emergency preparedness and the working environment in the petroleum activities. The Framework Regulations (2006) set out the principles according to which health, safety and environmental issues should be managed.

1.6.2 Recommended practice and the American Petroleum Institute (API)

The American Petroleum Institute (API) has contributed significantly to the technical standards associated with offshore oil and gas exploration and production. The API was established in 1919 with the objectives of developing an authoritative program of collecting industry statistics, standardization of oil field equipment and taxation. Today, the API maintains more than 500 standards and recommended practices covering all segments of the oil and gas industry to promote the use of safe, interchangeable equipment and sound, proven engineering practices.

Many of the API Recommended Practices, often referred to as API RPs, are widely accepted and applied internationally. The API PR2A (API 2002) is universally recognized for fixed structures, and is extensively referred to for floating structures as well. For example, many offshore structures in the UK sector of the North Sea have been designed according to the 100-year return condition requirements of API RP 2A, though the UK Statutory Instrument 289

© 2008 Woodhead Publishing Limited

required use of at least the individual 50-year return conditions in the evaluation of environmental loads.

NORSOK, the competitive standing of the Norwegian offshore sector, is the industry initiative to add value, reduce cost and lead-time and eliminate unnecessary activities in offshore field development and operations (NORSOK 2004). The NORSOK standards were developed by the Norwegian petroleum industry as a part of the NORSOK initiative and supported by the Norwegian Oil Industry Association and the Federation of Norwegian Engineering Industries. The standards are administered and issued by the Norwegian Technology Standards Institution.

1.6.3 Classification rules

Most mobile floating structures (some ship-shaped, some not) are classed by one of the classification societies. Floating production units may or may not be classed. ABS, Bureau Veritas, Det Norske Veritas, Lloyd's Register and other major classification societies have established rules specifically for MODUs and FPIs. Similar to ships, surveys of classification societies are typically made up of Annual Surveys, Intermediate Surveys and Special Surveys in a five-year cycle (ABS 2006). Classification rules for ship-shaped FPIs have relied heavily on the experiences of trading ships.

1.6.4 Design, inspection and maintenance of offshore structures

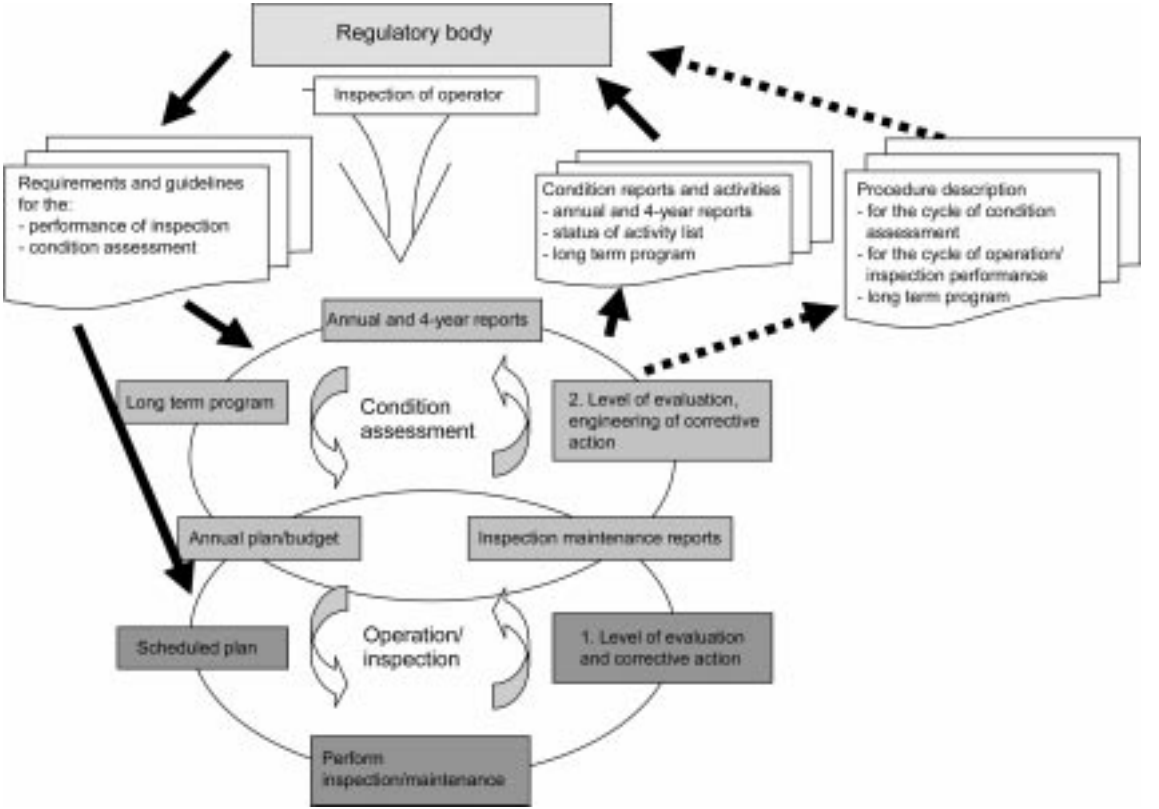
At the initial design stage, considerations are given to ensure that various structural limit state criteria are fulfilled and an initial inspection plan is established based on generic data (Moan 2005).

Corrosion is normally considered in the design process by providing a corrosion protection (coating, anodes, etc.) and a thickness allowance during new-build/construction. The purpose is to ensure that there will be a reasonable period of time during operation before the safety level of the structure is reduced to the extent that actions to maintain a safety level need to be carried out. This is essentially based on an economic consideration.

Fatigue criteria have been applied for fixed offshore platforms since the early 1970s. Several accidents with mobile units around 1980 made fatigue an important additional consideration for these structures. The fatigue design criteria depend upon inspectability and consequences of failure. A structural detail is designed to be of longer fatigue life if it is located in a less accessible area or the potential consequences of its fatigue failure are substantial.

The inspection and monitoring process coupled with, if necessary, maintenance and repairs are also important measures for maintaining adequate safety levels. Figure 1.9 shows the inspection and maintenance process within the

© 2008 Woodhead Publishing Limited



1.9 Inspection and maintenance process for offshore structures (ISSC 2003).

© 2008 Woodhead Publishing Limited

offshore sector in the North Sea. The regulatory body defines the framework for safety. The operator (the oil company or the rig owner) is responsible for safety during operation, defines the inspection and maintenance needed, reports on planned activity, and finds and evaluates conditions annually and every fourth year. The procedure for condition assessment, inspection and maintenance is available to the regulatory body, which in turn audits the operator.

Inspections of MODUs and FPIs are determined based upon accessibility. When considering the cost consequences a repair may entail, engineering analysis may be referred to for guiding the inspection scope and extent.

1.6.5 Operational experiences of floating offshore structures

Semi-submersibles saw fatigue failure in the period 1965–70. Fatigue design criteria were therefore implemented. Recent surveys revealed that some of the structural details had a design fatigue life of 2–6 years or a mean fatigue life of 6–18 years. Even today, the brace–column and column–pontoon connections for semi-submersibles with long pontoons present a challenge. The most fatigue-prone and critical areas of semi-submersible platforms are much more limited in number than for ships. Inspections can, to a large extent, be carried out from the inside of the structure. This has a significant effect on the quality and costs of inspections.

A *jackup drilling rig,* also called a self-elevating drilling unit, is a mobile bottom-supported offshore drilling structure with columnar or open-truss legs that support the deck and hull. When positioned over the drilling site, the hull is supported by spud can or mat resting on the seafloor. A jackup rig is towed or propelled to a location with its legs up. Once the legs are firmly positioned on the bottom, the deck and hull height are adjusted and leveled. The connections of brace to chord, connections located between leg guides, spud can brackets and stiffeners, and crane pedestal connections have all experienced cracking failure.

Tension leg platforms (TLPs) are buoyant installations connected to the seabed by pre-tensioned tendons. The tendons are normally parallel, near-vertical elements, acting in tension, which restrain the motions of the platforms in heave, pitch and roll. The TLP hull consists of buoyant columns, pontoons and intermediate structural bracings. Typical inspection locations include tendon interfaces with the foundations and the TLP hull, connections of tendons, connections of columns and pontoons.

Spars are cylindrical structures which have a deck containing the production facilities. The cylindrical structure houses all the tanks and may contain permanent ballast at the bottom for stability reasons. The cylindrical hull may incorporate a truss structure and heave plates. The internal inspection of the cylindrical hull is usually complemented by external inspections by remotely operated vehicles and divers.

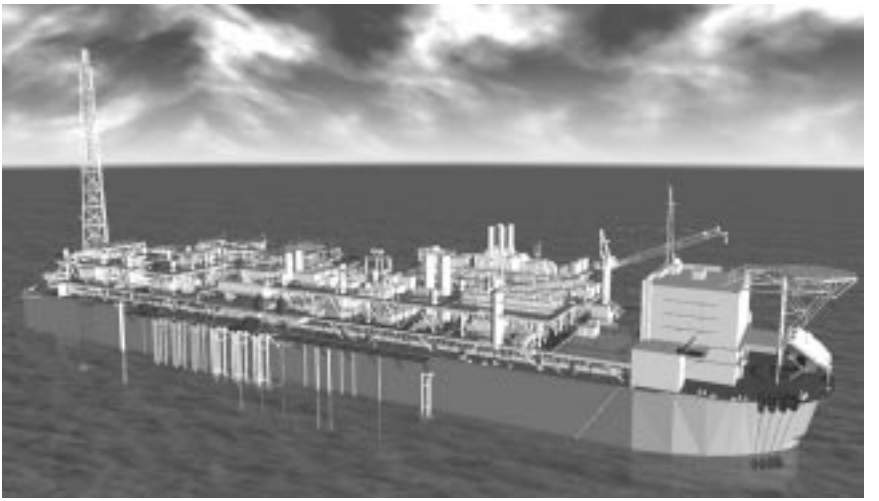
© 2008 Woodhead Publishing Limited

1.6.6 Floating production, storage and offloading units

Floating production, storage and offloading units are normally called FPSOs (Fig. 1.10). Ship-shaped FPSOs are by far the most widely used type of floating production unit, accounting for over 100 deployments globally. As operators are moving into deeper waters, FPSOs are continuing their popularity as the most cost-effective units. Design, maintenance and inspection of ship-shaped FPSOs have drawn upon the extensive experiences from tankers. The major difference between a trading tanker and an FPSO moored at a specific location is that dry-docking for inspections would be more complicated, and usually not possible, for FPSOs that need to be stationary at the offshore site.

The rules and guides of classification societies are usually utilized in assessing the fitness-for-purpose and are focused on safety aspects. These class requirements address the entire life cycle of FPSOs. Unlike the snapshot nature of certification, classification is an ongoing process by which the class periodically surveys the FPSO during its operating life to ensure compliance with the rules.

Hull structures of FPSOs experience structural failures typically seen in trading tankers. Operations and structural arrangement characteristics of FPSOs also place challenges on the brackets of some supporting structures on the longitudinal bulkheads and structures supporting a turret or topside modules. The industry has been using TSCF publications to better understand the structural performance and to guide FPSO hull structure maintenance, as well as starting to collect structural performance data to enhance the knowledge about FPSOs (Serratella and Spong 2007).



1.10 Floating production, storage and offloading unit (FPSO) (www.emersonprocess.com).

© 2008 Woodhead Publishing Limited

Most converted tankers were single-hull tankers built in the 1970s. With the number of candidate single-hull tankers shrinking, the industry has shown increasing interest in building new FPSOs and refurbishing double-hull tankers built since the 1990s.

1.7 Nondestructive examination and monitoring

The life-cycle management of ship and offshore structures is based on routine inspection, with the visual method being the primary means of inspection. Principles and tools of nondestructive examination (NDE) and monitoring have been developed. The offshore industry has been continuously introducing more advanced, nondestructive monitoring technologies.

1.7.1 Ultrasonic thickness measurement

In the early days of steel ships, people measured the remaining thickness of steel plates by drilling a hole. Over the years, ultrasonic thickness measurements have become the main means to measure plate thickness, and the measurement is done in a nondestructive manner.

Ultrasonic thickness measurement is the primary means of measuring the remaining thickness of structural members. By sending ultrasonic waves through the substrate and measuring reflection and transmission amplitudes, traveling time, and attenuation, the discontinuities or internal defects can be detected and the plate thickness can be accurately calculated.

It is a very time-consuming process to thoroughly measure large structures like ships. To overcome this disadvantage, many techniques have been developed (Rizzo *et al.* 2007). A *charge-coupled device* uses optical scanning devices to record the images and then processes them by computer. This technique can scan large areas and is relatively inexpensive. *Ultrasonic guided waves* have been used for large-area inspection as well. The advantage of this technique is the ability of guided waves to travel along the surface, making measurements faster than those made with the use of bulk waves.

1.7.2 Detection of cracks

Visual inspection is the primary means of detecting cracks. In addition, the following NDE tools are sometimes used in areas of high stress or areas of known cracks: magnetic particle inspection, eddy current inspection, ultrasonic flaw detection, dye-penetrant inspection, radiographic inspection, fluorescent lead test, acoustic emission, infrared thermography, laser shearography, potential drop test, alternating current field measurement (ACFM), crack propagation gauges, and automated ball indentation (Saidarasamoot *et al.* 2003, Lozev *et al.* 2003).

Magnetic particle inspection can be used to detect surface and near-surface

© 2008 Woodhead Publishing Limited

flaws in ferromagnetic materials such as steel and iron, e.g. casting, plates, machined components, welds and forgings. It is most often applied in identifying cracking at welded joints and in areas identified as being susceptible to environmental cracking, e.g., stress corrosion cracking or hydrogen-induced cracking, fatigue cracking or creep cracking.

Ultrasonic weld inspection is generally applied in the pulse–echo, shear wave mode. In this mode, an ultrasonic energy pulse is generated at a moveable transducer source (usually a commercially available piezoelectric material excited by a commercially available ultrasonic instrument). The sound pulse is transmitted at an angle into the material adjacent to a weld. Anomalies (cracks, inclusions, and porosity) reflect the sound energy back to the transducer, and the reflected energy is displayed on an oscilloscope or cathode ray tube.

Gamma radiography inspection uses radiant energy in the form of gamma rays to produce a two-dimensional image of an object on a sensitized film. This method has the ability to detect surface and subsurface discontinuities of structures and welds without causing damage or disassembly of the components. Gamma rays are emitted from radioactive isotopes in the form of iridium-192. Radiography film provides a permanent record.

Eddy current testing is an electromagnetic technique. When an energized coil is brought to the surface of a metal component, eddy currents are induced into the specimen. These currents set up a magnetic field that tends to oppose the original magnetic field. The impedance of the coil is in close proximity to that of the specimen. When the eddy currents in the specimen are distorted by the presence of the flaws or material variations, the impedance in the coil is altered. This change is measured and displayed in a manner that indicates the type of flaw or material condition. The application of eddy current testing ranges from crack detection to the rapid sorting of small components for flaws, size variations or material variation.

The ‘leak before break’ principle is sometimes used to detect cracks, if the hull structures have a higher level of redundancy and the cracks in the main hull structures can grow continuously until global rupture of the hull.

For the time being, only visual or close visual inspections are used to detect mechanical damage.

1.7.3 Probability of detection

The probability of detection, POD (HSE 2000), has been used to provide a baseline capability and confidence level that the NDE procedure can be reliably applied and will produce some confidence in detecting cracks (or other target anomalies). The elements of a reliable NDE procedure are *reproducibility* (addressed by a rigorous calibration protocol), *capability* (addressed by the POD analysis method), and *repeatability* (addressed by rigor in NDE procedure application, process control, and personnel skills).

© 2008 Woodhead Publishing Limited

1.8 Challenges and future trends

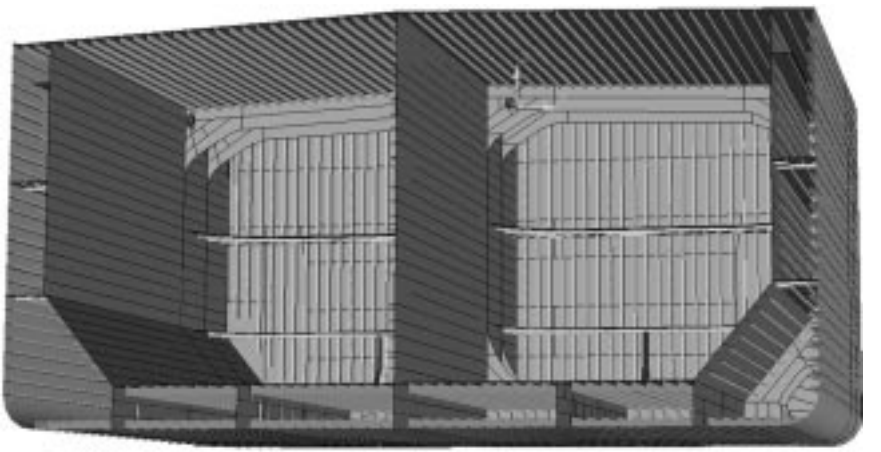
Both the shipping and offshore industries are becoming more and more proactive and are seeking better, more efficient ways of maintaining the structural integrity of ships and offshore installations. The concepts and methodologies of integrity management, asset integrity management, and risk-based inspection are applied in more and more projects. Many owners and operators are requesting vessel-specific inspection and maintenance guidance. The focus is progressing towards allocating inspection and maintenance resources to 'critical' or 'hot' areas where failure or damage is more likely to take place.

The offshore industry has also been applying risk-based approaches in inspection and maintenance decisions. The shipping industry is also progressively moving in the same direction. A systematic risk-based approach has been adopted directly for defining surveys or acceptance criteria (ISSC 2003, 2006a, 2009, Lee *et al.* 2006). Chapter 17 of this book provides further elaboration upon the subject of risk-based inspection.

The reliability-based approach is well suited to revealing the risks of structural failures and has been applied in risk-based inspection planning (Moan 2005, Ku *et al.* 2005, ISSC 2006b). Chapters 10–12 are devoted to structural reliability analysis.

Fleet and vessel management software systems are used to assist inspection and maintenance planning and storage of records. Figure 1.11 shows an example of a virtual ship model used for illustrating inspection areas and storing historical data and future inspection plans.

It is expected that more and more interest will be focused upon the application of the technologies of nondestructive examination and monitoring (ISSC 2003, 2006a, 2009, Rizzo *et al.* 2007, Saidarasamoot *et al.* 2003). NDE and monitoring



1.11 Virtual ship model used for managing structural integrity of a tanker (courtesy of ABS).

© 2008 Woodhead Publishing Limited

technologies are efficient risk control options and with their rapid advancement they will play an increasingly vital role in managing hull integrity.

1.9 Sources of further information and advice

American Bureau of Shipping (ABS), www.eagle.org
American Petroleum Institute (API), www.api.org
Bureau Veritas (BV), www.bureauveritas.com
China Classification Society (CCS), www.ccs.org.cn
Det Norske Veritas (DNV), www.dnv.com
European Maritime Safety Agency (EMSA), www.emsa.europa.eu
Germanischer Lloyd (GL), www.gl-group.com
Health and Safety Executive, www.hse.gov.uk
International Association of Classification Societies Ltd (IACS), www.iacs.org.uk/
International Association of Dry Cargo Shipowners (INTERCARGO), www.intercargo.org/
International Association of Independent Tanker Owners (INTERTANKO), www.intertanko.com
International Chamber of Shipping (ICS), www.marisec.org/ics/index.htm
International Maritime Organization (IMO), www.imo.org/
International Organization for Standardization, www.iso.org
Korean Register of Shipping (KR), www.krs.co.kr
Lloyd's Register (LR), www.lr.org
Minerals Management Service, US Department of Interior, www.mms.gov
Nippon Kaiji Kyokai (ClassNK or NK), www.classnk.or.jp
Oil Companies International Marine Forum (OCIMF), www.ocimf.com/
Registro Italiano Navale (RINA), www.rina.org
Russian Maritime Register of Shipping (RS), www.rs-head.spb.ru
United States Coast Guard (USCG), US Department of Homeland Security, www.uscg.mil/

1.10 Acknowledgments

The authors wish to express their appreciation to R. Basu, D. Browning, D. Liu, I. Simpson, J. Speed, K. Tamura, M. Unuvar and Q. Yu for reading the manuscript.

1.11 References

ABS (2006), *Mobile offshore drilling units*, Houston, TX, ABS.
ABS (2007), *Guidance notes on the inspection, maintenance and application of marine coating systems*, 3rd edition, Houston, TX, ABS.

© 2008 Woodhead Publishing Limited

API (2002), *API RP 2A-WSD*, *Planning, designing and constructing fixed offshore platforms – Working stress design*, Dallas, TX, American Petroleum Institute.

Contraros P D (2004), 'Diagnostics of coating breakdown in ballast tanks, testing – assessment – prevention (TAP)', Oslo, *Protective Coatings Conference in Oslo*.

Emi H (2006), *Illustrations of hull structures* (English/Japanese), Japan, Seizando-Soten Publishing Co.

EMSA (2005), *Double hull tankers high level of experts report,* European Maritime Safety Agency.

Harada S, Yamamoto N, Magaino A, Sone H (2001), 'Corrosion analysis and determination of corrosion margin, Part 1 & 2' (IACS discussion paper), London, International Association of Classification Societies.

Horn G, Baumans P (2007), 'The development, implementation and maintenance of IACS common structural rules for bulk carriers and oil tankers', *International Conference Developments in Classifications & International Regulations*, London.

HSE (2000), 'POD/POS curves for nondestructive examination', *Offshore Technology Report, OTO 2000-018*, London, Health and Safety Executive.

IACS (2002), *Guidelines for surveys, assessment and repair of hull structures – general cargo ships*, London, International Association of Classification Societies.

IACS (2004a), *Classification societies – what, why and how*, London, International Association of Classification Societies.

IACS (2004b), *Guidelines for surveys, assessment and repair of hull structures – bulk carriers Rec. No.76*, London, International Association of Classification Societies.

IACS (2004c), *Guidelines for coating maintenance & repairs for ballast tanks and combined cargo/ballast tanks on oil tankers*, *Rec. 87*, London, International Association of Classification Societies.

IACS (2005), *Unified requirements – enhanced survey program*; *UR Z7 & Z10*, London, International Association of Classification Societies.

IACS (2006), *Shipbuilding and repair quality standard*, *Rec. No. 47*, London, International Association of Classification Societies.

IMO (1989), *Code for the construction and equipment of mobile offshore drilling units* (IMO MODU Code), London, International Maritime Organization.

IMO (2006), *Performance standard for protective coatings for dedicated seawater ballast tanks in all types of ships and double-side skin spaces of bulk carriers, IMO PSPC 215(82)*, London, International Maritime Organization.

INTERTANKO (2003), *A guide to the vetting process*, 5th edition, London, International Association of Independent Tanker Owners.

INTERTANKO (2006), *Tanker performance* (presentation to World Maritime University by E Ranheim), London, International Association of Independent Tanker Owners.

ISO (2002), *Petroleum and natural gas industries – general requirements for offshore structures* ISO (19900), London, International Organization for Standardization.

ISSC (2003), 'Committee V.2, Inspection and monitoring' (prepared by Bruce G J, Duan M, Egorov G V, Folso R, Fujimoto Y, Garbatov Y, Le Hire J-C, Shin B C, Vardal O T), *Proceedings of 15th International Ship and Offshore Structures Congress*, 11–15 August 2003, San Diego, CA.

ISSC (2006a), 'Committee V.6, Condition assessment of aged ships' (prepared by Paik J K, Brennan F, Carlsen C A, Daley C, Garbatov Y, Ivanov L, Rizzo C M, Simonsen B C, Yamamoto N, Huang H Z), *Proceedings of 16th International Ship and Offshore Structures Congress*, 20–28 August 2006, Southampton, UK.

ISSC (2006b), 'Committee VI.1, Reliability based structural design and code development' (prepared by Moan T *et al.*), *Proceedings of 16th International Ship*

© 2008 Woodhead Publishing Limited

and Offshore Structures Congress, 20–28 August 2006, Southampton, UK.
ISSC (2009), 'Committee V.6, Condition assessment of aged ships', *Proceedings of 17th International Ship and Offshore Structures Congress*, Seoul, Korea.
Jones N (1989), *Structural Impact*, Cambridge, Cambridge University Press.
Ku A, Spong R E, Serratella C, Wu S, Basu R, Wang G (2005), 'Structural reliability application in risk-based inspection plans and their sensitivities to different environmental conditions', OTC 17535, *Offshore Technology Conference* (OTC'05), 2–5 May 2005, Houston, TX.
Lee A, Serratella C, Basu R, Wang G, Spong R E (2006), 'Flexible approaches to risk-based inspection of FPSOs', OTC 18364, *Offshore Technology Conference* (OTC'06), 1–4 May 2006, Houston, TX.
Lozev M G, Smith R W, Grimmett B B (2003), 'Evaluation of mathods for detecting and monitoring of corrosion damage in risers', *22nd International Conference on Offshore Mechanics and Arctic Engineering* (OMAE'03), 8–13 June 2003, Cancun, Mexico.
Melchers R E (2001), 'Probabilistic models of corrosion for reliability assessment an maintenance planning', *20th International Conference on Offshore Mechanics and Arctic Engineering*, 3–8 June 2001, Rio de Janeiro.
Moan T (2005), 'Reliability-based management of inspection, maintenance and repair of offshore structures', *Journal of Structures and Infrastructure Engineering*, 1(1), 32–62.
NORSOK (2004), *NORSOK Standards N-001 Structural Design*, Rev. 4, Standards Norway, Oslo.
Paik J K, Thayamballi A K (2007), *Ship-shaped Offshore Installations, Design, Building and Operation*, New York, Cambridge University Press.
Paik J K, Wang G, Thayamballi A K, Lee J M (2003), 'Time-variant risk assessment of aging ships accounting for general/pit corrosion, fatigue cracking and local dent damage', *SNAME Annual Meeting*, San Francisco, CA, Society of Naval Architects and Marine Engineers.
Paik J K, Lee J M, Shin Y, Wang G (2004), 'Design principles and criteria for ship structures under dynamic pressure arising from sloshing, slamming and green sea', *SNAME Annual Meeting*, 29 September–1 October 2004, Washington, DC.
Parker W J, Grove T W (2002), 'FPSO standards and recommended practices', *Offshore Technology Conference*, Houston, TX.
Rizzo C M, Paik J K, Brennan F B, Carlsen C A, Daley C, Garbatov Y, Ivanov L, Simonsen B C, Yamamoto N, Zhuang H Z (2007), 'Current practice and recent advances in condition assessment of aged ships', *Journal of Ships and Offshore Structures*, 2(3), 261–271.
Saidarasamoot S, Olson D, Mishra B, Spencer J, Wang G (2003), 'Assessment of the emerging technologies for the detection and measurement of corrosion wastage of coated marine structures', *22nd International Conference on Offshore Mechanics and Arctic Engineering* (OMAE'03), 8–13 June 2003, Cancun, Mexico.
Serratella C, Spong R E (2007), 'FPSO structural performance JIP, Phase II final report', *FPSO JIP Week*, May 2007, Houston, TX.
TSCF (1992), *Condition evaluation and maintenance of tanker structure*, London, Witherby & Co. and Tanker Structure Cooperative Forum.
TSCF (1995), *Guidance manual for the inspection and maintenance of double hull tanker structure*, London, Witherby & Co. and Tanker Structure Cooperative Forum.
TSCF (1997), *Guidance manual for tanker structures*, London, Witherby & Co. and Tanker Structure Cooperative Forum.

© 2008 Woodhead Publishing Limited

TSCF (2000), *Guidelines for ballast tank coating system and edge preparation*, London, Witherby & Co. and Tanker Structure Cooperative Forum.

UK DOE (1990), *Offshore installations: guidance on design, construction and certification*, 4th edition, London, UK Department of Energy.

UKOOA (2003), *UKOOA guidelines for ship/installation collision avoidance*, London, UK Offshore Operators Association.

Wang G, Tang S, Shin Y (2002), 'Direct calculation approach and design criteria for wave slamming of an FPSO bow', *International Journal of Offshore and Polar Engineering*, 12(4), 297–304.

Wang G, Spencer J, Sun H H (2003a), 'Assessment of corrosion risks to aging ships using an experience database', *22nd International Conference on Offshore Mechanics and Arctic Engineering* (OMAE'03), 8–13 June 2003, Cancun, Mexico.

Wang G, Spencer J, Elsayed T (2003b), 'Estimation of corrosion rates of oil tankers', *22nd International Conference on Offshore Mechanics and Arctic Engineering* (OMAE'03), 8–13 June 2003, Cancun, Mexico.

Wang G, Spencer S, Olson D, Mishra B, Saidarasamoot S, Thuanboon S (2005a), 'Tanker corrosion', Chapter 25 in Kutz M, *Handbook of Environmental Degradation of Materials*, Norwich, NY, William Andrew Publishing.

Wang G, Basu R, Chavda D, Liu S (2005b), 'Rationalizing the design of ice strengthened side structures', in Guedes Soares C, Garbatov Y, Fonseca N (eds), *Maritime Transportation and Exploitation of Ocean and Coastal Resources*, London, Taylor & Francis.

Wang G, Tamura K, Jiang D, Zhou J (2006), 'Design against contact damage for offshore supply vessels', *9th International Marine Design Conference (IMDC), Advancing Marine Design – Naval, Commercial, Inland/Great Lakes and Offshore*, 16–19 May 2006, Ann Arbor, MI.

Wang G, Lee A, Lynch T J, Ivanov L, Serratella C, Basu R (2008), 'A statistical investigation of time variant hull girder strength of aging ships and coating life', *Journal of Marine Structures*, 21, 240–256.

Yamamoto N, Ikegami K (1998), 'A study on the degradation of coating and corrosion of ship's hull based on the probabilistic approach', *Journal of Offshore Mechanics and Arctic Engineering*, 120, 121–128.

Yoneya Y, Shigemi T, Yamamoto N, Harada S, Harada M (2004), 'A comparative study on the practical strength assessment of tankers and bulk carriers structures', *SNAME Annual Meeting*, San Francisco, CA, Society of Naval Architects and Marine Engineers.

1.12 Appendix: abbreviations used in this chapter

ACFM	Alternating current field measurement
API	American Petroleum Institute
AS	Annual Survey
CAIP	Critical Area Inspection Plan
CAP	Condition Assessment Program
CAS	Condition Assessment Scheme
CNG	Compressed natural gas
CSR	Common Structural Rules
CVI	Close Visual Inspection

© 2008 Woodhead Publishing Limited

ESP	Enhanced Survey Program
FPI	Floating production installation
FPSO	Floating production, storage and offloading unit
GVI	General Visual Inspection
HSE	Health and Safety Executive
IACS	International Association of Classification Societies
IMO	International Maritime Organization
IS	Intermediate Survey
ISO	International Organization for Standardization
LNG	Liquefied natural gas
LPG	Liquefied petroleum gas
MIC	Microbially induced corrosion
MMS	Minerals Management Service
MODU	Mobile offshore drilling unit
NDCV	Nominal design corrosion values
NDE	Nondestructive examination
OCIMF	Oil Companies International Marine Forum
POD	Probability of detection
PSA	Petroleum Safety Authority
PSC	Port state control
PSPC	Performance Standards for Protective Coatings
SIRE	Ship Inspection Report Program
SS	Special Survey
TLP	Tension leg platform
TSCF	Tanker Structure Cooperative Forum
USCG	United States Coast Guard
VLCC	Very large crude carrier

© 2008 Woodhead Publishing Limited

2

Current practices in condition assessment of aged fixed-type offshore structures

I LOTSBERG, Det Norske Veritas (DNV), Norway

Abstract: This chapter gives an introduction to procedures for assessment of existing fixed offshore structures to demonstrate their fitness-for-purpose. An overview of some of the design standards frequently referred to for design of fixed offshore steel structures is presented. An overview of general safety considerations inherent in the design standards that are being used for design and for assessment during service life is also presented. The process for structural assessment is described. This chapter also gives some information related to situations that may trigger an assessment of structural integrity. A significant amount of data from design, fabrication, installation and in-service life is required for reliable assessment. Assessment of data for structural analysis for the Ultimate Limit State (ULS) and the Fatigue Limit State (FLS) is described. Considerations on in-service inspection and requirements to extension of service life of structures are presented. A section on mitigation of structures is included. Also some future trends related to assessment of fixed structures are discussed. Some sources for further information and advice are listed.

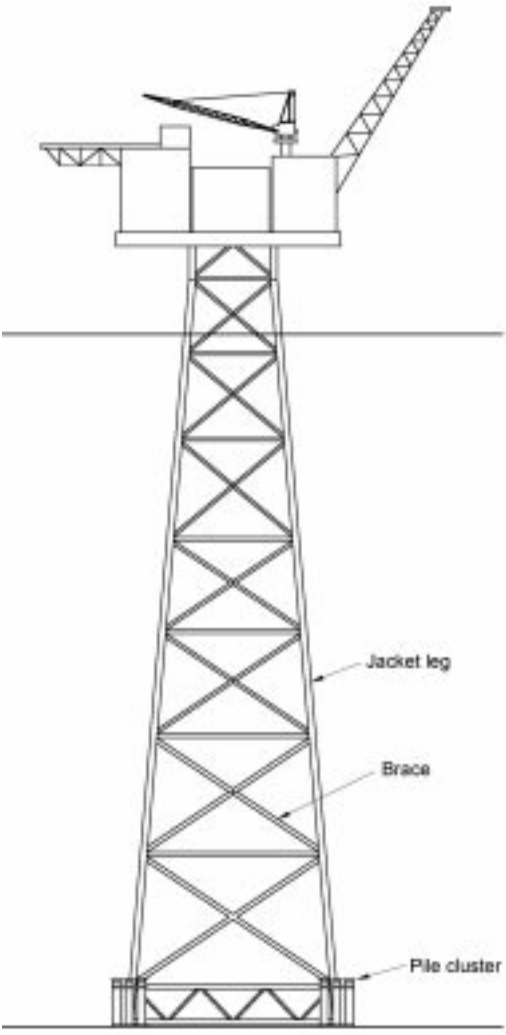
Key words: fixed structures, assessment, fitness-for-purpose, handling of data, ultimate strength analysis, fatigue strength analysis, in-service inspection, monitoring, extended life, mitigation, future trends.

2.1 Introduction

This chapter gives an introduction to procedures for assessment of existing fixed offshore structures to demonstrate their fitness-for-purpose.

Most fixed offshore structures are made of steel, but there are also some very large offshore structures made of concrete. Most steel platforms are designed as braced frame structures that are piled into the sea bottom. These platforms are denoted jackets or jacket structures. The platforms are prefabricated on land and transported to the installation site. Heavy jackets are launched from a barge before they are upended and placed on temporary foundation plates denoted mud mats on the sea bottom. Also a number of jackets have been lift-installed by crane ships. Then, in older jackets the piles were driven through the legs of the jackets and the annuli between the piles and the legs were grouted to achieve a connection that could transfer forces from the structure to the foundation. Later it has been found efficient to use clusters of piles at the main legs as shown in Fig. 2.1. After piling, the annuli between the piles and the pile sleeves are grouted as explained above. Shear keys are used on the piles and the pile sleeves

© 2008 Woodhead Publishing Limited



2.1 Jacket structure.

in order to keep the required length of the sleeves to a minimum for reliable transfer of forces. After installation of the substructure a module support frame or a deck structure is lifted onto the top and welded to the substructure. See also Veldman and Lagers (1997) for the historical development of structures used by the oil industry.

An overview of some of the design standards frequently referred to for design of fixed offshore steel structures is presented in Section 2.2. The same section also gives an overview of general safety considerations inherent in the design standards that are being used for design and for assessment during service life.

© 2008 Woodhead Publishing Limited

The process for structural assessment is described in Section 2.3. This also gives some information related to situations that may trigger an assessment of structural integrity. A significant amount of data from design, fabrication, installation and in-service life is required for reliable assessment. This is considered in more detail in Section 2.4. Assessment of data for structural analysis for the Ultimate Limit State (ULS) and the Fatigue Limit State (FLS) is described in Section 2.5. A section on mitigation is included in Section 2.6. Some future trends related to assessment of fixed structures are discussed in Section 2.7. Sources for further information and advice are included in Section 2.8.

2.2 Design standards and acceptance criteria for assessment

2.2.1 General

Mainly steel structures are considered in this chapter. Reference is made to ISO standard 19903 for assessment of concrete structures.

Most jackets have normally been designed according to recognised design standards such as API RP 2A (2000). This implies that the structures have been designed to meet certain safety levels that are inherent in the design standard. This design standard was first issued in 1969 and has later been revised several times based on lessons learned from research and development and also from in-service experience. Today the 21st version of API RP 2A is being used.

Design practices in different areas of the world have differed owing to differences in environmental climate and philosophy in operation of the platforms. Platform designs in the Gulf of Mexico and the North Sea are selected for exemplification. The ultimate loading in the Gulf of Mexico is due to hurricanes and the platforms are planned to be shut down and evacuated in such conditions. The platforms in the North Sea have traditionally been designed to meet the 100-year loading conditions together with additional safety coefficients. The platforms are normally not planned to be evacuated during these storms. The environmental climate in the North Sea is more homogeneous than in the Gulf of Mexico. This means that fatigue of structures in the North Sea becomes a larger challenge than for jacket structures in the Gulf of Mexico. These differences are reflected in developments of design standards for the different areas such as API RP 2A and the Norsok standards. The Norsok standards have been used for design in the Norwegian part of the North Sea for the last 10 years. However, much of the basic formulations for load and capacity calculation are similar to that in API RP 2A. These formulations are now included in the new ISO standard for fixed offshore structures (ISO/FDIS 19902). It is planned that contents that are specifically different from one area to another in terms of environment and operational philosophy will be included in regional annexes to this standard.

© 2008 Woodhead Publishing Limited

2.2.2 Assessment of risk of failure

In order to perform a sound assessment of structures, it is necessary to understand the basic design requirements and to assess changes made in operation of the platform during service life. When considering safety of structures it is found practical to group the risks of failure as follows:

- Risk of failure of the structure resulting from statistical variations in loads and structural load-bearing capacities
- Risk of failure due to accidents
- Risk of failure due to a gross error during design, fabrication, installation and operation of the structure.

The first of these is controlled by appropriate design standards with specified load and resistance coefficients. A low probability of failure is aimed for when design standards are developed. For welded offshore structures a target failure probability of less than 10^{-4}–10^{-5} is aimed for when load and material coefficients are calibrated for design codes for welded structures for the North Sea (Fjeld 1978). Thus, normally this probability of failure becomes small compared with the other risks for structural failure. This risk of failure is controlled by performing analysis according to the Ultimate Limit State (ULS) in design codes such as API RP 2A, ISO 19900 and Norsok N-001.

The risk of failure due to accidents is accounted for by appropriate risk assessment studies, denoted Quantified Risk Analysis (QRA). If the risk from an accidental event is high (typically higher than 10^{-4} on an annual basis), the event will be designed for. On the Norwegian Continental Shelf this is implemented by what is denoted the Accidental Limit State (ALS). Other codes recommend that the risk of failure due to accidents should be as low as is reasonably practicable. This is also known as the ALARP principle (HSE 1992).

The risk of failure due to gross error is the most difficult to handle, as this risk cannot be removed by additional safety coefficients (Lotsberg *et al.* 2005). Normally a detailed plan for verification and quality assurance of important items in the design, fabrication and installation process is required in order to keep the probability of gross errors in a project at an acceptable level. However, it is difficult to assess the risk of failure due to gross error because of its varied nature.

By gross errors are understood the following:

- Lack of human understanding of the methodology used for design
- Negligence of information
- Mistakes such as calculation errors (this can be input errors to the analysis programs used and also errors in computer software that are used for design)
- Lack of self-check and verification

© 2008 Woodhead Publishing Limited

- Lack of follow-up of material data testing, welding procedures, inspection during fabrication, etc.
- Mistakes resulting from lack of communication or misunderstanding in communication
- Lack of training of personnel onboard the platform that may lead to maloperation
- Errors in systems used for operation of the platform.

Thus, by gross errors are understood human mistakes. Different people are involved in each project and it becomes very difficult to predict the probability of a gross error in a project. However, from past history gross errors have been a significant contributor to the failure of structures, and a focus on these issues is considered to be important in order to ensure project success.

In-service inspection of structures is considered to be an important measure to reduce the probability of failure due to gross errors. This is accounted for by general visual inspection of the structure to ensure that the most important assumptions made during the design are fulfilled. This also includes degradation processes such as corrosion and fatigue. Corrosion may be assessed by general inspection, while fatigue cracks can hardly be detected by visual inspection before the cracks have grown large. Motives for in-service inspection have also been presented in ISO 19902 (2007): see Table 2.1.

Table 2.1 Examples of inspection motives (from ISO 19902, 2007)

Motive	Examples
Fabrication defects or installation damage	Weld defects (major and minor), material imperfections, dents, deformations
Degradation or deterioration	Corrosion, fatigue, scour, subsidence, sea floor stability
Design uncertainties or errors	Approximations (especially for oceanographic and seismic data), analysis uncertainties (especially for fatigue), underdesign, marine growth build-up
Environmental overload	Storm, earthquake, mud slide, tsunami, ice
Accidental events	Vessel impact, dropped objects, explosion, abrasion, floating debris, riser damage from anchor drag on pipeline
Modifications from original purpose	Addition of personnel, topsides equipment, support framing, risers or conductors, structure life extension
Repairs	Clamps, wet welds, bolting, adhesives

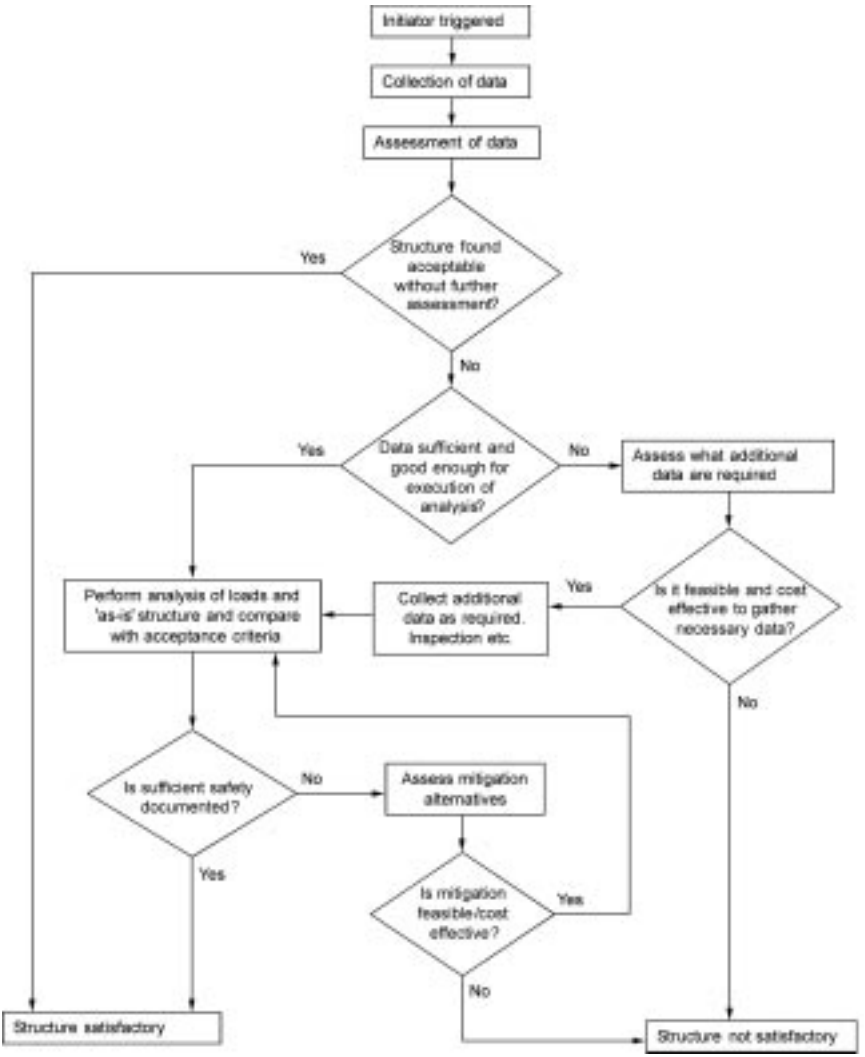
© 2008 Woodhead Publishing Limited

2.3 Process for structural assessment

The assessment process is illustrated in the flowchart in Fig. 2.2. This flowchart may be followed for assessment of the ultimate loading as well as fatigue loading.

An assessment of a fixed structure can be triggered by one or more of the following factors:

- Changes in deck loading
- New information on environmental criteria



2.2 Flowchart for the assessment process.

© 2008 Woodhead Publishing Limited

- New information about marine growth on the structure
- Subsidence of foundations resulting in increased environmental forces on the structure
- Modifications made with respect to structural members
- Accidents in terms of ship impact or lost objects that may have dented structural members
- Areas being more corroded than anticipated at the design stage and exceeding the corrosion allowance
- Cracks discovered during in-service inspection
- Elapsed service life and an extended life being considered
- Finding that the design basis is old and a more reliable assessment of the structural safety can be made based on design standards and analysis methodology of today.

Data collection is an important part of an assessment process – see Section 2.4. A further collection of data should be considered if significant data are missing. The feasibility/cost of collection of data should be considered. An initial assessment may be based on conservative assumptions. However, if such an assessment fails, more accurate data have to be provided. Structural analyses for assessment may be performed provided that a sufficient database for performing reliable analysis is available. Then the safety level of the structure can be assessed and it can be decided whether mitigation is required (see Section 2.6).

Evaluation of structural integrity and fitness-for-purpose requires consideration of numerous factors affecting the structural performance for the various structural components. According to ISO 19902 (2007) the following structural performance factors shall be considered, as appropriate:

- Structure age, condition, original design situations and criteria, and comparison with current design situations and criteria
- Analysis results and assumptions for original design or subsequent assessments
- Structure reserve strength and structural redundancy
- Fatigue sensitivity
- Degree of conservatism or uncertainty in specified environmental conditions
- Extent of inspection during fabrication and after transportation and installation
- Fabrication quality and occurrences of any rework or rewelding
- Damage (including fatigue damage) during transportation or installation
- Operational experience including previous in-service inspection results and learning from performance of other structures
- Modifications, additions and repairs or strengthening
- Occurrence of accidental and severe environmental events
- Criticality of structure to other operations

© 2008 Woodhead Publishing Limited

- Structure location (geographical area, water depth)
- Debris
- Structural monitoring, if available
- Potential reuse or removal intents.

In order to ensure the condition of a structure it is recommended to keep track of all relevant data in a systematic manner. This can be performed by development of Structural Integrity Management Systems (SIMS). Such systems should include all significant information related to

- data collection
- data evaluation
- development of inspection and maintenance strategy
- development and execution of an inspection programme and any consequent remedial work.

Structural Reanalysis Systems including updated structural analysis models (SRS models) ready for detailed analysis within a short notice are considered to be part of the SIMS.

2.4 Collection of data from design, fabrication, transportation, installation and in-service life

2.4.1 General

A reliable assessment of structures requires that a significant database is available. This database should include:

- As-built drawings of the structure
- New information on environmental data, if available
- Permanent loads and live loads
- Functional requirements
- Design and fabrication specifications
- Design, fabrication, transportation and installation reports, which should include information about material certificates (material yield strength and Charpy V test values), weld repairs during fabrication, non-destructive testing (extent and criteria used) and pile driving records (action effects during pile driving and number of blows)
- A weight report that is updated during service life
- In-service inspection history, including information on marine growth, corrosion, cracks, dents, deflections and scour
- Information about subsidence of bottom area versus mean water level
- Information about repair and strengthening if performed
- Experience from similar platforms during service life.

© 2008 Woodhead Publishing Limited

2.4.2 Condition monitoring by in-service inspection

General inspection

Shortly after installation it is recommended to perform a general visual inspection to map the condition of the structure. The different levels of in-service inspection are described by API RP 2A and ISO 19902. A level I inspection consists of a general below-water verification of the cathodic protection system and an above-water visual survey of the structure. If a level I inspection indicates that underwater damage is possible, a level II inspection should be conducted as soon as conditions permit. A level II inspection consists of general underwater visual inspection to detect the presence of any of the following:

- Excessive corrosion
- Effects of accidental or environmental overloading
- Scour, sea floor instability
- Damage detectable in a visual swim-around survey
- Design or construction deficiencies
- Presence of debris
- Excessive marine growth.

The inspection includes the measurement of cathodic potentials of preselected critical areas. Detection of significant damage during a level II inspection initiates a level III inspection as soon as conditions permit.

A level III survey consists of an underwater visual inspection of preselected areas and/or, based on results of the level II survey, areas of known or suspected damage. Such areas should be sufficiently cleaned of marine growth to permit thorough inspection. Preselection of areas to be surveyed should be based on an engineering evaluation of areas particularly susceptible to structural damage, or to areas where repeated inspections are desirable in order to monitor their integrity over time.

Flooded member detection (FMD) can provide an acceptable alternative to close visual inspection (level III) of preselected areas. Engineering judgement should be used to determine optimum use of FMD and/or close visual inspection of joints. Close visual inspection of preselected areas for corrosion monitoring should be included as part of the level III survey. Detection of significant structural damage during a level III survey should become the basis for initiation of a level IV survey in those instances where visual inspection alone cannot determine the extent of damage. The level IV survey, if required, should be conducted as soon as conditions permit.

A level IV survey consists of underwater non-destructive testing of preselected areas and/or, based on results of the level III survey, areas of known or suspected damage. A level IV survey should also include detailed inspection and measurement of damaged areas. A level III and/or level IV survey of fatigue-sensitive joints and/or areas susceptible to cracking could be necessary to

© 2008 Woodhead Publishing Limited

determine whether damage has occurred. Monitoring fatigue-sensitive joints and/or reported crack-like indications can be an acceptable alternative to analytical verification.

According to API RP 2A, in the US part of the Gulf of Mexico, cracking due to fatigue is generally not experienced. If cracks occur, they are most likely found at joints in the first horizontal conductor framing below water, normally resulting from fatigue degradation; or cracks may also occur at the main brace to leg joints in the vertical framing at the first bay above the mudline, normally due to environmental overload (for example, low cycle fatigue), or at the perimeter members in the vertical framing at the first bay below the water level, normally as a result of boat impact.

Condition monitoring principles are also outlined in Norsok N-005 (1997). It is the responsibility of the operator throughout the lifetime of the installation to ensure that the load-bearing structures are suitable for the intended purpose. The operator should monitor the condition of the operated offshore installation in a systematic manner. This may include development of an overall philosophy and strategy for condition monitoring, establishing in-service inspection systems and long-term inspection programmes, in-service inspection planning, offshore execution, data logging, evaluation and assessment, implementation of repair and mitigation measures, emergency preparedness, etc. Following Norsok N-005 the condition monitoring determines, within a reasonable level of confidence, the existence, extent and consequence of:

- Fabrication or installation damage
- Damage or component weakening due to strength overloading damage due to man-made hazards
- Excessive deformations
- Corrosion damage
- Degradation or deterioration due to fatigue or other time-dependent structural damage.

The condition monitoring programme is subject to continuous updating as it involves many factors in the nature of uncertainty such as environmental conditions, failure probabilities, damage development, etc. In addition, a revision of the programme may also be necessary as a result of development of tools and methods. Different inspection techniques and their efficiency described in Norsok N-005 are listed in Table 2.2.

In-service inspection for corrosion

Degradation of steel structures below the water level is generally not a large problem provided that the cathodic protection system is adequately designed and maintained. It is normal to perform readings of cathodic potential as part of a general inspection using a Remote Operated Vehicle (ROV). The consumption

© 2008 Woodhead Publishing Limited

Table 2.2 Below-water inspection methods (from Norsok N-005, 1997)

Methods/techniques	Capability	Technical description	ROV applicability	Cost-related aspects
Visual without cleaning	Scour, sea floor instability, gross damages, existence of anodes	Video-based reporting	ROV	Fast
Visual with cleaning	Follow-up investigation of general damage	Video-based reporting	Work class ROV	Time consuming
Electronic: MPI	Fatigue damage	Existence and length of surface crack	Work class ROV	Cleaning required, time consuming
Electronic: EC	Fatigue damage	Length of surface crack; may also be used for depth measurement; independent evaluation possible	ROV	Relatively fast, through coating up to *c.* 10 mm
Electronic: ACPD	Fatigue damage	Depth of surface crack, supporting MPI	Work class ROV	Cleaning required, time consuming
Electronic: ACFM	Fatigue damage	Both length and depth of surface crack; independent evaluation possible	ROV	Relatively fast, through coating up to *c.* 10 mm
Ultrasonic	Wall thickness, corrosion, fatigue and fabrication defect, post-repair inspection	Embedded defects	Work class ROV, usually performed by diver	Cost depends on different applications

© 2008 Woodhead Publishing Limited

FMD	Fatigue and post-event damage	Through-thickness crack; excellent tool for rapid screening	ROV	Fast, no cleaning necessary
Cathodic potential	Corrosion	Anode performance; often combined with visual inspection	ROV	Field calibration necessary, but the readings can be taken quickly
Dimensional measurement	Scour, subsidence, marine growth, dent, out-of-straightness, corrosion pit size, etc.	For special purposes	May be performed by ROV, but with limited capability	
Stress and deformation monitoring	Structural behaviour monitoring	For special purposes		
Radiography	E.g. testing of hyperbaric welds	Internal defects		

© 2008 Woodhead Publishing Limited

of the sacrificial anodes may be assessed by visual inspection. Above water, the condition of the coating is assessed by visual inspection. Recoating should be performed if the condition is not acceptable.

Monitoring of marine growth

Marine growth comes in different forms, broadly divided into hard (generally animal, such as muscles and barnacles) and soft (seaweeds and kelps). Hard growth is generally thinner (less effective increase in member diameter) but rougher (increase in drag coefficient) than soft growth. Marine growth measurements are in general unreliable, particularly for soft growth and for single estimates on large components. The size of marine growth is important for calculation of load on the members. The volume of the member is dependent on the diameter that is increased by marine growth. The fatigue loading on a jacket structure is very much dependent on the mass term in Morison's equation. In the splash zone region the fatigue loading is also significantly dependent on the drag term in Morison's equation. Also here the marine growth has some influence, as the effective diameter is increased with increasing marine growth. Some structures have antifouling claddings that have performed reliably for more than 20 years (ISO 19902, 2007).

In-service inspection for fatigue cracks

In general, large uncertainties are associated with fatigue analyses of offshore platforms. A design of offshore structures with respect to fatigue is normally based on S-N data (fatigue test data). In-service inspections for fatigue are performed in order to assure that the fatigue cracks in the structure do not exceed a critical size.

Risk-based inspection (RBI) may be recommended for planning of in-service inspection for fatigue cracks. The basis for this methodology is as follows. The reliability of a non-destructive examination is described by the ability to detect an existing crack as a function of the crack size and by the uncertainty associated with the sizing of an identified crack. Regardless of the inspection outcome (detection or no detection), each inspection provides additional information to that available at the design stage, which can be utilised to update the estimated fatigue reliability.

The acceptance criterion when planning in-service inspection for fatigue cracks based on RBI depends on the consequence of failure. The risk of a structural failure due to fatigue cracks should not be larger than the risk for other failure modes. Probabilities of failures are normally presented on an annual basis. Fatigue is a gradual process in which fatigue damage is accumulated. Thus, the probability of a fatigue failure will increase with time and can therefore be expressed in terms of the accumulated probability of fatigue failure

© 2008 Woodhead Publishing Limited

during the service life up to the time considered. In order to calculate the annual probability of failure, one can calculate the difference in the accumulated probability of failure within a time interval of one year and define this as an annual probability of failure.

An acceptance criterion for a connection with a large consequence of failure can be derived from a requirement that DFF = 10 (DFF = Design Fatigue Factor, a safety factor used on the number of load cycles) in case there is no access for in-service inspection and inspection is not possible (ISO 19902, 2007; Norsok N-004, 2004). From this a target probability level is derived that also depends on distributions used in the probabilistic analyses. For a connection with lesser consequences of fatigue failure, e.g. corresponding to DFF = 3, this value can similarly be used as the basis for establishing a target reliability level for such connections.

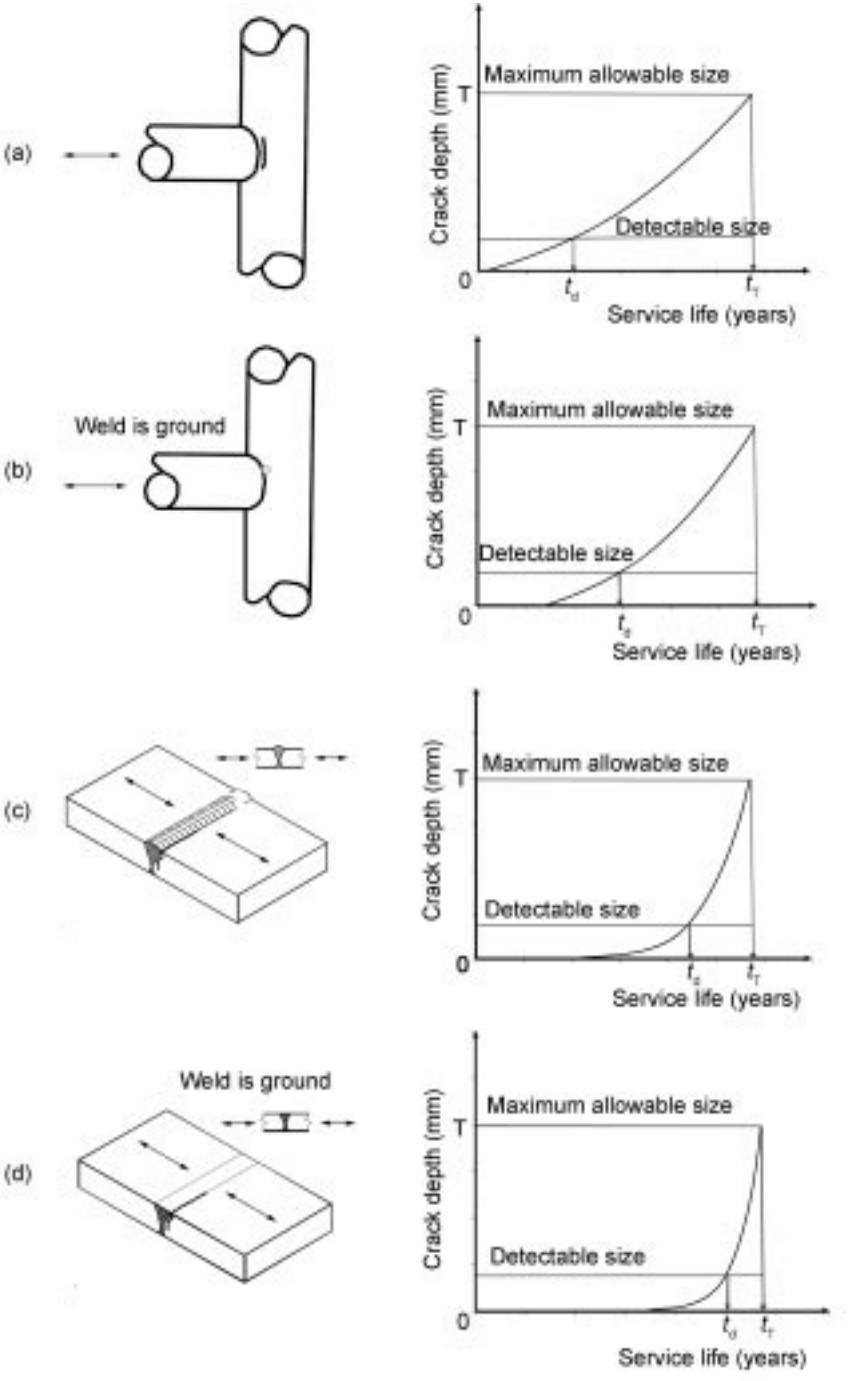
The time to the first inspection can be based on the results from the S-N approach, while the inspection intervals are based on the fracture mechanics approach (e.g. see BS 7910:1999). See also Chapter 11.

Examples of connections with different crack growth characteristics are shown in Fig. 2.3. It is seen that the time interval for a reliable inspection is dependent on the crack growth characteristics which again depend on the type of connection. Crack growth characteristics for a simple tubular joint in the as-welded condition are indicated in Fig. 2.3a. It is observed that there is a significant time interval (t_d to t_T) for detection of the crack before it grows through the chord thickness (T).

In some situations it is difficult to achieve sufficient calculated fatigue without weld improvement such as grinding of the weld toe. This means that the hot spot stress range is larger than if an acceptable fatigue life could be documented without grinding. After grinding, the crack initiation period becomes longer, but the crack growth period is shortened due to increased stress range (Fig. 2.3b). This reduces somewhat the time interval for detection of cracks.

Other details show less possibility of redistribution of stresses during crack growth. A butt weld subjected to pure axial loading is an example of this, as shown in Fig. 2.3c in the as-welded condition. It is observed that due to higher membrane stress the crack growth is faster and the time interval for detecting the fatigue cracks is reduced as compared with a simple tubular joint. If the nominal stress normal to a butt weld is so large that machining/grinding the weld is made flush with the base material, as shown in Fig. 2.3d, the initiation time will likely be longer but the crack growth will be even faster. This should be kept in mind when planning in-service inspection of such connections which are used, for example, in tethers of tension leg platforms. Similar examples with different details showing crack growth characteristics were also assessed using RBI methodology by Lotsberg and Marley (1992) and Lotsberg and Sigurdsson (2005).

© 2008 Woodhead Publishing Limited



2.3 Difference in crack growth for as-welded and ground connections.

© 2008 Woodhead Publishing Limited

It is recommended to use eddy current or magnetic particle inspection (MPI) for detection of surface cracks starting at hot spots such as weld toes. The cleaning and removal of the coating at the actual area is the main cost contribution in performing MPI. After inspection by MPI it is important to re-establish the coating such that corrosion of the inspected area is avoided. Eddy current may be used to detect fatigue surface cracks without removal of the coating, and is therefore less costly.

Ultrasonic techniques can be used to detect and size internal as well as surface defects, and to measure wall thickness and localised corrosion pits. Fatigue cracks can also be found using Flooded Member Detection (FMD) when cracks become through-thickness and are sufficiently open for flooding to occur. Through-wall damage on the leg (chord) side cannot be detected by FMD if there is a pile inside with grout in between or if the leg is water-filled from its installation.

In-service inspection is an integral part of structural integrity management, which is an ongoing process for ensuring the fitness-for-purpose of an offshore structure or of a group of structures; see also ISO 19902.

2.4.3 Measurements of load effects

Introduction

Instrumentation of members may be performed for measurement of platform behaviour such as deformations, load effect, motions, etc. to reduce uncertainties. Measurements of both global and local load effects can be performed. The latter are considered to be more challenging as they should also be combined with analysis, and local load effects are more sensitive to modelling of analyses such as joint flexibility, actual length of members, etc.

Hydrodynamic coefficients

The load mechanisms from waves, currents and wind are complex. The drag and inertia coefficients in the Morison equation are important parameters for the calculation of loads (see, e.g., Sarpkaya and Isaacson 1981). These parameters are a function of member geometry, member roughness, wave heights and periods, and position considered in the platform (see, e.g., the commentary section to API RP 2A, 2000). Due to this complexity it is of significant interest to compare calculated load effects with measured values for calibration of analysis methodology.

Full-scale measurements of jackets reported in the literature

Calculations of wave loads are associated with large uncertainties, e.g. due to the wave theory used, effect of marine growth/roughness, shielding, analysis

© 2008 Woodhead Publishing Limited

methods, etc. Since the mid-1970s a number of measurement programmes on jacket structures have been performed to reduce uncertainties, e.g. such as those of Kenley (1982), Langen *et al.* (1984), Inglis and Kint (1985), Bea *et al.* (1988), Webb and Corr (1989), Kanter *et al.* (2001) and Karunakaran and Haver (2007).

The relation between the drag and the inertia coefficient depends on water velocity and thus on wave height and wave periods. For space frame structures with slender members the inertia term in the Morison equation is important for small wave heights, i.e. for the Fatigue Limit State, while the importance of the drag term increases with increasing wave height and for increased water velocity. Thus, for joints in a region close to the water level, both drag and the mass term are important for calculated fatigue lives. For slender members it is the drag term that is important for the Ultimate Limit State.

Measurements should be performed over an interval of at least a year to provide representative load effects for fatigue assessment. It is also useful to get information about the corresponding environment. However, long-term stress range data from measured stress ranges also provide useful information.

In general, it has been found from actual measurements that the loading is calculated to be on the conservative side. It would also be expected that the basis for design is made to be on the conservative side. Similarly, the structures including foundations are normally found to be stiffer based on measured data than on those assessed during design. Depending on the situation it might be recommended to perform measurements of the load effects to better predict the actual structural behaviour. This can be especially relevant for a more reliable assessment of fatigue life and for requirements to make costly inspections underwater.

2.5 Assessment of data and structural analyses

2.5.1 The ultimate limit state

Structural integrity may be considered based on component check, system capability assessment or/and system safety assessment. Some guidance on assessment criteria can be found in Chapter 17 of API RP 2A and in ISO 19902.

Assessment of structural integrity is made in two steps. The first step is to check the structure according to the ordinary procedure used for new designs. If this criterion is not met or there are other factors, e.g. insufficient air gap, that violate this criterion, one should continue to the next step. The second step is to perform an ultimate strength analysis as a non-linear pushover analysis. These analyses are much more complex than ordinary linear analyses and guidance in codes and textbooks is scarce. Some guidelines for the use of non-linear techniques in ultimate strength analyses can be found in Ultiguide (1999), a result of a Joint Industry Project. See also Skallerud and Amdahl (2002) who give valuable guidance on non-linear analysis of offshore structures.

© 2008 Woodhead Publishing Limited

In order to determine reliable predictions of the ultimate strength by non-linear methods there are several important factors that are hardly described in ordinary design codes. Such factors are:

- Cyclic capacity of joints and members
- Ductility limits
- Modelling of stability failure modes
- Soil modelling
- Calculation of wave in deck loads (if relevant).

A large wave in a storm situation is normally followed by many smaller waves. This has to be considered when failure criteria are established for the different failure modes. Also the cyclic stress–strain relationship is different from that experienced during quasi-static loading (Heo *et al.* 2004, Urm *et al.* 2004). A procedure for low-cycle fatigue should be used for assessment of failure criteria for a storm loading. An S-N curve representative of the low-cycle region should be used. A design S-N curve in an air environment can be used for joints above water (Boge *et al.* 2007). For joints below water the effect of seawater and cathodic protection should be accounted for in the design S-N curve. See also Norsok N-006 (2008) for more detailed information on acceptance criteria related to low-cycle fatigue. Low-cycle fatigue in a storm should thus also be kept in mind if the Reserve Strength Ratio (RSR) concept in API RP 2A and ISO 19902 is considered. The RSR is defined as the platform's ultimate capacity against lateral loads divided by the 100-year environmental loading. By this definition it is understood that the air gap also becomes an important factor when the probability of structural failure is considered. This means that it is difficult to achieve a consistent safety level for different types of platforms using a single safety measure like that of the RSR. Thus, the RSR concept should be used with caution as indicated in ISO 19902.

Low-cycle fatigue is not considered to be a problem provided that the joint capacities are within those derived using design equations for static capacity in the API RP 2A, ISO 19902 or Norsok N-004 standards, where the failure criterion is capacity at first-observed cracking during the laboratory test.

2.5.2 The fatigue limit state

Uncertainties in fatigue analysis

A fatigue analysis procedure implies assessment of a number of different parameters, and each of these parameters may have a significant influence on calculated fatigue life for the considered structure. These parameters include:

- Environmental data (wave heights and associated wave periods and directionality)
- Wave theory

© 2008 Woodhead Publishing Limited

- Marine growth
- Hydrodynamic coefficients
- Analysis methodology (stochastic versus deterministic approach)
- Joint flexibility and structural modelling of members
- Stress concentration factors as functions of geometry and loading
- Combination of stresses into a hot spot stress taking into account direction of loading and multiplanar joints
- S-N curves
- Corrosion protection
- The Palmgren Miner rule.

The largest uncertainties for fatigue analysis of jacket structures are associated with the parameters leading to a hot spot stress, especially for joints in the splash zone area. The mean values of the S-N curves are rather accurately known based on laboratory tests, although S-N curves are also associated with significant uncertainty that influences the calculated probability of a fatigue failure. The loading on members in the splash zone is uncertain due to the presence of different load effects:

- Wave loading, as explained earlier
- Buoyancy forces when a wave passes the structure
- Slamming loads (Ridley 1982).

In order to account for these uncertainties it is normal practice to perform in-service inspection of joints with short calculated fatigue lives and/or joints where a failure might lead to large consequences with respect to human lives, pollution and/or cost.

Consistency of calculated fatigue lives

For the best possible effect of an in-service inspection of a joint, the selection of joints to be inspected should be based on a fatigue analysis that shows consistency in terms of calculated fatigue lives. By consistency is here understood that the calculated fatigue lives are considered to be based on a similar methodology for all the considered joints. This means that the calculated fatigue lives are considered to be associated with a similar bias relative to the actual fatigue life of the considered joint. A bias for fatigue life may be defined as the ratio between the calculated fatigue life and the actual life. An example of non-consistency could be a jacket with different types of joints, such as cast joints analysed in detail with finite element analysis and stiffened tubular joints which might have been assessed in a conservative manner. Consistency may also include differences in bias associated with the parametric equations that are used for different types of joints (X-joint, Y-joint and K-joint).

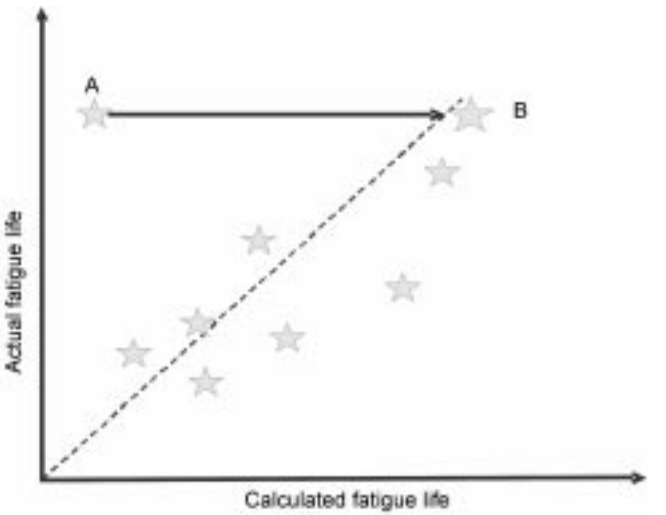
In a design situation it is normal practice to make different assumptions in the

© 2008 Woodhead Publishing Limited

analysis for different types of joints to document a fatigue life. Conservative simplifications are allowed as long as sufficient fatigue capacity can be demonstrated. For planning of joints to be inspected by detailed NDT one would normally select a joint with a short calculated fatigue life. The consequence of a fatigue failure can also be part of such an assessment. The result might be that joint A in Fig. 2.4 is selected for inspection as this joint shows the shortest calculated fatigue life. However, if a more refined fatigue analysis is performed, the calculated fatigue life may be moved to B, as an example. This means that this joint in reality has a long fatigue life; the probability of a fatigue crack is small, and one would more likely expect to find a crack at other joints shown in Fig. 2.4. Thus, in order to learn as much as possible from an in-service inspection of a joint in a platform, the selection should be based on fatigue analysis that is made for this purpose and that is consistent as far as possible. (For illustration purposes it is assumed that the calculated fatigue life in Fig. 2.4 does not include safety factors and that mean S-N curves are used.)

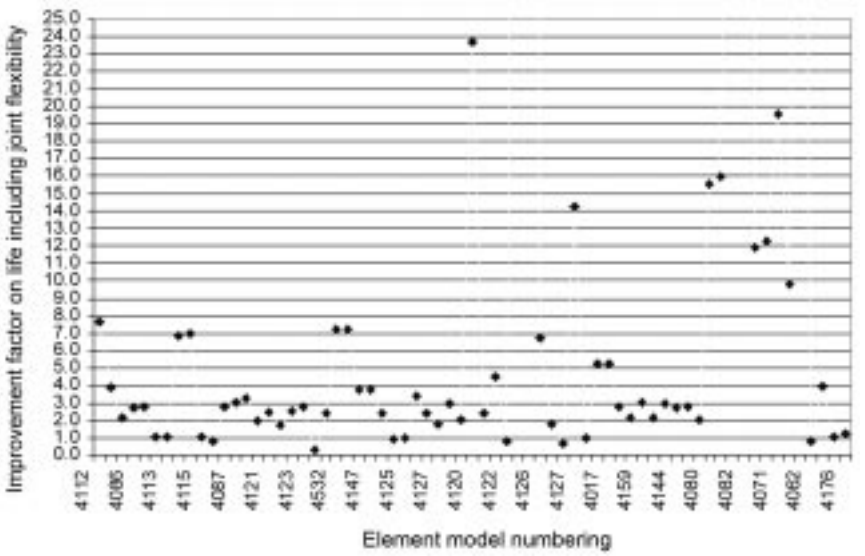
The objective of in-service inspection planning is to keep the structure at an acceptable safety level during the service life through a reasonable inspection and maintenance strategy. In-service inspections are performed in order to assure that the existing cracks in the structure, which may have been present from the initial delivery or have arisen at a later stage during the service time, do not exceed a critical size.

Stress concentration factors and derivation of hot spot stress for space frame structures are important factors in assessment of calculated fatigue lives. The stress concentration factors for simple tubular joints by Efthymiou (1988) are the basis for all hot spot stress calculation in ISO 19902 (2007); see also DNV-RP-



2.4 Example of calculated life versus actual life.

© 2008 Woodhead Publishing Limited



2.5 Factor on calculated fatigue life when including joint flexibility for joints in horizontal elevation in a jacket.

C203 (2005). These stress concentration factors depend on the type of joint and are based on geometry and on force flow through the joint. It is important that there is correspondence between the hot spot stress calculated as a basis for the equations for stress concentration factors and the actual stress in a real structure. Also the modelling of the joints in terms of joint flexibility is considered to be important for calculations of fatigue lives of simple tubular joints (Buitrago *et al.* 1993). Earlier it was normal practice to consider the joints in frame models as stiff. An example of calculated fatigue lives including flexible joints as compared with that of stiff joints is included in Fig. 2.5 for a horizontal frame in a jacket structure. It is observed that most of the joints show an increased fatigue life when including joint flexibility, as the moments at most of the joints are decreased when the joints are made flexible.

Consideration should also be given to the structural analysis methodology to be used. Should a deterministic approach be used as described in Norsok N-004 (2004), or should a stochastic analysis procedure be used, as in Vughts and Kinra (1976), API RP 2A and ISO 19902? A stochastic analysis procedure is used for slender structures and/or those with a large deck mass resulting in significant dynamic amplification (first natural period typically larger than 3 s). This methodology implies some techniques for linearisation of the loading in the waterline area. For this reason a deterministic approach may be preferred for joints in this area. The difference between calculated lives is considered to be less for joints in the lower part of the structures.

© 2008 Woodhead Publishing Limited

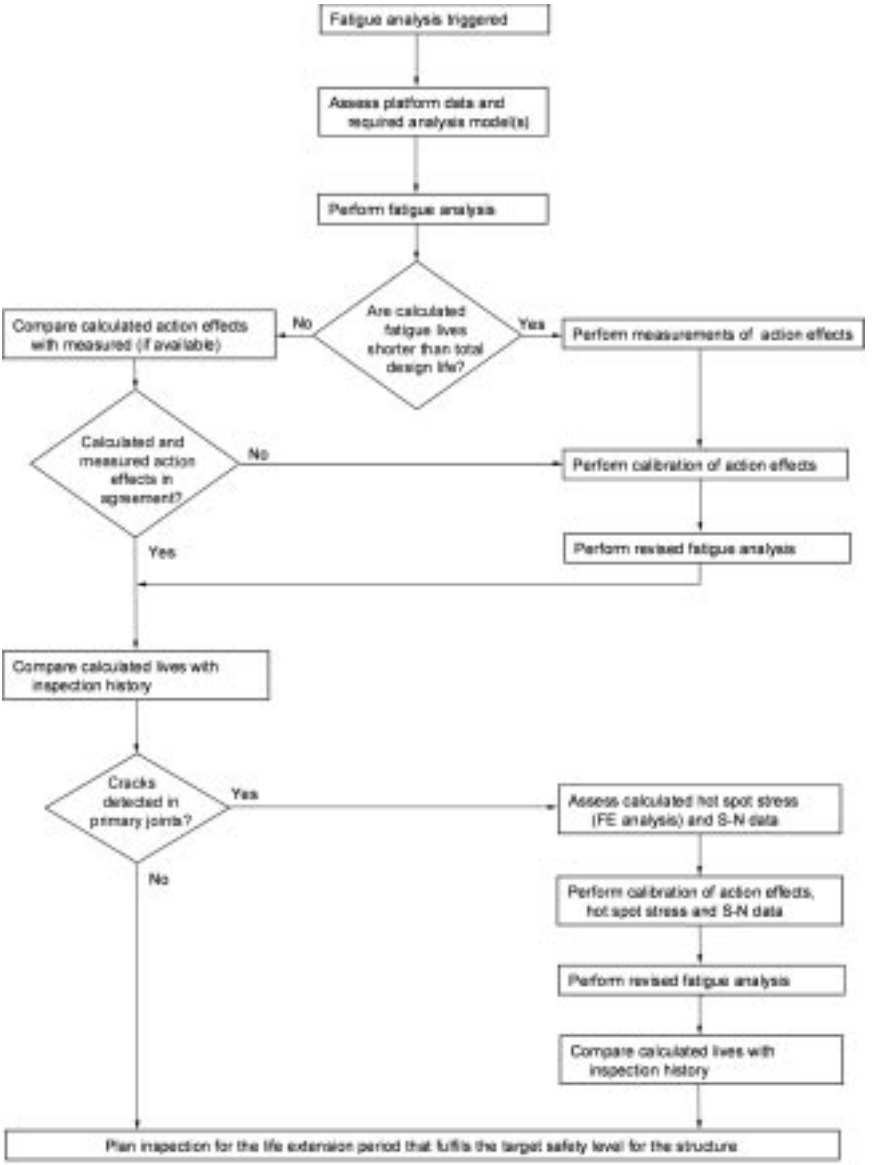
Extended fatigue life of a structure

An extended fatigue life is considered to be acceptable and within normal design criteria if the calculated fatigue life is longer than the total design life multiplied by the Design Fatigue Factor (e.g. see ISO 19902 and Norsok N-006, 2008). Otherwise an extended life may be based on a more detailed assessment, including results from performed measurements of action effects and/or inspections throughout the prior service life as shown in Fig. 2.6. Well-documented in-service records of joints with the shortest calculated fatigue lives can be used to document the fatigue reliability provided that fatigue cracks have not been detected.

A fatigue assessment should be based on the following principles and procedures.

1. Assessment of number of structural analysis models required. Different structural models may be required due to subsidence or modifications of the structure made during service life. When different analysis models are used, the total fatigue damage should be calculated by adding together the damages from the different models representing a defined time period.
2. A detailed and consistent fatigue analysis of the structure based on best practice for such analysis and use of S-N data.
3. If the calculated fatigue lives are short, it may be recommended to perform measurements of action effects of the global force flow in the structure. This means measurements of mainly axial forces in brace elements. In some cases measurements of action effects may already have been performed. Then calculated action effects should be compared with measured data and calibration of the analysis model can be performed. Then a revised fatigue analysis can be performed.
4. The calculated fatigue lives should be compared with results from in-service inspections with respect to fatigue cracks. If fatigue cracks are found in primary joints in the structure, it should be checked that this is in agreement with calculated lives. If calculated lives are not in agreement with observed fatigue cracking, it is recommended to look into the remaining uncertainties related to calculation of hot spot stress and fatigue capacity. This means assessment of relevance of stress concentration factors used in the case of complex joints and S-N data for the actual fabrication. Then a further calibration of data may be performed based on a total assessment of the most significant parameters contributing to uncertainty in calculated fatigue life. Finally, a revised fatigue analysis can be performed as a basis for planning in-service inspection for fatigue cracks during lifetime extension that fulfils the target safety level or the intended safety level in the design standard.
5. For planning of in-service inspection for fatigue cracks it is recommended to develop crack growth characteristics, i.e. calculated crack length/depth as

© 2008 Woodhead Publishing Limited



2.6 Guidance on assessment with respect to fatigue.

a function of time/number of cycles (depending on type of joint, type of loading, and possibility for redistribution of stress during crack growth).

6. The crack growth analysis based on fracture mechanics should be calibrated to that of the S-N data in such a manner that the crack growth characteristics will not be non-conservative when it is used for assessment of inspection intervals.

© 2008 Woodhead Publishing Limited

7. The acceptance criterion should be linked to consequence of failure as is implicit in the requirement for Design Fatigue Factors presented in ISO 19902 (2007) or Norsok N-001 (2004).
8. Assessment of maximum allowable crack size (corresponding to some defined maximum load effect) should be made. This includes assessment of maximum crack size when the ultimate capacity of the joints is considered (Stacey *et al.* 1996).
9. The inspection interval should depend on the reliability of the inspection method that is being used.
10. Elapsed time from earlier inspections should be accounted for in this assessment.

If no fatigue cracks have been found during inspection, there is good reason to believe that the structure is sound with respect to this failure mode. However, if fatigue cracks are found, it is reasonable to question the reliability of the joints that have not been inspected, and the inspection programme for these should be enhanced.

2.6 Mitigation

If the results from the risk assessment are unacceptable, remedial measures to reduce the risk of structural failure should be implemented. The choice of individual or combinations of remedial measures and their extent will depend on the source of risks to the structural integrity and their magnitude. Thus, measures may be taken both to reduce the load effects and to increase the resistance of the structure.

One or more of the following mitigations may be selected in case the assessment of the ultimate capacity of the structure has failed:

- Reinforcement of the structure in the form of grouting of members to increase buckling capacity
- Grouting of joints to increase joint capacity
- Installation of additional braces
- Installation of bolted and/or grouted clamps to strengthen dented and buckled members
- Reduction of wave loads by regular removal of marine growth
- Reduction of wave loads by removal of appurtenances or members that are no longer strictly required for operation of the platform
- Instrumentation of the structure to better calibrate the loads
- Use of material certificates or material testing in order to better estimate the structural resistance.

In some cases also a change in acceptance criterion may be considered. For example, if the operational strategy is changed from a manned platform to a

© 2008 Woodhead Publishing Limited

platform that is evacuated if extreme weather is expected, the acceptance criterion can be relaxed following design standards such as ISO 19902 (2007).

If crack indications are reported during inspections, they should be assessed by a qualified engineer familiar with the structural integrity aspect(s) of the platform.

Improvement methods can be used to improve fatigue lives of welded connections (Haagensen and Maddox 2007). If fatigue cracks are detected before they have grown through half the thickness of the tubular members or plates, they may be permanently repaired by grinding provided that the crack length is limited and the cracks do not significantly change the nominal stress flow at the considered connection; see also Norsok N-006 (2008).

2.7 Future trends

When evaluating future trends in engineering assessment of existing steel structures, one might get some perspective by looking back on the situation approximately 25 years ago. Around 1982 the author of this chapter was project manager for a joint industry project on 'Cost Effective Inspection Maintenance Offshore'. The author also participated at a petroleum conference in London where one of the main objectives was related to reduction of costs associated with in-service inspection and maintenance of offshore structures. At this conference a first procedure for risk-based inspection was presented by DNV (Sletten *et al.* 1982). The difference between the practices at that time compared with today is probably not as large as one might believe. The methodology for ultimate strength analysis and fatigue analysis was in principle well established; for example Vughts and Kinra (1976) had presented the basis for stochastic fatigue analysis, and Kinra and Marshal (1979) were using the methodology on a large jacket (Cognac) in the Gulf of Mexico. However, since that time there have been significant developments in numerical methods for more accurate calculation of loads and structural capacities. The methodologies have also been better calibrated to test data. This includes ultimate capacity of tubular joints, non-linear pushover analysis, joint flexibility and stress concentration factors for tubular joints. Computer capacity has been greatly increased, making it possible to carry out direct finite element modelling of joints and to include these in frame models to remove significant uncertainties related to hot spot stress in complex joints. It is believed that this trend will continue and that refined computer models of the structures will be made such that assessment with respect to ultimate capacity and fatigue can be more easily performed. As more reliable fatigue estimates can be derived from performed analysis, it is also believed that risk-based inspection methods for planning inspection as presented in Chapter 11 will become normal practice as part of the assessment process. During recent years there has also been a significant improvement in methodologies to directly measure the actual geometry of the

© 2008 Woodhead Publishing Limited

platforms, such that the actual geometry can be correctly included in structural analysis models.

As mentioned above, the possibility for more accurate calculation of loads on bodies with a complex shape has increased significantly in recent years. This now makes it possible to calculate action effects from waves hitting deck structures (Kleefsman *et al.* 2004). However, there are still uncertainties in calculating loads on slender members in jacket structures. Thus, more measurement of environmental data and load effects is recommended for reduction of uncertainties and for calibration of analysis models.

It is also believed that guidance on non-linear analysis together with acceptance criteria will be improved in the future. It is also possible to link these analyses to probabilistic methods. However, the use of these methods will require skilled engineers.

During recent years there has been much research and development work related to improvement methods. It is believed that there will be significant development of such methods also in the future.

There has been a trend to reduce inspection effort by divers. To achieve this, more efficient and automatic inspection methods and tools have been developed that are less dependent on the use of divers. It is believed that this trend will continue and that more advanced automatic inspection tools will be developed.

The engineering effort expended on assessing structures will likely continue to depend on the consequences of failure with respect to human life, pollution and cost. It is also believed that operators will put more investment into developing Structural Integrity Management Systems to more efficiently handle all the data involved in assessing structural integrity.

2.8 Sources of further information and advice

The new ISO standards for steel structures that are being developed are considered to be an important source with respect to assessment of fixed steel structures in the future. These include ISO 19900 and ISO 19902. The latter is developed for design of fixed steel structures but also includes information on in-service inspection, maintenance and repair. Clause 23 of ISO 19902 presents requirements for in-service inspection. This clause defines in-service inspection requirements for both the underwater and above-water parts of fixed steel offshore structures. In addition the structural integrity management requirements relating the inspection results to ongoing requirements for inspection, repairs and maintenance are given. In-service inspection is an integral part of structural integrity management, which is an ongoing process for ensuring the fitness-for-purpose of an offshore structure or of a group of structures. Clause 24 of ISO 19902 presents recommendations for assessment of existing structures.

Some guidance on reassessment of structures can be found in API RP 2A. Both ISO 19902 and the Norsok standards include some guidance on

© 2008 Woodhead Publishing Limited

strengthening of damaged members. The Norsok standards can be freely downloaded from the Internet. These also include DNV-RP-C203 Fatigue Design of Offshore Steel Structures. The electronic versions of these documents are regularly updated.

Work is also being carried out to prepare a new Norsok standard for life extension of offshore structures: Norsok N-006 Assessment of Structural Integrity for Existing Offshore Load-bearing Structures. It is planned that this document should be available during the first part of 2008. The purpose of this standard is to cover issues that are considered important for assessment of life extension of structures and that are not included in other reference standards such as ISO 19902 or other Norsok standards.

2.9 References

API RP 2A-WSD Recommended Practice for Planning, Designing and Constructing Fixed Offshore Platforms – Working Stress Design, 21st edition, December 2000.

Bea, R. G., Pawsey, S. F. and Litton, R. W. (1988), 'Measured and predicted wave forces on offshore platforms', OTC paper no. 5787.

Boge, F., Helland, T. K. and Berge, S. (2007), 'Low cycle fatigue of T-tubular joints with out-of-plane bending loading', OMAE2007-29351, *Proceedings of the 26th International Conference on Offshore Mechanics and Arctic Engineering, OMAE 2007*, June 2007, San Diego, CA.

BS 7910:1999 Guide on Methods for Assessing the Acceptability of Flaws in Fusion Welded Structures, British Standard.

Buitrago, J., Healy, B. E. and Chang, T. Y. (1993), 'Local joint flexibility of tubular joints', OMAE, Glasgow.

Det Norske Veritas DNV-RP-C203 (2005), 'Fatigue design of offshore steel structures', DNV, Oslo, August 2005.

Efthymiou, M. (1988), 'Development of SCF formulae and generalised influence functions for use in fatigue analysis', *Recent Developments in Tubular Joint Technology, OTJ'88*, October 1988, London.

Fjeld, S. (1978), 'Reliability of offshore structures', *Journal of Petroleum Technology*, pp. 1486–1496.

Haagensen, P. J. and Maddox, S. J. (2007), 'IIW recommendations on post weld improvement of steel and aluminium structures', IIW Doc. XIII-1815-00.

Health and Safety Executive (1992), *A Guide to the Offshore Installations (Safety Case) Regulations*, HMSO, London.

Heo, H. J., Kang, J. K., Kim, Y. I., Yoo, I. S., Kim, K. S., and Urm, H. S. (2004), 'A study on the design guidance for low cycle fatigue in ship structures', published in PRADS 2004, Hamburg, Germany.

Inglis, R. B. and Kint, T. E. (1985), 'Predicted and measured long term stress range distributions for the Fulmar A platform', in *Behaviour of Offshore Structures*, Delft, The Netherlands.

ISO 19900 General Requirements for Offshore Structures.

ISO/FDIS 19902 Fixed Steel Offshore Structures, 2007.

ISO 19903 Petroleum and Natural Gas Industries: Fixed Concrete Offshore Structures.

Kanter, P. A., Scherf, I., Pettersen, Ø., Osnes, J., Grigorian, H., Yu, W. G. and

© 2008 Woodhead Publishing Limited

Christensen, Ø. (2001), 'Instrumentation of Ekofisk platforms', OTC paper no. 13193.
Karunakaran, D. and Haver, S. (2007), 'Dynamic behaviour of Kvitebjørn jacket structure – Numerical predictions versus full-scale measurements', http://www.ivt.ntnu.no/imt/courses/tmr4195/, 17 October 2007.
Kenley, R. M. (1982), 'Measurement of fatigue performance of Forties Bravo', OTC paper no. 4402.
Kinra, R. K. and Marshal, P. W. (1979), 'Fatigue analysis of the Cognac platform', OTC paper no. 3378, Offshore Technology Conference, Houston, TX.
Kleefsman, K. M. T., Fekken, G. and Veldman, A. E. P. (2004), 'An improved volume-of-fluid method for wave impact problems', *ISOPE 2004*, paper no. 2004-JSC-365.
Langen, I., Spidsøe, N., Bruce, R. L. and Heavner, J. W. (1984), 'Measured dynamic behaviour of North Sea jacket platforms', OTC paper no. 4655.
Lotsberg, I. and Marley, M. (1992), 'Inservice inspection - Planning for steel offshore structures using reliability methods', BOSS 92, London.
Lotsberg, I. and Sigurdsson, G. (2005), 'Assessment of input parameters in probabilistic inspection planning for fatigue cracks in offshore structures', *Proceedings of the Ninth International Conference on Structural Safety and Reliability, ICOSSAR'05, Safety and Reliability of Engineering Systems and Structures* (edited by G. Augusti, G. I. Schuëller and M. Ciampoli), Rome, June 2005. Millpress, Rotterdam, Netherlands.
Lotsberg, I., Olufsen, O., Solland, G., Dalane, J. I. and Haver, S. (2005), 'Risk assessment of loss of structural integrity of a floating production platform due to gross errors', *Marine Structures*, Vol. 17, pp. 551–573.
Norsok N-001 Structural Design, rev. 4, February 2004.
Norsok N-004 Design of Steel Structures, Norsok Standard, rev. 02, 2004.
Norsok N-005 Condition Monitoring of Loadbearing Structures, rev. 01, December 1997.
Norsok N-006 Assessment of Structural Integrity for Existing Offshore Load-bearing Structures. Planned to be issued in 2008.
Ridley J.A. (1982), 'A study of some theoretical aspects of slamming', NMI report R 158, OT-R-82113, London.
Sarpkaya, T. and Isaacson, M. (1981), *Mechanics of Wave Forces on Offshore Structures*, Van Nostrand Reinhold, New York.
Skallerud, B. and Amdahl, J. (2002), *Nonlinear Analysis of Offshore Structures*, Research Studies Press, Baldock, Hertfordshire, UK.
Sletten, R., Mjelde, K., Fjeld, S. and Lotsberg, I. (1982), 'Optimization of criteria for design, construction and inspection of offshore structures based on resource allocation techniques', *European Petroleum Conference*, London, October 1982.
Stacey, A., Sharp, J. V. and Nichols, N. W. (1996), 'The influence of cracks on static strength of tubular joints', OMAE, Firenze.
Ultiguide (1999), *Best Practice Guidelines for Use of Non-linear Analysis Methods in Documentation of Ultimate Limit States for Jacket Type Offshore Structures*, DNV-SINTEF-BOMEL, DNV, Oslo, Norway.
Urm, H. S., Yoo, I. S., Heo, J. H., Kim, S. C. and Lotsberg, I. (2004), 'Low cycle fatigue strength assessment for ship structures', *PRADS, 9th International Symposium on Practical Design of Ships and Other Floating Structures* (edited by H. Keil and E. Lehman), Lübeck–Travemunde, Germany, 12–17 September 2004. Seehafen Verlag, Vol. 2.
Veldman, H. E. and Lagers, G. H. G. (1997), *50 Years Offshore*, published on behalf of Foundation for Offshore Studies, Delft, The Netherlands.

© 2008 Woodhead Publishing Limited

Vughts, J. H. and Kinra, R. K. (1976), 'Probabilistic fatigue analysis of fixed offshore structures', OTC paper no. 2608, Offshore Technology Conference, Houston, TX.
Webb, R. M. and Corr, R. B. (1989), 'Full scale measurements at Magnus', *Proceedings of E&P Forum Workshop on Wave and Current Kinematics and Loading*, Paris, 25–26 October 1989.

© 2008 Woodhead Publishing Limited

3

Definition and assessment of deficiencies in building construction

A VAN GRIEKEN, Connell Wagner Pty Ltd, Australia

Abstract: The assessment of land-based aged structures requires a historical knowledge of local structures and a clear definition of the types of deficiencies. This chapter provides a history of global and Australian construction developments from the early Mesopotamian to the Egyptian and Greek civilizations and to the current construction practices and materials.

There are three types of deficiencies. Deterioration is the reduction in material property characteristics and/or size due to exposure conditions. A defect is a reduction in structural capacity due to inadequate design, or variation from the design intent. Damage is the result of extraordinary loads which could not reasonably be foreseen or designed for. This chapter provides examples of deficiencies in concrete, steel, masonry, terracotta and timber structures or elements and of materials such as sealants and coatings. These deficiencies need to be assessed based on a logical approach and carefully selected scope. The age of a structure is of benefit in establishing the likely construction method and materials. This knowledge can influence the scope of the investigation into deficiencies.

Key words: construction history, Mesopotamia, Portland cement, Crystal Palace, Australian construction history, deficiencies, deterioration, defect, damage, scope and approach of deficiency assessment.

3.1 Historical perspective

When assessing a structure a number of questions come to mind immediately:

- The age of the structure
- The materials with which it was constructed
- Its function or purpose.

The age of the structure generally conjures up an expected image in terms of materials, architectural style and to some extent height. The mention of, for example, a very old church or railway workshop is likely to bring to mind images of the most commonly encountered structures such as these and the most common construction materials for these structures. Thus one does not expect to encounter a metal-clad three-storey-high church.

The current use of the structure may well vary from the intended purpose at the time of design and construction, as the structure may have evolved with the changes in society, and its requirements, in order to maximize its purpose or economic benefit. Thus an open mind is required, despite any initial thoughts

© 2008 Woodhead Publishing Limited

and assumptions related to the age of the structure and any materials which may have been used since construction. This leads to the question what is an aged structure.

Major building portfolio owners have construction-related divisions and asset management and maintenance divisions. As soon as a new building has been constructed by the former it is considered an existing building and taken over by the latter. Depending on the quality and type of structure and its exposure condition, the rate of aging varies considerably. Thus relatively modern buildings which have deteriorated rapidly may be considered aged and the concept of 'aged' can be related to date and condition.

For the purpose of assessment it is useful to identify the era during which the structure was built and to know the materials and methods which were predominant at that time. Many studies have been made into the history of a country from different perspectives including architectural styles. Economists will identify eras and key events that differ from those which sociologists consider significant.

Structures are the collective product of, amongst others, economic, political and sociological developments, and perhaps even climate change. The design and construction is heavily influenced by collective external factors which are relevant to structures such as architectural styles, materials availability, labor cost, 'boom and bust' economic cycles and new materials and construction techniques. This creates eras which are specific to construction and structures.

3.2 History of global construction developments

Mesopotamia was one of the earliest civilizations and developed between the rivers Tigris and Euphrates from around 5000 BC. This developed into the fabled *Babylonian* and *Assyrian* empires. It is not surprising that the 300-feet-high Tower of Babel was constructed with bricks made from the abundant source of clay. The Mesopotamians used a variety of bricks, some of which lasted 5000 years, and the most common of which used a straw binder (Kramer, 1981); the bricks were cemented with pitch. Outer surfaces of baked bricks were enameled and baked bricks were set in bitumen, a natural asphalt found in surface beds.

The *Egyptian* civilization developed over a similar period and used stone, their most abundant natural construction material, for their pyramids, temples and monuments. It is thought that their architects had been used to using mud bricks, possibly from the adjacent civilization, but adapted to the most abundant material, namely stone. The pyramids reached great heights, such as the 481-feet-high Great Pyramid, and have lasted to the present.

The *Greeks* also used natural stone to build large monuments and temples such as the Temple of Zeus, the soaring columns of which can still be inspected.

When the *Romans* absorbed the Greek empire around 500 BC, they adopted stone as the basic building material. They discovered the pozzolanic properties of clay and developed concrete to build structures which could span across vast

© 2008 Woodhead Publishing Limited

open spaces such as the 43.3-meter span lightweight aggregate dome above the Pantheon.

After the fall of Rome, *China* became the richest and most civilized power in the world over the seventh to the tenth centuries AD. Wood was the basic building material for houses, and stone was used only for public and religious structures. Incidentally it is of interest that their prosperous ninth-century houses were equipped with baths, heaters, mechanical fans, and ice-cooled rooms.

The expertise of making concrete was not rediscovered until around 1200 AD in Europe. The Eddystone lighthouse was built in 1756 in England and heralded a new era of construction using Portland cement. In the early nineteenth century, Portland cement began to be imported to America and the first building to be built with this new material is believed to be the 1844 Milton House in Wisconsin which lasted for over 100 years. The introduction of reinforcement in concrete was recognized in the first US building code in 1910.

The opening of Crystal Palace in 1851 in London heralded yet another era. The building used a total of 30,000 glass panels including the largest glass panels ever made. These were set in more than 5000 columns and girders of iron which were 'pre-shaped' in Birmingham foundries and set in place as little as 18 hours after being cast. This was one of the first instances of prefabrication and demonstration of mass production (Burchell, 1979).

Since then city buildings have grown ever taller using *in situ* concrete or steel superstructures. Bridges have spanned greater distances, some using steel such as the Sydney Harbour Bridge, and others a variety of concrete systems, mostly using pre-cast concrete elements.

The use of stone and timber has become less important and reinforced *in situ* concrete arguably the most dominant construction material.

3.3 The Australian experience

Each country has unique construction eras. These are unique due to the aforementioned factors and unique in length and time in history. Despite its relatively short post-settlement history, Australia is a good example in which a number of significantly different eras can be identified. For the condition assessment of aged Australian structures the following broad eras can be identified.

Era 1 – Early settlement to the 1850s gold rush

The location of raw materials greatly affected the type of early buildings. The lack of good hydrated lime or cement contributed to the prevalence of single-storey buildings in early Sydney and to their increased rate of deterioration. Occasionally concrete houses were built with crude thick walls using rubble bound in inferior lime (Lewis, 1988).

© 2008 Woodhead Publishing Limited

Some historians were of the opinion that the post-settlement nation hardly existed before the 1890s. As new settlements grew in size and number the increasing rural wealth created the need to construct more significant buildings. Minor gold finds from the 1820s to the 1850s injected further wealth into society. The structures of this period were low rise and generally simply constructed from an abundant source of natural stone and timber. However, this era of pastoral ascendancy was soon to be changed by the discovery of major deposits of gold.

Era 2 – 1850s to Federation in 1901

Wentworth said in July 1851 that 'the discovery of gold had opened up a new and unexpected era which must in a very few years precipitate us from a colony to a nation' (Clark, 1969). With the newfound wealth many traditional buildings of note were constructed in the late nineteenth and early twentieth centuries. Many of these reflected English architecture and used stone, brickwork and steel. Furthermore, structures in the major cities rose in height. The latter half of the nineteenth century was a great period of inventions and patents and developments in the colonies. For example, the first local patent for a form of hollow concrete building block was taken out in 1854. The first complete reinforced concrete building was constructed in Melbourne in 1905 (Lewis, 1988). Steel competed with *in situ* reinforced concrete for the construction of the most noteworthy bridges. For example in the late 1880s, the beautiful steel Princes Bridge was constructed across the River Yarra. The *in situ* reinforced concrete Morell Bridge was constructed further up this river in the same period and is equally elegant. Sadly both developed significant deficiencies over time.

Era 3 – Federation to 1960

During this period Australia was involved with two world wars and was severely affected by the depression in the thirties. However, typically after terrible events such as these, construction usually picks up as societies rebuild, restore and grow, with a new energy. The availability and cost of labor and the scarcity of some materials had a major influence on the choice of the type of structure and construction material. The introduction of reinforced concrete as a major building material in the US in the late 1800s is likely to have led to the construction of similar buildings in Australia. Many external concrete walls were rendered for aesthetic reasons. In 1907 modified regulations allowed both steel and concrete framed buildings to have thin non-structural walls. Steel-framed buildings supporting timber floors and masonry walls, and concrete-encased steel beams and *in situ* reinforced concrete structures became common.

© 2008 Woodhead Publishing Limited

The completion of the construction of the steel Sydney Harbour Bridge in 1933 heralded a new era of confidence and steel dominance. With ongoing maintenance and protective coating this magnificent bridge is still in good condition.

In 1945 the Housing Commission took a lease on a Commonwealth factory at Holmesglen, which had previously been making armored vehicles, and converted it into an industrial production line for precast concrete façades. Using load-bearing concrete walls, the heights of these buildings grew from two storeys in 1952 to 20 storeys in 1962, the tallest precast concrete structures in the world at that time (Lewis, 1988). However, these were also to develop significant defects over time due to exposure conditions and an incomplete understanding of the durability requirements for connections.

Era 4 – The terrible sixties

Many of the buildings which were constructed in the 1960s have developed significant deficiencies. Perhaps from a building construction perspective these could be termed the 'terrible sixties'. During this era there was an enormous demand for new buildings and structures. These were constructed under pressure with low quality control by today's standards, and with a limited understanding of the consequences of certain construction techniques and materials. Many *in situ* concrete structures with inadequate cover to the embedded reinforcement and inadequate concrete quality have since developed significant deficiencies due to corroding reinforcement.

The introduction of precast concrete elements for façades and new construction techniques led to accelerated construction programs. However, deficiencies developed in many buildings. Load-bearing brickwork buildings were also not uncommon but were slower to construct and more labor intensive.

The use of lightweight cladding systems such as curtain walls changed building structures and generally protected steel and concrete elements against the effects of exposure conditions. However, these lightweight façades involved new details, materials and construction methods and those which were not correctly designed or constructed created a new range of building façade deficiencies.

Era 5 – The magnificent 'glass' 80s and 90s

Over these two decades in the late twentieth century many spectacular high-rise buildings were constructed. Many of these featured an abundant use of glass façades and reached heights which were previously inconceivable. By this time concrete appeared to have won the ascendancy in the battle for the most commonly used construction material in infrastructure, resulting in many tall buildings supported by a concrete superstructure, long-span bridges and

© 2008 Woodhead Publishing Limited

spectacular elevated roadways though alpine areas and long tunnels through mountains.

Era 6 – Post 2000

Much energy and money was spent in preparing for anticipated problems with the change to the year 2000. The emphasis was on the electronic challenges and consequences of the perceived inability of computers to cope with the change into the third millennium, the dreaded 'Y2K' effect. However, once this short period of anxiety had passed a soft revolution started to gather. The focus was now on the need to produce more energy-efficient buildings, based on the recognition of the need to conserve our resources. In particular the need to minimize the use of our precious energy has gathered pace recently with the graphic examples and calamities due to what is considered to be 'climate change'. This has most profoundly affected the façades to buildings but has also led to research to minimize the energy embodied in materials and to minimize the energy required to construct buildings and structures.

Furthermore, natural stone is no longer commonly used as a structural material, precast concrete panels are largely used as non-load-bearing façade elements, and the quality of concrete and the protective concrete cover to reinforcement has been much improved.

3.4 The benefit of the historical perspective

In conclusion it is generally broadly possible to identify a type of structure and construction material with a particular era. Furthermore, the durability and deficiencies are often closely associated with these periods in construction history.

Stone structures have generally lasted the longest. However, they could not resist earthquake and have succumbed to hot humid climates where plants and organic matter slowly cause their decay. Reinforced concrete structures have not matched stone structures in terms of durability, due to the presence of the embedded steel reinforcing bars which corrode when not adequately protected. Fortunately, the greatly improved understanding of the durability requirements of reinforced concrete structures has led to more durable structures. Metal and steel structures have generally performed well, as the need to protectively coat or separate their elements was recognized from the outset.

3.5 General causes of deficiencies

Structures are being subjected to increasingly aggressive exposure conditions. The growth of populations and cities has created an increase in traffic and

© 2008 Woodhead Publishing Limited

carbon dioxide levels. These gases diffuse into the surfaces of building elements such as concrete and cause the carbonation of concrete. Furthermore, rain coupled with carbon dioxide pollution creates carbonic acid, commonly referred to as acid rain. This causes the initial pH of concrete to decrease to a level at which the concrete cannot protect the embedded reinforcement against corrosion. These aggressive exposure conditions also attack the various building construction elements and materials and cause their eventual deterioration, particularly in the case of older buildings and structures.

Other materials are being increasingly exposed to higher levels of ultraviolet radiation created by the shrinking ozone layer as evidenced by the well-known measured increase in the size of the 'ozone hole'. These increased levels of ultraviolet radiation have a profound effect on materials such as sealants and polymers. The severity of the ultraviolet attack was not foreseen by many manufacturers of building materials and has caused the total or partial breakdown of sealants, roof membranes and many plastic elements. In fact, after an international façade convention in Chicago in 1990 a number of manufacturers stated that they would decrease warranty periods.

Whilst Australia is relatively free from natural disasters such as earthquakes, the 1989 earthquake that struck Newcastle resulted in significant damage to mostly brittle masonry structures which could not adequately cope with these forces. This caused changes in national codes and earthquake provision requirements.

Thus there are a significant number of deficiencies which are the result of one or a combination of exposure conditions, and external forces or effects.

3.6 The three types of deficiencies: deterioration, defect and damage

It is important for those who assess structures and for designers of remedial solutions to clearly define the type of deficiency. Deficiencies can be grouped into three general groups.

Group A: Deterioration

Deterioration of buildings can be defined as the reduction in material property characteristics and/or size due to exposure conditions. Amongst others:

- Concrete can spoil and disintegrate due to sulfate attack, and reinforced concrete can crack and spall due to corroding reinforcement.
- Steel corrodes and swells and reverts to its original state under adverse exposure conditions.
- Masonry and terracotta can swell and change volumetrically due to water exposure.

© 2008 Woodhead Publishing Limited

- Timber when exposed to moisture will rot, develop fungal attack and split due to shrinkage.
- Sealants when exposed to ultraviolet can crack, debond and split.
- Coatings can blister and flake, chalk and change color largely due to ultraviolet exposure.
- Such deficiencies in the materials used can lead to material behavior that was not designed for or accommodated in construction.

Group B: Defect

This can be defined as reduction in structural capacity due to inadequate design or variation from the design intent during construction, leading to the visible manifestation of loads exceeding the structural capacity or to failure of elements or systems due to material deficiency and/or material behavior which was not designed for or accommodated in construction. Amongst others:

- The most notable example is arguably *foundation failure* as at the leaning tower of Pisa.
- Common examples are excessive *deflections* in floors and excessive deflections at cantilevering elements such as at balconies. Furthermore, excessive *vibrations* may occur due to impact loads or normal use.
- *Shrinkage*, particularly in the case of concrete, can cause cracks which result in leakage, corrosion of reinforcement and structural damage at interfaces with other materials. Polycarbonate roofs and domes can shrink and cause considerable damage. Products with a high cement content such as glass-reinforced cement or compressed cement sheets all have relatively high shrinkage characteristics and can cause fasteners to fail, edges to crack and water to ingress.
- *Expansion* can cause other defects. Brickwork undergoes almost irreversible volumetric expansion which is commonly labeled 'brick growth'. This can cause failure in the brickwork elements and failure of other elements which are trapped or moved by the expanding brickwork. Stainless steel has a relevantly high coefficient of expansion and can buckle, debond and cause failure in other elements. The following grouping provides an order of coefficients of thermal expansion (10^{-6}/ºC) (Sorenson, 1973):
  I. PVC: 50 to 185
  II. Fiberglass: 12 to 25
  III. Zinc, lead, copper, aluminum: 30, 29, 25, 17, respectively
  IV. Concrete, steel: 10, 11 (suitably close for reinforced concrete)
  V. Sandstone, granite: 11, 8.5.
- *Material deficiency*, most notably the presence of nickel sulfide in glass, causes spontaneous fracture and alkaline aggregate reactions in concrete, caused by the swelling of aggregates, causes concretes to crack, for which there is no cure.

© 2008 Woodhead Publishing Limited

- *Composite detachment*: the delamination of differing materials that have been veneered into a building material has been a common problem. This includes thin composite metal panels and thicker precast concrete panels.

Group C: Damage

This is the result of extraordinary loads which could not reasonably be foreseen and designed for:

- The best-known example is the destruction of the World Trade Center buildings in New York as a result of progressive collapse after *impact*.
- On a smaller scale the impact due to moving vehicles can also cause extensive significant and dangerous damage.
- Cyclones, tsunamis, accidents, explosions, etc., can cause damage, the extent and severity of which is often difficult to establish.

It may be difficult to classify a deficiency into only one of these three categories and each of the above three deficiency types can be prominent at a given structure. However, deterioration is common to most structures and damage arguably the least common.

3.7 Assessment of deficiencies

The condition of a structure and its deficiencies need to be assessed based on a logical approach. The scope of an assessment will need to be based on a number of key factors, including:

- The reason for the assessment (refer also to Chapter 14)
- The experience and 'historical' knowledge of the person conducting the assessment
- Prior knowledge of types of structure and building elements
- A thorough knowledge of material properties, including their strengths and weaknesses and prior failures
- A detailed understanding of testing methods, on site and in the laboratory
- Practical site constraints and opportunities.

The above will guide the scope and help to identify and locate specific tests and prevent 'over testing' and 'over inspections'. However, whilst there is no need to 'reinvent the wheel', one must keep an open mind as no two buildings are quite the same, and one must come to 'expect the unexpected'.

3.8 References

Building Statement, Australian Government Publishing Service, Canberra.
Burchell SC (1979), *Age of Progress*, Time-Life Books B.V.

© 2008 Woodhead Publishing Limited

Clark M (1969), *A Short History of Australia*, Sydney: Tudor Distributors.
Kramer SN (1981), *Cradle of Civilization*, Time-Life Books B.V.
Lewis M (1988), *Two Hundred Years of Concrete in Australia*, Concrete Institute of Australia.
Sorensen CP (1973), Technical Study, *The Weathering of City Buildings*, Canberra: AGPS.

© 2008 Woodhead Publishing Limited

Part II

Mechanisms, mathematical models and preventive measures for age-related deterioration

© 2008 Woodhead Publishing Limited

4

Corrosion wastage in aged structures

R E MELCHERS, The University of Newcastle, Australia

Abstract: Structural steel is widely used for critical infrastructure, such as offshore structures, ships, marine pipelines, coastal and harbour facilities, bridges, storage tanks, pipelines and conveyor systems. Protective coatings or cathodic protection, while often used, are not always effective and corrosion may threaten safety and performance through loss of material or through perforation by pitting. Recently developed quantitative models for marine immersion based on corrosion fundamentals including the effect of microbiological influences are described. These are useful for prediction of corrosion loss and for maximum pit depth. They can include the influence of various environmental and material composition factors and salinity levels. The models have been calibrated to in-situ data from a wide variety of sources, including ships, and are being extended to tidal, atmospheric and inland corrosion environments. It is shown that traditional extreme value analyses for maximum pit depth are not appropriate as the difference between meta-stable and stable pitting was not considered. A recent new interpretation is reviewed.

Key words: corrosion, marine, immersion, tidal, atmospheric, prediction, bacteria.

4.1 Introduction

Structural steel is widely used for critical infrastructure, including in harsh marine environments. Applications include offshore structures, ships, marine pipelines, coastal and harbour facilities such as sheet piling, cranes, bridges, storage tanks, pipelines and conveyor systems. It is standard practice in many cases to apply either protective coatings or cathodic protection or both. Moreover, in some applications such as offshore structures and ships, there are well-designed inspection and maintenance regimes. Despite this there is ample and usually very obvious evidence of corrosion, particularly for older structures for which maintenance practices have been less than optimal. Corrosion of steel can threaten the safety and the performance of infrastructures. It may cause loss of material and thereby affect the ultimate capacity, resistance or ductility of the structure and thus its safety. It may also change its elastic and dynamic properties, thereby affecting serviceability. Further, it may cause perforation such as through pitting or crevice corrosion, thereby affecting containment capacity. It is also of major economic significance. The economic cost for all forms of corrosion in advanced economies such as the USA was recently estimated at around 4% of GNP.

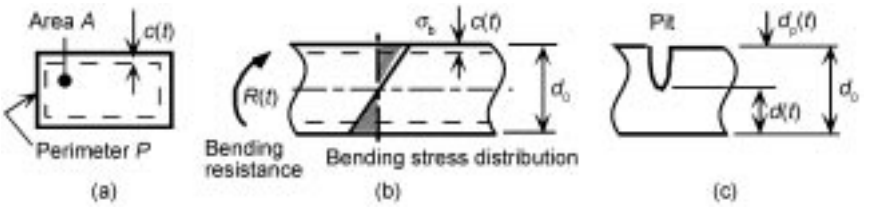
© 2008 Woodhead Publishing Limited

In the management of structures it ought to be possible to prevent corrosion commencing and an important practical question is how long it takes before this occurs under given environmental conditions, for a given thickness of a protective coating with known surface preparation. The life of protective coatings is a topic about which there is considerable practical experience and anecdotal information but, unfortunately, little quantitative data recorded or available in the open literature (Melchers and Jiang 2006). Also, laboratory studies of protective coating breakdown for research and for life expectancy studies tend to use accelerated testing including UV exposures and this renders comparisons with field behaviour problematic. Logically the process of in-service deterioration of protective coatings belongs to a completely different domain of investigation to that of corrosion progression and hence its modelling should be treated as such, despite the obvious interaction between coating and corrosion as the coating begins to fail (TSCF 2002). Until there is sufficient fundamental understanding of the breakdown of protective coatings under realistic operational conditions, any modelling attempt will remain essentially empirical. For this reason the coating deterioration phase is not considered herein.

In the management of structures already showing signs of corrosion typically three questions arise: (i) how serious is the visible corrosion, (ii) is immediate action required, and (iii) if not, how much longer can action be deferred? Clearly these are questions that extend beyond engineering. They involve both risk assessment and economic issues and criteria. Logical and justifiable responses to these questions require a reasonably degree of understanding of the corrosion process(es) and a quantitative understanding (i.e. a model) of how the corrosion process operates as a function of exposure time and under various environmental influences. Moreover, it is desirable to be able to predict the likely amount of corrosion in the future for defined conditions. In this context there are two main forms of corrosion of particular interest to infrastructure applications – general or 'uniform' corrosion and pitting corrosion (Fig. 4.1). The first directly influences structural strength (Fig. 4.1a, b). Pitting causes very localized and relatively severe penetration of the metal. Obviously, maximum pit depth is of most interest for loss of containment such as in pressure vessels and pipelines (Fig. 4.1c). Other forms of corrosion such as crevice corrosion and stress corrosion cracking are of significance for some specialized infrastructure applications and there are similar issues for the modelling and prediction of these forms of corrosion. However, these will not be discussed herein.

Surprising as it may seem, until quite recently the corrosion literature was not able to provide quantitative models for corrosion prediction that could be used with any degree of confidence. The reasons for this will be discussed below but may be summarized as being due to much fundamental corrosion research effort being dominated by the question of corrosion initiation, that is, whether or not corrosion will occur under given circumstances (often simply artificial laboratory conditions) and with much less effort being devoted to corrosion

© 2008 Woodhead Publishing Limited



4.1 Schematic corrosion loss $c(t)$ for (a) an immersed object and (b) a plate in bending; (c) maximum pit depth $d_p(t)$.

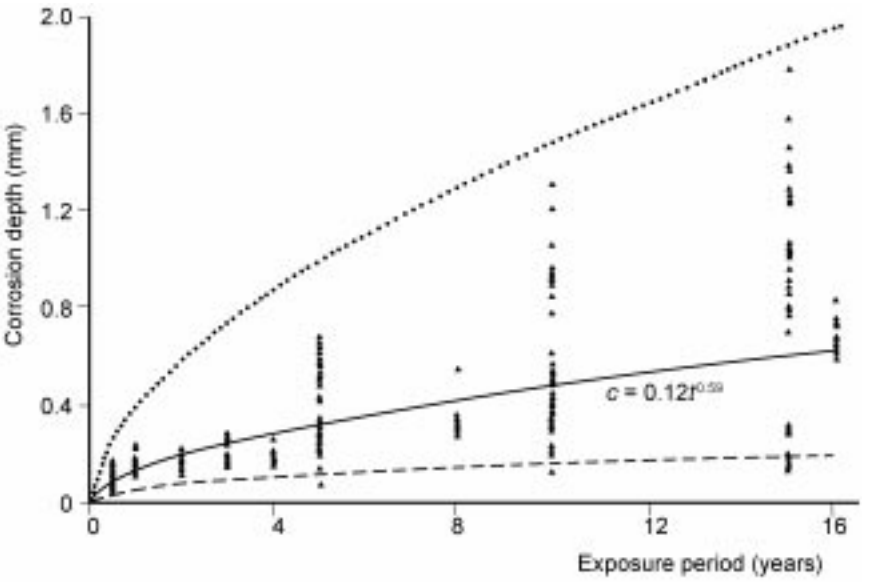
propagation. In practice, for most infrastructure applications it may be taken for granted that corrosion will occur eventually. Thus the question of main interest for deterioration is the rate of increase of corrosion losses and pitting depths with time.

Although there has been a lack of high-quality quantitative models, there is a considerable body of anecdotal and field observation of corrosion under quite widely varying practical climatic and exposure conditions. Good summaries are available (Kreysa and Eckermann 1992, Schumacher 1979, TSCF 2002). However, there has been little effort, until recently, of attempting to bring some coherence to the diversity of observations reported in the literature. As described below, both empirical models and models based on some degree of corrosion science fundamentals have been proposed, but with one important exception, they fail to capture longer-term corrosion behaviour. The typical models are able to describe only what might be expected to occur over a 2–3 year time span. This is clearly of little use in infrastructure applications. Nevertheless, the data are of considerable importance and reveal some interesting features as will be described below.

Figure 4.2 shows a collection of data (to 1994) of recorded corrosion losses for steel coupons exposed in marine tidal conditions (Melchers and Ahammed 1994). The losses have been converted from measured loss in coupon mass over time to the equivalent loss of metal from one side. Considerable experience by many investigators has shown that this is a reasonable approximation. Two observations are now of immediate interest. The first is that the amount of corrosion decreases slowly with time. This means that in practice there is no such thing as a 'corrosion rate' (i.e. a presumed constant rate of loss of material with time). The second important observation is that there is a high degree of scatter in the data and that this scatter increases considerably with time. This suggests, immediately, that there are factors at play that are not explicit in Fig. 4.2.

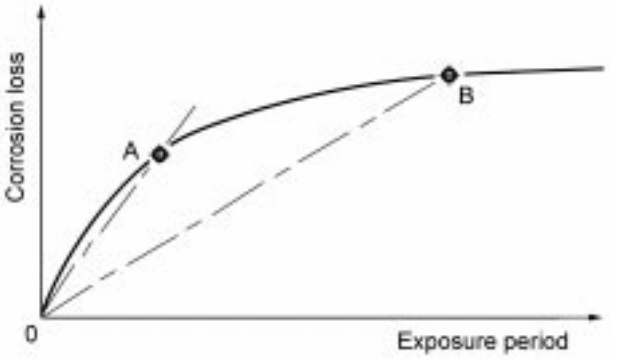
Both observations have practical implications. For example, the prediction of the future corrosion (thickness loss or pitting) can be very much in error if only a simplistic approach based on a 'corrosion rate' is used. For example, for ships typically thickness measurements of plates are made ultrasonically at some point in time, A, say. Assuming the time when corrosion first commenced can be

© 2008 Woodhead Publishing Limited



4.2 Collected data for tidal corrosion losses to 1994. The mean trend is shown together with the 10 percentile curves.

identified (e.g. time 0), the estimated future corrosion loss would be along the straight line through A, as shown in Fig. 4.3. Clearly it is different from what might be predicted from measurements at some other time (B, say). It follows that when data is collected from existing infrastructure an important challenge is how to interpret measurements such as made at A or B, to obtain the best estimate of the likely future amount of corrosion.



4.3 Schematic corrosion loss curve showing change in estimated corrosion rate from time at A to time at B.

© 2008 Woodhead Publishing Limited

4.2 Some fundamental corrosion principles

The discussion to follow will differ substantially from that usually found in corrosion texts. There is no discussion of electrochemistry despite its central position in corrosion science. Instead, a somewhat more classical approach will be used, based on the notion of the 'rate-controlling step' and the acceptance that the rate of corrosion is governed by diffusion issues, as will become clear. Moreover, it will not be necessary to enquire too much under what conditions corrosion may initiate – it will be assumed simply that it occurs, and for steel in marine environments common experience shows that this is a reasonable assumption, eventually. To understand why the corrosion rate is not constant in time and why there is so much scatter in the data, it is necessary to review what actually happens when a steel surface is exposed to natural seawater and how this process progresses with time.

4.2.1 First exposure (phase 1)

When a piece of steel is exposed to water or moisture such as seawater or seasprays, a complex series of reactions and processes occur more or less simultaneously. These include colonization by biofilms, bacteria and marine growth, establishment of incipient anodic regions (where the Fe goes into solution) and establishment of cathodic regions (where initial rust deposits form). As will be seen below, the timespan over which this occurs, while of considerable interest to corrosion scientists, is so short (days, weeks) compared to subsequent processes (years) that for infrastructure engineering purposes it may be (almost) ignored.

4.2.2 The development of rusts (phases 1 and 2)

Based on laboratory observations using fresh and salt water, the classical corrosion literature has shown that the key process for the corrosion of iron and steel is oxidation of the iron (ferrous iron). For seawater the process yields the commonly observed red-brown ferrous oxy-hydroxide (FeOOH) rusts for seawaters having a typical pH of around 8:

$$4Fe + 2H_2O + 3O_2 \rightarrow 4FeOOH \qquad 4.1$$

This shows immediately that both oxygen and water are essential for corrosion to occur by oxidation. It is generally accepted (Crolet 1992) that the rate of corrosion depends on the rate of supply of oxygen. The rate of iron ion diffusion away from the corroding surface is seldom limiting, at least for corrosion under normal temperatures and pressures.

At first the rate-controlling step is the rate at which oxygen can diffuse out of the bulk seawater to the metal surface. As a first approximation this scenario

© 2008 Woodhead Publishing Limited

may be modelled as an approximately linear function of time (Melchers and Jeffrey 2005). It can therefore be associated with the common use of a 'corrosion rate'. However, this situation does not last very long.

The oxidation of the metal causes a slow build-up of rust layers on the corroding steel and these layers increasingly impede the diffusion of oxygen to the corroding surface, causing a slowing of the oxidation process. This scenario may be modelled by assuming that the instantaneous rate of corrosion is controlled by the rate of oxygen diffusion through a uniform, homogeneous rust layer. This is a 'moving-boundary' diffusion problem described by Fick's second law of diffusion. Its solution was first presented by Tammann (1923) for tarnish layers on copper. Later refinements were made by Booth (1948), Evans (1960), Tomashev (1966) and others. The solution has the form

$$c = At^B \tag{4.2}$$

where A and B are constants. In ideal diffusion through a uniformly permeable layer theory predicts that $B = 0.5$. Attempts to fit Eqn (4.2) to empirical data have produced values of B somewhere between 0.3 and 0.8, depending on the data set (Benarie and Lipfert 1986, Feliu *et al.* 1993). Usually this is attributed to variations in and lack of knowledge of environmental conditions and non-perfect rust layers. Neither A nor B is particularly stable, showing very considerable changes in value, for example when the data set is increased from, say, 4 years to 8 years. There also are difficulties in fitting long-term corrosion data to this model, with the fitting error often greater in the earlier years. One consequence is that the resulting relationship has little meaning away from its source of data. Conventionally Eqn (4.2) is plotted on a log-log plot. This tends much to reduce variations of data with respect to the model and thus tends to hide its deficiencies. It also has allowed repeated claims that Eqn (4.2) is an appropriate model, with data that deviates too much often dismissed in the corrosion literature as caused by 'experimental error'.

Equation (4.2) has been used extensively in studies of atmospheric corrosion (e.g. Benarie and Lipfert 1986, Feliu *et al.* 1993). However, the difficulties outlined above suggest that its simple functional form is not sufficient to represent the corrosion process in its entirety with time. Already it has been shown that there are considerable theoretical and practical limitations implied in Eqn (4.2), including the assumption that it applies from time zero, despite the fact that at that time there is no rust layer present. Moreover, it has been shown that Eqn (4.2) with $B = 0.5$ is consistent with empirical data properly interpreted, and that it has an important role in the modelling of the progression of the corrosion of steel by oxygenation – that is, in Phase 2 (Melchers 2003a).

The role of salt in atmospheric corrosion of steel near the sea and its use on highway bridges in snow regions is widely held to be the most damaging agent in the corrosion process. However, it is clear that salt is not involved in the long-term corrosion process of Eqn (4.1). Chloride ions resulting from the dissolution

© 2008 Woodhead Publishing Limited

of NaCl in water are recognized to be very aggressive towards many metals, including iron. Reaction with iron (Fe) would be expected, thereby creating ferric chloride ($FeCl_3$). Since this is also highly aggressive, further reaction should result in ferrous chloride ($FeCl_2$). However, iron chlorides are seldom detected in rust layers both for immersion and for atmospheric corrosion (e.g. Gilberg and Seeley 1981). This has been attributed to their being washed out of the rust layers by the action of rainfall (Copson 1945). Moreover, the available evidence is that chloride activity does not last very long and that oxidation soon takes over as the rate-limiting reaction (Foley 1970). Certainly this fits careful experimental observations (Mercer and Lumbard 1995). One important feature of salt is that it is hygroscopic and able to draw moisture to the corroding surface under a range of humidity and temperature conditions. Since the moisture usually is highly oxygenated, this implies also a supply of oxygen to the corroding surface.

The rust layer generated by the corrosion process under oxygenation conditions is somewhat more complex than indicated by Eqn (4.1). FeOOH actually denotes a complex mix of different 'phases'. Of these the most commonly observed is a stable but brittle and flaky red-brown rust known as goethite (α-FeOOH) that is easily removed from the corroded surface. Under the goethite and next to the metal it is usual to find a hard, black rust known as magnetite (Fe_3OH_4). Usually it is very difficult to remove from the metal. Both goethite and magnetite are readily identified by scanning electron microscope (SEM) and X-ray diffraction (XRD) analysis. Occasionally these techniques also reveal different corrosion products, such as iron sulphides, FeS. Typically these are observed as black, soft and slimy and may emit H_2S gas ('rotten-egg gas'). Less frequently rusts known as 'green rusts' are revealed but only under anoxic observation conditions. Both the green rusts and FeS are unstable and usually oxidize quickly to goethite on exposure to air. Clearly Eqn (4.1) is not the only process involved in the corrosion of steel.

4.2.3 Bacteria in corrosion

The presence of FeS in the rusts of steel structures is the result of the activity of the anaerobic sulphate-reducing bacteria (SRB). Already in the late 1800s it was noted that iron pipes and other objects corroded at very high rates in waterlogged soils and this was identified as being caused by anaerobic bacteria. Subsequently a number of theories were proposed to explain the phenomenon but only relatively recently has some degree of consensus emerged about the mechanisms involved (Hamilton 1985, Crolet 1992). In brief, the SRB, which are obligatory anaerobes, are ubiquitous in nature and metabolize the (calcium and magnesium) sulphates abundantly present in seawater to hydrogen sulphide. This is highly aggressive to iron. The (partial) chemical reactions involved are

© 2008 Woodhead Publishing Limited

SRB metabolism: $SO_4^- + \rightarrow H_2S +$ 4.3

electrochemical reaction: $H_2S + Fe \rightarrow FeS + \ldots$ 4.4

The SRB are present in the rusts on or close to the steel surface but they do not directly attack the steel. The corrosion is the result of the bacterial metabolic products (metabolites). For metabolism, the SRB need appropriate conditions, including an anaerobic environment and sufficient food, including nutrients. Essential nutrients include Fe (available through the corrosion process), organic carbon (available in seawater and also available through the corrosion process and other bacterial involvement) and nitrogen, such as through nitrates, nitrites or ammonium. Sulphates normally are abundant in seawater and phosphates usually are not limiting. Typically the availability of nitrogen is limiting in seawater (Postgate 1984). In freshwaters sulphates may be limiting but this may not be the case in freshwaters polluted with sewage or fertilizers from, say, agricultural runoff.

There are many strains of SRB with various capabilities to withstand high and low temperatures and pressures. Mostly they operate optimally at moderate temperatures. In natural environments SRB invariably occur in consortia with other types of bacteria. The contribution to the nutrient and energy sources provided by the other bacteria in consortia has been proposed as the reason for the well-known observation that periodic exposure to oxygen greatly increases the metabolism of the SRB, despite the fact that they are obligatory anaerobes. It is also one reason why laboratory corrosion experiments with pure SRB cultures may produce totally misleading results (Little and Ray 2002).

4.2.4 Bacteria in short-term corrosion (phase 0)

When metal (and other) surfaces are first exposed to (sea)water they are colonized quickly by biofilms. Although these consist mainly of water, they do permit the development of niches of localized anaerobic conditions. Such anaerobic niches are associated with the harbouring of SRB. This has been demonstrated, both in the laboratory (Hamilton 1985, Lee *et al.* 1995) and from field data, to influence the rate of corrosion soon after first exposure. As would be expected, seawaters with elevated nutrient contents tend to show slightly higher rates of corrosion in the first few weeks to months. This phenomenon usually is not considered explicitly by corrosion engineers, yet has now been shown to have some influence in the early corrosion of steels (Melchers 2007a, b). However, identification of the precise mechanisms involved continues to be a topic of considerable research interest for microbiologists and for corrosion scientists.

4.2.5 Bacteria in long-term corrosion (phases 3 and 4)

In an important piece of observation and inference, not widely recognized either at the time or since, Southwell *et al.* (1979) proposed that the SRB are respon-

© 2008 Woodhead Publishing Limited

sible for long-term corrosion under marine immersion conditions. They based this conclusion on observations over 16 years of conditions in the Panama Canal Zone for a very wide range of steels and other metals and alloys. They represented these observations by a simple bilinear empirical model:

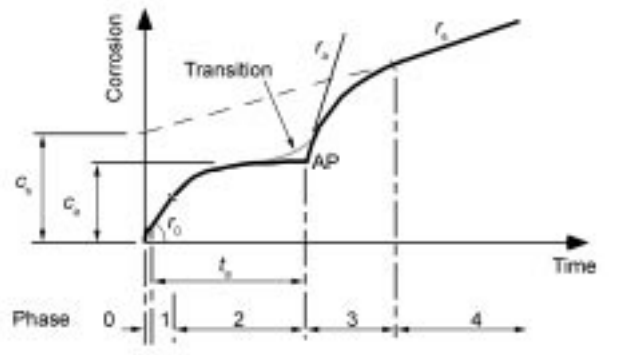
$$\begin{aligned} c &\leq a \qquad t = 0 \\ c &= a + bt \quad t > 0 \end{aligned} \tag{4.5}$$

where c is the mean corrosion loss (obtained from corrosion coupon weight-loss measurements) and a and b are constants.

Southwell *et al.* (1979) proposed that the SRB reside in the rust layers closest to the corroding steel surface and that they become active once anaerobic conditions are established, such as through sufficient thick rust layers having formed to retard the diffusion of oxygen. In the tropical conditions of the Panama Canal Zone this appeared to occur within about one year. However, they did not attempt to develop theory or extend the argument to other locations or conditions. Nevertheless they appear to have been the first to propose a relationship for the important influence of SRB in long-term marine immersion corrosion. Their work shows that the long-term corrosion rate is not necessarily related to the rate of very early corrosion. A similar conclusion can be drawn from the work of Mikhailovskii *et al.* (1980) who independently proposed at about the same time that there is a long-term corrosion rate K' not related to earlier corrosion rates. However, they did not attribute this to any particular cause. It arose simply from empirical observations.

4.3 A model based on fundamentals

The above preliminaries provide the background for the model for corrosion loss first proposed in 1997 (Melchers 1997) and since refined to that shown in Fig. 4.4 (Melchers 2003b). It is based on the notion that the corrosion process changes



4.4 Corrosion loss–exposure time model for immersion corrosion of steel in natural seawater showing the parameters for each of the phases.

© 2008 Woodhead Publishing Limited

Table 4.1 Summary description of the phases of the model (Fig. 4.4)

Phase	Corrosion process
0	Immediately upon first exposure the steel surface is colonized by biofilms, bacteria and marine organisms and is subject to a complex mix of influences. It takes a few days for the corrosion process to become fully established and it is then under 'activation' control, i.e., it is governed by the rate at which local chemical reactions can occur unhindered by external diffusion or transportation limitations.
1	Very soon the rate of corrosion becomes controlled by the rate of arrival of oxygen at the corroding surface. The critical constraint is now the maximum rate of oxygen diffusion from the waters adjacent to the corroding surface, hence 'oxygen concentration' control (Jones 1996). The resulting corrosion loss may be modelled, closely, as a linear function.
2	With continued corrosion a build-up of corrosion products (rust) occurs on the corroding surface. This tends to limit the rate of oxygen diffusion through the rust layer, and this now becomes the rate-controlling step. It is a non-linear function in time, described by the solution of the governing diffusion equation (Melchers 2003a).
3	The increasing thickness of the rust layer reduces the capability for oxygen to reach the corroding surface, thereby allowing localized anaerobic conditions to develop at the corroding surface. Sulphate-reducing bacteria (SRB) can flourish under such layers given the right nutrient conditions. The rate of corrosion depends on the rate of metabolism and this in turn depends on the rate of supply of nutrients.
4	A near-steady-state situation develops eventually over the corroding surface. The rate of corrosion depends on the balance between the rate of supply of nutrients (Melchers and Wells 2006) and the rate of loss of the rust layer through erosion and wear.

with the development of corrosion products with time. This progression is represented in a number of consecutive 'phases' as summarized in Table 4.1. The model recognizes that (i) oxygen diffusion through the rust layers cannot be the rate-controlling mechanism at the very start of immersion when there is no rust, (ii) corrosion controlled by oxygen diffusion through the rust layers as expressed by Eqn (4.2) with $B = 0.5$ is only part of the overall process, and (iii) long-term corrosion involves the activity of sulphate-reducing bacteria (SRB) and, following the idea of Southwell *et al.* (1979), can be modelled as a (near-)linear function of time.

In practice the corrosion loss will vary somewhat from point to point on a corroding surface and there will be some variation in time and over the surface for the transition from one phase to another. This is shown schematically in Fig. 4.4. The model has provided a consistent interpretation of immersion corrosion data (Melchers 2003b, 2004a) and has provided a link between empirical field

© 2008 Woodhead Publishing Limited

Table 4.2 Environmental factors **E** and material factors in immersion corrosion

Environmental factors	Metal-related factors
Bacteria	Steel composition
Biofouling	Surface roughness
Oxygen supply	Size
Carbon dioxide	Coupon edge ratio
Salinity	
pH	
Carbonate solubility	
Pollutants	
Temperature	
Pressure	
Suspended solids	
Wave action	
Water velocity	

observations and corrosion science principles. Nevertheless, there are many factors that may affect the corrosion loss with time. Table 4.2 provides a brief summary.

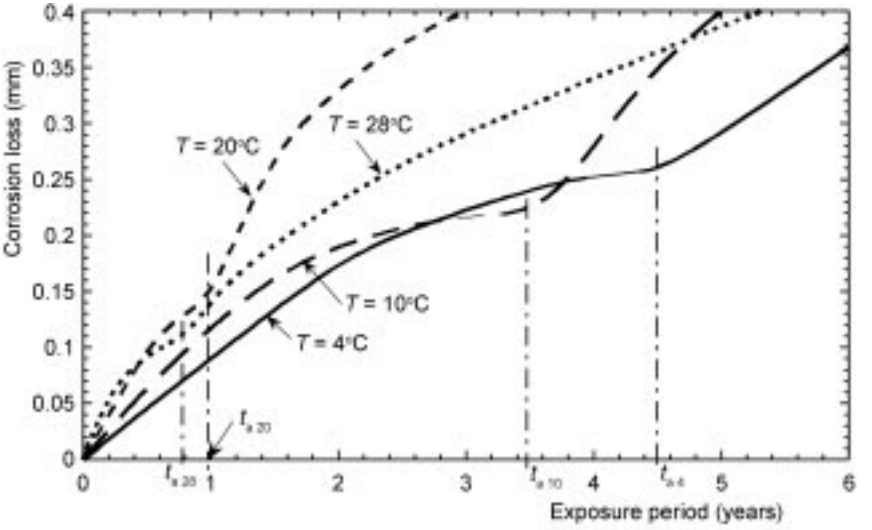
Fortunately, for marine immersion corrosion of structural steel exposed to essentially unpolluted seawater at low velocities, the components in **E** (the vector of environmental and material parameters – see Section 4.5 below) largely can be reduced to the average seawater temperature T (Melchers 2003b). As a result, the parameters describing the model also can be expressed as a function of T (Table 4.3).

Figure 4.5 gives an example of the changing nature of the corrosion loss curve with T. It is seen that seawater temperature has a significant effect on corrosion loss at all stages of the corrosion process. Referring to the parameters shown in Fig. 4.4, Fig. 4.6 shows this for the initial corrosion rate r_0. It illustrates that r_0 obeys the Arrhenius law for the effect of temperature on the kinetics of a

Table 4.3 Calibration of model parameters for general corrosion loss under immersion conditions in unpolluted low-velocity shallow waters as a function of annual average seawater temperature T (Melchers 2003b; Melchers and Wells 2006)

Model parameter	General corrosion
r_0 (mm/year)	$r_0 = 0.076\exp(0.054T)$
c_a (mm)	$c_a = 0.32\exp(-0.038T)$
t_a (year)	$t_a = 6.61\exp(-0.088T)$
r_a (mm/year)	$r_a = 0.066\exp(0.061T)$
c_s (mm)	$c_s = 0.141 - 0.00133T$
r_s (mm/year)	$r_s = 0.039\exp(0.0254T)$

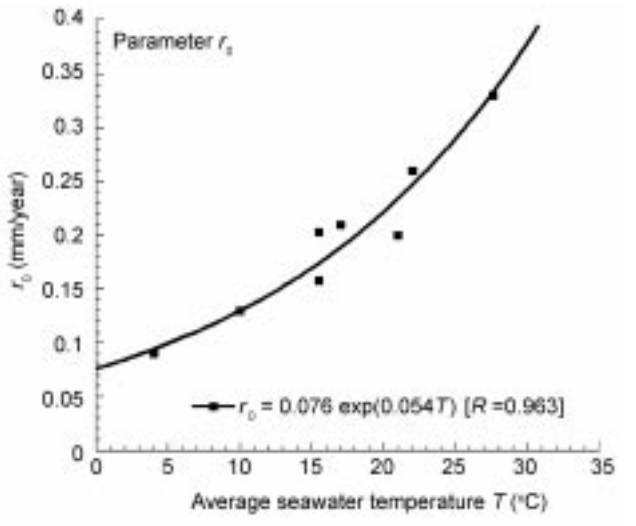
© 2008 Woodhead Publishing Limited



4.5 The shape of the theoretical corrosion loss curve for different mean water temperatures.

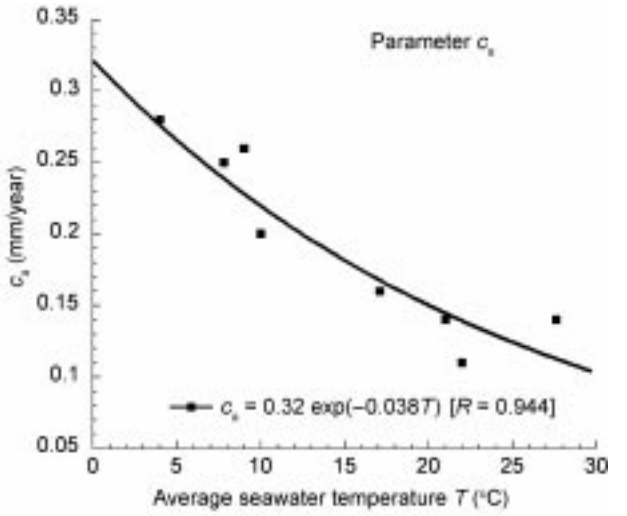
chemical reaction. Figure 4.7 shows the variation of the parameter c_a as a function of T, while Figs 4.8 and 4.9 show the dependence of the parameters c_s and r_s for long-term corrosion (Melchers and Wells 2006).

The parameter t_a (Fig. 4.4) that marks the idealized changeover from



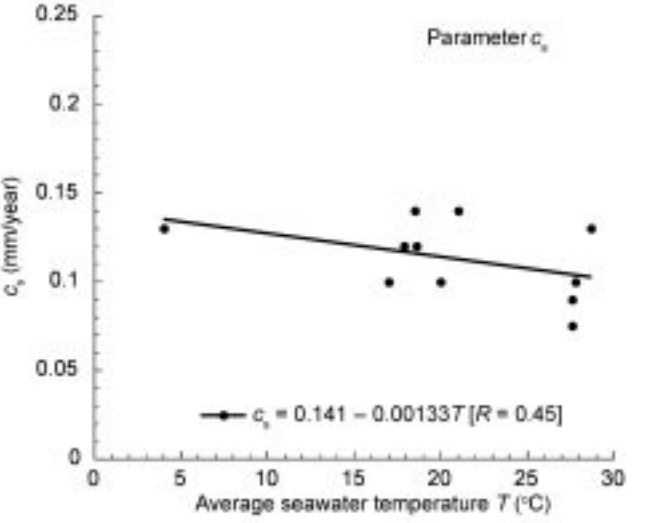
4.6 Variation of the initial corrosion rate r_0 as a function of T.

© 2008 Woodhead Publishing Limited



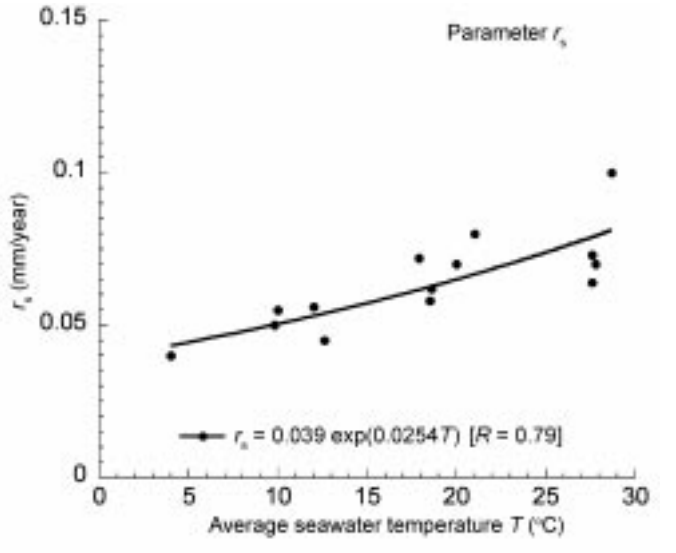
4.7 Variation of the parameter c_a as a function of T.

oxidation to anaerobic bacterial action is seen in Fig. 4.5 to be strongly dependent on average seawater temperature. This means that in tropical waters anaerobic conditions will be reached quite soon but it may take many years to reach this state in Arctic waters. Figure 4.10 shows its variation with T.

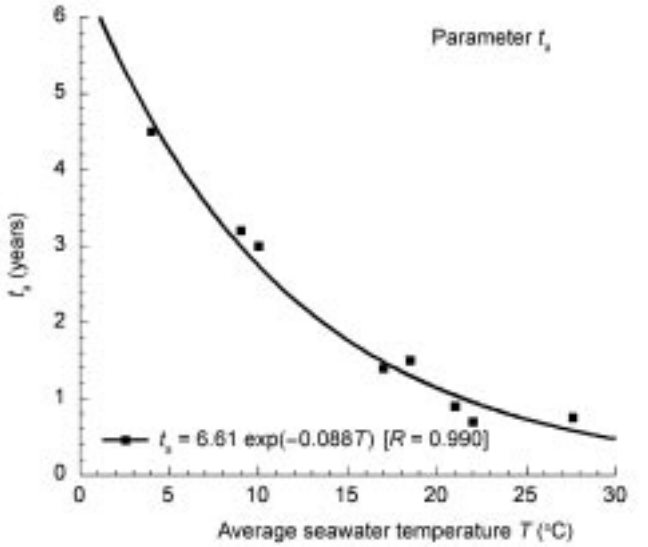


4.8 Variation of the parameter c_s for long-term corrosion as a function of T.

© 2008 Woodhead Publishing Limited



4.9 Variation of the parameter r_s for long-term corrosion as a function of T.



4.10 Variation of the parameter t_a that marks the idealized changeover from oxidation to anaerobic bacterial action, as a function of T.

© 2008 Woodhead Publishing Limited

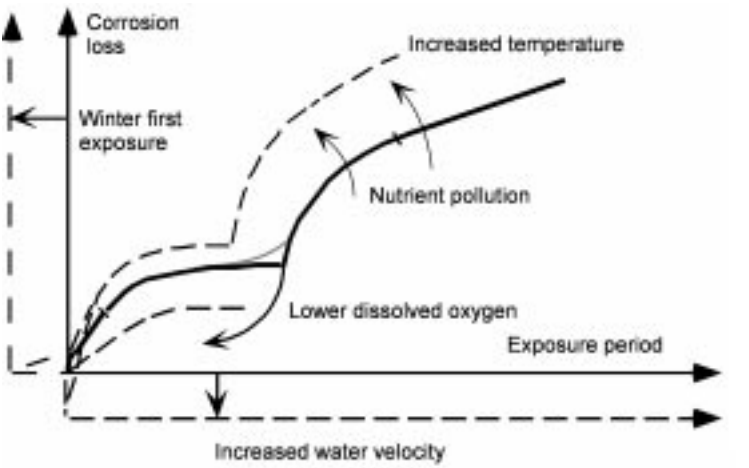
4.4 Environmental and other influences

The possible influences on immersion corrosion have recently been described in some detail in the literature. Figure 4.11 provides a qualitative summary for the effects of water (nutrient) pollution, water velocity, timing of first immersion and degree of water oxygenation (dissolved oxygen).

There is no evidence that increased water pressure has any noticeable effect on the corrosion of relatively small objects and that any effects on corrosion of immersion depth can be associated closely with the temperature, dissolved oxygen, water velocity and nutrient levels present at the given exposure depth and location (Melchers 2005a).

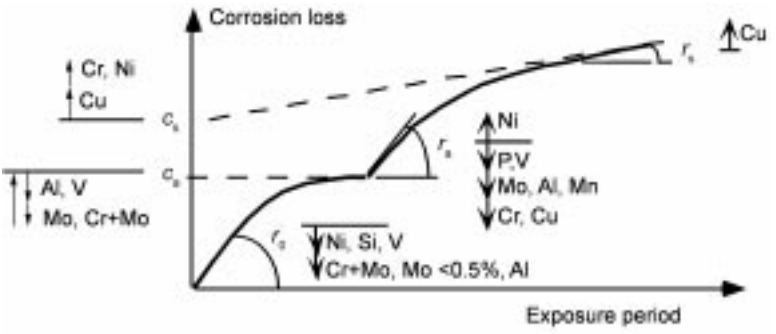
The effect of seawater salinity, conventionally considered to be very important, has been shown to be governed not by salinity *per se* but by the solubility of calcium carbonates (and to a lesser extent by magnesium carbonate) as governed by pH (Melchers 2006a). Calcium carbonate has been observed to be incorporated in rusts and is known to provide additional protection through reducing oxygen diffusivity. When 'hard' (high calcium carbonate, high pH) freshwaters cause the reduction of salinity in harbours and coastal areas, the higher pH causes lower solubility of the carbonates and these tend to deposit out in the rusts, thereby providing greater 'protection'. The apparent effect is that the brackish waters are less corrosive. However, this is not the case when the diluting waters are 'soft' (low or zero carbonates and pH around 7). These may be as corrosive as seawater or even more so.

The effects of small changes in steel composition are summarized in Fig. 4.12 (Melchers 2004b). It will be observed that for most alloying there is little effect



4.11 Qualitative summary of the effects of water (nutrient) pollution, water velocity, timing of first immersion and degree of water oxygenation (dissolved oxygen).

© 2008 Woodhead Publishing Limited



4.12 Summary of the effect on immersion corrosion loss of small changes in steel composition.

in phases 1 and 2 and this is consistent with these processes being controlled by the rate of oxygen diffusion to the corroding surface. Only alloys that have a significant effect on the diffusion properties of the rusts change the corrosion loss in these two phases.

An important observation in Fig. 4.12 is that alloying has different effects on different phases. Thus very few alloy changes affect the long-term corrosion rate r_s that is controlled by the rate of supply of nutrients to the SRB. Such behaviour would not have been predicted by any of the conventional corrosion models. It has also allowed quite conflicting empirical observations to be reconciled (Melchers 2004b). One further factor is the carbon content of steels. Traditionally there is conflicting evidence, with some investigators claiming no effect and others observing the opposite (Schultze and van der Wekken 1976). A detailed examination of all the available data shows that carbon content appears to have no effect on phases 1 and 2 (as would be expected since they are governed by oxygen diffusion) but that there is an effect for phases 3 and 4 (Melchers 2003c).

4.5 Variability and probabilistic models

Since only averaged environmental influences can be considered in any realistic (engineering) approach, it is to be expected that even with good accounting for the influencing factors, some uncertainty will remain in the relationship between corrosion loss, period of exposure and the environmental influences. A convenient and acceptable way of dealing with this is to invoke a probabilistic framework. To be sure, this is not conventional in the corrosion literature but it is consistent with structural reliability theory and the assessment of the safety of existing infrastructure (Melchers 1999). The approach is to consider the corrosion loss $c(t, \mathbf{E})$ to be a random variable dependent both on time t and on a vector $\mathbf{E}$ of environmental and material parameters (Melchers 1997, 2003b, d). This can be written as

© 2008 Woodhead Publishing Limited

$$c(t, \mathbf{E}) = b(t, \mathbf{E}) fn(t, \mathbf{E}) + \epsilon(t, \mathbf{E}) \quad 4.6$$

where $fn(t, \mathbf{E})$ is a mean-valued function or the 'expected' corrosion as a function of time and $\mathbf{E}$, $b(t, \mathbf{E})$ is a bias factor, expected to be unity for good-quality models, and $\epsilon(t, \mathbf{E})$ is a zero mean error function reflecting the uncertainty in $c(t, \mathbf{E})$ (sometimes known as a 'probability bucket'). Evidently, a good quality model has $\epsilon(t, \mathbf{E})$ as small as possible. Unfortunately the standard corrosion literature provides almost no information for its evaluation. Special tests with multiple coupons have been conducted in temperate waters to provide an initial assessment (Melchers 2003e). For the mean-value model $fn(t, \mathbf{E})$ the corrosion loss model described above may be taken as definitive. Previously it has been shown that this has the greatest influence on the evaluation of the probability of structural failure (Melchers 2003d).

4.6 Some other corrosion loss models

4.6.1 Models in the corrosion literature

For short-term corrosion when the influence both of biofilms and bacteria and of the build-up of corrosion products is ignored, electrochemistry theory leads directly to Faraday's law. It is theoretically equivalent to the Fickian oxygen diffusion equation used to derive Eqn (4.1) (Jones 1996). In Faraday's law the instantaneous corrosion rate $\mathrm{d}c/\mathrm{d}t$ is proportional to the corrosion current i:

$$\frac{\mathrm{d}c}{\mathrm{d}t} \propto i = \frac{nFDC}{\delta} \quad 4.7$$

where i is the limiting discharge current for oxygen diffusion (or 'corrosion current'), δ is the thickness of the diffusion layer immediately adjacent to the corroding surface, n is the number of electrons taking part in the discharge of the oxygen molecules, F is the Faraday constant, D is the diffusion coefficient for oxygen and C is the concentration of oxygen in the bulk seawater (i.e. away from the corroding surface).

Equation (4.7) is used widely in the corrosion literature and in some engineering literature. As described above, this is acceptable provided the corrosion products do not interfere with the rate of oxygen diffusion. Thus Eqn (4.7) is appropriate only for short-term corrosion. Some attempts have been made to modify Eqn (4.7) to allow for some environmental factors. Chernov (1990) expressed the diffusion coefficient as a function of temperature through the Arrhenius equation and proposed an empirical expression relating the thickness of the diffusion layer to water velocity. Oxygen concentration also was considered. However, attempts to fit the resulting model to two-year data (Chernov and Ponomarenko 1991) were not particularly successful.

© 2008 Woodhead Publishing Limited

4.6.2 Practical models: 'Ship corrosion wastage'

Particularly in the shipping research literature, empirical models derived only from data have been proposed under the terminology 'corrosion wastage' models. Their starting point is the assumption that the corrosion process and the many factors that influence it are too difficult for rational analysis and that therefore models should be developed only from data collected from ships (such as in the periodic classification society condition surveys).

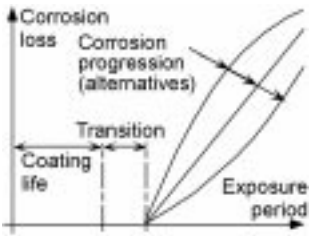
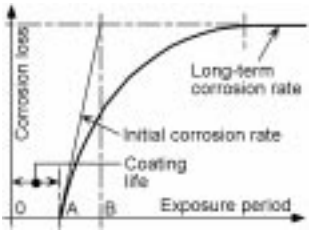
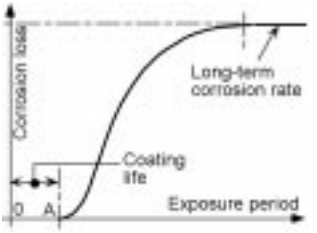
Most of the work published to date uses lumped historical data for a component of a ship, or for a type of ship. Typically it includes ships with widely differing sizes and operational profiles. The resulting lumped data means the population is not homogeneous as is usually required for detailed analysis (Melchers 2001, Gardiner and Melchers 2003). As a result, the data show very wide scatter (e.g. Yamamoto and Ikegami 1996), somewhat similar to Fig. 4.2. Unfortunately the shipping corrosion data does not come with the type and detail of information about the environmental conditions (e.g. temperature, humidity, sea states) necessary to interpret it in more detail and this will hamper model development. Nevertheless, models based on such lumped data have been proposed and applied in the estimation of structural reliability. A short summary of the empirical models is given in Table 4.4 (Paik *et al.* 1998, 2003; Guedes Soares and Garbatov 1999; Qin and Cui 2002).

Some effort is being made to account for environmental factors (Guedes Soares *et al.* 2005) but this is based mainly on short-term laboratory experimental observations without the use of natural seawater (Guedes Soares *et al.* 2006). However, it is now well established that artificial exposure conditions invariably produce completely misleading results compared to exposures under natural seawater conditions (Little and Ray 2002), even for short-term exposures. The reason is that natural seawater is a complex 'soup' of chemical and biological components. Both have important influences on corrosion as already noted above. Importantly, the realistic corrosion tests in the warm waters of the Panama Canal Zone and the interpretation of data given by Mikhailovskii *et al.* (1980) show clearly that there is no evidence of a levelling-out of corrosion loss with time, as proposed by Guedes Soares and Garbatov (1999) and Qin and Cui (2002). It also does not accord with actual experience with real structures. For example, if the corrosion process eventually stopped as proposed, the long-term deterioration and disintegration of shipwrecks and other steel objects in shallow seawaters simply would not occur.

Table 4.4 shows that some models attempt to include the loss of protection offered by protective coatings. As noted in Section 4.1, this is a complex matter with little objective field data in the open literature and for which laboratory studies are problematic. Logically, the modelling of protective coating deterioration belongs to a completely different domain of investigation. It is not considered herein.

© 2008 Woodhead Publishing Limited

Table 4.4 Corrosion 'wastage' models proposed for shipping

Format of model	Comments
	Yamamoto and Ikegami (1996) assumed that general corrosion results from pitting corrosion through the coalescence of many independent hemispherical pits. The result is a complex non-linear model showing corrosion loss levelling off with exposure time. Attempts to fit the model to data do not suggest that it provides a good fit (Melchers 2001).
	Paik *et al.* (1998, 2003) proposed that the corrosion loss with time be divided into three phases. The first is coating life, assumed to follow a lognormal distribution. The second, assumed to be exponentially distributed, is the transition when the coating breaks up and corrosion commences. The third is a corrosion loss curve that may be concave, convex or linear. The rationale for choosing between the corrosion curves, except empirically by fitting to data, is unclear. The model gives coefficients of variation for corrosion rates in bulk carriers typically in the range 0.5–2.0.
	Guedes Soares and Garbatov (1999) proposed a three-phase model. The first represents a period of no corrosion (such as due to protective coatings). The second phase is meant to signal damage of the corrosion protection system and the start of the corrosion process. However, in the diagram representing the model (on the left) and in expositions of the model, it is unclear how this phase differs from the third phase. The third phase shows a decrease in the rate of corrosion which eventually becomes zero. This is considered to be due to the build-up of protective rusts.
	Qin and Cui (2002) assumed that the coating protection system deteriorates gradually and allows corrosion to start by pitting. Corrosion loss is defined relative to the volume of pitting corrosion with pitting depth represented by Eqn (4.2). The long-term corrosion loss also is assumed to be represented by a function such as Eqn (4.2). The long-term instantaneous corrosion rate appears to tend asymptotically to zero.

© 2008 Woodhead Publishing Limited

Other examples using both empirical and more advanced models include the modelling of corrosion inside holds of bulk carrier ships used in the iron ore and coal trade (Gardiner and Melchers 2003) and the modelling of ballast tank corrosion for naval vessels (Gudze and Melchers 2006).

4.7 Coastal atmospheric corrosion

As noted earlier, the most widely accepted model for coastal atmospheric corrosion is Eqn (4.2) with A and B obtained by fitting to empirical data. There have been many attempts in the corrosion literature to apply it or a similar empirical model (Benarie and Lipfert 1986, Feliu *et al.* 1993), despite evidence that it has poor extrapolation powers and is often a poor fit to data. The problem is more complex than for immersion corrosion since there are more environmental parameters to be considered, including air temperature, salinity deposition rates, relative humidity, rainfall, wind effects, and perhaps air pollution inputs such as sulphur dioxide and nitrates (Roberge *et al.* 2002).

Others have attempted to perform linear or non-linear correlation studies between corrosion rates or annual corrosion loss and environmental factors. These efforts have not been wholly successful, with the importance of environmental factors varying considerably between studies (e.g. Duncan and Ballance 1988).

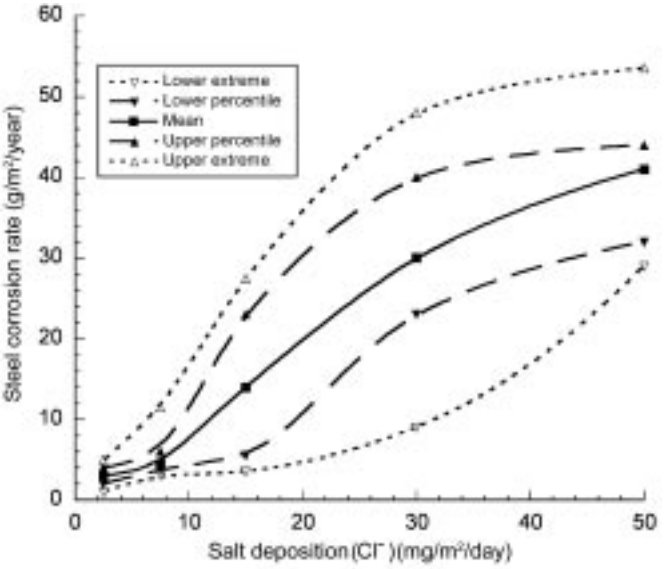
For coastal atmospheric corrosion a key input variable is considered to be the rate of salt deposition (Roberge *et al.* 2002). This derives from the classical studies on the Nigerian coast (Ambler and Bain 1955) and many subsequent observations. Correlation studies between one-year corrosion loss and salt deposition typically produce plots such as Fig. 4.13. This shows a very high degree of uncertainty (spread), indicating that there are other influencing factors involved. Also, the curves indicate that high levels of salt deposition have little extra effect.

The other influencing factor of significance is generally considered to be the relative humidity (RH), with RH greater than about 70% causing much greater 'time of wetness' (TOW), that is a greater proportion of time when the steel is sufficiently wet for corrosion to occur.

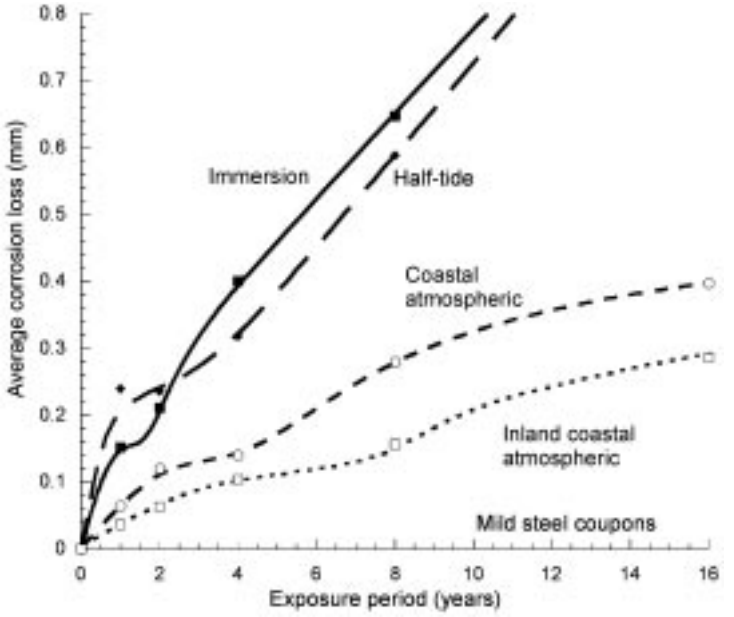
Despite the long and very extensive research that has been carried out on atmospheric corrosion, the present situation is still one of high levels of uncertainty between field observations and model predictions (Townsend 2002) and an inability to make predictions for locations other than where the measurements were made. Even then, predictions beyond a few years are not considered feasible.

There is some promise that the model shown in Fig. 4.4 is valid also for corrosion loss in the tidal and in the coastal atmospheric zone. Figure 4.14 shows an example (Melchers 2007c). It shows data for immersion and half-tide exposures in the Panama Canal Zone extracted from Forgeson *et al.* (1960) and

© 2008 Woodhead Publishing Limited



4.13 Correlation between corrosion loss (for the first year) as a function of salt deposition rate. It is evident that there is a very considerable spread in the relationship (based on data from Morcillo *et al.* 1999).



4.14 Example of trends of corrosion loss in the tidal and in the coastal atmospheric zones at the Panama Canal (Melchers 2007c).

© 2008 Woodhead Publishing Limited

Southwell *et al.* (1976) and for the coastal atmospheric exposure zone extracted from Southwell *et al.* (1958). Details of the sites involved and the weather and other conditions are given in the original references, but suffice to note here that the weather in the Panama Canal Zone is tropical with very stable temperature, RH and rainfall patterns. As before, the interpreted trend lines based on the model of Fig. 4.4 show progressive development from immersion through tidal to coastal atmospheric environments. These data are for small coupons and no account is taken of the known difference in corrosion loss for the sheltered side of coupons compared with the boldly exposed side. Similar trends have been interpreted for a variety of data sets covering sub-arctic to tropical conditions (Melchers 2007c).

More research is required to justify the possible application of the model of Fig. 4.4 to tidal and to coastal atmospheric corrosion loss. This work is in progress, including the calibration of the model against field data.

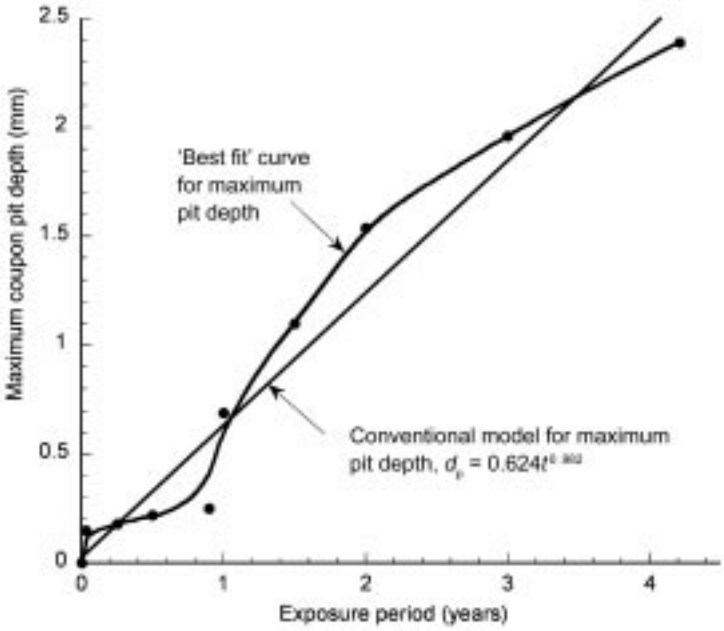
4.8 Inland atmospheric corrosion

Typically the marine environment is the most severe for the corrosion of mild steel. Inland the losses tend to be much less. Thus for high elevations extremely low corrosion rates have been observed – much lower than expected (Townsend 2002). Similarly, in the cold harsh Antarctic conditions very low but not negligible corrosion losses have been observed (Hughes *et al.* 1996). However, elevated corrosion losses occur in atmospheres polluted with industrial gases such as SO_2 and NO_2 (and their variants). SO_2 in particular has been implicated as causing 'acid rain' and this has been correlated with increased one-year corrosion rates as well as with longer-term corrosion losses (Roberge *et al.* 2002). As is the case for marine corrosion, there is as yet no systematic body of knowledge to allow development of universal models. Invariably field tests are required to establish likely local long-term corrosion losses (and pitting). Handbooks such as Kreysa and Eckermann (1992) and Schumacher (1979) may be helpful in estimating preliminary losses for design or assessment purposes.

4.9 Pitting corrosion

For liquid-retaining structures such as tanks and pipelines, or for ships, the maximum depth of pit determines the failure condition. Hence it has been conventional to seek the maximum depth of pitting as a function of the probability of its occurrence. The Gumbel extreme value distribution has been adopted widely in corrosion engineering following the pioneering work of Aziz (1956). Pitting is also widely quoted within the applied extreme value literature as a classic example (Galambos 1987). To illustrate, consider the pit depth data collected for mild steel coupons exposed to Pacific Ocean seawaters averaging 20 ºC, with multiple coupons (18 sides) exposed and recovered at each recovery

© 2008 Woodhead Publishing Limited



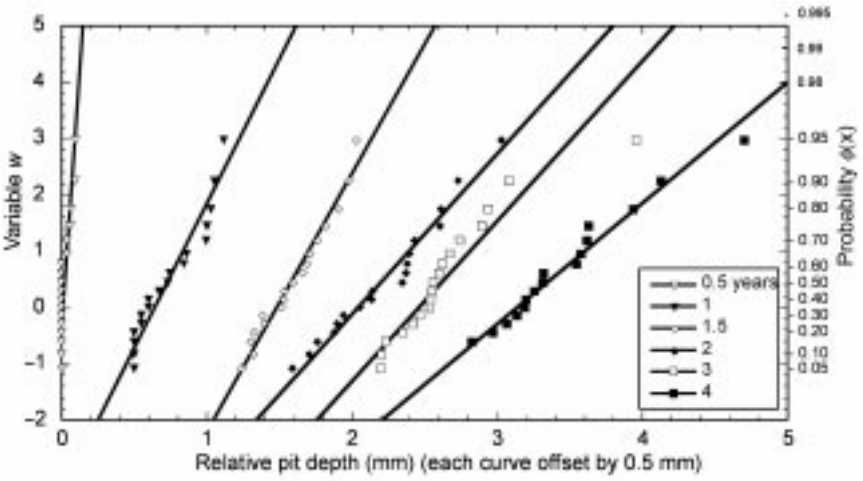
4.15 Maximum pit depth obtained from a set of 18 coupon faces as a function of exposure period showing best-fit curve and conventional model. Note the change from phase 2 to phase 3 at about 0.9 years.

time. Figure 4.15 shows typical data together with the model of Eqn (4.2) commonly assumed to apply to the progression of maximum pit depth with exposure time.

Figure 4.15 also shows the data interpreted according to the model of Fig. 4.4. One of the outstanding features is that phases 3 and 4 of the model are now much more pronounced (Melchers 2004a). By ranking the pit depth values for each recovery time and applying standard procedures for plotting a Gumbel plot, Fig. 4.16 is obtained. It will be seen that there is considerable deviation of the data from the straight line that would represent a Gumbel distribution on a Gumbel plot. In the past, if such deviation was noted, it was invariably dismissed as due to data or experimental problems or variability. However, a more detailed analysis of the data together with an understanding of the mechanics of pitting leads to a completely different interpretation. This is outlined briefly below.

The pitting process is known to generate two types of pits – those that initiate immediately and then continue to grow in depth with time (stable pits) and those that may initiate late or that may eventually stop growing ('die') in depth (metastable pits). Because pitting is a dynamic process, the distribution between each type of pitting changes with exposure time, with the distribution of stable pits increasing its mean value (and also its variability) and the metastable pits

© 2008 Woodhead Publishing Limited



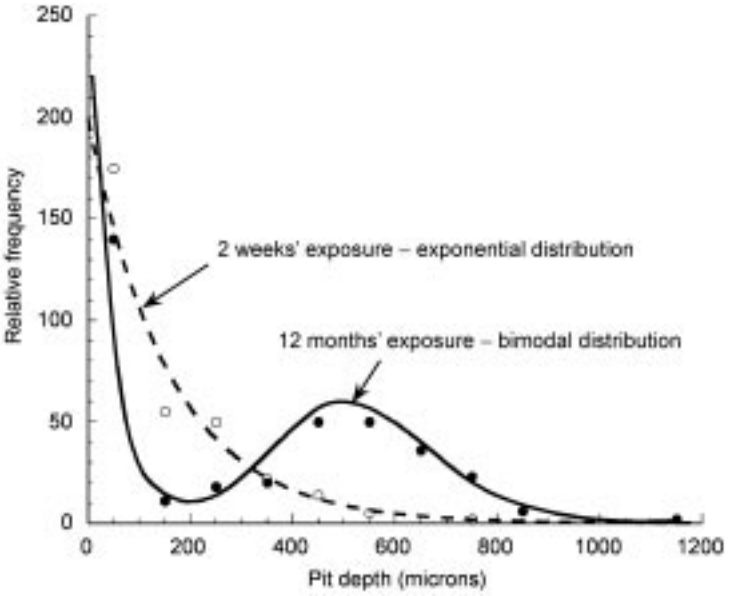
4.16 Maximum pit depths from each coupon face plotted on a Gumbel plot. Note that *w* is the standard reduced Gumbel parameter corresponding to the probabilities shown at right. The straight lines are the best fits to the data assuming the complete data set in each case is from a homogeneous population.

becoming relatively less important. Figure 4.17 shows the variation of typical bimodal pit depth distributions.

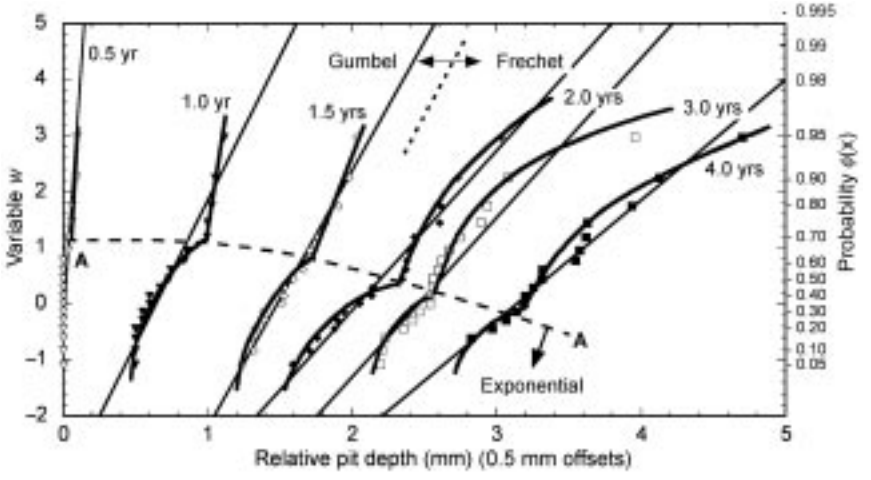
Earlier it was argued that only the stable pits could become extreme depth pits and of these only those that initiated very early and then grew in depth at the maximum rate consistent with pit growth mechanics. These have been termed 'super-stable' pits (Melchers 2005b). Moreover, detailed observation revealed that there is a significant change in both pit depths and pit geometries and that this change is consistent with the development of phase 3. It is also consistent with the observation of so-called 'broad' pits commonly noted in the empirical corrosion literature but not previously explained as being the result of bacterial activity (as in phase 3). Thus there is a change from pitting in phases 1 and 2 nominally under aerobic conditions external to the pits (irrespective of what may be the condition inside the pits themselves). This immediately implies a change in the population and hence, by fundamental statistical considerations, in the statistics of the population. To be specific, it can be shown using simple arguments that the extreme depth pits under phases 3 and 4 are more appropriately represented by the Frechet distribution than by the Gumbel distribution (Melchers 2006b). Figure 4.18 shows the differentiation between the distributions plotted on a Gumbel plot.

It is immediately evident from comparing Figs 4.16 and 4.18 that there are very significant systematic departures from the linear trends typically used to argue that the data is Gumbel distributed. Firstly, the data for the metastable pits (i.e. those below line AA in Fig. 4.18) should be disregarded in determining the

© 2008 Woodhead Publishing Limited



4.17 Typical bimodal pit depth distribution as a function of exposure period. Typically the exponential mode (dashed line) reduces to the left, and the right-hand mode moves towards the right and shows a wider spread.



4.18 Maximum pit depths from each coupon face plotted on a Gumbel plot. The light straight lines are the Gumbel lines for each data set (from Fig. 4.16). The heavy lines are subjective fits, with the straight lines above AA being consistent with the Gumbel extreme value distribution up to about 1.5 years' exposure, and thereafter consistent with the Frechet extreme value distribution. The curved lines below AA are generally consistent with the exponential distribution.

© 2008 Woodhead Publishing Limited

distribution of the extreme depth pits under all exposure phases. When exposure durations are still relatively short (i.e. in phases 1 and 2) the data for stable pitting is appropriately represented by the Gumbel distribution but only using the data above AA. It is easily seen that this results in lower probabilities of occurrence for a given extreme depth. However, in phases 3 and 4 the data is distinctly non-linear above AA and it is seen that the Frechet distribution is more appropriate. It also yields considerably greater probabilities of occurrence for given extreme pit depths. This has very significant practical implications (Melchers 2006c).

4.10 Discussion

The viewpoint taken herein is that sound progress in the development of mathematical (and probabilistic) models for corrosion loss and maximum pit depth under in-situ conditions cannot be made unless there is a good understanding of the fundamentals of corrosion under actual in-situ conditions. This must be coupled with fundamental laboratory observations but care should be exercised to ensure that the latter do not drive the former. It is now increasingly recognized that because of the complexity of natural seawater, laboratory tests must be used with care when attempting to extrapolate in time and to field conditions (Little and Ray 2002).

The use of coupons in developing corrosion loss and maximum pit depth models for larger structures is unlikely to be a significant issue. There is probably sufficient evidence in the corrosion literature that coupon size is not a significant variable within the one exposure environment (Evans 1960, Jeffrey and Melchers 2002). On the other hand, for atmospheric corrosion metal surface orientation is very important. This remains a topic about which there is little information (*cf.* Roberge *et al.* 2002) and much detailed investigation is still required.

An important corollary of the more advanced corrosion models introduced here is that they provide new insights as to the 'things to look for' in corrosion observations. This includes the possibility that bacterial activity may be involved. It also indicates that the conventional approach to monitoring corrosion loss by doubling the exposure time (e.g. 0.5, 1, 2, 4, 8 years) for coupon recovery may well miss the important transition from phase 2 to 3.

Regarding the input of environmental variables, it is important to observe that corrosion is an 'integration' process in that it smoothes out variations in the environmental conditions and (apart from very early, short-term corrosion) tends to be sensitive only to long-term trends. This means that only relatively short-term sampling of the environmental conditions is required. It means also that representative estimates may be sufficient. Both are much easier to obtain in practical applications.

© 2008 Woodhead Publishing Limited

4.11 Conclusions

An overview was given of the various approaches to modelling corrosion loss of mild steel as a function of time for application with deteriorating infrastructure, particularly where it is exposed to harsh marine conditions. Important points are that laboratory observations have little validity for predicting even short-term in-situ corrosion behaviour as a result of the complexity of natural seawaters and seawater aerosols. Moreover, short-term field observations may be misleading for the prediction of long-term corrosion as the process is distinctly non-linear in time. Hence a 'corrosion rate' has little meaning. An overview of pitting corrosion of mild steel was given and the dangers of the traditional use of the Gumbel distribution were outlined.

4.12 Acknowledgement

This chapter was prepared as part of a research project on structural reliability analysis under deterioration conditions that was financially supported by the Australian Research Council.

4.13 References

Ambler HR and Bain AAJ (1955) Corrosion of metals in the tropics, *Journal of Applied Chemistry* 5: 437–467.

Aziz PM (1956) Application of the statistical theory of extreme values to the analysis of maximum pit depth data for aluminum, *Corrosion (NACE)* 12(10): 495t–506t.

Benarie M and Lipfert FL (1986) A general corrosion function in terms of atmospheric pollutant concentrations and rain pH, *Atmospheric Environment* 20(10): 1947–1958.

Booth F (1948) A note on the theory of surface diffusion reactions, *Trans. Faraday Soc.* 44: 796–801.

Chernov BB (1990) Predicting the corrosion of steels in seawater from its physiochemical characteristics, *Protection of Metals* 26(2): 238–241.

Chernov BB and Ponomarenko SA (1991) Physiochemical modelling of metal corrosion in seawater, *Protection of Metals* 27(5): 612–615.

Copson HR (1945) A theory of the mechanism of rusting of low alloy steels in the atmosphere, *Proc. ASTM* 45: 554–590.

Crolet J-L (1992) From biology and corrosion to biocorrosion, in *Microbial Corrosion*, ed. CA Sequeira and AK Tiller, The Institute of Metals, London, 50–60.

Duncan JR and Ballance JA (1988) Marine salts contribution to atmospheric corrosion, in *Degradation of Metals in the Atmosphere*, ed. SW Dean and TS Lee, ASTM STP 965, American Society for Testing and Materials, Philadelphia, PA, 316–326.

Evans UR (1960) *The Corrosion and Oxidation of Metals: Scientific Principles and Practical Applications*, Edward Arnold, London.

Feliu S, Morcillo A and Feliu Jr S (1993) The prediction of atmospheric corrosion from meteorological and pollution parameters – 1. Annual corrosion, *Corrosion Science* 34(3): 403–422.

Foley RT (1970) Role of the chloride ion in iron corrosion, *Corrosion (NACE)* 26(2): 58–70.

© 2008 Woodhead Publishing Limited

Forgeson BW, Southwell CR and Alexander AL (1960) Corrosion of metals in tropical environments. Part 3 – Underwater corrosion of ten structural steels, *Corrosion (NACE)* 16(3): 87–96.

Galambos J (1987) *The Asymptotic Theory of Extreme Order Statistics*, 2nd edn, Krieger, Malabar, FL.

Gardiner CP and Melchers RE (2003) Corrosion analysis of bulk carriers, Part 1: Operational parameters influencing corrosion rates, *Marine Structures* 16(8): 547–566.

Gilberg MR and Seeley NJ (1981) The identity of compounds containing chloride ions in marine iron corrosion products: A critical review, *Studies in Conservation* 26: 50–56.

Gudze MT and Melchers RE (2006) Prediction of naval ship ballast tank corrosion using operational profiles, *Trans. Royal Institution of Naval Architects Part A: International Journal of Maritime Engineering* 148: 77–86.

Guedes Soares C and Garbatov Y (1999) Reliability of maintained, corrosion protected plate subjected to non-linear corrosion and compressive loads, *Marine Structures* 12: 425–445.

Guedes Soares C, Garbatov Y, Zayed A and Wang G (2005) Non-linear corrosion model for immersed steel plates accounting for environmental factors, *Trans. Society of Naval Architects and Marine Engineers* 111: 194–211.

Guedes Soares C, Garbatov Y, Zayed A, Wang G, Melchers RE, Paik JK and Cui W (2006) Non-linear corrosion model for immersed steel plates accounting for environmental factors, *Trans. Society of Naval Architects and Marine Engineers* 113: 306–329.

Hamilton WA (1985) Sulphate-reducing bacteria and anaerobic corrosion, *Ann. Rev. Microbiol.* 39: 195–217.

Hughes JD, King GA and O'Brien DJ (1996) Corrosivity in Antarctica – Revelations on the nature of corrosion in the world's coldest, driest, highest and purest continent, *Proc. 13th Int. Corrosion Conf.*, Melbourne, 25–29 November, Australasian Corrosion Association, Melbourne, Australia, Paper No. 24.

Jeffrey R and Melchers RE (2002) Shape and size effects for marine immersion coupons, *British Corrosion Journal* 37(2): 99–104.

Jones DA (1996) *Principles and Prevention of Corrosion*, 2nd edn, Prentice Hall, Upper Saddle River, NJ.

Kreysa G and Eckermann R (1992) *Dechema Corrosion Handbook*, Vol. 11, VCH Publishers, New York.

Lee W, Lewandowski Z, Nielsen PH and Hamilton WA (1995) Role of sulfate-reducing bacteria in corrosion of mild steel: A review, *Biofouling* 8: 165–194.

Little B and Ray R (2002) A perspective on corrosion inhibition by biofilms, *Corrosion (NACE)* 58(5): 424–428.

Melchers RE (1997) Modeling of marine corrosion of steel specimens, in *Corrosion Testing in Natural Waters*, ed. RM Kain and WT Young, ASTM STP 1300, American Society for Testing and Materials, Philadelphia, PA, 20–33.

Melchers RE (1999) *Structural Reliability Analysis and Prediction*, 2nd edn, John Wiley & Sons, Chichester.

Melchers RE (2001) Probabilistic models of corrosion for reliability assessment and maintenance planning, *Proc. Offshore Mechanics and Arctic Engineering Conf.*, Rio de Janeiro, 3–8 June 2001: paper OMAE2001/S&R-2108, CDRom.

Melchers RE (2003a) Mathematical modelling of the diffusion controlled phase in marine immersion corrosion of mild steel, *Corrosion Science* 45(5): 923–940.

© 2008 Woodhead Publishing Limited

Melchers RE (2003b) Modeling of marine immersion corrosion for mild and low alloy steels – Part 1: Phenomenological model, *Corrosion (NACE)* 59(4): 319–334.
Melchers RE (2003c) Effect on marine immersion corrosion of carbon content of low alloy steels, *Corrosion Science* 45(11): 2609–2625.
Melchers RE (2003d) A probabilistic model for marine corrosion of steel for structural reliability assessment, *J. Structural Engineering, ASCE* 129(11): 1484–1493.
Melchers RE (2003e) Modeling of marine immersion corrosion for mild and low alloy steels – Part 2: Uncertainty estimation, *Corrosion (NACE)* 59(4): 335–344.
Melchers RE (2004a) Pitting corrosion of mild steel in marine immersion environment – 1: maximum pit depth, *Corrosion (NACE)* 60(9): 824–836.
Melchers RE (2004b) Effect of small compositional changes on marine immersion corrosion of low alloy steel, *Corrosion Science* 46(7): 1669–1691.
Melchers RE (2005a) Effect of immersion depth on marine corrosion of mild steel, *Corrosion (NACE)* 61(9): 895–906.
Melchers RE (2005b) Statistical characterization of pitting corrosion – 1: Data analysis, *Corrosion (NACE)* 61(7): 655–664.
Melchers RE (2006a) Modelling immersion corrosion of structural steels in natural fresh and brackish waters, *Corrosion Science* 48(12): 4174–4201.
Melchers RE (2006b) Pitting corrosion of mild steel under marine anaerobic conditions – Part 2: Statistical representation of maximum pit depth, *Corrosion (NACE)* 62(12): 1074–1081.
Melchers RE (2006c) Probabilistic modelling of long-term pitting corrosion of structural steels under marine immersion conditions, *Proc. Corrosion & Prevention 2006*, Hobart, Tasmania.
Melchers RE (2007a) The influence of seawater nutrient content on the early immersion corrosion of mild steel – 1 Empirical observations, *Corrosion (NACE)* 63(1): 318–329.
Melchers RE (2007b) The influence of seawater nutrient content on the early immersion corrosion of mild steel – 2 The role of biofilms and SRB, *Corrosion (NACE)* 63(5): 405–415.
Melchers RE (2007c) The transition from marine immersion to coastal atmospheric corrosion for structural steels, *Corrosion (NACE)* 63(6): 500–514.
Melchers RE and Ahammed M (1994) *Non-linear modelling of corrosion of steel in marine environments*, Research Report 106.09.1994, Department of Civil Engineering and Surveying, The University of Newcastle.
Melchers RE and Jeffrey R (2005) Early corrosion of mild steel in seawater, *Corrosion Science* 47(7): 1678–1693.
Melchers RE and Jiang X (2006) Estimation of models for durability of epoxy coatings in water ballast tanks, *J. Ships and Offshore Structures* 1(1): 61–70.
Melchers RE and Wells PA (2006) Models for the anaerobic phases of marine immersion corrosion, *Corrosion Science* 48(7): 1791–1811.
Mercer AD and Lumbard EA (1995) Corrosion of mild steel in water, *British Corrosion Journal* 30(1): 43–55.
Mikhailovskii YN, Strekalov PV and Agafonov VV (1980) A model of atmospheric corrosion of metals allowing for meteorological and aerochemical characteristics, *Protection of Metals* 16(4): 308–323.
Morcillo M, Chico B, Itero E and Mariaca L (1999) Effect of marine aerosol on atmospheric corrosion, *Materials Performance* 38(4): 72–77.
Paik JK, Kim SK, Lee S and Park YE (1998) A probabilistic corrosion rate estimation model for longitudinal strength members of bulk carriers, *J. Ship and Ocean Technology* 2: 58–70.

© 2008 Woodhead Publishing Limited

Paik J, Lee J, Hwang J and Park Y (2003) A time-dependent corrosion wastage model for the structures of single and double hull tankers and FSOs and FPSOs, *Marine Technology* 40: 201–217.

Postgate JR (1984) *The Sulphate-reducing Bacteria*, 2nd edn, Cambridge University Press, Cambridge.

Qin S and Cui W (2002) Effect of corrosion models on the time-dependent reliability of steel plated elements, *Marine Structures* 15: 15–34.

Roberge PR, Klassen RD and Haberecht PW (2002) Atmospheric corrosion modeling – A review, *Materials & Design* 23: 321–330.

Schultze WA and van der Wekken CJ (1976) Influence of alloying elements on the marine corrosion of low alloy steels determined by statistical analysis of published literature data, *British Corrosion Journal* 11(1): 18–24.

Schumacher M (ed.) (1979) *Seawater Corrosion Handbook*, Noyes Data Corporation, Park Ridge, NJ.

Southwell CR, Forgeson BW and Alexander AL (1958) Corrosion of metals in tropical environments – Part 2 – Atmospheric corrosion of ten structural steels, *Corrosion (NACE)* 14(9): 53–59.

Southwell CR, Bultman JD and Alexander AL (1976) Corrosion of metals in tropical environments – Final report of 16-year exposures, *Materials Performance* 15(7): 9–25.

Southwell CR, Bultman JD and Hummer CW (1979) Estimating service life of steel in seawater, in *Seawater Corrosion Handbook*, ed. M Schumacher, Noyes Data Corporation, Park Ridge, NJ, 374–387.

Tammann G (1923) *Lehrbuch der Metallographie*, 2nd edn, Leipzig.

Tomashev ND (1966) *Theory of Corrosion and Protection of Metals*, MacMillan, New York.

Townsend HE (ed.) (2002) *Outdoor Atmospheric Corrosion*, STP 1421, ASTM International, West Conshohocken, PA.

TSCF (2002) *Guidelines for ballast tank coatings systems and surface preparation*, Tanker Structure Cooperative Forum, London.

Yamamoto N and Ikegami K (1996) A study on the degradation of coating and corrosion of ships hull based on the probabilistic approach, *Proc. 15th Int. Conf. on Offshore Mechanics and Arctic Engineering*, Vol. II, ASME, 159–166.

© 2008 Woodhead Publishing Limited

5

Fatigue cracking in aged structures

W C CUI, China Ship Scientific Research Center, China

Abstract: This chapter introduces the current state of the art concerning mechanisms, mathematical models and preventive measures against metal fatigue cracking. The chapter contains five sections. Section 5.1 is the introduction. Section 5.2 gives a brief historical overview of metal fatigue. Section 5.3 discusses the current understanding of fatigue mechanisms. Section 5.4 introduces the various fatigue life prediction methods, while Section 5.5 discusses the preventive measures against fatigue cracking.

Key words: fatigue cracking, cumulative fatigue damage, fatigue crack propagation, preventive measures.

5.1 Introduction

Fatigue is defined as a process of cycle by cycle accumulation of damage in a material undergoing fluctuating stresses and strains (Almar-Naess, 1985). A significant feature of fatigue is that the load is not large enough to cause immediate failure. Instead, failure occurs after a certain number of load fluctuations have been experienced, i.e. after the accumulated damage has reached a critical level.

Fatigue mechanism is different for different materials. In this chapter, it is confined to metal fatigue only. For fatigue mechanism of composite materials, readers are advised to refer to Carlson and Kardomateas (1996) and Mortensen (2006). The purpose of this chapter is to introduce the current state of the art concerning mechanisms, mathematical models and preventive measures against fatigue cracking. The chapter contains five sections. Section 5.1 is the introduction. Section 5.2 gives a brief historical overview of metal fatigue. Section 5.3 discusses the current understanding of fatigue mechanisms. Section 5.4 introduces the various fatigue life prediction methods, while Section 5.5 discusses the preventive measures against fatigue cracking.

5.2 Historical overview of metal fatigue

The history of fatigue was described in detail by Schutz (1996). According to him, the history of fatigue begins with Albert. In 1837, he published the first fatigue-test results known. In 1842, Rankine discussed the fatigue strength of railway axles. The term ‘fatigue’ was mentioned for the first time by the Englishman Braithwaite in 1854. In his paper, Braithwaite described many

© 2008 Woodhead Publishing Limited

service fatigue failures of brewery equipment, water pumps, propeller shafts, crankshafts, railway axles, levers, cranes, etc. Beginning in 1860, Wöhler published the results of fatigue tests with railway axles. In 1870, he presented a final report containing the following conclusions, often called 'Wöhler's laws': 'Material can be induced to fail by many repetitions of stresses, all of which are lower than the static strength. The stress amplitudes are decisive for the destruction of the cohesion of the material. The maximum stress is of influence in so far as the higher it is, the lower are the stress amplitudes which lead to failure.' Wöhler therefore stated the stress amplitudes to be the most important parameter for fatigue life, but a tensile mean stress also to have a detrimental influence.

Wöhler incidentally represented his test results in the form of tables. Not until 1910 did Basquin (1910) represent the finite life region in the form 'log σ_a on the ordinate, log N on the abscissa'. These curves were called 'Wöhler's curves' from 1936 and now they are called S–N curves.

The next step was the discovery of the Bauschinger effect in the period 1870–1905, 'the change of the elastic limit by often repeated stress cycles', which is the basis for the hypotheses of Coffin and Manson which originated in the 1950s and which are still being utilized today in the low cycle fatigue (LCF) field and for fatigue life prediction according to the local concept.

In the period 1920–1945, the foundations were laid for almost all the fatigue knowledge we enjoy today. These include the fatigue strength under variable amplitudes, the measurement of fatigue loads and load spectra, the realization that higher-strength materials do not result in higher fatigue strengths of components, the mechanical methods to improve fatigue strength by inducing compressive residual stresses, the damage accumulation hypotheses of Palmgren–Miner for fatigue life prediction under variable amplitudes, the statistical scatter of the static and fatigue strengths of materials, and the realization that it is difficult, if not impossible, to transfer the fatigue behavior of specimens to that of an actual component, which is true even today.

The period 1945–1960 was the time in which the harvest of the years 1920–1945 was brought in. In all industrial countries fatigue was investigated. Following the notorious crashes of the Comet airliners, many full-scale fatigue tests were carried out with fuselages. In this period, the 'safe life' concept was gradually replaced by the 'fail safe' concept. The scatter of the number of cycles to failure and of the fatigue limit was treated with the help of mathematical statistics.

From about 1950 onwards, doubts about the validity of Miner's rule began to appear in the literature. Damage sums between 0.1 and 10 were found in fatigue tests, which, however, were entirely unsuitable for this purpose. A genuine check of Miner's rule was only possible at the end of the 1950s, as only then had suitable test machines been developed.

Toward the end of the period 1945–1960, a large number of crack propagation tests were carried out and crack propagation hypotheses were developed,

© 2008 Woodhead Publishing Limited

still without employing fracture mechanics. However, in 1958, Irwin had realized that the stress-intensity factor $K = S\sqrt{\pi a}$ was the determining factor for static strength in the cracked state. With this concept, linear elastic fracture mechanics (LEFM) was born.

From 1960 onwards, the most significant progress in fatigue was made by applying LEFM. Various fatigue crack propagation (FCP) theories were proposed, although cumulative fatigue damage (CFD) theories were further developed and widely applied in most industries except the aircraft industry (Cui, 2002).

Paris (Paris *et al.*, 1961; Paris and Erdogan, 1963) established that fatigue crack propagation could be described by the following equation, soon erroneously called a 'law':

$$\frac{\mathrm{d}a}{\mathrm{d}N} = C(\Delta K)^n \qquad 5.1$$

This equation was widely accepted and is used even today. However, it contains neither the influence of mean stress on crack propagation, nor the static fracture on reaching the fracture toughness, K_{Ic}, nor the fatigue threshold ΔK_{th}, which is the stress intensity factor range below which no fatigue crack propagation occurs. The complex process of crack propagation is undoubtedly described much too simply by this equation.

In order to explain the stress ratio effect R (= $K_{\mathrm{min}}/K_{\mathrm{max}}$), Elber (1970) introduced the 'crack closure' concept based on his experimental observation that after a high tensile load the crack closes before the load is reduced to zero. This concept was highly appraised in the 1980s and 1990s and was used to explain various other effects, including the load sequence effect (e.g. McEvily *et al.*, 1999; McEvily and Ishihara, 2001; Newman *et al.*, 2006) but now it is subjected to some challenge (e.g. Hertzberg *et al.*, 1988). In particular, many people have agreed that the physical effects of crack closure have been greatly overestimated in the past (e.g. Vasudevan *et al.*, 1994). A partial crack closure model (Donald and Paris, 1999; Kujawski, 2001a, 2001b) was proposed to overcome the difficulty the crack closure model met. Later, Kujawski (2001c, 2001d) further found that without using the crack closure concept, it is possible to explain the stress ratio effect even better than by using the concept. Vasudevan, Sadananda and co-workers (e.g. Vasudevan *et al.*, 2001) had proposed the two-parameter unified approach. According to the unified approach it is both K_{max} (σ_{max}) and ΔK ($\Delta\sigma$) which are responsible for the fatigue crack propagation. Through their efforts the unified approach has been demonstrated that all the recognized special phenomena can be explained. Now more and more people tend to believe that this unified approach might be a correct way forward (Noroozi *et al.*, 2005; Stoychev and Kujawski, 2005; Kujawski, 2005; Zhang *et al.*, 2005; Maymon, 2005a, 2005b).

The load sequence effect might be the most challenging problem for the

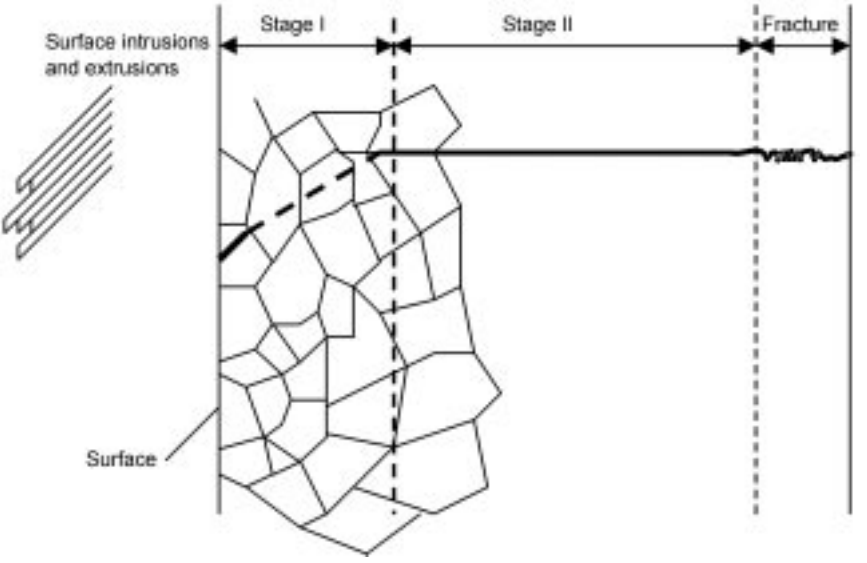
© 2008 Woodhead Publishing Limited

fatigue life prediction of engineering structures. Although the problem has been studied since the 1960s, the mechanism which causes the load sequence effect has not yet been understood (Skorupa, 1998, 1999). Generally speaking, three classes of mechanisms acting before, at or after the crack tip have been proposed in the literature. De Castro *et al.* (2005) have discussed extensively the three classes of mechanisms and found that 'plasticity-induced crack closure (behind the crack tip) cannot explain load sequence effects in various important problems and a damage accumulation model ahead of the crack tip based on ϵN cyclic properties can explain those effects in the absence of closure'. This point of view is similar to the two-parameter unified approach.

5.3 Current understanding of fatigue mechanisms

Fatigue cracks of metals usually initiate from the surface of a component, where fatigue damage initiates as shear cracks on crystallographic slip planes. The surface shows the slip planes as intrusions and extrusions. This is Stage I crack growth. After a transient period, Stage II crack growth takes place in a direction normal to the applied stress. Finally the crack becomes unstable and fracture occurs. Figure 5.1 shows a schematic representation of the two stages.

This two-stage process was first recognized by Forsyth (1969) and was one of the most important achievements in metal fatigue in the twentieth century (Miller, 1999). However, that division may be too rough for further discussion. So in some other sources, this process may be further divided. Schijve (1967)



5.1 Schematic representation of crack formation and growth in polycrystalline metals.

© 2008 Woodhead Publishing Limited

divided it into four phases: crack nucleation, microcrack growth, macrocrack growth and failure. Shang *et al.* (1998) divided it into five stages: (1) early cyclic formation and damage; (2) microcrack nucleation; (3) short crack propagation; (4) macrocrack propagation; and (5) final fracture. Miller (1987a, 1987b) divided the crack length into three regimes: microstructurally small crack, physically small crack, and long crack. A slightly different classification of small cracks has also been proposed by Ritchie (1986) as microstructurally small crack of critical microstructural dimension, e.g. grain size; physically small crack of the order of less than 1 mm; mechanically small crack of the order of plastic zone length (several millimeters); and chemically small crack of order up to 10 mm.

Based on these different divisions and applications in other papers, it is recommended in Cui (2002) that the total process of fatigue failure is divided into five stages: (1) crack nucleation ($a < a_m$); (2) microstructurally small crack propagation ($a_m < a \leq a_p$); (3) physically small crack propagation ($a_p < a \leq a_l$); (4) long crack propagation ($a_l < a \leq a_c$); and (5) final fracture, where a is the characteristic dimension of an equivalent crack in a component; a_m is the smallest crack length detectable by current technology, which is about 0.1 μm; a_p is the smallest crack length for physically small cracks, which is about 10 μm; a_l is the smallest crack length for long cracks, which is about 1 mm; and a_c is the critical crack length at which component fracture occurs. Obviously, these boundary divisions are subjective and depend on the ability of crack measuring systems. Traditionally, the processes before long crack propagation are named 'fatigue crack initiation' while long crack propagation is called 'fatigue crack propagation'. This division is also too rough and could not be expected to provide an accurate prediction of fatigue life. However, it may be worth pointing out here that depending on the initial crack length in a component, some of the early stages may be skipped for a practical problem. These five stages of fatigue process only exist in 'defect free' metal components.

Under the action of repeated loading, fatigue cracks can initiate in areas of stress concentration in a structure. Initial defects can form during fabrication and can conceivably remain undetected for a long time. Cracks may initiate from such defects, and propagate. In addition to propagation under repeated cyclic loading, cracks may also grow in an unstable way under monotonically increasing extreme loads, which can conceivably lead to catastrophic structural failure. This possibility is tempered by material ductility, and by the presence of reduced stress intensity regions that may serve as crack arresters (Paik *et al.*, 2006).

5.4 Fatigue life prediction methods

Since cracks can conceivably lead to catastrophic failure of a structure, it is essential to properly consider and establish relevant crack-tolerant design procedures for structures, in addition to implementation of close-up surveys and

© 2008 Woodhead Publishing Limited

maintenance strategies (Paik *et al.*, 2006). For reliability assessment of aging structures under extreme loads, it is often necessary to take into account a known (existing or assumed or anticipated) crack for the ultimate limit state analysis as a parameter of influence (Paik and Thayamballi, 2003). To make this possible, it is necessary to develop a time-dependent fatigue crack growth model which can predict crack damage in location and size as the ship ages.

Fatigue cracks propagate with time progressively in a ductile material. The time-variant cracking damage model is composed of the three separate models, namely: (a) crack initiation assessment or detection, (b) crack growth assessment, and (c) failure assessment. Crack initiation at a critical structural detail is typically predicted using cumulative fatigue damage (CFD) theories. Crack growth is often assessed by fracture mechanics based approaches, hereafter called fatigue crack propagation (FCP) approaches. In a FCP approach, a major task is to establish the relevant crack growth rate equations. The Paris–Erdogan equation (Eq. (5.1)) is the earliest and many other equations are available following later developments.

The main purpose of this section is to introduce various fatigue life prediction methods belonging to these two theories: CFD theory and FCP theory.

5.4.1 Cumulative fatigue damage (CFD) theories

Even up to today, cumulative fatigue damage analysis still plays a key role in life prediction of components and structures subjected to field load histories. Since the introduction of the damage accumulation concept by Palmgren (1924) and the 'linear damage rule' by Miner (1945), the treatment of cumulative fatigue damage (CFD) has received increasing attention. A comprehensive review on the development of cumulative fatigue damage theories has been conducted by Fatemi and Yang (1998) and Yang and Fatemi (1998).

Fundamentally speaking, fatigue damage is a result of material structural changes at the microscopic scale such as dislocations of the atomic structures. While bridging microscopic quantities and macroscopic experimental observations is still a long-term endeavor, it is reasonable to believe that microscopic parameters governing fatigue damage have an inherent relationship with the macroscopic stress and strain quantities based upon the continuum mechanics concepts. These macroscopic quantities can be used to account for crack nucleation and early growth. By choosing different macroscopic quantities such as stress, strain, energy density or combinations, different cumulative fatigue damage formulas are derived.

Stress-based approach (S–N curve approach)

The stress-based approach is the earliest but still the most frequently used approach for fatigue life prediction. In this approach, the fatigue life (number of

© 2008 Woodhead Publishing Limited

cycles N) is related to the applied stress range ($\Delta\sigma$ or S) or stress amplitude (σ_a). A plot of the fatigue life versus the true stress amplitude for a metal gives in general a curve of the Basquin form (Basquin, 1910):

$$\sigma_a = \frac{E \cdot \Delta\epsilon_e}{2} = \sigma'_f \cdot (2N)^b \qquad 5.2$$

where N is the number of cycles to failure, $2N$ is the number of load reversals to failure, σ'_f is the fatigue strength coefficient, and b is the fatigue strength exponent (the sign of b is negative).

In a component or structure, there are two types of stress concentration. One is due to the structural geometry change or discontinuity and the other is due to welding. Depending on how to account for the stress concentration effect, stress-based approaches can be further divided into the nominal stress approach, the hot-spot stress approach and the notch stress approach. Currently, the hot-spot stress approach seems to be the one most favored by ship classification societies (Wästberg *et al.*, 2006).

Traditional fatigue tests indicated a limit at about $N = 10^7$ cycles. If the applied stress range is lower than the limit, there will be no fatigue failure. However, recent giga-cycle fatigue tests performed on a cold rolled steel sheet ($E = 203\,\text{GPa}$, $\sigma_y = 225\,\text{MPa}$, $\sigma_u = 340\,\text{MPa}$, $\rho = 7.83\,\text{g/cm}^3$ and Hv = 95) (Wang *et al.*, 1999a), a high carbon chromium steel ($\sigma_u = 2316\,\text{MPa}$ and Hv = 750–795) (Sakai *et al.*, 1999) and an aluminum wrought alloy EN AW 6082 ($\sigma_y = 341\,\text{MPa}$, $\sigma_u = 356\,\text{MPa}$, elongation $\delta = 11.2\%$, reduction of area $\phi = 47.5\%$) (Berger *et al.*, 2006) showed that the fatigue limit does not appear until 10^9 cycles in the S–N curve or that the S–N curve tends to come down again in the long life region of $N > 10^7$ cycles. This poses questions on the existence of infinite fatigue life (Bathias, 1999). Marines *et al.* (2003) summarized the state of the art in this field and their conclusion is that the S–N curve in the giga-cycle regime must be determined in order to guarantee the real fatigue strength and safe life of mechanical components.

If a fatigue limit is assumed to exist, the relation expressed by Eq. (5.2) is only valid for the middle part. The stress amplitude is larger than the limit but the maximum stress should not exceed the ultimate tensile strength. A new function for the description of fatigue curves for both low and high fatigue regions, i.e. for the whole cycle region from tensile strength to fatigue limit, was proposed by Kohout and Vechet (1999). The function takes the following form:

$$\sigma(N) = \sigma_\infty \left(\frac{N + 10^7 \alpha\beta}{N + 10^7 \alpha} \right)^{-b} \qquad 5.3$$

where $$\alpha = \frac{\sigma_c^{-1/b} - \sigma_\infty^{-1/b}}{\sigma_u^{-1/b} - \sigma_c^{-1/b}}, \beta = \frac{\sigma_u^{-1/b}}{\sigma_\infty^{-1/b}}$$

© 2008 Woodhead Publishing Limited

where σ_u is the tensile strength, σ_∞ is the fatigue limit (both can be measured accurately), σ_c is the fatigue strength at 10^7 cycles, and $-b$ is the slope in the middle cycle region. σ_c and b can be determined by the least squares method.

Four parameters have to be determined for a complete S–N curve according to Eq. (5.3). In some practical situations, less information may be available. Wang *et al.* (1999b) proposed a simple and practical prediction method to estimate both the S–N curve and the crack growth rate curve using only the tensile strength.

In the high-cycle fatigue regime, Castillo and Fernandez-Canteli (2006) presented a similar general parametric lifetime model as Eq. (5.3) for predicting fatigue behavior at any stress level and amplitude. The problem of the design of the experimental laboratory test required for such a prediction is dealt with. The surprising and relevant result is that running two groups of tests for two different constant stress levels of σ_{max} or σ_{min} is sufficient to predict the whole collection of Wöhler fields for any possible stress level. However, some combinations of tests, such as one for a fixed value of σ_{max} and one for a fixed value of σ_{min}, are shown to be insufficient.

Generally, the basic fatigue behavior of materials and structures is determined by adopting constant amplitude loading resulting in various characteristic quantities and relationships such as S–N curves, cyclic stress–strain curves, fatigue crack growth rates, threshold values, etc. While constant amplitude loading is fully described by quite a few parameters (maximum/minimum or range/mean and number of load cycles), most structures experience in-service loading environments with variable amplitudes and mean loads. It is well established that fatigue response may be very sensitive to the specifics of the loading encountered.

Therefore, tests with realistic load sequences are often required in order to assess any susceptibility to that kind of phenomenon and to demonstrate the in-service integrity for given materials and structures. For this purpose standardized load–time histories (SLH) have been studied for 30 years since it has been recognized that the use of SLH provides a series of advantages – both for studies of a more generic nature and for practical applications. Heuler and Klätschke (2005) have presented an overview on SLH available. It details the principles applied for collection and analysis of appropriate load data, assessment of operating profiles and generation of the respective load spectra and sequences. The principles may also serve as guidelines for those cases where new load spectra and load–time histories have to be created, for example, for a given design problem.

Strain-based approach

In most practical cases of fatigue design, the critical location will be a notch in which plastic strains are imposed by surrounding elastic material. Thus, the

© 2008 Woodhead Publishing Limited

situation will be strain controlled with a total strain range composed of an elastic and a plastic part.

The plastic strain resistance is best described by the Coffin–Manson relationship (Coffin and Tavernelli, 1959; Manson and Hirschberg, 1964):

$$\frac{\Delta\epsilon_\rho}{2} = \epsilon'_{\mathrm{f}} \cdot (2N)^c \qquad 5.4$$

where ϵ'_{f} is the fatigue ductility coefficient and c is the fatigue ductility exponent – the sign of c is negative.

Manson and Hirschberg (1964) proposed that a metal's resistance to total strain cycling can be considered as a superposition of its elastic and plastic strain resistance. By combining Eqs (5.2) and (5.4),

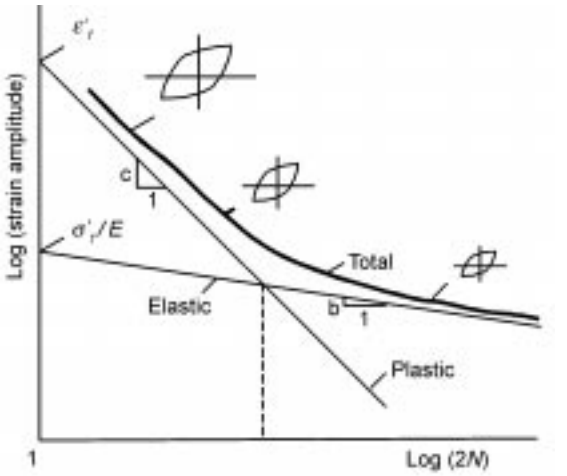
$$\frac{\Delta\epsilon_{\mathrm{T}}}{2} = \epsilon_{\mathrm{a}} = \frac{\Delta\epsilon_{\mathrm{e}}}{2} + \frac{\Delta\epsilon_{\mathrm{p}}}{2} = \frac{\sigma'_{\mathrm{f}}}{E}(2N)^b + \epsilon'_{\mathrm{f}} \cdot (2N)^c \qquad 5.5$$

The total strain life curve approaches the plastic strain life curve in the low cycle region and the stress life curve in the high cycle region as shown in Fig. 5.2.

For general low cycle and high cycle fatigue, the Coffin–Manson relationship, Eq. (5.5), has a strong curve-fitting ability but it needs to determine five material properties. Manson (1965) has simplified the equation even further with his method of universal slopes, where

$$\Delta\epsilon = 3.5\frac{S_{\mathrm{u}}}{E}N^{-0.1\epsilon} + \epsilon_{\mathrm{f}}^{0.6}N^{-0.6} \qquad 5.6$$

S_{u}, E and ϵ_{f} are all obtained from a monotonic tensile test. He assumed the two exponents are fixed for all materials and only S_{u}, E and ϵ_{f} control the fatigue behavior.



5.2 Representation of elastic, plastic and total strain resistance to fatigue loading.

© 2008 Woodhead Publishing Limited

Later, the above equation was further modified to the following expression (Muralidharan and Manson, 1988):

$$\Delta\epsilon = 0.0266D^{0.115}(S_u/E)^{-0.53}N_f^{-0.56} + 1.17(S_u/E)^{0.832}N_f^{-0.09} \qquad 5.7$$

where S_u is the ultimate strength of the metal, D is the ductility of the metal, E is the modulus of elasticity and N_f is the fatigue life. Good correlation between the fatigue life predicted by this equation and the fatigue test data has been found (Muralidharan and Manson, 1988).

Based on a detailed correlation study between monotonic tensile data and constant amplitude strain-controlled fatigue properties, the following simple strain-life formula is proposed by Roessle and Fatemi (2000):

$$\frac{\Delta\epsilon}{2} = \frac{4.25(HB) + 225}{E}(2N_f)^{-0.09} + \frac{0.32(HB)^2 - 487(HB) + 191\ 000}{E}(2N_f)^{-0.56} \qquad 5.8$$

This approximation uses only hardness and modulus of elasticity as inputs for strain-life approximation, both of which are either commonly available, or easily measurable.

The inclusion of mean stress or mean strain effects in fatigue life prediction methods involving strain-life data is very complex. One method is to replace σ'_f with $\sigma'_f - \sigma_m$ in Eq. (5.5), where σ_m is the mean stress such that

$$\frac{\Delta\epsilon}{2} = \frac{(\sigma'_f - \sigma_m)(2N)^b}{E} + \epsilon'_f(2N)^c \qquad 5.9$$

Here σ_m is taken positive for tensile values and negative for compressive values. Another equation suggested by Smith *et al.* (1970), based on strain-life test data at fracture obtained with various mean stresses, is

$$\sigma_{max}\epsilon_a E = (\sigma'_f)^2(2N)^{2b} + \sigma'_f\epsilon'_f E(2N)^{b+c} \qquad 5.10$$

where $\sigma_{max} = \sigma_m + \sigma_a$ and ϵ_a is the alternating strain. If σ_{max} is zero, Eq. (5.10) predicts infinite life, which implies that tension must be present for fatigue fractures to occur. Both Eqs (5.9) and (5.10) have been used to handle the mean stress effect.

In Ong (1993a), fatigue lives were calculated for 49 steels using published values of σ'_f, ϵ'_f, b and c. These lives were compared with lives calculated using some of the approximation methods described above. These include the original and modified versions of the Four-Point Correlation method, the original Universal Slopes method, and the Mitchell method. The lives covered a range from 10 to 10^7 reversals. The steels covered values of UTS from 345 MPa to 2585 MPa, and Brinell hardness values from 80 to 660. They included the steels SAE1005, SAE1015 and SAE1045.

In all cases correlation between the 'experimental' and the 'estimated' lives

© 2008 Woodhead Publishing Limited

was poor. The modified Four-Point Correlation method was found to be slightly better than the original Universal Slopes method and to be the best within the methods studied.

In another study conducted by Park and Song (1995), six such methods were evaluated and compared. These consisted of the Universal Slopes and Four-Point Correlation methods by Manson (1965), the Modified Universal Slopes method by Muralidharan and Manson (1988), the Uniform Material method by Baumel and Seeger (1990), the Modified Four-Point Correlation method by Ong (1993b), and the method proposed by Mitchell *et al.* (1977). A total of 138 materials were used in the study, including unalloyed steels, low-alloy steels, high-alloy steels, aluminum alloys and titanium alloys, with low-alloy steels providing the most data. Amongst the correlations compared, those proposed by Muralidharan and Manson (1988), Baumel and Seeger (1990) and Ong (1993b) yielded good predictions according to Park and Song (1995). They concluded that the Modified Universal Slopes method provided the best correlation.

In the study carried out by Roessle and Fatemi (2000), they also compared their simple formula which uses only hardness and modulus of elasticity for estimation of the strain-life curve with the Modified Universal Slopes method and found their simple formula resulted in somewhat better and more conservative predictions over the entire fatigue life regime. A similar study was carried out by Lee and Song (2006). They found that the (direct) hardness method proposed by Roessle and Fatemi (2000) provides excellent estimation results for steels, but the indirect hardness methods utilizing the ultimate tensile strength predicted from hardness were proposed by them and successfully applied to estimate fatigue properties for aluminum alloys and titanium alloys. The medians method proposed by Meggiolaro and Castro (2004) has been found to provide the best estimation results for aluminum alloys. Based on the results obtained, some guidelines are provided for estimating fatigue properties from simple tensile data or hardness. In addition, a new relationship of ultimate tensile strength versus hardness is proposed for titanium alloys.

Most of the existing methods for estimating ϵ–N parameters are based on a relatively limited amount of experimental data. In addition, sound statistical evaluation of the popular rules of thumb used in practice to estimate fatigue properties is scarce, if available at all. Meggiolaro and Castro (2004) presented an extensive statistical evaluation of the existing Coffin–Manson parameter estimates based on monotonic tensile and uniaxial fatigue properties of 845 different metals, including 724 steels, 81 aluminum alloys, and 15 titanium alloys. The studied Coffin–Manson estimates include the methods proposed by Muralidharan and Manson, Baumel and Seeger, Roessle and Fatemi, Mitchell, Ong, Morrow, and Raske, as well as Manson's universal slope and four-point correlation methods. From the collected data, it is shown that all correlations between the fatigue ductility coefficient ϵ'_f and the monotonic tensile properties are very poor, and that it is statistically sounder to estimate ϵ'_f based on constant

© 2008 Woodhead Publishing Limited

values for each alloy family. Based on this result, a new estimation method which uses the medians of the individual parameters of the 845 materials is proposed.

Energy-based approach

A historical description of the energy-based approaches is given by Fatemi and Yang (1998). For using this type of failure criteria, it was realized that an energy-based damage parameter can unify the damage caused by different types of loading such as thermal cycling, creep and fatigue. In conjunction with Glinka's rule (Glinka, 1988), it is possible to analyze the damage accumulation of a notched specimen or components with the energy approach. Energy-based damage models can also include mean stress and multiaxial loads, since multiaxial fatigue parameters based on strain energy have been developed.

Recently, Pan *et al.* (1999) proposed the following fatigue strain energy density parameter for the critical plane to predict the fatigue life of various materials under multiaxial loading:

$$W^* = \frac{\Delta\sigma_{12}}{2}\frac{\Delta\gamma_{12}}{2} + k_1 k_2 \frac{\Delta\epsilon_{22}}{2}\frac{\Delta\sigma_{22}}{2} \qquad 5.11$$

where $\Delta\sigma_{12}$ and $\Delta\sigma_{22}$ are the shear and normal stress ranges in the critical plane, $\Delta\gamma_{12}$ and $\Delta\epsilon_{22}$ are the shear and normal strain ranges in the critical plane, and k_1 and k_2 are two weight constants for strain and stress amplitudes which are defined as follows:

$$k_1 = \frac{\gamma'_{\mathrm{f}}}{\epsilon'_{\mathrm{f}}}, \quad k_2 = \frac{\sigma'_{\mathrm{f}}}{\tau'_{\mathrm{f}}} \qquad 5.12$$

where σ'_{f} is the uniaxial fatigue strength coefficient, ϵ'_{f} is the uniaxial fatigue ductility coefficient, τ'_{f} is the torsional fatigue strength coefficient, and γ'_{f} is the torsional fatigue ductility coefficient.

By using the concept of volume influencing fatigue crack initiation proposed by Palin-Luc and Lasserre with an energy-based approach, a new criterion is presented by Banvillet *et al.* (2003). Based on the strain-work density given to the material, this proposal is usable whatever the constant amplitude loading: in-phase and out-of-phase combined loadings, with or without mean stress. Its predictions are compared both with a total of 38 experiments on four materials (a mild steel, two high-strength steels and a spheroidal graphite cast iron) and with the predictions of local criteria. The comparison shows that the predictions of the volumetric proposal are very good and less scattered than those of the local approaches, especially for loadings with mean stresses or under non-proportional loadings.

Gasiak and Pawliczek (2003) applied an energy model for fatigue life prediction of construction steels under bending, torsion and synchronous bending

© 2008 Woodhead Publishing Limited

and torsion, and good agreement between the calculated and experimental results was obtained.

An energy parameter accounting for normal and shear deformation was used by Lee *et al.* (2003) to predict fatigue lives under variable amplitude multiaxial loading. Fatigue damage was computed as a function of orientation of the plane, and the maximum damage plane was considered as the critical plane. The linear damage rule was employed with rainflow cycle counting either on the shear or on the normal strain history depending on which gives more damage when evaluated individually. The method yields fatigue life correlations comparable to those by existing methods for materials failing in shear mode (S45C, SNCM439, SNCM630). However, a noticeable improvement is found for stainless steel 304 that exhibits a mixed normal and shear fracture behavior.

On the basis of the analysis of energy of an elastic–plastic body subjected to monotonic and cyclic loading, a physical relationship between Neuber's rule and the equivalent strain energy density (ESED) method is found by Ye *et al.* (2004). It is shown that Neuber's rule is actually a particular case of the ESED method, namely when the dissipation of the plastic strain energy at the notch root is neglected in the ESED method. The reason for the overestimation of the local strains using Neuber's rule is thus explained essentially, and the physical meaning of the ESED method in both monotonic and cyclic forms is further defined. In terms of the real physical behavior occurring at the notch root during cyclic plastic deformation, a modified version of the ESED method, in which only the heat energy is considered as a dissipation and the stored energy is regarded as a contribution to local stress and strain ranges, has been developed by Ye *et al.* (2004). It is shown that, for the case of cyclic loading, the modified ESED method further improves the accuracy of the original ESED method in prediction of the nonlinear stress/strain behavior of notches. It is also shown that the relation can easily be used for a simulation of the local strain–stress history near a notch root.

Jahed and Varvani-Farahani (2006) addressed the problem of using an energy-based parameter to evaluate the fatigue life of metallic components subjected to multiaxial loading conditions. Cyclic strain–life data and corresponding Coffin–Manson coefficients for both normal and shear strain lives were first defined. Energy–fatigue life curves were then generated from strain–fatigue life properties. The upper and lower limits of life are estimated using the proposed life equations. The upper life limit is obtained by assuming that the dominant cracking mechanism is Case A and the lower life limit is obtained by assuming that the dominant cracking mechanism is Case B. The proposed method was developed based on physical evidence of crack initiation and growth as well as the amount of dissipated energy over life cycles. The fatigue life data fall between the upper and the lower limits, resulting in a promising life prediction. The proposed method has been used to evaluate the fatigue life of various metallic materials of SAE 1045, AISI 304, Inc 718 and Haynes 188

© 2008 Woodhead Publishing Limited

reported in the literature. Results of fatigue life predictions were found to be in good agreement with experimental life data.

Continuum damage mechanics (CDM) approaches

Continuum damage mechanics (CDM) is a relatively new subject in engineering mechanics and deals with the mechanical behavior of a deteriorating medium at the continuum scale. The general concepts and fundamental aspects of this subject can be found in Kachanov (1986). Chaboche and Lesne (1988) were the first to apply CDM to fatigue life prediction. For the one-dimensional case, Kachanov postulated that fatigue damage evolution per cycle can be generalized by a function of the load condition and damage state. By measuring the changes in tensile load-carrying capacity and using the effective stress concept, he formulated a nonlinear damage evolution equation as:

$$D = 1 - [1 - r^{1/(1-\alpha)}]^{1/(1+\beta)} \qquad 5.13$$

where β is a material constant, α is a function of the stress state and r is the damage state. This damage model is highly nonlinear in damage evolution and is able to account for the mean stress effect. It is, therefore, called a nonlinear continuous damage (NLCD) model. The main features, advantages and some deficiencies of the NLCD model are summarized by Chaboche and Lesne (1988). Based on the CDM concept, many other forms of fatigue damage equations have been developed. More information can be found in Fatemi and Yang (1998). Basically, all these CDM-based approaches are very similar to the Chaboche NLCD model in both form and nature. The main differences lie in the number and the characteristics of the parameters used in the model, in the requirements for additional experiments, and in their applicability.

Dattoma *et al.* (2006) presented a nonlinear continuum damage mechanics model based on the general thermodynamic framework developed by Lemaitre and Chaboche (1990). The proposed model has been formulated to take into account the material damage evolution at different load levels and it allows the effect of the loading sequence to be included; by means of a recurrence formula derived for multilevel loading, complex load sequences can be considered. The fatigue test data for a hardened and tempered steel have been used to verify the model proposed and the results show good agreement in predicting fatigue life under complex load sequences.

The CDM models were mainly developed for uniaxial fatigue loading. Some difficulties arise when these models are extended to multiaxial loading. Due to the complexity of non-proportional multiaxial fatigue problems, a three-dimensional anisotropic CDM model does not yet exist. Great efforts are still needed to obtain an appropriate generalized prediction model for cumulative fatigue damage under multiaxial loading.

© 2008 Woodhead Publishing Limited

Memon *et al.* (2002) discussed the prediction of fatigue lives for 3-D problems in the elastoplastic range with variable load amplitude. The effect of loading sequence on the fatigue life of a structure member and the validity of Miner's rule are studied. The computational method is derived according to damage mechanics, theory of plasticity and finite element analysis (FEA). A two-block cyclic loading is considered with high–low and low–high load sequences. To consider the effect of the high stress level beyond the yielding point of the material in one load block, deformation theory and the iteration method are applied to the stress analysis of the first load cycle. The damage evolution under given stress and damage field for each block loading is determined by a damage evolution equation. Furthermore, an additional loading method is introduced to perform the stress analysis with a given damage field to avoid the reassembling of the stiffness matrix of the structure member. In this research, the damage increment at a critical element is considered as the step length instead of the load cycle increment.

Summary

For many years, design engineers have used the Palmgren–Miner law, the linear damage rule (LDR), and its modifications to predict fatigue life of components in the case of variable loading (Dattoma *et al.*, 2006). This method is based on the assumption of constant work absorption per cycle independent of the loading levels. The main deficiencies with LDR are the load-level independence character, the lack of damage contribution for stress below the fatigue limit, and the lack of load interaction accountability; this can produce a discrepancy of up to an order of magnitude between the predicted and the experimental life and this calculation may be non-conservative. Many researchers have tried to modify Miner's rule, but, due to its intrinsic deficiencies, no matter which version is used, life prediction based on this rule is often unsatisfactory (Fatemi and Yang, 1998).

In summary, no matter what quantities are used, fatigue criteria based on cumulative fatigue damage (CFD) theory suffer from another significant deficiency in addition to the above. That is, they have not consistently defined whether life to failure is the life to a small detectable crack, the life to a certain percentage decrease in load amplitude, or the life to fracture. Differences in fatigue life depending on these three criteria may be small or appreciable. More accurately, the following factors will affect the fatigue life:

- Quality of material processing (size and distribution of inclusions, voids, etc.)
- Procedure of material processing (annealed, quenched, tempered, etc.)
- Procedure of specimen manufacture (specimen shape, machining method)
- Quality of specimen manufacture (scratch, surface condition)
- Material properties (yield strength, ultimate strength, strain at failure, σ–ϵ curve)

© 2008 Woodhead Publishing Limited

- Geometry (length, width, thickness, diameter, transition radius, constraint effect)
- Stress state (uniaxial, multiaxial, stress ratio, mean stress)
- Effect of environment (temperature, corrosive environment).

Accurate prediction of fatigue life must take all these factors into account. For example, the effect of different surface conditions on the fatigue properties of cyclically loaded bending specimens of the case-hardened steel SAE 5115 was investigated by Laue *et al.* (2006). On the basis of a well-defined adjustment of different surface conditions, the effect of internal oxidation, surface roughness and residual stresses on fatigue crack initiation and growth were assessed. The effect of different parameters on the endurance limit has been quantified by the application of a fracture mechanics and a weakest-link approach. The result of fatigue testing was that internal oxidation has a detrimental influence on the endurance limit, which becomes stronger when the surface roughness is raised. Microhardness measurements within the oxidized layer showed a strong decrease of hardness due to the oxidation of alloying elements. The removal of the damaged zone results in an increase of the endurance limit, although the newly generated surface is more sensitive against surface roughness due to its higher hardness. In the case of the electrolytically polished variant it became apparent that it is very difficult to examine the influence of a single parameter on the endurance limit. The removal of the oxidized layer resulted in a modification of the surface hardness, surface roughness and residual stresses all at the same time. Shot peening of carburized specimens resulted in an increase of the endurance limit due to the generation of a pronounced maximum of compressive residual stresses. An explanation for this was found by the observation of small fatigue cracks arresting in front of the maximum of compressive residual stresses. The experimental results suggested the use of a fracture mechanics approach for the fatigue of case-hardened steels. If the internal oxidation is taken as the initial crack for fatigue crack growth and the residual stress state at the crack tip is taken into consideration as well, one can calculate the endurance limit of case-hardened steels. The calculations contributed to a deeper insight into the complex interaction between the parameters governing the fatigue process.

Many critical mechanical components experience multiaxial cyclic loading during their service life. In recent decades, numerous attempts to develop multiaxial fatigue damage modeling have been reported. There are two main causes of the multiaxial fatigue problem of engineering materials. In isotropic materials, the multiaxial stress within the material is due to the complex applied loading history. In anisotropic materials, a multiaxial stress state is obtained even if the applied loading is uniaxial. Different from the uniaxial fatigue problem, the multiaxial fatigue problem is more complex due to the complex stress states, loading histories and possible anisotropy of the material. A unified

© 2008 Woodhead Publishing Limited

multiaxial fatigue damage model based on a characteristic plane approach is proposed by Liu and Mahadevan (2007), integrating both isotropic and anisotropic materials into one framework. Compared with most available critical plane-based models for the multiaxial fatigue problem, the physical basis of the characteristic plane does not rely on the observations of the fatigue crack in the proposed model. The cracking information is not required for multiaxial fatigue analysis and the proposed model can automatically adapt for very different materials experiencing different failure modes. The effect of the mean normal stress is also included in the proposed model. The results of the proposed fatigue life prediction model are validated using experimental results of metals as well as unidirectional and multidirectional composite laminates.

Up to now, no CFD models are available which could consider all these influencing factors. A consequence of this is that fatigue data are subjected to large scatter. However, the fuzzy definition of fatigue failure in CFD theory can be overcome through a fracture mechanics approach. Fatigue crack propagation (FCP) theory, introduced in the next section, could eliminate this deficiency.

5.4.2 Fatigue crack propagation (FCP) theories

Long crack growth

The earliest theory for predicting the fatigue crack propagation length is the linear elastic fracture mechanics (LEFM) approach. The LEFM approach was first introduced by Paris and co-workers (1961) who equated fatigue crack growth rate to the cyclic elastic stress intensity factor range at the tip of a long crack subjected to a low value of cyclic stress, as in Eq. (5.1). Later, people found that the crack growth rate curve is not linear for all the ranges of ΔK. The general crack growth rates for Mode I cracks in metals are as shown in Fig. 5.3.

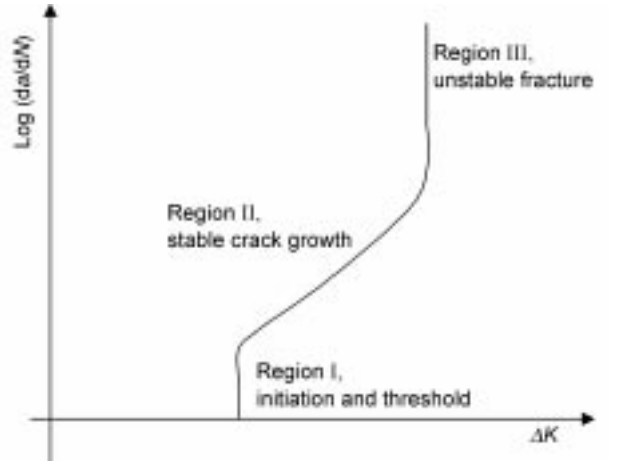
The sigmoidal shape of the crack growth curve in Fig. 5.3 suggests a subdivision into three regions. In region I, the crack growth rate goes asymptotically to zero as ΔK approaches a threshold value $\Delta K_{\text{th.}}$ This means that for stress intensities below ΔK_{th}, there is no crack growth, i.e. there is a fatigue limit.

The crack growth relation in the threshold region has been proposed by Donahue *et al.* (1972) as

$$\frac{\mathrm{d}a}{\mathrm{d}N} = C \cdot (\Delta K - \Delta K_{\text{th}})^m \qquad 5.14$$

Region II crack growth follows a power law, the so-called Paris–Erdogan crack growth law (Paris and Erdogan, 1963) as given in Eq. (5.1). Region III crack growth exhibits a rapidly increasing growth rate towards 'infinity', i.e. ductile tearing and/or brittle fracture. This has led to the relation proposed by Forman *et al.* (1967):

© 2008 Woodhead Publishing Limited



5.3 Crack growth rate curve showing the three regions.

$$\frac{\mathrm{d}a}{\mathrm{d}N} = \frac{C(\Delta K)^m}{(1-R)K_c - \Delta K} \tag{5.15}$$

where K_c is the fracture toughness of the material.

Relations combining the departures from power law behavior at high and low ΔK values also exist (Kanninen and Popelar, 1985; Carpinteri, 1994). The most representative might be the following one, proposed by McEvily and Groeger (1977):

$$\frac{\mathrm{d}a}{\mathrm{d}N} = A(\Delta K - \Delta K_{th})^2\left(1 + \frac{\Delta K}{K_c - K_{max}}\right) \tag{5.16}$$

In order to explain the effects of the load ratio ($R = K_{min}/K_{max}$) on fatigue crack growth, Elber (1970) introduced the concepts of crack closure and the effective cyclic stress intensity factor ΔK_{eff} as the dominant driving force for fatigue:

$$\Delta K_{eff} = K_{max} - K_{op} \tag{5.17}$$

where K_{max} is the stress intensity calculated for the maximum load, and K_{op} is the stress intensity calculated for the crack opening load. This concept was highly appraised in the 1980s and 1990s but now it is subjected to some challenge (e.g. Hertzberg *et al.*, 1988). In particular, many people have agreed that the physical effects of crack closure have been greatly overestimated in the past (e.g. Vasudevan *et al.*, 1994). A partial crack closure model (Donald and Paris, 1999; Kujawski, 2001a, 2001b) was proposed to overcome the difficulty the crack closure model met. The modified effective stress intensity factor range is defined as (Kujawski, 2001b):

$$\Delta K_{effM} = K_{max} - K_{op}\left[1 + \left(\frac{2}{\pi} - 1\right)g\right] \tag{5.18}$$

© 2008 Woodhead Publishing Limited

where $g = \exp\left[-\left(\frac{K_{\max}}{K_{\max TH}} - 1\right)\right]$

and $K_{\max TH}$ is the maximum stress intensity factor (SIF) at threshold for a given R-ratio.

Later, Kujawski (2001c, 2001d) further found that without using the crack closure concept, it is possible to explain the stress ratio effect even better than by using the concept. He defined the following parameter as the fatigue crack driving force:

$$\Delta K^* = (K_{\max})^{\alpha}(\Delta K^+)^{1-\alpha} \tag{5.19}$$

where ΔK^+ is the positive part of the applied SIF range. Using this parameter, the threshold value can be expressed as

$$\Delta K^*_{th} = \begin{cases} \Delta K^*_{th0}(1-R)^{\alpha} & \text{for } R > 0 \\ \Delta K^*_{th0}(1-R) & \text{for } R \leq 0 \end{cases} \tag{5.20}$$

where ΔK^*_{th0} is the threshold value corresponding to $R = 0$.

Sadananda and Vasudevan (2003) criticized the FCP methods based on the crack closure concept. They pointed out that the drawbacks in the current fatigue life prediction methods stem from several sources: (1) the assumption of plasticity-induced crack closure, (2) the lack of terms in the model that relates to the environmental effects and slip deformation behavior, and (3) several adjustable parameters needed to fit the observed data. In order to overcome these drawbacks and develop a more reliable fatigue life prediction model, Vasudevan, Sadananda and co-workers have proposed a two-parameter unified approach. This will be presented on pages 129–132.

Physically small crack growth

It is well agreed that for physically small crack growth, elastic–plastic fracture mechanics (EPFM) must be employed. The EPFM approach was first introduced by Tomkins in 1968 (Miller, 1999) who equated da/dN to crack tip decohesion (from knowledge of the cyclic stress–strain curve) and thence to the bulk plastic strain field as occurs, for example, under high strain fatigue, thus:

$$\frac{da}{dN} = B\left(\Delta\epsilon_p\sqrt{\pi a}\right)^m - \Xi \tag{5.21}$$

where Ξ is the threshold condition in this crack regime.

Others established the relation between the rate of fatigue crack growth, da/dN, and some functions of the range of the stress intensity factor ΔK by modifying the crack growth relation for long cracks. In order for the constitutive relationship to be able to explain the six phenomena of anomalous fatigue crack growth, fatigue crack growth under compression–compression cycling, the delay due to an overload, the two-step cyclic loading, the effect of mean stress on

© 2008 Woodhead Publishing Limited

fatigue life, and the small fatigue crack growth, McEvily *et al.* (1999) and McEvily and Ishihara (2001) proposed the following modified constitutive relationship for fatigue crack growth:

$$\frac{\mathrm{d}a}{\mathrm{d}N} = A\left\{\left[\sqrt{\pi\gamma_{\mathrm{e}}\left(\sec\frac{\pi}{2}\cdot\frac{\sigma_{\max}}{\sigma_{\mathrm{y}}}+1\right)}+Y\sqrt{\frac{\pi}{2}a\left(\sec\frac{\pi}{2}\frac{\sigma_{\max}}{\sigma_{\mathrm{y}}}+1\right)}\right]\Delta\sigma - \left(1-\mathrm{e}^{-ka}\right)\left(K_{\mathrm{op\ max}}-K_{\min}\right)-\Delta K_{\mathrm{effth}}\right\}^2 \tag{5.22}$$

where

$$\gamma_{\mathrm{e}} = \left(\frac{\Delta K_{\mathrm{effth}}}{\Delta\sigma_{\mathrm{EL}}}\right)^2\cdot\frac{1}{\pi\left(\sec\frac{\pi}{2}\cdot\frac{\sigma_{\max}}{\sigma_{\mathrm{y}}}+1\right)} \tag{5.23}$$

A is a material and environmentally sensitive constant, $(\mathrm{MPa})^{-2}$; $\Delta K_{\mathrm{effth}}$ is the effective range of the stress intensity factor at the threshold level, $\mathrm{MPa}\sqrt{\mathrm{m}}$; $K_{\mathrm{op\,max}}$ is the maximum stress intensity factor at the opening level for a macroscopic crack, $\mathrm{MPa}\sqrt{\mathrm{m}}$; $K_{\min}$ is the minimum stress intensity factor applied, $\mathrm{MPa}\sqrt{\mathrm{m}}$; k is a material constant which reflects the rate of crack closure development with crack advance; Y is a geometrical factor; a is the actual crack length, m; σ_{y} is the yield strength of the material, MPa; $\Delta\sigma$ is the stress range applied, MPa; $\sigma_{\max}$ is the maximum stress applied, MPa; and $\Delta\sigma_{\mathrm{EL}}$ is the stress range of the endurance limit, MPa. Comparison with some experimental data showed that this constitutive relationship is able to explain the six phenomena concerned.

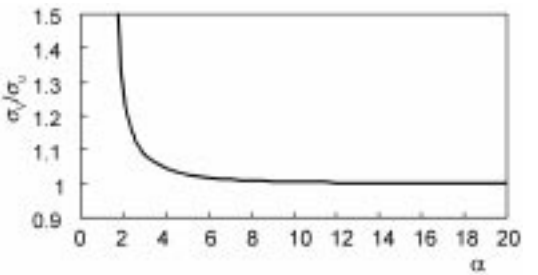
It is well known that a general crack growth rate curve exhibits a sigmoidal shape from the near-threshold region to unstable fracture (Kanninen and Popelar, 1985). Equation (5.22) is certainly only for the near-threshold region. For a cracked body, the unstable fracture condition is often defined by the condition (Kanninen and Popelar, 1985):

$$K_{\max} = K_{\mathrm{c}} \tag{5.24}$$

where K_{c} is the fracture toughness of the material. Use of Eq. (5.22) to define $K_{\max}$ implies that the stress will never exceed the yield stress σ_{y} even at static failure for 'uncracked' plain specimens. In order to make Eq. (5.22) also valid for uncracked plain specimens, an empirical approach is adopted by replacing the yield strength σ_{y} by another 'virtual strength' (σ_{V}) (Cui and Huang, 2003). The 'virtual strength' (σ_{V}) is defined by the condition that the maximum stress of the uncracked (i.e. $a = r_{\mathrm{e}}$) plain specimen is equal to the ultimate strength (σ_{u}) of the material in the unstable fracture condition. Based on this definition, the virtual strength can be determined from the following equation:

$$\left(1+\frac{Y(r_{\mathrm{e}})}{\sqrt{2}}\right)\sqrt{\pi r_{\mathrm{e}}\left(\sec\frac{\pi}{2}\frac{\sigma_{\mathrm{u}}}{\sigma_{\mathrm{V}}}+1\right)}\sigma_{\mathrm{u}} = K_{\mathrm{c}} \tag{5.25}$$

© 2008 Woodhead Publishing Limited



5.4 Variation of virtual strength versus parameter α.

The solution of Eq. (5.25) is

$$\frac{\sigma_V}{\sigma_u} = \frac{\pi}{2} \cdot \frac{1}{\cos^{-1}\left(\frac{1}{\alpha^2 - 1}\right)}, \quad \alpha = \frac{K_c}{\sigma_u \sqrt{\pi r_e}\left(1 + \frac{Y(r_e)}{\sqrt{2}}\right)} > \sqrt{2} \qquad 5.26$$

From Eq. (5.26) it can be seen that the virtual strength of the material will depend on the crack type (Y) together with three material parameters σ_u, K_c and r_e. Four of them form a new parameter α. Figure 5.4 shows the influence of the parameter α on the ratio of virtual strength over ultimate strength. As α increases, the ratio approaches unity.

The virtual strength of the material may represent the material strength at the limit of the 'perfect' condition ($r_e = 0$) while the actual ultimate strength of the material (σ_u) represents the strength under the condition that the defect size is equal to the inherent flaw length ($r_e > 0$), a minimum crack size for engineering metals. What this means is that the virtual strength is only an ideal value when all the inherent flaws have been removed. However, for any existing engineering metal, the inherent flaws exist and its maximum strength is the ultimate strength, which will be lower than its virtual strength. The essence of this modification is a small change in the defined length of the plastic zone size. The new modified crack length is expressed as

$$a = \frac{a_{act}}{2}\left(\sec\frac{\pi}{2}\frac{\sigma}{\sigma_V} + 1\right) \qquad 5.27$$

which is slightly shorter than the Dugdale expression using σ_y instead of σ_V. If σ is less than $0.9\sigma_y$, the effect of modification is small, but when σ approaches σ_y, the Dugdale expression will give a crack length of infinity, which is also not very meaningful. The new empirical formula of Eq. (5.27) will give a finite value of the crack length and this may be more reasonable. Obviously this conclusion needs physical confirmation, although measurement of the plastic zone at high stress levels is a difficult task.

When a body contains a crack, its ultimate strength (σ_{ua}) will be lower than the ultimate strength of the material (σ_u) and this ultimate strength can be determined from the following equation:

© 2008 Woodhead Publishing Limited

$$\sqrt{\pi r_e\left(\sec\frac{\pi}{2}\frac{\sigma_{ua}}{\sigma_V}+1\right)}\left(1+Y(a)\sqrt{\frac{a}{2r_e}}\right)\sigma_{ua}=K_c \tag{5.28}$$

It can be seen that σ_{ua} will depend on K_c and a together with the crack type $Y(a)$. As crack length increases, the ultimate strength will decrease.

Thus the general constitutive relation for fatigue crack growth of metals can be expressed as follows (Cui and Huang, 2003):

$$\frac{da}{dN}=\frac{AM^2}{1-\left(\frac{K_{max}}{K_c}\right)^n} \tag{5.29}$$

where

$$M=\sqrt{\pi\gamma_e\left(\sec\frac{\pi}{2}\frac{\sigma_{max}}{\sigma_V}+1\right)}\left(1+Y\sqrt{\frac{a}{2r_e}}\right)\sigma_{max}(1-R)$$
$$-(1-e^{-ka})(K_{op\,max}-RK_{max})-\Delta K_{effth} \tag{5.30}$$

and

$$K_{max}=\sqrt{\pi r_e\left(\sec\frac{\pi}{2}\frac{\sigma_{max}}{\sigma_V}+1\right)}\left(1+Y(a)\sqrt{\frac{a}{2r_e}}\right)\sigma_{max} \tag{5.31}$$

As mentioned before, both ΔK_{effth} and $K_{op\,max}$ are functions of the stress ratio R. Let us use the following general format used in describing the threshold effective stress range to describe these two quantities:

$$\Delta K_{effth}=\Delta K_{effth0}(1-R)^{\gamma} \tag{5.32}$$

$$K_{op\,max}=K_{op\,max0}(1-R)^{\gamma} \tag{5.33}$$

where $K_{op\,max0}$ and ΔK_{effth0} are corresponding values at zero stress ratio. Different exponents γ_1 and γ_2 could be used, but for simplicity they are assumed to be the same following the assumption implicitly made by McEvily and co-workers that these two quantities are close to each other. According to Schijve (1979), γ is between 0.5 and 1.0. γ can also take different values for positive R and negative R (Kujawski, 2001d). Thus, the independent model parameters for this general constitutive relation are A, n, σ_u, r_e, K_c, ΔK_{effth0}, $K_{op\,max0}$, k and γ, a total of nine parameters.

From the condition of $M=0$, the fatigue limit ($\sigma_{\infty a}$) in terms of the maximum stress for a body containing a crack can be determined from the following equation:

$$\sqrt{\pi\gamma_e\left(\sec\frac{\pi}{2}\frac{\sigma_{\infty a}}{\sigma_y}+1\right)}\left(1+Y(a)\sqrt{\frac{a}{2r_e}}\right)\sigma_{\infty a}$$
$$=\frac{[(1-e^{-ka})K_{op\,max0}+\Delta K_{effth0}](1-R)^{\gamma}}{1-Re^{-ka}} \tag{5.34}$$

© 2008 Woodhead Publishing Limited

$\sigma_{\infty a}$ is a function of σ_u, r_e, K_c, ΔK_{effth0}, $K_{op\,max0}$, k, γ, a and R. If the crack length a is set to be equal to r_e, then this equation will give the fatigue limit of the material (σ_∞), i.e. the plain specimen fatigue limit. As crack length increases, the fatigue limit under a given crack length will decrease.

The extended constitutive relation can be applied from low cycle fatigue (LCF) down to static failure and from high cycle fatigue (HCF) up to the fatigue limit, and from 'crack-free' plain specimens to cracked bodies. For a body containing an existing initial crack of length a_0, the maximum fatigue stress has to be in the range between the fatigue limit ($\sigma_{\infty a}$) and the ultimate strength (σ_{ua}). If the stress is lower than the fatigue limit, the fatigue crack will not propagate. If the stress approaches the ultimate strength, static failure will occur. Therefore, a sigmoidal shape of the general crack growth rate curve also reflects a sigmoidal shape of an S–N curve as expressed by Eq. (5.2). This implies that if a threshold exists there is a fatigue limit.

For a given maximum stress between the fatigue limit and ultimate strength, Eq. (5.29) can also be used to find out the maximum crack length at failure, a_f. When a is smaller than a_f, the crack propagation is stable. The fatigue life for a constant amplitude test can be calculated from the following equation:

$$N_f = \int_{a_0}^{a_f} \frac{1 - \left(\frac{K_{max}}{K_c}\right)^n}{AM^2} da \qquad 5.35$$

Microstructurally small crack growth

Microstructural fracture mechanics (MFM) was proposed to handle crack propagation at the microcrack level. The MFM approach was first introduced by Hobson *et al.* (1986) and was followed by Navarro and de los Rios (1988). The crack growth law is expressed as

$$\frac{da}{dN} = C\Delta\gamma^\beta(d - a) \qquad 5.36$$

where d is a microstructural dimension. It should be noted that Eq. (5.36) indicates a zero crack speed when the crack depth, a, is equal to d, and that prior to this state the crack will continuously decelerate until it either stops or continues to propagate according to an overlapping continuum mechanics description.

Two-parameter unified approach for fatigue crack growth

The fundamental assumptions made in the 'unified approach' (Vasudevan *et al.*, 2001) are that: (1) the true material behavior is represented by the long crack growth properties, (2) fatigue damage must be described by two driving force

© 2008 Woodhead Publishing Limited

parameters ΔK and K_{max} instead of one, and (3) the deviations from the long crack growth behavior arise from the *internal stresses* present ahead of the crack tip which contribute to K_{max}. These internal stresses are responsible for the accelerated growth in the short crack, underload region and for decelerated growth during overloads.

Since there are two driving forces required to obtain fatigue crack growth, K_{max} and ΔK, there are two fatigue thresholds, $K_{max\,th}$ and ΔK_{th} corresponding to two driving forces. These are asymptotic values in the ΔK–K_{max} plot. Both must be satisfied simultaneously for fatigue crack growth to occur. The existence of dependence of ΔK_{th} on R is a trivial consequence of the existence of two thresholds. Extrinsic mechanisms (such as crack closure) therefore are not necessary to account for the dependence of ΔK_{th} on R. Crack growth is driven by total crack tip stresses, i.e., the superimposition of the externally applied stress and any internal stress that exists. Internal stresses exist due to, for example, defects, scratches, inclusions or other stress concentrators, residual stresses such as from welding or heat treatments, cold work, transformation-induced stresses, and plasticity, including overload plasticity. The basic effect of internal stress is to offset the total stress intensity at the crack tip relative to the externally applied stress, so that both K_{min} and K_{max} would generally be affected similarly. Consequently, the primary effects of internal stress manifest through K_{max} and not the ΔK parameter. Environmental effects manifest primarily in the K_{max} term. This is because the K_{max} driving force is what opens and increments the crack, therefore it is more sensitive to environmental modification of the material at the crack tip.

Physically, although both driving forces are essential, only one will be the controlling parameter for a given range of R. For example, at low R, K_{max} is the controlling force, and at high R, ΔK is the controlling force. Crack arrest occurs if either of the two forces falls below its respective threshold. The experimental validity for the existence of a K_{max} threshold, in addition to threshold ΔK, has been demonstrated for a variety of materials. A broad classification of material behavior has been presented (Sadananda and Vasudevan, 2003, 2004a).

The two-parameter unified approach was proposed by Vasudevan, Sadananda and co-workers and described in many papers (Vasudevan *et al.*, 1994, 2001, 2005; Sadananda and Vasudevan, 1997, 2003, 2004a, 2004b, 2005; Vasudevan and Sadananda, 1999, 2001; Sadananda *et al.*, 1999, 2001, 2003; Sadananda and Sreenivasan, 2001). Although many papers have been published that use the two-parameter unified approach to explain various special phenomena, there are no unified expressions for the two-parameter crack growth rate law.

In Vasudevan *et al.* (1994), the following general expression was given:

$$\frac{da}{dN} = f\left[\left(\Delta K - \Delta K^*_{th}\right), \left(K_{max} - K^*_{max\,th}\right)\right] \qquad 5.37$$

In Sadananda and Vasudevan (1997), the following specific expression was given:

© 2008 Woodhead Publishing Limited

$$\frac{da}{dN} = A\left(\Delta K - \Delta K_{th}^{*}\right)^{n}\left(K_{max} - K_{max\,th}^{*}\right)^{m} \tag{5.38}$$

Note that $K_{max\,th}^{*}$ and ΔK_{th}^{*} depend on da/dN, and the general expressions are:

$$K_{max\,th}^{*} = K_{max\,th0}\, f_1\left(\frac{da}{dN}\right), \quad \Delta K_{th}^{*} = \Delta K_{th0}\, f_2\left(\frac{da}{dN}\right) \tag{5.39}$$

This expression can only describe the behavior near the threshold region. Maymon (2005a) used it to study an aluminum 2024-T351 and the detailed values for the model parameters are given there.

In order to describe the sigmoidal shape of the crack growth rate curve, Bukkapatnam and Sadananda (2005) proposed the following expression:

$$\frac{da}{dN} = C_1 \Psi(\Delta K, K_{max}) \tag{5.40}$$

where

$$\Psi(\Delta K, K_{max}) = [s_0 - 2\gamma(\Delta K, \Delta K_0, K_{max})]K_{max}^{n}$$

and

$$\gamma(\Delta K, \Delta K_0, K_{max}) = \frac{e^{b(\Delta K_0 - \Delta K)^m}}{e^{b(\Delta K_0 - \Delta K)^m} + e^{b(\alpha_1 K_{max} + \alpha_2 \Delta K + \alpha_3 \Delta K_0)^m}}$$

Here, b determines the flatness of the cusp of the sigmoidal function, m is a real number between 0 and 1, n is a real number between 1 and 5, ΔK_0 is the initial value of ΔK, s_0 is related to the value of da/dN at which the curve reaches the cusp before accelerated fatigue growth takes place, and α_1, α_2 and α_3 determine the relative contributions of ΔK and K_{max}. These parameters can be adjusted to accurately capture the relative influences of these two drivers. As stated in the foregoing, this structure offers flexibility in capturing the complicated fatigue crack growth profiles prevailing in certain material systems, as well as the multifarious environment–fatigue interactions. Furthermore, the structure can correctly capture the relative contributions of the two drivers ΔK and K_{max} under various loading conditions and environments.

Although their expression can capture the sigmoidal shape, the physical meanings of the parameters are unclear. We recommend writing the general expression of the two-parameter unified approach following the same idea as Eq. (5.22) as follows:

$$\frac{da}{dN} = \frac{A\left(\Delta K - \Delta K_{th}^{*}\right)^{n}\left(K_{max} - K_{max\,th}^{*}\right)^{m}}{1 - \left(K_{max}/K_{cf}\right)^{\gamma_1}} \tag{5.41}$$

where A, n, m, γ, K_{cf}, ΔK_{th}^{*} and $K_{max\,th}^{*}$ are the model parameters. In this model we specifically differentiate K_{cf} from K_c measured in a static fracture toughness test. This is the consequence of fatigue loading history. Schijve (2003) has specifically pointed out this problem but it has not received adequate attention in the literature. ΔK_{th}^{*} and $K_{max\,th}^{*}$ can be functions of da/dN similar to those in Eq. (5.39) (Maymon, 2005a) or can be functions of R (Kujawski, 2001d) such as

© 2008 Woodhead Publishing Limited

$$\begin{cases} \Delta K_{\text{th}}^{*} = \Delta K_{\text{th0}}(1-R)^{\gamma_2} \\ K_{\text{max th}}^{*} = K_{\text{max th0}}(1-R)^{\gamma_2} \end{cases} \quad 5.42$$

Knowledge of fatigue thresholds is very important since most fatigue life is spent close to the threshold regime, where crack growth rates are low. The procedures and standards for measurement of fatigue threshold, ΔK_{th0}, are available but there are no equivalent ones for $K_{\text{max th0}}$. Based on a comprehensive study, Sadananda and Vasudevan (2003) found that for all the steels, ΔK_{th0} is independent and is of the order of $2.6 \pm 0.2\,\text{MPa}\sqrt{\text{m}}$, while K_{maxth0} varies significantly for different steels (2.6 to $10\,\text{MPa}\sqrt{\text{m}}$). The experimental evidence they collected indicated that (1) $K_{\text{max th0}}$ is much larger than ΔK_{th0} and they are nearly equal in an inert environment; (2) $K_{\text{max th0}}$ decreases with increase in yield stress, and increases with increase in grain size; (3) at some critical combination of yield stress and grain size, there is a minimum in the threshold; (4) $K_{\text{max th0}}$ varies significantly with temperature, sometimes showing a minimum at some critical temperature depending on the environment; and (5) it also varies with frequency and microstructure. Similar results may exist for other metals.

K_{max} can be either defined within linear elastic fracture mechanics or modified by elastic–plastic fracture mechanics as given in Eq. (5.31). The total number of model parameters is 11, namely A, n, m, γ_1, γ_2, r_e, K_c, K_{cf}, σ_u, ΔK_{th0} and $K_{\text{max th0}}$. The performance of this two-parameter crack growth rate curve, Eq. (5.41), was studied through a simple example of a center crack in a finite width plate in Cui *et al.* (2007).

5.5 Preventive measures for fatigue cracking

In general, fatigue damage at a crack initiation site is affected by many factors such as material properties (e.g., elastic modulus, ultimate tensile stress), high local stresses (e.g., stress concentration, residual stresses), size of components, nature of stress variation (e.g., stress variation during the loading and unloading cycles, number of wave-induced stress range cycles), and environmental and operational factors including corrosion and performance of coatings. Potential flaws (e.g., poor materials, porosity, slag inclusions, undercuts, lack of fusion, incomplete weld root penetration) and misalignments can also significantly increase stress concentrations at weld toes.

To achieve greater fatigue durability in a structure, therefore, stress concentrations, flaws and structural degradation including corrosion and fatigue effects should be avoided or minimized. In an active marine environment, this is very challenging. Thus, in practice the best that can be achieved is that their levels and effects must be anticipated in design, and must be monitored and effectively controlled during construction and service. At the design stage the effect of stress concentrations intentionally present is assessed in order to ensure

© 2008 Woodhead Publishing Limited

that the fatigue life of the structure is longer than the design service life with an adequate factor of safety. Construction defects are in practice to be monitored and controlled by appropriate construction standards. However, to the extent that such standards are often generic to a type of vessel and based mainly on what can be economically achieved, they need to be selectively enhanced in many cases depending on individual structural characteristics.

Structural fracture modes associated with cracks can often be classified into three groups: brittle, ductile and rupture. When the strain at fracture of a material is very small, it is called brittle fracture. In steel structures made of ductile material with adequately high fracture toughness, however, the fracture strain can be comparatively large. When the material is broken by necking associated with large plastic flow, it is called rupture. As a failure mode, ductile fracture is an intermediate phenomenon between brittle fracture and rupture.

Welded structures are susceptible to fatigue failure (Borzecki *et al.*, 2006). This is due to a combination of tensile residual stresses in the weld region and the presence of macroscopic cracks at the weld, initiated during the welding.

5.5.1 Fatigue crack detection and measurement

Fatigue cracking is a localized problem, and therefore local detection is needed (Paik *et al.*, 2006). Cracks are most efficiently detected visually as too many locations in practical structures like ships would need to be monitored by individual sensors. A visual examination should determine the type of crack and assess whether it is likely to propagate. Dye penetrant and magnetic particle tests can also be used after visual inspection, providing approximate measures of surface crack length but not of crack depth. Photographic records of both may be kept.

Assessment methods other than visual inspections are generally seldom used for ship structures because a single crack does not impair structural safety due to redundancy. Tiku and Pussegoda (2003) compare several NDE methods for fatigue and fracture of ship structures. Conventional techniques are ranked as in Table 5.1. Other, more advanced, techniques include acoustic emission, infrared thermography, laser shearography, potential drop test (ACPD or DCPD), alternating current field measurement (ACFM), crack propagation gauges, and automated ball indentation. Other methods are commonly used in the offshore field for inspection as well as monitoring. Eddy current, ultrasonics, ACPD and DCPD are generally able to characterize crack dimensions and locations with different degrees of accuracy, and better than visual inspection (Ditchburn *et al.*, 1996).

Generally, crack detection needs off-service inspections. Ultrasonic surface-guided waves are proposed by Vanlanduit *et al.* (2003) for in-service monitoring. One of the advantages of this method is that working stresses do not need to be released and therefore open cracks can be detected, making this method much

© 2008 Woodhead Publishing Limited

Table 5.1 Methods for fatigue crack measurements (Tiku and Pussegoda, 2003)

	Ultrasonics	X-ray	Eddy current	Magnetic particle	Liquid penetrant
Capital cost	Medium to high	High	Low to medium	Medium	Low
Consumable cost	Very low	High	Low	Medium	Medium
Time of results	Immediate	Delayed	Immediate	Short delay	Short delay
Effect of geometry	Important	Important	Important	Less important	Less important
Access problems	Important	Important	Important	Important	Important
Type of defect	Internal	Most	External	External	Surface breaking
Relative sensitivity	High	Medium	High	Low	Low
Formal record	Expensive	Standard	Expensive	Unusual	Unusual
Operator skill	High	High	Medium	Low	Low
Operator training	Important	Important	Important	Important	–
Training needs	High	High	Medium	Low	Low
Portability of equipment	High	Low	High to medium	High to medium	High
Dependent on material composition	Very	Very	Very	Magnetic only	Little
Ability to automate	Good	Fair	Good	Fair	Fair
Capabilities	Thickness gauging	Thickness gauging	Thickness gauging	Defects only	Defects only

more sensitive. Talei-Faz *et al.* (2004) introduced a novel digital photogrammetric method. The technique allows for real-time three-dimensional measurements of local deformations.

5.5.2 Fatigue crack protection measures

Methods to prevent fatigue failure may again be classified into two types, namely active and passive (Paik *et al.*, 2006). Active methods directly improve

© 2008 Woodhead Publishing Limited

the fatigue performance of the material or the weld joint itself, while passive methods improve fatigue performance by reducing the applied stress.

Resistance to crack initiation can be increased by hardening the surface of the material. This is normally done with machine parts. Carburizing, case hardening and hardening/tempering are typical examples of this method. The degree of fatigue strength improvement depends on the hard layer thickness, the processing temperature of the surface layer and the heat treatment (Tokaji *et al.*, 2004; Farfan *et al.*, 2004). It is recognized that carburizing can also improve the corrosion resistance (Tokaji *et al.*, 2004).

Resistance to fatigue crack growth can be increased by controlling the microstructure of the material (Nakajima *et al.*, 2004; Konda *et al.*, 2003, 2004). Such innovative structural steels have already been put into practical use and applied to ship structures.

In the first stage of cracking, including crack initiation, the effects of residual stress are significant. In the case of machinery elements, in order to improve fatigue strength, the method of creating a compressive residual stress field in the surface layer by shot peening is often used. In the case of welded joints, where fatigue strength is decreased due to the existence of large weld residual tensile stresses, fatigue strength can be improved by relaxing the weld residual stress (Cheng *et al.*, 2003). In this case, the degree of improvement in fatigue strength depends on the relation between the mean stress including residual stress, the applied stress range and the yield stress of the material. The improvement in fatigue strength by relaxation of weld residual stress is greater in the low stress/high cycle region (Huo *et al.*, 2005).

An investigation on the use of a post-weld cold working process to improve fatigue strength of low carbon steel resistance spot welds was carried out by Spitsen *et al.* (2004). The cold working process generates uniform and consistent large zones of compressive residual stresses in resistance spot-welded low carbon steel structures using a specially designed indentation device. The effect of the indentation process parameters on the mechanical properties of the resistance spot-weld was investigated. The mechanical properties and qualitative results for the as-resistance spot-welded specimens and the post-weld cold worked resistance spot-welded specimens were compared in this investigation. Fatigue testing was also conducted to evaluate the effect of the post-weld cold working process on the fatigue characteristics of resistance spot-welds. Preliminary results showed that a significant improvement in the fatigue endurance limit was achieved through the post-weld cold working process.

A compressive stress induced by post-weld treatment may be beneficial by eliminating the tensile residual stresses and introducing compression residual stresses which improve the fatigue strength of welded structures. Stresses in a welded structure are a combination of applied stress due to load and the locked-in weld residual stresses which are independent of the load. When the applied stress is superimposed on the residual stress at a point in the material, the tensile

© 2008 Woodhead Publishing Limited

component of the combined stress will contribute to fatigue crack development and is defined as effective stress range. Conventional post-weld treatment techniques include grinding, air hammer peening, shot peening, needle peening and TIG (tungsten inert gas) remelting. Grinding and TIG dressing can well improve the weld toe profile and reduce stress concentration effects. However, tensile residual stresses remain due to the heat produced in the treatment operation. Peening techniques can both improve the weld toe profile and induce beneficial compressive stresses at weld toes. A modern treatment technique, ultrasonic impact treatment (UIT), is a possible way to effectively improve the residual stress conditions near a detail weld toe. UIT is a treatment technique that utilizes ultrasonic impulses at a frequency of 27 kHz to treat metals or weld toe surfaces. The treatment causes plastic deformation near the weld toe, improves weld toe profile and introduces compressive stresses. The weld toe geometry improvement is caused by the mechanical cold working from tool pins at about 100 Hz. The residual stress improvement is caused by transferring the ultrasonic wave vibration during the pin impact. Limited studies have examined the residual stress modification quantitatively (Janosch *et al.*, 1996; Statnikov, 2000), but no studies have examined weld toe profile and hardness change that result from UIT.

The shot peening process is a cold working process in which the surface of the metal material is bombarded with small spherical shot. Each piece of shot striking the material acts as a tiny peening hammer, imparting a small indentation or dimple to the surface. Overlapping dimples develop an even layer of metal in compressive stress and cold works on the surface, which increases fatigue life. Unlike UIT and air hammer peening in which treatment is focused locally along a weld toe, shot peening is focused on a surface of an area. In the study carried out by Cheng *et al.* (2003), residual stresses induced by UIT and shot peening were examined on the specimens with more suitable geometry and materials often used in bridge and ship structures by employing both X-ray and neutron diffraction techniques for the first time. Residual stresses were measured on three base metal samples treated by UIT and shot peening, and on one welded sample treated by UIT. The experimental conditions and results of these stress measurements were presented. Based on the information on compressive stress level and depth introduced by the post-weld treatments, the effect of residual stress modification on fatigue strength was examined from the point of view of fracture mechanics. The beneficial effect of UIT has been verified by fatigue test results on large-scale welded girders. The major findings can be summarized as follows (Cheng *et al.*, 2003):

1. The peak compressive residual stress induced by the treatments exceeded the yield stress of the base material near the surface.
2. The compressive stress region by UIT alone was 1.5–1.7 mm in depth and $\sim \pm 15$ mm in width. For welded specimen the compressive layer was reduced to 1 mm deep due to the existence of tensile weld residual stress.

© 2008 Woodhead Publishing Limited

3. Shot peening treatment induced compressive stress comparable to UIT in magnitude, but the compressive stress layer was about half the depth (0.8 mm) of UIT.
4. Beneficial compressive stress induced by the post-weld treatments can modify tensile weld stress distribution and reduce internal stress ratio to negative near the weld toe.

The crack growth threshold value, ΔK_{th}, is increased after the treatments and thus fatigue resistance is enhanced. Because the compressive stress layer is thin, the beneficial effect is significant in fatigue crack initiation and early stage crack growth rather than Stage II crack propagation. UIT may have more beneficial effects on crack initiation life than shot peening due to its deeper compressive stress layer. So far there is not enough evidence showing that the intensity of UIT and shot peening treatment has a significant effect on compressive residual stresses in magnitude and distribution. Further study in this aspect is desirable. Study on relaxation of beneficial compressive stress with cyclic loading is also needed.

Enhancement of the fatigue resistance of welded transverse stiffeners and cover plate details by ultrasonic impact treatment (UIT) was evaluated by Roy *et al.* (2003) in 18 full-scale W27 × 129 rolled beam specimens. Fatigue tests were conducted under constant amplitude loading at various stress range levels and at two minimum stress levels simulating the effect of sustained load. The test specimens were investigated for fatigue crack initiation and propagation. Distributions of residual stresses adjacent to the weld toe were determined before and after the treatment. Test results indicated that UIT enhanced the fatigue performance of all treated details by improving the weld toe profile, changing microstructure and introducing beneficial compressive residual stresses at the treated weld toe. The treatment effectively elevated the fatigue crack growth threshold and the fatigue limit without changing the slope of the S–N curve.

Weld toe treatment by ultrasonic peening or TIG dressing improves the fatigue performance of welded joints and structures significantly. This has been verified by many constant amplitude fatigue tests. However, there is the need to check their benefits for structures subjected to variable-amplitude loading. Therefore, fatigue tests were performed by Huo *et al.* (2005) on fillet welded joints in 16Mn steel for three different conditions: as-welded, TIG dressed and after treatment by ultrasonic peening. The beneficial effects of both TIG dressing and ultrasonic peening were found to be less under variable amplitude than under constant amplitude loading. In particular, under constant amplitude loading TIG dressing increased the fatigue strength by 37% and the fatigue life by 2.5 times. In contrast, under variable-amplitude loading the corresponding benefits were 34% increase in fatigue strength and 1.7–1.9 times increase in fatigue life. The improvement in fatigue performance due to ultrasonic peening

© 2008 Woodhead Publishing Limited

depended on the applied stress, being negligible at stresses approaching yield, but greater than that due to TIG dressing in the low stress/high-cycle regime. Under constant amplitude loading, ultrasonic peening increased the fatigue strength by up to 84% and the fatigue life by 3.5–27 times. In contrast, under variable-amplitude loading the corresponding benefits were 80% increase in fatigue strength and 2.5–17 times increase in fatigue life. For either constant or variable-amplitude loading, the improvement in fatigue strength of the welded joints due to ultrasonic peening was greater than that due to TIG dressing, but only in the low stress/high-cycle regime.

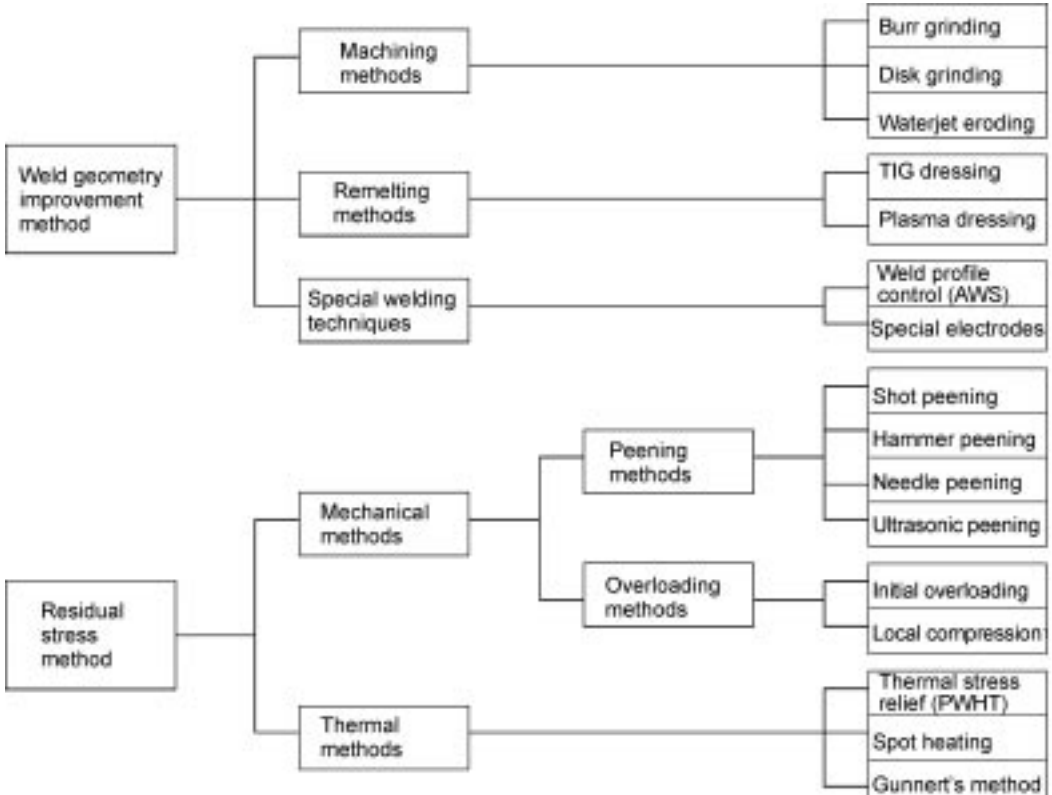
Shot peening improvement of high cycle fatigue (HCF) behavior of metal inert gas (MIG) welded T-joints made from 5083 H11 Al-alloy plates using 5183 Al-alloy welding wires was evaluated by means of four-point bending fatigue tests by Sidhom *et al.* (2005). The enhancement of the fatigue limits at 2×10^6 cycles were 135% and 59% for stress ratios $R_1 = 0.1$ and $R_2 = 0.5$, respectively. The properties of near weld toe surfaces, where the microcrack nucleation occurred, were characterized before and after shot peening. The metallurgical modifications were monitored by micro-hardness measurements, and the in-depth residual stresses were determined by the hole drilling technique. The surface integrity was examined using a scanning electronic microscope (SEM). Based on the multiaxial HCF criterion of Sines and taking into account the different surface properties, a local predictive approach was developed. It allows correlating quantitatively the influence of MIG welding and shot peening on the HCF performance of the Al-alloy 5083 H11. The characteristic parameters of the proposed approach have been calibrated, in order to obtain accurate predictions, for the two cases of welded and peened welded T-joints.

The role of fatigue quality enhancers is to delay or if possible eliminate crack nucleation. The best known fatigue quality enhancers are cold working, shot peening and controlled interference fit fastening. Ofsthun (2003) discussed the theory behind these common fatigue quality enhancers. But more importantly, he pointed out conditions where the fatigue quality enhancers did not delay crack nucleation and in some cases sped up crack nucleation. He emphasized the need to support the analytical benefits of fatigue quality enhancers with test data.

Decreasing the stress concentration at a hot spot area contributes to the improvement of fatigue strength because the initiation and progress of fatigue cracks are influenced by the local stress condition. Especially in the case of welded joints, removing the undercut or notch, which results in stress concentrations at the weld toe, is very effective. Grinding, dressing, profile control, etc. are often employed for improving or avoiding the undercut or notch (Kirkhope *et al.*, 1997). These fatigue strength improvement methods in welded joints are summarized in Fig. 5.5.

The above method refers to the notch stress. Fatigue strength can also be improved by decreasing the hot spot stress, which is caused by a structural

© 2008 Woodhead Publishing Limited



5.5 Classification of some weld improvement methods (Kirkhope *et al.*, 1997).

© 2008 Woodhead Publishing Limited

discontinuity. In a hull structure, a nominal stress level is generally determined by the arrangements and the scantlings of the structural members. Therefore, improvement in fatigue strength can be achieved by decreasing the stress concentration due to a structural discontinuity, by altering the structural detail around the hot spot area. Since fabrication errors such as misalignment, angular misalignment and plate distortion cause secondary bending stresses, it is important to control fabrication errors to improve the fatigue performance (Kendrick *et al.*, 2005).

5.5.3 Steels with improved fatigue properties

Prevention of fatigue problems can also be achieved by using fatigue-resistant materials (Borzecki *et al.*, 2006). Suzuki *et al.* (2004) have used newly developed high fatigue property steel plates to reduce the life-cycle cost of ships. The anti-fatigue damage ('AFD') steel plates have a fatigue propagation life more than twice as long as that of conventional steel plates, as well as showing improved fatigue strength. The developed steels have already been applied to some ships and vessels, and a new bulk carrier has recently used steels developed by Nippon Kaiji Kyokai with resistance to fatigue fracture (Katsumoto *et al.*, 2005). From further studies, it was found that the developed steels also had high resistance to fatigue crack initiation as well as growth even in welded structures. It was clarified that the fatigue strength of the heat-affected zone, where fatigue cracks generally initiate, in the developed steel was higher than that in the conventional steel, and the stress concentration at the weld toe in the developed steel was smaller than in the conventional steel. The newly developed steel can effectively extend the fatigue fracture life of welded structures from the viewpoint of material. Hirota *et al.* (2005) developed a new functional steel plate with superior resistance against fatigue crack growth, and proposed that fatigue strength could be improved using the improved material. A part of the conventional steel plate was replaced with the one developed, to give higher reliability on fatigue strength.

5.6 Conclusions

In this chapter, an introduction to fatigue-related problems has been presented. These included the current state of the art about mechanisms, mathematical models and preventive measures of fatigue cracking. Efforts have been made to include materials as recently developed as possible. However, from the above sections one can see that research into fatigue has entered another new era of fast development. The understanding of fatigue mechanisms will become deeper and deeper due to the availability of more accurate crack measuring systems. Some of the traditional concepts and methods such as crack closure are subjected to challenges and new theories will be developed for the prediction of fatigue crack

© 2008 Woodhead Publishing Limited

propagation. Readers are advised to monitor the progress of this field closely and to update the information presented in this chapter in due course.

5.7 References

Almar-Naess, A. (1985), *Fatigue Handbook*, Tapir, Trondheim, Norway.

Banvillet, A., Palin-Luc, T. and Lasserre, S. (2003), 'A volumetric energy based high cycle multiaxial fatigue criterion', *International Journal of Fatigue*, 25, 755–769.

Basquin, O.H. (1910), 'The exponential law of endurance tests', *Proc. ASTM*, 10 (Part II), 625–630.

Bathias, C. (1999), 'There is no infinite fatigue life in metallic materials', *Fatigue Fract. Engng Mater. Struct.*, 22, 559–565.

Baumel, A. Jr. and Seeger, T. (1990), *Materials Data for Cyclic Loading, Supplement 1*, Amsterdam, Elsevier Science Publishers.

Berger, C., Pyttel, B. and Trossmann, T. (2006), 'Very high cycle fatigue tests with smooth and notched specimens and screws made of light metal alloys', *International Journal of Fatigue*, 28, 1640–1646.

Borzecki, T. *et al.* (2006), Report of Specialist Committee V.3: Fabrication Technology, in *Proceedings of the 16th International Ship and Offshore Structures Congress*, edited by P.A. Frieze and R.A. Shenoi, 20–25 August, Southampton, UK, 2, 117–167.

Bukkapatnam, S.T.S. and Sadananda, K. (2005), 'A genetic algorithm for unified approach-based predictive modeling of fatigue crack growth', *International Journal of Fatigue*, 27, 1354–1359.

Carlson, R.L. and Kardomateas, G.A. (1996), *An Introduction to Fatigue in Metals and Composites*, London and New York, Chapman & Hall.

Carpinteri, A. (ed.) (1994), *Handbook of Fatigue Crack Propagation in Metallic Structures*, Vols 1 and 2, Amsterdam, Elsevier.

Castillo, E. and Fernandez-Canteli, A. (2006), 'A parametric lifetime model for the prediction of high-cycle fatigue based on stress level and amplitude', *Fatigue Fract. Engng Mater. Struct.*, 29, 1031–1038.

Chaboche, J.L. and Lesne, P.M. (1988), 'A non-linear continuous fatigue damage model', *Fatigue Fract. Engng Mater. Struct.*, 11(1), 1–7.

Cheng, X., Fisher, J.W., Prask, H.J., Gnaupel-Herold, T., Yen, B.T. and Roy, S. (2003), 'Residual stress modification by post-weld treatment and its beneficial effect on fatigue strength of welded structures', *International Journal of Fatigue*, 25(9–11), 1259–1269.

Coffin, L.F. and Tavernelli J.F. (1959), 'The cyclic straining and fatigue of metals', *Trans. Metallurgical Society of American Institute of Mechanical Engineers*, 215, 794.

Cui, W.C. (2002), 'A state-of-the-art review on fatigue life prediction methods for metal structures', *Journal of Marine Science and Technology*, 7(1), 43–56.

Cui, W.C. (2003), 'A feasible study of fatigue life prediction for marine structures based on crack propagation analysis', *Journal of Engineering for the Maritime Environment*, 217(M1), 11–23.

Cui, W.C. and Huang, X.P. (2003), 'A general constitutive relation for fatigue crack growth analysis of metal structures', *Acta Metallurgica Sinica (English Letters)*, 16(5), 342–354.

Cui, W.C. and Wu, Y.S. (2002), 'Towards a more rational first-principle-based strength

© 2008 Woodhead Publishing Limited

assessment system for ship structures', presented at ASRANET Conference in Glasgow, 8–10 July.
Cui, W.C., Bian, R.G. and Huang, X.P. (2007), 'Application of the two-parameter Unified Approach for fatigue life prediction of marine structures', to be presented in *PRADS2007*.
Dattoma, V., Giancane, S., Nobile, R. and Panella, F.W. (2006), 'Fatigue life prediction under variable loading based on a new non-linear continuum damage mechanics model', *International Journal of Fatigue*, 28, 89–95.
de Castro, J.T.P., Meggiolaro, M.A. and de Oliveira Miranda, A.C. (2005), 'Singular and non-singular approaches for predicting fatigue crack growth behavior', *International Journal of Fatigue*, 27, 1366–1388.
Ditchburn, R.J., Burke, S.K. and Scala, C.M. (1996), 'NDT of welds: state of the art', *NDT&E International*, 29(2), 111–117.
Donahue, R.J., Clark, H.M., Atanmo, P., Kumble, R. and McEvily, A.J. (1972), 'Crack opening displacement and the rate of fatigue crack growth', *International Journal of Fracture Mechanics*, 8, 209–219.
Donald, K. and Paris, P.C. (1999), 'An evaluation of ΔK_{eff} estimation procedure on 6061-T6 and 2024-T3 aluminum alloys', *International Journal of Fatigue*, 21, S47–S57.
Elber, W. (1970), 'Fatigue crack closure under cyclic tension', *Engineering Fracture Mechanics*, 2, 37–45.
Farfan, S., Rubio-Gonzalez, C., Cervantes-Hernandez, T. and Mesmacque, G. (2004), 'High cycle fatigue, low cycle fatigue and failure modes of a carburized steel', *International Journal of Fatigue*, 26(6), 673–678.
Fatemi, A. and Yang, L. (1998), 'Cumulative fatigue damage and life prediction theories: a survey of the state of the art for homogeneous materials', *International Journal of Fatigue*, 20(1), 9–34.
Forman, R.G., Kearney, V.E. and Engle, R.M. (1967), 'Numerical analysis of crack propagation in cyclic-loaded structures', *Journal of Basic Engineering*, 89, 459–464.
Forsyth, P.J.E. (1969), *The Physical Basis of Metal Fatigue*, New York, American Elsevier Publishing Co.
Fricke, W., Cui, W.C., Kierkegaard, H., Kihl, D., Koval, M., Lee, H.L., Mikkola, T., Parmentier, G., Toyosada, M. and Yoon, J.H. (2002), 'Comparative fatigue strength assessment of a structural detail in a containership using various approaches of classification societies', *Marine Structures*, 15(1), 1–13.
Gasiak, G. and Pawliczek, R. (2003), 'Application of an energy model for fatigue life prediction of construction steels under bending, torsion and synchronous bending and torsion', *International Journal of Fatigue*, 25, 1339–1346.
Glinka, G. (1988), 'Relations between the strain energy density distribution and elastic–plastic stress–strain fields near cracks and notches and fatigue life calculation', in *Low Cycle Fatigue*, ASTM STP 942, Philadelphia, PA, American Society for Testing and Materials, 1002–1047.
Hertzberg, R.W., Newton, C.H. and Jaccard, R. (1988), 'Crack closure: correlation and confusion', in *Mechanics of Fatigue Crack Closure*, ASTM STP 982, Philadelphia, PA, American Society for Testing and Materials, 139–148.
Heuler, P. and Klätschke, H. (2005), 'Generation and use of standardised load spectra and load–time histories', *International Journal of Fatigue*, 27, 974–990.
Hirota, K., Sugimura, T., Arimochi, K., Konda, N. and Katsumoto, H. (2005), 'A study on fatigue life of local structure using steel plate with superior resistance against

© 2008 Woodhead Publishing Limited

fatigue crack growth', *Trans. West-Japan Society of Naval Architects*, 109, 49–56 (in Japanese).

Hobson, P.D., Brown, M.W. and de los Rios, E.R. (1986), in *The Behaviour of Short Fatigue Cracks*, K.J. Miller and E.R. de los Rios (eds), EGF (ESIS) Publ. No. 1, London, Mechanical Engineering Publications Ltd, 441–459.

Huo, L., Wang, D. and Zhang, Y. (2005), 'Investigation of the fatigue behaviour of the welded joints treated by TIG dressing and ultrasonic peening under variable-amplitude load', *International Journal of Fatigue*, 27, 95–101.

Ishihara, S. and McEvily, A.J. (1999), 'A coaxing effect in the small fatigue crack growth regime', *Scripta Materialia*, 40(3), 617–622.

Jahed, H. and Varvani-Farahani, A. (2006), 'Upper and lower fatigue life limits model using energy-based fatigue properties', *International Journal of Fatigue*, 28, 467–473.

Janosch, J.J., Koneczny, H., Debiez, S., Statnikov, E.C., Troufiakov, V.J. and Mikhee, P.P. (1996), 'Improvement of fatigue strength in welded joint (in HSS and in aluminum alloy) by ultrasonic hammer peening', *Welding in the World, Le Soudage dans le Monde*, 37(2), 72–83.

Kachanov, L.M. (1986), *Introduction to Continuum Damage Mechanics*, The Hague, Martinus Nijhoff.

Kanninen, M.F. and Popelar, C.H. (1985), *Advanced Fracture Mechanics*, New York, Oxford University Press.

Katsumoto, H., Hirota, K., Sakano, M., Konda, N., Isoda, A., Yajima, H., Arimochi, K. and Kitada, H. (2005), 'Development of structural steel with high resistance to fatigue crack initiation and growth', Part 3, *Proceedings of the 24th International Conference on Offshore Mechanics and Arctic Engineering – OMAE2005*, 3, 143–151.

Kendrick, A., Ayyub, B. and Assakkaf, I. (2005), 'The effect of fabrication tolerances on fatigue life of welded joints', *Ship Structure Committee Report*, SSC-437, Washington, DC.

Kirkhope, K.J., Bell, R., Caron, L. and Basu, R.I. (1997), 'Weld detail fatigue life improvement techniques', *Ship Structure Committee Report*, SSC-400, Washington, DC.

Kohout, J. and Vechet, S. (1999), 'New functions for description of fatigue curves and their advantages', in *Proceedings of the Seventh International Fatigue Congress (Fatigue'99)*, ed. X.R. Wu and Z.G. Wang, Beijing, China, Higher Education Press, 783–788.

Konda, N., Arimochi, K., Hirota, K., Watanabe, E., Toda, M., Kitada, H., Fukui, T., Yamamoto, M., Koh, Y. and Yajima, H. (2003), 'Development of structural steel with superior resistance against fatigue crack growth', *Proceedings of the International Conference on Offshore Mechanics and Arctic Engineering – OMAE*, 3, 35–44.

Konda, N., Arimochi, K., Hirota, K., Watanabe, E., Toda, M., Kitada, H., Fukui, T., Yamamoto, M., Koh, Y. and Yajima, H. (2004), 'Development of structural steel with superior resistance against fatigue crack growth (part 2)', *Proceedings of the 23rd International Conference on Offshore Mechanics and Arctic Engineering – OMAE*, 2, Safety and Reliability, Materials Technology Workshop, 689–701.

Kujawski, D. (2001a), 'Correlation of long- and physically short-cracks growth in aluminum alloys', *Engineering Fracture Mechanics*, 68, 1357–1369.

Kujawski, D. (2001b), 'Enhanced model of partial crack closure for correlation of *R*-ratio effects in aluminum alloys', *International Journal of Fatigue*, 23, 95–102.

© 2008 Woodhead Publishing Limited

Kujawski, D. (2001c), 'A new $(\Delta K^{+}K_{\max})^{0.5}$ driving force parameter for crack growth in aluminum alloys', *International Journal of Fatigue*, 23, 733–740.

Kujawski, D. (2001d), 'A new fatigue crack driving force parameter with load ratio effects', *International Journal of Fatigue*, 23, S239–S246.

Kujawski, D. (2005), 'On assumptions associated with ΔK_{eff} and their implications on FCG predictions', *International Journal of Fatigue*, 27, 1267–1276.

Laue, S., Bomas, H. and Hoffmann, F. (2006), 'Influence of surface condition on the fatigue behaviour of specimens made of a SAE 5115 case-hardened steel', *Fatigue Fract. Engng Mater. Struct.*, 29, 229–241.

Lee, B.L., Kim, K.S. and Nam, K.M. (2003), 'Fatigue analysis under variable amplitude loading using an energy parameter', *International Journal of Fatigue*, 25, 621–631.

Lee, K.S. and Song, J.H. (2006), 'Estimation methods for strain-life fatigue properties from hardness', *International Journal of Fatigue*, 28, 386–400.

Lee, S.Y. and Song, J.H. (2000), 'Crack closure and growth behavior of physically short fatigue cracks under random loading', *Engng Fract. Mech.*, 66(3), 321–346.

Lemaitre, J. and Chaboche, J.L. (1990), *Mechanics of Solid Materials*, Cambridge, Cambridge University Press.

Liu, Y.M. and Mahadevan, S. (2007), 'A unified multiaxial fatigue damage model for isotropic and anisotropic materials', *International Journal of Fatigue*, 29, 347–359.

Manson, S.S. (1965), 'Fatigue: a complex subject – some simple approximations', *Exp. Mech., Journal of the Society for Experimental Stress Analysis*, 5(7), 193–226.

Manson, S.S. and Hirschberg, M.H. (1964), *Fatigue: An Interdisciplinary Approach*, Syracuse, NY, Syracuse University Press, 133.

Marines, I., Bin, X. and Bathias, C. (2003), 'An understanding of very high cycle fatigue of metals', *International Journal of Fatigue*, 25, 1101–1107.

Martinez, F., Liu, S. and Edwards, G.R. (2005), 'Development of compressive residual stress in structural steel weld toes by means of weld metal phase transformations', presented at the *International Trends in Welding Research Conference Proceeding*, Pine Mountain, GA, May.

Maymon, G. (2005a), 'A "unified" and a $(\Delta K^{+}.K_{\max})^{1/2}$ crack growth models for aluminum 2024-T351', *International Journal of Fatigue*, 27, 629–638.

Maymon, G. (2005b), 'Probabilistic crack growth behavior of aluminum 2024-T351 alloy using the "unified" approach', *International Journal of Fatigue*, 27, 828–834.

McEvily, A.J. and Groeger, J. (1977), 'On the threshold for fatigue-crack growth', *Fourth International Conference on Fracture*, Waterloo, Ontario, University of Waterloo Press, 2, 1293–1298.

McEvily, A.J. and Ishihara, S. (2001), 'On the dependence of the rate of fatigue crack growth on the $\sigma_a^n(2a)$ parameter', *International Journal of Fatigue*, 23, 115–120.

McEvily, A.J., Bao, H. and Ishihara, S. (1999), 'A modified constitutive relation for fatigue crack growth', in *Proceedings of the Seventh International Fatigue Congress (Fatigue'99)*, ed. X.R. Wu and Z.G. Wang, Beijing, China, Higher Education Press, 329–336.

Meggiolaro, M.A. and Castro, J.T.P. (2004), 'Statistical evaluation of strain-life fatigue crack initiation predictions', *International Journal of Fatigue*, 26, 463–476.

Memon, I.R., Zhang, X. and Cui, D.Y. (2002), 'Fatigue life prediction of 3-D problems by damage mechanics with two-block loading', *International Journal of Fatigue*, 24, 29–37.

Miller, K.J. (1987a), 'The behavior of short fatigue cracks and their initiation. Part I – A review of two recent books', *Fatigue Fract. Engng Mater. Struct.*, 10(1), 75–91.

Miller, K.J. (1987b), 'The behavior of short fatigue cracks and their initiation. Part II – A

© 2008 Woodhead Publishing Limited

general summary', *Fatigue Fract. Engng Mater. Struct.*, 10(2), 93–113.
Miller, K.J. (1999), 'A historical perspective of the important parameters of metal fatigue and problems for the next century', in *Proceedings of the Seventh International Fatigue Congress (Fatigue'99)*, ed. X.R. Wu and Z.G. Wang, Beijing, China, Higher Education Press, 15–39.
Miner, M.A. (1945), 'Cumulative damage in fatigue', *J. Appl. Mech.*, 67, A159–A164.
Mitchell, M.R., Socie, D.F. and Caulfield, E.M. (1977), 'Fundamentals of modern fatigue analysis', *Fracture Control Program Report No. 26*, University of Illinois, USA, 385–410.
Mortensen, A. (ed.) (2006), *Concise Encyclopedia of Composite Materials*, 2nd edn, Elsevier Science.
Muralidharan, U. and Manson, S.S. (1988), 'A modified universal slopes equation for estimation of fatigue characteristics of metals', *J. Eng. Mat. Tech. – Trans. ASME*, 110, 55–58.
Nakajima, K., Nose, T. and Ishikawa, T. (2004), 'Effects of hard secondary phase on fatigue crack growth properties and fatigue properties of welded joint in heavy steel plate', *Proceedings of Symposium on Welding Structures,* Japan Welding Society, 335–342.
Navarro, A. and de los Rios, E.R. (1988), 'A microstructurally short fatigue crack growth equation', *Fatigue Fract. Engng Mater. Struct.*, 11(5), 383–396.
Newman Jr, J.C. (1998), 'The merging of fatigue and fracture mechanics concepts: a historical perspective', *Progress in Aerospace Sciences*, 34, 347–390.
Newman Jr, J.C., Phillips, E.P. and Swain, M.H. (1999), 'Fatigue-life prediction methodology using small-crack theory', *International Journal of Fatigue*, 21, 109–119.
Newman Jr, J.C., Irving, P.E., Lin, J. and Le, D.D. (2006), 'Crack growth predictions in a complex helicopter component under spectrum loading', *Fatigue Fract. Engng Mater. Struct.,* 29, 949–958.
Noroozi, A.H., Glinka, G. and Lambert, S. (2005), 'A two parameter driving force for fatigue crack growth analysis', *International Journal of Fatigue*, 27, 1277–1296.
Ofsthun, M. (2003), 'When fatigue quality enhancers do not enhance fatigue quality', *International Journal of Fatigue*, 25, 1223–1228.
Ong, J.H. (1993a), 'An evaluation of existing methods for the prediction of axial fatigue life from tensile data', *International Journal of Fatigue*, 15(1), 13–19.
Ong, J.H. (1993b), 'An improved technique for the prediction of axial fatigue life from tensile data', *International Journal of Fatigue*, 15(3), 213–219.
Oystein, A. (2004), *Fatigue of Welded High Strength Steels*, MSc Thesis, NTNU, Norway.
Paik, J.K. and Thayamballi, A.K. (2003), *Ultimate Limit State Design of Steel-plated Structures*, Chichester, John Wiley & Sons.
Paik, J.K., Wang, G., Thayamballi, A.K., Lee, J.M. and Park, Y.I. (2003), 'Time-dependent risk assessment of aging ships accounting for general/pit corrosion, fatigue cracking and local denting damage', *Transactions SNAME*, 111, 159–197.
Paik, J.K. *et al.* (2006), 'Report of Specialist Committee V.6: Condition Assessment of Aged Ships', in *Proceedings of the 16th International Ship and Offshore Structures Congress*, edited by P.A. Frieze and R.A. Shenoi, 20–25 August, Southampton, UK, 2, 269–320.
Palmgren, A. (1924), 'Die Lebensdauer von Kugellagern (Durability of ball bearings)', *ZDVDI*, 68, Bo.14, 339 (in German).
Pan, W.F., Hung, C.Y. and Chen, L.L. (1999), 'Fatigue life estimation under multiaxial

© 2008 Woodhead Publishing Limited

loadings', *International Journal of Fatigue*, 21, 3–10.
Paris, P.C. and Erdogan, F. (1963), 'A critical analysis of crack propagation laws', *Journal of Basic Engineering*, 85, 528–534.
Paris, P.C., Gomez, M.P. and Anderson, W.P. (1961), 'A rational analytical theory of fatigue', *The Trend in Engineering*, 13, 9–14.
Park, J.H. and Song, J.H. (1995), 'Detailed evaluation of methods for estimation of fatigue properties', *International Journal of Fatigue*, 17(5), 365–373.
Ritchie, R.O. (1986), 'Small fatigue cracks: a statement of the problem and potential solutions', *Materials Science and Engineering*, 84, 11–16.
Roessle, M.L. and Fatemi, A. (2000), 'Strain-controlled fatigue properties of steels and some simple approximations', *International Journal of Fatigue*, 22, 495–511.
Roy, S., Fisher, J.W. and Yen, B.T. (2003), 'Fatigue resistance of welded details enhanced by ultrasonic impact treatment (UIT)', *International Journal of Fatigue*, 25, 1239–1247.
Sadananda, K. and Sreenivasan, R. (2001), 'Analysis of fatigue crack growth behavior in niobium–hydrogen alloys using the unified approach to fatigue damage', *International Journal of Fatigue*, 23, S357–S364.
Sadananda, K. and Vasudevan, A.K. (1997), 'Short crack growth and internal stresses', *International Journal of Fatigue*, 19(93), S99–S108.
Sadananda, K. and Vasudevan, A.K. (2003), 'Fatigue crack growth mechanisms in steels', *International Journal of Fatigue*, 25, 899–914.
Sadananda, K. and Vasudevan, A.K. (2004a), 'Crack tip driving forces and crack growth representation under fatigue', *International Journal of Fatigue*, 26, 39–47.
Sadananda, K. and Vasudevan, A.K. (2004b), 'Non-propagating incipient cracks from sharp notches under fatigue', *Acta Materialia*, 52, 4239–4249.
Sadananda, K. and Vasudevan, A.K. (2005), 'Fatigue crack growth behavior of titanium alloys', *International Journal of Fatigue*, 27, 1255–1266.
Sadananda, K., Vasudevan, A.K., Holtz, R.L. and Lee, E.U. (1999), 'Analysis of overload effects and related phenomena', *International Journal of Fatigue*, 21(s1), S233–S246.
Sadananda, K., Vasudevan, A.K. and Holtz, R.L. (2001), 'Extension of the Unified Approach to fatigue crack growth to environmental interactions', *International Journal of Fatigue*, 23, S277–S286.
Sadananda, K., Vasudevan, A.K. and Kang, I.W. (2003), 'Effect of superimposed monotonic fracture modes on the ΔK and K_{max} parameters of fatigue crack propagation', *Acta Materialia*, 51, 3399–3414.
Sakai, T. *et al.* (1999), 'Experimental evidence of duplex S–N characteristics in wide life region for high strength steels', in *Proceedings of the Seventh International Fatigue Congress (Fatigue'99)*, ed. X.R. Wu and Z.G. Wang, Beijing, China, Higher Education Press, 573–578.
Schijve, J. (1967), 'Significance of fatigue cracks in micro-range and macro-range', *ASTM STP 415*, 415–459.
Schijve, J. (1979), 'Four lectures on fatigue crack growth', *Engineering Fracture Mechanics*, 11, 167–221.
Schijve, J. (2003), 'Fatigue of structures and materials in the 20th century and the state of the art', *International Journal of Fatigue*, 25, 679–702.
Schutz, W. (1996), 'A history of fatigue', *Engineering Fracture Mechanics*, 54(2), 263–300.
Shang, D.G., Yao, W.X. and Wang, D.J. (1998), 'A new approach to the determination of fatigue crack initiation size', *International Journal of Fatigue*, 20(9), 683–687.

© 2008 Woodhead Publishing Limited

Sidhom, N., Laamouri, A., Fathallah, R., Braham, C. and Lieurade, H.P. (2005), 'Fatigue strength improvement of 5083 H11 Al-alloy T-welded joints by shot peening: experimental characterization and predictive approach', *International Journal of Fatigue*, 27, 729–745.

Skorupa, M. (1998), 'Load interaction effects during fatigue crack growth under variable amplitude loading – a literature review, Part I: empirical trends', *Fatigue and Fracture of Engineering Materials and Structures*, 21(8), 987–1006.

Skorupa, M. (1999), 'Load interaction effects during fatigue crack growth under variable amplitude loading – a literature review, Part II: qualitative interpretation', *Fatigue and Fracture of Engineering Materials and Structures*, 22(8), 905–926.

Smith, K.N., Watson, P. and Topper, T.H. (1970), 'A stress–strain function for the fatigue of metals', *J. Mater.*, 5(4), 767–778.

Spitsen, R., Kim, D., Ramulu, M., Flinn, B. and Easterbrook, E.T. (2004), 'The effects of post-weld cold working processes on the fatigue strength of low carbon steel resistance spot welds', *American Society of Mechanical Engineers, Manufacturing Engineering Division, Manufacturing Engineering and Materials Handling – 2004*, 15, 107–113.

Statnikov, E.S. (2000), 'Applications of operational ultrasonic impact treatment (UIT) technologies in production of welded joints', *Welding in the World*, 44(3), 11–21.

Stoychev, S. and Kujawski, D. (2005), 'Analysis of crack propagation using ΔK and K_{max}', *International Journal of Fatigue*, 27, 1425–1431.

Suzuki, S., Muraoka, R., Obinata, T., Endo, S. Horita, T. and Omata, K. (2004), 'Steel products for shipbuilding', *JFE Technical Report*, 2, 41–48.

Talei-Faz, B., Brennan, F.P. and Dover, W.D. (2004), 'Residual static strength of high strength steel cracked tubular joints', *Marine Structures*, 17, 291–309.

Tiku, S. and Pussegoda, N. (2003), 'In service non destructive evaluation of fatigue and fracture properties for ship structures', *Ship Structure Committee*, SSC-428, Washington, DC.

Tokaji, K., Kohyama, K. and Akita, M. (2004), 'Fatigue behaviour and fracture mechanism of a 316 stainless steel hardened by carburising', *International Journal of Fatigue*, 26, 543–551.

Vanlanduit, S., Guillaume, P. and van der Linden, G. (2003), 'On-line monitoring of fatigue cracks using ultrasonic surface waves', *NDTE International*, 36(8), 601–607.

Vasudevan, A.K. and Sadananda, K. (1999), 'Application of unified fatigue damage approach to compression–tension region', *International Journal of Fatigue*, 21(s1), S263–S273.

Vasudevan, A.K. and Sadananda, K. (2001), 'Analysis of fatigue crack growth under compression–compression loading', *International Journal of Fatigue*, 23, S365–S374.

Vasudevan, A.K., Sadananda, K. and Louat, N. (1994), 'A review of crack closure, fatigue crack threshold and related phenomena', *Materials Science and Engineering*, A188, 1–22.

Vasudevan, A.K., Sadananda, K. and Glinka, G. (2001), 'Critical parameters for fatigue damage', *International Journal of Fatigue*, 23, S39–S53.

Vasudevan, A.K., Sadananda, K., and Holtz, R.L. (2005), 'Analysis of vacuum fatigue crack growth results and its implications', *International Journal of Fatigue*, 27, 1519–1529.

Wang, Q.Y., Sun, Z.D., Bathias, C., Berard, J.Y. and Rathery, S. (1999a), 'Fatigue crack initiation and growth behavior of a thin steel sheet at ultrasonic frequency', in

© 2008 Woodhead Publishing Limited

Proceedings of the Seventh International Fatigue Congress (Fatigue'99), ed. X.R. Wu and Z.G. Wang, Beijing, China, Higher Education Press, 169–174.

Wang, X.S. *et al.* (1999b), 'Prediction of fatigue life of carbon steel using only the tensile strength', in *Proceedings of the Seventh International Fatigue Congress (Fatigue'99)*, ed. X.R. Wu and Z.G. Wang, Beijing, China, Higher Education Press, 845–850.

Wästberg, S. *et al.* (2006), 'Fatigue and fracture', TC III.2 Report, *Proceedings of 16th International Ship and Offshore Structures Congress*, ed. P.A. Frieze and R.A. Shenoi, 20–25 August, Southampton, UK, 1, 459–541.

Yang, L. and Fatemi, A. (1998), 'Cumulative fatigue damage mechanisms and quantifying parameters: A literature review', *Journal of Testing and Evaluation*, 26(2), 89–100.

Ye, D.Y., Matsuoka, S., Suzuki, N. and Maeda,Y. (2004), 'Further investigation of Neuber's rule and the equivalent strain energy density (ESED) method', *International Journal of Fatigue*, 26, 447–455.

Zhang, J.Z, He, X.D. and Du, S.Y. (2005), 'Analyses of the fatigue crack propagation process and stress ratio effects using the two parameter method', *International Journal of Fatigue*, 27, 1314–1318.

© 2008 Woodhead Publishing Limited

6

Local denting and other deterioration in aged structures

N Y A M A M O T O, Research Institute of Nippon Kaiji Kyokai, Japan

Abstract: This chapter outlines the generation mechanism, causes and features of damage by local deformation which might be caused in hull structural members, and the measures that can be taken to prevent it. This chapter includes two types of local deformation damage, one caused by mechanical external causes and the other by deterioration with age due to corrosion and wastage. Local deformation damage does not usually exert an immediate influence on the structural strength of the hull structure. However, as the ship ages, the amount and severity of such damage may increase.

Key words: local denting, mechanical damage, grooving corrosion, general corrosion, buckling.

6.1 Introduction

Ship hulls are occasionally damaged due to an unexpected accident such as collision or grounding, causing a large deformation of the hull structure and threatening both structural safety and the environment. Therefore, many studies have been performed on the consequences of collision and grounding. For instance, the committee that investigates the collision and grounding of ships has been established four times in the International Ship and Offshore Structures Congress (ISSC 1994, 1997, 2003, 2006a).

On the other hand, local deformation of structural members such as local denting occurs due to mechanical external cause and/or strength degradation caused by corrosion and wastage. Such local deformation damage does not usually exert an immediate influence on the structural strength of the hull structure. However, as the ship ages, the amount and severity of such damage may increase, and this type of damage often becomes the cause of other types of damage. The committee that treats local denting in association with the condition assessment of aged ships was established in ISSC (2006b).

This chapter outlines the generation mechanism, causes and features of damage by local deformation which might be caused in hull structural members and the measures that can be taken to prevent it. The causes of generation of local deformation damage can be roughly divided into mechanical external causes and deterioration with age due to corrosion and wastage of a structural member.

© 2008 Woodhead Publishing Limited

In Section 6.2, damage caused by mechanical external cause is outlined. The most typical example of this damage is local denting in hold structural members of bulk carriers during loading and unloading work using grabs, and local collapse due to the concentrated heavy cargo load.

In Section 6.3, damage caused by deterioration with age due to corrosion and wastage is outlined. The most typical example of this damage is local buckling along with thickness diminution of structural members due to corrosion and wastage.

6.2 Local deformation damage caused by mechanical external cause

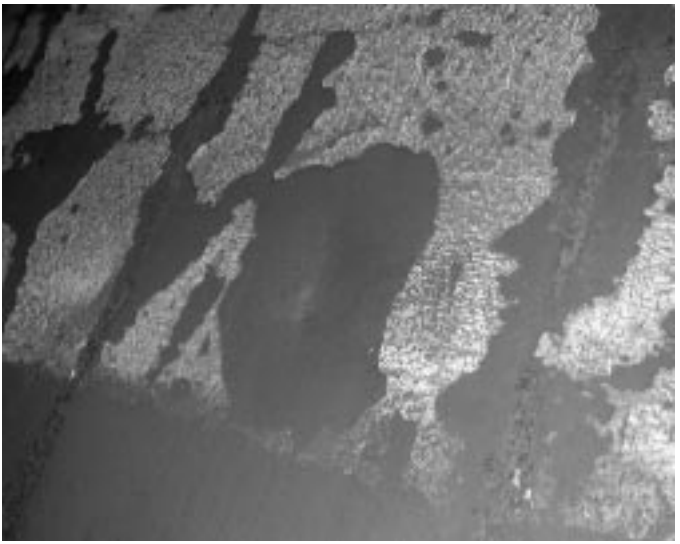
Local denting due to contact with quaysides, ice, underwater objects, etc., is a kind of mechanical damage. In the case of damage due to contact with other objects, although damage to the shell plating may look small from the outboard side, in many cases the internal members are heavily damaged (IACS 1999, 2002). On the other hand, since a cylindrical structure is axially loaded in offshore structures composed of steel pipes, the influence of local denting on structural strength is significant (Harding and Onoufriou 1995).

A local dent that is also a kind of mechanical damage may occur during regular loading and unloading work using a grab (Fig. 6.1). Especially in the case of bulk carriers, not only a local dent (Fig. 6.2) but also a continuous dent over the tank top plate (Fig. 6.3) is generally caused by collision between the grab and the structural members, contact between the bucket of the wheel loader



6.1 Grab loading.

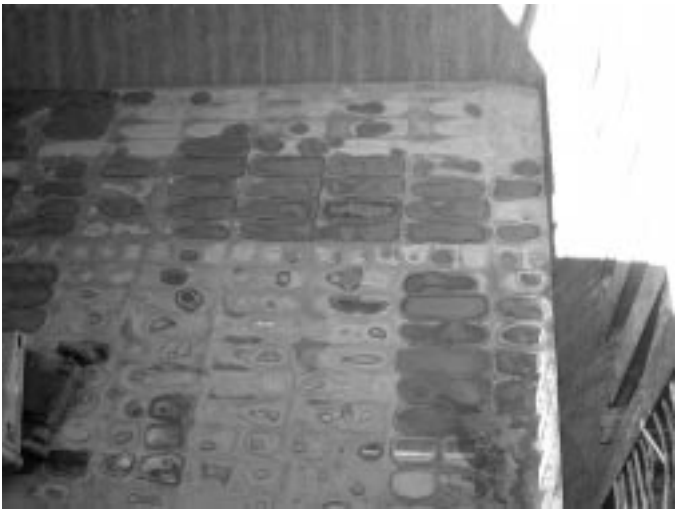
© 2008 Woodhead Publishing Limited



6.2 Local dent due to collision with the grab.

and the structural members during unloading work, the dead weight of the wheel loader, etc.

Moreover, in the case of a local dent due to the claw of the grab (Fig. 6.4), the extent of denting to the dented area can be large. A local dent due to the claw of the grab locally causes damage to the paint coating on the back side, and corrosion occurs in such paint-damaged areas (Fig. 6.5). However, although



6.3 Continuous dent over the tank top.

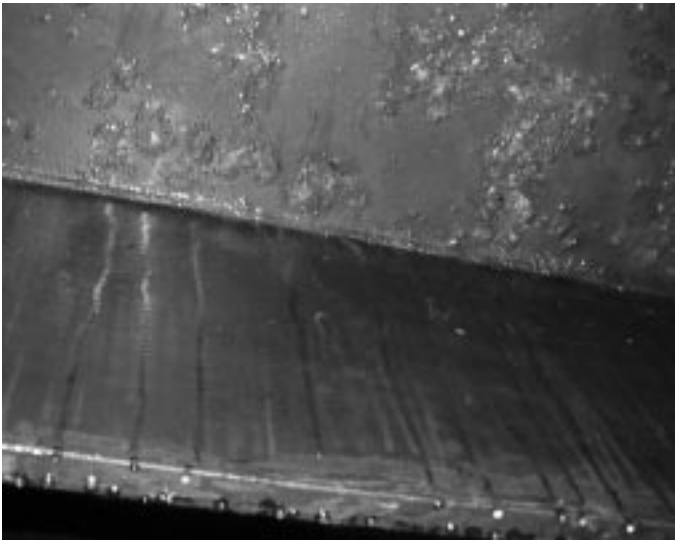
© 2008 Woodhead Publishing Limited



6.4 Local dent due to the claw of the grab.

local denting such as dimple imperfections seems to have little impact on the collapse strength (Dow and Smith 1984), the influence on strength of the local denting caused on the plate should not be disregarded (Luis *et al.* 2007).

In order to prevent the mechanical damage described above, careful operation of the grab crane is necessary. However, collision of the grab with structural



6.5 Damage of paint coating due to local dent.

© 2008 Woodhead Publishing Limited



6.6 A new unloading system.

members is unavoidable in unloading work when considering the handling efficiency. With regard to local denting caused by the collision of the grab with the structural members in the case of bulk carriers, a new unloading system (Fig. 6.6) might be preferable to the conventional system. However, such a new system would incur additional cost and is limited by the availability of suitable quays; it is not a fundamental procedure.

Since it can be assumed that a structure does not deform until it is directly compressed, a plate can be analyzed independently from its supporting structures due to the characteristic localization of deformation (Wang 2002). Therefore, having enough structural scantling in the inner bottom plate to withstand the grab load is both practical and fundamental. IACS (2005) set the requirements for plate thickness considering the weight of grab in the Common Structural Rules for Bulk Carriers (CSR-B). According to these rules, it is mandatory that the hold of a bulk carrier that carries dry bulk cargoes of cargo density 1.0 t/m^3 and above is designed considering a grab weight of more than 20 tonnes.

On the other hand, if the compressive load is acting in a plane of the structure, the load does not spread much and is limited for a certain length. Therefore, if the web girder structure is subjected to the locally compressed load, the structure would bend and form local dents due to buckling.

In the case of bulk carriers, extremely heavy cargoes such as steel coils may cause local denting. When an extremely heavy cargo is loaded in the hold of a bulk carrier, the arrangement of dunnage to distribute the concentrated load is important. In this case, it is necessary to decide the scantlings of structural members considering the concentrated load through the arranged dunnage. IACS (2005) also set out the requirements for plate thickness in a hold loaded by steel coils on a wooden support in the CSR-B.

The plate or the stiffener might collapse due to buckling by the local concentrated load. However, when such a local concentrated load is acting on the stiffeners, etc., the influence of local grooving corrosion on the strength should

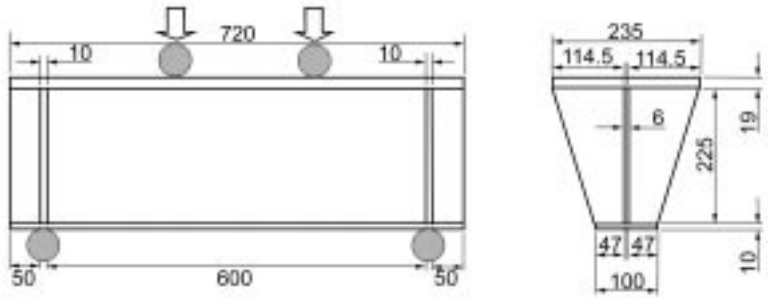
© 2008 Woodhead Publishing Limited



6.7 Conditions of the experiment.

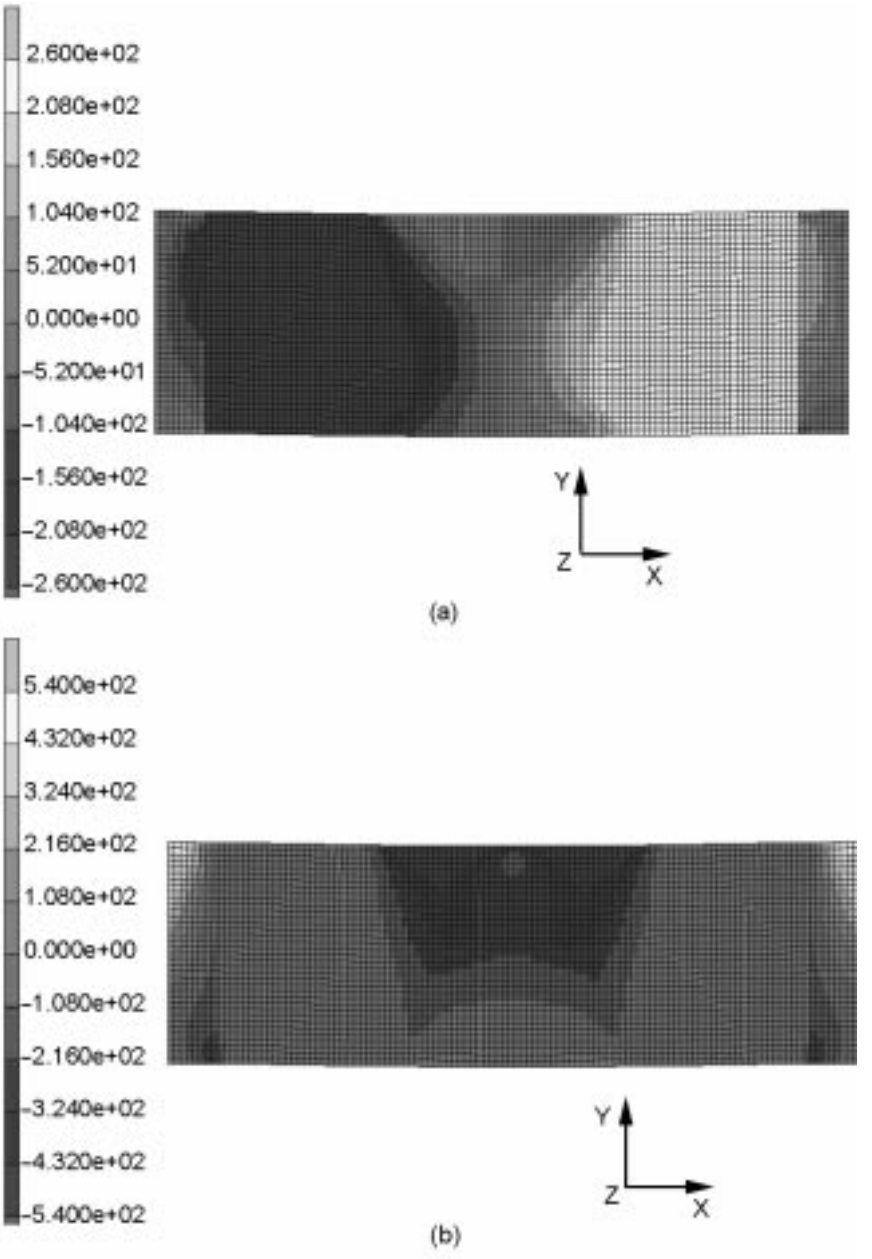
be taken into account in the case of aged ships, because grooving corrosion is usually observed along the weld line of aged welded structures. The strength depends on the form of collapse, which changes according to the progress of the grooving corrosion.

Matsushita *et al.* (2006) experimentally investigated the effect of grooving corrosion on the strength of fillet-welded joints for ship structures under compressive stress conditions. The experiments were done as shown in Fig. 6.7 by using almost a half-scale model of the hold frame of a cape size bulk carrier as shown in Fig. 6.8. Various artificial grooving corrosions were made along the welded joint between the hold frame and the shell plate to investigate the effect of grooving corrosion on the strength. Figure 6.9 shows the stress distribution in the web plate assessed by the finite element analysis. A large compressive stress due to the locally concentrated load was evaluated. According to their report, the buckling point in the web plate of the hold frame tends to shift toward the intersection according to the progress of grooving corrosion as shown in Fig. 6.10, and the ultimate strength of the stiffened panel decreases along with this. As schematically shown in Fig. 6.10, it is necessary to pay attention to the



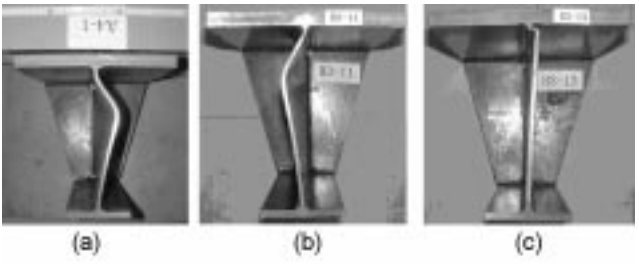
6.8 Model specimen (dimensions in mm).

© 2008 Woodhead Publishing Limited



6.9 Stress distribution in the web plate: (a) shear stress; (b) normal stress in the *Y*-direction.

© 2008 Woodhead Publishing Limited



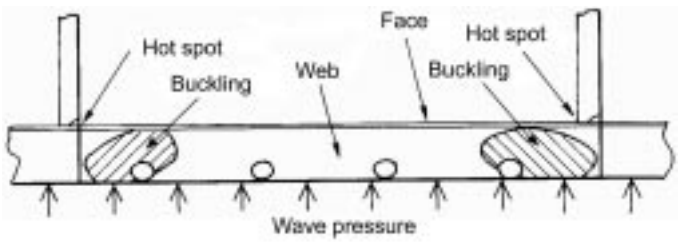
6.10 Different shapes of collapse depending on the progress of grooving corrosion: (a) no grooving corrosion; (b) grooving of 0.75 mm depth and 15 mm width; (c) grooving of 1.5 mm depth and 15 mm width (web thickness 6 mm).

change in the collapse form according to the local corrosion condition. This may affect the strength deterioration.

6.3 Local deformation damage caused by corrosion

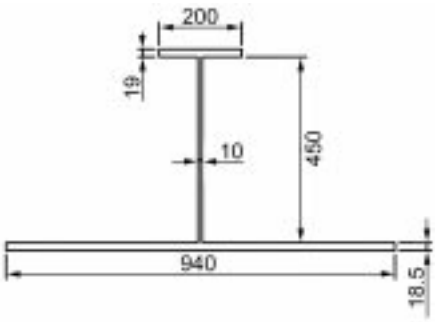
Corrosion is an unavoidable problem for aged ship structures. Its influence on the deterioration of strength becomes increasingly evident as corrosion generates and progresses. As a result, the form of damage may change from the one considered at the design stage. For instance, a longitudinal stiffener subjected to wave-induced pressure is generally designed according to the fatigue strength assessment of the connection of the longitudinal stiffener with the web frame and transverse bulkhead indicated as a 'hot spot' in Fig. 6.11. In general, the web of a stiffener is originally comparatively thin, and in addition is usually in a relatively corrosive environment because of the deposit of rusty sludge. Therefore, its deterioration in strength due to the generation and progress of corrosion becomes a problem. In this case, buckling would occur at the end of the span where the shear stress is high, as shown in Fig. 6.11, because of the deterioration of buckling strength of the web of the stiffener as the corrosion progresses.

When the deformation of the web by buckling is repeated due to wave load fluctuation, the progress of corrosion becomes accelerated and, finally, breaking



6.11 An example of the damage to the side longitudinal stiffener.

© 2008 Woodhead Publishing Limited



6.12 Cross-sectional view of the analyzed hold frame (dimensions in mm).

fracture might occur at the buckling area. Moreover, the fatigue crack might be initiated at the hot spot location because of the increased stress of the face plate of the stiffener caused by the decrease of rigidity in the web of the stiffener.

Evaluation of the ultimate strength by FEM analysis which models the hold frame of a bulk carrier subjected to lateral hydraulic pressure is introduced here (Matsushita *et al.*, 2007). In their study, the effect of grooving corrosion on the ultimate strength of hold frames subjected to lateral pressure was investigated based on a series of elastoplastic large deflection FE analyses.

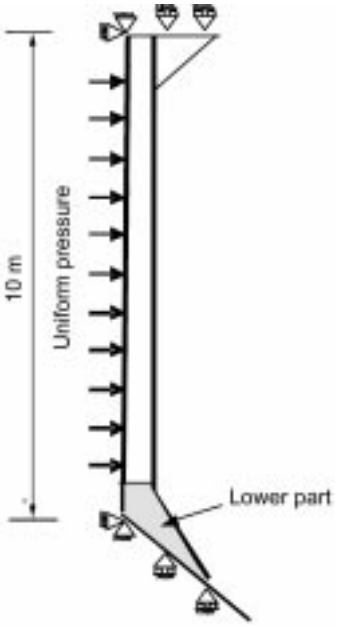
One hold frame with a half-frame space of side shell plate on both sides of the hold frame is modeled. The tripping bracket is not modeled in the analyses. Figure 6.12 shows the cross-sectional view of analyzed hold frames that consist of web, face and side shell plates with thicknesses of 10 mm, 19 mm and 18.5 mm, respectively, where the web thickness at the lower part of the hold frame is 12 mm.

Symmetrical conditions are assumed in the direction of the ship length. The simplified boundary conditions are applied at the upper and lower edges of the model and a uniformly distributed load is applied to the side shell plate from the outside as schematically shown in Fig. 6.13. The geometrical model of the hold frame used in the FE analyses is shown in Fig. 6.14. Small elements are used in the vicinity of the connection between the web and side shell plates for modeling the grooving corrosion. The depth and width of grooving corrosion in the web and side shell plates are assumed to be the same.

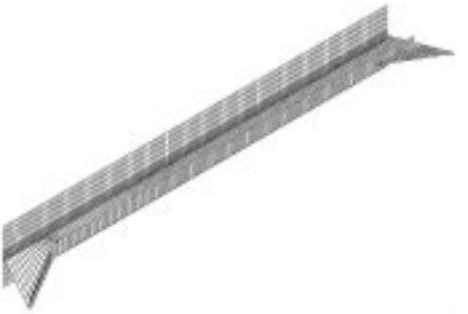
Figure 6.15 shows the deformation of the hold frame with general corrosion in the web plate when it reached ultimate strength. In this simulation case, a thickness diminution of 2.5 mm, which is 25% of the original thickness, is assumed, but no grooving corrosion is assumed. Local denting occurs due to buckling at the end of the span as well as in the example shown in Fig. 6.11.

Figure 6.16 shows the degradation of ultimate strength as a function of the diminution in thickness of the web plate. The results show that the degradation of ultimate strength is almost proportional to the progress of corrosion wastage of the web plate. Where only general uniform corrosion exists in the web plate,

© 2008 Woodhead Publishing Limited



6.13 Boundary conditions of the analyzed hold frame.

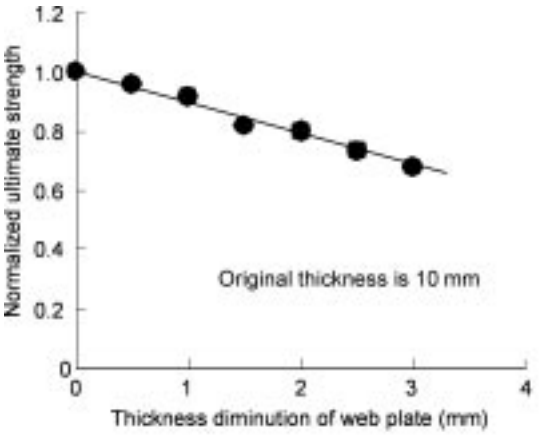


6.14 Geometrical model in FE analysis.



6.15 Collapse mode of the hold frame with general corrosion in the web plate.

© 2008 Woodhead Publishing Limited

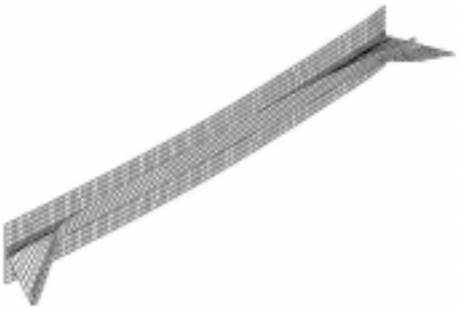


6.16 Degradation of ultimate strength according to the general uniform thickness diminution of the web plate.

local buckling at the upper and lower parts of the hold frame can be observed as shown in Fig. 6.15.

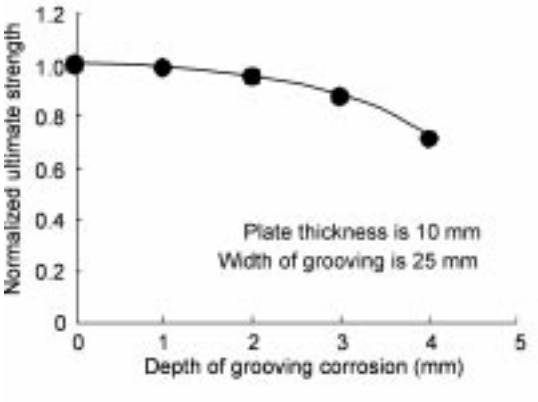
The grooving corrosion is usually generated along the weld line in an actual structure. In the study of Matsushita *et al.* (2007), grooving corrosion is modeled assuming that the depth and width of the grooving corrosion in the web and side shell plates are the same. Figure 6.17 shows the deformation of the hold frame with grooving corrosion along the weld line when it reached ultimate strength. In this simulation case, a grooving depth of 3 mm and a grooving width of 25 mm, which is a relatively excessive grooving corrosion condition, are assumed. The collapse mode of the hold frame is lateral–torsional deformation.

Figure 6.18 shows the degradation of ultimate strength as a function of the progress of grooving corrosion. The results show that the degradation of ultimate strength is gradual at the beginning of grooving corrosion but accelerates as



6.17 Collapse mode of the hold frame with grooving corrosion along the weld line.

© 2008 Woodhead Publishing Limited

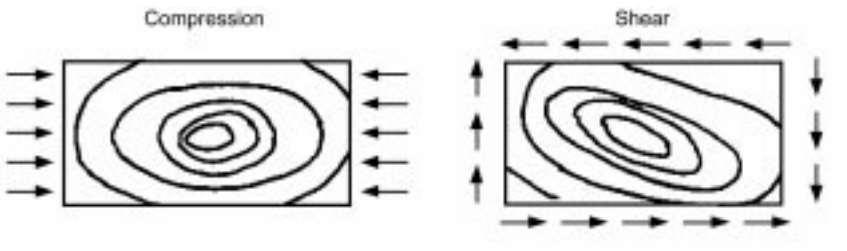


6.18 Degradation of ultimate strength according to the progress of grooving corrosion.

grooving corrosion progresses. Although the collapse mode of the hold frame is local buckling at the end of the hold frame at the start of grooving corrosion, the collapse mode changes to lateral–torsional deformation as grooving corrosion progresses, and this change of collapse mode causes a large degradation of ultimate strength. However, such a change of collapse mode from local buckling to lateral–torsional deformation was said to be a condition in which grooving progresses excessively.

Moreover, attention needs to be paid to the strength degradation of the panel which composes the hull structure due to corrosion. Since the buckling strength of the panel is proportional to the factor of (plate thickness/spacing between the stiffeners)^2, corrosion has a major influence on the thickness diminution of the plate. Special attention needs to be paid to the buckling strength degradation due to corrosion for the primary strength member. Even though elastic buckling does not cause permanent deformation, it may cause coating damage (IACS 1999, 2002). Since the coating damage encourages the progress of corrosion, the buckling strength will decrease if early maintenance is not done.

In order to prevent the occurrence of buckling in which an overall reduction in thickness due to corrosion is observed, additional internal stiffening may need



6.19 Convex deformation due to buckling.

© 2008 Woodhead Publishing Limited

to be provided (IACS 1999, 2002). In general, as shown in Fig. 6.19, the form of convex deformation of the plate due to buckling depends on the type of buckling. In the case of compressive buckling, a ridge of convex deformation is formed perpendicular to the side. On the other hand, in the case of shear buckling, a ridge of convex deformation is formed at an angle to the side. Since it is necessary to arrange an additional stiffener perpendicular to the ridge of convex deformation due to buckling, the load pattern of the object part needs to be considered when an additional stiffener is arranged.

6.4 Conclusions

The influence of local deformation damage in hull structures on the structural integrity of the hull may be limited, but it may cause damage of other types. Local deformation damage includes damage caused by mechanical external causes and damage caused along with buckling as a result of degradation of strength due to corrosion. Mechanical external causes include unexpected causes such as contact with floating objects and regular causes such as contact with grabs and the concentrated heavy load in bulk carriers. Prior measures to minimize the effects of regular causes can be taken at the design stage.

It is important to consider the change of collapse form caused by the influence of local grooving corrosion when a concentrated load is loaded, as well as by progressive damage caused by degradation of strength due to such corrosion. Thus, measures to counter local deformation damage should be examined in association with a local corrosion situation.

Up to now, local denting has received less attention, with the exception of local denting in cylindrical pipework in offshore structures composed of steel pipes. Local denting in ship structures, especially in relation to aging, has hardly been considered, because its influence on structural integrity is small. However, it seems desirable to examine the influence of local corrosion on the generation of local denting in the future in association with further research on deterioration due to aging of such structures.

6.5 References

Dow, R. S. and Smith, C. S., 1984, 'Effects of localized imperfections on compressive strength of long rectangular plates', *Journal of Constructional Steel Research*, Vol. 4, pp. 51–76

Harding, J. E. and Onoufriou, A., 1995, 'Behavior of ring-stiffened cylindrical members damaged by local denting', *Journal of Constructional Steel Research*, Vol. 33, Issue 3, pp. 237–257

IACS, 1999, General Cargo Ships – Guidelines for surveys, assessment and repair of hull structures, Witherby

IACS, 2002, Bulk Carriers – Guidelines for surveys, assessment and repair of hull structures, Witherby

© 2008 Woodhead Publishing Limited

IACS, 2005, IACS Common Structural Rules for Bulk Carriers
ISSC, 1994, International Ship and Offshore Structures Congress, Report of Committee V.6 Structural Design for Pollution Control
ISSC, 1997, International Ship and Offshore Structures Congress, Report of Committee V.4 Structural Design against Collision and Grounding
ISSC, 2003, International Ship and Offshore Structures Congress, Report of Committee V.3 Collision and Grounding
ISSC, 2006a, International Ship and Offshore Structures Congress, Report of Committee V.1 Collision and Grounding
ISSC, 2006b, International Ship and Offshore Structures Congress, Report of Committee V.6 Condition Assessment of Aged Ships
Luis, R. M., Witkowska, M. and Guedes Soares, C., 2007, 'Collapse behavior of damaged panels with a dimple imperfection', *Proc. OMAE 2007*
Matsushita, H., Nakai, T. and Yamamoto, N., 2006, 'Effect of grooving corrosion on static strength of fillet welded joints for hull structures under compression induced by patch loading', *Proc. ISOPE 2006*
Matsushita, H., Nakai, T. and Yamamoto, N., 2007, 'Effect of grooving corrosion in the vicinity of fillet welded joint on ultimate strength of hold frame', *Proc. ISOPE 2007*
Wang, G., 2002, 'Some recent studies on plastic behavior of plates subjected to large impact loads', *Trans. ASME, Journal of Offshore Mechanics and Arctic Engineering*, Vol. 124, pp. 125–131

© 2008 Woodhead Publishing Limited

Part III

Residual strength of aged structures

© 2008 Woodhead Publishing Limited

7

Corroded structures and residual strength

T NAKAI, Nippon Steel Corporation, Japan and
N YAMAMOTO, Research Institute of Nippon Kaiji Kyokai, Japan

Abstract: This chapter discusses a method of probabilistic modeling of corrosion to predict corrosion diminution behavior that is probabilistic in nature. This chapter also discusses the effect of general corrosion on overall strength such as hull girder strength under longitudinal bending, and the effect on local strength of localized corrosion such as pitting corrosion observed in structural members in cargo holds of bulk carriers.

Key words: probabilistic model of corrosion, general corrosion, pitting corrosion, hull girder strength, ultimate strength.

7.1 Introduction

It is generally said that corrosion is one of the dominant life-limiting factors of ships because hull structural members are exposed to corrosive environments after commissioning and aging effects such as thickness diminution due to corrosion may be unavoidable. In order to ensure the structural integrity of ships, it is of crucial importance to understand the corrosion process, estimate the corrosion rate and evaluate the effect of corrosion wastage not only on overall strength but also on local strength accurately. Since a corrosion phenomenon is probabilistic in nature, probabilistic modeling is necessary when predicting corrosion diminution behavior. When assessing the effect of corrosion on overall strength such as hull girder strength under longitudinal bending, the amount of thickness diminution due to corrosion of each member must be predicted, because the thickness diminution behavior depends on the corrosive environment each member is subjected to. Furthermore, a difficulty in evaluating the effect of localized corrosion such as pitting corrosion on local strength is that the shape, size and distribution of the corrosion pits must be precisely predicted.

This chapter presents a method of probabilistic modeling of corrosion, the effect of general corrosion on hull girder strength and the effect on local strength of pitting corrosion observed in structural members in cargo holds of bulk carriers.

7.2 Probabilistic modeling of corrosion

Corrosion in ship structures is affected by many factors such as coatings, cargoes, temperature, humidity, chlorides, sulfur dioxide, oxygen, pH, flow

© 2008 Woodhead Publishing Limited

velocity and so on. Studies on modeling of the corrosion process are found in Paik (2004), Paik *et al.* (1998, 2003a, 2003b, 2004a), Guedes Soares and Garbatov (1999), Garbatov *et al.* (2004, 2005) and Qin and Cui (2002, 2003), among others. In order to evaluate the corrosion condition of ship structural members, Yamamoto and Ikegami (1998) developed a probabilistic corrosion model which could evaluate the generation and progress of corrosion quantitatively. In the probabilistic corrosion model, the following assumptions were made:

1. Corrosion does not occur as long as the anti-corrosive paint coating remains effective, because it is general practice to apply anti-corrosive paint coating to hull structural members. When the effectiveness of the anti-corrosive paint coating deteriorates, active pitting points which have a potential to turn into progressive pitting points are generated.
2. The active pitting points thus generated transform into progressive pitting points associated with the progress of actual corrosion over time.
3. In the specific areas where progressive pitting points are generated, they start growing individually.

A state of no corrosion is assumed before the generation of pitting points. Generally, it is considered that corrosion and wear observed in structural members are assumed to be the consequences of an extremely large number of generated progressive pitting points growing individually (Tsuji *et al.*, 1983).

Since the above-mentioned three processes are probabilistic, the following probabilistic models can be introduced individually. In general, a log-normal distribution is applied to describe the probabilistic characteristics of life. Hence, it is assumed that the life of an anti-corrosive paint coating T_0, which is defined as the period before active pitting points are generated, follows the log-normal distribution as given below:

$$f_{T_0}(t) = \frac{1}{\sqrt{2\pi}\sigma_0 t} \exp\left\{-\frac{(\ln t - \mu_0)^2}{2\sigma_0^2}\right\} \tag{7.1}$$

where μ_0 is the mean of $\ln(T_0)$, and σ_0 is the standard deviation of $\ln(T_0)$.

The transition time from active pitting points to progressive pitting points T_r is assumed to follow the exponential distribution (Matoba *et al.*, 1994):

$$g_{T_r}(t) = \alpha \cdot \exp(-\alpha t) \tag{7.2}$$

where α is the inverse of mean transition time.

The progress behavior of pitting points after generation can be expressed by the following equation (Shreir, 1976):

$$z(\tau) = a \cdot \tau^b \tag{7.3}$$

where τ denotes the time elapsed after the generation of progressive pitting

© 2008 Woodhead Publishing Limited

points, z is the depth of pitting, and a and b are coefficients which govern the characteristics of the corrosion progress. Coefficient a in Eq. (7.3) is a random variable following the log-normal distribution:

$$h_a(x) = \frac{1}{\sqrt{2\pi}\sigma_a x} \exp\left\{-\frac{(\ln x - \mu_a)^2}{2\sigma_a^2}\right\} \qquad 7.4$$

where μ_a is the mean of $\ln(a)$, and σ_a is the standard deviation of $\ln(a)$. The exponent coefficient b depends on the environmental conditions, etc. (Komai *et al.*, 1987; Kondo, 1987; Masuda *et al.*, 1986).

Corrosion found in ships' hull structures is generally divided into two types, general corrosion and localized corrosion. Pitting corrosion is categorized as one form of localized corrosion. It is assumed that the shape of a pit is a part of a sphere with a ratio of diameter to depth of 5:1 in order to describe the phenomena of generation and progress of corrosion pits which lead to general corrosion (Yamamoto and Ikegami, 1998), based on the findings by Matoba *et al.* (1994). Parameters included in the probabilistic corrosion model can be identified using the plate thickness measurement records. When the effect of surface unevenness due to predominant pitting corrosion on local strength is evaluated, it is necessary to reproduce the shape of corrosion pits accurately. In handling such problems, such as the effect on local strength of predominant pitting corrosion observed in structural members in cargo holds of bulk carriers, it is necessary to reconsider the shape of pit as will be described later.

7.3 Degradation of hull girder strength

Once parameters in the probabilistic corrosion model are identified for each structural member based on the plate thickness measurement records, etc., the corrosion diminution behavior of each structural member can be predicted. The predicted results can be used to assess the effect of corrosion on the overall strength such as hull girder longitudinal strength.

In order to demonstrate the scatter of the amount of diminution considering the effect of corrosion, examples of statistics such as average, standard deviation and coefficient of variance in the corrosion condition of the sample Single Hull Very Large Crude oil Carrier (SHVLCC, length 315 m, breadth 59 m, depth 30.53 m, DWT 281,018 ton) at the age of 20 years calculated by the probabilistic corrosion model are summarized in Table 7.1 (Yamamoto and Yao, 2001). In this table, 'Area' denotes the sectional area of each structure composed of panel plates and stiffeners. In this analysis, initial collapse load and ultimate strength were obtained by a simplified progressive analysis (Yao and Nikolov, 1991, 1992) based on the Smith method (Smith, 1977; Smith and Dow *et al.*, 1981).

Statistics show that the scatter of the amount of thickness diminution in each member due to corrosion is very large. On the other hand, scatter of sectional

© 2008 Woodhead Publishing Limited

Table 7.1 Statistics of diminution due to corrosion (adapted from Yamamoto and Yao, 2001)

			Average	Standard deviation	Coefficient of variance
Diminution	Upper	Plate	1.57	0.955	60.85%
		Stiffener web	1.52	0.968	63.86%
	Side	Plate	0.78	0.498	63.65%
		Stiffener web	1.08	0.501	46.53%
		Stiffener face	1.34	0.842	62.76%
	Bottom	Plate	2.39	1.773	74.06%
		Stiffener web	1.12	0.561	49.92%
		Stiffener face	1.16	0.572	49.47%
	Left bulkhead	Plate	1.24	0.910	73.50%
		Stiffener web	1.12	0.484	43.15%
		Stiffener face	1.13	0.523	46.08%
Area*		Upper	1,403,241	5,233	0.37%
		Side	1,781,982	3,798	0.21%
		Bottom	1,714,416	8,722	0.51%
		Left bulkhead	1,572,933	4,984	0.32%
Section modulus		Upper	62.37	0.161	0.26%
		Bottom	71.76	0.230	0.32%
Initial collapse load			1.64E+06	2.11E+04	1.29%
Ultimate strength			1.78E+06	5.91E+03	0.33%

* 'Area' denotes the sectional area of each structure (m^2) composed of panel plates and stiffeners.

area, cross-section modulus and ultimate strength are negligibly small. This means that the effect of the stochastic nature of corrosion phenomena can be neglected in the assessment of hull girder strength taking into account corrosion effects. This result confirmed that it is possible to satisfactorily assess the hull girder strength taking into account corrosion effects by assuming a uniform corrosion condition based on the average amount of thickness diminution in each structural member. It is also confirmed that the hull girder strength diminishes almost deterministically, even if there is a wide scatter in the thickness diminution of each structural member.

7.4 Pitting corrosion

Pitting corrosion is categorized as one form of localized corrosion. For example, corrosion pits with a conical shape are typically observed in coated structural members in cargo holds of bulk carriers which carry coal and iron ore (Nakai and Yamamoto, 2007; Nakai *et al.*, 2004b, 2005, 2007b, 2007c). In a typical case, pitting corrosion of this type is generated under heavy blisters, and when

© 2008 Woodhead Publishing Limited

the heavy blisters are removed by sand-blasting, an unevenly corroded surface with pitting corrosion will appear. The DOP (degree of pitting intensity), which is defined as the ratio of the pitted surface area to the entire surface area, is a promising parameter for the evaluation of residual strength/thickness of plates with pitting corrosion, because this parameter could be identified from observation of the surface corroded conditions of pitted plates while parameters such as average thickness loss or average thickness loss at the minimum cross-section could not be determined directly from observation. Each corrosion pit is hidden under a rust blister, and the diameters of the rust blister and the corresponding pit are almost the same. This fact suggests that it is possible to obtain DOP values by estimating the degree of rust blister intensity (ratio of the surface area covered with rust blisters to the entire surface area). Figure 7.1 gives examples of corroded webs taken from a 13-year-old bulk carrier with a wide variety of DOP after sand-blasting. This figure demonstrates well the generation and progress of pitting corrosion. Figure 7.2 shows an example of a cross-sectional view of an extremely corroded web. It can be seen that the surfaces of the webs are very uneven due to pitting corrosion. It has been shown that the ratio of the diameter to the depth of typical pits is approximately in the range between 8:1 and 10:1.

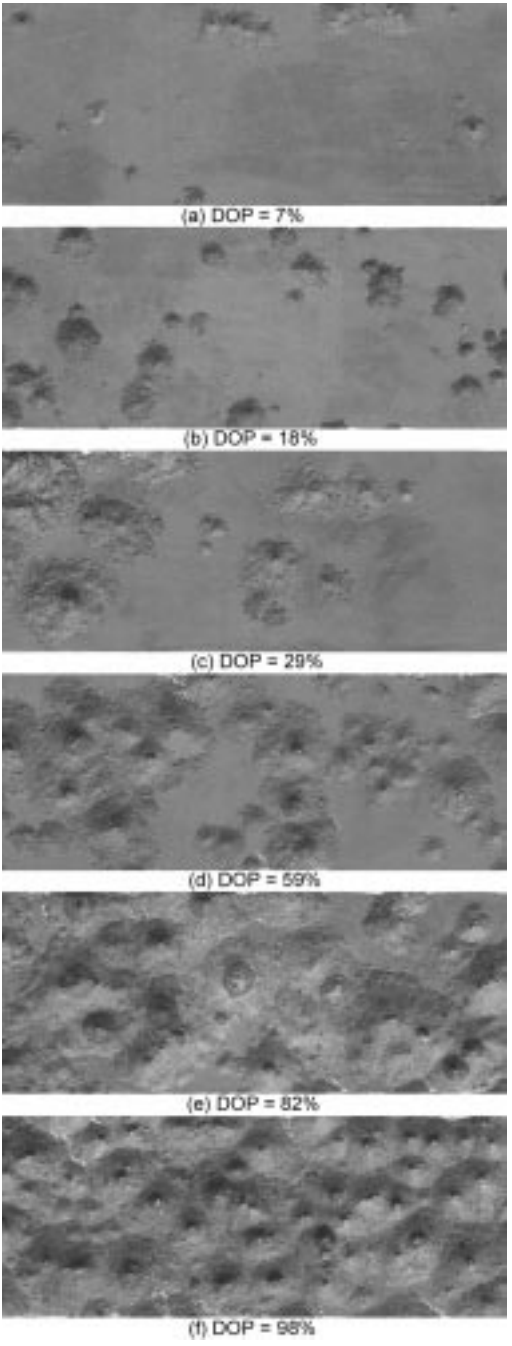
The geometrical characteristics of pitted hold frames can be investigated in detail using laser displacement sensors, etc. Figure 7.3 shows the relationship between statistics of corroded condition and DOP for the webs and face plates taken from the 13-year-old bulk carrier, where the measured area of the webs is 80 mm × 200 mm (see Fig. 7.1) and that of the face plates is 50 mm × 200 mm. It can be seen that the average thickness diminution and standard deviation of thickness diminution vary with small scatter bands, and the DOP reaches 100% when the average thickness diminution on one side exceeds approximately 2 mm. A trend is observed in that the form of corrosion changes from pitting corrosion to general corrosion with further progress of corrosion after DOP reaches 100%. The probability distribution of diminution varies from exponential to normal depending on DOP and thickness diminution (Nakai and Yamamoto, 2007) and it is considered that the probability distribution of diminution follows a normal distribution when the form of corrosion changes almost completely to general corrosion with the progress of corrosion. Evaluation of residual strength of pitted plates is difficult, because corroded and non-corroded regions coexist and the plates have uneven surfaces due to pitting corrosion.

7.4.1 Probabilistic modeling of pitting corrosion

Formulation of pit shape

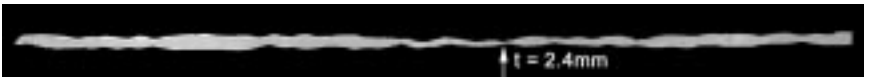
For the purpose of establishing a method for the strength evaluation of corroded structural members, it is necessary to conduct a series of tests and/or numerical

© 2008 Woodhead Publishing Limited



7.1 Examples of corroded surface conditions of webs of hold frames (80 mm × 200 mm, 13-year-old bulk carrier): (a) DOP = 7%; (b) DOP = 18%; (c) DOP = 29%; (d) DOP = 59%; (e) DOP = 82%; (f) DOP = 98%.

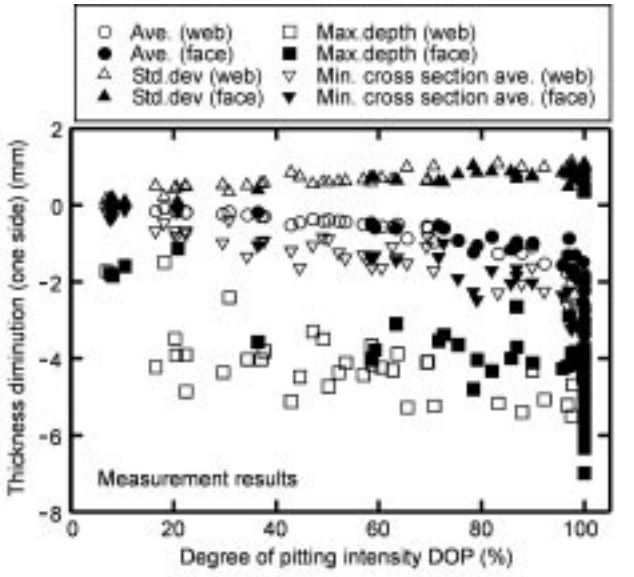
© 2008 Woodhead Publishing Limited



7.2 Cross-sectional view of actual corroded web (original thickness t_0 = 10 mm, 13-year-old bulk carrier).

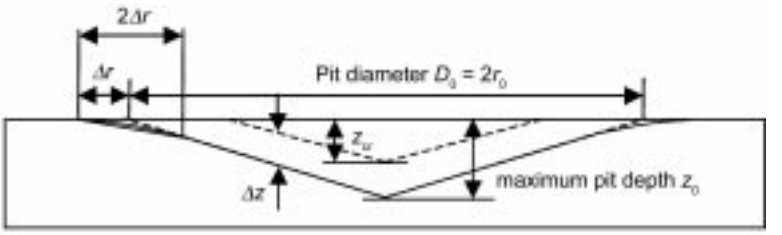
analyses with structural members having a wide variety of corroded surface conditions. Since the corrosion phenomenon is probabilistic and time-variant in nature, it is quite difficult to obtain corroded members fitting the objective of the investigation. For this reason, it is important to develop a simulation method which can reproduce the corroded surfaces.

In the corrosion model described earlier, the shape of corrosion pits is assumed to be a part of a sphere, and the ratio of the pit diameter to its depth is 5:1. It is well known that the shape of corrosion pits varies depending on the corrosive environment, etc., and when surface unevenness due to pitting corrosion is predominant, it significantly affects the reduction of local strength of corroded structural members. Therefore, when the effect of predominant pitting corrosion on the local strength of hull structural members is evaluated, the shape of the corrosion pit must be precisely described. The corrosion model described earlier can be updated to reproduce the generation and progress of pitting corrosion observed in hold frames of bulk carriers by appropriately modeling the shape of corrosion pits. As mentioned earlier, the shape of typical corrosion pits observed in hold frames of bulk carriers is basically a circular



7.3 Relationship between statistics of corroded condition and DOP (measurement results, adapted from Nakai and Yamamoto, 2007).

© 2008 Woodhead Publishing Limited



7.4 Schematic cross-sectional view of corrosion pit.

cone and the ratio of diameter to depth is in the range between 8:1 and 10:1. The edge of a corrosion pit becomes dull as it gets larger, as schematically shown in Fig. 7.4. Therefore, it is assumed that pits grow keeping a similar figure when the maximum pit depth z_0 is less than the critical pit depth z_{cr} (= 3 mm). When z_0 becomes larger than or equal to z_{cr}, the rate of corrosion progress at the pit edge is assumed to be twice as great as in the case where pits grow keeping a similar figure. The shape of the corrosion pit can be modeled as follows:

$$W(\mathbf{x}-\mathbf{x_0}, r_0, \delta_0) = \max\{W_0(\mathbf{x}-\mathbf{x_0}, r_0, \delta_0), W_d(\mathbf{x}-\mathbf{x_0}, r_0, \delta_0)\} \quad 7.5$$

where

$$W_0(\mathbf{x}-\mathbf{x_0}, r_0, \delta_0) = \delta_0\left(\max\left\{0, r_0 - \sqrt{(x-x_0)^2+(y-y_0)^2}\right\}\right) \quad 7.6$$

$$W_d(\mathbf{x}-\mathbf{x_0}, r_0, \delta_0, r_{cr}) = \frac{\delta_0}{2}\left(\max\left\{0, 2r_0 - r_{cr} - \sqrt{(x-x_0)^2+(y-y_0)^2}\right\}\right) \quad 7.7$$

$$\mathbf{x_0} = (x_0, y_0), \mathbf{x} = (x, y) \quad 7.8$$

$$\delta_0 = \frac{z_0}{r_0} = 2\frac{z_0}{D_0} = \frac{\Delta z}{\Delta r}, r_{cr} = \frac{z_{cr}}{\delta_0} \quad 7.9$$

where $\mathbf{x_0}$ and $\mathbf{x}$ are the vector of the pit center and that of the evaluated point, respectively; z_0 and r_0 are the depth and radius, respectively, of a corrosion pit at $\mathbf{x_0}$; and r_{cr} is the radius of a pit with a depth of z_{cr}. It is assumed that δ_0 is a random variable following the normal distribution, as follows:

$$f_\delta(x) = \frac{1}{\sqrt{2\pi}\lambda\mu_\delta}\exp\left\{-\frac{(x-\mu_\delta)^2}{2(\lambda\mu_\delta)^2}\right\} \quad 7.10$$

Calculation procedure

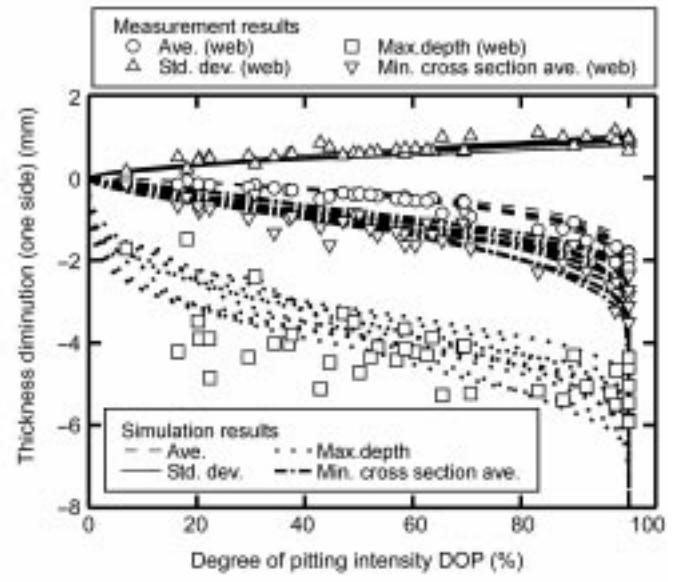
A procedure of simulating pit distributions using the probabilistic corrosion model can be described as follows:

© 2008 Woodhead Publishing Limited

1. Set an expected number of active pitting points in a unit area and the area size under consideration, and determine the positions of active pitting points, which are assumed to be randomly distributed.
2. The effective coating life T_0, the transition time from active pitting points to progressive pitting points T_r, the coefficient a in the corrosion growth law, and parameters in the shape function of each active pitting point are independently determined.
3. The generation and progress of pitting points are calculated with respect to time.
4. When some corrosion pits overlap each other, the thickness diminution at the points in the overlapped area is represented by the largest diminution among the overlapping pits.

Simulation results

Ten simulations have been made to obtain corroded plate surface conditions, where the target area is 200 mm × 80 mm. The simulated thickness diminution behavior in terms of DOP is shown in Fig. 7.5, where measurement results are also plotted. It is seen from this figure that the trend of thickness diminution behavior can be reproduced well by the probabilistic corrosion model.



7.5 Relationship between statistics of corroded condition and DOP (comparison of simulation results with measurement results, adapted from Nakai and Yamamoto, 2007).

© 2008 Woodhead Publishing Limited

7.5 Equivalent thickness of plates with pitting corrosion

As for the effect of pitting corrosion on the ultimate strength of structural members, Daidola *et al.* (1997) proposed a mathematical model to estimate the residual thickness of pitted plates using the average and maximum values of pitting data or the effect of thickness reduction due to pitting data or the number of pits and the depth of the deepest pit, and presented a method to assess the effect of thickness reduction due to pitting on local yielding and plate buckling based on the probabilistic approach. Paik *et al.* (2004b, 2004c) studied the ultimate strength reduction behavior of pitted plate elements under axial compressive loads and in-plane shear loads, and developed closed-form formulae for the ultimate strength. Amlashi and Moan (2005) investigated the residual strength of pitted stiffened plates under combined loading. The shape of corrosion pits is assumed to be cylindrical in these studies. It is well known that the shape of corrosion pits varies depending on the corrosive environment, etc. Therefore, investigation of the actual state of pitting corrosion observed in target structural members is quite important, and it is necessary to take into account the shape of corrosion pits when the effect of pitting corrosion on strength is investigated. Up until now, corrosion pits with a circular cone shape observed in hold frames of bulk carriers have been treated in only a few studies (Nakai and Yamamoto, 2007; Nakai *et al.* 2004a, 2004b, 2005, 2006, 2007a, 2007b, 2007c).

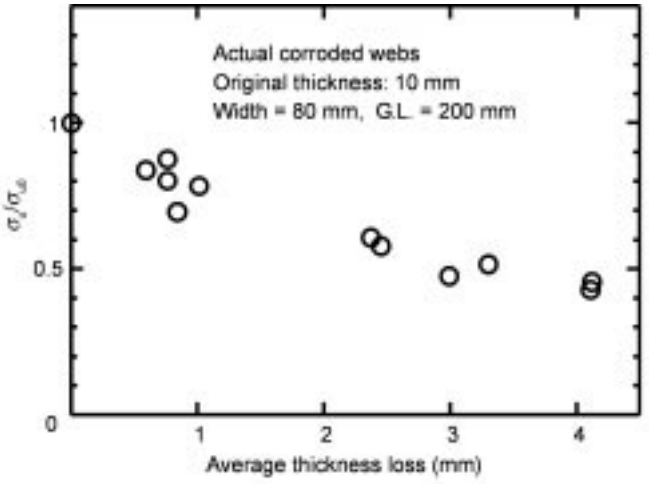
Two approaches were suggested by Paik *et al.* (2004b) to evaluate the ultimate strength of steel plates with pitting corrosion. One approach is to evaluate the equivalent thickness t_e which is defined as the thickness of a uniformly corroded plate with the same ultimate strength as the plate with pitting corrosion. The other approach is to directly evaluate the ultimate reduction due to pitting corrosion. When the ultimate strength of a pitted plate is considered from the viewpoint of when to renew, the equivalent thickness t_e is a more useful parameter because it can be directly compared with the allowable thickness diminution specified in rules for uniformly corroded plates, and it is possible to determine whether the diminution level of the pitted plates reaches the maximum allowable level or not.

7.5.1 Residual strength of local structural members

Tensile strength of plate elements

This section investigates the effect of pitting corrosion on the tensile strength of plate elements with pitting corrosion. Test specimens were taken from actual corroded hold frames of a bulk carrier which carries coal and iron ore. Figure 7.6 gives the relationship between nominal tensile strength and average thickness loss, where nominal tensile strength $\sigma_{nominal}$ is defined by the following equation:

© 2008 Woodhead Publishing Limited



7.6 Normalized tensile strength vs. average thickness loss (t_0 10 mm, width 80 mm, G.L. 200 mm).

$$\sigma_{\text{nominal}} = \frac{P_{\max}}{A_0} \tag{7.11}$$

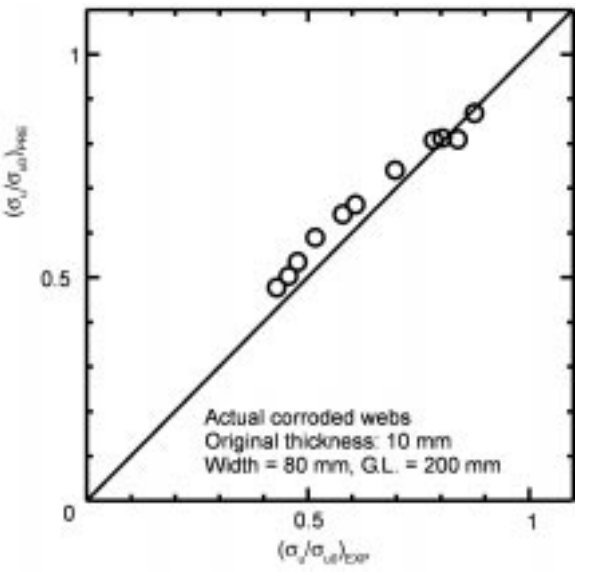
where $P_{\max}$ and A_0 are the maximum load and the original cross-sectional area, respectively, and the original cross-sectional area A_0 is defined as the original thickness multiplied by the width of specimens. As shown in this figure, nominal tensile strength decreases with the increase of average thickness loss. A trend for the uniformly corroded plates is shown by a solid line in this figure, when it is assumed that the tensile strength of uniformly corroded plates is proportional to residual thickness. It is clear that the reduction of nominal tensile strength of the plates with pitting corrosion is larger than those with general (uniform) corrosion in terms of average thickness loss. It has been shown that total elongation decreases drastically in the case where pitting corrosion exists (Nakai *et al.*, 2004b). It is noted that the deformation capacity of plates with pitting corrosion under tensile load is small. It is considered that the reduction of total elongation is closely related to localization of plastic deformation at the corrosion pits (Sumi *et al.*, 2006).

Figure 7.7 shows the prediction results of tensile strength, where normalized tensile strength is predicted using the following equation:

$$\left(\frac{\sigma_{\text{u}}}{\sigma_{\text{u0}}}\right)_{\text{PRE}} = \frac{t_{\text{ave,min}}}{t_0} \tag{7.12}$$

where $t_{\text{ave,min}}$ and t_0 depict the average thickness at the minimum cross-section and the original thickness, respectively. As can be seen in Fig. 7.7, the results predicted by Eq. (7.12) show good agreement with the experimental ones. Average thickness at the minimum cross-section is one of the dominant factors affecting the tensile strength of members with pitting corrosion. The equivalent

© 2008 Woodhead Publishing Limited



7.7 Prediction of tensile strength using average thickness at minimum cross-section (t_0 10 mm, width 80 mm, G.L. 200 mm).

thickness of plates with pitting corrosion for tensile strength is almost equal to the average thickness at the minimum cross-section, where the equivalent thickness t_e is defined by the thickness of a uniformly corroded plate with the same tensile strength as a plate with pitting corrosion, as follows:

$$t_e = t_{ave,min} \qquad \text{for tensile strength} \qquad 7.13$$

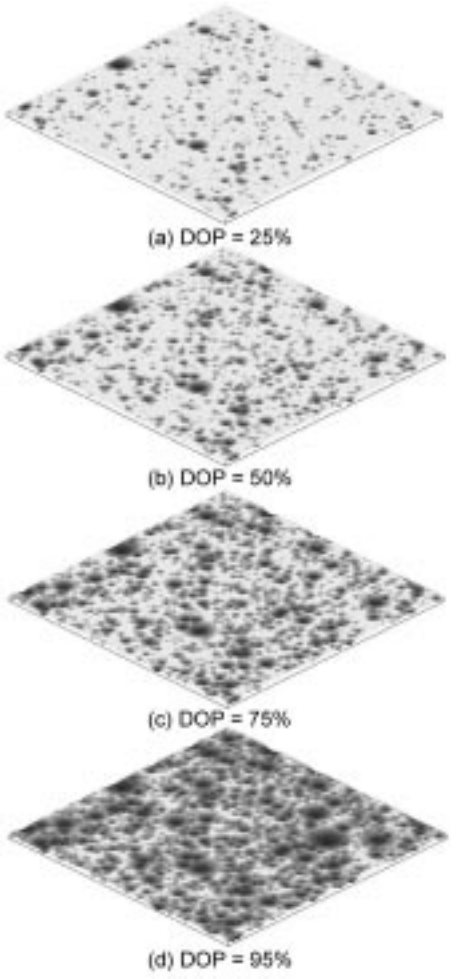
Therefore, the equivalent thickness loss t_{el}, which is defined by the thickness loss of a uniformly corroded plate with the same tensile strength as a plate with pitting corrosion, can be given by

$$t_{el} = t_0 - t_{ave,min} \qquad \text{for tensile strength} \qquad 7.14$$

Ultimate strength of plate elements under uniaxial compression

This section discusses the effect of pitting corrosion on the ultimate strength of simply supported square plates under uniaxial compressive loading using non-linear FEA. Pit distributions of the analyzed square plates were the ones calculated by the aforementioned updated probabilistic corrosion model. It is assumed that pitting corrosion exists on both sides of the plate and the DOP of both sides of the plate is the same, but different pit distributions are assumed for each side. Examples of the pit distributions used in the analyses are depicted in Fig. 7.8. While an average level of initial deflection is assumed, no welding residual stresses are considered.

© 2008 Woodhead Publishing Limited



7.8 Examples of simulated surface with pitting corrosion: (a) DOP = 25%; (b) DOP = 50%; (c) DOP = 75%; (d) DOP = 95%.

The pitted plates can be modeled with shell elements with small mesh size. The thickness at each node was calculated based on the pit distribution on both sides, and the average value of the thickness at the four nodes which form an element was used as the thickness of the element. The validity of this modeling method can be checked by comparative calculations using geometrical models with solid elements and shell elements with very fine mesh (Nakai *et al.*, 2006).

It should also be noted that eccentricity due to pitting corrosion exists because corrosion pits are distributed differently on each side of the plate. The eccentricity due to pitting can be taken into account by shifting the node at the center of the thickness. The following three types of modeling are used to

© 2008 Woodhead Publishing Limited

examine how the modeling methods affect the calculated deformation behavior:

- Considering the eccentricity due to pitting and initial imperfection with convex on side A.
- Considering the eccentricity due to pitting and initial imperfection with convex on side B.
- Taking into consideration only the initial imperfection.

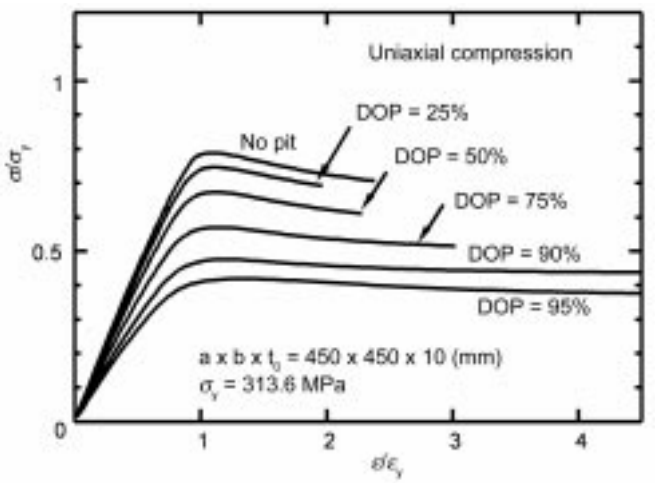
The difference in estimated ultimate strength using these three modeling methods is within 4.5%. It can be said that the effect of eccentricity due to pitting corrosion on the calculated ultimate strength is small.

Curves of average stress against average strain for plates with original thicknesses of 10 mm with pitting corrosion are plotted in Fig. 7.9. As shown by these curves, the ultimate strength decreases with the increase of DOP.

Figure 7.10 shows the relationship between the equivalent thickness t_e and the DOP, where the equivalent thickness t_e is defined by the thickness of a uniformly corroded plate with the same ultimate strength as a plate with pitting corrosion. In this figure, a dashed line gives the prediction results using the following equation:

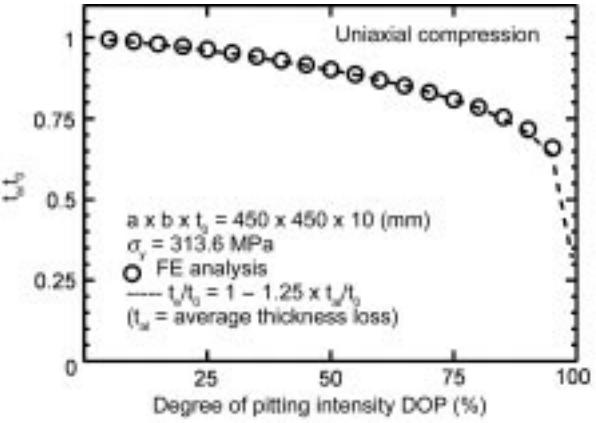
$$\frac{t_e}{t_0} = 1 - \frac{1.25 t_{al}}{t_0} \qquad \text{for uniaxial compression} \qquad 7.15$$

where t_{al} denotes average thickness loss. It is seen that the equivalent thickness of the pitted plates for the ultimate compressive strength can be well predicted by Eq. (7.15). From Eq. (7.15), equivalent thickness loss for the ultimate compressive strength can be expressed as



7.9 Average stress–average strain curves (uniaxial compression, t_0 = 10 mm, adapted from Nakai and Yamamoto, 2007).

© 2008 Woodhead Publishing Limited



7.10 Relationship between equivalent thickness and DOP (uniaxial compression, $t_0 = 10$ mm, adapted from Nakai and Yamamoto, 2007).

$$t_{el} = 1.25t_{al} \qquad \text{for uniaxial compression} \qquad 7.16$$

where t_{el} is defined by the thickness loss of a uniformly corroded plate with the same ultimate strength as a plate with pitting corrosion. This means that the ultimate strength of the pitted plates is smaller than that of the uniformly corroded plates with the same thickness as the average thickness of the pitted plates, and it is apparent that unevenness of the plate surface due to pitting corrosion affects the ultimate strength. There is no or little dependency of equivalent thickness loss t_{el} on original thickness t_0.

Ultimate strength of plate elements under shear

This section discusses the effect of pitting corrosion on the ultimate strength of simply supported square plates under shear using non-linear FEA. Pit distributions and modeling methods of the analyzed square plates were the same as those mentioned in the previous section. The reduction behavior of the equivalent thickness for the shear ultimate strength can be well described by Eq. (7.17). From Eq. (7.17), the equivalent thickness loss for the ultimate shear strength can be expressed by Eq. (7.18):

$$\frac{t_e}{t_0} = 1 - \frac{1.20t_{al}}{t_0} \qquad \text{for shear} \qquad 7.17$$

$$t_{el} = 1.20t_{al} \qquad \text{for shear} \qquad 7.18$$

Ultimate strength of plate elements under combined loads

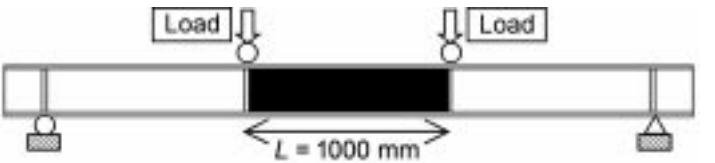
The ultimate strength of simply supported plates with pitting corrosion under combined loads has also been investigated by Nakai *et al.* (2007b). From these

© 2008 Woodhead Publishing Limited

analytical results including those in the previous sections, the equivalent thickness loss t_{el} for the ultimate strength under various loading conditions such as uniaxial compression, biaxial compression, shear and combinations of these is smaller than or equal to 1.25 times the average thickness loss t_{al}.

Ultimate strength of beams

This section investigates the effect of pitting corrosion on the ultimate strength of structural models (monosymmetric I-beams) under four-point bend using non-linear FEA. The structural model consists of shell, web and face plates simulating hold frames of bulk carriers. The cross-section of the structural models corresponds approximately to one half-scale of that of hold frames of cape-size bulk carriers. When the local strength of hold frames is considered, the effect of corrosion of the webs is more severe than that of the shell and face plates because the webs are generally thinner than the shell and face plates. Therefore, the effect of pitting corrosion of the webs is considered here. The analyzed structural model and loading condition are schematically shown in Fig. 7.11. In this figure, the pitted area is shaded black. The pit distributions in the pitted area were the ones calculated by the aforementioned updated probabilistic corrosion model. It is assumed that pitting corrosion exists on both sides of the plate and the DOP of both sides of the plate is the same, but the different pit distributions are assumed for each side. While initial deflection is given to the structural model, no welding residual stresses are considered. Geometrical models used in the FEA are shown in Fig. 7.12.

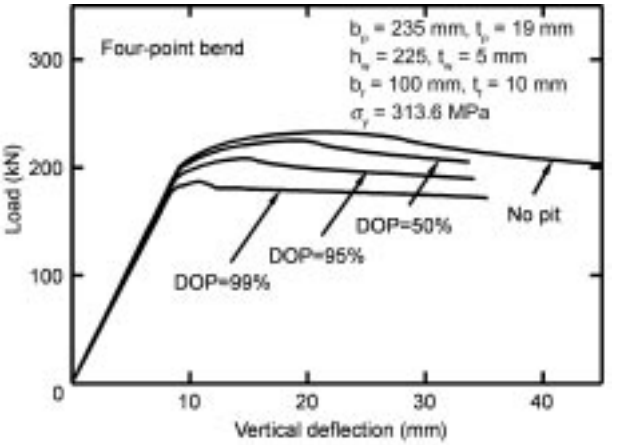


7.11 Loading conditions and pitted area (four-point bend).



7.12 Geometrical modeling of structural models (four-point bend).

© 2008 Woodhead Publishing Limited



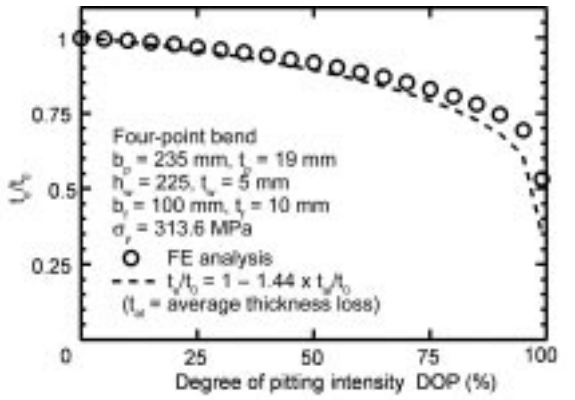
7.13 Load–vertical deflection curves (four-point bend).

Load–deflection curves of the structural models under four-point bend are given in Fig. 7.13. Figure 7.14 presents the relationship between the equivalent thickness of the webs and the DOP. Dashed lines in these figures show the results predicted using the following equation:

$$\frac{t_e}{t_0} = 1 - \frac{1.44 t_{al}}{t_0} \qquad 7.19$$

As shown in Fig. 7.14, the reduction behavior of the equivalent thickness of the webs can be well reproduced by Eq. (7.19). From Eq. (7.19), the equivalent thickness loss of the webs for the ultimate strength of the structural models can be expressed as

$$t_{el} = 1.44 t_{al} \qquad 7.20$$



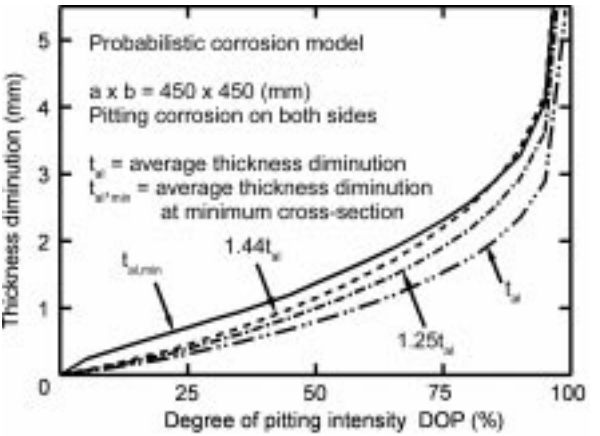
7.14 Relationship between equivalent thickness of web and DOP (structural models, four-point bend).

© 2008 Woodhead Publishing Limited

7.5.2 Evaluation of residual strength of members with pitting corrosion

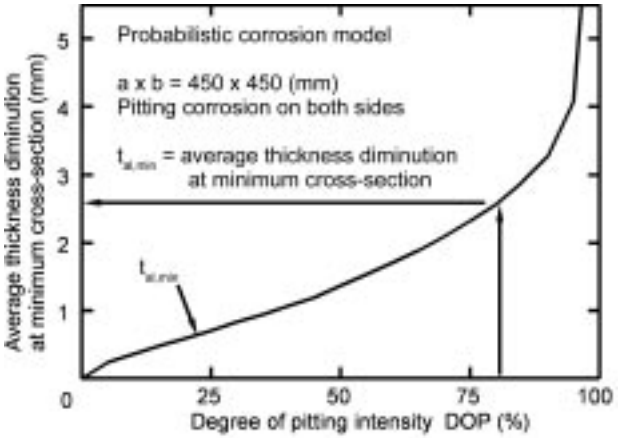
Figure 7.15 shows the thickness diminution behavior as a function of the DOP for the plates (450 mm × 450 mm) analyzed in the previous section. The increase of the average thickness diminution (t_{al}), the equivalent thickness loss for ultimate strength under combined loading of compression and shear ($1.25t_{al}$), the equivalent thickness loss for ultimate strength of structural models ($1.44t_{al}$) and the equivalent thickness loss for tensile strength ($t_{al,min}$) are plotted in this figure. A trend can be seen that the equivalent thickness loss increases almost linearly with increase of the DOP when the DOP is smaller than approximately 75%, and when the DOP exceeds 90% all these losses increase drastically. It is clear from this figure that the equivalent thickness loss for the tensile strength is larger than those for other loading conditions. Therefore, it is possible to ensure the structural integrity if the average thickness loss at the minimum cross-section is within the allowable corrosion level specified in rules for uniformly corroded members. The relationship of equivalent thickness loss to DOP shown in Fig. 7.16 is quite useful from a practical point of view, because the allowable DOP for plates with pitting corrosion could be determined by comparing the allowable diminution level specified for uniformly corroded plates with the equivalent thickness of the pitted plates. It is kept in mind that safety factors should be taken into account, because this evaluation method includes both probabilistic uncertainty in the progress of corrosion and uncertainty in visual determination of the DOP.

A method for the visual assessment of thickness diminution of pitted webs of hold frames of bulk carriers could be developed taking into account the residual strength as mentioned above. The shape and size of corrosion pits depends on the corrosive environment, etc. However, it is considered that a concept/



7.15 Relationship between thickness diminution and DOP estimated by probabilistic corrosion model.

© 2008 Woodhead Publishing Limited



7.16 Relationship between average thickness diminution at minimum cross-section and DOP estimated by probabilistic corrosion model (adapted from Nakai *et al.,* 2007b).

procedure of developing the method can be applied to other structural members in which predominant pitting corrosion is observed. This evaluation method is useful for the evaluation of the residual thickness of local structural members. However, when evaluating the residual strength of overall structures with pitting corrosion, pitting locations, patterns and intensity should be properly taken into consideration. Further research is necessary from such a point of view.

7.6 Conclusions

In this chapter, a method of probabilistic modeling of corrosion, the effect of general corrosion on hull girder strength and the effect of pitting corrosion observed in structural members in cargo holds of bulk carriers on local strength have been presented. It is considered that the procedure of developing a method for the evaluation of corrosion could be applied to many structures in which strength degradation due to corrosion needs to be accurately evaluated.

7.7 References

Amlashi, H.K.K. and Moan, T. 2005, On the strength assessment of pitted stiffened plates under biaxial compression loading, *Proceedings of the 24th International Conference on Offshore Mechanics and Arctic Engineering* (*OMAE2005*), OMAE2005-67232, Halkidiki, Greece.

Daidola, J.C., Parente, J., Orisamolu, I.R. and Ma, K.T. 1997, Residual Strength Assessment of Pitted Plate Panels, SSC-394, Ship Structure Committee.

Garbatov, Y., Vodkadzhiev, I. and Guedes Soares, C. 2004, Corrosion wastage assessment of deck structures of bulk carriers, *Proceedings of the International Conference on Marine Science and Technology*, 24–33.

© 2008 Woodhead Publishing Limited

Garbatov, Y., Guedes Soares, C. and Wang, G. 2005, Non-linear time dependent corrosion wastage of deck plates of ballast and cargo tanks of tankers, *Proceedings of the 24th International Conference on Offshore Mechanics and Arctic Engineering* (*OMAE2005*), OMAE2005-67579, Halkidiki, Greece.

Guedes Soares, G. and Garbatov, Y. 1999, Reliability of maintained, corrosion protected plate subjected to non-linear corrosion and compressive loads, *Marine Structures*, 10, 629–653.

Komai, K., Minoshima, K. and Kim, G. 1987, Corrosion fatigue crack initiation behavior of 80 kgf/mm^2 high-tensile strength steel weldment in synthetic seawater, *Journal of the Society of Materials Science Japan*, 36(401), 141–146 (in Japanese).

Kondo, Y. 1987, Prediction method of corrosion fatigue crack initiation life based on corrosion pit growth mechanism, *Transactions of the Japan Society of Mechanical Engineers*, 53(495), 1983–1987 (in Japanese).

Masuda, C., Abe, T., Hirukawa, H. and Nishijima, S. 1986, Corrosion fatigue life prediction for SUS403 stainless steel in 3% NaCl aqueous solution, *Transactions of the Japan Society of Mechanical Engineers*, 52(480), 1764–1769 (in Japanese).

Matoba, M., Yamamoto, N., Watanabe, T. and Umino, M. 1994, Effect of corrosion and its protection on hull strength, *Journal of the Society of Naval Architects of Japan*, 175, 271–280 (in Japanese).

Nakai, T. and Yamamoto, N. 2007, Pitting corrosion – probabilistic modeling and its effect on the ultimate strength of steel plates subjected to uni-axial compression, *Proceedings of the 10th International Conference on Applications of Statistics and Probability in Civil Engineering* (*ICASP10*).

Nakai, T., Matsushita, H. and Yamamoto, N. 2004a, Effect of pitting corrosion on local strength of hold frames of bulk carriers (2nd report), *Marine Structures*, 17, 612–641.

Nakai, T., Matsushita, H., Yamamoto, N. and Arai, H. 2004b, Effect of pitting corrosion on local strength of hold frames of bulk carriers (1st report), *Marine Structures*, 17, 403–432.

Nakai, T., Matsushita, H. and Yamamoto, N. 2005, Pitting corrosion and its influence on local strength of hull structural members, *Proceedings of the 24th International Conference on Offshore Mechanics and Arctic Engineering* (*OMAE2005*), OMAE2005-67025, Halkidiki, Greece.

Nakai, T., Matsushita, H. and Yamamoto, N. 2006, Effect of pitting corrosion on the ultimate strength of steel plates subjected to in-plane compression and bending, *Journal of Marine Science and Technology*, 11, 52–64.

Nakai, T., Matsushita, H. and Yamamoto, N. 2007a, Effect of pitting corrosion on ultimate strength of web plates subjected to shear loading, *Key Engineering Materials*, 340–341, 489–494.

Nakai, T., Matsushita, H. and Yamamoto, N. 2007b, Visual assessment of corroded condition of plates with pitting corrosion taking into account residual strength – in the case of webs of hold frames of bulk carriers, *Proceedings of the 26th International Conference on Offshore Mechanics and Arctic Engineering* (*OMAE2007*), OMAE2007-29159, San Diego, CA.

Nakai, T., Matsushita, H. and Yamamoto, N. 2007c, Pitting corrosion on epoxy-coated surface of ship structures, *Proceedings of International Symposium on Shipbuilding Technology – Coatings and Fabrication*, Osaka, Japan.

Paik, J.K. 2004, Corrosion analysis of seawater ballast tank structures, *International Journal of Maritime Engineering*, 146(A1), 1–12.

Paik, J.K., Kim, S.K. and Lee, S.K. 1998, Probabilistic corrosion rate estimation model

© 2008 Woodhead Publishing Limited

for longitudinal strength members of bulk carriers, *Ocean Engineering*, 25, 837–860.

Paik, J.K., Lee, J.M., Hwang, J.S. and Park, Y.I. 2003a, A time-dependent corrosion wastage model for the structures of single and double hull tankers and FSOs and FPSOs, *Marine Technology*, 40, 201–217.

Paik, J.K., Lee, J.M., Park, Y.I., Hwang, J.S. and Kim, C.W. 2003b, Time-variant ultimate longitudinal strength of corroded bulk carriers, *Marine Structures*, 16, 567–600.

Paik, J.K., Thayamballi, A.K., Park, Y.I., Hwang, J.S. and Kim, C.W. 2004a, A time-dependent corrosion wastage model for seawater ballast tank structures of ships, *Corrosion Science*, 46, 471–486.

Paik, J.K., Lee, J.M. and Ko, M.J. 2004b, Ultimate compressive strength of plate elements with pit corrosion wastage, *Journal of Engineering for the Maritime Environment*, 217(M4), 185–200.

Paik, J.K., Lee, J.M. and Ko, M.J. 2004c, Ultimate shear strength of plate elements with pit corrosion wastage, *Thin-Walled Structures*, 42, 1161–1176.

Qin, S. and Cui, W. 2002, A discussion of the ultimate strength of ageing ships, with particular reference to the corrosion model, *Journal of Engineering for the Maritime Environment*, 216(M2), 155–160.

Qin, S. and Cui, W. 2003, Effect of corrosion models on the time-dependent reliability of steel plated elements, *Marine Structures*, 16, 15–34.

Shreir, F.F. 1976, *Corrosion*, Vol. 3, Newnes-Butterworths, London.

Smith, C.S. 1977, Influence of local compressive failure on ultimate longitudinal strength of a ship's hull, *Proceedings of the International Symposium on Practical Design in Shipbuilding*, Tokyo, Japan.

Sumi, Y., Yamamura, N. and Yamamuro, Y. 2006, On the strength and deformability of corroded steel plates by using reproduced specimens, *Journal of the Japan Society of Naval Architects and Ocean Engineers*, 4, 239–245 (in Japanese).

Tsuji, K., Hisada, T. and Kitagawa, H. 1983, *Transactions of the Japan Society of Mechanical Engineers* A, 49(439), 331–340 (in Japanese).

Yamamoto, N. and Ikegami, K. 1998, A study on the degradation of coating and corrosion of ship's hull based on the probabilistic approach, *Transactions of the ASME*, *Journal of Offshore Mechanics and Arctic Engineering*, 120, 121–128.

Yamamoto, N. and Yao, T. 2001, Hull girder strength of a tanker under longitudinal bending considering strength diminution due to corrosion, *Structural Safety and Reliability, Proceedings of the 8th International Conference* (*ICOSSAR2001*).

Yao, T. and Nikolov, P.I. 1991, Progressive collapse analysis of a ship's hull under longitudinal bending, *Journal of the Society of Naval Architects of Japan*, 170, 449–461.

Yao, T. and Nikolov, P.I. 1992, Progressive collapse analysis of a ship's hull under longitudinal bending (2nd report), *Journal of the Society of Naval Architects of Japan*, 172, 437–446.

© 2008 Woodhead Publishing Limited

8

Cracked structures and residual strength

F WANG and W C CUI,
China Ship Scientific Research Center, China

Abstract: This chapter is primarily concerned with the residual strength assessment of steel plated structures with existing crack damage and under monotonic extreme loading. It describes the fundamentals and some results of the residual strength evaluation of cracked ship structures, aiming at obtaining insights into the ultimate strength behavior of structures given one or more cracks under different types of cracks and loads, and indicating how to use such knowledge within the current framework of ultimate strength calculation for a complex structural system and ship hull girder. The main contents include (i) residual tensile/compressive strength assessment method of cracked unstiffened plates, (ii) residual tensile/compressive strength assessment method of cracked stiffened panels, and (iii) residual strength assessment of ship hull girders.

Key words: residual strength, cracked structures, unstiffened plates, stiffened panels, ship hull girder.

8.1 Fundamentals of residual strength of cracked structures

Under the action of repeated loading, fatigue cracks may be initiated in the stress concentration areas of the structure. Initial defects or cracks may also be formed in the structure by inappropriate fabrication procedure and may conceivably remain undetected over time. In addition to propagation under repeated cyclic loading, cracks may also grow in an unstable way under monotonically increasing extreme loads, a circumstance which eventually can lead to catastrophic failure of the structure. This possibility is of course tempered by the ductility of the material involved, and the presence of reduced stress intensity regions in a complex structure that may serve as crack arresters even in an otherwise monolithic structure (Paik and Thayamballi, 2002a).

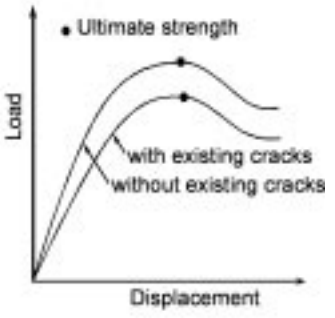
Therefore, residual strength evaluation when cracks exist is playing a significant role in damage tolerance analysis of structures. For aging ships, the fatigue cracks will degrade the ultimate strength of stiffened panels and unstiffened plates. The damage degree of fatigue cracks should be determined properly at first to assess the strength of aging ships. It is essential to seek a rational standard for structural integrity of aging structures without economic penalties with respect to the repair and maintenance costs incurred over the life

© 2008 Woodhead Publishing Limited

cycle of the structure, while a risk or reliability assessment scheme is normally applied for that purpose.

For residual strength assessment of aging steel structures under extreme loads as well as under fluctuating loads, it is often necessary to take into account a known or existing crack as a parameter of influence (Paik and Thayamballi, 2002b). In the usual situation where the deformations of cracked structures are not considerable, ductile fracture related to stable crack growth may be a predominant mode in ductile steel structures. In the rare situation when the structure has been weakened by large cracks or large-scale plasticity associated with cracks, resulting in decrease of structural stiffness, large deformations are likely to develop. For a very ductile material and/or a very slow loading rate, yielding can spread to the specimen boundary prior to crack growth and failure can occur by plastic collapse without macro-cracking (net section yield) or with macro-cracking (yield under fully plastic behavior) (Sih, 1991). The general failure process with large plasticity of a cracked plate is that a plastic zone first forms in the vicinity of the crack tips and with the load increasing, the plastic zone will be enlarged continuously and result in the decrease of strength. In this regard, the maximum loading point in the load–displacement relationship of a structure with a premised crack damage and under monotonic extreme loading may not exceed the ultimate strength of the uncracked structure. Figure 8.1 shows a schematic representation of the nonlinear behavior of cracked steel structures. It is noted that, for similar structures, the stiffness and ultimate strength of cracked structures are smaller than those of uncracked structures.

Moreover, strength assessment methods of cracked structures are quite different from those of uncracked structures. There have been few systematic contributions in this regard until now but more and more extensive studies are currently being carried out. Several techniques are in use including the theoretical method based on fracture mechanics, FE analysis, a simplified theoretical model based on net section static failure and other methods for



8.1 Schematic representation of the cracking damage effect on the ultimate strength behavior of steel structures (Paik and Thayamballi, 2002a).

© 2008 Woodhead Publishing Limited

practical engineering structures such as Feddersen's method (Feddersen, 1971) and the methodology proposed by Li *et al.* (2003). Usually, fracture mechanics are highlighted in its use on crack problems. With the development of the modern era of fracture mechanics from the work of Griffith (1920), several failure criteria expressing the relationship of the working stress and the ultimate strength are established, and many studies and works are concentrating on fracture parameter analyses considering the ductility of materials used in modern practical engineering (e.g. O'Dowd *et al.*, 1999; Krawczuk *et al.*, 2001), which makes more use of fracture mechanics for residual strength assessment of cracked engineering structures. The details of fracture mechanics can be found in various textbooks and other literature (e.g. Cotterell, 2002). FE analysis provides a convenient way to solve more complicated problems such as calculating structural residual strength under different types of cracks and loads, while if one presupposes a very ductile material, one may postulate a simple and intuitive model to simply calculate the ultimate strength of cracked structures. For instance, for a center or edge cracked plate under controlled displacement conditions, constructed of ductile material, one may predict the ultimate strength on the basis of the reduced cross-sectional area, accounting for the loss of load-carrying material due to the crack damage. A series of extensive studies have been done concentrating on validating a simplified theoretical model for residual strength assessment of cracked structural elements including unstiffened plates and stiffened panels (Paik and Thayamballi, 2002a, 2002b; Paik *et al.*, 2003; Paik and Satish Kumar, 2006). The simplified crack damage model has been tested by a series of experiments and FE simulations on steel plates and panels with existing cracks under monotonic tensile and compressive loading.

Some extensive work has been done by Cui and co-workers. Hu *et al.* (2004) proposed a methodology to assess the time-variant ultimate strength of a ship hull girder with crack damage in which FE analysis results for the tensile and compressive residual strength of center-cracked and edge-cracked plates are adopted. Considering varieties of influential parameters on residual strength of cracked plates, non-dimensional parametric FE analyses on the effects of crack types, crack position, plate dimensions, material properties and boundary conditions are carried out to provide a basis for residual strength assessment of more complicated structures and ship hull girders (Wang and Cui, 2006). The cases of multi-cracks have also been briefly studied (Wang *et al.*, 2006) based on the works of Moukawsher *et al.* (1996), Cherry *et al.* (1997) and Smith *et al.* (2000). The multi-crack problem was studied mainly in the field of aging aircraft structures and the problem attracted attention due to the Aloha accident in 1988 (Hendricks, 1991). In recent years, research efforts have been undertaken to assess the residual strength of panels with multiple cracks (Labeas *et al.*, 2005), though most of them are on collinear cracks characterized by a leading crack interacting with one or more multiple site damage (MSD) cracks. Up to now, several crack link-up criteria have been supposed for the residual strength of

© 2008 Woodhead Publishing Limited

cracked plates and panels with MSD (e.g. Swift, 1993; Jeong and Brewer, 1995). Tests have also been carried out to validate the supposed failure criteria (Cherry *et al.*, 1997).

The studies on residual strength of basic fundamental structural elements such as unstiffened plates and stiffened panels will provide a foundation for residual strength assessment of ship hull girders. The ultimate bending moment of a ship hull girder is associated with the compressive and tensile ultimate strength of stiffened panels between bulkheads or web frames and unstiffened plates between stiffeners (Hu *et al.*, 2004). Combining those with current ship structure assessment procedures, the residual strength assessment methodology of a ship hull girder under crack damage can thus be set up.

This chapter is primarily concerned with the residual strength assessment of steel plated structures with existing crack damage and under monotonic extreme loading. It describes the fundamentals and some results of the residual strength evaluation of cracked ship structures, aiming at obtaining insights into the ultimate strength behavior of structures given one or more cracks under different types of cracks and loads, and indicating how to use such knowledge within the current framework of ultimate strength calculation for a complex structural system and ship hull girder. Considering that axial tension/compression are primary load components in ships, offshore structures and other steel structures, residual strength corresponding to load types of axial tension and compression will be addressed in this chapter. The main contents will include (i) residual tensile/compressive strength assessment method of cracked unstiffened plates, (ii) residual tensile/compressive strength assessment method of cracked stiffened panels, and (iii) residual strength assessment of ship hull girders.

8.2 Residual ultimate strength of cracked plates

Thin plates are among the main components in ship structures. The ultimate strength of the plate components is very important from the design and safety viewpoint because the collapse loads of these elements can often act as an indicator of the ultimate strength of the whole stiffened panel. Assessing the strength of cracked plates exactly is significant for reducing the manufacture and maintenance costs of ships and increasing ship life and safety.

8.3 Plates with a single crack under ultimate tensile loads

8.3.1 Theoretical method based on fracture mechanics

Fracture mechanics deals with the strength behavior of materials and structures with cracks by applying structural mechanics and relevant fracture criteria. Basic concepts of fracture mechanics include the energy-based concept, the

© 2008 Woodhead Publishing Limited

stress intensity-based concept and the crack growth-based concept, which can be found in many textbooks, e.g. Anderson (1995). To predict the ultimate strength of steel plated structures with existing cracks, it is sometimes considered that the structures reach their ultimate limit states if any fracture criterion described in the following is satisfied.

The main fracture criteria based on fracture mechanics based concepts are as follows:

$$G = G_C \tag{8.1}$$

$$K_I = K_{IC} \tag{8.2}$$

$$J = J_C \tag{8.3}$$

$$\delta = \delta_C \tag{8.4}$$

where G = strain energy release rate; K_I = mode I stress intensity factor for a crack body with a linear elastic material; J = a path-independent integral around the crack tip as the energy that is extracted through the crack tip singularity; and δ = crack tip opening displacement. G_C, K_{IC}, J_C and δ_C are critical values of the four parameters above respectively, which may be empirically determined as a function of the material properties based on the test data. Among them, Eq. 8.2 is for a crack body with a linear elastic material while Eqs 8.3 and 8.4 can be used to solve elasto-plastic problems with a ductile material.

8.3.2 Simplified theoretical model based on net section static failure

A simplified model based on net section static failure is a simple and intuitive model to predict the ultimate strength of structures presupposing a very ductile material. For instance, for a center or edge cracked plate constructed of ductile material under controlled displacement conditions, one may predict the ultimate strength on the basis of the reduced cross-sectional area, accounting for the loss of load-carrying material due to the crack damage. In this case, the ultimate strength of a steel plated structural component with existing cracks and under monotonic extreme loading may be approximately obtained by

$$\sigma_u = \frac{A_c}{A_0}\,\sigma_{u0} \tag{8.5}$$

where σ_u, σ_{u0} = ultimate strengths of cracked or original (uncracked) structure, and A_c, A_0 = cross-sectional areas of cracked or original (uncracked) structural component.

As a typical example, Fig. 8.2 shows a steel plate component with an existing crack damage and subject to monotonic axial tensile loads. Using the simplified

© 2008 Woodhead Publishing Limited



8.2 Schematic of a simply supported steel plate with existing crack (Paik and Thayamballi, 2002b).

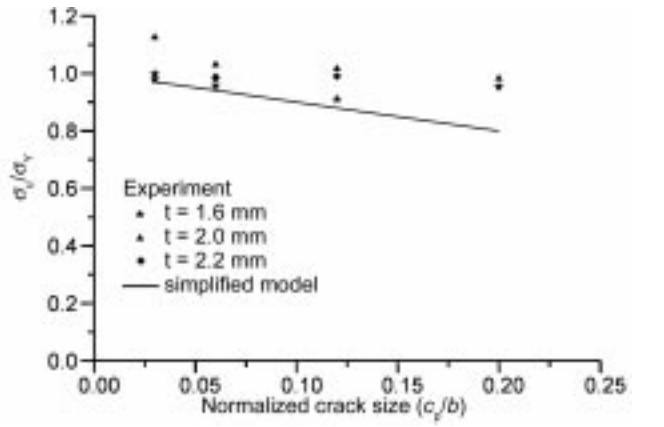
model noted in Eq. 8.5, the residual tensile strength can then be predicted as follows:

$$\sigma_u = \frac{b - c_p}{b}\,\sigma_{u0} \qquad 8.6$$

where $\sigma_{u0} = \sigma_{YP}$ = material yield stress of the plate; b = plate width; and c_p = crack length in the plate.

The applicability of Eq. 8.6 can be verified by a series of experiments on steel plates with an existing crack under room temperature (Paik and Thayamballi, 2002b). In the structural testing related to residual strength, a small hole is mechanically made first either at the center or at the edge of the plate, and axial fatigue loading is then applied in the plane of the plate until a crack of the desired size is achieved. Finally, increasing controlled displacements corresponding to different levels of monotonic uniaxial tensile loads are applied and are progressively increased in a quasi-static condition until the cracked plate is split into two pieces.

Figure 8.3 shows the variation of the ultimate tensile strength of steel plates as a function of the crack length as obtained by the experiments and by the simplified model noted above, i.e., reducing the cross-sectional area to account



8.3 Variation of the ultimate tensile strength as a function of the crack length, as obtained by the experiments and by the simplified model, σ_Y being the measured yield stress (Paik and Thayamballi, 2002b).

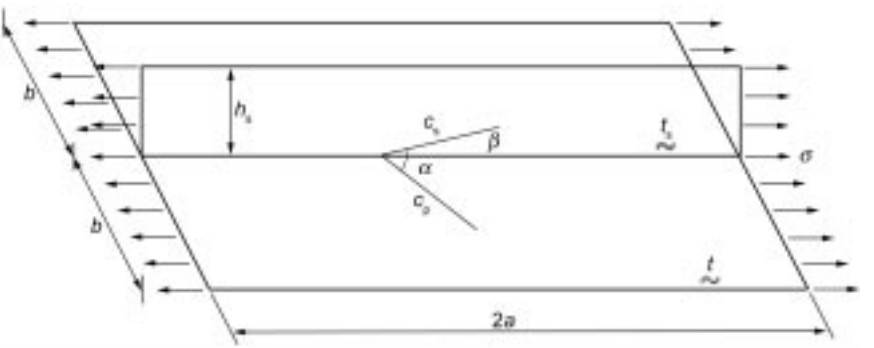
© 2008 Woodhead Publishing Limited

for the crack damage. It is evident that the simplified model provides adequate results on the pessimistic side.

8.3.3 Finite element (FE) analysis

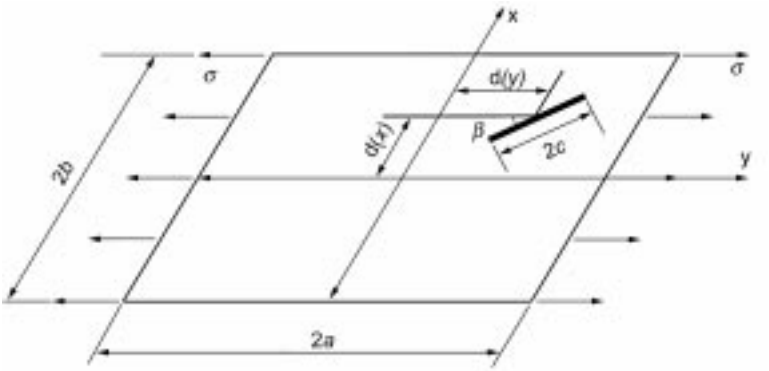
FE analysis provides a convenient way to solve more complex crack problems. The simplified model above simply uses the cross-sectional method to calculate the residual strength of a cracked plate by considering only two crack locations at edge and center and neglecting the strain hardening effect of material and other influential parameters. When a small crack is initiated in the welding position of panels, it usually propagates along a random direction under complicated loading circumstances. Therefore, different crack forms with inclinations shown in Fig. 8.4 should be considered in a simple and intuitive mode. It can be shown that the ultimate tensile strength can be affected by parameters including material properties, crack characteristics, the plate's geometrical dimensions, and the boundary loading conditions (uniform stress or constant displacement). Moreover, the mesh refining order should also be examined first to conduct a parametric finite element study.

The basic FE model of parametric study (Wang and Cui, 2006) is the rectangular plate with a through-thickness crack subjected to uniform tensile stress on the boundary of the plate, illustrated in Fig. 8.5. The normalized influential parameters include the yield ratio σ_s/σ_b, Poisson's ratio ν, the crack length c/b, the crack angle β, the eccentric ratio in the x-direction $e_x = \mathrm{d}(x)/b$, the eccentric ratio in the y-direction $e_y = \mathrm{d}(y)/b$, the plate's aspect ratio a/b, and the plate thickness t/b.



8.4 Schematic representation of stiffened panel with inclined cracks in welding position under tensile loads ($2a$ = plate length; $2b$ = plate width; h_s = stiffener height; t = plate thickness; t_s = stiffener thickness; c_p = crack length in the plate; c_s = crack length in the stiffener; α = crack angle in the plate; β = crack angle in the stiffener).

© 2008 Woodhead Publishing Limited



8.5 Schematic representation of a steel plate with an existing crack for parametric analysis.

Effects of material properties

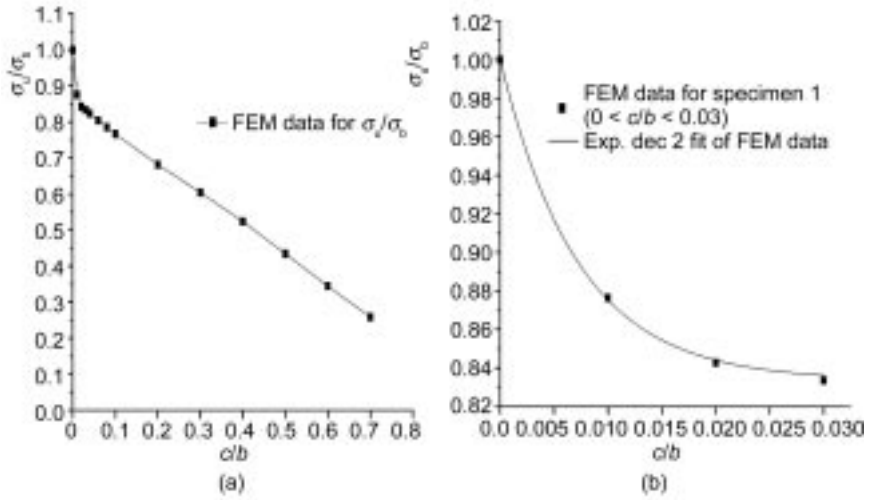
Material properties, including the yield ratio and Poisson's ratio, are the most important factors influencing the characteristics of the cracked plate. The ultimate tensile strength of uncracked plates is σ_b. When cracks are initiated, there will be local stress concentration in the vicinity of the crack tip and different yield ratios will affect stress redistribution when yielding initiates. Due to the hardening property of the material, the cracked plates could endure an additional extent of load when yielded, which makes the average stress in the plastic zone between σ_s and σ_b. So the residual tensile strength can be different with variation of the hardening extent indicated by the yield ratio. The effect of Poisson's ratio should be examined, because a larger Poisson's ratio will be expected to develop more compressive stresses in the vicinity of crack tips under tensile stress, which may affect the ultimate tensile strength of the plate.

Figure 8.6(a) shows the variation of the normalized ultimate tensile strength of the plate as a function of the nominal crack length. The changing tendency has been divided into two phases. When the crack length is relatively small, the curve can be poly-fitted by a first-order exponential decreasing function as illustrated in Fig. 8.6(b), while the phase related to a relatively large crack length is apparently linear.

The material properties used in the FEM calculation are shown in Table 8.1, and Fig. 8.7 illustrates the calculation results. It shows the evident difference between the three specimens with different yield ratios. There is an apparent tendency for the results related to a higher yield ratio to lie above the results with a lower one.

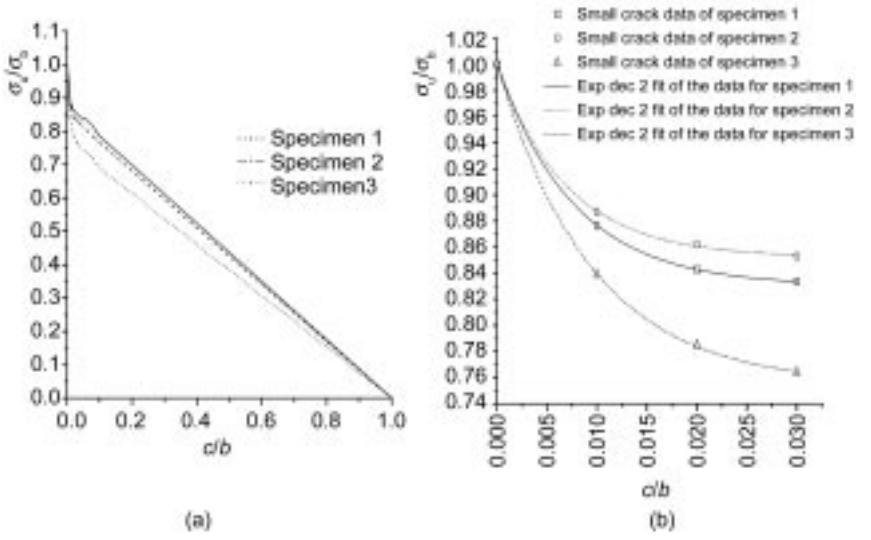
As another important material property parameter, Vafai and Estekanchi (1999) discussed the effect of Poisson's ratio on the lateral displacement of a cracked plate, showing that lateral deformation varies obviously for different

© 2008 Woodhead Publishing Limited



8.6 Normalized ultimate tensile strength versus (a) c/b (0–0.7), (b) c/b (0–0.03).

Poisson's ratios. But a series of analyses (Wang and Cui, 2006) show that the ultimate tensile strength of the cracked plate will almost not be altered even though the Poisson's ratios do change the stress field and the deformation of the plate.



8.7 The changing tendency of normalized ultimate tensile strength versus (a) c/b (0–1) for three specimens, (b) c/b (0–0.03) for three specimens.

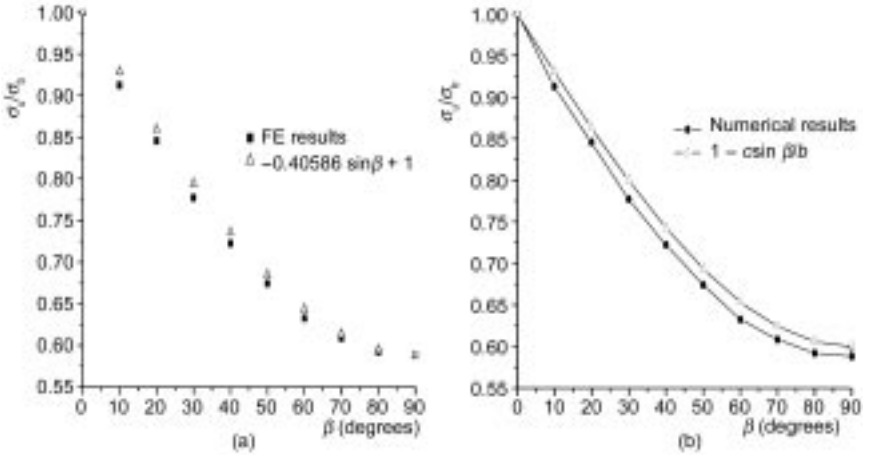
© 2008 Woodhead Publishing Limited

Table 8.1 Material properties of test specimens

Specimen no.	σ_s (MPa)	σ_b (MPa)	E (GPa)	Elongation (%)	Yield ratio
1	296.1	362.1	198.3	36.9	0.81773
2	328.8	396.6	207.4	36.8	0.829047
3	249.7	345.4	202.2	43.6	0.72293

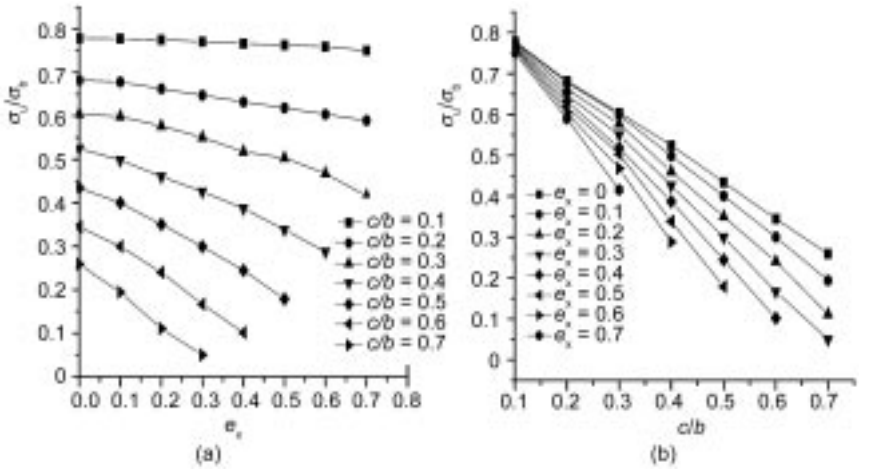
Effects of crack characteristics

Crack characteristics including the crack length, crack angle and crack position illustrated in Fig. 8.5 are the most important factors influencing the ultimate strength of a cracked plate. The effect of crack length is illustrated in Figs 8.6 and 8.7. Figure 8.8 illustrates the effect of crack inclination. From the depiction, a sinusoidal curve is approximately supposed in Fig. 8.8(a), which reaches a maximum value of 1 when β is 0 and a minimum value when β is 90º. It can be seen from the two series of data that the changing tendency of the ultimate tensile strength of a cracked plate with an inclined crack can certainly be regarded as being sinusoidal, thereby the ultimate strength of an inclined cracked plate can be approximately calculated through treating the plate as a center through-thickness crack with dimension of $(c/b)' = (c/b)\sin\beta$ and then the failure mode can be regarded as the net section yielding. The validated comparison curves are given in Fig. 8.8(b). The hypothesis is testified by the good agreement between the two curves representing the calculated results and the normalized net section width of the cracked plate.



8.8 Normalized ultimate tensile strength versus crack angle compared with (a) the sinusoidal curve; (b) the normalized net section width method ($c/b = 0.4$, $e_x = 0$, $e_y = 0$, $a/b = 1$, $E = 2.1 \times 10^5$ MPa, $\nu = 0.3$, $\sigma_s = 300$ MPa).

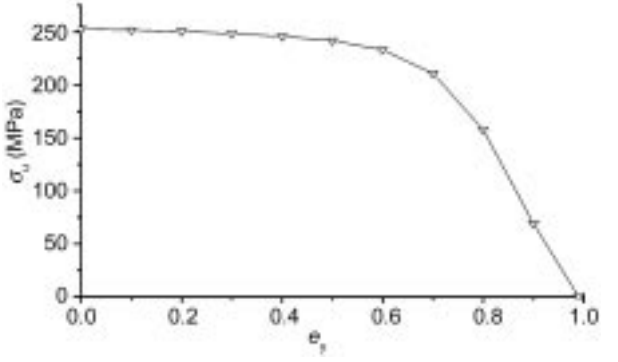
© 2008 Woodhead Publishing Limited



8.9 (a) Normalized ultimate strength versus e_x; (b) nominal ultimate strength versus c/b ($\beta = 90^{\circ}$, $e_y = 0$, $a/b = 1$).

The effect of eccentricity e_x is shown in Fig. 8.9. The eccentricity ratio has a distinct influence on the ultimate tensile strength of the cracked plates. As the eccentricity ratio increases, the ultimate tensile strength decreases significantly for a given crack length, and this changing trend is more and more evident with increase of c/b. For a certain eccentricity ratio, the effect is approximately supposed to be a linear equation in c/b. The points of intersection between the coordinate axis y and the normalized ultimate strength line with the variation of c/b keep approximately constant when the eccentricity ratio changes.

The effect of eccentricity e_y is shown in Fig. 8.10. The eccentricity ratio e_y goes from 0 to 0.99. It can be seen that the ultimate tensile strength of the plate decreases with variation of e_y, and the curve shows a rapidly descending tendency when the eccentric ratio e_y exceeds 0.6, perhaps because the applied



8.10 Ultimate tensile strength versus e_y ($\beta = 90^{\circ}$, $c/b = 0.2$, $e_x = 0$, $a/b = 1$).

© 2008 Woodhead Publishing Limited

loading condition in the above numerical model is uniform stress but not constant displacement. When the crack is near a plate boundary under uniform tensile stress, there will be additional bending moments acting on the crack tip, and the effects will be more evident for the ultimate tensile strength of plates with larger cracks.

Effects of plate geometrical dimensions and boundary conditions

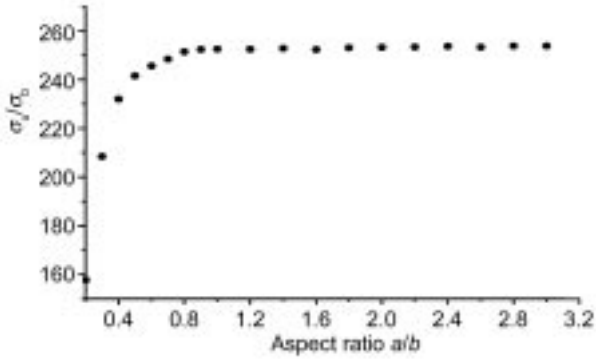
The plate geometry, especially the aspect ratio a/b, may affect the ultimate strength of cracked plates. It can be assumed intuitively that when the aspect ratio of the plate is large enough, the ultimate tensile strength of the same cracked plate will be as if the plate were regarded as a plate strip. But as the aspect ratio is relatively small, it can greatly affect the ultimate strength of the plate, especially when $a/b \leq 1$. Two different loading conditions, of uniform stress and of constant displacement on the boundary of the plate, should be taken into account. It is believed that the difference between the two loading conditions is correlated to the aspect ratio of the plate, and when the aspect ratio is sufficiently large, the loading conditions will become the same.

A simple calculation is conducted first to initially examine the effects of aspect ratio by the y-displacements of the nodes on the boundary versus the x-coordinates when the plates are subjected to a uniform stress load. It can be concluded that when the aspect ratio of the plate is increasing, the displacements along the boundary gradually become uniform. There is only a small discrepancy when the aspect ratio exceeds 1.0. As the aspect ratio is over 2.0, the displacements can be neglected for this plate model with a crack length of $c/b = 0.2$. So it could be assumed that the two loading conditions of uniform stress and constant displacement will approximately produce the same results if the aspect ratio of the plates exceeds 2.0.

The ultimate tensile strength of the plate with a crack of $c/b = 0.2$ with variation of the plate's aspect ratio is illustrated in Fig. 8.11. As expected, it increases rapidly from a very small aspect ratio of 0.2 to a relatively large one of 1.0. When the aspect ratio reaches 1.0, the ultimate tensile strength gradually becomes uniform but with a very small fluctuation, while it approaches a constant value approximately when the aspect ratio exceeds 2.0. Hence, when the crack is not very large, the ultimate strength of the cracked plate can be modeled and calculated by considering the plate as a plate strip, neglecting the boundary effects.

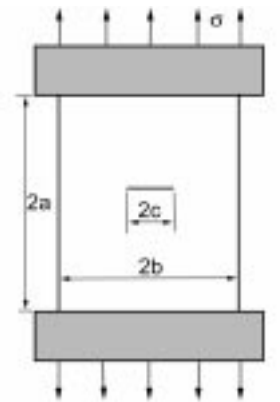
To exhibit the discrepancy in the results induced by the two loading conditions of uniform stress and constant displacement, a series of plate models with center crack of $c/b = 0.2$ were calculated. The plate models were modified by adding two rigid plates on the boundaries of the original cracked plate to control the displacements of the plate boundaries and keep the displacement constant along the boundary, as can be seen in Fig. 8.12.

© 2008 Woodhead Publishing Limited



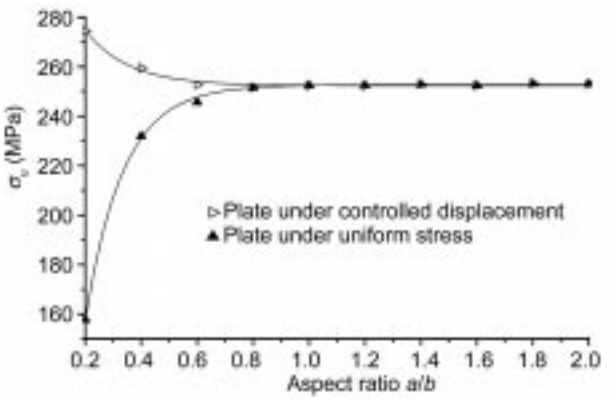
8.11 Ultimate tensile strength versus aspect ratio of the plate.

Figure 8.13 compares the results under the two different loading conditions. Obviously, the results for the two loading conditions approach their constant value from the opposite directions. Namely, when the plate is subjected to uniform stress, its ultimate tensile strength will go up rapidly and then reach a constant value when the aspect ratio of the plate approximately exceeds 1.0, but the opposite tendency applies under constant displacement loading conditions. When the constant displacement is implemented on the plate boundary, the ultimate tensile strength for the cracked plate with a smaller aspect ratio will be higher than for that with a larger one. The discrepancy may be explained by existing conclusions. Vafai and Estekanchi (1999) have discussed the effects of boundary conditions on the crack open displacement (COD) and the membrane stress before the cracked plate reaches its limit strength condition. There is an interesting conclusion that the COD approaches its limiting value from the



8.12 Cracked thin plate constrained by rigid plates on the two boundaries.

© 2008 Woodhead Publishing Limited



8.13 Ultimate tensile strength versus plate aspect ratio considering two loading conditions of uniform stress and constant displacement.

opposite sides of the horizontal asymptotic line for the two loading conditions. It is initially higher for uniform stress and lower for constant displacement than the limiting value. So perhaps when the plate is under uniform stress, the value of the COD will reach the critical value of the material more rapidly for the cracked plate with a smaller aspect ratio and make the ultimate tensile strength lower, but the situation is the opposite for the cracked plate under constant displacement.

Empirical formulas for cracked plates

According to the effects of influential parameters, the empirical formula for the ultimate tensile strength of a cracked plate can be obtained (Wang and Cui, 2006), namely,

$$\frac{\sigma_u}{\sigma_b}\left(\frac{\sigma_s}{\sigma_b}, x_e, c/b, \beta\right) = \begin{cases} Y_0(c/b,\beta) + Y_1\left(\dfrac{\sigma_s}{\sigma_b}, c/b, \beta\right) & 0 \le c\sin\beta/b < 0.03 \\ \left(0.012 + 1.04\dfrac{\sigma_s}{\sigma_b}\right) \times \left(1 - \dfrac{1}{x_e} \times c\sin\beta/b\right) & 0.03 \le c\sin\beta/b < 1 \end{cases} \quad 8.7$$

where

$$Y_0(c/b,\beta) = 0.8336 + 0.1666\exp\left(-138.3 \times \frac{c\sin\beta}{b}\right)$$

$$Y_1\left(\frac{\sigma_s}{\sigma_b}, c/b, \beta\right) = \left[8.82 - 68.78 \times \frac{\sigma_s}{\sigma_b} + 71.43 \times \left(\frac{\sigma_s}{\sigma_b}\right)^2\right] \times \frac{c\sin\beta}{b}$$

$$x_e = 1.00589 - 1.02488e_x + 0.61096e_x^2$$

© 2008 Woodhead Publishing Limited

8.3.4 Other methods for practical engineering structures

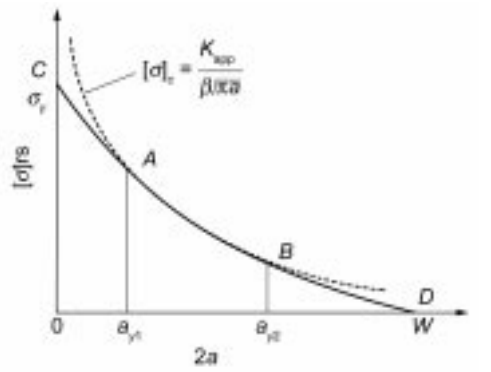
As fracture mechanics has been developed for many years, many researchers are concentrating on combining it with conventional evaluation methods such as the static mechanics method. Usually, three types of failure modes are generally considered for practical engineering structures, namely the linear elastic fracture mode, the static mode (fully plastic fracture mode) and the elastic–plastic fracture mode. The common process determining residual strength is the elastic–plastic correction and fully plastic examination on the basis of linear elastic fracture estimation. A commonly used method is Feddersen's evaluation method (Feddersen, 1971). The basic concept of this method is that the elastic–plastic fracture mode dominates when the crack length is very small, since the residual strength $[\sigma]_{rs}$ is restricted by the yield strength of the material, while the fully plastic fracture mode dominates when the crack is very long. As illustrated in Fig. 8.14, for a center-cracked plate with width W and crack length $2a$, tangent lines to the linear elastic fracture strength curve are plotted from $C(0, \sigma_y)$ and $D(W, 0)$ and the tangent points are A and B respectively. Then the full residual strength evaluation curve consists of lines CA, AB and BD.

Another simple formula, evaluated by Li *et al.* (2003), is:

$$[\sigma]_{rs} = \frac{[\sigma]_n [\sigma]_c}{\sqrt{[\sigma]_n^2 + [\sigma]_c^2}} \qquad 8.8$$

where $[\sigma]_c$ = elastic fracture strength, $[\sigma]_n$ = net section static strength, and $[\sigma]_{rs}$ = residual strength at a certain crack length.

Equation 8.8 was developed based on the consideration that the strength of a cracked body is controlled by mechanisms of both linear elastic fracture and net section static failure. The linear elastic fracture strength is determined in terms of apparent fracture toughness criteria, and the static failure equals the ultimate load that would result in the entire breaking of the ligament beyond the crack tips.



8.14 Feddersen's method for residual strength evaluation (Li *et al.*, 2003).

© 2008 Woodhead Publishing Limited

8.4 Plates with a single crack under ultimate compressive loads

8.4.1 Theoretical model

As a crack in a panel under axial compressive loading may lead to buckling, it is also possible that some lateral deflection may take place because of either initial deformations or additional local out-of-plane loading. After buckling, lateral deformation is a near certainty. In such cases with lateral deformation, the crack can affect (reduce) the panel collapse strength as out-of-plane deformation increases. It may, therefore, be pessimistically assumed that the effect of the cracking damage on the panel's ultimate compressive strength is similar to that on the panel's ultimate tensile strength, as in Eq. 8.5. Here, Eq. 8.5 can be transformed to:

$$\sigma_{xu} = \frac{A_c}{A_0}\,\sigma_{xuo} \tag{8.9}$$

where σ_{xuo} and σ_{xu} are the ultimate axial compressive strengths of uncracked (intact) or cracked plating, and A_c and A_0 mean the same as in Eq. 8.5.

The ultimate compressive strength formulae of uncracked plates σ_{xuo} can be expressed as follows (Paik *et al.*, 2003). For $a/b \geq 1$, the ultimate strength of an intact (uncracked) plating with an average level of fabrication-related initial imperfections under uniaxial compression in the loading direction alone may be predicted as a function of the plate slenderness ratio β', as

$$\frac{\sigma_{xuo}}{\sigma_s} = \begin{cases} -0.032\beta'^4 + 0.002\beta'^2 + 1.0 & \text{for } \beta' \leq 1.5 \\ 1.274/\beta' & \text{for } 1.5 < \beta' \leq 3.0 \\ 1.248/\beta'^2 + 0.283 & \text{for } \beta' > 3.0 \end{cases} \tag{8.10}$$

where $\beta' = \dfrac{b}{t}\sqrt{\dfrac{\sigma_s}{E}}$.

On the other hand, the ultimate compressive strength formula of the imperfect plating (i.e. with an average level of initial imperfections) under uniaxial compression in the direction of vertical loading alone may be predicted as a function of the plate aspect ratio and the slenderness ratio β', as

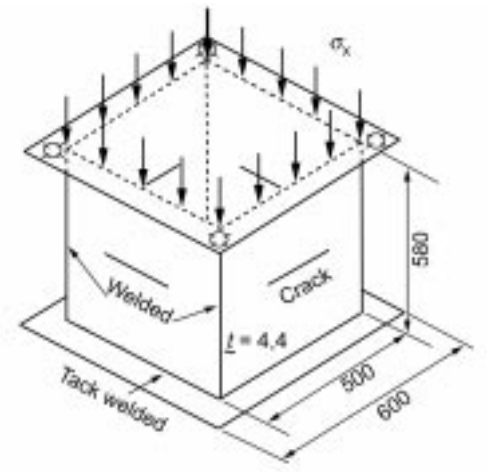
$$\frac{\sigma_{yuo}}{\sigma_s} = \frac{b}{a}\frac{\sigma_{xuo}}{\sigma_s} + \frac{0.475}{\beta'^2}\left(1 - \frac{b}{a}\right) \qquad \text{for } \frac{a}{b} \geq 1 \tag{8.11}$$

where σ_{xuo} is the ultimate strength of the plating under uniaxial compression in the loading direction alone, which is obtained from Eq. 8.10.

8.4.2 Structural model test

To verify the simplified theoretical model, a series of collapse tests on box-type

© 2008 Woodhead Publishing Limited

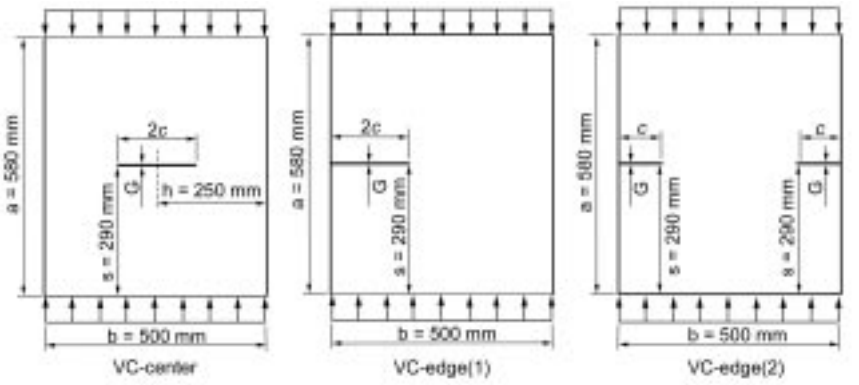


8.15 A schematic view of the test structure with cracking damage and under axial compressive loads (Paik *et al.,* 2005).

plated structures with premised cracking damage and under axial compressive loads were undertaken in a quasi-static loading condition.

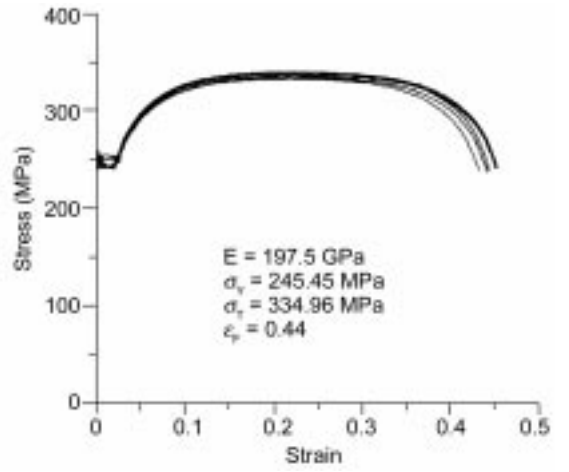
Figure 8.15 gives a schematic presentation of the test structure with cracking damage and under axial compressive loads, which includes the structural dimensions. A set of the same through-thickness cracking is artificially made in each of the four plates of the test structure. Three types of crack locations are considered, namely VC-Center, VC-Edge(1) and VC-Edge(2), as shown in Fig. 8.16. VC-Center represents a crack located at the plate center; VC-Edge(1) and VC-Edge(2) represent edge cracking, where VC-Edge(1) has a crack on one side of the plate and VC-Edge(2) has a crack on each side of the plate.

It is considered that the ultimate strength behavior of a plate with cracking damage may also be affected by the size of the gap between the crack faces,



8.16 Various crack locations considered in the test structure (Paik, 2005).

© 2008 Woodhead Publishing Limited



8.17 Stress–strain curves of the material as obtained by the tensile coupon test (E = elastic modulus; σ_Y = yield stress; σ_T = ultimate tensile stress; ϵ_F = fracture strain) (Paik *et al.*, 2005).

denoted by G. Therefore, two types of crack gap size, namely 0.3 and 3.0 mm, are considered in the present tests. Figure 8.17 shows the stress–strain curves of the material as obtained by the tensile coupon test. Maximum initial deflections were measured for each of the four plates in the test structure.

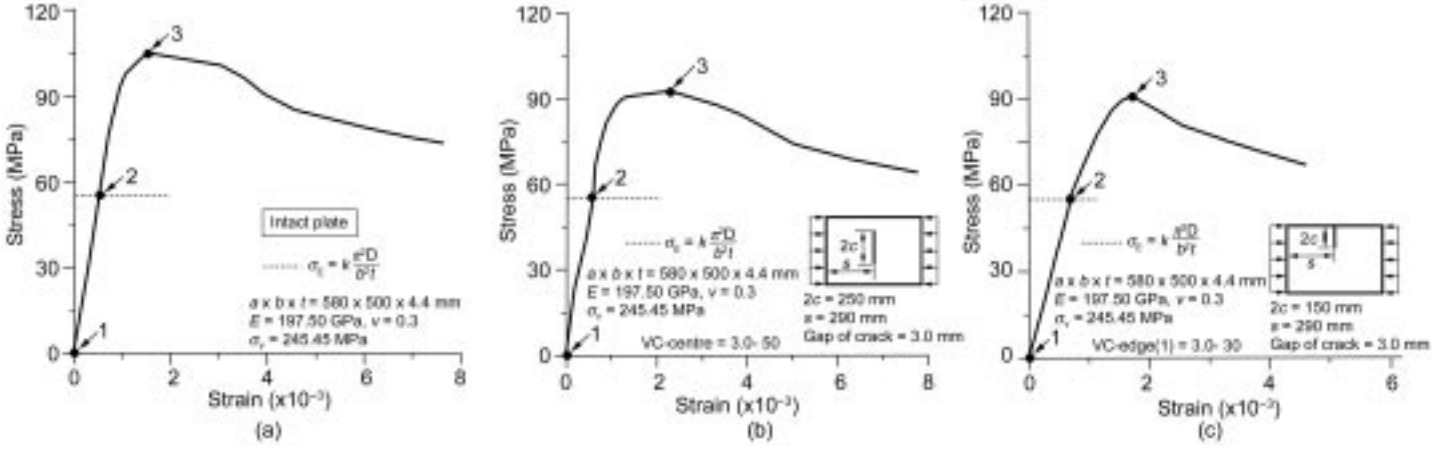
Figure 8.18(a–c) shows the average axial compressive stress–strain curves and the associated deformed shapes of the uncracked and cracked structures under axial compressive loading such as those obtained by the present experiment. An average value of the ultimate compressive strength of the four individual plates making up the test structure is then calculated by dividing the applied loads by the total cross-sectional area of the structure.

Table 8.2 summarizes the ultimate strength of the cracked plates with varying crack size and location, obtained from the present experiments. The ultimate strength predictions for the test structures can also be made using Eq. 8.9. Figure 8.19 shows the ultimate compressive strength reduction characteristics of plates due to varying crack size, obtained from the present experiment. Figure 8.20 compares the ultimate compressive strength of the cracked plates between the experiment and the simplified formula of Eq. 8.9. It is apparent that Eq. 8.9 predicts reasonably well the ultimate compressive strength of the cracked plates on the somewhat pessimistic side.

8.4.3 Finite element (FE) analysis

A series of ANSYS elastic–plastic large deflection finite element analyses for steel plates with cracking and under axial compressive loads in the x direction were undertaken, varying the crack sizes and locations so that the validity of Eq.

© 2008 Woodhead Publishing Limited



8.18 The average axial compressive stress versus strain relation and the associated deformed shapes of (a) the intact (uncracked) structure as obtained from the experiment; (b) the cracked structure VC-Center-3.0-50, as obtained from the experiment; (c) the cracked structure VC-Edge(1)-3.0-30, as obtained from the experiment (Paik *et al.*, 2005).

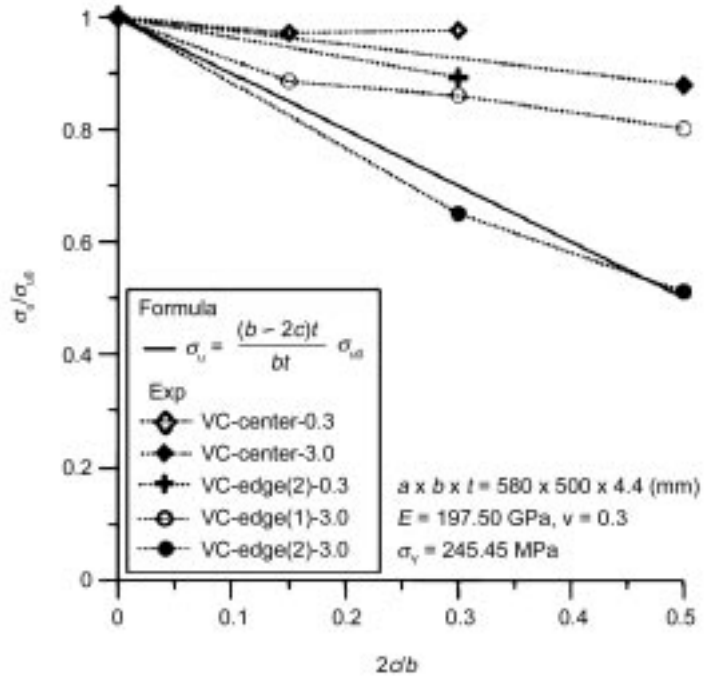
© 2008 Woodhead Publishing Limited

Table 8.2 Ultimate strength of cracked plates obtained from the experiment

Crack type	σ_{xu} (MPa)	σ_{xu}/σ_Y	σ_{xu}/σ_{xu0}
Intact	105.3	0.429	1.0
VC-Center-0.3-15	102.27	0.417	0.971
VC-Center-0.3-30	102.89	0.419	0.977
VC-Center-3.0-50	92.65	0.377	0.880
VC-Edge(1)-3.0-15	93.38	0.380	0.887
VC-Edge(1)-3.0-30	90.55	0.369	0.860
VC-Edge(1)-3.0-50	84.40	0.344	0.802
VC-Edge(2)-0.3-30	94.11	0.383	0.894
VC-Edge(2)-3.0-30	68.60	0.279	0.651
VC-Edge(2)-3.0-50	53.64	0.219	0.509

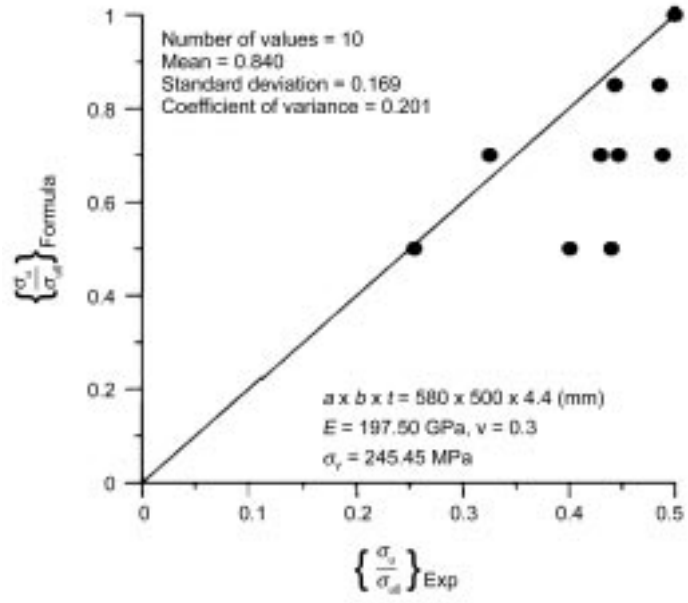
8.9 would be further checked by comparison with the computed results, and the ultimate strength characteristics of the plate with cracks and under axial compression were studied.

Figures 8.21 and 8.22 show the average axial compressive stress–strain curves of a plate with center crack (i.e. $s = 0.5a$, $h = 0.5b$), with varying crack

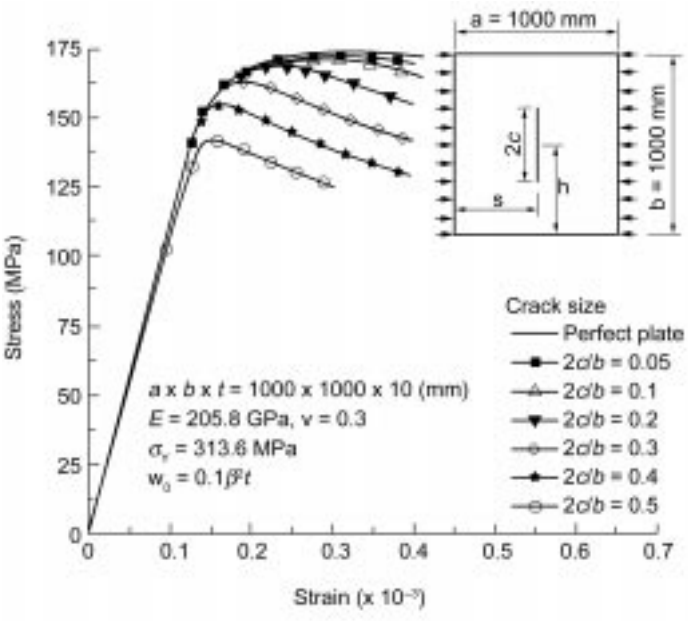


8.19 The ultimate compressive strength reduction characteristics of steel plates as a function of the crack size (σ_{uo}, σ_u = ultimate strengths of uncracked or cracked plate elements) (Paik *et al.*, 2005).

© 2008 Woodhead Publishing Limited

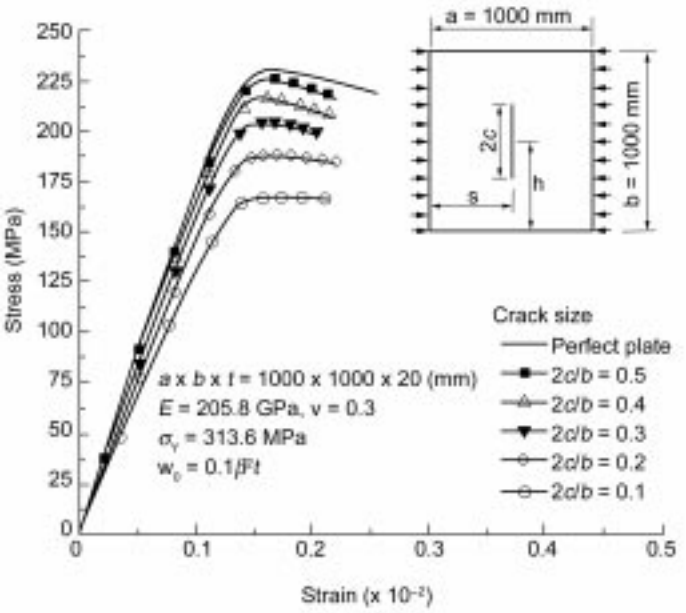


8.20 Comparison between the experiment and Eq. (8.9) for the ultimate compressive strength of steel plates with cracking damage (Paik *et al.,* 2005).



8.21 Average axial compressive stress–strain curves for a plate with center crack, $t = 10$ mm (Paik *et al.,* 2005).

© 2008 Woodhead Publishing Limited



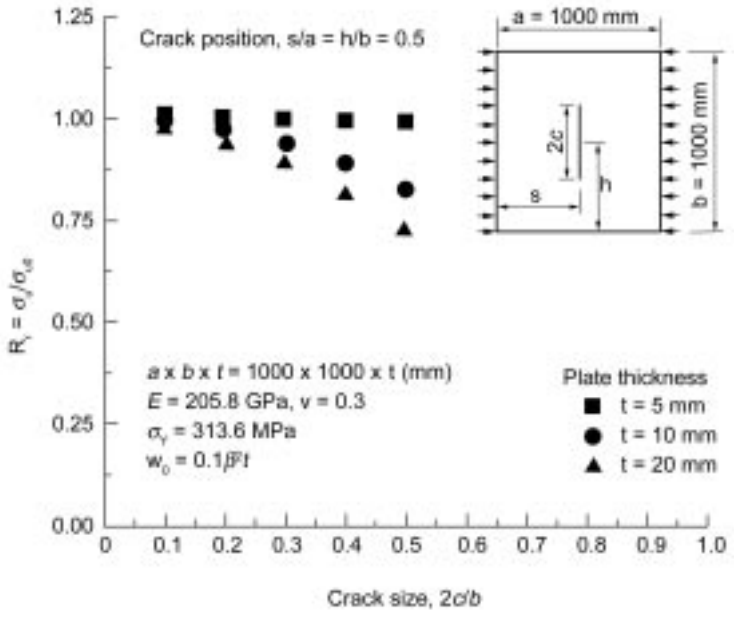
8.22 Average axial compressive stress–strain curves for a plate with center crack, $t = 20$ mm (Paik *et al.*, 2005).

lengths and different plate thicknesses. It is observed from Fig. 8.21 that a crack with size $2c/b \leq 0.2$ causes an insignificant reduction in the ultimate strength of the plate, whereas a crack of size $2c/b > 0.2$ reduces the strength moderately, while Fig. 8.22 shows that the ultimate strength of 20 mm thick plate is found to decrease with increase in crack size, unlike that of 10 mm thick plates as shown in Fig. 8.21. In the case of 10 mm thick plates, the ultimate strength is found to decrease moderately with change in crack size.

Figure 8.23 plots the reduction factor of the ultimate strength for vertical center-cracked plates with thickness $t = 5$, 10 and 20 mm, which is defined as the ratio of the cracked plate ultimate strength to the perfect plate ultimate strength. The ultimate strength reduction characteristics are more significant as plate thickness increases. Plates with thickness $t = 5$ mm are not influenced by the crack, and their ultimate strength is similar to that of a perfect plate. Plates with thickness $t = 10$ mm show a moderate reduction in ultimate strength compared to that of perfect plates, whereas plates with thickness $t = 20$ mm show a significant decrease in ultimate strength with increase in crack size.

Figure 8.24 shows the average axial compressive stress–strain curves of an edge-cracked plate under axial compression. The crack size was varied from $2c/b = 0.1$ to 0.5 and also the crack location was varied from $s/a = 0.0$ to 0.5, where $s/a = 0$ indicates that the crack is located at $x = 0$ and $s/a = 0.5$ indicates that the crack is located at the center of the bottom horizontal edge of the plate.

© 2008 Woodhead Publishing Limited



8.23 The ultimate compressive strength reduction characteristics of a center-cracked plate as a function of the crack size (Paik *et al.,* 2005).

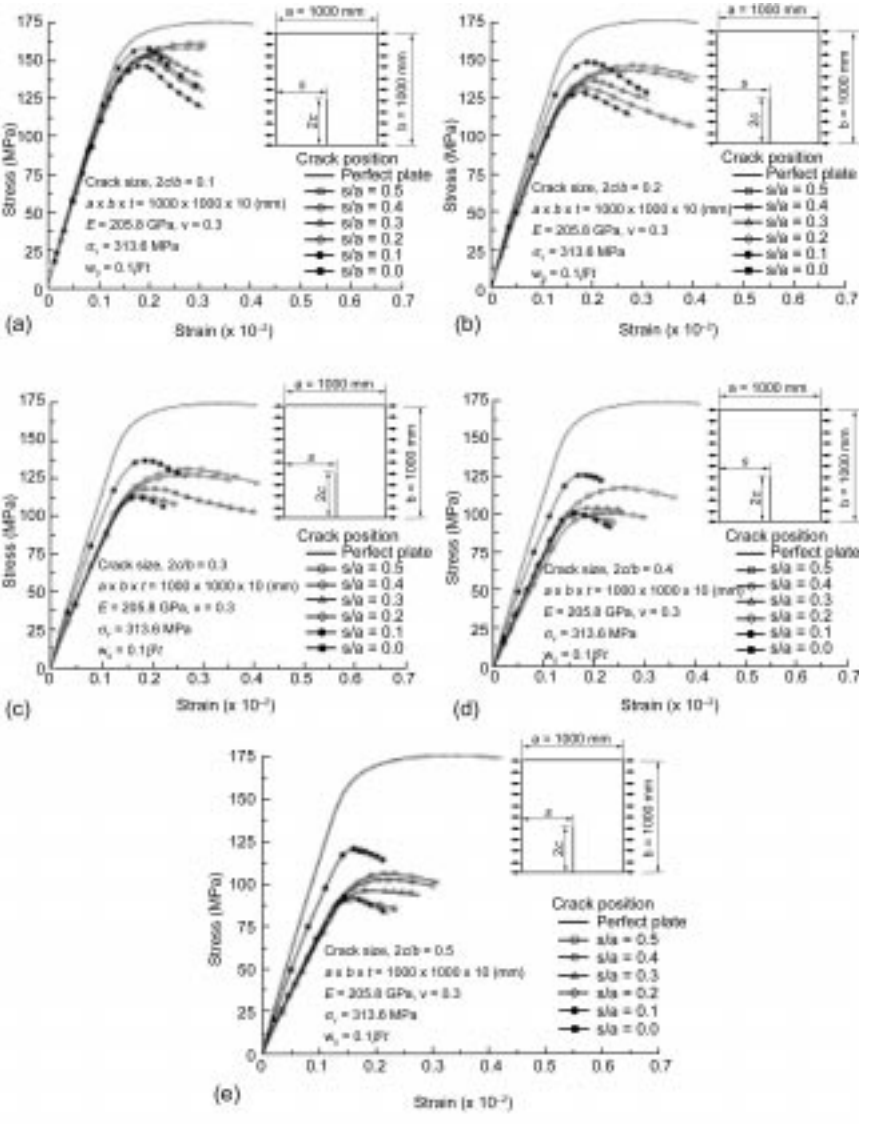
The ultimate strengths are found to remain constant irrespective of the location of the crack. However, when the crack is located at $s/a = 0.0$, the ultimate strength of the plate is found to be higher than when the crack is located elsewhere. The minimum value of the ultimate strength is noticed when the crack is located at $s/a = 0.1$.

Figure 8.25 shows the stress–strain curves of a plate with 20 mm thickness. The crack size was varied from $2c/b = 0.1$ to 0.5. The location of the crack was varied from $s/a = 0.0$ to 0.5. The ultimate strength of the plate was found to remain constant irrespective of location of the crack. However, the strength of the plate was higher when the crack was located at $s/a = 0.0$.

Figure 8.26 shows the reduction characteristics in ultimate strength of plates with thickness $t = 10$ and 20 mm. The reduction factor is found to increase with increase of the thickness of the plate. The reduction in ultimate strength is a minimum when the crack is located at either $s/a = 0.1$ or $s/a = 0.2$.

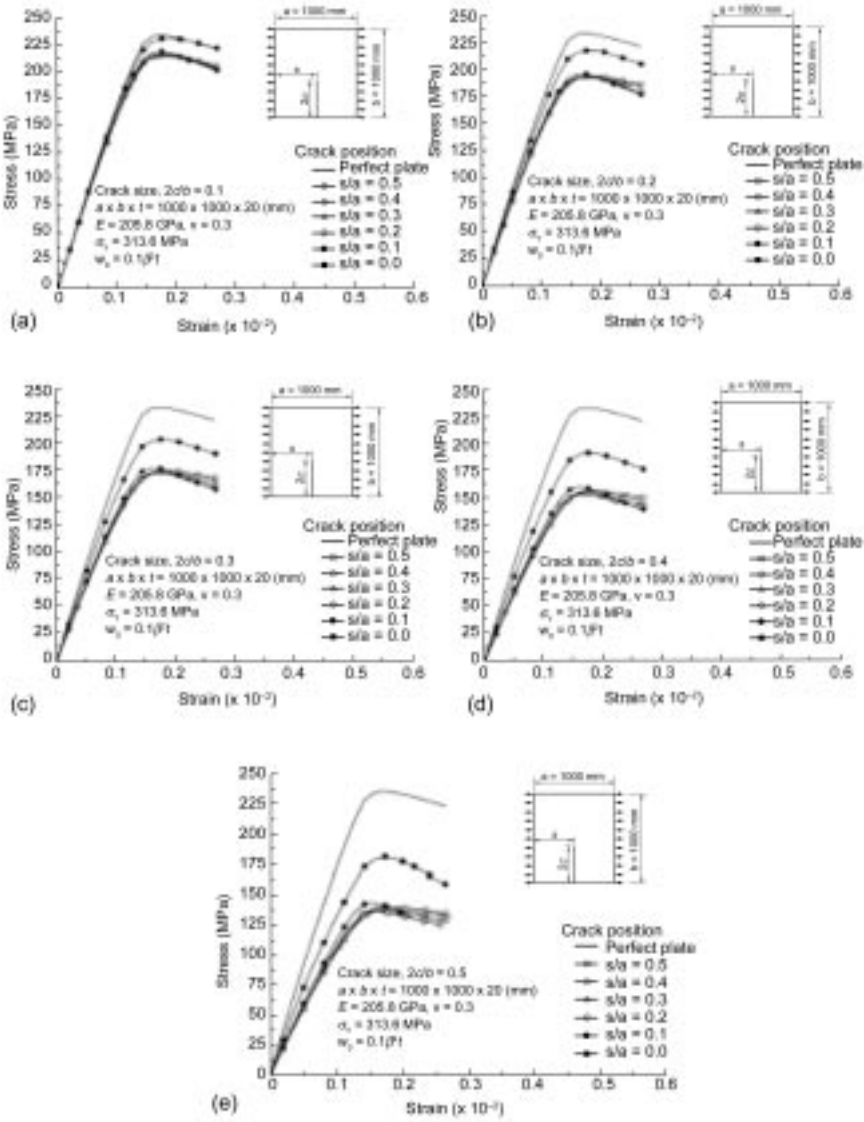
The behavior of edge-cracked plates is different from that of center-cracked plates for varying thickness of the plate. The reduction factor in center-cracked plates is found to decrease with increase in plate thickness, whereas the reduction factor in edge-cracked plates is found to increase with increase in plate thickness.

© 2008 Woodhead Publishing Limited



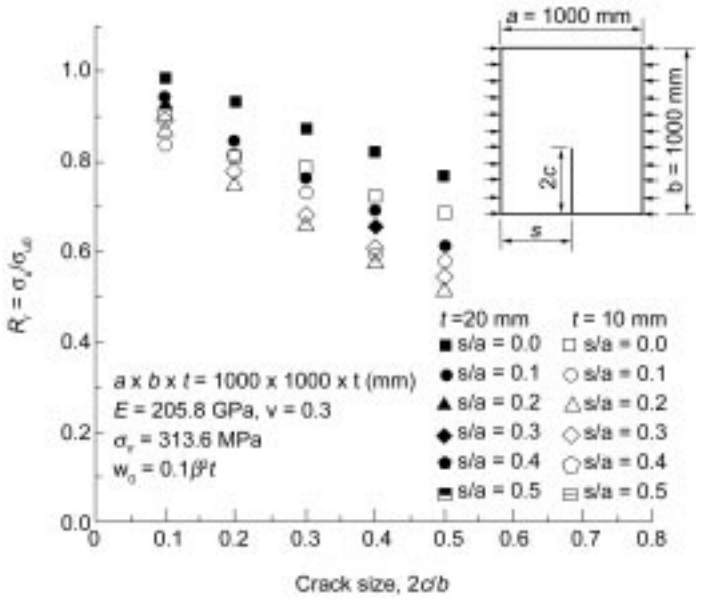
8.24 Average axial compressive stress–strain curves for edge-cracked plate ($t = 10$ mm) for varying locations of the crack with crack size (a) $2c/b = 0.1$, (b) $2c/b = 0.2$, (c) $2c/b = 0.3$, (d) $2c/b = 0.4$, (e) $2c/b = 0.5$ (Paik *et al.*, 2005).

© 2008 Woodhead Publishing Limited



8.25 Average axial compressive stress–strain curves for edge-cracked plate ($t = 20$ mm) for varying locations of the crack with crack size (a) $2c/b = 0.1$, (b) $2c/b = 0.2$, (c) $2c/b = 0.3$, (d) $2c/b = 0.4$, (e) $2c/b = 0.5$ (Paik *et al.*, 2005).

© 2008 Woodhead Publishing Limited



8.26 The ultimate compressive strength reduction characteristics of edge-cracked plates (Paik *et al.,* 2005).

8.5 Residual strength of plates with multiple collinear cracks

The residual strength of plates with multiple collinear cracks has been investigated mainly in aging aircraft since the Aloha accident in 1988 but is gradually attracting attention as part of fracture study for aging ships. Multiple collinear cracks can be characterized by the interaction of a lead crack with several short cracks located collinearly in the same structural element, which may become critical when cracks are of sufficient size and density to exceed the residual strength of the structural element (Labeas *et al.*, 2005). When multiple cracks are present, the residual strength may decrease well below that which would otherwise be expected with a single lead crack (Cherry *et al.*, 1997). Several analytical techniques have been proposed to predict the failure load of a panel with multiple cracks when subjected to a monotonically increasing load. Five of these techniques are briefly described below.

8.5.1 Failure criteria

Net ligament loss criterion

The net ligament loss criterion, also referred to as net section yield, predicts failure based on the amount of material available to carry the load. Con-

© 2008 Woodhead Publishing Limited

sequently, the failure load is a function of the material's yield strength, and the number of flaws included in the gage section. The failure load is the load that causes the net section stress to equal or exceed the material's yield strength. The calculation formula is similar to Eqs 8.5 and 8.9 for a single crack.

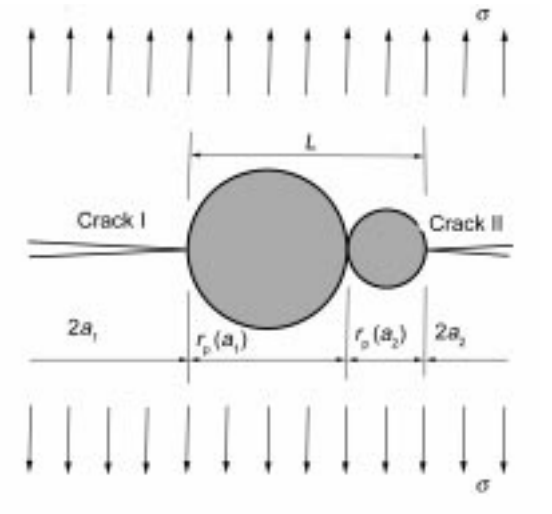
K-apparent criterion

The *K*-apparent criterion is based on linear elastic fracture mechanics. The primary assumption for this criterion is that there exists an effective fracture toughness for the thin sheet which allows more yielding than that under the plane strain condition. This is referred to here as K_{app} (*K*-apparent). Unlike the fracture toughness K_{IC}, K_{app} is not strictly a material property, but can vary with different geometries and crack configurations. The following equation was used to determine K_{app}:

$$K_{app} = \sigma \sqrt{\pi a \beta_w} \qquad 8.12$$

where σ = applied stress at fracture; W = specimen width; a = half of lead crack length; and $\beta_w = \sec(\pi a/W)$ = finite width correction factor.

To determine the predicted failure load by this criterion, the stress intensity factor of the lead crack, including crack interaction effects from multiple cracks, was used to determine the remotely applied load that would produce a stress intensity factor equal to or greater than the measured K_{app}.



8.27 Schematic of plastic zones for ligament yield criterion (Xu and Yao, 2001).

© 2008 Woodhead Publishing Limited

Ligament yield criterion

The ligament yield criterion (Swift, 1993) predicts the residual strength of the panel with lead crack and multiple cracks as the stress level causes the lead crack's plastic zone to touch the plastic zone of the multiple cracks, as shown in Fig. 8.27. The size of the plastic zone is equal to Irwin's plastic zone radius. The criterion can be expressed as:

$$r_p(a_1) + r_p(a_2) = L_s \tag{8.13}$$

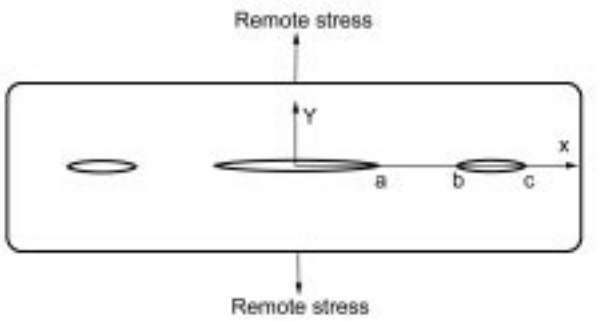
where $r_p(a_1)$ and $r_p(a_2)$ are the sizes of the plastic zone for cracks 1 and 2, and L_s is the ligament length. The size of the plastic zone is equal to Irwin's plastic zone radius:

$$r = \frac{1}{2\pi}\left(\frac{K}{\sigma_s}\right)^2 \tag{8.14}$$

where r = plastic zone diameter in front of the crack; K = stress intensity factor at the crack tip; and σ_s = yield strength of the material.

Average displacement criterion

The average displacement criterion (Jeong and Brewer, 1995) assumes that the stress across the ligament is uniform and equal to the material's ultimate strength. According to Jeong and Brewer, prior to specimen failure, the displacement of the crack faces is assumed to be zero in the direction parallel to the crack. The configuration with a single large lead crack surrounded by smaller multiple cracks was modeled as the superposition of two known cases. The two cases used were a single crack (from $x = 0$ to $x = c$) in an infinite medium subjected to remote tension, and the same single crack subjected to pressure loading on its crack faces. The locations of the crack tips used in this criterion and in the next criterion also by Jeong and Brewer can be seen in Fig. 8.28. Since the displacement of the crack faces along the ligament (from $x = a$ to



8.28 Locations of crack tips for average stress and average displacement criterion (Cherry *et al.*, 1997).

© 2008 Woodhead Publishing Limited

$x = b$) after superposition should be zero, this criterion then becomes:

$$\int_0^a \nu_1(x)\mathrm{d}x + \int_a^b \nu_2(x)\mathrm{d}x = 0 \tag{8.15}$$

where:

$\nu_1(x)$ = displacement of the crack face perpendicular to the crack (finite body uniform tension);

$\nu_2(x)$ = displacement of the crack face perpendicular to the crack (infinite body pressure loading).

$$\nu_1(x) = \frac{2\sigma}{E}\sqrt{c^2 - x^2} \tag{8.16}$$

$$\begin{aligned}\nu_2(x) = \frac{2\sigma_{\text{ult}}}{\pi E}\Bigg[&(b-x)\cos h^{-1}\frac{c^2 - bx}{c(b-x)} - (a-x)\cos h^{-1}\frac{c^2 - ax}{c(x-a)} \\ &+(b+x)\cos h^{-1}\frac{c^2 + bx}{c(x+b)} - (a+x)\cos h^{-1}\frac{c^2 + ax}{c(x+a)} \\ &+2\left(\sin^{-1}\left(\frac{b}{c}\right) - \sin^{-1}\left(\frac{a}{c}\right)\right)\sqrt{c^2 - x^2}\Bigg]\end{aligned} \tag{8.17}$$

The predicted failure load, P_{avgd}, of the panel according to the average displacement criterion becomes:

$$P_{\text{avgd}} = \frac{2\sigma_{\text{ult}} W_{\text{asd}} t}{\pi} \frac{\displaystyle\int_a^b \nu_2(x)\mathrm{d}x}{b\sqrt{c^2 - b^2} - a\sqrt{c^2 - a^2} + c^2\left[\sin^{-1}\left(\frac{b}{c}\right) - \sin^{-1}\left(\frac{a}{c}\right)\right]} \tag{8.18}$$

where a, b and c = locations of the crack tips shown in Fig. 8.28; and W_{asd} = appropriate width for average displacement and average stress criterion.

Average stress criterion

The average stress criterion (Jeong and Brewer, 1995) postulates that the stress in the ligament between the lead crack and its nearest neighboring multiple cracks is uniform and equal to the material ultimate strength immediately prior to failure of the specimen. The average stress criterion models the various cracks individually. Linkup between the two adjacent cracks is assumed to occur when the average stress in the ligament between the crack tips is equal to the ultimate tensile strength of the material. The criterion can be expressed as:

$$P_{\text{avgst}} = \sigma_{\text{ult}} W_{\text{asd}} t \frac{b - a}{\displaystyle\int_a^b \frac{\left[(c^2 - a^2)\dfrac{E(k)}{K(k)} + a^2\right]x - x^3}{\sqrt{(x^2 - a^2)(b^2 - x^2)(c^2 - x^2)}}\mathrm{d}x} \tag{8.19}$$

where:

© 2008 Woodhead Publishing Limited

P_{avgst} = specimen failure load based on the average stress criterion;
$E(k)$ = complete elliptic integral of the first kind;
$K(k)$ = complete elliptic integral of the second kind;

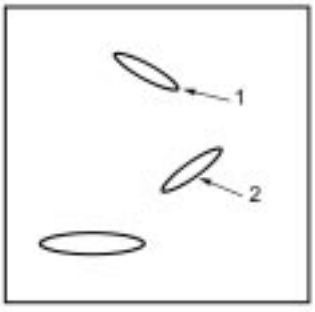
$$k = \text{geometry factor} = \sqrt{\frac{c^2 - b^2}{c^2 - a^2}}$$

8.5.2 Residual strength prediction using different criteria

Among all the criteria, the most extensively applied is the ligament yield criterion, known as the 'plastic zone touch' model, because its results are conservative in the majority of the cases for which it has been applied (Labeas *et al.*, 2005). Comparisons between different criteria with experimental results on narrow and wide panels with MSD were done by Cherry *et al.* (1997). Results show that the K-apparent approach produced the most unconservative results and the net ligament loss criterion produced the most accurate residual strength predictions. The net ligament loss criterion also gave good results, but it was unconservative for the wider panels and conservative for the narrow ones. The average stress and average displacement criterion consistently produced excessively conservative predictions of residual strength. Only the net ligament loss criterion showed a difference in the prediction of residual strength between the narrow and wide panels.

8.6 Random cracks

In actual structures, multiple cracks commonly exist with random length, inclination, number and distribution and even random boundary and loading conditions. The crack number, length and orientation at the onset of fracture are usually treated as random variables. Few studies have been carried out on the residual strength of cracked structures with random cracks, though some theories have been derived for brittle fracture and fatigue problems (e.g. Ni, 1996; Nicholson and Ni, 1997). The studies on elasto-plastic problems are mainly concentrated on fracture parametric analysis such as the *J*-integral when random



8.29 Cracked plate with random disturbing cracks (Wang *et al.*, 2006).

© 2008 Woodhead Publishing Limited

disturbing cracks exist (e.g. Wang and Cui, 2006). As in Fig. 8.29, a lead crack exists with two small disturbing cracks which will influence the value of the *J*-integral around the crack tip of the lead crack, which will eventually affect the residual strength of the cracked plate. But in contrast with a single crack or collinear multi-cracks, random cracks may not definitely reduce the strength of cracked bodies. The disturbing cracks can sometimes increase the strength of cracked bodies with only lead cracks.

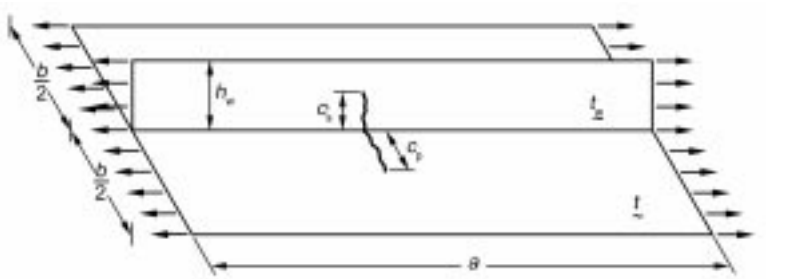
8.7 Ultimate strength of cracked stiffened panels

8.7.1 Ultimate tensile strength reduction characteristics of cracked panels

For a typical steel stiffened panel with existing vertical crack damage as in Fig. 8.30, with increasing tensile load the effect of the crack propagation on the ultimate behavior of the cracked panel will be of significance. In this regard, LS-DYNA3D is employed, taking account of the crack propagation to exhibit the ultimate tensile strength reduction characteristics of cracked panels. In the analysis, two types of panel material models are employed, as follows:

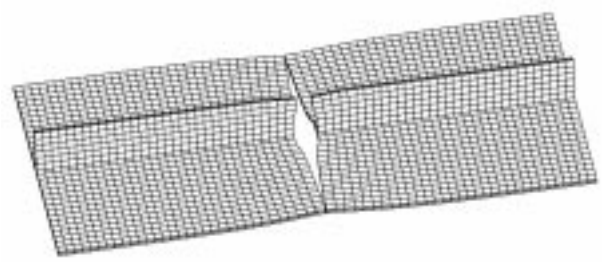
1. The stress–strain relationship of the panel material obtained by the tensile coupon test is used, meaning that the effects of strain-hardening, necking and ductile fracture are accounted for as far as possible.
2. The elastic–perfectly plastic material model is used by neglecting the effect of strain-hardening, but taking into account ductile fracture.

For all analyses, the effect of crack extension by tearing is taken into consideration as the external tensile loads monotonically increase. Figure 8.31 shows a typical deformed shape immediately before the panel is entirely fractured, that is, the panel is broken into two pieces. Figure 8.32 shows the LS-DYNA3D results for the average stress–strain relation for the stiffened panel under monotonically applied axial tensile loads until the panel is broken into two pieces.

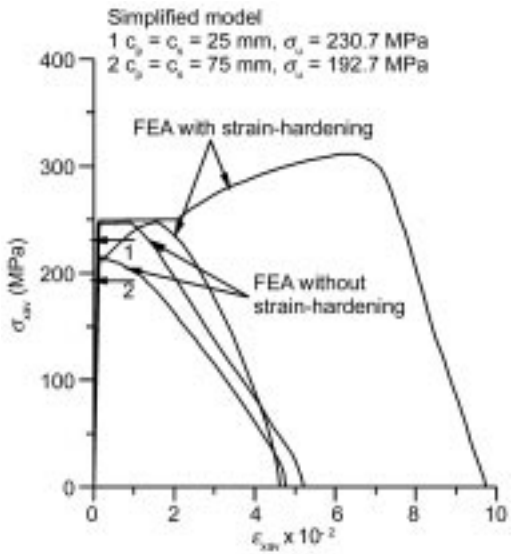


8.30 A typical stiffened steel panel component with existing vertical crack (Paik and Satish Kumar, 2006).

© 2008 Woodhead Publishing Limited



8.31 Deformed shape immediately before the entire fracture of the stiffened panel under monotonic tensile loads, as obtained by LS-DYNA3D ($b = 400$ mm, $a = 1600$ mm, $t = 15$ mm, $h_w = 150$ mm, $t_w = 12$ mm, $\sigma_{Yp} = \sigma_{Ys} = 249.7$ MPa, $E = 202.2$ GPa and $\nu = 0.3$; $2c_p = 50$ mm or 150 mm at plating and $c_s = 25$ mm or 75 mm at stiffener) (Paik and Satish Kumar, 2006).

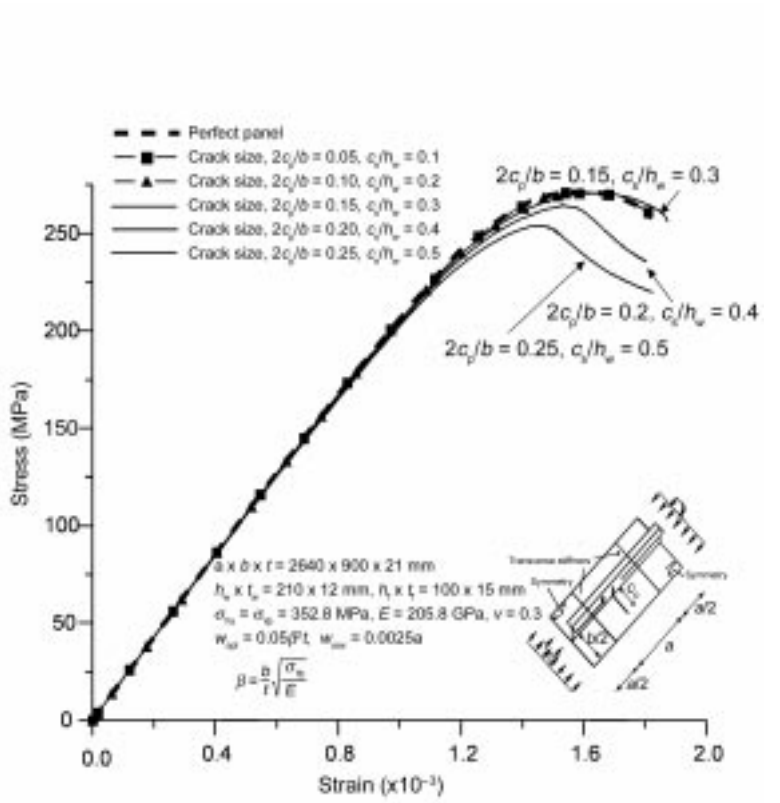


8.32 The elastic–plastic behavior of a stiffened panel with premised cracks and under monotonic tensile loads (Paik and Satish Kumar, 2006).

8.7.2 Ultimate compressive strength reduction characteristics of cracked panels

In contrast to the cracked panel under axial tension, the effect of crack propagation on the panel's ultimate strength behavior is considered to be small when axial compressive loads are predominant (Paik *et al.*, 2003). In this regard, ANSYS (2003) is employed, considering the crack propagation in this part to exhibit the ultimate compressive strength reduction characteristics of cracked

© 2008 Woodhead Publishing Limited



8.33 Average axial compressive stress–strain curves of a stiffened panel with vertical cracks on one side of stiffener and web, as those obtained by ANSYS (w_{opl} = plate initial deflection, w_{osx} = maximum global initial deflection of stiffener) (Paik and Satish Kumar, 2006).

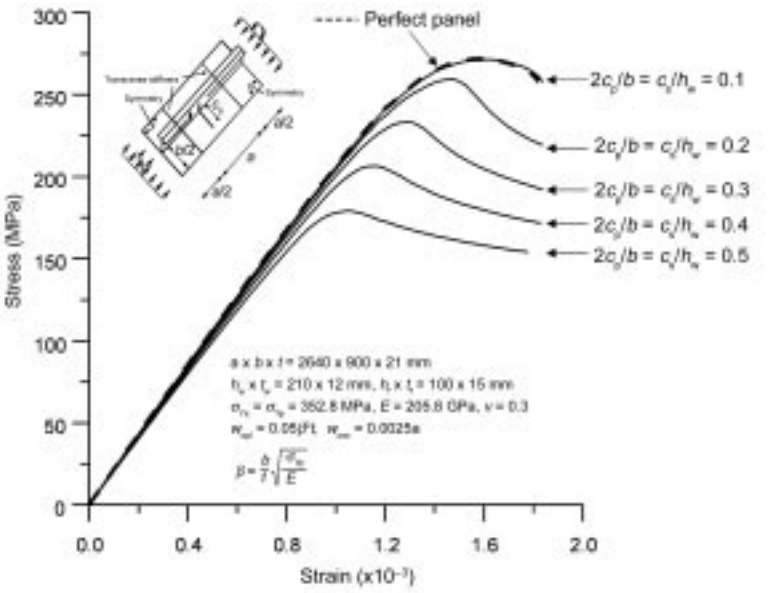
panels. Figures 8.33 and 8.34 show the average axial compressive stress–strain curves for a stiffened panel under axial compressive loads and with a single edge crack and a double crack. It is considered that the stiffener web always has a crack in each case. It can be seen that the ultimate compressive strength of the stiffened panel decreases significantly with increase in the crack size.

8.7.3 Theoretical model

As for the case of the cracked unstiffened panel, the ultimate strength of a cracked stiffened panel can also be pessimistically predicted using the simplified theoretical model noted in Eq. 8.5 (tensile strength) and Eq. 8.9 (compressive load), as follows:

$$\sigma_u = \frac{(b - c_p)t\sigma_{Yp} + (h_w - c_s)t_w\sigma_{Ys}}{bt + h_w t_w} \qquad 8.20$$

© 2008 Woodhead Publishing Limited



8.34 Average axial compressive stress–strain curves of a stiffened panel with vertical cracks on both sides of stiffener and web, as those obtained by ANSYS (w_{opl} = plate initial deflection, w_{osx} = maximum global initial deflection of stiffener) (Paik and Satish Kumar, 2006).

where c_p = crack length for the plating, c_s = crack length for the stiffener, $\sigma_{Yp} = \sigma_Y$ = yield strength of the plating, and σ_{Ys} = yield strength of the stiffener.

Tables 8.3 and 8.4 indicate the ultimate tensile and compressive strengths of the panel respectively obtained by FE analysis compared with results from the simplified Eq. 8.20. Based on the results of FE analysis and the simplified theoretical model, additional insights can be obtained as follows:

- It is evident that the cracking damage reduces the ultimate strength of a stiffened panel significantly.
- The theoretical model is characterized by the reduced cross-sectional area associated with the cracking damage being equal to that area multiplied by the yield strength (i.e., ultimate strength of uncracked panel) for a cracked panel under tensile loads. The validity of the simplified model can be confirmed numerically. The ultimate strength of cracked panels under axial compressive loads decreases as out-of-plane deformation increases. The effect of the cracking damage on the panel's ultimate compressive strength is similar to that of the cracking damage on the panel's ultimate tensile strength. Therefore, Eq. 8.20 can be used to predict the ultimate tensile/compressive strength on the somewhat pessimistic side.

© 2008 Woodhead Publishing Limited

Table 8.3 Comparison of the simplified model solutions with FEA

c_p (mm)	c_s (mm)	σ_u (MPa)		A/B	Effect of strain-hardening
		A	*B*		
25	25	230.7	311.4	0.741	Included
			246.8	0.935	Not included
75	75	192.7	247.8	0.778	Included
			212.9	0.905	Not included

A = simplified model, *B* = LS-DYNA3D. The simplified model does not account for the effect of strain-hardening.

- The results and insights in this part can be used for the ultimate limit state-based risk or reliability assessment of steel-plate structures with cracking damage.

8.7.4 Residual tensile strength of stiffened panels with multiple cracks

Multiple cracks in stiffened panels may include two types, namely multiple site damage (fatigue cracks existing simultaneously in the same structural element) and multiple element damage (fatigue cracks existing simultaneously in different but similar structural elements). The residual strength of a cracked stiffened panel in this case can be similarly predicted using criteria introduced in Section 8.5 but should be equivalently transformed by an equivalent rigidity method. The generally used criterion for a cracked stiffened panel is the equivalent net ligament loss criterion, expressed as follows:

$$\sigma \frac{A_{w0} + \frac{E_s}{E_w} A_{s0}}{A_w + \frac{E_s}{E_w} A_s} \geq \sigma_s \tag{8.21}$$

where σ is the applied stress; A_{w0} and A_w are the initial area and the remaining area of the web plate, respectively; A_{s0} and A_s are the initial area and the remaining area of stiffeners, respectively; E_w and E_s are the rigidities of the web plate and stiffener, respectively; and σ_s is the material yield stress.

Other criteria for an unstiffened plate with multiple cracks can also be transformed for stiffened panels as crack tip ligament yield criteria, which are referred to in some works (e.g. Wang *et al.*, 2004). As prediction of the coalescence of adjacent cracks is critical for the residual strength estimation of structures under multiple site damage conditions, an energy-based methodology successfully developed for the case of crack linkup prediction of unstiffened plates (Labeas *et al.*, 2005) is extended to the case of typical cracked stiffened aircraft panels (Labeas and Diamantakos, 2006). The proposed linkup criterion

© 2008 Woodhead Publishing Limited

Table 8.4 Ultimate compressive strength of a stiffened panel with cracking damage as obtained by ANSYS

Crack position in plate	Crack size		σ_{xu} by FEM	σ_{xu} by formula	$\left(\frac{\sigma_{xu}}{\sigma_{Yeq}}\right)$ by FEM	$\left(\frac{\sigma_{xu}}{\sigma_{Yeq}}\right)$ by formula	$\left(\frac{\sigma_{xu}}{\sigma_{xuo}}\right)$ by FEM	$\left(\frac{\sigma_{xu}}{\sigma_{xuo}}\right)$ by formula
	$2c_p/b$	c_s/h_w						
Perfect panel	0.00	0.0	271.76	271.76	0.770	0.770	1.000	1.000
On one side of stiffener	0.05	0.1	271.61	257.57	0.770	0.730	1.000	0.948
	0.10	0.2	271.13	243.37	0.769	0.689	0.997	0.896
	0.15	0.3	270.71	229.18	0.767	0.649	0.996	0.843
	0.20	0.4	264.95	214.99	0.751	0.609	0.975	0.791
	0.25	0.5	254.05	200.79	0.720	0.569	0.935	0.739
On both sides of stiffener	0.10	0.1	271.45	246.36	0.769	0.698	0.999	0.907
	0.20	0.2	259.19	220.97	0.735	0.626	0.954	0.813
	0.30	0.3	233.16	195.57	0.661	0.554	0.858	0.719
	0.40	0.4	206.22	170.17	0.585	0.482	0.759	0.626
	0.50	0.5	178.90	144.77	0.507	0.410	0.658	0.533

© 2008 Woodhead Publishing Limited

is based on the quantity of the 'specific' strain energy increase, i.e. the strain energy increment due to the ligament area.

8.8 Ultimate strength of cracked ship hull girder

The International Maritime Organization (IMO), classification societies and ship owners continue to seek acceptable standards for the structural integrity of aging ships without excessive economic penalties with respect to repair and maintenance costs incurred over the ship's life cycle. The ultimate strength of ship hull girders will be slowly reduced due to the degradation effects of fatigue cracks. Assessing the residual strength of a ship structure, it has been common to consider three main strength components, which are longitudinal strength, transverse strength and local strength. Among these strengths, longitudinal strength, that is hull girder strength, is the most fundamental and important strength to ensure the safety of a ship structure. With the increase of the applied longitudinal bending moment, the structural members composing a hull cross-section begin to collapse one by one due to buckling and yielding. The unsteady propagation of fatigue cracks may induce rapid reduction of the residual ultimate strength of ship structures, and the unsteady period of crack propagation is very short compared to the inspection interval. The ultimate bending moment of the ship hull girder is associated with the compressive and tensile ultimate strength of stiffened panels between bulkheads or web frames and of unstiffened plates between stiffeners. The residual strength of a cracked ship hull girder can be assessed by the following method.

8.8.1 Residual strength calculation of unstiffened and stiffened panels with crack damage

The residual ultimate strength of unstiffened plates and stiffened panels with crack damage can be assessed using simplified models or empirical formulas introduced in previous sections of this chapter. The critical crack length can be determined for a given external load using Eq. 8.5, 8.7, 8.9, 8.20 or 8.21.

8.8.2 Crack propagation prediction

To predict the crack propagation and fatigue life, the Paris–Erdogan equation is often used:

$$\frac{\mathrm{d}a(t)}{\mathrm{d}N} = C\Delta K^m \qquad 8.22$$

where $a(t)$ is the crack length at given time t, N is the number of cycles, ΔK is the stress intensity factor range, and C and m are material parameters. The stress intensity factor range is given by

© 2008 Woodhead Publishing Limited

$$\Delta K = \Delta\sigma Y(a)\sqrt{\pi a} \tag{8.23}$$

where $\Delta\sigma$ is the stress range and $Y(a)$ is the geometry function. If $Y(a) = Y$ is a constant and $N = v_0 t$ where v_0 is the mean zero uncrossing rate and t is the time, then integration of Eq. 8.22 gives

$$\begin{aligned} a(t) &= \left[a_0^{1-m/2} + \left(1 - \frac{m}{2}\right) C\Delta\sigma^m Y^m \pi^{m/2} v_0 t\right]^{2/(2-m)}, \quad m \neq 2 \\ a(t) &= a_0 \exp\left(CY^2 \Delta\sigma^2 \pi v_0 t\right), \qquad m = 2 \end{aligned} \tag{8.24}$$

The complete fatigue life T_f is equal to the sum of the time of crack propagation T_p with the time of crack initiation T_i (Guedes Soares and Garbatov, 1998):

$$T_\mathrm{f} = T_\mathrm{i} + T_\mathrm{p} \tag{8.25}$$

The probability distribution of the time of crack initiation is approximated by a Weibull distribution (Guedes Soares and Garbatov, 1998):

$$F_{T_\mathrm{i}}(t_\mathrm{i}) = 1 - \exp\left[-\left(\frac{t_\mathrm{i}}{\beta_{T_\mathrm{i}}}\right)\right] \tag{8.26}$$

It is practical and sufficiently accurate to assume that the time to crack initiation is related to the time to reach a critical size a_cr by

$$T_\mathrm{i} = kT_\mathrm{p} \tag{8.27}$$

where k can vary between 0.1 and 0.15 (Guedes Soares and Garbatov, 1998).

To calculate the time of crack propagation, the critical crack length a_cr should be determined first. When the residual ultimate strength of the unstiffened plate or stiffened panel is lower than the maximum external load, the crack will propagate unstably.

Using Eq. 8.24, the mean value and variance of the crack propagation length are given by

$$\overline{a(t)} = \left[\overline{a_0}^{1-m/2} + \left(1 - \frac{m}{2}\right)\overline{C\Delta\sigma}^m Y^m \pi^{m/2} v_0 t\right]^{2/(2-m)} \tag{8.28}$$

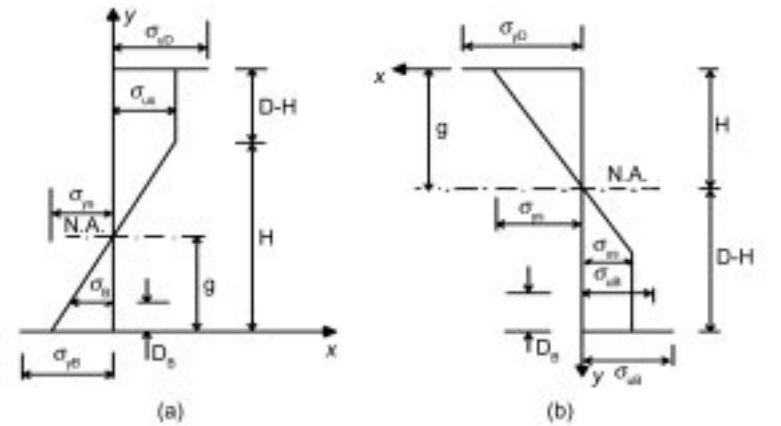
$$\begin{aligned} D_{a(t)} = &\left[\frac{\overline{a_0}^{m/2}\overline{a(t)}}{\overline{a_0}^{1-m/2} + \left(1 - \frac{m}{2}\right)\overline{C\Delta\sigma}^m Y^m \pi^{m/2} v_0 t}\right]^2 D_{a(0)} \\ &+ \left[\frac{\overline{\Delta\sigma}^m Y^m \pi^{m/2} v_0 t\overline{a(t)}}{\overline{a_0}^{1-m/2} + \left(1 - \frac{m}{2}\right)\overline{C\Delta\sigma}^m Y^m \pi^{m/2} v_0 t}\right]^2 D_\mathrm{C} \\ &+ \left[\frac{\overline{C\Delta\sigma}^m Y^m \pi^{m/2}}{\overline{a_0}^{1-m/2} + \left(1 - \frac{m}{2}\right)\overline{C\Delta\sigma}^m Y^m \pi^{m/2} v_0 t}\right]^2 D_{a(0)} \end{aligned} \tag{8.29}$$

© 2008 Woodhead Publishing Limited

8.8.3 Ultimate strength of ship hulls

Vasta (1958) assumed that the ship hull would reach the ultimate limit state when the compression flange, i.e. the upper deck in the sagging condition or the bottom plating in the hogging condition, collapses, and that the relationship between the bending moment and curvature is linear. Caldwell (1965) took into account buckling in compression and yielding in tension. The ship hull cross-section was idealized as an equivalent section with uniform plate thickness in deck, bottom or sides. When the ship hull reached the ultimate limit state, the entire material in compression was assumed to have reached its ultimate buckling strength and the entire material in compression was assumed to have reached full yielding. However, in the immediate vicinity of the final neutral axis, the side shells will often remain in the elastic state up to the overall collapse of the hull girder. So Paik and Mansour (1995) developed Caldwell's method further. They assumed a more credible distribution of longitudinal stresses of the hull cross-section in the collapse state: see Fig. 8.35. Based on this assumption, the formulae for prediction of the ultimate strength can be derived.

In Fig. 8.35 and the discussion that follows, AB is the total sectional area of the outer bottom, $A'B$ is the total sectional area of the inner bottom, A_D is the total sectional area of the deck, A_S is the half-sectional area of all sides, D is the hull depth, D_B is the height of the double bottom, g is the neutral axis position above the base line in the sagging condition or below the deck in the hogging condition, H is the depth of the hull section in the linear elastic state, M_{uh} and M_{us} are the ultimate bending moments in hogging or sagging conditions respectively, σ_{yB}, σ'_{yB}, σ_{yD} and σ_{ys} are the yield strength of the outer bottom, inner bottom, deck and side shell, respectively, and σ_{uB}, σ'_{uB}, σ_{uD} and σ_{us} are the ultimate buckling strength of the outer bottom, inner bottom, deck and side shell, respectively.



8.35 Assumed distribution of longitudinal stresses in a hull cross-section at the overall collapse state: (a) sagging, (b) hogging.

© 2008 Woodhead Publishing Limited

If the x–y coordinates are taken as shown in Fig. 8.35, the stress distribution can be expressed as follows:

In sagging condition:

$$\begin{aligned}
\sigma_x &= \sigma_{yB} && \text{at } y = 0 \\
&= -\frac{1}{H}[(\sigma_{uS} + \sigma_{yS})y - H\sigma_{yS}] && \text{at } 0 < y < H \\
&= \sigma'_B \\
&= -\frac{1}{H}[(\sigma_{uS} + \sigma_{yS})D_B - H\sigma_{yS}] && \text{at } y = D_B \\
&= -\sigma_{uS} && \text{at } H \le y < D \\
&= -\sigma_{uD} && \text{at } y = D
\end{aligned} \tag{8.30}$$

In hogging condition:

$$\begin{aligned}
\sigma_x &= \sigma_{yD} && \text{at } y = 0 \\
&= -\frac{1}{H}[(\sigma_{uS} + \sigma_{yS})y - H\sigma_{yS}] && \text{at } 0 < y < H \\
&= -\sigma_{uS} && \text{at } H \le y < D \\
&= -\sigma'_{uB} && \text{at } y = D - D_B \\
&= -\sigma_{uB} && \text{at } y = D
\end{aligned} \tag{8.31}$$

From the condition that no axial force acts on the hull girder, the depth of the collapsed sides $(D - H)$ can be obtained from

$$\int \sigma_x(t)\mathrm{d}A(t) = 0 \tag{8.32}$$

$$H(t) = \frac{C_1(t)D + \sqrt{C_1^2(t)D^2 + 4C_2(t)D}}{2} \tag{8.33}$$

where
$$C_1(t) = \frac{A_D(t)\sigma_{uD}(t) + 2A_S(t)\sigma_{uS}(t) - A_B(t)\sigma_{yB}(t) - A'_B(t)\sigma_{yS}(t)}{A_S(t)[\sigma_{uS}(t) + \sigma_{yS}(t)]}$$

$$C_2(t) = \frac{A'_B(t)D_B}{A_S(t)}$$

The position of the neutral axis where the longitudinal stress is zero can be determined by substituting Eqs 8.30 and 8.32 into the following equation:

$$g(t) = y \mid \sigma(t)_{x=0} \tag{8.34}$$

namely

$$g(t) = \frac{[C_1(t)D + \sqrt{C_1^2(t)D^2 + 4C_2(t)D}]\sigma_{yS}(t)}{2[\sigma_{uS}(t) + \sigma_{yS}(t)]} = H(t)\frac{\sigma_{yS}(t)}{\sigma_{uS}(t) + \sigma_{yS}(t)} \tag{8.35}$$

© 2008 Woodhead Publishing Limited

Similarly, in the hogging condition, $g(t)$ and $H(t)$ can be obtained as follows:

$$H(t) = D\frac{A_B(t)\sigma_{uB}(t) + A'_B(t)\sigma'_{uB}(t) + 2A_S(t)\sigma_{uS}(t) - A_D(t)\sigma_{yD}(t)}{A_S(t)[\sigma_{uS}(t) + \sigma_{yS}(t)]} \quad 8.36$$

$$g(t) = D\frac{A_B(t)\sigma_{uB}(t)\sigma_{yS}(t) + A'_B(t)\sigma'_{uB}(t)\sigma_{yS}(t) + 2A_S(t)\sigma_{uS}(t)\sigma_{yS}(t) - A_D(t)\sigma_{yD}(t)\sigma_{yS}(t)}{A_S(t)[\sigma_{uS}(t) + \sigma_{yS}(t)]^2}$$

$$= H(t)\frac{\sigma_{yS}(t)}{\sigma_{uS}(t) + \sigma_{yS}(t)} \quad 8.37$$

The ultimate moment capacity of the hull under sagging bending moment is

$$M_{uS}(t) = A_D(t)[D - g(t)][-\sigma_{uD}(t)] + \frac{2A_S(t)}{D}[D - H(t)]\frac{D + H(t) - 2g(t)}{2}[-\sigma_{uS}(t)]$$

$$+ A_B(t)[-g(t)\sigma_{yB}(t)] + \frac{A'_B(t)}{H(t)}[g(t) - D_B(t)]\{[\sigma_{uS}(t) + \sigma_{yS}(t)]D_B - H(t)\sigma_{yS}(t)\}$$

$$- \frac{A_S(t)H(t)}{3D}\{[2H(t) - 3g(t)]\sigma_{uS}(t) - [H(t) - 3g(t)]\sigma_{yS}(t)\} \quad 8.38$$

In the hogging condition, the ultimate moment capacity of the hull is

$$M_{uh}(t) = A_B(t)[D - g(t)]\sigma_{uB}(t) + \frac{2A_S(t)}{D}[D - H(t)]\frac{D + H(t) - 2g(t)}{2}\sigma_{uS}(t)$$

$$+ A'_B(t)[D - g(t) - D_B]\sigma'_{uB}(t) + A_D g(t)\sigma_{yD}(t)$$

$$+ \frac{A_S(t)H(t)}{3D}\{[2H(t) - 3g(t)]\sigma_{uS}(t) - [H(t) - 3g(t)]\sigma_{yS}(t)\} \quad 8.39$$

To calculate Eq. 8.38 or 8.39, the ultimate strength of the stiffened panel and the unstiffened plate must be known. Equations 8.5, 8.7, 8.9, 8.20 and 8.21 are used to predict the ultimate strength of the stiffened panel and the unstiffened plate with crack damage.

The variance of the ultimate moment capacity of the hull girder under the sagging condition can be calculated using standard theory. The detailed formulas can be found in Hu *et al.* (2004).

8.8.4 Time variant reliability of the ship hull girder

The limit state for global hull failure is defined as:

$$M_T > M_u(t) \quad 8.40$$

where M_T is the total vertical bending moment acting on the hull, and $M_u(t)$ is the ultimate bending moment of the ship hull girder. M_T can be decomposed into two components, the stillwater bending moment M_s and the wave-induced bending moment M_w. Since detailed load calculation is not the purpose of this study, we take a simplified approach to estimate the extreme total bending

© 2008 Woodhead Publishing Limited

moment on the hull girder. The maximum wave-induced bending moment M_w is calculated from the IACS design guidance formula (IACS, 2006):

$$M_w = \begin{cases} 190 F_M f_P C L^2 B C_b \times 10^{-3}\,(\text{kNm}) & \text{for hogging} \\ 110 F_M f_P C L^2 B (C_b + 0.7) \times 10^{-3}\,(\text{kNm}) & \text{for sagging} \end{cases} \quad 8.41$$

The maximum stillwater bending moment is calculated by:

$$M_s = \begin{cases} 175 C L^2 B (C_b + 0.7) \times 10^{-3} - M_w\,(\text{kNm}) & \text{for hogging} \\ 175 C L^2 B (C_b + 0.7) \times 10^{-3} - M_w\,(\text{kNm}) & \text{for sagging} \end{cases} \quad 8.42$$

where F_M and f_P are the distribution factor and probability coefficient respectively, defined in the design guidance, L is the ship length, B is the ship breadth, C_b is the block coefficient, and C is related to L:

$$C = \begin{cases} 0.0792L & L < 90\,\text{m} \\ 10.75 - [(300 - L)/100]^{1.5} & 90\,\text{m} \le L \le 300\,\text{m} \\ 10.75 & 300\,\text{m} < L \le 350\,\text{m} \\ 10.75 - [(L - 300)/100]^{1.5} & L > 350\,\text{m} \end{cases} \quad 8.43$$

The ratio range between the mean stillwater bending moment $\overline{M_s}$ and the extreme stillwater bending moment M_s is from 0.4 to 0.6 and the coefficient of variation of M_s is from 0.3 to 0.9.

There will be a failure if Eq. 8.40 is fulfilled, and the probability of the vertical bending moment M_T exceeding $M_u(t)$ during the period of time $[0, T]$ is

$$P_f(T) = 1 - \exp\left[-\int_0^T v[M_u(t)]\mathrm{d}t\right] \quad 8.44$$

where $v[M_u(t)]$ is the mean upcrossing rate of the threshold $M_u(t)$. The mean upcrossing rate is assumed to follow the Weibull distribution:

$$v[M_u(t)] = v_0 \exp\left[-\left(\frac{M_u(t) - E[M_T]}{\lambda}\right)^{\alpha}\right] \quad 8.45$$

where α and λ are the Weibull parameters.

Substituting

$$R(t) = 1 - p_f(t) \quad 8.46$$

in Eq. 8.44, the reliability after and before crack initiation respectively can be derived as

$$R_a(t) = \exp\left(-\int_0^t v[M_u(\tau)]\mathrm{d}\tau\right), t > t_i \quad 8.47$$

$$R_b(t) = \exp\left(-\int_0^t v[M_u(\tau)]\mathrm{d}\tau\right), t \le t_i \quad 8.48$$

where t_i is the time of the first initiation of crack propagation.

© 2008 Woodhead Publishing Limited

The total reliability $R(T)$ includes the reliability of the hull with cracks plus the reliability of the hull without cracks. The final expression is given by:

$$R(T) = [1 - F_{T_i}(T)]R_b(T) + \int_0^T R_b(t_i)R(T - t_i)f_{T_i}(t_i)dt_i \qquad 8.49$$

The first term of this equation represents the probability that no cracks are present and that failure does not occur in time $[0, T]$. The second term represents the probability of non-failure under the condition that the cracks are initiated.

8.9 Conclusions

Residual strength evaluation for cracked structures plays a significant role in damage tolerance analysis of structures. For aging ships, fatigue cracks will degrade the ultimate strength of stiffened panels and unstiffened plates. The damage degree of fatigue cracks should be determined properly at first to assess the strength of aging ships. It is essential to seek a rational standard for structural integrity of aging structures without economic penalties with respect to the repair and maintenance costs incurred over the life cycle of the structure, while a risk or reliability assessment scheme is normally applied for that purpose.

In this chapter, the residual strength assessment of steel-plated structures with existing crack damage and under monotonic extreme loading has been extensively discussed. The chapter has described the fundamentals and some results of the residual strength evaluation of cracked ship structures, with the intention of obtaining insights into the ultimate strength behavior of structures given one or more cracks under different types of cracks and loads, and indicating how to use such knowledge within the current framework of ultimate strength calculation for a complex structural system and ship hull girder. Considering that axial tension/compression are the primary load components in ships, offshore structures and other steel structures, residual strength corresponding to load types of axial tension and compression has been mainly addressed. The main contents of the chapter included the residual tensile/compressive strength assessment method for cracked unstiffened plates, the residual tensile/compressive strength assessment method for cracked stiffened panels, and the residual strength assessment of ship hull girders. The methods and procedures presented in this chapter may act for demonstration purposes since actual problems are often different from the examples studied.

8.10 References

Anderson T L (1995), *Fracture Mechanics: Fundamentals and Applications*, Second Edition, London, CRC Press.

Caldwell J B (1965), 'Ultimate longitudinal strength', *Trans RINA*, 107, 411–430.

Cherry M C, Mall S, Heinimann B, Grandt Jr. A F (1997), 'Residual strength of

© 2008 Woodhead Publishing Limited

unstiffened aluminum panels with multiple site damage', *Engineering Fracture Mechanics*, 57(6), 701–713.
Cotterell B (2002), 'The past, present, and future of fracture mechanics', *Engineering Fracture Mechanics*, 69, 533–553.
Feddersen C E (1971), 'Evaluation and prediction of the residual strength of center cracked tension panels', ASTM STP 486, 50–78.
Griffith A A (1920), 'The phenomena of rupture and flow in solids', *Philosophical Transactions*, Series A, 221, 163–198.
Guedes Soares C, Garbatov Y (1998), 'Reliability of maintained ship hull girders subjected to corrosion and fatigue', *Structural Safety*, 20, 201–219.
Hendricks W R (1991), 'The Aloha airline accident – a new era for aging aircraft', in: Atluri S N, Sampath S G, Tong P (eds), *Structural Integrity of Aging Airplane*s, Heidelberg, Berlin, Springer Verlag, 153–166.
Hu Y, Cui W, Pedersen P T (2004), 'Maintained ship hull girder ultimate strength reliability considering corrosion and fatigue', *Marine Structures*, 17, 91–123.
IACS (2006), *Common Structural Rules for Bulk Carriers*.
Jeong D Y, Brewer J C (1995), 'On the linkup of multiple cracks', *Engineering Fracture Mechanics*, 51(2), 233–238.
Krawczuk M, Wieslaw A Z, Ostachowicz (2001), 'Finite element model of plate with elasto-plastic through crack', *Computers and Structures*, 79, 519–532.
Labeas G, Diamantakos J (2006), 'Residual strength prediction of multiple cracked stiffened panels', *Fatigue Fract Engng Mater Struct*, 29, 365–371.
Labeas G, Diamantakos J, Kermanidis T (2005), 'Crack link-up for multiple site damage using an energy density approach', *Theoretical and Applied Fracture Mechanics*, 43, 233–243.
Li Y, Huang Q, Fu X (2003), 'Methodology for residual strength evaluation of cracked structures', *Journal of Mechanical Strength*, 25(1), 071–075 (in Chinese).
Moukawsher E J, Heinimann M B, Grandt Jr. A F (1996), 'Residual strength of plates with multiple site damage', *Journal of Aircraft*, 33(5), 1014–1021.
Ni P (1996), 'Probabilistic theory for mixed-mode brittle fracture and fatigue with random cracks', Doctoral dissertation, University of Central Florida, Orlando, FL.
Nicholson D W, Ni P (1997), 'Extreme value probabilistic theory for mixed mode brittle fracture', *Engineering Fracture Mechanics*, 58, 121–132.
O'Dowd N P, Kolednik O, Naumenko V P (1999), 'Elastic–plastic analysis of biaxially loaded center-cracked plate', *International Journal of Solids and Structures*, 36, 5639–5661.
Paik J K, Mansour A E (1995), 'A simple formulation for predicting the ultimate strength of ships', *Journal of Marine Science and Technology*, 1, 52–62.
Paik J K, Satish Kumar Y V (2006), 'Ultimate strength of stiffened panels with cracking damage under axial compression or tension', *Journal of Ship Research*, 50(3), 231–238.
Paik J K, Thayamballi A K (2002a), *Ultimate Limit State Design of Steel Plated Structures*, London, John Wiley & Sons.
Paik J K, Thayamballi A K (2002b), 'Ultimate strength of ageing ships', *J Eng Marine Environ*, 216(M1), 57–77.
Paik J K, Thayamballi A K, Lee J M (2003), 'Effect of initial deflection shape on the ultimate strength behavior of welded steel plates under biaxial compressive loads', *Journal of Ship Research*, 48(1), 45–60.
Paik J K, Satish Kumar Y V, Lee J M (2005), 'Ultimate strength of cracked plate elements under axial compression or tension', Thin-walled Structures, 43(2), 237–272.

© 2008 Woodhead Publishing Limited

Sih G C (1991), *Mechanics of Fracture Initiation and Propagation*, Dordrecht/Boston/London, Kluwer Academic Publishers.

Smith B L, Saville P A, Mouak A, Myose R Y (2000), 'Strength of 2024-T3 aluminum panels with multiple site damage', *Journal of Aircraft*, 37(2), 325–331.

Swift T (1993), 'Widespread fatigue damage monitoring issues and concerns', *Fifth International Conference on Structural Airworthiness of New and Aging Aircraft*, Hamburg, Germany, June.

Vafai A, Estekanchi H E (1999), 'A parametric finite element study of cracked plates and shells', *Thin-Walled Structures*, 33, 211–229.

Vasta J (1958), 'Lessons learned from full-scale structural tests', *Trans SNAME*, 66, 165–243.

Wang F, Cui W (2006), 'Parametric finite element analysis of the ultimate strength of through-thickness cracked plates', *Journal of Ship Mechanics*, 10(6), 76–93.

Wang Q, Huang X, Cui W (2006), 'Interaction and influence between cracks in different positions through finite element analysis', *Journal of Jiangsu University of Science and Technology (Natural Science Edition)*, 1120(11), 16–19 (in Chinese).

Wang Z, Chen L, Nie X (2004), 'Residual strength analysis for widespread fatigue damage in stiffened panel', *Journal of Mechanical Strength*, 26(S), 254–257 (in Chinese).

Xu X, Yao W (2001), 'Analysis of residual strength for multiple site damage structure', *Hongdu Science and Technology*, 4, 8–13 (in Chinese).

© 2008 Woodhead Publishing Limited

9

Dented structures and residual strength

J K PAIK, Pusan National University, Korea

Abstract: In aging structures, mechanical damage such as local denting is often caused by accidental loading or impact and can reduce the load-carrying capacity of the structure. Therefore, it is very important to develop a relevant scheme of inspection and maintenance because repair or renewal of damaged structural parts is in general complex and costly. This chapter addresses the mechanisms of local denting damage based on experimental observations and numerical computations. The effect of local denting damage on residual ultimate strength of plated structures is also discussed.

Key words: local denting, mechanical damage, aging structures, residual ultimate strength, dropped objects, probability of detection (POD), probability of sizing (POS).

9.1 Introduction

Aging steel structures have reportedly suffered various types of damage. Some types of damage such as corrosion and fatigue cracking are related to age, but others are more likely to be mechanical damage caused by accidental loading or impact. Structural damage can reduce load-carrying capacity of the structure and lead to catastrophic failure (Paik and Thayamballi 2003, 2007). Once structural damage is detected the operator will need to judge if relevant repair and maintenance should be done. In fact, repair or renewal of damaged structural parts is in general complex and costly (Paik *et al.* 2006).

The present chapter is focused on mechanical damage caused by impacts such as from dropped objects. Mechanical damage may occur in plate panels of steel-plated structures in many ways depending upon where such plates are used. In inner bottom plates of cargo holds of bulk carriers, mechanical damage can take place by mishandled loading or unloading of cargoes; inner bottom plates suffer mechanical damage during loading of iron ore, because iron ore cargo strikes the plates. In unloading of bulk cargoes such as iron ore or coal, the excavator hits the inner bottom plates mechanically.

Deck plates of offshore platforms may be subjected to impacts due to objects dropped from a crane. Figure 9.1(a) shows a photo of local denting damage formed in inner bottom plates of a bulk carrier, and Fig. 9.1(b) shows a photo of local denting at deck plates caused by dropped objects.

Numerous studies related to formation of local denting itself in steel cylinders or offshore tubular members and its influence on structural behavior are found in

© 2008 Woodhead Publishing Limited



9.1 Photos of local denting damage: (a) inner bottom plate of a bulk carrier; (b) deck plate of an offshore platform.

the literature (Ellinas *et al.* 1984, Smith 1984, Reid and Goudie 1989, Paik and Shin 1989, Paik *et al.* 1989, Moussouros and Hoo Fatt 1995, Harding and Onoufriou 1995, Park and Kyriakides 1996, among others). Some useful contributions to denting in steel-plated structures (Smith and Dow 1981, Jones 1997, Muscat-Fenech and Atkins 1998) and its effect on the residual ultimate strength (Paik *et al.* 2003, Paik 2005) are also found.

In this chapter, mechanisms of local denting damage are presented based on experimental observation and numerical computations. The effect of local denting damage on residual ultimate strength of plated structures is also addressed.

9.2 Mechanism of local denting damage

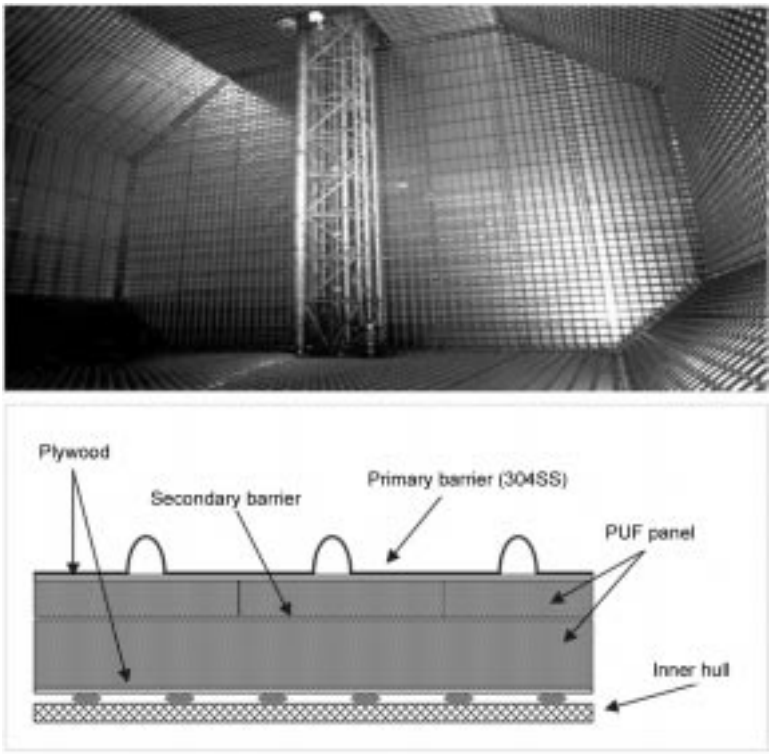
Local denting damage in steel-plated structures may normally involve various features such as local deformation, cracking, residual stresses or strains due to plastic deformation, and coating damage. Some illustrative examples of local denting damage caused by impacts are now presented.

9.2.1 Cargo tank damage in membrane type liquid natural gas (LNG) carriers

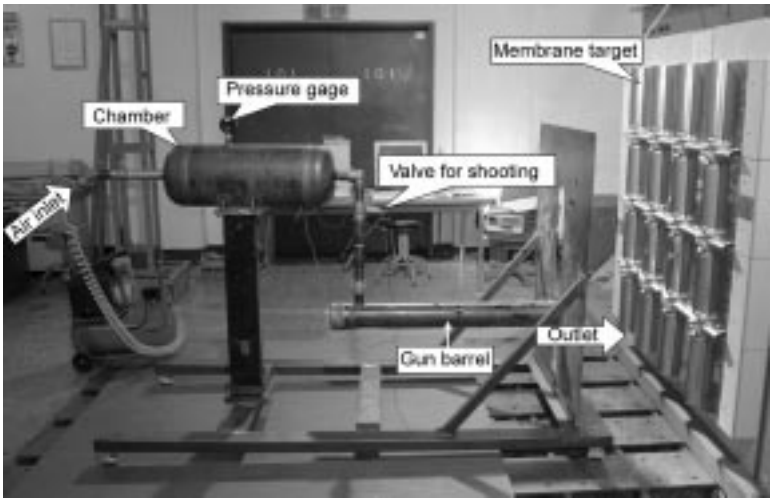
It has reportedly been experienced that membrane sheets of primary barrier inside cargo tanks of liquefied natural gas (LNG) carriers have suffered local denting damage caused by dropped objects such as bolts or nuts mishandled during building. Local denting damage can lead to leaking of LNG during operation. Figure 9.2 shows the cargo tank structure of membrane type LNG carriers.

Figure 9.3 shows the gun-type impact test facility at the Ship and Offshore Structural Mechanics Laboratory of Pusan National University in Korea. An

© 2008 Woodhead Publishing Limited

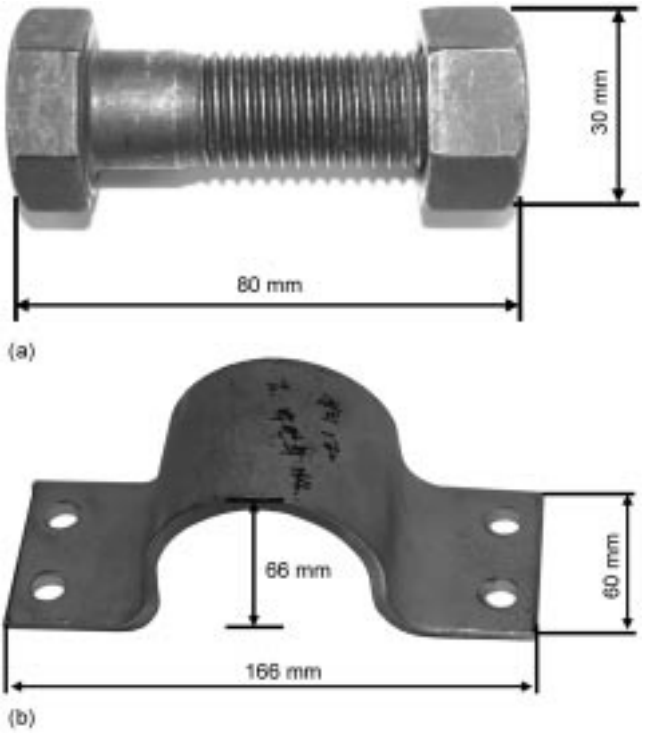


9.2 Cargo tank structure of membrane type LNG carriers.



9.3 Gun-type impact test system at Ship and Offshore Structural Mechanics Laboratory in Pusan National University, Korea.

© 2008 Woodhead Publishing Limited



9.4 Impacted objects used for the impact test: (a) bolt together with nut weighing 280 g; (b) pipe support weighing 555 g.

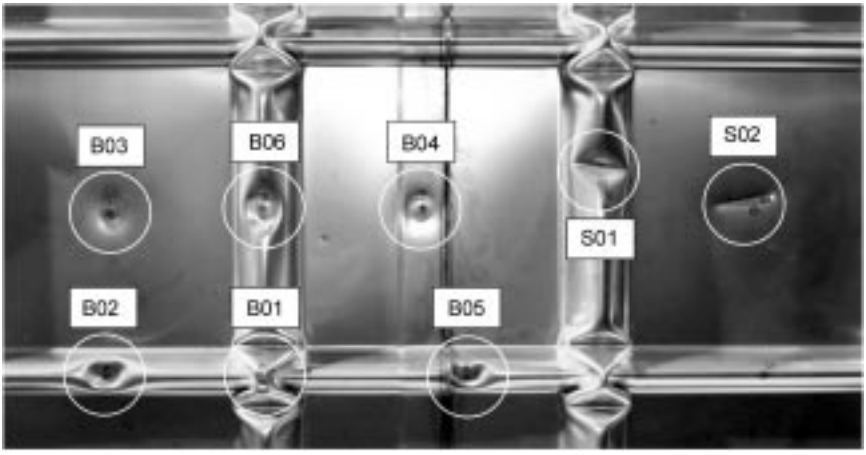
impact test was performed to investigate the local denting damage characteristics for a primary barrier sheet of LNG cargo tank impacted by two types of objects, namely a bolt together with a nut and a pipe support such as those shown in Fig. 9.4. The primary barrier sheet is made of SUS 304 material. The weights of the bolt with nut and pipe support are 280 g and 555 g, respectively. The tested primary barrier structure at full scale includes an insulation system made of PUF (polyurethane foam) panels and a secondary barrier as shown in Fig. 9.2, but without an inner hull plate. The impact speed of objects is 23 m/s.

Figure 9.5 shows local denting damage caused by the impacts. Depending on the location of impacts and type of impacted objects, the maximum dent depth was over 20 mm. Although rupture was not found in the primary barrier sheet, it is certain that the dented plates must be replaced to avoid any catastrophic accident due to gas leakage during operation.

9.2.2 Deck stiffened-plate damage in offshore platforms

In deck structures of offshore platforms, drill-collars (pipes) must be handled by crane, and it has been reported that such drill-collars often drop accidentally to

© 2008 Woodhead Publishing Limited



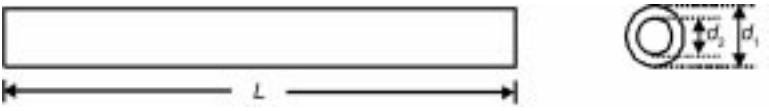
9.5 Local denting damage at the primary barrier sheet of LNG cargo tank.

the deck plate. Figure 9.6 shows a schematic of a drill-collar pipe. For typical dimensions used for the work in offshore platforms, $L = 2000$ mm, $d_1 = 241.3$ mm, and $d_2 = 76.2$ mm. The weight of a drill-collar made of high tensile steel with yield stress of 690 MPa is 442 kg.

A numerical simulation by the LS-DYNA3D nonlinear finite element method was carried out to investigate the local denting damage characteristics of deck stiffened-plate structures impacted by drill-collar. The simulation considers that the drill-collar freely falls to the deck structure.

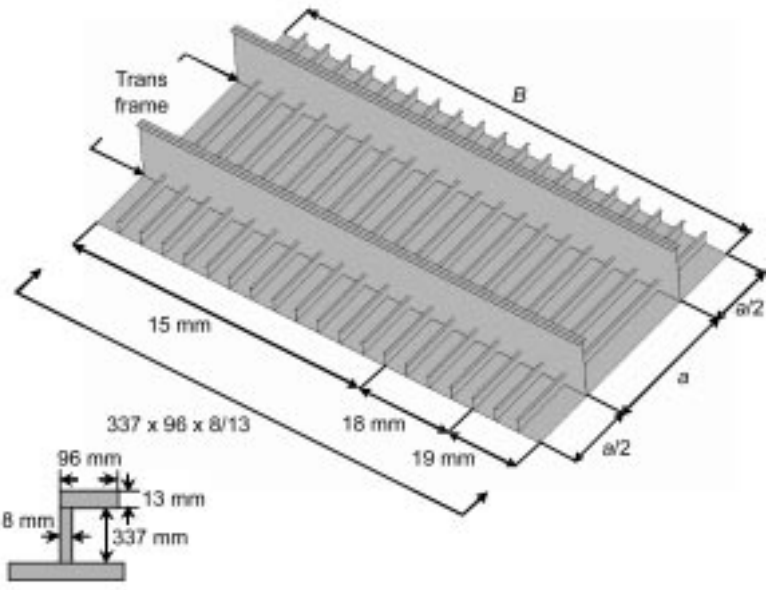
Figure 9.7 shows the geometric dimension of the deck stiffened-plate structure. The deck structure is made of high tensile steel with yield stress of 315 MPa. Longitudinal stiffeners and transverse frames as well as deck plates are all included in the finite element modeling as shown in Fig. 9.8. The drill-collar can also be damaged during the impact, and thus the drill-collar is also modeled as shown in Fig. 9.9. The height of the drill-collar is varied in the computations in the range of 1 m to 3 m.

Figure 9.10 shows the reaction force versus time history in the impact structure for three different heights of dropped drill-collar. Rebounding is allowed in the computations so that some post-impact responses are also seen in Fig. 9.10. Figure 9.11 shows the corresponding dent depth (deflection) versus time history for the three different drop heights. Figure 9.12 shows the deformed shapes of the structure before and after impact when the drop height is 3 m. It is

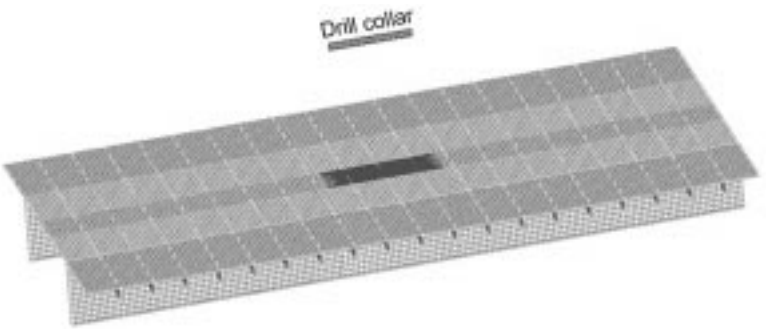


9.6 Schematic of a drill-collar pipe.

© 2008 Woodhead Publishing Limited



9.7 Stiffened deck-plate structure of an offshore platform ($B = 16300$ mm, $a = 4300$ mm).

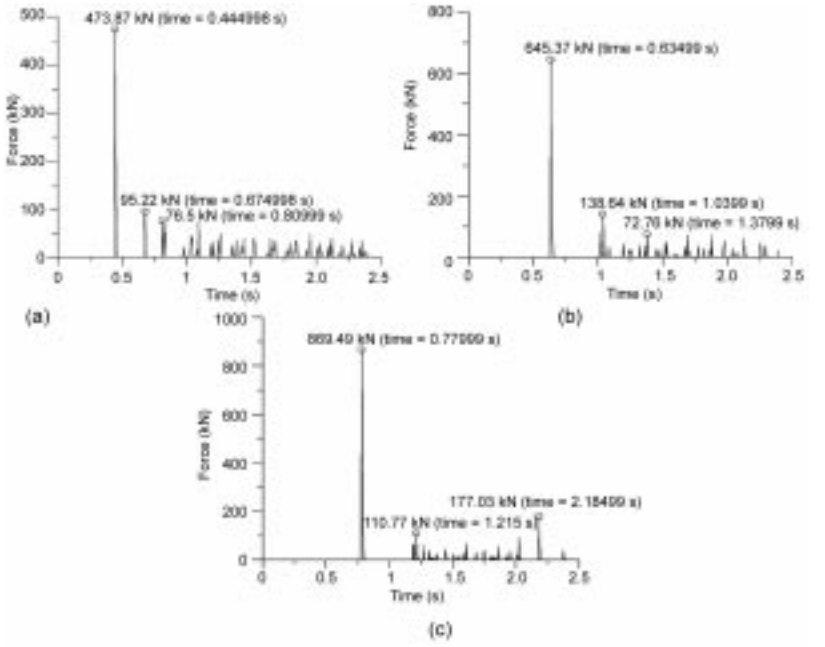


9.8 Nonlinear finite element model using plate-shell elements for stiffened deck-plate structure impacted by free fall of drill-collar pipe.

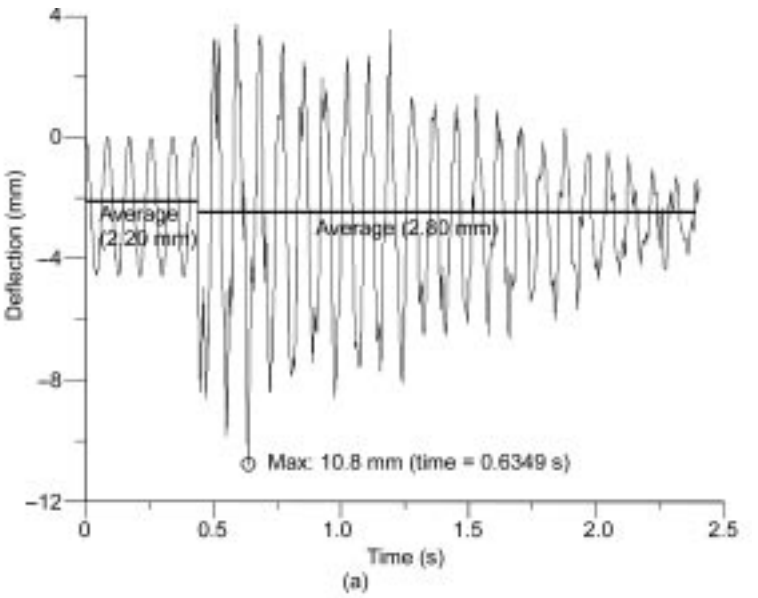


9.9 Nonlinear finite element model using plate-shell elements for the drill-collar.

© 2008 Woodhead Publishing Limited

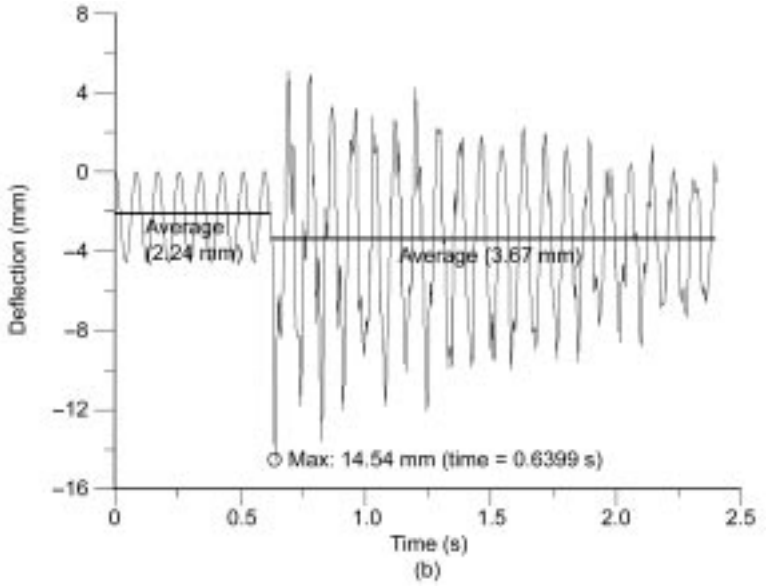


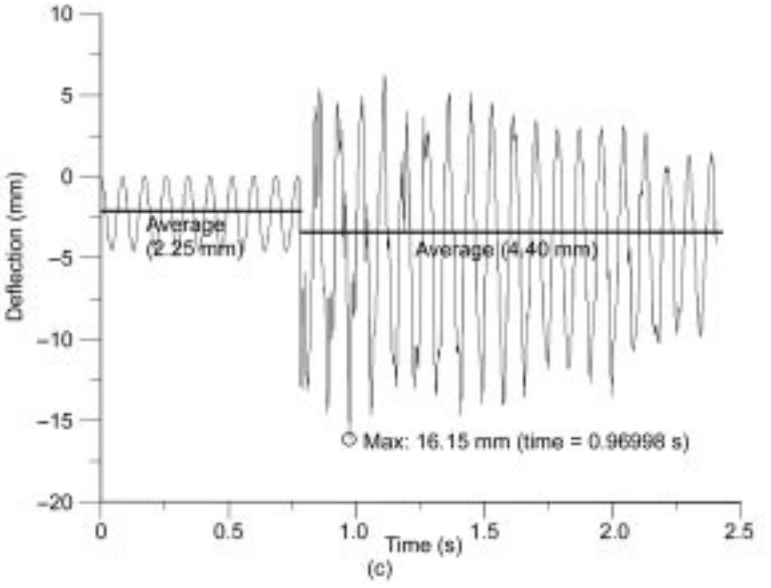
9.10 Reaction force versus time history for drop heights of (a) 1 m, (b) 2 m, (c) 3 m.



9.11 Dent depth (deflection) versus time history for drop heights of (a) 1 m, (b) 2 m, (c) 3 m.

© 2008 Woodhead Publishing Limited

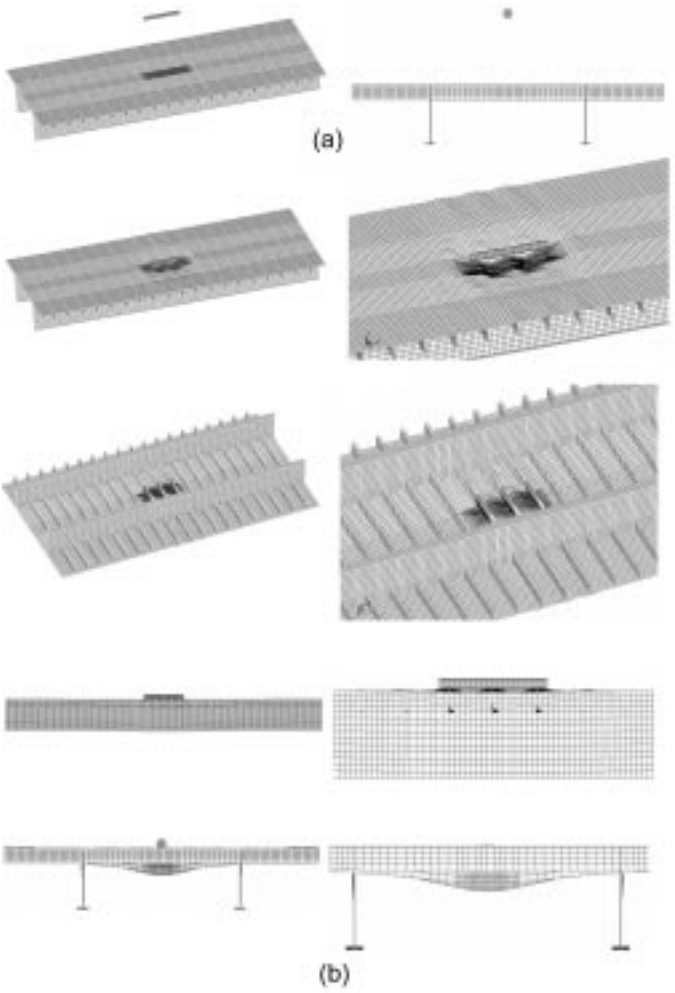




9.11 Continued.

seen from the figures that the local denting damage can be very serious, significantly affecting the structural integrity in terms of reducing load-bearing capacity. Therefore, it is very important to establish a relevant method for assessment and management of denting damage in the structures.

© 2008 Woodhead Publishing Limited



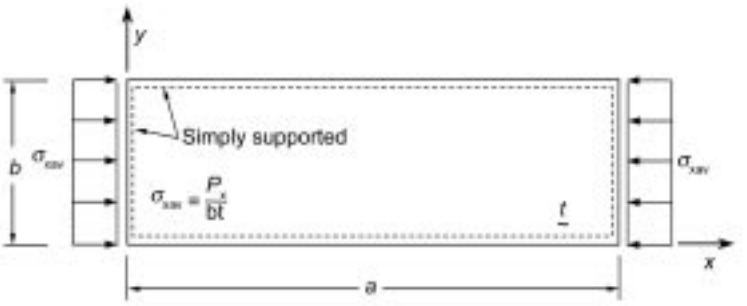
9.12 (a) Initial state of the structure before free fall at $t = 0$ s; (b) deformed shapes of the structure after free fall at $t = 0.78$ s.

9.3 Residual ultimate strength characteristics of dented plates

Load-carrying capacity of dented structures will of course be reduced compared to that of intact structures. In this section, residual ultimate strength characteristics of dented plates are presented based on nonlinear finite element computations.

Figure 9.13 shows a steel plate under axial compressive loads considered in this section. In a continuous steel stiffened plate structure, plating is surrounded by support members (stiffeners) which are typically designed so that they should

© 2008 Woodhead Publishing Limited

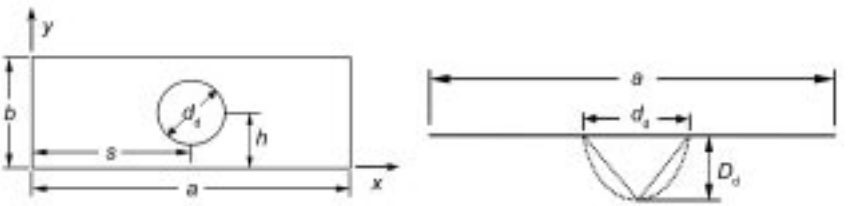


9.13 A simply supported rectangular plate under axial compressive loads (P_x = axial compressive load, σ_{xav} = average axial compressive stress).

not fail prior to plating. In this regard, the plate in the present study is considered to be simply supported at all (four) edges which are kept straight until the ultimate strength is reached. This boundary condition is usually adopted for ultimate strength design of ship plating.

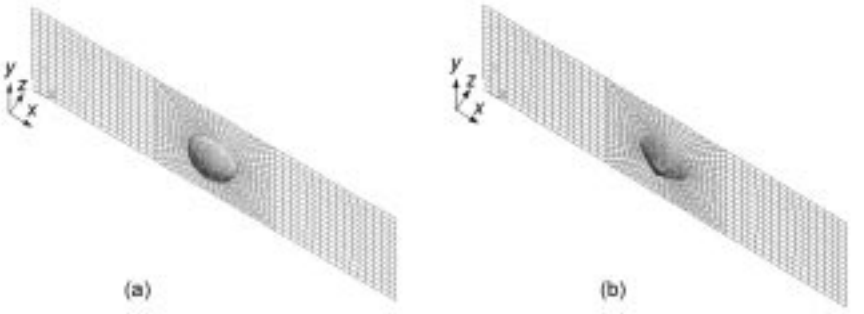
Two types of dent shapes, namely spherical and conical, are considered. Geometric parameters of the dent damage are defined in Fig. 9.14. The center of the localized dent is located at s in the x-coordinate and h in the y-coordinate as shown in Fig. 9.14. The plate breadth (b) is 800 mm, while the plate length (a) and the plate thickness (t) are varied in the computations. The size (diameter) of local dent varies from $d_d/t = 0.0$ to 0.8 and the depth of the local dent varies from $D_d/t = 0.0$ to 10. The material of the plate considered for the numerical computations is high tensile steel with yield stress of $\sigma_Y = 352.8$ MPa. The elastic modulus, E, is 205.8 GPa and the Poisson ratio, ν, is 0.3.

Figure 9.15 shows nonlinear finite element models for dent plates with different shape of local dent. Figure 9.16 shows the deformed shape of a steel plate with or without denting and under axial compressive loads immediately after the ultimate strength is reached. Figure 9.17 shows the membrane stress distribution inside the plate at the ultimate limit state. It was observed from Figs 9.16 and 9.17 and also some additional investigations made in the present

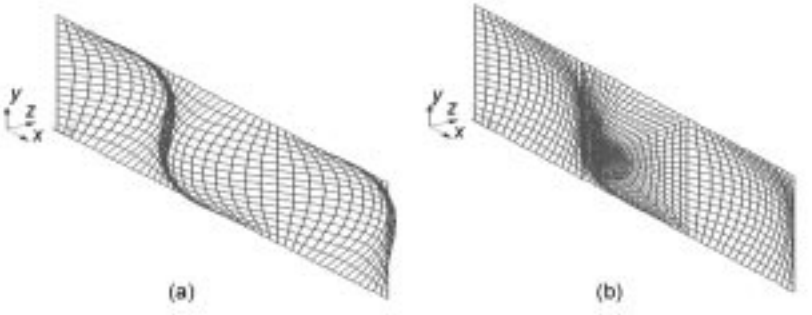


9.14 Geometric parameters of local denting in plate.

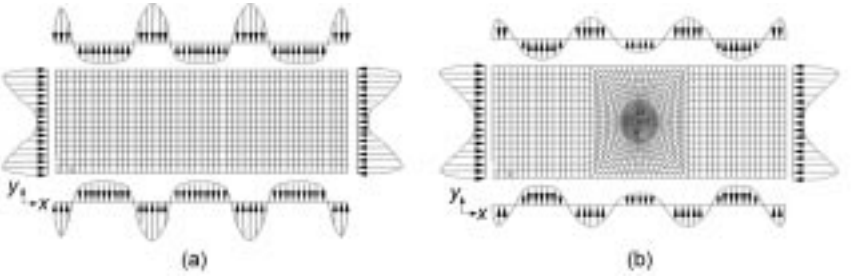
© 2008 Woodhead Publishing Limited



9.15 Nonlinear finite element models for a steel plate with local denting: (a) spherical shape, (b) conical shape.



9.16 Deflected shape of a steel plate with or without denting at the ultimate limit state under axial compressive loading ($a \times b = 2400 \times 800$ mm): (a) undented plate, (b) dented plate.

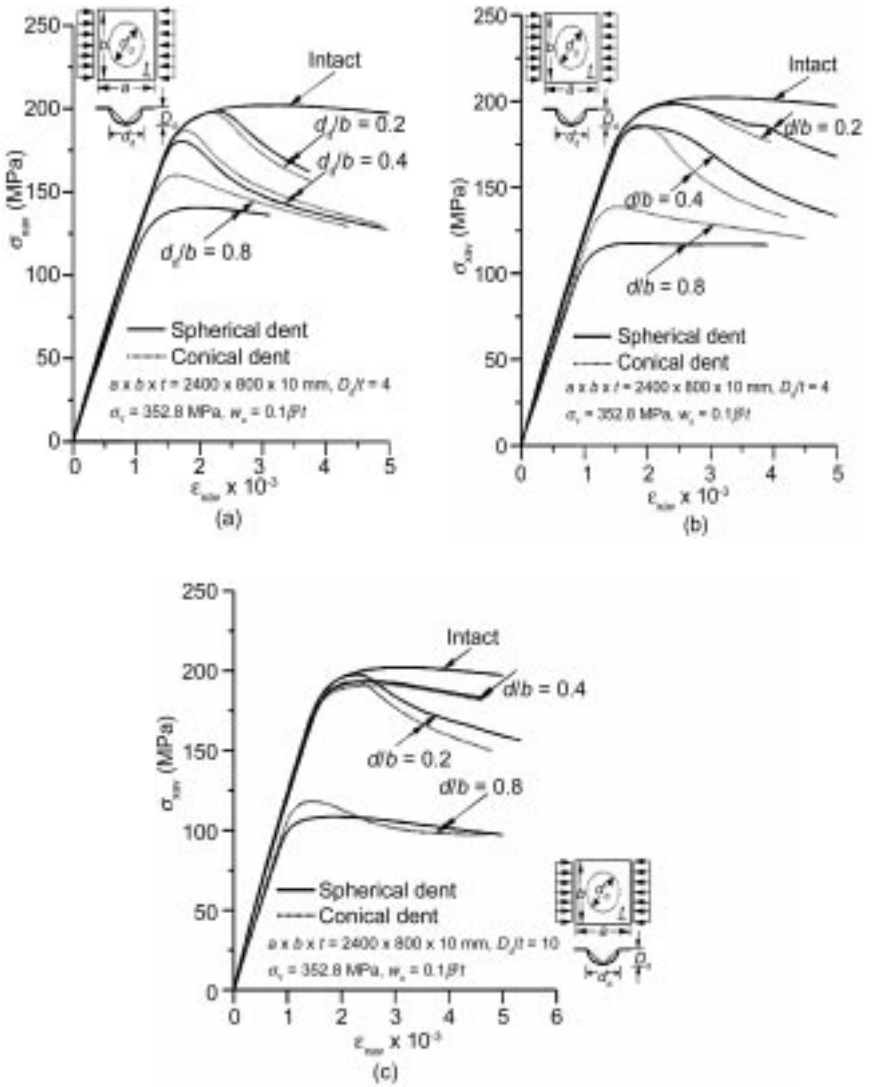


9.17 Membrane stress distribution of a steel plate with or without denting at the ultimate limit state under axial compressive loading ($a \times b = 2400 \times 800$ mm): (a) undented plate, (b) dented plate.

© 2008 Woodhead Publishing Limited

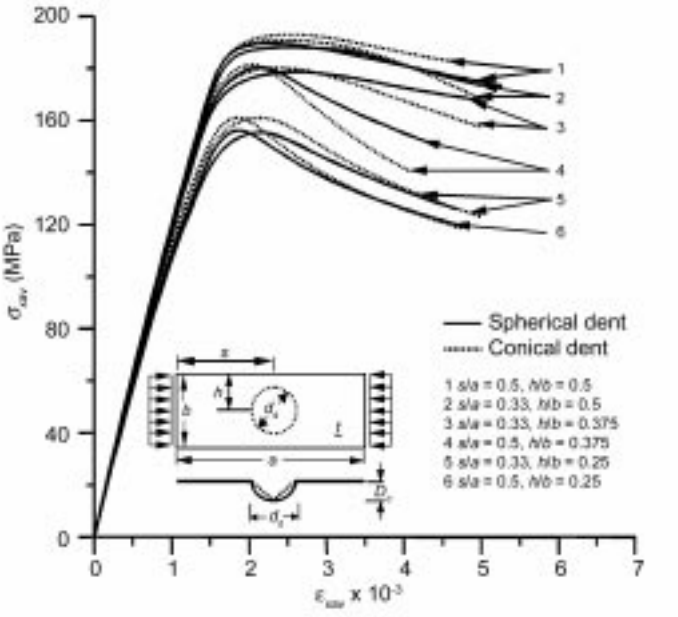
computations that the deflected patterns and membrane stress distributions of dented plates are similar to those of undented (intact) plates as long as dent damage is limited to some local region.

Figure 9.18 shows the elastic–plastic large deflection behavior of plates with spherical or conical shape of local denting and under axial compressive loads,



9.18 Average stress versus average strain curves for a dented steel plate under axial compressive loads, varying the dent depth and diameter, for (a) $D_d/t = 2$, (b) $D_d/t = 4$, (c) $D_d/t = 10$.

© 2008 Woodhead Publishing Limited



9.19 Average stress versus average strain curves for a dented steel plate under axial compressive loads, varying the dent location.

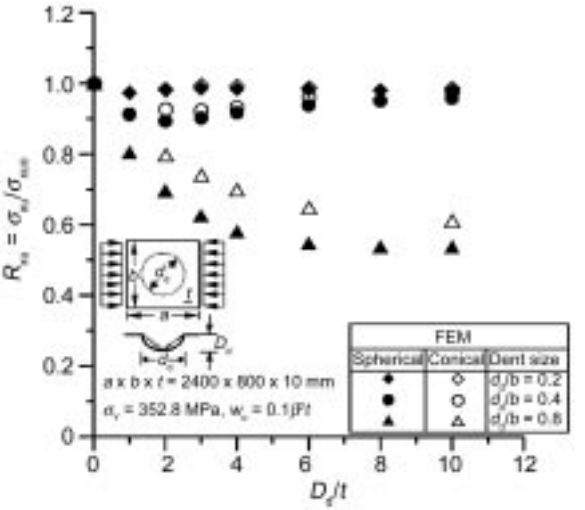
varying the dent size (i.e., depth and diameter). It is seen from Fig. 9.18 that the ultimate compressive strength decreases significantly as the depth and/or diameter of local denting increases. Also, it is apparent that the collapse behavior for a spherical dent is similar to that for a conical dent, while the former case is more likely to reduce the load-carrying capacity than the latter as long as the depth and diameter of denting are the same.

Figure 9.19 shows the effect of dent location on the collapse behavior of dented plates. It is found from Fig. 9.19 that the plate falls in the worst situation in terms of the load-carrying capacity when the local denting is located at the plate center rather than other places.

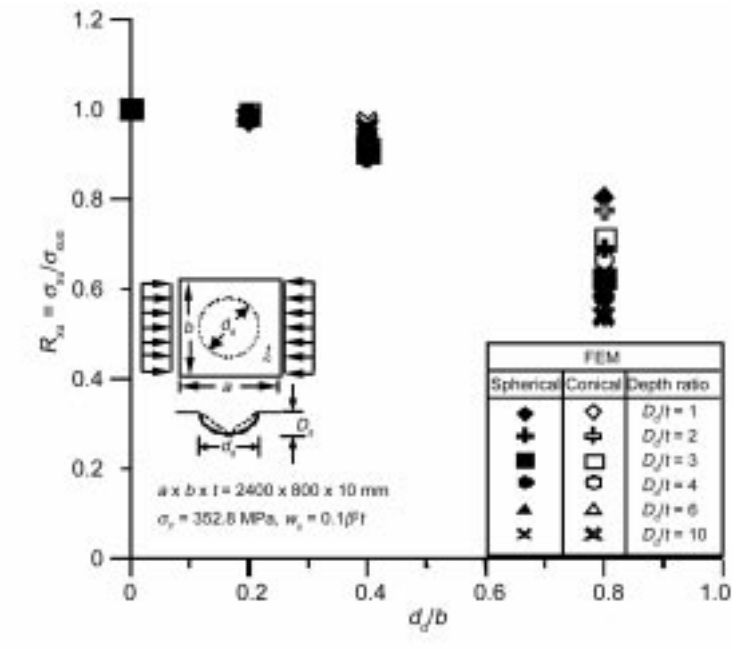
A series of elastic–plastic large deflection analyses on dented steel plates were undertaken varying the dent depth, the dent diameter, the dent location, the plate thickness and the plate aspect ratio. Figures 9.20 to 9.24 show the variations of the ultimate strength of a dented plate under axial compressive loads as a function of the D_d/t ratio, the d_d/b ratio, the dent location, the plate thickness and the plate aspect ratio, respectively. In these figures, σ_{xu} and σ_{xuo} are the ultimate compressive strengths for a dented or undented (intact) plate, respectively.

It is evident that the size (depth, diameter) and location of local denting are generally quite sensitive to the normalized ultimate compressive strength, i.e.,

© 2008 Woodhead Publishing Limited

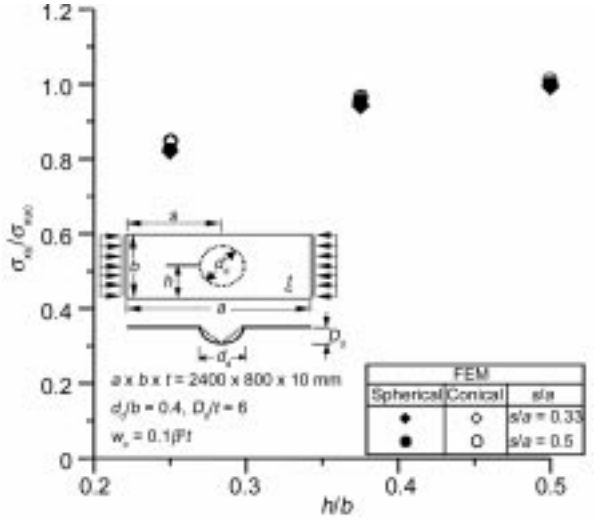


9.20 Variations of the ultimate compressive strength of a dented plate as a function of the D_d/t ratio.

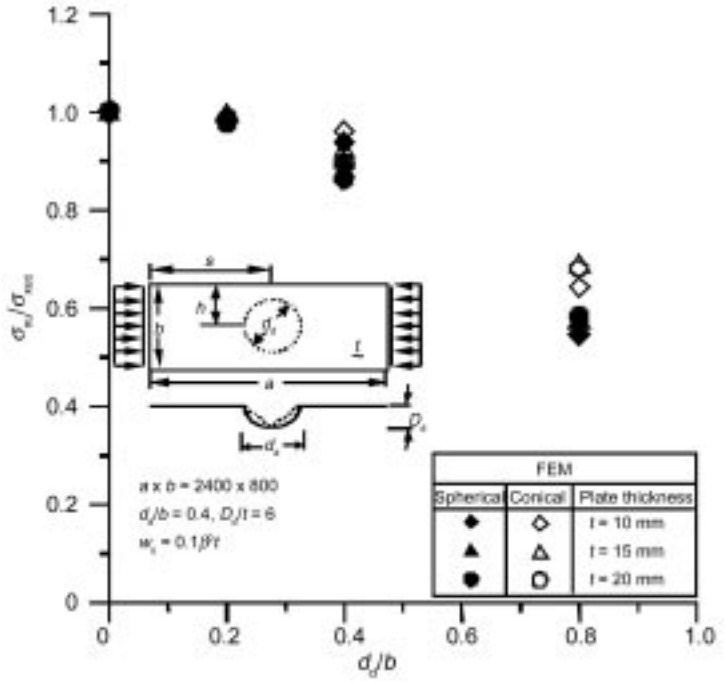


9.21 Variations of the ultimate compressive strength of a dented plate as a function of the d_d/b ratio.

© 2008 Woodhead Publishing Limited

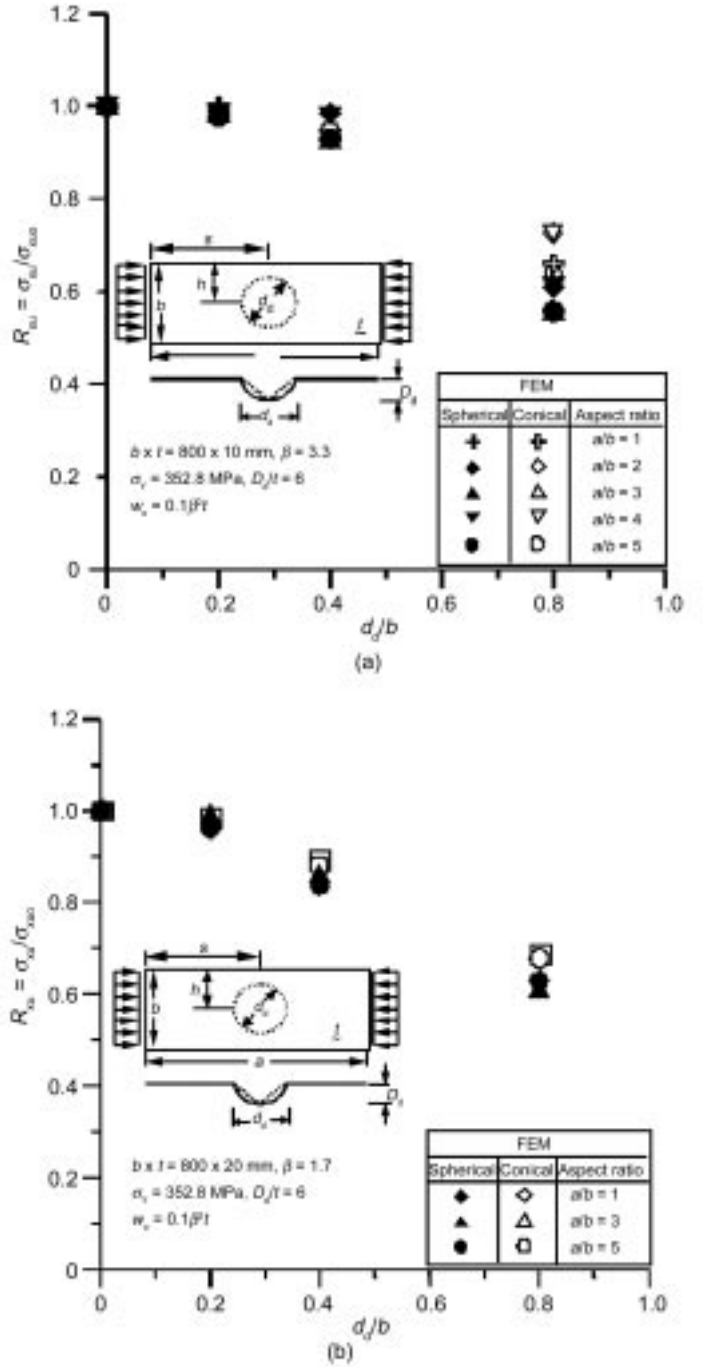


9.22 Variations of the ultimate compressive strength of a dented plate as a function of the dent location (σ_{xuc} = ultimate strength of the plate with local denting at center).



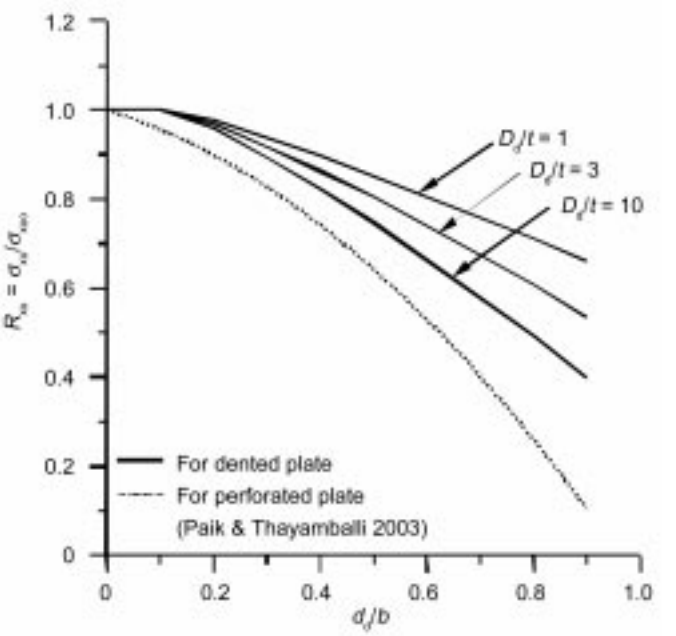
9.23 Variations of the ultimate compressive strength of a dented plate as a function of the plate thickness.

© 2008 Woodhead Publishing Limited



9.24 Variations of the ultimate compressive strength of a dented plate as a function of the plate aspect ratio for (a) $t = 10$ mm, (b) $t = 20$ mm.

© 2008 Woodhead Publishing Limited



9.25 Comparison of the ultimate compressive strength factor for a dented plate (spherical type) vs a perforated plate (with a circular hole) for $h/b = 0.5$.

$R_{xu} = \sigma_{xu}/\sigma_{xuo}$, while the influence of the dent depth on the plate's ultimate compressive strength is not significant as long as the dent diameter is small.

Since the plate collapse behavior for a spherical dent is similar to that for a conical dent and the former is slightly worse than the latter, the spherical dent may be taken as representative of the local dent shape for the purpose of the plate's ultimate strength prediction, regardless of the actual shape of denting. As the dent location becomes closer to the unloaded plate edges the ultimate strength is decreased by 20%, compared to that of the dent located at the plate center. On the other hand, it is found that the plate thickness and the aspect ratio are not influential parameters to the strength reduction factor, R_{xu}. It is interesting to note that the residual ultimate strength of dented plates becomes closer to that of perforated plates (with a circular hole) as the dent size becomes larger, as shown in Fig. 9.25.

9.4 Methods of damage detection and their uncertainties

Visual inspections have usually been applied for detection of denting damage in terms of extension and dent depth to assess whether they are within specified limits. It is, however, important to realize that denting damage due to an impact

© 2008 Woodhead Publishing Limited

can affect material properties and stiffness of structural components. In this regard, structural analysis applying nonlinear structural mechanics is essentially needed to evaluate the integrity of dented structures. Also, the uncertainties of damage detection and measurement must be properly identified.

Babbar *et al.* (2005) studied a technique to measure dent geometry and stresses using the magnetic flux leakage (MFL) inspection method. Song *et al.* (2003) presented a guided waves-based technique to detect denting damage. An approximate image of damage together with a discontinuity locus map is constructed using the guided waves reflected from the damage.

Uncertainties in the methods for detecting and measuring structural deterioration are associated with various sources such as geometry, material properties, location of structural components, life of coating, type of cargo, operational conditions and loading cycles, seawater and internal temperature, humidity and environment, measuring sensors and so on.

Some useful guidelines for nondestructive methods to detect various types of damage are available (Halmshaw 1997, Porter 1992, Berens 1989, Bøving 1989). It is interesting to note that scatter is largely due to operators and practical difficulties rather than measuring equipment. Typically, gages used to measure residual plate thickness have inherent errors mainly due to errors in sensor location (Ma *et al.* 1999). The latter uncertainties are more difficult to identify. Statistical analysis of measured data can identify statistical distributions of probability of detection (POD) and probability of sizing (POS) (Rudlin and Wolstenholme 1992, Rummel *et al.* 1989, HSE 2000).

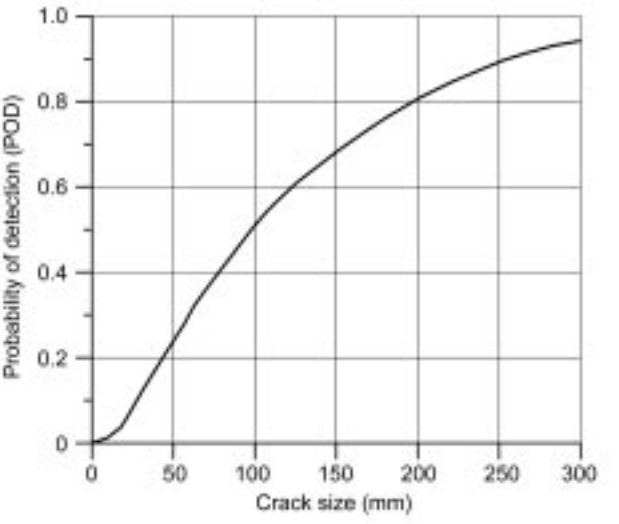
The human factors in damage detection of ship structures are discussed by Demsetz *et al.* (1996) and Demsetz and Cabrera (1999). Statistical distributions of POD in tank structures are compared with those in related engineering fields. Visual damage detections by different inspectors show that POD is greater with prior knowledge of likely damage locations, indicating that human factors are a key to POD. As the size of damage becomes larger, it will be generally much easier to detect, as shown in Fig. 9.26.

9.5 Conclusions

Industrial structures such as ships, offshore platforms, and land-based structures can suffer local denting damage in service. In some cases, leaks of oil or gas stored in the space can take place due to the dent damage. Also, the load-bearing capacity of dented structures will be reduced compared to that of intact structures.

During operation of the structures stakeholders such as owners or operators must judge whether maintenance of dented structures including replacement or repair must be performed in a relevant way, while repair or renewal of damaged structural parts is in general complex and costly. Such considerations must also be necessary during structural design and building. Therefore, it is of importance

© 2008 Woodhead Publishing Limited



9.26 Probability of detection (POD) as a function of crack size (HSE 2000).

to establish a relevant procedure for assessment and management of local denting damage, which must be composed of (1) the mechanism and prediction of local denting damage, and (2) the effect of local denting damage on load-carrying capacity.

9.6 References

Babbar, V., Bryne, J. and Clapham, L. (2005). Mechanical damage detection using magnetic flux leakage tools: the effect of dent geometry and stress. *NDT&E International*, 38: 471–477.

Berens, A.P. (1989). NDE reliability data analysis. *Nondestructive Evaluation and Quality Control in Metals Handbook*, 9th edn, Vol.17, ASM International.

Bøving, K. (ed.) (1989). *NDE Handbook: Non-destructive Examination Methods for Condition Monitoring*. Woodhead Publishing, Cambridge.

Demsetz, L. and Cabrera, J. (1999). *Detection probability assessment for visual inspection of ships*. Ship Structure Committee, SSC-408, Washington, DC.

Demsetz, L., Carlo, R. and Schulte-Strathaus, R. (1996). *Inspection of marine structures*. Ship Structures Committee, SSC-389, Washington, DC.

Ellinas, C.P., Supple, W.J. and Walker, A.C. (1984). *Buckling of Offshore Structures: A State-of-the-art Review*, Gulf Publishing, Houston, TX.

Halmshaw, R. (1997). *Introduction to the Non-destructive Testing of Welded Joints*. Woodhead Publishing, Cambridge.

Harding, J.E. and Onoufriou, A. (1995). Behavior of ring-stiffened cylindrical members damaged by local denting. *Journal of Constructional Steel Research*, 33: 237–257.

HSE (2000). *POD/POS curves for non-destructive examination*. Offshore Technology Report, OTO 2000-018, Health and Safety Executive, UK.

© 2008 Woodhead Publishing Limited

Jones, N. (1997). Dynamic plastic behaviour of ship and ocean structures. *RINA Transactions*, The Royal Institution of Naval Architects, London, 139: 65–97.

Ma, K., Orisamolu, I.R. and Bea, R.G. (1999). *Optimal strategies for inspections of ships for fatigue and corrosion damage*. Ship Structure Committee, SSC-407, Washington, DC.

Moussouros, M. and Hoo Fatt, M. (1995). Effect of shear on plastic denting of cylinders. *International Journal of Mechanical Sciences*, 37(4): 355–371.

Muscat-Fenech, C.M. and Atkins, A.G. (1998). Denting and fracture of sheet steel by blunt and sharp obstacles in glancing collisions. *International Journal of Impact Engineering*, 21(7): 499–519.

Paik, J.K. (2005). Ultimate strength of dented steel plates under edge shear loads. *Thin-Walled Structures*, 43: 1475–1492.

Paik, J.K. and Shin, B.C. (1989). Damage effects on the ultimate strength of offshore tubular members. *Journal of Ocean Engineering and Technology*, The Korea Committee for Ocean Resources & Engineering, 3(2): 577–586.

Paik, J.K. and Thayamballi, A.K. (2003). *Ultimate Limit State Design of Steel-plated Structures*, John Wiley & Sons, Chichester.

Paik, J.K. and Thayamballi, A.K. (2007). *Ship-shaped Offshore Installations: Design, Building, and Operation*. Cambridge University Press, Cambridge.

Paik, J.K., Shin, B.C. and Kim, C.Y. (1989). Damage estimation for offshore tubular members under quasi-static loading. *Journal of the Society of Naval Architects of Korea*, 26(4): 81–93.

Paik, J.K., Lee, J.M. and Lee, D.H. (2003). Ultimate strength of dented steel plates under axial compressive loads. *International Journal of Mechanical Sciences*, 45: 433–448.

Paik, J.K. *et al.* (2006). Report of ISSC Committee V.6 Condition Assessment of Aged Ships. *International Ship and Offshore Structures Congress*, University of Southampton, August.

Park, T.D. and Kyriakides, S. (1996). On the collapse of dented cylinders under external pressure. *International Journal of Mechanical Sciences*, 38(5): 557–578.

Porter, R. (1992). Non-destructive examination in shipbuilding. *Welding Review*, 11(1): 9–10.

Reid, S.R. and Goudie, K. (1989). Denting and bending of tubular beams under local loads, in: *Structural Failure*, ed. T. Wierzbicki and N. Jones, John Wiley & Sons, New York, 331–364.

Rudlin, J.R. and Wolstenholme, L.C. (1992). Development of statistical probability of detection models using actual trial inspection data. *British Journal of Non-Destructive Testing*, 34(12).

Rummel, W.D., Hardy, G.L. and Cooper, T.D. (1989). Applications of NDE reliability to systems. *Nondestructive Evaluation and Quality Control in Metals Handbook*, 9th Edition, Vol. 17, ASM International.

Smith, C.S. (1984). Assessment of damage in offshore steel platforms, in: *Marine and Offshore Safety*, ed. P.A. Frieze, R.C. McGregor and I.E. Winkle, Elsevier, New York, 279–307.

Smith, C.S. and Dow, R.S. (1981). Residual strength of damaged steel ships and offshore structures. *Journal of Constructional Steel Research*, 1(4): 1–15.

Song, W.J., Rose, J.L. and Whitesel, H. (2003). An ultrasonic guided wave technique for damage testing in a ship hull. *Material Evaluation*, 61(1): 94–98.

© 2008 Woodhead Publishing Limited

Part IV

Reliability of aged structures

© 2008 Woodhead Publishing Limited

10

Reliability of aged ship structures

Y GARBATOV and C GUEDES SOARES,
Technical University of Lisbon, Portugal

Abstract: The chapter reviews recently developed mathematical tools for the reliability assessment of ship hulls subjected to the degrading effect of corrosion and fatigue. The model allows for the existence of multiple cracks both in the stiffeners and in the plating and models the cracks and corrosion growth as a time-dependent process. The long-term stress range acting on the elements is defined as a function of the local pressure combined with the hull girder bending stresses. The effect of corrosion and fatigue deterioration on the section modulus is accounted for and is used as the reference variable to measure the reliability of the ship hull against collapse. The effects of maintenance actions and different repair policies are also discussed.

Key words: fatigue, corrosion, reliability, inspection, maintenance.

10.1 Introduction

The process of ship structural design goes from the primary structure (midship section) to the detailed design of substructures and components such as plates and welded joints. Design of primary load-carrying structures is mainly governed by fatigue and ultimate strength. Fatigue analysis is based on different principles than ultimate collapse.

Currently, there is a trend to consider explicitly the effect of degradations such as corrosion and fatigue. Fatigue is a strength degradation phenomenon that can also increase with corrosion. Fatigue is one of the most complicated problems in engineering, especially for the structural components subjected to stochastic loading. A practical method of predicting component reliability under the fatigue failure mode is generally difficult, not only because of the difficulty in describing the mechanics of fatigue crack growth but also because of the complexity of the reliability model.

Both the environmental loads and the corresponding stress in a structural component vary with time and can be modelled as stochastic processes. Theory and methods of reliability assessment have been developed significantly in the last two decades and now there are two main types of reliability methods. Time-invariant methods consider that both the strength of the component and the loads do not change with time, i.e. they are random variables. Time-dependent formulations are able to model the case when a component is subjected to a random fluctuating load and its capacity deteriorates with time.

© 2008 Woodhead Publishing Limited

The developments of structural reliability theory, which occurred in the late 1960s, started being applied to ship structures in the 1970s. Since then several improvements have occurred in the theoretical formulations and in the computational methods of structural reliability, some of which have been applied to the analysis of ship structures.

Presently the first-order reliability method takes into account the information about the type of distribution of the basic variables, and these analytically based methods have been extended to combine their capabilities with Monte-Carlo simulation methods which in turn have been made efficient through different strategies. Non-linear limit state functions are adequately dealt with and the analysis of systems, either in parallel or in series, can be performed with current methods. Furthermore, various interesting formulations for time-varying reliability have been proposed.

In light of these developments of the computational methods, one can justifiably raise the question of how to formulate specific reliability problems and how to interpret the results of the analysis. At a given moment the most appropriate methodology is the one that best compromises between the required extent and quality of input data, the accuracy of the calculation methods, and the likely use of the results. Very advanced methods are not justified when the input data involves large uncertainties or when the output is used for relative ranking of various alternatives which would be kept unchanged when using a simpler method.

One interesting problem to study is the behaviour of the whole hull girder of a ship and in particular the way in which the structural design process is addressed from the point of view of the regulatory agencies. Several reliability studies have concentrated on ship components, such as, for example, a plate element under compressive load or a welded joint under fatigue.

Classification societies have been interested in the subject since the early days, as can be seen in the papers of Abrahamsen *et al.* (1970), Akita *et al.* (1976), Goodman and Mowatt (1997), Planeix *et al.* (1977), Stiansen *et al.* (1980), Ostergaard and Rabien (1981), and Ferro and Cervetto (1984). The interest of classification societies is very important, since one of the main applications of reliability theory is in design codes which, in the case of ships, are elaborated by the classification societies.

The formulations that have been used for the safety check of the primary ship structure adopt the same approach as prescribed in the rules of the classification societies. The main difference is that in those studies the basic variables are modelled as being random, while the rules of the classification societies specify their nominal value as a function of ship parameters.

Basically the ship hull is considered to behave globally as a beam under transverse load subjected to the still-water and wave-induced load effects. In general the governing variable is the vertical bending moment which will induce the longitudinal bending of the hull. The resulting stresses are distributed

© 2008 Woodhead Publishing Limited

linearly across the depth of the hull and their intensity at bottom and deck is the ratio of the applied moments by the respective section modulus.

Thus in this formulation the strength variables are the yield strength of the material and the section modulus, while the load variables are the still-water and the wave-induced bending moments. This formulation has the limitation that the system behaviour of the hull girder is not taken into account. In fact, when the whole girder is subjected to a bending moment the stiffened plate elements in the deck and bottom are subjected to cyclic tension and compression. Since the different elements may have different dimensions and different levels of initial defects, some will fail before others. This means that some elements will fail before the hull girder is able to develop its full ultimate load-carrying capacity as quantified by Caldwell (1965).

Depending on the geometry of the hull cross-section, the relation between the load corresponding to the initial yield stress at deck or bottom and the ultimate collapse load will vary. This means that the elastic stress that is used as the reference value is not a consistent parameter for comparative purposes of hull collapse. However, this has been the basic approach used in the classification societies' checking procedure and in the former reliability formulations.

The first reference to structural safety of ships dates back to 1962 and is due to Abrahamsen (1962). He provided an interesting discussion about the role of safety factors, which is still applicable. However, the first reported work on ship structural reliability dates from 1971 and is due to Nordenstrom (1971). He formulated the reliability problem between a normally distributed stillwater load, a Weibull-distributed wave-induced load and a normally distributed resistance. He calculated the probability of failure, i.e., he defined the three variables by their probability distribution functions and calculated the probability of failure by integrating them in the appropriate failure domain.

The first complete reliability analysis of a ship structure was not made before 1972 (Mansour 1972). Mansour and Faulkner (1973) developed a probabilistic model for ship strength and analysed a Mariner ship, a tanker and a warship. They adopted Nordenstrom's model for wave-induced loads, considering different modes of failure of the structure.

Another major contribution is the introduction of second moment methods by Mansour (1974) and by Faulkner and Sadden (1979). Mansour adopted the reliability index formulation of Cornell (1969) and applied it to 19 merchant ships.

To assess the reliability of the structure, it is necessary to compare the values of the load effects in the various components with their respective load-bearing capacity. In view of the different load components present and of the corresponding different behaviour of the structural elements, several modes of failure or limit states must be considered.

In general, the modes of failure of the structural components are due to yielding and plastic flow, to elasto-plastic buckling and to crack growth by

© 2008 Woodhead Publishing Limited

fatigue or fracture, as discussed for example by Mansour (1972). When considering the primary hull structure, reference is usually made to the midship section, and checks on the capability of secondary structures were only made in some studies.

Akita (1988) used a FORM approach to predict the strength of square panels. He used an implicit formula to predict plate strength, which took explicit account only of plate slenderness and amplitude of initial distortions.

Bonello and Chryssantoloulos (1993) used the concept of system reliability to access the reliability of one plate element; they assumed that, for collapse, the plate must simultaneously have reached the collapse load, and the strain at the edges of the plate must be sufficiently large in the post-collapse region. This is sometimes what happens in large panels: one plate element is in the post-collapse region, but the rest of the structure does not allow it to develop excessive strain.

Hart *et al.* (1986) used a FORM method to assess the reliability of stiffened plates in ship structures which were subjected to combinations of time-varying loads representative of ship structures. The stiffened plates were idealised as a stiffener with an effective width of plating.

The developments made in the load and in the strength models as well as in reliability theory have been incorporated in more recent reliability formulations.

Ferro and Cervetto (1984) went beyond the use of the Cornell reliability index and adopted a first-order reliability method to assess the hull girder reliability.

Interesting developments can also be identified in the application of systems reliability to ship structures. The initial applications have used frame models and looked at the transverse strength of ships (Murotsu *et al.*, 1995). However an approach has now been presented of systems reliability using plate elements, which has been applied to a tanker (Okada, 1996).

The time-variant formulation of ship reliability results from modelling the problem with stochastic processes that represent the random nature of the load and strength parameters. In general, failure is seen as the upcrossing of a threshold level that separates a safe from an unsafe state.

To design the marine structure with respect to fatigue damage, the hot spot stress approach is one of the most practical methods and is usually combined with detailed finite element analysis (Fricke and Petershagen, 1992). It has to be pointed out that the calculated local stress around the structural singularities depends very much on the structural idealisation, the element types used and the mesh subdivision. Some application of the approach can be found by Janssen (2000) and by Garbatov *et al.* (2004).

Two main corrosion mechanisms are generally present in steel plates. One is a general wastage that is reflected in a generalised decrease of plate thickness. Another mechanism is pitting, which consists of much localised corrosion with very deep holes appearing is the plate.

© 2008 Woodhead Publishing Limited

Various models of corrosion deterioration have been proposed. Melchers (1998) suggested a steady-state trilinear model for corrosion wastage thickness. In fact, experimental evidence of corrosion reported by various authors shows that non-linear models are appropriate. Yamamoto and Ikagaki (1998) proposed a corrosion model based on analysing data collected from plate thickness measurements. Guedes Soares and Garbatov (1999) proposed one model that describes the growth of corrosion wastage by a non-linear function of time in three phases. Paik's 2003 corrosion model (Paik *et al.*, 2003a, b) also categorises the corrosion behaviour into three phases: durability of coating, transition to visibly obvious corrosion, and progress of such corrosion. A probabilistic model has been developed by Melchers (2003a, b), which divides the corrosion process into four stages: initial corrosion, oxygen diffusion controlled by corrosion products, micro-organic growth, and limitation on food supply for aerobic activity and anaerobic activity.

Engineering systems such as ship structures are designed to ensure an economical operation throughout the anticipated service life in compliance with given requirements and acceptance criteria. Deterioration processes such as fatigue crack growth and corrosion are always present to some degree, and depending on the adapted design philosophy in terms of degradation allowance and protective measures the deterioration processes may reduce the performance of the system beyond what is acceptable. In order to ensure that the given acceptance criteria are fulfilled throughout the service life of the engineering systems, it is necessary to control the development of deterioration and, if required, to install corrective maintenance measures resulting in inspection in the most relevant and effective means of deterioration control.

The initial formulations of the time-variant approach to ship structural reliability were developed in connection with the fatigue problem, in particular to be able to deal with the time degradation of reliability by Guedes Soares and Garbatov (1996b) and with the improvements made by maintenance actions by Guedes Soares and Garbatov (1996b, d).

Planning of inspections concerns the identification of what to inspect, how to inspect, where to inspect and how often to inspect. Even though inspections may be used as an effective means for controlling the degradation of the considered engineering system and thus imply a potential benefit, they may also have considerable impact on the operation of the system and other economic consequences themselves. For this reason, it is necessary to plan the inspections such that a balance is achieved between the expected benefit of the inspections and the corresponding economic consequences implied by the inspections themselves.

During the last 10 to 15 years reliability-based and risk-based approaches have been developed for the planning of inspections as reported by Skjong (1985), Madsen *et al.* (1986) and Fujita *et al.* (1989). These approaches are based on the decision theory to minimise the overall service life costs including direct and implied costs of failures, repairs and inspections.

© 2008 Woodhead Publishing Limited

The consequence of component failure, e.g. in terms of potential loss of lives or costs, will depend on the component and its importance for the operation of the structure. The risk associated with the component is the product of the probability of component failure and the consequence of failure. The risk-based inspection approach is based on a quantification of risk not only on a component basis but also for all components in the installation as a whole. Different inspection strategies with different inspection effort, inspection quality and costs will have different effects on the risk. By comparing the risk associated with different inspection strategies, the inspection strategy implying the smallest risk can be identified.

Formulating the inspection and maintenance planning problem as a problem where the overall service life costs are minimised, the pre-posterior analysis from the classical decision theory was given by Raiffa and Schaifer (1982) and Benjamin and Cornell (1970), providing a consistent and systematic framework for its solution.

Following the more recent work of Rackwitz (2000), the acceptable probability of failure for an engineering system, or any other activity for that matter, should be established on the basis of an optimisation where the consequences of failure are assessed in terms of preferences expressed, e.g., in monetary terms. This approach is based on the fundamental work by Nathwani *et al.* (1997) addressing the value of the individual to society by means of the Life Quality Index. However, the implementation of such approaches in practice still lags behind, and approaches resting on the (less optimal) judgemental power of the individual decision-maker must be pursued in the meanwhile.

The decision to repair a ship is based not on the status of one specific crack or one specific corroded plate, but instead on a generalised state of deterioration. This can be modelled by a global variable such as, for example, the midship section modulus, which changes with time with the growth of both strength degradation phenomena. Therefore, the expected values of both crack sizes and plate thickness as a function of time have to be described. Consequently, the midship section modulus is also modelled as a random variable whose mean and standard deviation change with time.

The need of such approach has been recognised by Guedes Soares and Garbatov (1996c), who developed a method to assess the reliability of the ship hull subjected to potential cracks initiated at the weldments between stiffeners and the plating. The crack propagation is governed by the effect of the longitudinal stresses associated with the overall bending of the hull. The simultaneous effect of a random number of cracks was accounted for by considering the decrease in the net sectional area that is available to resist the vertical bending of the hull.

The inspection and repair work performed during the ship lifetime never allows a very dramatic spreading of cracks to be developed. This effect was incorporated in the time-variant formulation of ship hull reliability by Guedes

© 2008 Woodhead Publishing Limited

Soares and Garbatov (1996a), which yields the required information to assess the effect of inspections and repairs at different points in time on the reliability of the hull girder, as shown for tankers by Guedes Soares and Garbatov (1996d). The effect of repair with plate replacement in ship hulls subjected to corrosion was modelled in a similar way to the fatigue problem by equating the repaired state of the structure to the state that the structure had at an earlier time in its life, as shown by Guedes Soares and Garbatov (1996b).

Normally both fatigue and corrosion will be present and their combined effect needs to be considered in that the decreased net section due to corrosion will increase the stress levels, which in turn increases the rate of crack growth. This effect has been considered by Guedes Soares and Garbatov (1998), who showed that, depending on the repair policy adopted, one of the two phenomena would be the dominating one.

Garbatov and Guedes Soares (2002) have adopted a Bayesian approach to update some of the parameters of the probability distributions governing the reliability assessment of maintained floating structures. The description of the time to crack initiation, crack growth law and probability of crack detection were updated using the information from the inspections.

Risk-based methods for inspection and maintenance can reduce lifecycle cost by basing inspection and repair intervals on the risk of incurring damage rather than on arbitrary periods. Risk-based methods for inspection and maintenance can reduce inspection cost and downtime and may actually increase ship reliability and safety by defining explicit failure probabilities for all important components and functions. The cost justification for embedding inspection and monitoring devices into structures is the reduction in the total ownership cost. The components of total cost can be affected by the cost of periodic inspections, the frequency of inspections, the restoration cost saved by earlier detection, and the reduction in failure probability given constraints in the cost of frequency of inspections. In some cases, the structure may be out of service during the time of the inspection, in which case the cost of the inspection is also affected by the capability of the inspection methods and internal devices used in the structure.

In maintenance planning, optimisation can be achieved by appropriate selection of inspection interval, inspection methods, repair, quality, and so on. The interval between inspections in the case of floating structures depends on economic considerations, on expected losses due to maintenance downtime and on the requirements of classification societies. In general, classification societies require fixed intervals between inspections, but owners may decide on shorter intervals based on economic considerations.

The approach that was presented by Garbatov and Guedes Soares (2001) has defined the optimal strategy for maintenance planning in comparison with cost considerations. The approach has demonstrated how repair cost can be used as a criterion in reliability-based maintenance planning and, in particular, how to vary the inspection interval in order to obtain the minimum intensity of repair

© 2008 Woodhead Publishing Limited

cost. In some cases to keep the reliability level above a certain acceptable value, the costs will not dominate and the reliability criterion will be the governing one. Several inspection strategies have been studied and reliability and repair cost have been discussed.

The simulated strategies for inspection planning pointed out that the application of repair cost optimisation for floating structures involves many uncertainties related to the costs of the shipyard that would perform the repair, with the inspection procedures.

Evaluation of alternative criteria for maintenance planning in terms of the intensity of repair cost and availability of the platform to perform its intended functions is difficult to achieve. The minimum required intensity or repair cost could be related to the requirements of classification societies. However, this does not mean that the maintenance effort is optimised. When maintenance is intensified, the costs associated with inspection and repairs increase. The search for a maintenance effort that will optimise the use of available resources should consider the lifetime cost of the solution.

The problems related to assessing the serviceability and safety of aged steel ships including the assessment of their structural condition (in view of corrosion, fatigue cracking and local denting), methods for repair, quantification of strength of deteriorated and repaired ships (as well as criteria for acceptable damage), accounting for the uncertainties involved and cost–benefit and risk-based decision procedures for remedial actions, have been the main objective in two consecutive reports of ISSC, 2003, Specialist Committee V.2 Inspection and Monitoring (Bruce *et al.*, 2003) and ISSC, 2006, Committee V.6 Condition Assessment of Aged Ships (Paik *et al.*, 2006).

However, a balance between reliability and economic criteria could be the key to inspection strategy as has been defined by Garbatov and Guedes Soares (2001). Repair cost can be used as a criterion in reliability-based maintenance planning and, in particular, how to vary the inspection interval in order to obtain the minimum intensity of repair cost. In some cases to keep the reliability level above a certain acceptable value, the costs will not dominate and the reliability criterion will be the governing one. The approach was used as a base case to define the optimal strategy for maintenance planning using cost considerations. Simulated strategies for inspection planning showed that the application of repair cost optimisation for floating structures involves many uncertainties, including the costs of the shipyard making the repairs, and the inspection procedures.

This chapter reviews the approach adopted in recent years by the authors, in which crack growth was governed by the loading from vertical horizontal bending moments and local pressures resulting from internal and external wave-induced pressures. A two-failure mode is applied. The local criterion addresses the fact that the cracks in the longitudinal elements are growing under combined loading. The combined loading includes the global loading from vertical and horizontal bending moments and the local loading which is governed by the

© 2008 Woodhead Publishing Limited

cargo loading and external transverse water pressure. The failure of the ship structure is modelled by a global criterion, which includes only direct stresses as given by a ratio of vertical bending moments and midship section modulus.

10.2 Time-dependent hull section modulus subject to crack growth

The conditions governing the fatigue crack growth are the geometry of the structure, the crack initiation size a_0, the material characteristics, the environmental conditions, and the loading $\Delta\sigma$. In general, these conditions are of a random nature.

The time for a crack to reach the critical crack size is calculated by applying the Paris–Erdogan law which indicates that crack propagation depends on a_0, $\Delta\sigma$, C and m. Since both C and m are material properties that are likely to be highly negatively correlated, only one parameter will be modelled here as a random variable. These three random variables are considered statistically independent, which is a reasonable assumption since they depend on different sources. The initial crack size a_0 depends on the fabrication of the weldment, m is a material property and $\Delta\sigma$ depends on the external loading. The distributions of a_0 and m are considered to follow a normal distribution and the wave loading is assumed to have an exponential distribution.

The mean and standard deviation of the crack size can be given by first-order second moment methods, which are based on the application of an expansion in a Taylor series given for example in Benjamin and Cornell (1970). The mean and variance of the time of crack propagation are approximated by:

$$E[T_p] = \frac{a_{\text{cr}}^{1-\frac{m}{2}} - \{E[a_o]\}^{1-\frac{m}{2}}}{\left(1-\frac{m}{2}\right)E[C]E[\Delta\sigma^m]Y^m\pi^{m/2}\nu_o}$$
$$\sigma_{T_p}^2 = \left(\frac{\partial T_p}{\partial a_o}\right)^2\sigma_{a_o}^2 + \left(\frac{\partial T_p}{\partial C}\right)^2\sigma_c^2 + \left[\frac{\partial T_p}{\partial(\Delta\sigma^m)}\right]\sigma_\Delta^2 \qquad 10.1$$

as derived by Guedes Soares and Garbatov (1996a), where $E[\ ]$ is the mean value operator, T_p is the time for a crack to reach the critical size, and $\sigma_{a_o}^2$, σ_c^2 and σ_Δ^2 are the variance of a_o, C and $\Delta\sigma^m$, respectively. The derivatives, given as:

$$\frac{\partial T_p}{\partial a_o} = \frac{-a_o^{-\frac{m}{2}}\left(1-\frac{m}{2}\right)}{\left[a_{\text{cr}}^{1-\frac{m}{2}} - a_o^{1-\frac{m}{2}}\right]}T_p, \quad \frac{\partial T_p}{\partial C} = -\frac{1}{C}T_p \quad \text{and} \quad \frac{\partial T_p}{\partial(\Delta\sigma^m)} = -\frac{1}{\Delta\sigma^m}T_p \qquad 10.2$$

are to be evaluated at the mean values of the random variables.

The crack size at an arbitrary point in time is a random variable too. Its mean and variance are taken as:

© 2008 Woodhead Publishing Limited

$$E[a(t)] = \left[\{E[a_o]\}^{1-\frac{m}{2}} + \left(1 - \frac{m}{2}\right) E[C] E[\Delta\sigma^m] Y^m \pi^{m/2} \nu_o t\right]^{1/(1-\frac{m}{2})} \quad 10.3$$

$$\sigma^2_{a(t)} = \left[\frac{\{E[a_o]\}^{-m/2} a(t)}{\{E[a_o]\}^{1-\frac{m}{2}} + \left(1 - \frac{m}{2}\right) E[C] E[\Delta\sigma^m] Y^m \pi^{m/2} \nu_o t}\right]^2 \sigma^2_{a_o}$$

$$+ \left[\frac{E[\Delta\sigma^m] Y^m \pi^{m/2} \nu_o t\, a(t)}{\{E[a_o]\}^{1-\frac{m}{2}} + \left(1 - \frac{m}{2}\right) E[C] E[\Delta\sigma^m] Y^m \pi^{m/2} \nu_o t}\right]^2 \sigma^2_c$$

$$+ \left[\frac{E[C] Y^m \pi^{m/2} E[\Delta\sigma^m]}{\{E[a_o]\}^{1-\frac{m}{2}} + \left(1 - \frac{m}{2}\right) E[C] E[\Delta\sigma^m] Y^m \pi^{m/2} \nu_o t}\right]^2 \sigma^2_\Delta \quad 10.4$$

where no correlation was assumed between the three random variables.

The crack size is assumed to have a normal distribution, which is truncated at zero to ensure that negative crack sizes will not occur, although the values of the parameters of the distribution make this event very unlikely.

This approach is applied to a ship hull girder where two different types of cracks are considered, both in stiffeners and in plates. It is assumed that a crack can be initiated at the weld between the plate and the stiffener and can propagate in each of them.

In the plate, the crack will be a through-thickness crack that propagates away from the stiffener in a transverse direction, decreasing the net section of the plate that resists longitudinal loading. In the stiffener, the crack initiates on the edge connected to the weld and propagates across the stiffener, decreasing its net effective area to resist the longitudinal loads.

The stiffener is considered to be a flat bar with height h_{so} and thickness b_s. The variation of the net sectional area with time will be dependent on crack size, $a(t)$. The net area of the stiffener is the product of the thickness b_s, which is considered constant, by the height $h_s(t)$, which decreases with time as the crack size increases:

$$h_{si}(t) = h_{so} - a(t) \quad 10.5$$

The area of stiffener i is given by:

$$A_i(t) = b_{si} h_{si}(t) \quad 10.6$$

The moment of inertia of the stiffener with respect to its centre of gravity is given by:

$$i_{oi}(t) = \frac{b_{si} h^3_{si}(t)}{12} \quad 10.7$$

© 2008 Woodhead Publishing Limited

The plate has breadth b_{po} and thickness h_p. The crack will decrease the net sectional area of the plate, which will be given as:

$$A_i(t) = h_{pi} b_{pi}(t) \tag{10.8}$$

where the net plate breadth varies with time:

$$b_{pi}(t) = b_{poi} - a(t) \tag{10.9}$$

The mean and variance of the net area and the moment of inertia of the structural elements can be determined by second moment methods as already done with T_p.

The mean value and variance of the geometric characteristics of the midship section depend on the size $a_i(t)$ of the crack in each element i. The mean and variance of the area of the midship section at a specific point in time are given by:

$$E[A(t)] = \sum_{i=1}^{n} E[A_i(t)], \qquad \sigma_A^2(t) = \sum_{i=1}^{n} \sigma_{A_i}^2(t) \tag{10.10}$$

The mean value and standard deviation of the midship section properties are obtained by first-order second moment methods. The mean value of the ordinate of the neutral axis Z_n is given by the ratio of the mean moment of area, $E[M(t)]$, to the mean value of the total area, $E[A(t)]$:

$$E[Z_n(t)] = \frac{E[M(t)]}{E[A(t)]} \tag{10.11}$$

The mean value of the area and the moment of area are given by:

$$E[A(t)] = \sum_{i=1}^{n} E[A_i(t)], \qquad E[M(t)] = \sum_{i=1}^{n} z_i E[A_i(t)] \tag{10.12}$$

where z_i is the ordinate of the centre of gravity of each element and $E[A_i(t)]$ is the expected area at an instant of time t.

The variance of the moment of area is:

$$\sigma_M^2(t) = \sum_i z_i^2 \sigma_{A_i}^2(t) = \sum_{i=1}^{n} \sum_{j=1}^{n} z_i z_j \sigma_{A_i}(t) \sigma_{A_j}(t) \rho_{ij} \tag{10.13}$$

where ρ_{ij} is the correlation coefficient between plate elements, which is equal to 1 when $i = j$. It is important to account for the correlation between different plate elements because the elements that will be subjected to the same conditions will be likely to have similar corrosion rates and crack growth rates.

The variance of Z_n is obtained from:

$$\sigma_{Z_n}^2(t) = \frac{\sigma_M^2(t)}{\{E[A(t)]\}^2} + \frac{\{E[M(t)]\}^2}{\{E[A(t)]\}^4} \sigma_A^2(t) + \frac{E[M(t)]}{E[A(t)]} \sigma_A(t) \sigma_M(t) \rho_{AM} \tag{10.14}$$

© 2008 Woodhead Publishing Limited

where the correlation coefficient ρ_{AM} is expected to be very high and as an approximation can be taken equal to 1.0.

The moment of inertia of the hull section is obtained from the product of the area of the plate elements multiplied by their ordinates and from their own inertia and mean value and variance are given by:

$$E[I_b(t)] = \sum_{i=1}^{n} \{z_i^2 E[A_i(t)] + E[i_{oi}(t)]\} \tag{10.15}$$

$$\sigma_{I_b}^2(t) = \sum_{i=1}^{n} \sum_{j=1}^{n} \left[z_i^2 z_j^2 \, \sigma_{A_i}(t) \, \sigma_{A_j}(t) + \sigma_{i_{oi}}(t) \, \sigma_{i_{oj}}(t) \right] \rho_{ij} \tag{10.16}$$

The moment of inertia with respect to the neutral axis is obtained by transporting the moment of inertia in relation to the base line by the ordinate of the neutral axis:

$$E[I_n(t)] = E[I_b(t)] - \{E[Z_n(t)]\}^2 E[A(t)] \tag{10.17}$$

and the variance is obtained from:

$$\sigma_{I_n}^2(t) = \sigma_{I_b}^2(t) + \{E[Z_n(t)]\}^4 \sigma_A^2(t) + 4\{E[Z_n(t)]\}^2 \{E[A(t)]\}^2 \sigma_{Z_n}^2(t) \tag{10.18}$$

Finally the probabilistic descriptors of the section modulus, $W(t)$, are obtained from:

$$\sigma_{W_{\mathrm{D}}}^2(t) = \frac{\sigma_{I_n}^2(t)}{\{E[Z_n(t)]\}^2} + \frac{\{E[I_n(t)]\}^2}{\{E[Z_n(t)]\}^4} \sigma_{Z_n}^2(t) \tag{10.19}$$

where $$E[W_{\mathrm{D}}(t)] = \frac{E[I_n(t)]}{E[Z_n(t)]}$$

$$\sigma_{W_{\mathrm{B}}}^2(t) = \frac{\sigma_{I_n}^2(t)}{\{D - E[Z_n(t)]\}^2} + \frac{\{E[I_n(t)]\}^2}{\{D - E[Z_n(t)]\}^4} \sigma_{Z_n}^2(t) \tag{10.20}$$

where $$E[W_{\mathrm{B}}(t)] = \frac{E[I_n(t)]}{D - E[Z_n(t)]}$$

where subscripts B and D stand for bottom and deck respectively, and D is the depth of the hull as derived by Guedes Soares and Garbatov (1996b).

The probability distribution function of the midship section modulus is approximated by a normal distribution with the mean value and variance indicated in the latter expressions and is truncated at 0 to neglect the negative values of the midship section modulus.

© 2008 Woodhead Publishing Limited

10.3 Effect of corrosion on the hull section modulus

The variable that controls the resistance of the hull girder to longitudinal bending is the midship section modulus, since the nominal longitudinal stresses will be the ratio of the applied bending moments by the hull section modulus. This section will examine how the section modulus will vary in time because of corrosion.

It is considered that general corrosion will occur in all structural elements, both in the plating and in the stiffeners, by decreasing the plate thickness at a rate that may be different from element to element. In the foregoing formulation, localised pit corrosion will not be accounted for.

For each plate element i the area, A_i, is given by the product of its breadth b_i by the thickness, $h_i(t)$:

$$A_i = b_i\, h_i(t) \tag{10.21}$$

The plate thickness starts from an initial design value, h_{oi}, and decreases with a corrosion depth $d(t)_{\mathrm{cor},i}$ as a function of time:

$$h_i(t) = h_{oi} - d(t)_{\mathrm{cor},i} \tag{10.22}$$

The corrosion depth in each element is, however, a random quantity.

The vertical moment of inertia of the plate element with respect to its centre of gravity is given by:

$$i_{oi}(t) = \frac{b_i\, h_i(t)^3}{12} \tag{10.23}$$

in the case of the horizontal plate elements found in the bottom and intermediate decks, and by:

$$i_{oi}(t) = \frac{b_i^3\, h_i(t)}{12} \tag{10.24}$$

in the case of vertical plates in the side shell and longitudinal bulkheads.

To assess the properties of stiffeners it is enough to note that they are made of plate elements to which the above formulas can be applied.

The mean value and standard deviation of the midship section properties are obtained by first-order second moment methods similar to Eqns 10.8 to 10.22. The variance of the moment is

$$\sigma_M^2(t) = \sum_i z_i^2\, \sigma_{A_i}^2(t) = \sum_{i=1}^{n} z_j^2\, \sigma_{A_i}^2(t) + 2\sum_{i=1}^{n}\sum_{j=1, j>i}^{n} z_i\, z_j\, \sigma_{A_i}(t)\sigma_{A_j}(t)\rho_{ij} \tag{10.25}$$

where ρ_{ij} is the correlation coefficient between plate elements i and j. It is equal to 1.0 when $i = j$. It is assumed that the correlation of corrosion wastage in neighbouring plate elements decreases with increasing distance between them.

© 2008 Woodhead Publishing Limited

If the location of each pair of elements can be represented by two vectors $\vec{r}_i$ and $\vec{r}_j$, then the distance between them can be calculated as the modulus of:

$$\Delta\vec{r}_{ij} = \vec{r}_i - \vec{r}_j \tag{10.26}$$

Normalising Eqn 10.26, with the maximum vector, and transforming into a real coordinate system, gives a non-dimensioned distance. The correlation coefficient is then proposed as a function of the distance between elements, decreasing as distance increases:

$$\rho_{ij} = \begin{cases} 1 & \text{if } r_i = r_j \\ \left[1 - \left|\dfrac{\sqrt{y_i^2+z_i^2} - \sqrt{y_j^2+z_j^2}}{\sqrt{y_{\max}^2+z_{\max}^2}}\right|\right]^n \end{cases} \tag{10.27}$$

where $y_{\max}$ and $z_{\max}$ are maximum values of y and z, and n is a coefficient. When $\Delta\vec{r}_{ij} = 0$ the correlation coefficient refers to one plate and this corresponds to $\rho_{ij} = 1$.

10.4 Time-dependent section modulus of a hull with cracks and corrosion

The stiffening elements are considered to be a flat bar. The crack will propagate across its width, decreasing therefore its net sectional area available to carry longitudinal stresses. The variation of the area with time will be dependent on the crack size $a_i(t)$ and on the corrosion depth $d_{\text{cor},i}(t)$. The net area of the element, which decreases with time, is the product of the horizontal dimension of the plate $s_{yi}(t)$ by the vertical dimension $s_{zi}(t)$:

$$A_i(t) = s_{yi}(t)\, s_{zi}(t) \tag{10.28}$$

The dimensions of the elements start from initial values s_{yoi} and s_{zoi} and decrease with time at a rate of corrosion r_i and due to a crack size $a_i(t)$:

$$s_{yi}(t) = s_{yoi} - a_{11}a_i(t) - a_{12}d_{\text{cor},i}(t) \tag{10.29}$$

$$s_{zi}(t) = s_{zoi} - a_{21}a_i(t) - a_{22}d_{\text{cor}.i}(t) \tag{10.30}$$

where the coefficients in Eqns 10.29 and 10.30 are given depending on the location of an element as $a_{11} = 0$, $a_{12} = 1$, $a_{21} = 1$ and $a_{22} = 0$ for the vertical elements, and $a_{11} = 1$, $a_{12} = 0$, $a_{21} = 0$ and $a_{22} = 1$ for the horizontal elements respectively.

The mean value and standard deviation of the net sectional area of the elements are given by:

$$E[A_i(t)] = E[s_{yi}(t)]E[s_{zi}(t)] \tag{10.31}$$

$$\sigma^2_{A_i(t)} = s^2_{zi}(t)\,\sigma^2_{s_{yi}(t)} + s^2_{yi}(t)\,\sigma^2_{s_{zi}(t)} \tag{10.32}$$

© 2008 Woodhead Publishing Limited

and the mean value and variance of the moment of inertia are presented below:

$$E[i_i(t)] = \frac{E[s_{yi}(t)]E[s_{zi}(t)]^3}{12} \tag{10.33}$$

$$\sigma^2_{i_i(t)} = \left(\frac{s^3_{zi}}{12}\right)^2 \sigma^2_{s_{yi}(t)} + \left(\frac{s_{yi}s^2_{zi}}{4}\right)^2 \sigma^2_{s_{zi}(t)} \tag{10.34}$$

The variances that are considered are given by:

$$\sigma^2_{s_{yi}(t)} = p_{11}\sigma^2_C + p_{12}\sigma^2_{d_{\text{cor}.i}} + p_{13}\sigma^2_{a_o} + p_{14}\sigma^2_{\Delta\sigma} + p_{15}\sigma^2_{s_{yoi}} \tag{10.35}$$

$$\sigma^2_{s_{zi}(t)} = p_{21}\sigma^2_C + p_{22}\sigma^2_{d_{\text{cor}.i}} + p_{23}\sigma^2_{a_o} + p_{24}\sigma^2_{\Delta\sigma} + p_{25}\sigma^2_{s_{zoi}} \tag{10.36}$$

where $\sigma^2_{s_{yoi}}$ and $\sigma^2_{s_{zoi}}$ are the variances of the initial geometry s_{yoi} and s_{zoi} of an element.

In the case of a vertical element the coefficients will be given as $p_{1k} = m_{2k}$ for $k = 1$ to 5, and $p_{2k} = m_{1k}$ for $k = 1$ to 5. In the case of a horizontal element they can be written as $p_{1k} = m_{1k}$ for $k = 1$ to 5, and $p_{2k} = m_{2k}$ for $k = 1$ to 5.

The parameters included in the above equations are described by:

$$m_{11} = \left[\frac{E[\Delta\sigma^m]Y^m\pi^{m/2}\nu_o t\, a(t)}{\{E[a_o]\}^{1-\frac{m}{2}} + \left(1-\frac{m}{2}\right)E[C]E[\Delta\sigma^m]Y^m\pi^{m/2}\nu_o t}\right]^2 \tag{10.37}$$

$$m_{12} = 0 \tag{10.38}$$

$$m_{13} = \left[\frac{\{E[a_o]\}^{-m/2}a(t)}{\{E[a_o]\}^{1-\frac{m}{2}} + \left(1-\frac{m}{2}\right)E[C]E[\Delta\sigma^m]Y^m\pi^{m/2}\nu_o t}\right]^2 \tag{10.39}$$

$$m_{14} = \left[\frac{E[C]Y^m\pi^{m/2}E[\Delta\sigma^m]}{\{E[a_o]\}^{1-\frac{m}{2}} + \left(1-\frac{m}{2}\right)E[C]E[\Delta\sigma^m]Y^m\pi^{m/2}\nu_o t}\right]^2 \tag{10.40}$$

$$m_{15} = m_{21} = m_{23} = m_{24} = 0, \quad m_{22} = 1, \quad m_{25} = 1 \tag{10.41}$$

The mean value and standard deviation of the midship section properties are obtained by first-order second moment methods applying the procedure which was already presented in previous sections.

10.5 Time-dependent reliability of the ship hull girder

The limit state for global hull failure is defined as:

© 2008 Woodhead Publishing Limited

$$\frac{M_T}{W} > \sigma_s \tag{10.42}$$

where M_T is the vertical bending moment, W is the midship cross-section modulus and σ_s is the allowable stress. After transformation, Eqn 10.42 may be written:

$$M_T > \varsigma(t) \quad \text{where } \varsigma(t) = \sigma_s W(t) \tag{10.43}$$

There will be a failure if Eqn 10.42 is true, and the probability of failure during the period of time T is:

$$P_{\mathrm{f}}(T) = 1 - \exp\left[-\int_0^T \nu[\varsigma(t)]\mathrm{d}t\right] \tag{10.44}$$

where $\nu[\varsigma(t)]$ is the mean upcrossing rate of the threshold, $\varsigma(t)$.

The probability of failure, $P_{\mathrm{f}}[T|\varsigma(t)]$, is just a conditional probability, on the threshold, $\varsigma(t)$. Therefore, the probability of failure, $P_{\mathrm{f}}(t)$, may be obtained by unconditioning on $\varsigma(t)$:

$$P_{\mathrm{f}}(T) = 1 - \int_0^\infty f_{\varsigma(t)}[\varsigma(t)]P_{\mathrm{f}}[T|\varsigma(t)]\mathrm{d}[\varsigma(t)] \tag{10.45}$$

If σ_s and $W(t)$ are not correlated then the probability density function of the threshold limit may be represented by:

$$f_{\varsigma(t)}[\varsigma(t)] = \int_0^\infty f_{\sigma_s}(\sigma_s)\, f_{W(t)}\left[\frac{\varsigma(t)}{\sigma_s}\right] \frac{\mathrm{d}\sigma_s}{|\sigma_s|}, \varsigma(t) \geq 0 \tag{10.46}$$

where $f_{\varsigma(t)}(\ )$, $f_{\sigma_s}(\ )$ and $f_{W(t)}(\ )$ are probability density functions of the threshold limit, the allowable stress and the midship section modulus respectively. It is considered that the allowable stress follows a normal probability density function and the midship section modulus is described by a normal probability function truncated at zero, which is written as:

$$f_{\sigma_s}(\sigma_s) = \frac{1}{\sqrt{2\pi\sigma_{\sigma_s}^2}} \exp\left\{-\frac{[\sigma_s - E(\sigma_s)]^2}{2\sigma_{\sigma_s}^2}\right\}, -\infty \leq \sigma_s \leq \infty \tag{10.47}$$

$$f_{W(t)}\left[\frac{\varsigma(t)}{\sigma_s}\right] = \frac{c}{\sqrt{2\pi\sigma_{W(t)}^2}} \exp\left\{-\frac{\left[\dfrac{\varsigma(t)}{\sigma_s} - E[W(t)]\right]^2}{2\sigma_{W(t)}^2}\right\}, \quad \text{for } \frac{\varsigma(t)}{\sigma_s} \geq 0 \tag{10.48}$$

where the parameter c equals 2 when $W(t) \geq 0$.

If the amplitudes or the peaks $\varsigma(t)$ of M_T follow the Weibull distribution the upcrossing rate may be written:

$$\nu[\varsigma(t)] = \nu_o \exp\left[-\left(\frac{\varsigma(t) - \mu_{M_T}}{\beta_L}\right)^{\alpha_L}\right] \tag{10.49}$$

© 2008 Woodhead Publishing Limited

where α_L and β_L are the Weibull parameters. The two main components of the vertical bending moment are the still water (M_{SW}) and the wave-induced (M_W). Both can be modelled as a stochastic process but the first one has a much larger typical duration than the wave-induced cycles. Therefore, in a voyage, for example, one can consider that the still water load is constant and, since the mean of the wave-induced load is zero, the mean of the total moment will be equal to the still-wave value.

Considering now that during the ship lifetime the still water loads can be described by a normal distribution, the upcrossing rate can be calculated by unconditioning on the still water:

$$\nu[\varsigma(t)] = \int_{-\infty}^{\infty} \nu_o[\varsigma(t)|m_{SW}] f_{M_{SW}}(m_{SW}) \mathrm{d}m_{SW} \tag{10.50}$$

where $f_{M_{SW}}(m_{SW})$ will be a normal distribution of still water load effects.

Using now Eqn 10.50 and substituting μ_{M_W} by m_{SW} results in

$$\nu[\varsigma(t)] = \int_{-\infty}^{\infty} \nu_o \exp\left[-\left(\frac{\varsigma(t) - m_{SW}}{\beta_L}\right)^{\alpha_L}\right] f_{M_{SW}}(m_{SW}) \mathrm{d}m_{SW} \tag{10.51}$$

Since the process of fatigue failure is separated into two parts depending on the status of crack growth, the probability of non-failure after crack initiation is given by the following equation:

$$R_a(T) = 1 - P_f(T) \tag{10.52}$$

It has been shown on several occasions that an exponential distribution is an adequate approximation for the long-term distribution of wave-induced loads. Therefore, this distribution is adopted and making $\alpha = 1$, Eqn 10.51 becomes:

$$R_a(t) = \exp\left\{-\left[\exp\left(-\int_0^t \nu[\varsigma(\tau)]\mathrm{d}\tau\right)\right]\right\}, \quad t > t_{i1} \tag{10.53}$$

where t_{i1} is the time of the first initiation of crack propagation. This approximation is correct for a stationary process but the long-term distribution considered here is non-stationary. Therefore, this result is only approximate in this case.

For $t \leq t_{i1}$ the midship section is still intact and the section modulus is equal to its value at $t = 0$:

$$W(t) = W(0) \quad \text{for} \quad t \leq t_{i1} \tag{10.54}$$

and $\varsigma(t)$ becomes a constant ς_o. Therefore, the reliability before crack initiation is given by:

$$R_b(t) = \exp\{-\exp[-\nu(\varsigma_o)]t\}, \quad \text{for} \quad t \leq t_{i1} \tag{10.55}$$

since the upcrossing rate is now constant.

It is assumed that at each connection between stiffener and plating a potential

© 2008 Woodhead Publishing Limited

crack exists. At a given point in time, there will be a probability that a crack will start propagating. This can be described by a probability density function following the results observed by Antoniou (1977).

The probability density function of the time for crack initiation was derived assuming $T_i = 0.15T_p$ and was fitted by a Weibull density function:

$$f_{T_i}(t_i) = \frac{\alpha_{T_i}}{\beta_{T_i}} \left(\frac{t_i}{\beta_{T_i}}\right)^{a_{T_i}-1} \exp\left[-\left(\frac{t_i}{\beta_{T_i}}\right)^{\alpha_{T_i}}\right] \qquad 10.56$$

Since the time to crack initiation is a random variable, the reliability given in Eqns 10.53 and 10.55 is in fact conditional on the probability of time to crack initiation, $R(T|t_i)$. Therefore, the unconditional reliability of a hull with cracks is given by:

$$R(T) = \int_0^\infty R(T|t_i) f_{T_i}(t_i) \mathrm{d}t_i \qquad 10.57$$

where $R(T|t_i)$ is given by Eqns 10.53 and 10.55.

The total reliability $R(t)$ is given by the reliability of the hull with cracks plus the reliability of the hull without cracks, which has a probability of $[1 - F_{T_i}(T)]$. Thus, the final expression is given by:

$$R(T) = [1 - F_{T_i}(T)]R_b(T) + \int_0^T R_b(t_i)R_a(T - t_i) f_{T_i}(t_i) \mathrm{d}t_i \qquad 10.58$$

10.6 Modelling crack inspections and reliability

The inspection of ship details during their lifetime aims at detecting any cracks that may have initiated. Despite details being designed to be free from cracks, the practice has shown that cracks do occur and thus inspection procedures are essential.

The policy to be adopted in deciding how often inspection is to be performed, which inspection methods to adopt and where to inspect must be a trade-off between the cost of inspection and the probability of detecting cracks.

The probability of crack detection increases with the probability of cracks existing in the details inspected, with increasing accuracy of the inspection method and with the number of inspections. However, in general the cost of inspection also increases with the number of inspections and with the sophistication of the method of inspection.

The immediate question that an inspector will have after detecting a crack is what is the remaining life. The growth of an existing crack can be calculated using fracture mechanics concepts that are included in the following section.

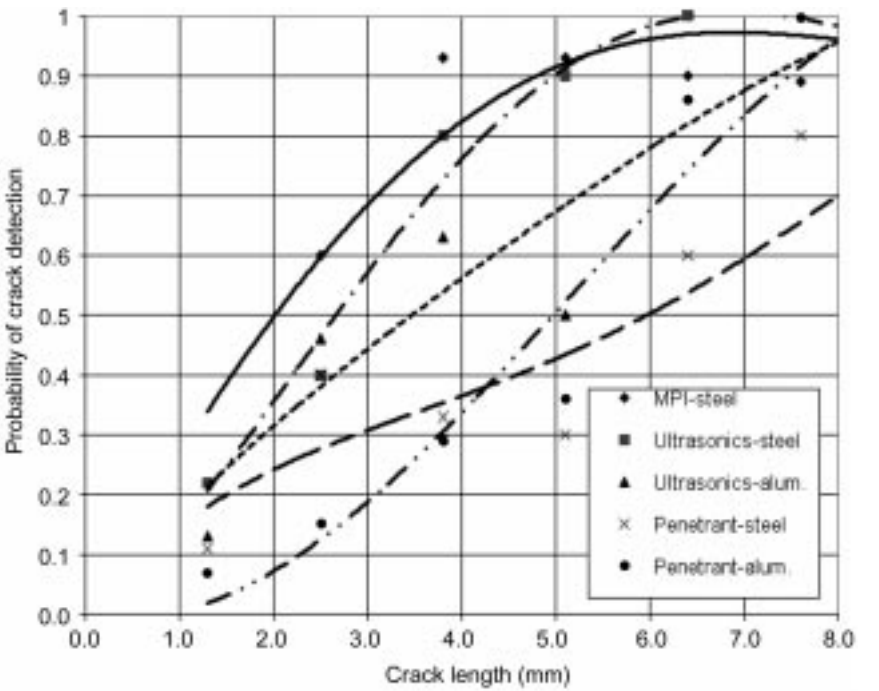
Any non-destructive testing (NDT) method consists of an inspection technique, equipment and a set of rules or inspection procedures for using the equipment. Appling a NDT technique should consider material characteristics,

© 2008 Woodhead Publishing Limited

types of defects, component configuration and surface condition, thickness, presence of abrupt geometrical changes, accessibility of critical regions, human factors including variation in inspector skill, interpretation of results, variation of calibration of equipment, variation between equipment, variations in inspection procedures and sequencing of operations, and different inspection environments including laboratory, factory and field and the corresponding required detection confidence level.

There are different inspection approaches (see Fig. 10.1). Visual inspection covers a wide field ranging from sophisticated monitoring systems to simple hand operations. Under most conditions visual inspection with either the unaided eye or magnifiers is the least expensive method available for detecting surface cracks in structural components. It can be used for all materials, but the results depend on surface and environmental conditions, as well as the skill of operators. To achieve higher sensitivity the surface coating including dirt, rust and paint should be removed.

The capability of an inspection technique can be described in terms of two aspects: sensitivity in detecting cracks, and accuracy in interpreting detected cracks. Both are uncertain aspects that depend on material characteristics, human factors and inspection environment.



10.1 Probability of detection using different inspection techniques.

© 2008 Woodhead Publishing Limited

Inspections are routinely made for structures in service and may result in the detection or non-detection of the cracks. For welded structures, cracks are generally assumed to be present after fabrication. Fatigue damage is expressed with a fatigue crack size that increases with time.

The purpose of periodic inspections is to detect fatigue cracks. It is assumed that if a fatigue crack is detected, it is repaired and its contribution to the midship section modulus is restored, thus increasing the reliability of the ship's structure.

The inspection quality depends on detection of the crack and crack size. In principle, each detection technique will have a limit size of detection, $a_{d,o}$, under which cracks cannot be detected.

The inspection procedure is not a deterministic one because of measuring inaccuracies and therefore the inspection capability may be described by the probability of detection:

$$P_{d,\mathrm{cr},i}(t) = 1 - \exp\left[-\frac{E[a_i(t)] - a_{d,o}}{\lambda_d}\right], \quad E[a_i(t)] > a_{d,o} \tag{10.59}$$

where $E[a_i(t)]$ is a mean value of crack size.

The inspection quality is characterised by the parameter λ_d which has values between zero and infinity. The smallest limit corresponds to a perfect inspection, and when $\lambda_d = \infty$ the structure has not been inspected.

It is assumed that all elements will be inspected every five years. For example, if a_d is a crack size with probability of detection $P_d(a_d)$ then every crack larger than a_d can be found. The elements with initiated cracks may be divided into three groups. The first group consists of elements with cracks not detected (with crack size less than $a_{d,o}$). The second group comprises elements with cracks that may be detected with crack size less than a_d. The probability of detection is less than $P_d(a_d)$ and the element with the crack is not repaired. The third group consists of elements with cracks detected (the crack is larger than a_d) and repaired. After repair, the crack size will be a_o, which is their initial size. It should be noticed that as the crack size is larger, the probability of its detection increases very much.

The average probability of detection of cracked elements is given as:

$$\bar{P}_{d,\mathrm{cr}}(t) = \frac{\sum_{i=1}^{n_{o,\mathrm{cr}}} P_{d,\mathrm{cr},i}(t)}{N_{\mathrm{tot}}} \tag{10.60}$$

where $n_{o,\mathrm{cr}}$ is the number of elements that have cracks larger than $a_{d,o}$. From the $n_{o,\mathrm{cr}}$ elements that have cracks larger than $a_{d,o}$ only $n_{d,\mathrm{cr}}$ will be detected, i.e.:

$$n_{d,\mathrm{cr}} = n_{d,o}\bar{P}_{d,\mathrm{cr}}(t) \tag{10.61}$$

The number of elements that will be repaired is $n_{d,\mathrm{cr}}$ because it is assumed that all detected elements will be repaired.

The probability of repair at time of inspection T_j is the ratio of the repaired elements by the total number of elements N_{tot}:

© 2008 Woodhead Publishing Limited

$$P_{r,\mathrm{cr}}(T_j) = \frac{n_{d,\mathrm{cr}}}{N_{\mathrm{tot}}} = \frac{n_{d,o}}{N_{\mathrm{tot}}}\,\bar{P}_{d,\mathrm{cr}}(T_j) \tag{10.62}$$

The state of the ship structure is 'as bad as old' because only $n_{d,\mathrm{cr}}$ of N_{tot} elements are replaced with new.

The reliability of the hull after repair will be smaller than the initial value for the new ship because it will contain some undetected cracks. After repair, cracks start to propagate again. This implies that the time-dependent reliability will still be applicable for the period after inspection. However, the time scale must be changed so that a new period starts after repair.

The reliability after the jth inspection at time T_j is the same as the reliability of the hull before repair at time $t_{\mathrm{e}j}$. Therefore, the reliability of the repaired hull for times larger than T_j is the same as the reliability of the unrepaired hull for times larger than $t_{\mathrm{e}j}$.

To assess the reliability of a hull girder after inspection, the repaired midship of section modulus will be denoted by $W_r(t_{\mathrm{e}})$, where t_{e} is the effective time that is related to the status of the midship section modulus without repair. This means that the more extensive the repairs are made the smaller t_{e} will be, i.e. the section modulus will be restored to a condition close to when it is defined. Until the time T_1 of the first inspection, $t_{\mathrm{e}} = t$:

$$W_r(t_{\mathrm{e}}) = W(t) \quad 0 \le t < T_1 \tag{10.63}$$

At the first repair, the midship section is restored to a situation that it had some years earlier. The effective age of the structure t_{e} will now be reduced according to the repair that was made. From then on $t_{\mathrm{e}} < t$ and the repaired midship section modulus decreases at a rate that depends on t_{e} instead of t, i.e.

$$W_r(t_{\mathrm{e}}) = W(t) \quad \text{for} \quad T_{j-1} \le t < T_j \tag{10.64}$$

where the effective time is given by:

$$t_{\mathrm{e}} = t - Tr_{j-1} \quad \text{and} \quad Tr_{j-1} = \sum_{k=1}^{j-1} \Delta T_k \tag{10.65}$$

where the T_j is the time of the jth inspection, and Tr_j is the total 'recovered' time that at the jth inspection has been accumulated due to all previous repairs. The repair at time T restored the structure to the condition ΔT_j years earlier, for example the first inspection $Tr_1 = \Delta T_1$, and if there is no repair then $\Delta T_1 = 0$.

The reliability for each period between inspections is a function of the effective time:

$$\begin{aligned} R(t) = {} & [1 - F_{T_i}(t - Tr_{j-1})]R_b(t - Tr_{j-1}) \\ & + [1 - P'_{d,\mathrm{cr}}(Tr_{j-1})] \int_0^{t-Tr_{j-1}} R_b(t_i)R_a(t - Tr_{j-1} - t_i) f_{T_i}(t_i)\mathrm{d}t_i \\ & \text{for} \quad T_{j-1} \le t < T_j \end{aligned} \tag{10.66}$$

© 2008 Woodhead Publishing Limited

where R_a and R_b are also functions of t_e. It is important to note that t_e is a discontinuous function of the real time t because at each inspection j, Tr_j changes its value and remains constant until the next repair.

The effect of each repair is represented by a value of ΔT_k determined by assessing the age of the structure that has a section modulus equal to the value that resulted from the repair. This value will represent the decrease of the effective age of the structure, and will update Tr_{j-1} as given by Eqn 10.65. This updated value is substituted in Eqn 10.66 and the reliability can be evaluated for the inspection cycle. In Eqn 10.66 the first term denotes the probability of non-failure when some cracks are not initiated in the service interval before $[T_{j-1}, T_j]$ and the second term denotes the probability of non-failure when some cracks are initiated in the service interval $[T_{j-1}, T_j]$.

The approach presented may be used for the solution of several problems based on the reliability of the ship structure. Different assumptions have been made in this formulation and it is important to verify how the results are sensitive to each of them.

10.7 Modelling corrosion inspection and reliability

The state of general corrosion in a panel is assessed by measuring the plate thickness at several points. There are two sources of uncertainty in this procedure. One results from the precision of the measuring instrument and the other from sampling variability. Measurements are made at a few points of a panel and they are considered to be representative of the thickness in the whole plate. The uncertainty of this method of detection is considered small and in this work it is assumed not to influence plate detection.

Inspections routinely made for structures in service may or may not uncover plate with a thickness smaller than the acceptable value, normally expressed as a fraction k of the as-built thickness:

$$s_i(t) \leq k s_{oi}, \quad k \leq 1.0 \tag{10.67}$$

The probability of detection of a corroded element may be approximated by the exponential distribution function:

$$P_{d,\mathrm{cor}}(t) = 1 - \exp\left(-\frac{\mathrm{d}s}{\lambda_s}\right), \quad t > t_0 \tag{10.68}$$

where the parameter λ_s is defined as:

$$\lambda_s = \frac{\mathrm{d}s_p}{\ln(1-p)} \quad \text{and} \quad \mathrm{d}s = 1 - \frac{s(t) - s_0}{s_0} \tag{10.69}$$

in which $\mathrm{d}s_p$ is the fraction of the as-built thickness associated with a probability of detection p.

It is assumed that all elements will be inspected every five years, which is the

© 2008 Woodhead Publishing Limited

present practice. It is further assumed that the method of inspection is such that all plates with thickness smaller than a limit value are detected. At the inspection, the detected plates will be replaced and after replacement their thickness will return to their original value s_{oi}.

The average probability of detection of the corroded elements in a ship section is given as:

$$P^t_{d,\mathrm{cor}}(t) = \frac{\sum_{j=1}^{n_2} P_{d,\mathrm{cor},j}(t)}{n_2} \tag{10.70}$$

where n_2 is the number of elements with corrosion.

To assess the reliability of the hull girder after inspection, the formulation developed for fatigue phenomena can also be applied here. The reliability is computed for each period between inspections by:

$$\begin{aligned} R(t) &= [1 - F_{T_o}(t - Tr_{j-1})]R_{b,\mathrm{cor}}(t - Tr_{j-1}) \\ &\quad + [1 - P^t_{d,\mathrm{cor}}(Tr_{j-1})] \int_0^{t-Tr_{j-1}} R_{b,\mathrm{cor}}(t_i) R_{a,\mathrm{cor}}(t - Tr_{j-1} - t_o) f_{T_i}(t_o) \mathrm{d}t_0 \\ &\quad \text{for} \quad T_{j-1} \le t < T_j \end{aligned} \tag{10.71}$$

where f_{t_o}, F_{t_o}, $R_{b,\mathrm{cor}}$ and $R_{a,\mathrm{cor}}$ are the probability density and cumulative functions of the time when the coating protection loses its effectiveness and thus corrosion starts, and the reliability before and after the start of corrosion respectively.

10.8 Time-dependent reliability of ship hull subjected to fatigue and corrosion failure

Applying the principles presented in previous chapters, the equations for reliability can be derived for fatigue and corrosion. Since the time to crack initiation and the life of the protective coating are random variables, the reliability is conditional on the probability of time to initiation of crack and corrosion, $R(T|t_i, t_o)$. Therefore, the unconditional reliability of a hull with cracks and corrosion is given by:

$$R(T) = \int_0^\infty \int_0^\infty R(T|t_i, t_o) f_{T_i}(t_i) f_{T_o}(t_o)\, \mathrm{d}t_i\, \mathrm{d}t_o \tag{10.72}$$

The total reliability $R(T)$ is given by the reliability of the hull without cracks and corrosion, which has a probability of $[1 - F_{T_i}(T)][1 - F_{T_o}(T)]$, plus the reliability of the hull under the condition that corrosion has occurred but no cracks, which has probability $[1 - F_{T_i}(T)]$, plus the reliability of the hull with cracks and without corrosion, with probability $[1 - F_{T_o}(T)]$, plus the reliability of the hull with cracks and corrosion. Thus the final expression is given by:

© 2008 Woodhead Publishing Limited

$$R(T) = R_1(T) + R_2(T) + R_3(T) + R_4(T) \tag{10.73}$$

where the components which are included in the above equations are written as:

$$R_1(T) = [1 - F_{T_i}(T)][1 - F_{T_o}(T)]R_{b,i,o}(T) \tag{10.74}$$

$$R_2(T) = [1 - F_{T_i}(T)] \int_0^T R_{b,i,o}(t_o) R_{b,i;a,o}(T - t_o) f_{T_o}(t_o) \mathrm{d}t_o \tag{10.75}$$

$$R_3(T) = \int_0^T R_{b,i,o}(t_i) R_{a,i;b,o}(T - t_i) f_{T_i}(t_i) \mathrm{d}t_i [1 - F_{T_o}(T)] \tag{10.76}$$

$$R_4(T) = \int_0^T f_{T_i}(t_i) \int_0^T R_{b,i,o}(t_o|t_i) R_{a,i,o}(T - t_o|t_i) f_{T_o}(t_o) \mathrm{d}t_o \, \mathrm{d}t_i \tag{10.77}$$

in which subscripts *a, b, i* and *o* represent reliability before and after, time to crack initiation and coating life respectively.

Since the time to crack initiation and the coating lifetime are independent random variables, then:

$$R_4(T) = \int_0^T R_{b,i,o}(t_i) R_{a,i,o}(T - t_i) f_{T_i}(t_i) \mathrm{d}t_i \int_0^T R_{b,i,o}(t_o) R_{a,i,o}(T - t_o) f_{T_o}(t_o) \, \mathrm{d}t_o \tag{10.78}$$

Inspections are routinely made for structures in service and may result in the detection or non-detection of cracks or corrosion thickness less than a certain value. The size of a detected crack is measured by a non-destructive method. For welded structures, cracks are generally assumed to be present after fabrication. Fatigue damage is expressed in terms of fatigue crack size that increases with time.

One of the purposes of periodic inspections is to detect fatigue cracks. It is assumed that if a fatigue crack is detected, it is repaired and its contribution to the midship section modulus is restored, thus increasing the reliability of the ship's structure. The full discussion for the two methods of detection has already been given by Guedes Soares and Garbatov (1997).

Combining repairs of both cracks and corrosion, four hypotheses may be formulated for the repair status of the structure: H_0 (without repair of cracks and corrosion), H_1 (repair only because of corrosion), H_2 (repair only because of cracks) and H_3 (repair due to both).

The probabilities of repair in the case of corrosion and cracks are already formulated. Applying those definitions, the probabilities of the different hypotheses are written as:

$$P(H_0) = [1 - P_{r,\mathrm{cr}}(T_j)][1 - P_{r,\mathrm{cor}}(T_j)] \tag{10.79}$$

$$P(H_1) = P_{r,\mathrm{cr}}(T_j)[1 - P_{r,\mathrm{cor}}(T_j)] \tag{10.80}$$

© 2008 Woodhead Publishing Limited

$$P(H_2) = [1 - P_{r,\mathrm{cr}}(T_j)]P_{r,\mathrm{cor}}(T_j) \tag{10.81}$$

$$P(H_3) = P_{r,\mathrm{cr}}(T_j)P_{r,\mathrm{cor}}(T_j) \tag{10.82}$$

Repair r would be successful in the case when:

$$\{P(r|H_1) \cup P(r|H_2) \cup P(r|H_3) = 1\} \cap \{P(r|H_0) = 0\} \tag{10.83}$$

The probability of every event may be presented by applying the conditional probabilities:

$$P(H_i|r) = \frac{P(H_i)P(r|H_i)}{\sum_{i=1}^{3} P(H_i)P(r|H_i)} \tag{10.84}$$

The probability of repair of cracks or corrosion may be obtained taking into account the total probability expression:

$$P(r) = \sum_{i=1}^{3} P(H_i)P(r|H_i) \tag{10.85}$$

After substituting Eqns 10.80–10.82 into Eqn 10.85, finally the total probability of repair is written as:

$$P_r(T_j) = P_{r,\mathrm{cr}}(T_j)[1 - P_{r,\mathrm{cor}}(T_j)] + [1 - P_{r,\mathrm{cr}}(T_j)]P_{r,\mathrm{cor}}(T_j) + P_{r,\mathrm{cr}}(T_j)P_{r,\mathrm{cor}}(T_j) \tag{10.86}$$

The reliability for each period between inspections is a function of the effective time:

$$\begin{aligned} R(t) = {} & R_1(t - Tr_{j-1}) + R_2(t - Tr_{j-1})[1 - P_{r,\mathrm{cor}}(T_{j-1})] \\ & + R_3(t - Tr_{j-1})[1 - P_{r,\mathrm{cr}}(T_{j-1})] + R_4(t - Tr_{j-1})[1 - P_r(T_{j-1})] \\ & \text{for} \quad T_{j-1} \le t < T_j \end{aligned} \tag{10.87}$$

The approach presented may be used for the solution of several problems based on the reliability of the ship structure (Guedes Soares and Garbatov, 1997).

10.9 Numerical example

The approaches reviewed here have been applied to the reliability assessment of a tanker with the following characteristics: length $L = 236$ m, breadth $B = 42$ m, depth $D = 19.2$ m, and block coefficient $C_b = 0.805$. The mean and standard deviation of yield stress are considered to be $E[\sigma_y] = 315$ MPa and $\sigma_{\sigma_y} = 31$ MPa respectively. The mean and standard deviation of the still-water bending moment are $E(M_{\mathrm{SW}}) = 584$ MN.m and $\sigma_{M_{\mathrm{SW}}} = 109$ MN.m.

The mean value and standard deviation of the initial crack sizes are considered to be $E(a_o) = 1.5$ mm and $\sigma_{a_o} = 0.15$ mm respectively. The material parameter m is 3, the mean value of C is $E(C) = 1.7\mathrm{E}{-11}$ and the standard

© 2008 Woodhead Publishing Limited

deviation is $\sigma_C = 1.8\text{E}{-12}$. The limit value of a detectable crack size $a_d = 0.15\,\text{m}$ and the detected crack size with probability 0.999 is $a_{d,0.999} = 0.3\,\text{m}$, which are in agreement with the data from visual observation presented by Packman *et al.* (1969). The limit of detectable corrosion thickness is $t_d = 0.75 t_{\text{nom}}$, of the nominal thickness (as-built) t_{nom}. The corrosion rate is considered invariant but uncertain in the example here, although the formulation could account for a time-varying corrosion rate. The covariance of corrosion rate is taken as $\text{COV}_{\text{cor}} = 0.1$. In fact, the coefficient of variation of the corrosion rate varies in time, and Loseth *et al.* (1994) showed that it may have a value from 10% in the 10th year to 63% in the 20th year of the service life of the ship. The parameters of the probability distribution of the coating life are considered to be $\alpha_{t_o} = 2$ and $\beta_{t_o} = 4.2$ years.

The parameters of the probability density function of the time to crack initiation are taken as suggested by Guedes Soares and Garbatov (1996a) as $\alpha_{t_i} = 1.8$ and $\beta_{t_i} = 13$ years. The time to crack propagation is calculated based on the assumption that the critical crack size is 95% of the plate breadth or stiffener height. In fact this value depends on several parameters and will be different for the various hull elements. However, studying the exact value of the critical crack size of each element is not the main objective of the method presented here. The allowable stress is taken as 85% of the yield stress of the material. The inspections are made every five years. The mean long-term period of the wave-induced bending moment, $T_m = 9.4$ s, is calculated by an equation given by Bach-Gansmo *et al.* (1987).

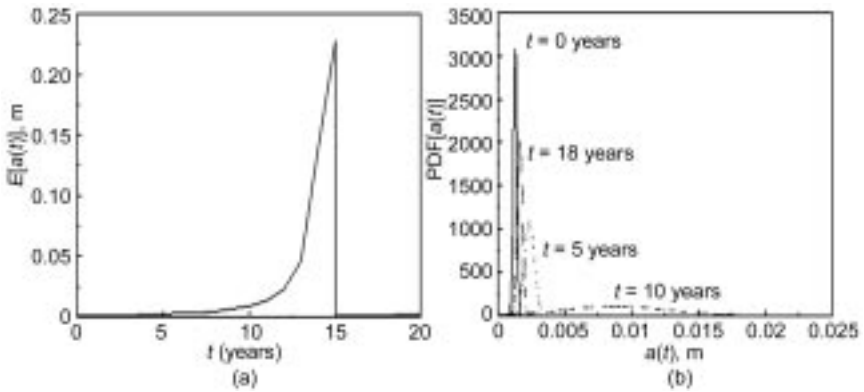
The method aims at deciding when to perform inspections in view of the overall state of the cracks and corroded plates or qualifying the structural reliability of the overall structure given the inspection interval. The elements at the ship side will be subjected to global loading resulting from vertical and horizontal bending moments and local lateral pressure.

The crack size is assumed to have a truncated normal distribution. This implies that this distribution will be changing in time, which reflects the increase in the mean and standard deviation that starts being noticeable at 12 years and increases extremely rapidly from 15 years. The normal distribution of crack size is truncated at $a = 0$ in order to avoid negative crack sizes. Alternatively, a log-normal distribution could be adopted.

Figure 10.2(a) shows the mean value of the crack size including the effect of a repair action at $t = 15$ years. The crack size is assumed to be a normal distribution function with a mean value and standard deviation governed by those parameters.

Applying Eqns 10.19 and 10.20, the calculated time variation of the mean section modulus and its standard deviation are shown in Fig. 10.2(b); at each time instant they define a normal distribution function. However, it should be pointed out that in some cases, depending on the information input about the quality of the manufacturing process, deterioration, inspection intervals and

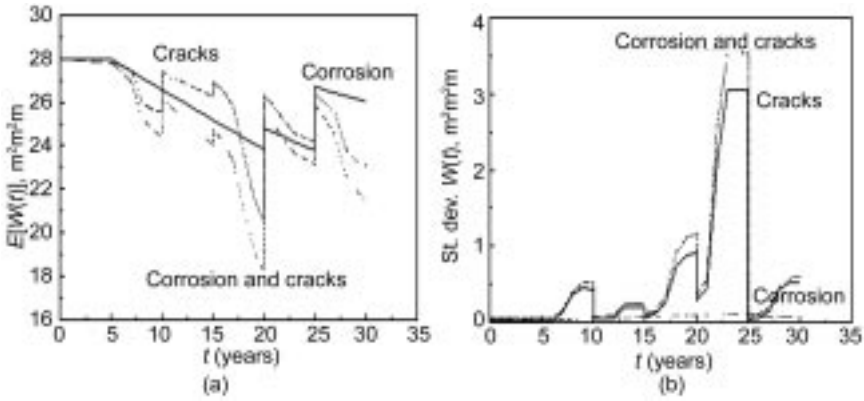
© 2008 Woodhead Publishing Limited



10.2 (a) Mean value and (b) probability density function of crack size as a function of time, including a repair at $t = 15$ years (only vertical bending loading).

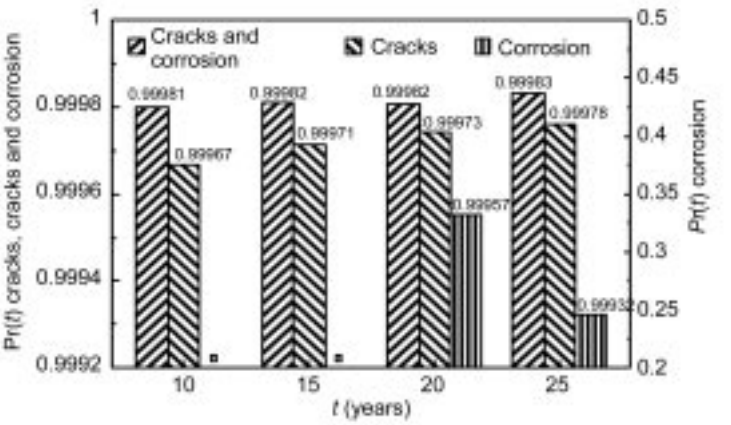
tools for inspection, the midship section modulus may be reduced by more than 75% with respect to as-built. To avoid such a situation, special inspection policies and improvement of repairs should be induced (see Fig. 10.3).

Figure 10.4 shows that during the 10th year, most of the cracks in the deck and bottom will be reaching the lower limit of detection, and because of this the probability of repair shows a marked peak. From then on, the increase is at a much smaller rate, and at 15 years the number of elements with crack size larger than the lower limit of detection is not much greater than at 10 years and also depends on the inspection policies. The probability of repair of corroded plates appears at the 25th year after the first inspection with restoring actions (only the corrosion phenomenon) and drops because a large number of elements were replaced and the process of corrosion initiation restarts from the beginning. The case of 'cracks and corrosion' in Fig. 10.4 demonstrates the combined effect of



10.3 (a) Mean value and (b) standard deviation of the midship section modulus as a function of time (only vertical bending loading).

© 2008 Woodhead Publishing Limited

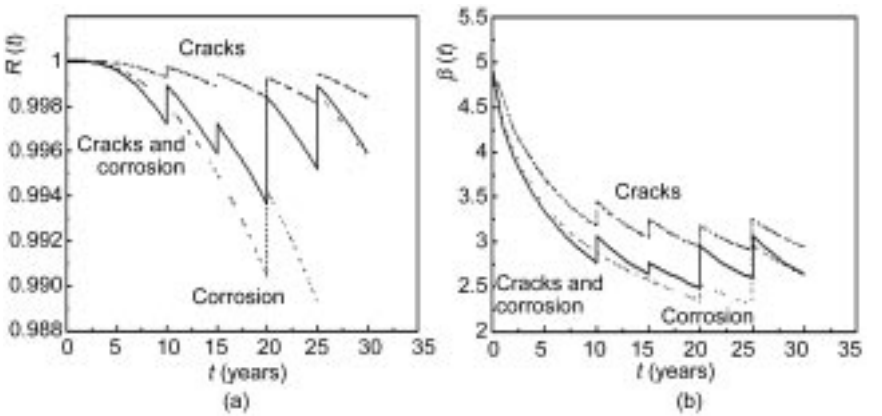


10.4 Probability of detection as a function of inspection time (only vertical bending loading).

repair in the presence of corrosion and cracks that contributes to a larger total probability of repair. The probability of repair reflects directly the reliability during the next interval before the next inspection.

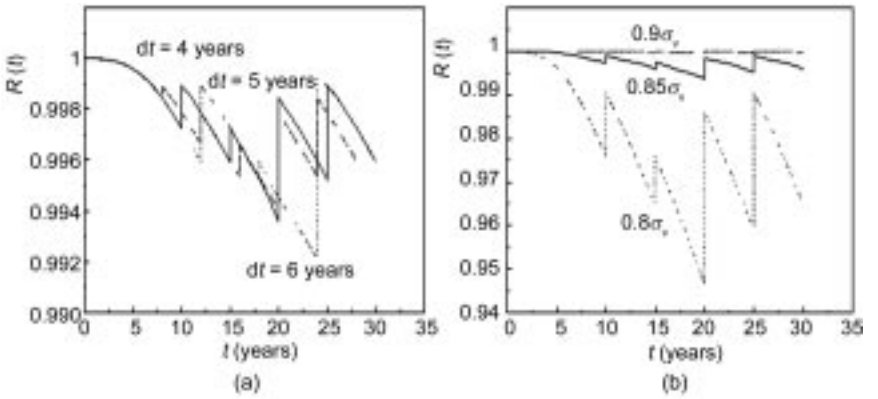
The method presented here has been applied to predict the reliability of a tanker. The results of the calculations are shown in Fig. 10.5(a) and the corresponding reliability beta index is taken in Fig. 10.5(b), which is preferred by some authors. These results show very distinct differences between predictions of the reliability resulting from the consideration of both cracks and corrosion and predictions when only one effect is accounted for.

The formulation just presented can be used to assess the effect of different parameters on the reliability. The typical interval between inspections in



10.5 (a) Reliability and (b) beta index as a function of time (only vertical bending loading).

© 2008 Woodhead Publishing Limited

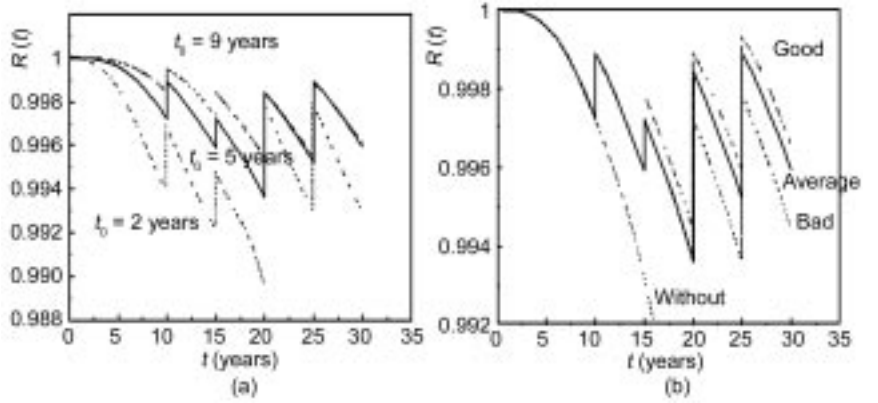


10.6 Influence of (a) the different time interval for inspection and (b) the allowable stress on the reliability function (only vertical bending loading).

shipbuilding is five years. Decreasing the time interval will have less effect on the reliability than if the time interval is allowed to become longer. This can be seen clearly in the results of the calculations shown in Fig. 10.6(a) for inspection intervals of four, five and six years.

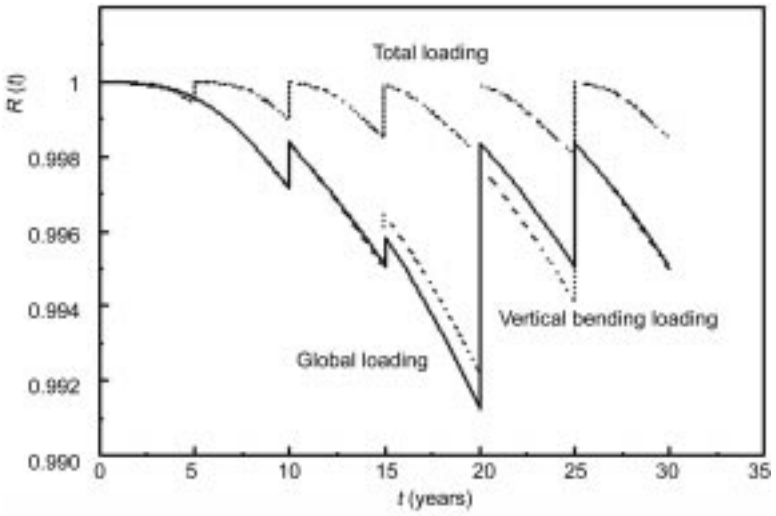
The effect of using different allowable stress levels is shown in Fig. 10.6(b) for reference values of 0.8, 0.85 and 0.9 of the yield stress of the material. It is quite clear that allowable stresses have a significant influence on the reliability, directly influencing the upcrossing limit state for which the structure will be accounted.

Another important aspect with respect to corrosion is the coating lifetime. Increasing the coating life will increase the reliability. This can be seen in the result of the calculation shown in Fig. 10.7(a) for coating lifetimes of two, five and nine years. It is interesting to note that a higher coating life leads to a higher reliability



10.7 Influence of (a) the coating time and (b) the inspection policy on the reliability function.

© 2008 Woodhead Publishing Limited



10.8 Influence of the loading on the reliability function.

level, since general corrosion will occur after a longer time interval and decrease of the net section of the midship will be delayed. The variation of this parameter shows that the coating life has a significant effect on the reliability.

Four different inspection policies were created for comparative analysis. They reflect good, average, bad and no-maintenance actions. A graphical illustration of reliability is shown in Fig. 10.7(b). Different characteristics of inspection policies keep reliability on different levels. It can be seen that the effect of different maintenance actions appears at just 15 years, during the second inspection. The inspections at 20 and 25 years show clearly that applying bad maintenance or none at all results in low reliability levels (see Fig. 10.8).

The formulation already presented was also applied to the same tanker but with combined loading. The combined loading includes the stresses from vertical and horizontal bending wave-induced moment and seawater-induced pressure and cargo loading. The full discussion of the correlation between different loadings and their final composition has already been presented by Garbatov and Guedes Soares (1998). It is assumed that this tanker is fully loaded with a full central tank and empty ballast tanks in the area of the midship.

The calculated reliability considering each load component and their combination is shown in Fig. 10.8. It can be seen that applying global loading becomes more destructive and leads to more frequent repairs.

10.10 Discussion and conclusions

A time-variant formulation for the reliability of a ship hull was presented taking into account the degrading effects of crack growth and corrosion and the

© 2008 Woodhead Publishing Limited

improvements obtained by repair operations. The midship section modulus is described by a time-dependent process including the effect of crack propagation and corrosion.

Different assumptions were made about loading and material properties that are not essential to the method but are needed for the example calculation of the tanker that was also presented.

The effects of different variables on the reliability of the ship hull are easily determined with this formulation. The significant effects on the inspection interval, allowable bending stress and coating time have been demonstrated also. The average probability of detection during inspection was taken into account.

The effect of different loading results in a different distribution of the relative rate of replacements around the net section. It is shown that applying the total loading, which includes the global loading governed by vertical and horizontal bending moments and the local loading caused by external seawater loading and internal cargo loading, the maximum replacement rate of structural elements is incurred around the waterline for the side shell and in the corners formed by the longitudinal bulkhead and deck and bottom.

Applying the presented formulation for the reliability assessment leads to a solution to manage ship inspections and repair activities that will improve the control of the technical condition of the ship hull. However, to achieve these objectives accurate information about loading conditions, deterioration processes and inspection methodology should be given.

It has been recognised that for practical application of fatigue analysis of ship structures there is still a need for development of realistic load models in terms of magnitude, expected number of cycles and frequency content, including combinations of different loading sources that account for dynamic effects. The methods for stress determination based on the nominal stress approach, local stress or stress intensities in the case of fracture mechanics also need to be improved.

Greater emphasis should be given to structural monitoring systems to create an improved database of structural information, to provide increased safeguards against sudden structural failure and to obtain useful design feedback and condition maintenance assessment. Such data should be stored in an appropriate information database and be made available to be used to optimise maintenance over the structural life of the ship.

It is also necessary to identify the variation of material parameters as a function of temperature and stress field patterns as well as appropriate test methods for their quantification.

10.11 Acknowledgements

This work has been performed within the project ‘MARSTRUCT – Network of Excellence on Marine Structures’ (http://www.mar.ist.utl.pt/marstruct/) and has

© 2008 Woodhead Publishing Limited

been partially funded by the European Union through the Growth programme under contract TNE3-CT-2003-506141.

10.12 References

Abrahamsen, E., 1962, Structural safety of ships and risks to human life, *European Shipbuilding*, Vol. 11, pp. 134–146.

Abrahamsen, E., Nordenstrom, N. and Roren, E., 1970, Design and reliability of ship structures, *Proceedings Spring Meeting*, SNAME.

Akita, Y., 1988, Reliability and damage of ship structures, *Marine Structures*, Vol. 1, pp. 89–114.

Akita, Y., Yamaguchi, I., Nitta, A. and Arai, H., 1976, Design procedure based on reliability analysis of ship structures, *J. Soc. Nav. Arch. Japan*, Vol. 140.

Antoniou, A. C., 1977, Survey on cracks in tankers under repair, *Proceedings of the International Symposium on Practical Design in Shipbuilding (PRADŚ77)*, Tokyo, pp. 143–150.

Bach-Gansmo, O., Carlsen, C. A. and Moan, T., 1987, Fatigue assessment of hull girder for ship type floating production vessels, *Proceedings of the Mobile Offshore Structure*, Elsevier Science, pp. 297–319.

Benjamin, J. and Cornell, C., 1970, *Probability, Statistics and Decision for Civil Engineers*, McGraw-Hill, New York.

Bonello, M. and Chryssantoloulos, M., 1993, Buckling analysis of plated structures using reliability concept, *Proceedings of the 12th International Conference on Offshore Mechanics and Arctic Engineering (OMAE)*, New York, ASME, Vol. II, pp. 313–321.

Bruce, G., Duan, M., Egorov, G., Folso, R., Fujimoto, Y., Garbatov, Y., Le Hire, J.-C. and Shin, B.-C., 2003, Inspection and monitoring, *Proceedings of the 15th International Ship and Offshore Structures Congress, Committee VI.2*, A. Mansour and R. Ertekin, editors, Elsevier, Vol. 2, pp. 37–69.

Caldwell, J. B., 1965, Ultimate longitudinal strength, *Transactions of the Royal Institution of Naval Architects (RINA)*, Vol. 107, pp. 411–430.

Cornell, C. A., 1969, A probability based structural code, *American Concrete Institute Journal*, Vol. 66, pp. 974–985.

Faulkner, D. and Sadden, J., 1979, Toward a unified approach to ship structural safety, *Transactions of the Royal Institution of Naval Architects (RINA)*, Vol. 121, pp. 1–38.

Ferro, G. and Cervetto, D., 1984, Hull girder reliability, *Proceedings of the Ship Structural Symposium (SNAME)*, New York, pp. 89–110.

Fricke, W. and Petershagen, H., 1992, Detail design of welded ship structures based on hot-spot stresses, *Proceedings of the Practical Design of Ships and Mobile Units*, J. B. Caldwell and G. Ward, editors, Elsevier Science, Vol. 2, pp. 1087–1100.

Fujita, M., Schall, G. and Rackwitz, R., 1989, Adaptive reliability-based inspection strategies for structures subject to fatigue, *Proceedings of the International Conference on Structural Safety and Reliability (ICOSSAR)*, A. H.-S. Ang, M. Shinozuka and G. I. Schueller, editors, San Francisco, American Society of Civil Engineers, Vol. 2, pp. 1619–1626.

Garbatov, Y. and Guedes Soares, C., 1998, Fatigue reliability of maintained welded joints in the side shell of tankers, *Journal of Offshore Mechanics and Arctic Engineering*, Vol. 120, pp. 2–9.

© 2008 Woodhead Publishing Limited

Garbatov, Y. and Guedes Soares, C., 2001, Cost and reliability based strategies for maintenance planning of floating structures, *Reliability Engineering and System Safety*, Vol. 73, pp. 293–301.

Garbatov, Y. and Guedes Soares, C., 2002, Bayesian updating in the reliability assessment of maintained floating structures, *Journal of Offshore Mechanics and Arctic Engineering*, New York, ASME, Vol. 124, pp. 139–145.

Garbatov, Y., Rudan, S. and Guedes Soares, C., 2004, Assessment of geometry correction functions of tanker knuckle details based on fatigue tests and finite-element analysis, *Journal of Offshore Mechanics and Arctic Engineering*, Vol. 126(1), pp. 139–145.

Goodman, J. and Mowatt, G., 1997, Application of strength research to ship design, *Steel Plated Structures*, Crosby Lockwood Staples, London, pp. 676–712.

Guedes Soares, C. and Garbatov, Y., 1996a, Fatigue reliability of the ship hull girder, *Marine Structures*, Vol. 9, pp. 495–516.

Guedes Soares, C. and Garbatov, Y., 1996b, Fatigue reliability of the ship hull girder accounting for inspection and repair, *Reliability Engineering and System Safety*, Vol. 51, pp. 341–351.

Guedes Soares, C. and Garbatov, Y., 1996c, Fatigue reliability of the ship hull girder, *Marine Structures*, Vol. 9, pp. 495–516.

Guedes Soares, C. and Garbatov, Y., 1996d, Influence of inspection and repair on the fatigue reliability of oil tankers, *Proceedings of the 15th International Conference on Offshore Mechanics and Arctic Engineering (OMAÉ96)*, New York, ASME, Vol. II, pp. 245–254.

Guedes Soares, C. and Garbatov, Y., 1997, Reliability assessment of maintained ship hull with correlated corroded elements, *Marine Structures*, Vol. 10, pp. 629–653.

Guedes Soares, C. and Garbatov, Y., 1998, Reliability of maintained ship hull subjected to corrosion and fatigue, *Structural Safety*, Vol. 20, pp. 201–219.

Guedes Soares, C. and Garbatov, Y., 1999, Reliability of maintained, corrosion protected plate subjected to non-linear corrosion and compressive loads, *Marine Structures*, Vol. 12, pp. 425–445.

Hart, D., Rutherford, S. and Wichham, A., 1986, Structural reliability analysis of stiffened panels, *Transactions of the Royal Institution of Naval Architects (RINA)*, Vol. 128, pp. 293–310.

Janssen, G., 2000, Fatigue based design rules for the application of high tensile steel in ships, *Proceedings of the Seventh International Marine Design Conference*, Kyongju, Korea, pp. 317–328.

Loseth, R., Sekkesaeter, G. and Valsgard, S., 1994, Economics of high-tensile steel in ship hulls, *Marine Structures*, Vol. 7, pp. 31–50.

Madsen, H., Krenk, S. and Lind, N., 1986, *Methods of Structural Safety*, Prentice-Hall, Englewood Cliffs, NJ.

Mansour, A., 1972, Probabilistic design in ship structural safety and reliability, *Transactions of the Society of Naval Architects and Marine Engineers (SNAME)*, New York, Vol. 80, pp. 64–97.

Mansour, A., 1974, Approximate probabilistic method of calculating ship longitudinal strength, *Journal of Ship Research*, Vol. 18, pp. 203–213.

Mansour, A. and Faulkner, D., 1973, On applying the statistical approach to extreme sea loads and ship hull strength, *Transactions of the Royal Institution of Naval Architects (RINA)*, Vol. 115, pp. 277–314.

Melchers, R., 1998, Probabilistic modelling of immersion marine corrosion, *Structural Safety and Reliability (ICOSSAŔ98)*, N. Shiraishi, M. Shinozuka and Y. K. Wen,

© 2008 Woodhead Publishing Limited

editors, Balkema, Leiden, The Netherlands, pp. 1143–1149.
Melchers, R., 2003a, Probabilistic models for corrosion in structural reliability assessment. Part 1: Empirical models, *Journal of Offshore Mechanics and Arctic Engineering*, Vol. 125, pp. 264–271.
Melchers, R., 2003b, Probabilistic models for corrosion in structural reliability assessment. Part 2: Models based on mechanics, *Journal of Offshore Mechanics and Arctic Engineering*, Vol. 125, pp. 272–280.
Murotsu, Y., Okada, H., Hibi, S., Niho, O. and Kaminaga, H., 1995, A system for collapse and reliability analysis of ship hull structures using a spatial plate element model, *Marine Structures*, Vol. 8, pp. 133–149.
Nathwani, J., Lind, N. and Pandey, M., 1997, *Affortable Safety by Choice: the Life Quality Method*, Institute for Risk Research, University of Waterloo, Waterloo, Ontario.
Nordenstrom, N., 1971, 'Methods for predicting long-term distributions of wave loads and probability of failure for ships', Report No. 71-2-S, Det Norske Veritas, Oslo.
Okada, H., 1996, A method for reliability-based sensitivity analysis of ship's hull structures using combined plate and frame structure models, *Proceedings of the I5th International Conference on Offshore Mechanics and Arctic Engineering (OMAE)*, ASME, Vol. II, pp. 235–243.
Ostergaard, C. and Rabien, U., 1981, Reliability techniques for ship design (in German), *Trans. Schiffbau Tech. Gesellsch.*, Vol. 75, pp. 303–339.
Packman, P. F., Pearson, H. S., Owens, J. S. and Young, G., 1969, Definition of fatigue cracks through non-destructive testing, *Journal of Materials*, Vol. 4, pp. 666–700.
Paik, J., Lee, J., Hwang, J. and Park, Y., 2003a, A time-dependent corrosion wastage model for the structures of single and double hull tankers and FSOs, *Marine Technology*, Vol. 40, pp. 201–217.
Paik, J., Wang, G., Thayamballi, A., Lee, J. and Park, Y., 2003b, Time-dependent risk assessment of ageing ships accounting for general/pit corrosion, fatigue cracking and local dent damage, *SNAME 2003 Annual Meeting*, San Francisco, Vol. 111, pp. 159–197.
Paik, J., Brennan, F., Carlsen, C., Daley, C., Garbatov, Y., Ivanov, L., Rizzo, C., Simonsen, B., Yamamoto, N. and Zhuang, H., 2006, Condition assessment of aged ships, *Proceedings of the 16th International Ship and Offshore Structures Congress, Committee V.6*, P. Frieze and R. Shenoi, editors, University of Southampton, Vol. 2, pp. 255–306.
Planeix, J., Raynaud, J. and Huther, M., 1977, New outlooks for guardians of safety – Explicit versus implicit risk analysis in classification certification, *Symposium of Safety at Sea, RINA*, pp. 71–82.
Rackwitz, R., 2000, Optimization – the basis for code-making and reliability verification, *Journal of Structural Safety*, Vol. 22(1), pp. 27–60.
Raiffa, H. and Schaifer, R., 1982, *Applied Statistical Decision Theory*, Harvard University Press, Boston, MA.
Skjong, R., 1985, Reliability based optimization of inspection strategies, *Proceedings of ICOSSAR 85*, Vol. 3, pp. 614–618.
Stiansen, S., Mansour, A., Jan, H. and Thayamballi, A., 1980, Reliability methods in ship structures, *Trans. RINA*, Vol. 122, pp. 381–397.
Yamamoto, N. and Ikagaki, K., 1998, A study on the degradation of coating and corrosion on ship's hull based on the probabilistic approach, *Journal of Offshore Mechanics and Arctic Engineering*, Vol. 120, pp. 121–128.

© 2008 Woodhead Publishing Limited

11

Reliability of aged offshore structures

T MOAN, Norwegian University of Science and Technology (NTNU), Norway

Abstract: This chapter deals with methods for reliability analysis of offshore structures subjected to strength degradation due to crack growth and corrosion. It is shown how the effect of inspection and repair on the reliability level can be accounted for. Methods for reliability assessment of both component and simple systems are considered. Moreover, it is discussed how this methodology can be applied in making decisions about design as well as inspection and repair.

Key words: offshore steel structures, reliability updating, fatigue and corrosion, life cycle decision making.

11.1 Introduction

In general, adequate structural safety is ensured by proper design, fabrication and operational criteria as well as inspection and monitoring and possible repair during fabrication and the service life of 20 to 40 years. Modern design codes of structures include dimensioning (design) checks based on calculated effects due to different types of loads and the resistance, corresponding to different failure modes. Separate sets of calculations are required to check that the structure will not attain each limit state for each structural component. Limit state criteria are classified in two groups, namely serviceability and safety requirements (ISO 19900, 1994; ISO 2394, 1998; NORSOK N-004, 1998; NORSOK N-001, 2002). Serviceability requirements refer to motions, deformations, vibrations etc. that can hamper the operation, but do not represent a threat to the safety. Safety means the absence of failures and damage and is ensured by fulfilling requirements to overall stability and ultimate strength and fatigue failure under repetitive loading to avoid ultimate consequences such as fatalities, environmental damage or property damage. The corresponding criteria are defined by limit states for ultimate failure and fatigue, respectively. In addition to the limit states mentioned above, modern codes for offshore structures include so-called Accidental collapse Limit State (ALS), addressing the survivability of the structures as a whole after accidental damage due to, e.g., fires, explosions or ship collisions. While strength degradation due to crack growth is explicitly designed for, corrosion is not expressed by a separate limit state but affects the ultimate and fatigue failure limit states.

© 2008 Woodhead Publishing Limited

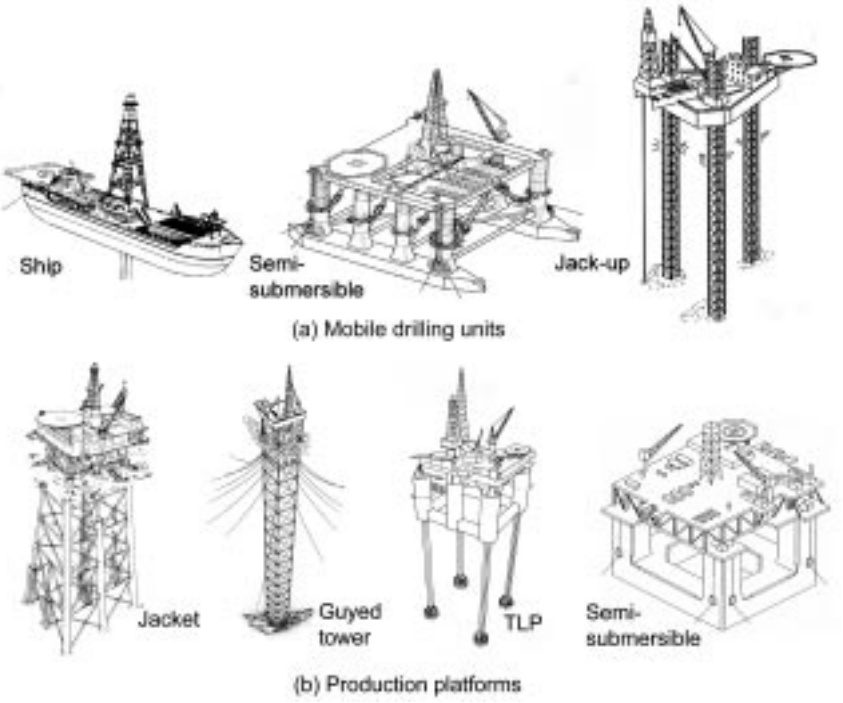
As mentioned above, adequate safety is ensured by proper actions during design, fabrication and operation. During design scantlings, with possible corrosion allowance, corrosion protection system and inspection plan, are decided. During fabrication, compliance (with maximum allowable geometrical tolerances and weld defects) is ensured by inspection to identify possible repairs. During operation inspection to detect cracks and corrosion, and remedial repair or replacement of possible degradation damage, are essential. Since the damage needs to be of a certain size to be detected and takes some time to repair, effective inspection and repair requires a certain damage tolerance. This implies that there is an interrelation between design criteria (fatigue life, damage tolerance) and the inspection and repair criteria.

It is often found more economical to use existing rather than new structures. Hence, there might be a need to reassess existing offshore structures during operation, for instance, because of a planned change of function or occurrence of damage or a need to extend service life; see ISO 2394, ISO 19900, Dunlap and Ibbs (1994) and Moan (2000). A majority of the 5000 fixed offshore production platforms in the world have been operated for longer than the initially planned service life of 20 years. About 40% of mobile drilling platforms have exceeded their planned service life. Since structural modifications to maintain an acceptable safety level are much more expensive for existing structures than during the initial fabrication, other strategies to achieve the necessary safety for existing structures are pursued. For instance, the information about material and geometrical properties that can be collected during fabrication and the information about structural response that can be recorded during operation imply modified estimates of possible bias and random uncertainties in predicted resistance and load effects. Hence smaller safety margins than those used at the design stage can be demonstrated to be acceptable. Since many conventional design methods are simple and conservative, use of more refined analysis methods for loads, load effects and strength than those used in initial design is another strategy to document adequate safety for existing structures (Moan, 2000).

The risk associated with cracks depends on how fast they develop to failure of a component (say, a brace) and the residual system strength after failure. Welded joints in ship hulls and jackets represent extreme cases. Ships are monocoque structures where the cracks in the hull plating grow until fracture of the hull. In particular there is a residual life between a through-thickness crack (TTC) and final fracture (e.g. Bin and Moan, 2005). After fatigue failure in tubular joints in jackets, residual ultimate strength is normally available. Moreover, there is residual fatigue life after through-thickness cracks (which typically defines the failure criterion for S-N curves which are used in fatigue design) in most types of joints.

The offshore industry (see Fig. 11.1) early recognized that loads and their effects as well as the resistance are subjected to uncertainties. Since about 1970

© 2008 Woodhead Publishing Limited



11.1 Selected offshore platforms: (a) mobile drilling units; (b) production platforms.

this industry, therefore, has been concerned with a rationalization of safety measures through application of risk and reliability methods. Initial efforts were focused upon establishing risk-based storm load criteria (e.g. Marshall, 1969), but also application of structural reliability to calibrate ULS code requirements (Fjeld, 1977; Moses, 1987; Lloyd and Karsan, 1988) to develop a reliability-based load and resistance factor design code for fixed platforms is noted. In certain situations when a new design falls outside the scope of existing codes, reliability analysis has been applied ad-hoc to establish design criteria. This was the case when the first offshore production ship was designed some years ago (Moan, 1988). An evaluation of previous efforts on calibration of offshore codes was provided by Moan (1995) in conjunction with the ISO effort to harmonize codes for offshore structures (ISO 19900, 1994).

The uncertainties associated with the basic load effects and resistances are amplified by the significant scatter in the degradation processes and inspection approaches. Reliability methods are hence crucial to support decision making regarding safety and economy relating to design and inspection criteria. Such Bayesian reliability methods have been developed for offshore structures in the last two decades, partly by implementing approaches applied in the aeronautical industries (e.g. Shinozuka and Deodatis, 1989; Yang, 1994) and partly by novel

© 2008 Woodhead Publishing Limited

approaches (e.g. Madsen *et al.*, 1987; Jiao and Moan, 1990). Reliability-based fatigue codes have also developed. The code calibrations described above all refer to ultimate strength criteria. Because fatigue in offshore structures is mainly caused by one type of loading, there is limited merit in calibrating fatigue criteria in the same sense as ULS criteria are calibrated to yield the same safety level for different load combinations. However, to achieve consistent design and inspection criteria, fatigue design criteria should be calibrated to reflect the consequences of failure and inspection plan. Moan (1994) showed how the allowable cumulative fatigue damage in design can be relaxed when inspection is carried out.

This calibration of fatigue criteria and corrosion allowance is done on a generic basis to achieve a balance between the desired lifetime safety and economy, based on the data available at the design stage. It is important that information obtained, e.g., by inspections during operation is used and the inspection plan is updated accordingly for each individual structure. By, for instance, ensuring that the characteristic fatigue life is at least 20 years (i.e. mean life is about 60 years) fatigue cracks will develop slowly, so there would normally be ample time to detect and remedy them during operation. Similarly, adequate design would normally also ensure that corrosion would develop relatively slowly and become a safety problem only in case of lack of follow-up.

Structural reliability analysis (SRA), however, can only be applied to estimate the probability of structural failures induced by natural and man-made hazards resulting from normal operations. To account for the effect of accidental events, typically induced by human errors, a quantitative risk analysis (QRA) (e.g. Vinnem, 1999) needs to be used considering all uncertainties that affect the risk in the life cycle. In this process, the effects of ageing and the role of inspections and maintenance must be anticipated in an integrated manner. While this approach is required to assess the efficiency of ALS requirements (Moan, 2007), it is outside the scope of this chapter.

The aim of this chapter is to describe reliability modelling and analysis of offshore structures. Reliability methods can be used at the design stage to assess the optimal choice of scantlings and materials as well as the inspection plan. A more important application of reliability analyses is to continuously assess the safety during operation to provide information to update the inspection plan and other safety measures to maintain the safety level. The first updating of reliability could be based on information obtained during the inspection of the as-fabricated structure. It is important that the assessment during operation is consistent with current design practice. This means that the reliability approaches used should imply the safety level corresponding to the semi-probabilistic methods that are currently used in design codes for offshore structures.

Against this background Sections 11.2–11.4 briefly outline the current basis for design codes and inspection planning of offshore structures. Examples of design criteria are described in terms of limit states, which serve as a basis for

© 2008 Woodhead Publishing Limited

both semi-probabilistic and fully probabilistic criteria. Relevant semi-probabilistic criteria are summarized in conjunction with the limit states. System failure criteria are discussed in Section 11.5. Section 11.6 deals with uncertainty modelling in general, while uncertainties in loads and load effects are classified and characterized in probabilistic terms in Section 11.7. Sections 11.8–11.10 briefly deal with the basic principles of reliability analysis of components and systems. Section 11.11 describes how the reliability of ageing structures can be updated based on inspection and applied in connection with structural reassessment and inspection planning and gives a brief overview of reliability software. Finally, Sections 11.12–11.14 outline how reliability methods are used to achieve decisions during design and operation of offshore structures.

11.2 Current design practice for offshore structures: limit states

11.2.1 Ultimate limit states

Modern codes are based on application of explicit limit state criteria and semi-probabilistic design formats in terms of characteristic load effects and resistances and partial safety factors. Assuming a component with resistance R and assuming that S_1 and S_2 are extreme load effects in a reference period of 100 years due to different types of loads, e.g. payload and wave load, respectively, R and S refer to the same physical quantity, e.g. a stress or an axial force or a bending moment. Since R, S_1 and S_2 are subject to uncertainty and variability, the design format applied is:

$$R_c/\gamma_R \geq \gamma_{S1} S_{1c} + \gamma_{S2} S_{2c} \tag{11.1a}$$

where subscript c refers to characteristic value and γ_R, γ_{S1} and γ_{S2} are resistance and load factors. The characteristic resistance is obtained by, e.g., using the 95% fractile material strength, while the characteristic load effects due to payload and waves correspond to a specified value and to the load with annual probability exceeding 10^{-2}, respectively. Equation (11.1a) implies that the failure probability

$$P_f = P[R \leq S] \tag{11.1b}$$

for the present problem becomes sufficiently small when load and resistance factors and characteristic values are properly chosen. Ultimate limit state criteria in modern design codes are based on the design formats like Eq. (11.1a). This approach is denoted semi-probabilistic while design based on direct calculation of the failure probability is a probabilistic approach. Then R and S are considered random variables which represent the uncertainties and variability in R and S. Some design codes permit direct probabilistic design for particular situations. Even more importantly, probabilistic approaches are used to calibrate the semi-probabilistic approaches.

© 2008 Woodhead Publishing Limited

An appreciation of the philosophy underlying such provisions is essential: in the presence of uncertainty, absolute reliability is an unattainable goal. However, probability theory and reliability-based design provide a formal framework for developing criteria for design which ensure that the probability of unfavourable performance is acceptably small.

More general expressions than Eq. (11.1a–11.1b) would be required to describe ultimate failure of beams, panels and shell structures under multiple loading. Also design formats relating to brittle fracture and fatigue need to be described.

Also, when S_1 and S_2 represent two time-varying loads, such as the still-water and wave loading on an FPSO, the fact that their maxima in a given period do not occur at the same time necessitates particular analysis to determine the maximum of the combined load. Using stochastic process theory, the characteristic values of the combined loads may be expressed by $(\psi_{S1}S_{1c}, S_{2c})$ or $(S_{1c}, \psi_{S2}S_{2c})$ where ψ_{Si} are load reduction factors and the individual load effects are still defined separately with respect to the 10^{-2} exceedance probability.

The basic case is a structural component with one resistance R and two load effects S_1 and S_2. This case could relate to ductile collapse of a member. Overall stability check of a rigid body can be formulated by two destabilizing load effects and a stabilizing load effect (resistance). The corresponding limit state function $g(\ )$ is given by

$$g(R, S_1, S_2) = R - S_1 - S_2 \tag{11.2a}$$

The design criterion (11.1a) is then given by

$$g(R_d, S_{1d}, S_{2d}) \geq 0 \tag{11.2b}$$

where $R_d = R_c/\gamma_R$, $S_{1d} = \gamma_{S1}S_{1c}$, $S_{2d} = \gamma_{S2}S_{2c}$ are the design values of resistance and load effects, respectively. Similarly, the expression for failure event is given by

$$g(R, S_1, S_2) < 0 \tag{11.2c}$$

As another example of ultimate limit state, consider a steel beam-column subject to axial force and bending moment. The failure probability in this case may be formulated as

$$\begin{aligned} g(R_1, R_2, R_3, S_1, S_2) &= 1 - \left[\frac{S_1}{R_1} + \frac{S_2}{\left(1 - \dfrac{S_1}{R_2}\right)R_3}\right] \\ &= 1 - \left[\frac{X_1}{X_2} + \frac{X_3}{\left(1 - \frac{X_1}{X_4}\right)X_5}\right] = g(X) \end{aligned} \tag{11.3}$$

where S_i and R_i are load effect and resistance parameters, respectively. Clearly Eq. (11.3) is based on a Perry–Robertson approach, and represents one alternative.

© 2008 Woodhead Publishing Limited

Many other problems can be formulated by a multiple set $\boldsymbol{X}$ of random variables.

Brittle fracture due to overload in welded metal structures has often been treated in a simple manner, with choice of material quality based upon environmental temperature and plate thickness but not a formal explicit design check analogous to Eq. (11.1a). However, by fracture mechanics approaches formal criteria can be established and treated in a semi-probabilistic or fully probabilistic manner; see, e.g., Almar-Næss (1985).

11.2.2 Fatigue limit states

Fatigue is an important consideration for structures in areas with more or less continuous storm loading and especially for dynamically sensitive structures. The fatigue design check is normally based on resistance defined by S-N data ($N = KS^{-m}$) that have been obtained by laboratory experiments, and the use of Miner and Palmgren's hypothesis of linear cumulative damage. A simple expression for the cumulative damage can be obtained by assuming that the S-N curve is defined by $NS^m = K$ and the number $n(s)$ of stress ranges is given by the two-parameter Weibull distribution. The distribution of stress ranges s can then be described by

$$F_S(s) = 1 - \exp\left[-\left(\frac{s}{A}\right)^B\right] \tag{11.4}$$

where

$$A = s_0/(\ln N_0)^{1/B} \tag{11.4a}$$

$$P[S \geq s_0] = 1/N_0 \tag{11.4b}$$

where A and B are the scale and shape parameters, respectively. The damage D in a period T with N_T cycles is then

$$\begin{aligned} D &= \sum_i \frac{n_i}{N_i} = \sum \frac{n(s_i)}{N(s_i)} = \frac{N_T}{K}\left[\frac{s_0}{(\ln N_0)^{1/B}}\right]^m \Gamma(m/B+1) \\ &= \frac{N_T}{K} A^m \Gamma(m/B+1) = \frac{N_T}{K}\bar{S}^m \end{aligned} \tag{11.5}$$

where A is given by Eq. (11.4a–b). Guidance on the magnitude of the shape parameter B is available, e.g. as indicated by Marshall and Luyties (1982). The scale parameter A, which is directly related to the extreme response value required for ULS design checks, can be estimated in connection with this kind of analysis. In this way, fatigue loading at least for initial design and screening to identify the importance of fatigue can be easily accomplished.

$\bar{S}$ may be interpreted as an equivalent constant amplitude loading of the variable amplitude loading. The expression (11.5) is valid for a single slope S-N

© 2008 Woodhead Publishing Limited

curve. For other types of S-N curves different expressions apply (e.g. Ayala-Uraga and Moan, 2007a).

The failure function for reliability analysis based on the S-N approach is given by

$$g(\ ) = \Delta - D \tag{11.6a}$$

where Δ describes the damage at fatigue failure. The design check

$$g(\Delta_{\text{all}}, D_{\text{c}}) \geq 0 \tag{11.6b}$$

is normally based upon the expected long-term distribution of stress cycles, i.e. A and B. K is taken to be the characteristic K_{c}, the characteristic value of K, typically corresponding to 97.7% probability of exceedance (mean minus two standard deviations), and Δ_{all} is the acceptable fatigue damage, usually between 0.1 and 1.0. In the calculation of the failure probability A, K, Δ, etc., in $g(\ )$ are taken as random variables.

The failure function may be also expressed in terms of time by reformulating Eq. (11.6a), by using Eq. (11.5) as follows:

$$g(\ ) = \frac{K \cdot \Delta}{\nu_0 \cdot A^m \cdot \Gamma(m/B + 1)} - \frac{N}{\nu_0} = T_{\text{f}} - \tau \leq 0 \tag{11.7}$$

where T_{f} and τ are the time to failure (resistance) and the time elapsed with fatigue loading (load effect), and ν_0 is the mean frequency of the stress cycles (ranges).

11.2.3 Fracture mechanics model of fatigue

Instead of the S-N curve together with the Miner–Palmgren approach, a fracture mechanics approach needs to be adopted to assess more accurately the different stages of crack growth, including calculation of residual fatigue life beyond through-thickness cracking, which is normally defined as fatigue failure. Such detailed information about crack propagation is also required to plan inspections and repair. A model that includes the crack depth as a variable also gives the opportunity to better compare predicted with observed fatigue behaviour. However, it is crucial that the fracture mechanics approach is calibrated to the S-N approach for the initial stage of the fatigue life, to ensure that the initial crack size and local geometry are properly represented.

The fracture mechanics approach is often based on the Paris crack propagation law in a bilinear form:

$$\frac{\mathrm{d}a}{\mathrm{d}N} = \begin{cases} C_1(\Delta K)^{m_1} & \text{for } \Delta K > \Delta K_0 \\ C_2(\Delta K)^{m_2} & \text{for } \Delta K_0 \geq \Delta K \geq \Delta K_{\text{th}} \\ 0 & \text{for } \Delta K < \Delta K_{\text{th}} \end{cases} \tag{11.8a}$$

where a is crack depth, N is number of cycles, C is crack growth parameter, m is

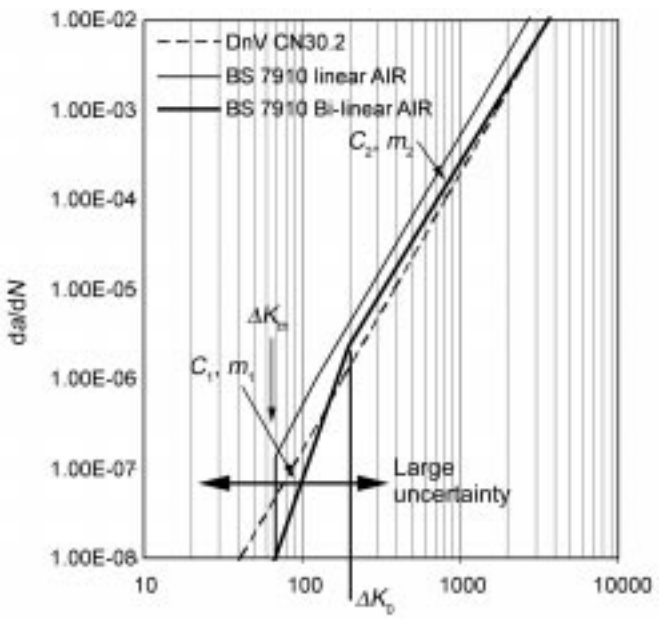
© 2008 Woodhead Publishing Limited

the inverse slope of the S-N curve, and ΔK_{th} is a threshold for $\Delta K =$ the stress intensity factor (SIF) range given by

$$\Delta K = \left[Y_{\text{m,plate}} S_{\text{m}} + Y_{\text{b,plate}} S_{\text{b}}\right] \sqrt{\pi a} \qquad 11.8\text{b}$$

where S is stress range and subscripts m and b refer to membrane and bending, respectively.

Compliance functions for semi-elliptical surface cracks in flat plates, $Y = Y_{x,\text{plate}}(a/t, a/c, c/w, \phi)$, $x =$ m or $x =$ b (Newman and Raju, 1981), are used, where c is one half of the crack length, w is plate width, and the angle ϕ measured from the surface defines a point on the elliptical crack boundary. For applications to tubular joints, $Y_{\text{m,plate}}$ and $Y_{\text{b,plate}}$ are corrected by a magnification factor M_k in order to account for effects from welds based on upper bound (conservative) values; see, e.g., Almar-Næss (1985). Details of $Y(a)$ may be found, e.g., in handbooks and some design codes such as BS 7910 (1999). In general, the $Y(a)$ function needs to be determined by a 3D FE model. This represents a significant challenge. BS 7910 specifies a linear and bilinear log (da/dN) vs. ΔK relationship. In Fig. 11.2 alternative crack propagation data are compared, and a significant difference especially for low ΔK is observed. Equation (11.8a) may be generalized by representing da/dN as $C_i(\Delta K)^{mi}$ for segments i among a set of segments for ΔK (e.g. Celant *et al.*, 1983). Codified data for a bilinear crack propagation law are given in BS 7910 (1999).



11.2 Crack propagation data.

© 2008 Woodhead Publishing Limited

The failure function for fatigue can be written

$$g(\ldots) = a_{\mathrm{f}} - a(t) \tag{11.9}$$

where a_{f} and $a(t)$ are the crack size at failure and the crack size at time t respectively. In the time t the number of cycles is equal to the time t multiplied by the average stress cycle frequency, ν_0.

By assuming a linear $\mathrm{d}a/\mathrm{d}N$ vs. ΔK relationship in log scale and a constant geometry function $Y(a)$ and $\Delta K_0 = \Delta K_{\mathrm{th}} = 0$ in Eq. (11.8a),

$$a(t) = \left[a_0^{1-m/2} + \left(1 - \frac{m}{2}\right) C \Delta\sigma^m Y^m \pi^{m/2} N\right]^{1/(1-m/2)} \tag{11.10}$$

As pointed out by, e.g., Moan *et al.* (2004), $g(\ )$ in Eq. (11.9) needs to be reformulated when introducing $a(t)$ according to Eq. (11.10) when FORM/SORM is applied to determine P_{f}. In general, when $Y(a)$ is a function of a, $g(\boldsymbol{X})$ can be reformulated as a function of time (Madsen *et al.*, 1986). For the case when $C_1 = C$, $m_1 = m$, $\Delta K_0 = \Delta K_{\mathrm{th}} = 0$ in Eq. (11.8a),

$$\begin{aligned} g(X) = M(t) &= \int_{a_0}^{a_{\mathrm{f}}} \frac{\mathrm{d}a}{[Y(a)\sqrt{\pi a}]^m} - C \cdot \nu_0 \cdot A^m \Gamma\left(1 + \frac{m}{B}\right) \cdot t \\ &= \int_{a_0}^{a_{\mathrm{f}}} \frac{\mathrm{d}a}{[Y(a)\sqrt{\pi a}]^m} - C \cdot \nu_0 \cdot \bar{S}^m \cdot t \end{aligned} \tag{11.11}$$

where a_0 and a_{f} are initial crack size and the crack size at failure, respectively. The crack size a_{f} that corresponds to fatigue failure according to S-N curves for plated structures is approximately equal to the plate thickness. $\Gamma(\cdot)$ is the Gamma function. Failure functions for other, more general cases of Eq. (11.8a) have been formulated by Kam and Dover (1989) and Hovde and Moan (1994).

Let a mobile offshore structure initially be designed and installed in a stress environment j and later be transferred to another environment k. The difference in stress in the two environments can be due to the wave conditions or load shedding in the structure after partial failure. The safety margin for this kind of situation is (Moan *et al.*, 2004):

$$\begin{aligned} M_{j\to k}(t) = \int_{a_0}^{a_{\mathrm{f}}} \frac{\mathrm{d}a}{[Y(a) \cdot \sqrt{\pi a}]^m} &- C \cdot \nu_{0,j} \cdot A_j^m \cdot \Gamma(1 + m/B_j) t_{\mathrm{change}} \\ &- C \cdot \nu_{0,k} \cdot A_k^m \cdot \Gamma(1 + m/B_k)(t - t_{\mathrm{change}}) \end{aligned} \tag{11.12}$$

The first two terms apply for $t < t_{\mathrm{change}}$ while the whole expression is valid for $t > t_{\mathrm{change}}$. A_i and B_i represent the Weibull parameters of the long-term stress range corresponding to the climatic conditions j, and $\nu_{0,j}$ is the average frequency corresponding to the sea climate i. t_{change} is the time at which the vessel changes location, i.e. between when it is installed under initial climatic conditions j until it is moved to different climatic conditions k.

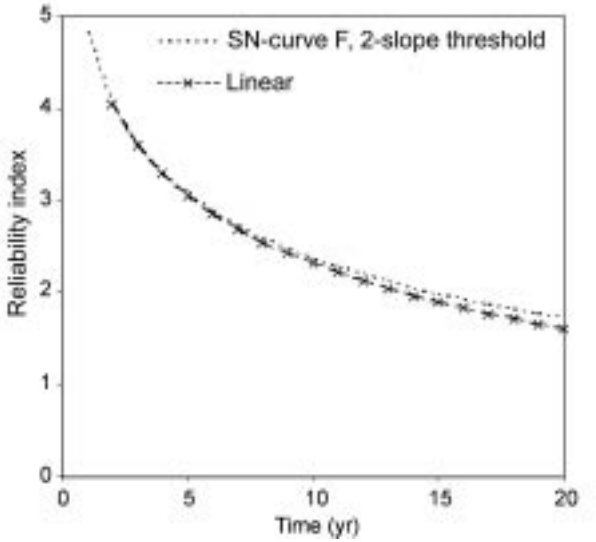
The formulation (11.13) is also applicable when a change in the loading

© 2008 Woodhead Publishing Limited

occurs due to failure of a structural component and redistribution of loading. However, then the deterministic value of t_{change} is changed with the (random) time to failure of the component to fail. The formulation is also easily generalized to n sequential climatic conditions.

11.2.4 Calibration of fracture mechanics models for fatigue

Before FM formulations can be applied for small crack sizes they need to be calibrated based upon S-N data. This is because the initiation of cracks and its initial stages are subjected to uncertainties which are hard to quantify. This calibration can be performed by a semi-probabilistic or probabilistic (reliability) approach, e.g. Moan *et al.* (1993). Ayala-Uraga and Moan (2007a) applied a probabilistic calibration to various S-N curves using BS 7919 FM data. Figure 11.3 shows the reliability index curves obtained with the linear FM model for an F-joint, calibrated with respect to their corresponding two-slope S-N curve. The calibration procedure is achieved by disregarding the initiation time, i.e. $T_0 = 0$ years. The mean value of the initial crack size for the F joint was found to be 0.2 mm, while the mean initial crack size for the C joint was 0.15 mm. The crack aspect ratio was found to be larger for the F joint. Calibration of the bilinear FM model to the S-N model was found to be more complex and a calibration strategy based upon two or three parameters may be necessary. The effect of inspection of reliability, i.e. reliability updating, for the bilinear FM model needs to be carried out by means of Monte Carlo simulation, as the FORM/SORM



11.3 Reliability calibration of the linear FM model for an F joint (Ayala-Uraga and Moan, 2007a).

© 2008 Woodhead Publishing Limited

approaches are found to be non-conservative. In order for the reliability calculations to be conservative when applying the bilinear crack growth law, it is recommended to assume both segments to be highly correlated.

It is popular to apply this initial crack size of 0.11 mm in fracture mechanics-based inspection planning. This crack size relates cracks that occur at a rate of 16 per m (Bokalrud and Karlsen, 1981). Moan *et al.* (1997) found that the mean initial crack depth for tubular joints for jackets was 0.94 mm. However, these data were obtained by underwater inspections *in situ* and the probability of detection was less than in Bokalrud and Karlsen's study under laboratory conditions. Hence the occurrence rate was one per three tubular joints. This initial crack depth was transformed by using extreme value statistics into a mean initial crack depth of 0.38 mm.

Kountouris and Baker (1989) collected and analysed a large database of weld defects in an offshore structure which sheds some light on the defect size.

11.2.5 Corrosion effects

The fatigue crack growth rate increases because of increased stress and possibly an increased crack propagation rate. The effect of corrosion on the crack propagation rate may be shown by the S-N curves or by introducing a correction factor C_{corr} to the material or crack growth parameter C used in the fracture mechanics models. The crack growth rate under free corrosion conditions may correspond to a factor C_{corr} of the order of 3.

To account for the plate thinning effect, the scale parameter A in the Weibull distribution of long-term stress range is taken to vary with time due to corrosion. A fixed annual thickness reduction rate due to corrosion is assumed throughout the service life. The plate thickness may be modelled, assuming a constant corrosion rate R_{corr}, by

$$h(t) = h_0 - R_{\text{corr}} \cdot \alpha(t - t_0) \quad \text{for } t \geq t_0 \tag{11.13}$$

where h_0 is the initial value of the wall thickness. In view of the significant uncertainty in R_{corr} a constant corrosion rate is considered a reasonable choice. α is a factor equal to 1 if the corrosion rate is one-sided or to 2 if it is two-sided. It is assumed that h_0 includes the corrosion allowance.

The stress range due to axial forces is therefore $S(t) = S_0 \cdot h_0/h(t)$. Using the definition of equivalent stress $\bar{S}$ implied by Eqs (11.5) and (11.13) in this expression, the effective stress range of $\bar{S}$, $\bar{S}_{\text{eff}}$ for a period $t \geq t_0$, can be determined by assuming linear cumulative damage, i.e. the value of $\bar{S}^m$ for each period is weighted according to the duration of the period. The resulting $\bar{S}_{\text{eff}}$ is (Moan and Ayala-Uraga, 2006):

© 2008 Woodhead Publishing Limited

$$\bar{S}_{\text{eff}}^{m} = \begin{cases} \bar{S}^{m} & \text{for } 0 \le t \le t_0 \\ \bar{S}^{m}\left[t_0/t + \frac{1}{(m-1)k \cdot t}\left\{(1-k(t-t_0))^{-m+1} - 1\right\}\right] & \text{for } t \ge t_0 \end{cases} \quad 11.14$$

where

$$k = \alpha \cdot R_{\text{corr}}/h_0$$

The effect of corrosion on the fatigue reliability can therefore be obtained by applying the time-varying fatigue stress $\bar{S}_{\text{eff}}$ instead of $\bar{S}$ in Eq. (11.11) and other expressions for the failure function based on a single slope S-N (or fracture mechanics) formulation.

It is important to note that fatigue failure could be defined in various ways. S-N curves are obtained by referring to a visible crack or a through-thickness crack, or to loss of capacity for the (small-scale) specimen applied, and do not reflect the possibly significant amount of material surrounding the crack, especially in steel-plated structures.

If Δ_{all} is taken to be 1.0, it is indicated later that the implied $P_{\text{f}}(t)$ would be of the order of 10% in the service life. With a large number of possible crack sites, the likelihood of having one or more fatigue failures becomes significant. Such a design criterion can therefore be applied only under the condition of either:

- the existence of a significant amount of surrounding material and the use of visual inspection to detect cracks, followed by repair, or
- non-destructive examination to detect even small cracks, which are then repaired.

Semi-probabilistic methods need to be calibrated by reliability analysis to account for the effect of inspection results, and possible repair (grinding, welding and replacement), on safety. For instance, by a given inspection plan (inspection method, frequency of inspection) the fatigue criterion may be relaxed. This effect would have to be estimated at the design stage. Another situation occurs when inspections are carried out during use of the structure. In such cases the outcome of the inspection (e.g. crack not found) will be known.

11.3 Inspection and maintenance of offshore structures

So far the focus has been on achieving serviceability and safety by structural design. However, inspections and all kinds of actions during fabrication and operation to maintain the intended quality of the structure are crucial to ensure safety, especially in connection with deterioration phenomena such as fatigue and corrosion. Such actions may include repair and replacement of components and corrosion protection systems. But the effect of inspections on reliability depends upon its quality, e.g. in terms of detectability vs. size of the damage. Hence inspection, repair and replacement measures can contribute to safety only

© 2008 Woodhead Publishing Limited

Table 11.1 Fatigue design factor FDF $= 1/\Delta_{all}$ to multiply the planned service life to obtain the required design fatigue life (NORSOK N-001, 2002). The consequences are substantial if the Accidental Collapse Limit State (ALS) criterion is not satisfied in case of a failure of the relevant welded joint considered in the fatigue check

Classification of structural components based on damage consequence	Access for inspection and repair		
	No access or in splash zone	Accessible (inspection according to generic scheme is carried out)	
		Below splash zone	Above splash zone or internal
Substantial consequences	10	3	2
Without substantial consequences	3	2	1

Note: Slightly different criteria have been proposed by API (Karsan, 2005).

when there is a certain damage tolerance. This implies that there is an interrelation between design criteria (fatigue life, damage tolerance) and the inspection and maintenance criteria. To some extent these issues are reflected in fatigue design criteria in offshore codes (NORSOK N-001, 2002; ISO 19900, 1994) where the fatigue design check depends upon the consequences of failure and access for inspection. NORSOK N-001 (2002) specifies an allowable cumulative damage Δ_{all} between 0.1 and 1.0, or a fatigue design factor FDF $= 1/\Delta_{all}$ between 10 and 1, as indicated in Table 11.1. The consequence measure is based on whether the structure has sufficient residual strength after fatigue failure of the relevant joint to resist expected functional loads and 100-year sea loads and is thus linked to the Accidental Collapse Limit State, as briefly described in Section 11.2.3. The treatment of both the consequence and inspection issues, however, could be improved, e.g. by taking Δ_{all} to be dependent on a more precise measure of reserve strength and explicit measure of the effect of inspection.

Anyway, the fabrication and operation imply features unique to each structure that need to be observed in planning of inspection and maintenance during operation. By continuously updating the safety measure (P_f) depending on actions initiated during use, decisions regarding inspection scheduling, maintenance and repair can be properly made, to ensure an acceptable safety level.

Normally, a fatigue design factor FDF $= 1.0$ is applied for ships, including FPSOs. However, it may be reasonable to apply more restrictive criteria when the consequences of, e.g., a through-thickness crack may be high. This may be the case when the crack causes leaks from cargo tanks into ballast tanks, which may lead to an explosion hazard. Even if cracks in hulls do not represent an immediate risk of global failure, they can cause leaks of oil which can lead to explosion risk and environmental damage as well as reduced quality of the oil

© 2008 Woodhead Publishing Limited

cargo. This fact together with the large number of potential crack sites in a complex hull with difficult access suggests a larger FDF, say in the range of 2 or 3. This issue is even more important in the case of tension leg platforms, which are designed with an FDF of 10. LNG tanks on gas carriers are preferably designed based on the 'leak-before-failure' principle. This means that potential cracks shall propagate through the thickness before reaching a critical size. A gas detection system shall therefore be arranged to detect potential gas leaks. After a through-thickness leak the tanks shall have a sufficient time window (e.g. two weeks) for the vessel to go to port and unload her cargo.

11.4 Concluding remarks on component design criteria

The verification of a structure with respect to a particular failure mode may be expressed by a model describing the limit state in terms of a function (called the limit state function) whose value depends on all design parameters. In general terms, attainment of the limit can be expressed as

$$g(\boldsymbol{X}) = 0 \tag{11.15a}$$

where $\boldsymbol{X}$ represents the vector of design parameters (also called the basic variable vector) that are relevant to the problem, and g($\boldsymbol{X}$) is the limit state function. Conventionally, $g(\boldsymbol{X}) \leq 0$ represents failure (i.e. an adverse state).

For many structural engineering problems, the limit state function, $g(\boldsymbol{X})$, can be separated into one resistance function, $g_R(\cdot)$, and one loading (or action effect) function, $g_S(\cdot)$, in which case Eq. (11.6a) can be expressed as

$$g_R(\mathbf{r}) - g_S(\mathbf{s}) = 0 \tag{11.15b}$$

where **s** and **r** represent subsets of the basic variable vector, usually called loading and resistance variables respectively.

11.5 System failure criteria for offshore structures

Ultimate and fatigue design criteria in current codes for offshore structures are based on component failure modes (limit states), and a linear global model of the structure is used to determine the load effects in the components. However, a design approach which is based on global (system) failure modes of the structure is desirable because significant failure consequences, e.g. fatalities, will primarily be caused by global failure. A proper systems approach is also necessary to obtain the optimal balance between design and inspection plan since an inspection and repair strategy is normally based on a certain damage tolerance, especially when the inspections rely on detecting flooded or failed members.

However, NORSOK N-001 (2002) specifies a quantitative Accidental Collapse Limit State (ALS) mainly intended to prevent progressive failure of

© 2008 Woodhead Publishing Limited

the structural system initiated by accidental loads such as fires, explosions, ship impacts or fabrication defects. The design check is a two-step procedure. The first step is to estimate the damage due to accidental loads with an annual exceedance probability of 10^{-4} which should be identified by risk analysis methods as described, e.g., by Vinnem (1999). In principle the accidental damage includes abnormal strength. The second step is to check that the structure survives the various damage conditions without global failure, considering environmental loads with an annual exceedance probability of 10^{-2}. As mentioned above, some fatigue design criteria in some codes depend upon the consequence of the fatigue failure, i.e. Δ depends on whether the system satisfies an ALS criterion with respect to fatigue failure of the relevant member.

System failure is then expressed mathematically by load and resistance parameters relating to all failure modes for all components. The systems failure probability is calculated by the probabilistic properties of these parameters. Broadly speaking, this may be achieved by a failure mode (or survival mode) analysis or direct simulation methods.

Inspection plans may be optimized at the design stage as shown, for example, by Madsen and Sørensen (1990) as well as Faber *et al.* (1992).

11.6 Uncertainty measures used in reliability analysis

The failure probability P_f according to Eq. (11.25) is dependent upon the joint distribution $f_{\boldsymbol{X}}(\boldsymbol{x})$ of the state variables. The uncertainties used in reliability analyses should include all variables that may affect reliability. These would include 'inherent' statistical variability in basic strength or action parameters. Additional sources of uncertainty arise due to modelling and prediction errors and incomplete information; included in these 'modelling uncertainties' would be errors in estimating the parameters of the distribution function, idealizations of the actual load effect process in space and time, uncertainties in calculation, and deviations in the application of standard and material specification from the idealized cases considered in their development. While occasionally there may be some data available with which to estimate these latter uncertainty measures, frequently they must be estimated on the basis of professional judgement and experience. The key test in differentiating between the 'inherent' and 'modelling' uncertainties is in whether the acquisition of additional information would materially reduce their estimated magnitude. If the variability is intrinsic to the problem, additional sampling is not likely to reduce its magnitude, although the confidence interval on the estimate would contract. In contrast, uncertainties due to 'modelling' should decrease as improved models and additional data become available. The main categories of basic variables may be described as mechanical properties of the materials, structural dimensions and geometry, loads and methods for load effect analysis.

© 2008 Woodhead Publishing Limited

If the variables are independent from each other, their marginal distributions, $f_{Xi}(x_i)$, are enough to identify the joint distribution. In a few specific cases, such as for normal and log-normal joint distributions, the mean values, variance and covariance are enough to define $f_{\boldsymbol{X}}(\boldsymbol{x})$ completely. For other cases the same data provide only approximate information. Reference is made to textbooks, e.g. Thoft-Christensen and Baker (1982), Madsen *et al.* (1986) and Melchers (1999).

In many cases, important variations exist over time (and sometimes space), which have to be taken into account in specifying basic variables. In probabilistic terms, this may lead to a random process rather than random variable models for some of the basic variables. However, simplifications might be acceptable, thus allowing the use of random variables whose parameters are derived for a specified reference period (or spatial domain).

The joint probability distribution of state variables in principle reflects all relationships among variables. In the case of a dependence or correlation between variables (e.g. due to a common cause such as the strength of a panel subjected to axial and horizontal loads) it may not be possible to describe the dependence in analytical terms. In such cases, the dependence is modelled by a Response Surface Method (RSM).

In reliability analyses the means or characteristic extremes have been normalized with respect to their nominal values. This is done for convenience and makes the statistics applicable to a wide range of design situations. The statistics of the action or resistance variable can easily be computed for each design situation that is defined by nominal action and resistances, since if

$$X = (X/X_n) \cdot X_n \tag{11.16}$$

then

$$\mu_X = \mu_{(X/X_n)} \cdot X_n; \quad V_X = V_{(X/X_n)} \tag{11.17a,b}$$

Consider, for example, the ultimate capacity of a member with axial compression force. The predicted normalized ultimate capacity f_u/f_y (where f_y is the yield strength) is obtained as a function of member slenderness from curves determined experimentally and given in design codes. The true resistance R is then expressed by

$$R = N_u = f_u \cdot A = R_{\text{pred}} \cdot X_R \cdot X_A \cdot X_{fy} \tag{11.18}$$

where

$$X_R = \left(\frac{f_u}{f_{yn}}\right) \Big/ \left(\frac{f_u}{f_{yn}}\right)_{\text{pred}}, \quad X_A = \left(\frac{A}{A_n}\right), \quad X_{fy} = \left(\frac{f_y}{f_{yn}}\right) \tag{11.18a–c}$$

are the model uncertainty and parameter uncertainty in cross-section area (A) and yield strength (f_y), respectively. Typically X_R would have a mean value of 1.0 to 1.1 and a COV in the range of 0.05 to 0.10 depending upon type of

© 2008 Woodhead Publishing Limited

member and slenderness. X_A is close to 1.0 with a small uncertainty. The mean and COV are 1.0 to 1.1 and 0.05–0.10, respectively.

The model uncertainty is defined as the true value divided by the value predicted by the model, i.e.

$$X_{\mathrm{m}} = \frac{\text{actual behaviour}}{\text{predicted behaviour}} = \frac{X_{\mathrm{true}}}{X_{\mathrm{pred}}} \qquad 11.19$$

Such a model uncertainty X_{m} should be considered a random variable which needs to be assessed by tests on full-scale structures or representative models. Frequently the model uncertainty is the dominant uncertainty and should be estimated carefully.

There may be a tendency to focus on the sensitivity of the reliability results on the random uncertainty (COV), but it is emphasized that a 10% change of bias has a larger effect on the P_{f} than a 10% change of COV.

The values of the uncertainties are crucial to the estimates of the reliability. It is therefore important that authoritative uncertainty measures are applied. Data processed in connection with code calibration and assessed by an expert committee, with knowledge about the mechanics of the phenomena as well as the probabilistic characteristics, are most relevant. A general treatment on uncertainties may be found in Ang and Tang (1984).

Uncertainties relating to resistances and extreme load effects relating to ULS are reported, e.g., by Fjeld (1977), Lloyd and Karsan (1988), Moses (1987) and Moan (1995) in connection with code calibrations. Data relating to fatigue loading and resistance of offshore structures have been assessed, e.g., by Wirsching (1983), Kirkemo (1989) and Moan *et al.* (1993).

11.7 Load effects on offshore structures

11.7.1 General description

For permanent actions, which are assumed to remain constant for the life of the structure (e.g. densities of the construction materials), the statistical distribution function should be assumed to be normal. The self-weight of the structure itself is generally not treated as a basic variable, as it is a function of two other types of more fundamental quantities (dimensions and densities).

Environmental loads are time variant. For wave loads, for example, it is convenient to use such statistics as the long-term variation of sea states in terms of scatter diagrams or some joint probability distribution. The load effects are obtained by a frequency domain analysis for a linear problem or a time domain analysis when important nonlinearities affect the load effects. In general a Weibull distribution is found to accurately describe different types of long-term load effects in structures in extratropical areas well. Extreme values corresponding to one-year or 100-year periods can then be readily established based on extreme value theory. However, for certain types of load effects such

© 2008 Woodhead Publishing Limited

as forces obtained by Morison's equation, different phenomena prevail at different load levels. In connection with Morison's equation, this is borne out by the fact that inertia forces dominate at moderate wave heights while drag forces may dominate at large wave heights. In such cases Weibull-tail or POT methods are recommended for use in connection with predicting extreme values.

If a single load process depends on time, it can be substituted, without loss of generality, by its extreme value in the reference period. The new variable takes a single value in the period, thus yielding a time-invariant formulation. When more than one time-varying load is present, it is unlikely that each load will reach its peak lifetime value at the same moment. Consequently, a structural component could be designed for a total load which is less than the sum of the peak loads. If several time-variant loads are dealt with, a proper combination of these loads within the failure equation can be treated only by means of Monte Carlo simulations. Alternatively, the combination problem can be solved before evaluating the probability of failure, substituting in the limit function the single loads with their combined effect.

11.7.2 Load combination

The combination of loads and their effects should be handled by applying the theory of stochastic processes, which accounts for the stochastic nature and correlation of the actions in space and time. Various methods can be applied. Turkstra's rule (Turkstra, 1970) is the simplest but may not be accurate enough. In this case the maximum of two loads is taken as the maximum of one load and a random point in time value (expected value) of the other one. Wen (1990) gives an overview of general methods for combining load processes based on stochastic process theory.

For ship-type offshore structures, combinations of still-water and wave loads are of main concern. For FPSOs, where both still-water and wave loads vary continuously, Wang and Moan (1996) found that the Ferry Borges and Castanheta (1972) model gave good results for load combination. Turkstra's rule was found to be non-conservative. Recently, Huang and Moan (2006) studied load combinations for FPSOs and refined and extended this approach. By writing the characteristic values

$$M_c = M_{wc} + \psi_{sw} M_{swc};\ M_c = \psi_w M_{wc} + M_{swc} \tag{11.20}$$

where the subscripts w, sw and c refer to wave, still-water and characteristic value, respectively, it was found that the ψ_{sw} and ψ_w were about 0.7 for operations in extratropical areas.

11.7.3 Uncertainty in wave load effects

The uncertainty in the effects of wave loads often dominates in the reliability analysis. It is necessary to distinguish between the uncertainties in extreme load

© 2008 Woodhead Publishing Limited

effects – affecting ultimate failure – and those in fatigue load effects. Extreme values for conventional ULS design checks typically correspond to a value which is exceeded by an annual probability of 10^{-2}, while fatigue loads are represented by the total cyclic load history (in the service life). The following factors contribute to this uncertainty:

- environmental conditions
- stochastic model adopted
- hydrodynamic loading model
- structure–fluid (and possible foundation–soil analysis model) to determine member forces and moments

and especially for fatigue load effects:

- stress concentration factors in welded joints.

The environmental conditions are described by the macroscopic (meteorological) and microscopic variation of ocean waves, winds and currents. The uncertainty is especially associated with the data for the long-term variation of sea states and the kinematics of the waves for the relevant site.

The stochastic modelling of, e.g., wave loads is obtained by the following means:

- Stochastic analysis considering all relevant sea states in a long-term period of, say, 20 years, typically using crude structural models to identify the load pattern (forces or nominal stress) that can be used to determine the extreme response
- Stochastic analysis considering a single or a few sea states
- Deterministic analysis using a hierarchy of refined models of the structure, e.g. a single regular design wave.

The first two approaches reflect stochastic dynamic effects in the most proper manner and should be applied when, e.g., structural dynamic effects are important. The latter two approaches need to be calibrated by the first one, typically using simplified structural models. The rationale behind the second approach is described by, e.g., Winterstein *et al.* (1993) and Videiro and Moan (1999). For instance, the design wave for bottom-supported platforms corresponding to a 100-year return period is calibrated by using the 100-year design wave height and varying the wave period within a reasonable range. For floating platforms usually the wave period is the most critical wave parameter. The stochastic features of waves are especially of importance when dynamic effects due to rigid body motions or flexible structural modes are significant.

Obviously, the latter two approaches are primarily intended to be used to determine the extreme load effects. However, by combining this information with knowledge about the (Weibull) distribution of response amplitudes (or more precisely stress ranges), fatigue load effects can be modelled.

The stochastic analysis is normally based on modelling the wave elevation as

© 2008 Woodhead Publishing Limited

a Gaussian process, comprising regular waves with different frequency, phase lag and direction. For linear systems the stochastic response is most efficiently and accurately obtained in the frequency domain. The distribution of individual response peaks and their maximum is known to be a Rayleigh distribution and a Gumbel distribution, respectively, for narrowband Gaussian response, and the distribution parameters are readily obtained from the response spectrum, $S_X(\omega)$. The stochastic long-term analysis becomes especially challenging when nonlinearities are important, especially phenomena like wave slamming and green water effects. It is then necessary to apply time-domain simulation. Since proper account of frequency-dependent mass and damping in general requires an integral–differential equation (convolution of, e.g., mass with time and acceleration), such analyses become very time-consuming.

The hydrodynamic analysis is carried out by the semi-empirical Morison's equation for structures consisting of slender members. For large volume structures it is important to apply 3D theory at least for validating possible simplified methods. Load effects are determined in a hierarchy of analyses. When dynamic effects are of concern, a model which recognizes the stochastic features of waves is important.

A hierarchy of structural models, based on finite elements, is commonly used to analyse marine structures. Coarse models are used to establish simplified load conditions (e.g. in terms of design waves) for calculating extreme load effects. The models used to determine stress for ULS design criteria can be coarser that those used to determine load effects for fatigue design checks.

The geometric stress concentration is determined by strain gauge measurements or by refined finite element analysis based on shell or solid elements. Based on systematic studies of unstiffened tubular joints with different configurations and relative scantlings, parametric formulae for the stress concentration factor have been developed, see e.g. NORSOK N-004 and the forthcoming ISO 19900.

11.7.4 Fatigue load effect analysis

The local stress for fatigue design needs to be determined with due account of the temporal and spatial variation. For offshore structures the main parameter to represent the variation in time is the stress range. This approach is based on the assumption that tensile residual stresses are always present and that all stress cycles effectively drive the crack. Fatigue design criteria for marine structures are based on two alternative definitions of load effects and the corresponding strength (S-N curves). This is the nominal and the so-called hot spot stress method (e.g. Almar-Næss, 1985; Karsan, 2005; Halkyard, 2005). Hot spot stress places many different connection geometries on a common basis by incorporating the microscopic notch effects, metallurgical degradation, and incipient cracks at the toe of the weld into the S-N curve. While the nominal stress

© 2008 Woodhead Publishing Limited

approach requires many S-N curves, a single S-N curve is applied for the hot spot approach. Stresses have to be calculated with due account of weld geometry.

The primary cyclic stress that causes fatigue is induced by the external wave loading and is calculated based on the environmental conditions. Three-dimensional hydrodynamic effects may be important because the waves that contribute fatigue loading may be short compared to the size of the structure, implying diffraction and radiation effects. Since moderate sea states contribute most to fatigue, linear analyses often suffice. In some cases fatigue load effects are influenced by nonlinear effects and time-domain simulation combined with rain flow counting of stress ranges is necessary. Detailed guidance for load effect analyses is given in design codes, and reviews were presented by Karsan (2005) and Halkyard (2005).

Systematic studies carried out for offshore structures in, e.g., extratropical regions suggest that the long-term response of the response variables can be well described by a two-parameter Weibull distribution. Equation (11.4) is convenient as a basis for an early screening of fatigue proneness, using a simple (conservative) estimate of the extreme response s_0 and assuming the shape parameter B of the Weibull distribution. The parameter B depends upon the environmental conditions, the relative magnitude of drag and inertia forces and possible dynamic amplification. For a quasi-static response in an extratropical climate like the North Sea, B may be around 1.0, while it may be as low as 0.4–0.6 for Gulf of Mexico platforms subjected to infrequent hurricanes. For structures with predominantly drag forces B will be smaller than for those with predominantly inertial forces. Structural dynamics may affect load effects when the natural period of flexible modes of vibration exceeds 2.0 s. Normally offshore platforms are designed so as to avoid natural periods of flexible modes that exceed 5.0 s. Commonly, load effects for fatigue design checks are more affected by dynamics than extreme values. Increasing the natural period from 2 s to 4 s may increase B from 0.7 to 1.1 and from 0.9 to 1.3 for Gulf of Mexico and North Sea structures respectively, implying a factor of the order of 10 on fatigue damage.

The long-term stress ranges are described by the Weibull distribution, Eq. (11.4). The uncertainty model applied for the distribution of S is to describe $(\ln A, 1/B)$ by a joint normal distribution with correlation coefficient ρ.

In the assessment of damaged structures regarding their performance in say one winter (year), it is important to note the variability in environmental conditions from year to year. This fact would have an effect on the fatigue damage as illustrated by Moan *et al.* (2005).

Table 11.2 shows typical uncertainty levels for fatigue of steel plated joints in marine structures.

© 2008 Woodhead Publishing Limited

Table 11.2 Uncertainty measures for plated joint with shifting environmental conditions (benign to harsh or vice-versa) assumed in the case study (Moan *et al.*, 2004)

Parameter	Distribution	Mean	Std dev. (COV)
Scale parameter ln$A$ (Benign conditions)	Normal	2.0288	0.198
Shape parameter B (Benign conditions)	Normal	0.66	0.044
Scale parameter ln$A$ (Harsh conditions)	Normal	3.2288	0.198
Shape parameter B (Harsh conditions)	Normal	1.14	0.044
Average stress cycle frequency, ν_0	Fixed	0.158	
Material parameter ln$C$	Normal	−29.97	0.514
Material parameter m	Fixed	3.1	
Geometry function, *GFactor*	Normal	1.0	0.05
Crack aspect ratio, a/c	Fixed	0.83	
Stress ratio, $S_m/(S_m + S_b)$	Fixed	1.0	
Initial crack size, a_0	Exponential	0.11	0.11
Detectable crack size, a_d	Exponential	2.0	2.0
Wall thickness, critical crack size	Fixed	20	
Corrosion wastage rate, R_{corr} (mm/yr)	Normal	0.1–0.2	(0.5)
Thickness measurement, *ThM*	Normal	1.0–5.0	(0.3)
Time of coating, T_0	Normal	5.0	(0.5)

11.7.5 Illustration of uncertainty modelling of extreme load effects

According to Eq. (11.16) a basic variable X may be expressed by

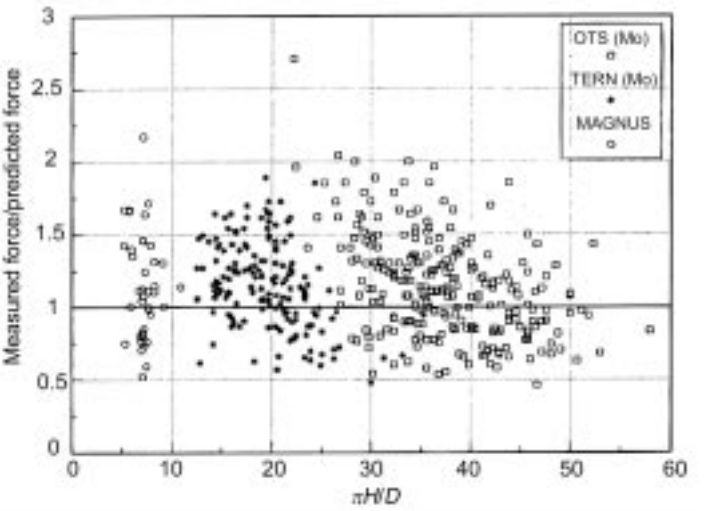
$$X = X_{\text{m}} \cdot X_{\text{pred}} \tag{11.21a}$$

where X_{m} and X_{pred} are the model uncertainty and the predicted value, respectively. X_{pred} may normally be a function of several variables. For instance, consider X to be the wave load effect for a submerged member in a jacket with static behaviour. Assume that the method for predicting X is the design wave method specified in the API RP2A/ISO code. This method is based on a regular wave with height H and appropriately chosen wave period. Wave kinematics is described by Stokes's fifth-order theory and the wave forces on the wetted structure are obtained by Morison's equation. X_{pred} may then be expressed for instance by (e.g. Moan, 1995)

$$X_{\text{pred}} = k \cdot C(C_{\text{d}}, C_{\text{m}};\ \text{wave kinematics}) \cdot H^{\alpha} \tag{11.21b}$$

where k = influence coefficient, reflecting the transformation of action into its effect; C = coefficient that depends upon the coefficients appearing in Morison's equation and wave kinematics; and α = exponent depending upon the dimensions of the platform members, which should be determined by regression analysis for the range of H most relevant for extreme loading.

© 2008 Woodhead Publishing Limited



11.4 Model uncertainty for the ISO design wave approach for predicting wave loading on jackets. Mean value and COV are 1.06 and 0.25, respectively, for the Tern jacket (Heideman and Weaver, 1992).

In this case X_m needs to reflect the model uncertainty in all factors, and it may be necessary to split the factor X_m into different contributions. Figure 11.4 shows how the model uncertainty for the predicted load on jackets in service can be estimated (Heideman and Weaver, 1992).

In most instances the basic resistance variable is taken as the strength of the structural member in question, and the basic load variable is the load effect (moment, shear, etc.) dimensionally consistent with the resistance. These can be used directly when the limit state is formulated as a linear combination of resistance and load variables. The linear formulation is quite common in practice.

11.8 Structural reliability analysis: elementary case

11.8.1 Elementary reliability analysis

The term *structural reliability* should be considered as having two different meanings – a general one and a mathematical one.

- In the most general sense, the *reliability* of a structure is its ability to fulfil its design purpose for some specified time under specified conditions. This interpretation is used in the ISO 2394 code.
- In a narrow sense it is the *probability* that a structure will not attain each specified limit state (ultimate or serviceability) during a specified *reference period*.

© 2008 Woodhead Publishing Limited

In this context the focus will be on structural reliability in the narrow sense, as the complementary quantity to *failure probability* P_f defined by Eq. (11.1b). Hence, the *reliability* may be determined as

$$\Re = 1 - P_f = P[R > S] = 1 - P[R \leq S] \tag{11.22}$$

which may be interpreted as a long-run survival frequency or long-run reliability and is the percentage of a notionally infinite set of nominally identical structures which survive for the duration of the reference period T. $\Re$ may therefore be called a *frequentist reliability*. If, however, the attention is focused on one particular structure (and this is generally the case for unique civil or marine structures), $\Re$ may also be interpreted as a measure of the reliability of that particular structure.

Depending upon how R and S are related to time, the failure probability also will be defined with respect to some reference time period, say one or more years or the service lifetime. This issue is explored later. First, the basic reliability problem – i.e. the calculation of P_f – is examined.

In some special cases the failure probability can be expressed analytically. This applies for cases when both R and S have normal distribution and both R and S have lognormal distribution. The failure probability can generally be written as

$$P_f = \int\int_{R \leq S} f_R(r) f_S(s) dr ds = \int_0^\infty f_S(s) F_R(s) ds = \Phi(-\beta) \tag{11.23}$$

and $\Phi(u)$ is the cumulative probability of a standard normal variable. Tabulated values of this function may be found in handbooks on mathematics and textbooks on reliability analysis. Hence, the *reliability index* β is uniquely related to the *failure probability*, P_f.

The reliability index β for the special case of $P_f = P(R - S \leq 0)$, when both R and S are lognormal variables, is

$$\beta = \beta_{LN} = \frac{\ln\left[(\mu_R/\mu_S) \cdot \sqrt{(1 + V_S^2)/(1 + V_R^2)}\right]}{\sqrt{\ln(1 + V_R^2)(1 + V_S^2)}} \approx \frac{\ln(\mu_R/\mu_S)}{\sqrt{V_R^2 + V_S^2}} \tag{11.24}$$

The β is denoted the reliability index and is an important quantity since it is uniquely related to the failure probability, P_f. Table 11.3 shows the corresponding values of P_f and β.

If R and S have a lognormal and a normal distribution, respectively, it is not possible to determine P_f analytically as for the cases treated above. In this case P_f may be obtained by numerical integration of the third term of Eq. (11.23). However, more general and effective methods are available as subsequently indicated in Section 11.8.4.

© 2008 Woodhead Publishing Limited

Table 11.3 Relation between β and P_f

β	1.0	1.1	1.2	1.3	1.4	1.5	1.6	1.7	1.8	1.9
P_f	0.16	0.14	0.12	0.097	0.081	0.067	0.055	0.045	0.036	0.029
β	2.0	2.1	2.2	2.3	2.4	2.5	2.6	2.7	2.8	2.9
P_f	0.023	0.018	0.014	0.011	$8.2 \cdot 10^{-3}$	$6.2 \cdot 10^{-3}$	$4.7 \cdot 10^{-3}$	$3.5 \cdot 10^{-3}$	$2.6 \cdot 10^{-3}$	$1.9 \cdot 10^{-3}$
β	3.0	3.1	3.2	3.3	3.4	3.5	3.6	3.7	3.8	3.9
P_f	$1.4 \cdot 10^{-3}$	$0.97 \cdot 10^{-3}$	$0.69 \cdot 10^{-3}$	$0.48 \cdot 10^{-3}$	$0.34 \cdot 10^{-3}$	$0.23 \cdot 10^{-3}$	$0.16 \cdot 10^{-3}$	$0.11 \cdot 10^{-3}$	$0.72 \cdot 10^{-4}$	$0.48 \cdot 10^{-4}$
β	4.0	4.1	4.2	4.3	4.4	4.5	4.6	4.7	4.8	4.9
P_f	$0.32 \cdot 10^{-4}$	$0.21 \cdot 10^{-4}$	$0.13 \cdot 10^{-4}$	$0.85 \cdot 10^{-5}$	$0.54 \cdot 10^{-5}$	$0.34 \cdot 10^{-5}$	$0.21 \cdot 10^{-5}$	$0.13 \cdot 10^{-5}$	$0.79 \cdot 10^{-6}$	$0.48 \cdot 10^{-6}$

© 2008 Woodhead Publishing Limited

11.8.2 Example of implied failure probability by design equations

Despite the simplicity of the expression for P_f by Eq. (11.23) with $\beta = \beta_{LN}$ (Eq. (11.24)), it has been extensively used in calibration of design codes, as described later. Here, it will be used to illustrate the failure probability implied by Eq. (11.1a), with only one load effect S. Let the random load effect S and resistance R be defined by

$$\mu_S = B_S S_C, B_S \geq 1; V_S = 0.15 - 0.30$$
$$\mu_R = B_R R_C, B_R \geq 1; V_R = 0.1$$

The B_S reflects the ratio between the mean load (which refers to an annual maximum if the annual failure probability is to be calculated) and the characteristic load effect (typically the 100-year value) as well as possible bias in predicting wave load effects. The reliability index is determined by inserting the design equation Eq. (11.1a) into the approximate expression of Eq. (11.24). With $\gamma_R \gamma_S = 1.5$, a typical $B_S = 0.8$ for wave-induced load effects, $B_R = 1.1$ and $V_R = 0.1$, it is found that β_{LN} is about 2.7 and 3.2 for a V_S of 0.25 and 0.20, respectively. These reliability indices correspond to a P_f of 35×10^{-4} and 7×10^{-4}, respectively. By inspection of the expression for β_{LN} it is seen that when V_S dominates over V_R, β_{LN} is inversely proportional to V_S, and hence very sensitive.

11.8.3 Tail sensitivity of P_f

It is interesting to compare the β (and implicitly the P_f) obtained by different assumptions about distributions. Figure 11.5 shows the comparison when the βs are obtained under the following assumptions:

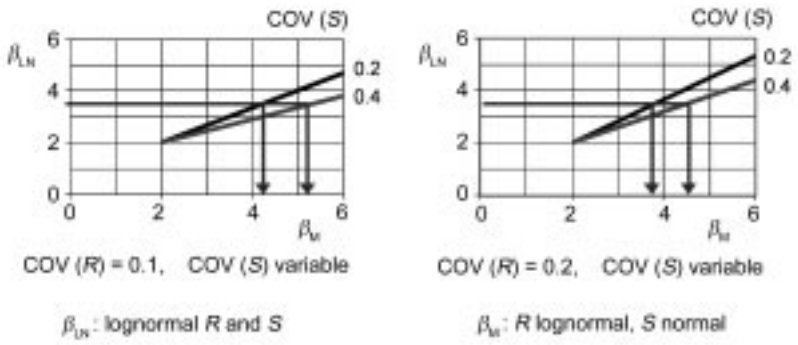
- R and S both with lognormal distribution
- R and S with lognormal and normal distribution, respectively.

With a typical $V_R = 0.15$, $V_S = 0.3$ and μ_R/μ_S given such that β_N is in the range 3 to 4, β_{LN} varies in the range 2.6 to 3.3, corresponding to probabilities differing by a factor of 10. These results clearly show the sensitivity of reliability to the shape of the distribution tail.

11.8.4 Reliability problems formulated by multiple load and resistance variables

The methods for calculating the failure probability outlined above have resulted in a one-dimensional integral, Eq. (11.23). The failure probability may be expressed as the integral of the probability density function for R and S over the area which corresponds to failure, i.e. $S \geq R$. Instead of doing the integration of

© 2008 Woodhead Publishing Limited



11.5 Comparison of reliability indices determined by different assumptions about the distributions of R and S.

$f_{RS}(r,s)$ in the (r,s) domain, the variables may be transformed into a space (u_1,u_2) such that these variables are independent and have a standard normal distribution.

An important class of limit states is those for which all the variables are treated as time independent, either by neglecting time variations in cases where this is considered acceptable or by transforming time-dependent processes into time-invariant variables (e.g. by using extreme value distributions). The failure probability for a *time-invariant* reliability problem may in general be expressed by:

$$P_{\mathrm{f}} = P[g(\mathbf{x}) \leq 0] = \iint_{g(\mathbf{x})\leq 0} f_{\mathbf{x}}(\mathbf{x})\mathrm{d}\mathbf{x} = \iint_{\mathbf{x}} I[g(\cdot)] f_{\mathbf{x}}(\mathbf{x})\mathrm{d}\mathbf{x} \qquad 11.25$$

where $g(\mathbf{x})$ is the limit state function, $\boldsymbol{X}$ is the set of n random variables used to formulate the problem, and $f_{\boldsymbol{x}}(\boldsymbol{x})$ is the joint probability density of the vector $\mathbf{X}$. $I[g(\cdot)]$ is an indicator function, which is 0 and 1 for $g(\boldsymbol{x}) > 0$ and $g(\boldsymbol{x}) \leq 0$, respectively, the expression $g(\boldsymbol{x}) \leq 0$ corresponding to failure. Examples of failure functions, $g(\boldsymbol{x})$, are given in Section 11.2. The integral of Eq. (11.25) may be calculated by direct integration, simulation or FORM/SORM methods (First Order/Second Order Reliability Methods) as described in, e.g., textbooks such as Madsen *et al.* (1986) and Melchers (1999). A brief account of the reliability calculation is given here.

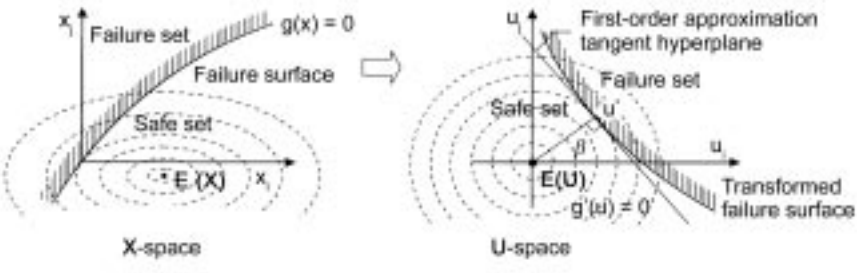
The reliability index, β, is defined as:

$$\beta \equiv -\Phi^{-1}(P_{\mathrm{f}}) \qquad 11.26$$

where $\Phi(\cdot)$ is the cumulative standard normal distribution. Hence, the *reliability index* β is uniquely related to the *failure probability*, P_{f}.

FORM is an efficient method which determines the integral by transforming the problem from the space $\mathbf{x}$ of physical variables to a standard normal space $\mathbf{u}$ and approximates the failure surface by a linear surface which is a tangent to the

© 2008 Woodhead Publishing Limited



11.6 Schematic illustration of FORM analysis for general $g(\mathbf{x})$ function.

initial failure surface at the point with the shortest distance from the origin. This point is called the *β-point* or the *design point*. Schematically, the procedure is illustrated in Fig. 11.6, where the first step is to map the limit state from the real space to the standard normal space. The SORM correction takes the curvature of the failure surface at the design point into account.

11.8.5 Time-variant *R* and *S*

In general, R and S are functions of the time. For instance, the ultimate resistance may be a slowly decreasing function with time due to crack growth (fatigue) or corrosion. Load effects due to waves clearly vary with time, and a stochastic process model is required to describe these phenomena.

If there is no strength degradation and the load effect is stationary, the annual probability of overload failure in the time t_L may be determined by taking the mean load effect as the expected maximum value in the reference period t_L, e.g. the annual maximum, and by including the statistical uncertainty of this maximum together with other (model) uncertainties in the load (effects).

The relation between the failure probability per year and n years can be investigated by formulating the probability in n years as follows:

$$P_f(T) = P[(M_I \leq 0) \cup (M_2 \leq 0) \ldots \cup (M_n \leq 0)] \qquad 11.27$$

where M_i refers to the failure function for year i (annual failure). The failure probability is bounded by $P(M_i \leq 0)$ and $n \cdot P(M_i \leq 0)$, depending upon the correlation between failure in individual years. Consider in this connection, for instance, Eqs (11.21a, b) that describe the load on fixed platforms. Here the model uncertainty X_m will be identical from year to year while the annual maximum wave height, relevant as the variable for H when calculating the annual failure probabilities, is independent from year to year. If only these two variables are considered as random with lognormal distribution, the correlation between the load (effects) in two different years will approximately be:

$$\rho = \frac{V_{Xm}^2}{V_{Xm}^2 + \alpha^2 V_H^2} \qquad 11.28$$

© 2008 Woodhead Publishing Limited

For $V_{X\mathrm{m}} = 0.3$, $\alpha = 1.6$ and $V_H = 0.15$, ρ becomes approximately 0.6.

While reliability problems involving a single, time-variant load effect $X(t)$ and otherwise time-independent variables ($\boldsymbol{Z}$) can be readily formulated in terms of Eq. (11.25), this is not the case when the load effects are a vector process, $\boldsymbol{X}(t)$. Under such circumstances, the conditional failure probability $P_{\mathrm{f}}(\boldsymbol{z})$ for a given $\boldsymbol{Z} = \boldsymbol{z}$ can be determined by estimating the rate of crossing from the safe to the failure domain; see, e.g., Hagen and Tvedt (1991) and Beck and Melchers (2004). Instead of formally considering the vector outcrossing, the scalar $g(X(t), \boldsymbol{z})$ can be sampled for given $\boldsymbol{z}$ (Videiro and Moan, 1999). The unconditional P_{f} is then obtained by taking the expectation of $P_{\mathrm{f}}(\boldsymbol{Z})$ over $\boldsymbol{Z}$.

Determination of the failure probability when the resistance is degrading and the structure is subjected to a stochastic loading requires a truly time-variant approach; see, e.g., Madsen *et al.* (1986). Fortunately, accurate simplified methods are available, e.g. that of Ayala-Uraga and Moan (2007b), who deal with the time-variant reliability problem in which degradation is due to crack growth. This issue is briefly described in Section 11.9.4.

11.8.6 Concluding remarks concerning calculation of reliability

In general it should be noted that FORM and SORM are approximate reliability methods. The advantage of these methods is that they are fast. FORM and SORM have proved to be useful tools for evaluating reliability of marine structures. But these methods need to be verified by simulation. Simulation can then be used to verify if this local estimate is sufficient as an estimate of the global reliability when there is more than one estimation point. Simulations by crude Monte Carlo and importance sampling methods should be carried out with a number of simulation samples not less than $100/P_{\mathrm{f}}$ where P_{f} denotes the failure probability.

In connection with system reliability (Section 11.10) as well as Bayes' statistics (Section 11.11), it is necessary to determine the probability of union and intersection of failure or inspection events. FORM/SORM and Monte Carlo simulation methods may be applied. Particular caution should then be exercised when linearizing the failure functions in FORM or SORM analyses.

Besides providing an estimate of the failure probability, reliability methods also give importance and sensitivity measures. The parametric sensitivity factor gives the change in failure probability (through change in reliability index) to an increment $\Delta\theta$ of the parameter θ, whether it is a statistical distribution parameter or a deterministic parameter. Hence, the sensitivity of the reliability index is given by Eq. (11.26) is expressed by

$$\Delta\beta = \frac{\partial\beta}{\partial\theta} \cdot \Delta\theta \tag{11.29a}$$

where $\partial\beta/\partial\theta$ for the approximate reliability index in Eq. (11.24) is:

© 2008 Woodhead Publishing Limited

$$\frac{\partial\beta}{\partial\mu_R} = \frac{1/\mu_R}{\sqrt{V_R^2 + V_S^2}}, \frac{\partial\beta}{\partial V_R} = -\frac{\ln(\mu_R/\mu_S)}{\sqrt{V_R^2 + V_S^2}} \cdot \frac{V_R}{V_R^2 + V_S^2} = -\beta\frac{V_R}{V_R^2 + V_S^2} \qquad 11.29b$$

The FORM and SORM methods give parametric sensitivity factors and uncertainty importance factors for the reliability index. The directional simulation method provides parametric sensitivity factors of the reliability index.

11.8.7 Application of reliability methods to calibrate ultimate limit state (ULS) criteria in codes

Time-invariant reliability methods have been extensively used to calibrate ultimate strength code checks based on partial safety factors, to comply with a certain target reliability level (Melchers, 1999). This application is centred on current design practice, in the sense that the $g(\ )$ function can be based on the relevant design equations in an existing code. The main result of the calibration is more consistent safety factors.

In the previous section it is shown that P_f is uniquely defined by the reliability index β. It may also be shown that, for a specific case (design equation, uncertainty measures of R and S, etc.), a unique relationship between β and partial factors γ can be established, so that the design values are given by $Q_d = \gamma Q_c$. However, this would imply that a safety factor will vary depending upon the case at hand. Such an approach, however, will not be convenient to use in practical design. For this reason design codes are established by specifying a set of partial factors γ_i that would yield a P_f or β as close as possible to the desired target level, P_{ft} or β_t for different design cases.

This feature will be illustrated by a simple example, by considering the design format in Eq. (11.1a) and by assuming that the characteristic values are expressed by the (true) mean values of the random variables R and S_i as $\mu_R = B_R R_c$ and $\mu_{Si} = B_{Si} S_{ic}$ where B_R and B_{Si} are 'bias' factors. Table 11.4 illustrates a typical set of uncertainty measures.

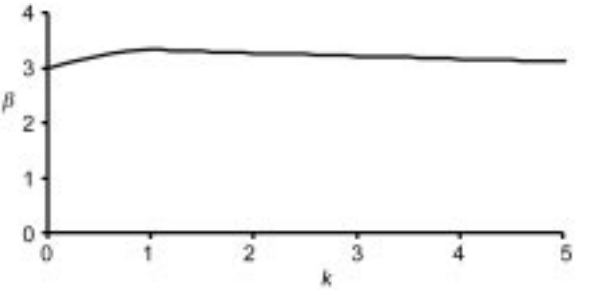
The aim of this example is then to determine one set of $\{\gamma_R, \gamma_{S1}, \gamma_{S2}\}$, with $\gamma_R = 1.15$, which should be applied to all combinations of action effects S_{1c} and S_{2c}, and yield a P_f and β as close as possible to the target values. Here the reliability is estimated by assuming that the R and S_i have a normal distribution.

This task is commonly denoted 'calibration of partial factors' or 'code

Table 11.4 Probabilistic character of random variables

Variable X_i	$\beta_{X_i} = \dfrac{\mu_{X_i}}{X_{i(k)}}$	Coefficient of variation V_{X_i}
R	1.15	0.12
S_1 (permanent)	1.05	0.10
S_2 (variable)	0.75	0.30

© 2008 Woodhead Publishing Limited



11.7 Safety index β as a function of the action ratio k for an 'optimal' set of action factors $\gamma_{S1} = 1.4$ and $\gamma_{S2} = 1.3$.

calibration'. γ_1 and γ_2 are then determined so that $|(\beta - \beta_t)|_{min}$ for, say, an assumed range of $k = S_{1c}/S_{2c} = (B_{S2}/B_{S1})(\mu_{S1}/\mu_{S2})$ for $0.2 < k < 5.0$. Here,

$$\Pi = \sum_{i=1}^{9} (\beta_i - \beta_t)^2,\ \beta_t = 3.0,\ \text{is minimized} \qquad 11.30$$

The relatively high γ_1 in this case is due to the large 'bias' (B_{S1}) of S_1. A plot of β as a function of k is shown in Fig. 11.7.

In the above example of calibration, one set of partial factors $\{\gamma_R, \gamma_{S1}, \gamma_{S2}\}$ was applied. It would normally be necessary to apply several sets to ensure a close fit to the target level, $\beta_t(P_{ft})$ for the relevant range of S_{ic}/S_{2c}.

Structural reliability methods have been applied to calibrate ULS code requirements (Fjeld, 1977; NPD, 1977). Later there was significant effort by API (Moses, 1987; Lloyd and Karsan, 1988) and Jordaan and Maes (1991) to develop a load and resistance factor design for jackets. In certain situations when a new design falls outside the scope of existing codes, reliability analysis has been applied ad-hoc to establish design criteria. This was the case when the first offshore production ship was designed some years ago. It then became clear that application of the ship rules for merchant vessels and existing offshore codes differed significantly, implying a difference in steel weight of the order of 20–30%. Moan (1988) conducted a study to establish ultimate strength criteria for this type of vessel, which complied with the inherent safety level in the existing NPD code for offshore structures. An evaluation of previous calibration efforts for offshore codes was provided by Moan (1995) in conjunction with the ISO effort to harmonize codes for offshore structures (ISO 19900, 1994).

11.9 Fatigue reliability

11.9.1 Elementary reliability format

The elementary reliability format (11.24) may also be used to obtain an estimate for the fatigue reliability based on S-N formulation. It is then noted from Eqs (11.2a) and (11.6a) that Eq. (11.24) can be used with $R = \Delta$ and $S = D$.

© 2008 Woodhead Publishing Limited

Moreover, if only the dominant variables s_0 and K are taken as random variables with lognormal distribution and other parameters are taken as constants, the accumulated D, according to Eq. (11.5), is characterized by

$$\mu_D = k \cdot \frac{\mu_{S0}^m}{\mu_K} \cdot \sqrt{\frac{1 + V_K^2}{1 + m^2 V_{S0}^2}} \tag{11.31a}$$

$$V_D^2 = \ln\left(1 + V_K^2\right)\left(1 + m^2 V_{S0}^2\right) \approx V_K^2 + m^2 V_{S0}^2 \tag{11.31b}$$

$$k = N_T \cdot \Gamma(m/B + 1)/(\ln N_0)^{m/B} \tag{11.31c}$$

The failure probability refers to the time period T, with N_T stress cycles.

The implicit P_f in the fatigue design check (Eq. 11.6b) $D_\mathrm{c} \leq \Delta_\mathrm{all}$ can be estimated using the β_LN in Eq. (11.24) as a measure of reliability. Based on the equality in the design equation and using $D_\mathrm{c} = k \cdot \mu_{S0}^m / K_\mathrm{c}$ and $\mu_D \approx k \cdot \mu_{S0}^m / \mu_K$, Eq. (11.24) may be written as

$$\beta_{\mathrm{LN(fatigue)}} \approx \frac{\ln\left(\mu_\Delta / \mu_D\right)}{\sqrt{V_\Delta^2 + V_D^2}} = \frac{\ln\left[\left(\mu_\Delta / \Delta_\mathrm{all}\right)\left(\mu_K / K_\mathrm{c}\right)\right]}{\sqrt{V_\Delta^2 + V_D^2}} \tag{11.32}$$

Typically $\mu_\Delta = 0.6$–0.9 and $V_\Delta = 0.2$–0.3 (Wirsching, 1983). Here, it is assumed that $\mu_\Delta = 0.8$ and $V_\Delta = 0.25$. The characteristic value K_c is determined as the mean value minus two standard deviations. With the relevant uncertainty in S-N curves this implies a μ_K / K_c of the order 2.5 to 3.3. Here this ratio is taken as 3.0. The uncertainty in the S-N curves typically corresponds to a V_K of 0.4–0.5. The uncertainty in V_{S0} consists of contributions from the load and global load effect calculation, and the total uncertainty would correspond to a V_{S0} in the range 0.15–0.30. Based on Eq. (11.32) V_D would be of the order of 0.75. Hence, $\beta_\mathrm{LN} = 1.33 \cdot [0.88 - \ln(\Delta_\mathrm{all})]$. This means that $\beta_\mathrm{LN} = 1.2$ when $\Delta_\mathrm{all} = 1.0$, implying a P_f in the service life that is about 0.12. A value of $\Delta_\mathrm{all} = 0.1$ on the other hand corresponds to $\beta_\mathrm{LN} = 4.2$ and a P_f in the service life that is about 0.13×10^{-4}.

More refined fatigue reliability models can be established by using fracture mechanics to model the fatigue behaviour or by modelling the random variables in a more refined manner. Such models are especially relevant in connection with reliability analysis involving additional information due to inspection, as discussed in Section 11.11.

11.9.2 Hazard rate

Time-dependent reliability problems may be solved by means of the hazard function, which is based on conditional probability theory. In principle the hazard function or hazard rate may be interpreted as the frequency of failure per unit of time. Let $F(t)$ be the distribution function of the time-to-failure of a

© 2008 Woodhead Publishing Limited

random variable T, and let $f(t)$ be its probability density function. Then the hazard rate $h(t)$ is defined as (see e.g. Melchers, 1999)

$$h(t) = \frac{f(t)}{1 - F(t)} \tag{11.33}$$

This expression represents the probability that the structure of age t will fail in the interval $t + \Delta t$, given that it has survived up to time t, namely

$$h(t) = P[T \leq (t + \Delta t) | T > t] = \frac{P[t \leq T \leq t + \Delta t]}{\Delta t \cdot (1 - P[T \leq t])}$$

$$= \frac{\mathrm{d}P_{\mathrm{f}}(t)/\mathrm{d}t}{1 - P_{\mathrm{f}}(t)} = -\frac{\phi(-\beta(t))}{1 - \Phi(-\beta(t))} \cdot \frac{\mathrm{d}\beta(t)}{\mathrm{d}t} \tag{11.34}$$

It is therefore an advantage to use hazard rates in time-dependent problems, such as fatigue, over the traditional procedure of cumulative failure probabilities, since hazard rates consider the history of the structure, e.g. the degrading effect is accounted for.

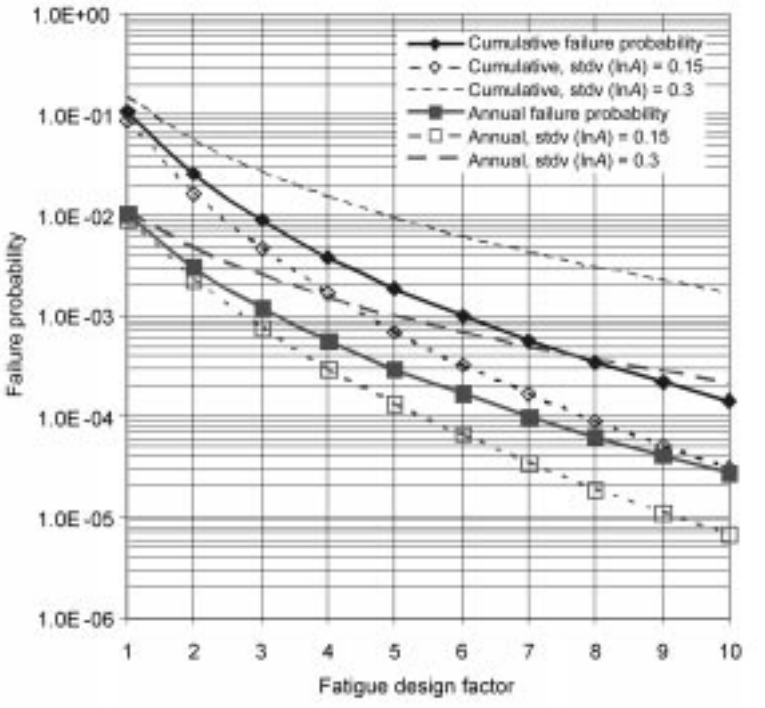
11.9.3 Fatigue reliability as a function of fatigue design factor

Figure 11.8 shows the cumulative failure probability and the (maximum) hazard rate after 20 years as a function of the fatigue design factor, FDF $= 1/\Delta_{\mathrm{all}}$, when the design equation (11.6) is applied. For the base case of uncertainty measures it is seen that the difference between the implied probabilities for a FDF of 1 and 10 is nearly three orders of magnitude. The maximum hazard rate is about 1/10 to 1/4 of the cumulative probability, while the average hazard rate in 20 years is 1/20 of the cumulative probability. The sensitivity of the implied hazard rate and cumulative failure probability to the uncertainty in the loading is investigated. While in the base case the standard deviation of $\ln A$ (where A is the scale parameter of the Weibull distribution of stress ranges) is 0.198, a lower bound of 0.15 and an upper bound of 0.30 are considered. The effect of the uncertainty measure is particularly significant for large FDFs.

11.9.4 Time-variant interaction between strength degradation and overload failure

In the fatigue analysis the cyclic loading is assumed to be steady, without account of sequence effect and the occurrence of extreme stresses that can cause fracture before the fatigue life is exhausted. For instance, S-N curves refer to constant amplitude loading and the approach used implies that variable amplitude loading is represented by an equivalent constant amplitude loading. However, the resistance to fracture or rupture decreases as the crack grows. Fracture failure may be expressed by the stress intensity factor K_{I} as follows:

© 2008 Woodhead Publishing Limited



11.8 Reference values for fatigue failure probability and hazard rate for a structure in a harsh environment, as a function of the fatigue design factor FDF, which is multiplied by the service life to get the design fatigue life. The major uncertainties are $\sigma \ln C = 0.514$ while the uncertainty of the scale parameter A is varied. The mean value of A is chosen to give the relevant FDF (Moan, 2004).

$$K_I = Y(a(t)) \cdot S \cdot \sqrt{\pi \cdot a(t)} \geq K_{IC} \tag{11.35}$$

where $a(t)$ is the crack size at time t, $Y(a)$ is a function of the geometry adjacent to the crack, and K_{IC} is a material parameter. S is the stress range that varies randomly with time.

Failure can then occur when a high stress occurs at a crack size well below the critical one from a fatigue point of view. The problem of calculating the reliability under these circumstances is truly a *time-variant* reliability problem and is very time consuming, especially when the long-term variability of sea states is to be taken into account (Madsen *et al.*, 1986). However, it has been demonstrated (Marley and Moan, 1992; Ayala-Uraga and Moan, 2007b) that the reliability in many situations can be efficiently calculated by replacing the time-variant problem with a time-invariant one. This is achieved by calculating the probability of fracture in the service life using the fatigue crack size at the end of the service period. This approach is conservative, but only slightly.

© 2008 Woodhead Publishing Limited

11.10 Systems reliability

11.10.1 General

Ultimate and fatigue design criteria in current codes are based on component failure modes (limit states) and commonly a linear global model of the structure to determine the load effects in the components. However, an approach based on global (system) failure modes of the structure is desirable because significant consequences, e.g. fatalities, will primarily be caused by global failure. A suitable systems approach is also necessary to obtain the optimal balance between design and the inspection plan since it is normally based on a certain damage tolerance, especially when the inspections rely on detecting flooded or failed members.

In the systems approach the relevant structure is assumed to be composed of different physical components (members, joints, piles, etc.) which may each have different failure modes, e.g. different collapse, fracture or fatigue modes.

System failure is then expressed mathematically by load and resistance parameters relating to all failure modes for all components, and the systems failure probability is calculated by the probabilistic properties of these parameters, e.g. Melchers (1999). Broadly speaking, this may be achieved by a failure mode (or survival mode) analysis, or direct-simulation methods as illustrated for offshore structures by Karamchandani (1990) and Moses and Liu (1992).

The failure mode analysis consists of the following steps:

1. Identifying the various sequences of component failures (system failure modes), ES_i, considering members, joints and other components.
2. Establishing a mathematical expression for the events of each sequence, ES_i, based on structural mechanics. The ith event sequence (ES_i) may involve failure of n_i components such that

$$ES_i : E_{i_1}^{(\ldots)} \cap E_{i_2}^{(\ldots)} \cap \ldots \cap E_{i_n}^{l \ldots ni-l} \tag{11.36}$$

   where $E_{i_j}^{(\ldots)}$ is the event that component j fails given that $j - l$ components have already failed. The numbers of these components are listed in the superscript $(\ldots)$.
3. Establishing probabilistic measures for the random variables involved.
4. Calculating the failure probability of the system.

In the following section, general system reliability analyses based on the failure mode approach are briefly reviewed to establish a basis for the simplified methods currently applied for jacket structures, e.g. in PIA (Kirkemo, 1989).

Failure of redundant offshore structures may also be initiated by a fatigue failure or a fatigue-induced fracture. If repair is not accomplished, a second fatigue or overload failure may occur. Even if the damage is detected, it may not

© 2008 Woodhead Publishing Limited

be repaired until some time later, depending upon weather conditions. The increased stress in the remaining members will contribute to this second failure. While progressive overload failures are assumed to take place instantly (during the 18–20 s period of a storm wave), fatigue failures occur at different points in time.

For each sequence (i) of fatigue failures, the failure functions for successive failures in each mode should be established (Shetty, 1992; Dalane, 1993). This task is even more complex than for overload failure, because the successive failures depend upon the (random) time between different failure events (memory effect).

Modelling the uncertainties in loads and resistances in the components of the system is a crucial task. The system approach in addition requires an estimate of the uncertainty of the system model as well as the correlation between variables in the different failure functions that represent the system.

Correlation in strength variables is provided if joints belong to the same 'batch', since the between-batch variability is predominant. Correlation in stress due to common hydrodynamic factors depends upon location in the same vertical truss plane, and closeness in space. Correlation in stress concentration factors depends upon geometric similarity. The correlation will be 1.0 for joints with identical geometry.

While the failure probability of a series system with n components may vary by a factor of n depending upon the correlation, the failure probability of a parallel system may vary even more, depending upon correlation and component characteristics.

Typically, load uncertainties predominate in the calculation of the probability of wave overload of jackets, while load and resistance uncertainties are of the same order of magnitude in fatigue problems. Also, the correlation between component failure modes is less in fatigue. For fatigue failure modes the ratio of the probability of the first failure and the system failure probability will, hence, be large. Similarly, the small correlation between fatigue and overload failure events implies large systems effects for failure modes comprising fatigue events and a single overload failure.

Having established the limit state $g_{ij}^{(\ldots)}(\ )$ and uncertainty measures for all random variables, the failure probability may be calculated using

$$P_{\mathrm{fSYS}} = P[F_{\mathrm{SYS}}] = P\left[\bigcup_{i=l}^{N}\bigcap_{j=l}^{ni}\left(g_{ij}^{(\ldots)}(\ ) \le 0\right)\right] \qquad 11.37$$

by considering N system failure modes, each mode involving a sequence of ni component failures. The probability is estimated by FORM/SORM, bounding techniques or simulation methods. Due to the effort involved, it is important to apply some kind of technique to limit the number (N) of failure modes.

© 2008 Woodhead Publishing Limited

11.10.2 Simplified systems analysis of framed offshore tower structures

For special cases simplified methods may be applied to estimate the system failure probability. For instance, the ultimate (overload) system failure probability for jackets under extreme sea loading can be estimated by considering only few systems modes, i.e. by referring both the load and resistance to a given load pattern and using the (overall) base shear as variable. This model has been validated for cases where the load uncertainties are dominant and the component forces are highly correlated (Wu and Moan, 1989; De *et al.*, 1989).

This approach may be extended to include fatigue failure modes, using the basic overload case as the reference case. A variety of failure sequences should then in principle be considered. A first approximation to P_{fSYS}, considering both overload and fatigue failure modes, may be achieved by

$$P_{\mathrm{fSYS}} = P[F_{\mathrm{SYS}}] \approx P[F_{\mathrm{SYS(U)}}] + \sum_{j=l}^{n} P[F_j] \cdot P[F_{\mathrm{SYS(U)}}|F_j] \qquad 11.38$$

where $F_{\mathrm{SYS(U)}}$ is the overload system failure and F_j is the fatigue failure of component j. It is noted that the first term then accurately covers all pure overload failure sequences, i.e. all kinds of failure modes such as $F_{\mathrm{SYS}(\mathrm{U}_i)}$, $F_{\mathrm{SYS}(\mathrm{U}_j)}$, $F_{\mathrm{SYS}(\mathrm{U}_k)}$, …. The main approximation in Eq. (11.38) is the neglecting of sequences initiated by component overload followed by component fatigue failure, or of sequences initiated by fatigue failure and followed by more fatigue or overload failures. This approximation is non-conservative. On the other hand, disregarding the correlation between the failure modes that are included, Eq. (11.38) is conservative.

The first two terms of Eq. (11.38) are easily interpreted and calculated. The failure probability P_{fSYS} may most conveniently be referred to the service life or a period of a year. $P(F_j)$ is then conservatively computed as the probability of fatigue failure in the service life. In principle $P(F_{\mathrm{SYS(U)}}|F_j)$ should be calculated as the probability of overload failure in the remaining time of the service life after fatigue failure. However, if it is assumed that inspection is carried out and that fatigue failures (of the complete member) can be reliably detected, e.g. by an annual visual inspection, the latter failure probability may be calculated as an annual overload probability.

To estimate P_{fSYS} as an annual probability, the fatigue failure event F_j could be split into mutually exclusive events F_{jk}, which denote fatigue failure of component j in year k, given survival up to that time. The conditional probability of $F_{\mathrm{SYS(U)}}$ given F_{jk} is then calculated as the probability of overload failure in the period from year k to the end of the service life. Alternatively, if inspections with reliable detection of member failure are assumed, the probability of overload failure could be referred to all annual values, as mentioned above.

The probability of ultimate failure of an intact or damaged system may be

© 2008 Woodhead Publishing Limited

calculated by a single mode approach, based on a single resistance (R_{sys}) and load effect (S_{sys}) both referred to the base shear force. While FORM/SORM and simulation methods can be applied for this purpose, a simple approach based on log-normally distributed resistance and load effect is applied herein. The *annual* reliability index β is

$$\beta = \frac{\ln\left(\frac{\mu_R}{\mu_S}\right)}{\sqrt{V_{R_{\text{sys}}}^2 + V_{S_{\text{sys}}}^2}} = \frac{\ln\left(\frac{B_R}{B_S}\text{REF}\right)}{\sqrt{V_{R_{\text{sys}}}^2 + V_{S_{\text{sys}}}^2}} \tag{11.39}$$

where μ and V denote mean and COV, respectively. The mean values for strength and load are related to their respective characteristic (nominal) values by

$$\mu_{R,\text{sys}} = B_R R_{\text{c,sys}}, \quad \mu_{S,\text{sys}} = B_S S_{\text{c,sys}} \tag{11.40}$$

where B_R and B_S are bias factors. Subscript c indicates characteristic (nominal) values. For S_{sys}, the characteristic value $S_{\text{c,sys}}$ is defined as the most probable 100-year maximum load from the pushover analysis. For R_{sys}, the characteristic value $R_{\text{c,sys}}$ is defined according to characteristic material properties. REF is defined as $R_{\text{c,sys}}/S_{\text{c,sys}}$. The ultimate strength of jackets and other framework platforms can efficiently and accurately be calculated by nonlinear finite element analysis (Moan *et al.*, 2002b).

The main contribution to the base shear load variable S_{sys} stems from wave loads. The load effect may be approximated by a design regular wave approach, with a fixed ratio between wave height and length, as expressed by

$$S_{\text{sys}} = c\psi H^{\alpha} \tag{11.41}$$

where c is a constant, ψ is the model uncertainty, H is the wave height and α is a wave force exponent for the given structure. The uncertainty in S is then given by the model uncertainty and that in the wave height. If these variables are assumed to be lognormal,

$$\mu_{S,\text{sys}} \cong c \cdot \mu_{\psi} \cdot \mu_{H_1}^{\alpha} \tag{11.42a}$$

$$V_{S,\text{sys}}^2 = V_{\psi}^2 + \alpha^2 V_{H_1}^2 \tag{11.42b}$$

where $\mu_{S,\text{sys}}$ is the mean value of the annual maximum wave height. The characteristic value of S_{sys} with annual exceedance probability of 10^{-2} is given by

$$S_{\text{c,sys}} = c \cdot H_{100}^{\alpha} \tag{11.43}$$

This implies that $B_S = \mu_{\psi}(\mu_{H1}/H_{100})^{\alpha}$.

This simplified approach has especially been applied in connection with inspection planning as discussed by, for example, Kirkemo (1989) and Moan *et al.* (1999).

© 2008 Woodhead Publishing Limited

11.11 Updating of variables in reliability analysis

11.11.1 General principle

Reliability measures may be updated based on additional information by updating variables, updating events (such as probability of failure), and updating statistics at large.

The distribution of a variable can be updated by procedures developed by Itagaki *et al.* (1983), Shinozuka and Deodatis (1989), and others, as reviewed by Yang (1994). Over the last decade FORM/ SORM techniques have been used to develop general and efficient techniques for event updating; see, e.g., Madsen *et al.* (1986). When the variables are updated, the failure probability can be easily calculated based on the new safety margin in which the updated variables are used to replace the original ones. However, if several variables are updated based on the same inspection event, the change of correlation between the updated variables due to the common information used should be accounted for.

This updating of A given the information B is based on Bayes's theorem:

$$P(A|B) = P(A \cap B)/P(B) \tag{11.44a}$$

where A and B are arbitrary events, '|' indicates the start of a conditioning event, and the operator '$\cap$' means intersection, i.e. both of the events A and B shall occur. The theorem may also be written as:

$$P[A_j|B] = P[B|A_j]P[A_j] \Big/ \left(\sum_{i=1}^{n} P[B|A_i]P[A_i] \right) \tag{11.44b}$$

11.11.2 Example of updating distribution of variables

First, updating of variables is illustrated by a simple example. Consider that the initial crack depth follows an exponential distribution, with the mean crack size λ_0 as parameter. The probability of crack detection, POD, curve is often approximated by a cumulative exponential function, with the crack depth λ and the minimum detectable crack size a_{th} as parameters. By assuming a_{th} equal to zero, the density function for the initial crack depth, $f_{A0}(a)$, and POD curve, $P_{\text{D}}(a)$, are given by:

$$f_{A0}(a) = \frac{1}{\lambda_0} \mathrm{e}^{-a/\lambda_0} \tag{11.45}$$

$$P_{\text{D}}(a) = 1 - \mathrm{e}^{-a/\lambda} \tag{11.46}$$

The unknown parameters λ_0 and λ can be determined by using the results of the first and second inspection, where the first inspection resulted in a no-finding. In principle this method may be based on fabrication and fatigue cracks. However, if fatigue cracks are used, they would have to be backtracked to the time of the respective inspection due to the crack propagation. In the work by Moan *et al.*

© 2008 Woodhead Publishing Limited

(2002a), only fabrication defects were used to estimate the two parameters. By using Bayes's theorem and defining the events A_j and B to be that the crack size is in an interval $(a,\ a + \mathrm{d}a)$ and detection of a crack with size $(a,\ a + \mathrm{d}a)$, the updated probability density of the crack depth may be obtained by Eq. (11.44b):

$$f_{A,\mathrm{D}}(a) = \frac{f_A(a)P_\mathrm{D}(a)}{\int_0^\infty f_A(a)P_\mathrm{D}(a)\mathrm{d}a} \tag{11.47a}$$

$$f_{A,\mathrm{ND}}(a) = \frac{f_A(a)(1 - P_\mathrm{D}(a))}{\int_0^\infty f_A(a)(1 - P_\mathrm{D}(a))\mathrm{d}a} \tag{11.47b}$$

where the subscripts D and ND refer to the updated density functions of cracks detected and not detected, respectively. Analogous expressions apply for the probability density $f_{A,\mathrm{ND1,D2}}(a)$ of the sizes of cracks that were not detected in the first inspection but were detected in the second inspection. The expected values of cracks detected in the first and second inspections, denoted by $E[A|\mathrm{D1}] = E[A, \mathrm{D1}]$ and $E[A|\mathrm{ND1}, \mathrm{D2}] = E[A, \mathrm{ND1}, \mathrm{D2}]$, respectively, were used to determine the two unknown parameters, λ_0 and λ, based on about 4000 inspections in-service (Moan *et al.*, 2002a).

$$E[A, \mathrm{D1}] = \frac{\lambda + \lambda_0}{\lambda_0}\left[\lambda_0 - \frac{\lambda}{\lambda + \lambda_0}\left(\frac{\lambda\lambda_0}{\lambda + \lambda_0}\right)\right] \tag{11.48a}$$

$$E[A, \mathrm{ND1}, \mathrm{D2}] = \frac{1}{\left(\dfrac{1}{\lambda + \lambda_0} - \dfrac{1}{\lambda + 2\lambda_0}\right)} \times \left[\frac{1}{\lambda + \lambda_0}\left(\frac{\lambda\lambda_0}{\lambda + \lambda_0}\right) - \frac{1}{\lambda + 2\lambda_0}\left(\frac{\lambda\lambda_0}{\lambda + 2\lambda_0}\right)\right] \tag{11.48b}$$

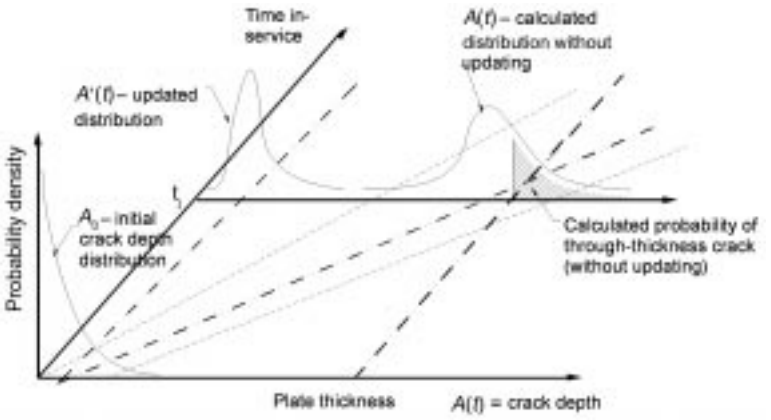
The mean crack sizes in the first and second inspections were determined by correcting the rough data for measurement bias. The actual crack size used is $a = a_\mathrm{rep} - 0.5 + \Delta a$ where a_rep is the reported crack size, 0.5 mm is the grinding increment carried out to size the crack, and Δa is a parameter characterizing the measurement uncertainty, taken to be 0.3. Based on the reported mean values of 1.77 and 1.31 mm, respectively, the unknown parameters mean crack size λ_0 and mean detectable crack size λ were determined to be $\lambda_0 = 0.94$ and $\lambda = 1.95$. A sensitivity study was made (Moan *et al.*, 2002a) to determine the robustness of the data, involving possibly using a threshold value for the POD curve.

11.11.3 Updating of failure probability associated with fatigue crack growth

Reliability updating is relevant in connection with deterioration phenomena such as crack growth, corrosion, etc. Here, crack growth serves as an illustration.

The crack depth may be represented by a random variable $A(t)$, being a

© 2008 Woodhead Publishing Limited



11.9 Initial distribution of crack depth A_0, simulated crack depth $A(t_i)$ at time t_i and updated distribution of crack depth $A'(t_i)$.

function of time t: see Fig. 11.9. The distribution of the crack size at the initial time and a time t are given in the figure. The inspection may be used for updating the distribution function for $A(t)$ into a distribution function representing the variable $A'(t)$ accounting for the inspection. The updating is undertaken by using Bayesian statistics, as discussed below.

The failure probability at time t (N cycles) can be formulated as:

$$P_f = P[a_f - a_N \leq 0] = 1 - F_{A_N}(a_f) \qquad 11.49$$

where a_f and a_N are the crack size at failure and after N cycles, respectively, and $F_{A_N}(a)$ is the cumulative distribution function of the crack size a_N. In general, $a(t)$ is not known explicitly and it would have been difficult to determine this distribution explicitly when taking into account all uncertainties that affect the distribution as well as the effect of inspections. The basic expression for the probability of fatigue failure, therefore, is based upon

$$P_f = P[a_f - a_N \leq 0] = P[M(t) \leq 0] \qquad 11.50$$

where $M(t)$ is given by Eq. (11.11).

If inspection is made at time t_i, our belief in the probability of large cracks must be changed in accordance with the inspection result. The change in our belief of the probability of large cracks depends on the quality of the inspection method, the experience of the operator, and the conditions in which the inspections are carried out. The size of the minimum detectable crack is also represented by a random variable A_d. The distribution of A_d depends on the probability of detection (POD) data valid for the inspection method in question.

For instance, what is the probability of failure (TTC) at time t_2 given that inspection without any finding was carried out at time t_1? The outcomes of inspections are assumed to be no crack detection (ND) or crack detection (D) after N cycles, which can be described by events like:

© 2008 Woodhead Publishing Limited

$$I_{\mathrm{ND}} = a_N - a_{\mathrm{d}} \leq 0 \tag{11.51}$$

$$I_{\mathrm{D}} = a_N - a_{\mathrm{d}} \geq 0 \tag{11.52}$$

The events can be reformulated analogous with the transition from Eq. (11.9) to Eq. (11.11).

The failure probability of a given joint (i) may be updated on the basis of a given inspection event:

$$P_{\mathrm{f,up}} = P[M_i(t) \leq 0 | \mathrm{IE}_j] = P[(M_i(t) \leq 0) \cap \mathrm{IE}_j] / P[\mathrm{IE}_j] \tag{11.53}$$

where $M(t)$ is the failure function for joint i in time period t and IE_j stands for a mathematical expression of inspection events such as, e.g., detection or non-detection of a crack, e.g. Eqs (11.51–11.52).

Bayesian statistics can be applied to update the reliability, for instance, in connection with proof testing of structures or by accounting for inspection results associated with deterioration due to corrosion or crack growth. In this context only the latter issue will be pursued.

To indicate the effect of updating more explicitly, it is convenient to express Eq. (11.44) in terms of reliability indices. Terada and Takahashi (1988) showed that the following approximation is reasonable if the correlation ρ between the events $(M \leq 0)$ and $(\mathrm{IE} \leq 0)$ is less than 1:

$$\beta_{\mathrm{up}} = \frac{\beta_M - \rho A}{\sqrt{1 - \rho^2 B}} \tag{11.54}$$

where $\rho = \alpha_M^{\mathrm{T}} \alpha_{\mathrm{IE}}$, $A = \phi(-\beta_E)/\Phi(-\beta_{\mathrm{IE}})$ and $B = A(A - \beta_{\mathrm{IE}})$, $0 \leq B \leq 1$.

Figure 11.10 illustrates results for reliability updating based on consecutive inspections. When the inspections result in no-finding in situations when cracks are expected, the reliability is increased.

11.11.4 *A priori* versus *a posteriori* effect inspections

The effect of inspection may be viewed in two different ways, depending upon whether it is assessed before inspections are done – i.e. at the design stage – or after the inspection has been carried out. If the effect of inspections is estimated before they are carried out, two outcomes need to be considered, namely (i) crack detection and repair, or (ii) no crack detection. The exact outcome is not known, but the probability of the outcomes can be estimated based on the reliability method.

For the failure probability in time period t, when a single inspection is made at time t_1 and possible cracks detected are repaired, the failure probability in the period $t \geq t_I$ is

$$\begin{aligned} P_{\mathrm{f}}(t) = {} & P[F(0,t_1)] + P[S(0,t_1) \text{ and } F(t_1,t) | I_{\mathrm{D}}(t_1)] \cdot P[I_{\mathrm{D}}(t_1)] \\ & + P[S(0,t_1) \text{ and } F(t_1,t) | I_{\mathrm{ND}}(t_1)] \cdot P[I_{\mathrm{ND}}(t_1)] \end{aligned} \tag{11.55}$$

© 2008 Woodhead Publishing Limited

where $F(t_1, t_2)$ and $S(t_1, t_2)$ mean failure and survival in time period (t_1, t_2); and $I_D(t_1)$ and $I_{ND}(t_1)$ refer to crack detection and non-detection, respectively, at time t_1. It is assumed that repair is carried out when cracks are detected. This fact implies a change in the failure function. Equation (11.55) can be generalized to cover cases with several inspections, with two alternative outcomes.

If, on the other hand, no failure has occurred before time t_1 and no crack is detected at time t_1, the failure probability in the period $t \geq t_1$ is

$$P_f(t) = P[F(t_1, t)|I_{ND}(t_1)] \tag{11.56}$$

The knowledge of survival up to time t_1 and no crack detection at time t_1 reduces the uncertainty and makes the failure probability drop and the reliability index β increase at the time of inspection, as illustrated by the example shown in Fig. 11.10.

It is observed that the two methods described above yield very different values just after inspection. The reliability index for the first method is continuous after updating but exhibits a change in slope after inspection and has almost a horizontal tangent. This means that the failure rate immediately after an inspection is small, for one of two reasons: either the inspection has not revealed a crack or repair has taken place.

A crack with a size close to the critical one is detected with a large probability, and when no crack is detected there is a small probability that the crack can grow to a critical size in a short period, i.e. the time between inspections. If a crack is repaired, the crack size after repair is also expected to be much smaller than the critical size. Also in this case there is a very small probability that the crack can grow to the critical size within a short period after the inspection.

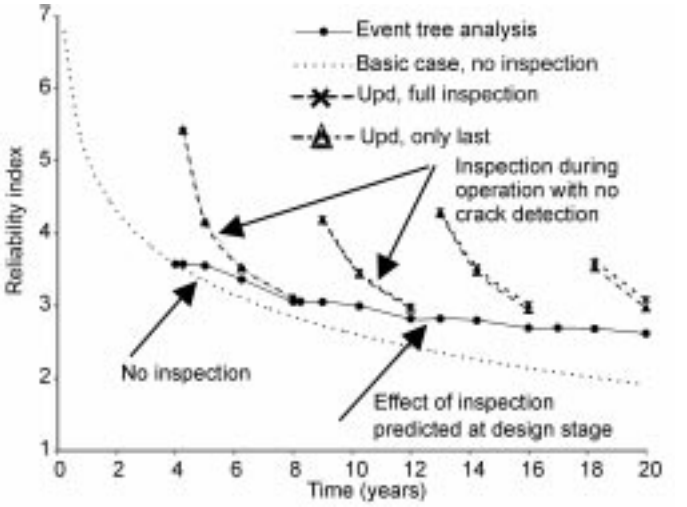
Figure 11.10 shows fatigue reliability curves updated both at the design stage and during operation. The updated probability at the design stage is assessed by means of an event tree analysis approach, assuming that four inspections are carried out every fourth year. Two possible outcomes are assumed at every inspection. The updating during operation is made under the assumption that no crack is found. It is observed that, as the structure ages, the effect of updating is larger.

In the example in Fig. 11.10 with in-service inspections the effect of all inspections with no crack detection is accounted for. It was shown that it is only the last inspection that dominates and needs to be accounted for when the previous inspection outcomes are *no detection*.

11.11.5 Reliability updating associated with service life extension

The updating methodology is useful in connection with extension of service life for structures with joints governed by the fatigue criterion. In such cases the

© 2008 Woodhead Publishing Limited



11.10 Fatigue failure probability updated at the design stage (event tree analysis) and with in-service inspection (no crack found) using typical uncertainty measures. The major uncertainties are $\sigma_{\ln C} = 0.514$ and $\sigma_{\ln A} = 0.198$. Mean detectable crack depth is 1.5 mm (Ayala-Uraga and Moan, 2002).

design fatigue life is in principle exhausted at the end of the planned service life. However, if no cracks have been detected during inspections, a remaining fatigue life can be demonstrated. However, it is not possible to bring the structure back to its initial condition by inspection only. This is because the mean detectable crack size typically is 1.0–2.0 mm, while the initial crack size is 0.1–0.4 mm. The fatigue damage D actually caused in the service-life can be estimated by updating the fatigue damage, based on the inspection results. When a Bayesian updating of the remaining fatigue life is made, further improvement of the fatigue life can be achieved by grinding to remove the possible crack.

By bringing the fatigue life towards the initial value, inspection can be kept at a minimum. Alternatively, if the members possess sufficient residual strength after development of through-thickness cracks, less effort can be devoted to documenting the remaining fatigue life and an inspection strategy based on flooded member detection could be used to ensure adequate safety. If the global system is sufficiently damage-tolerant, another alternative is to utilize a systems (reliability) approach, as indicated below.

In the approach described above, inspection results are used to update the initial estimates of fatigue loading, crack growth parameters and initial crack size based on an assumed probabilistic nature of these variables. Since only fundamental randomness and 'normal' uncertainties are considered, the updated hazard rate will be very conservative if, e.g., the initial crack size had been accidentally large due to a gross fabrication defect. Additional information about

© 2008 Woodhead Publishing Limited

loads – maybe a second measurement of the crack size, etc. – would then be necessary to achieve a better estimate.

11.11.6 Effect of crack inspection quality

The quality of NDE methods for detection of cracks in metal structures is expressed by a probability of detection (POD) curve, which corresponds to the distribution function of the detectable crack size a_D. POD curves for various NDE methods obtained from different industrial projects have been compiled by Silk *et al.* (1987) and Visser (2002). The continued efforts of UCL (Dover and Rudlin, 1996; Rudlin and Austin, 1996) to assess POD curves for offshore structures are particularly noted. Besides MPI, eddy current, alternate current methods (ACFM and ACPD) and ultrasonic inspection are also considered. Typically, these projects indicate a mean detectable depth of 1.4–1.8 mm if an exponential POD curve is assumed. Moan *et al.* (1997, 2002a) inferred a POD curve with exponential distribution with a mean detectable depth of 1.95 mm, based on data from 3411 underwater NDE inspections of tubular joints in jackets. It is reasonable to consider the data from the latter reference to represent an 'upper bound' of the mean detectable crack size, considering the difficult environmental conditions under which inspections are made. Fujimoto *et al.* (1996, 1997) showed POD curves for Close Visual Inspection (CVI) of ships. The mean detectable crack length is of the order of 40–120 mm, depending upon the access to the crack site.

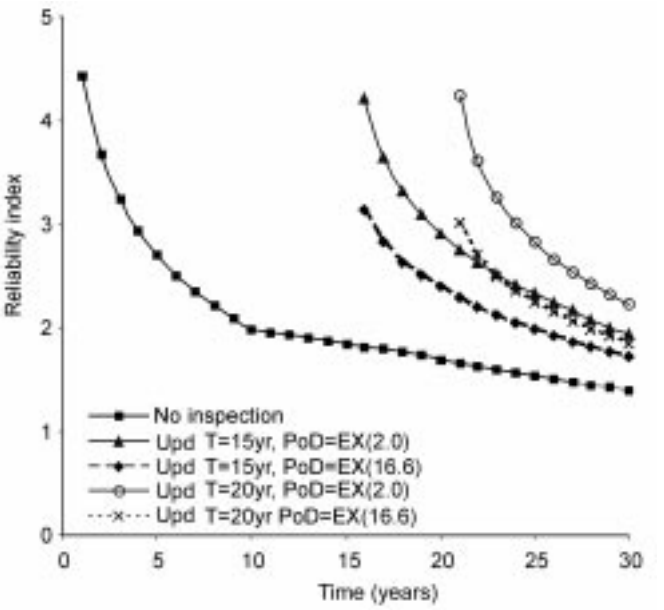
To illustrate the effect of inspection quality on the reliability, consider the use of magnetic particles inspection (MPI) or eddy current technique as compared to a visual inspection (CVI) procedure. The POD curves for NDE and CVI are assumed to be exponentially distributed with mean detectable crack depth of 2.0 and 16.6 mm, respectively. The CVI value corresponds to a mean detectable length of 40 mm. It is assumed that no crack is detected in inspections carried out at 15 and 20 years of service. The results are shown in Fig. 11.11.

Other cases involving inspection with respect to both crack growth and loss of plate thickness due to corrosion, as well as structures exposed to different environmental climates, are shown by Moan and Ayala-Uraga (2008).

11.11.7 Effect of correlation between variables, safety margins and inspection events

The use of inspection results from inspected joints to make statements about inspected and uninspected joints is based on the correlation between inspection events and safety margins. For instance, Eq. (11.53) expresses the failure probability of joint i given an inspection event j which may refer to joint i or another joint. Due to common or correlated variables entering the expressions of safety margins and inspection events, this leads to a certain degree of correlation between them.

© 2008 Woodhead Publishing Limited

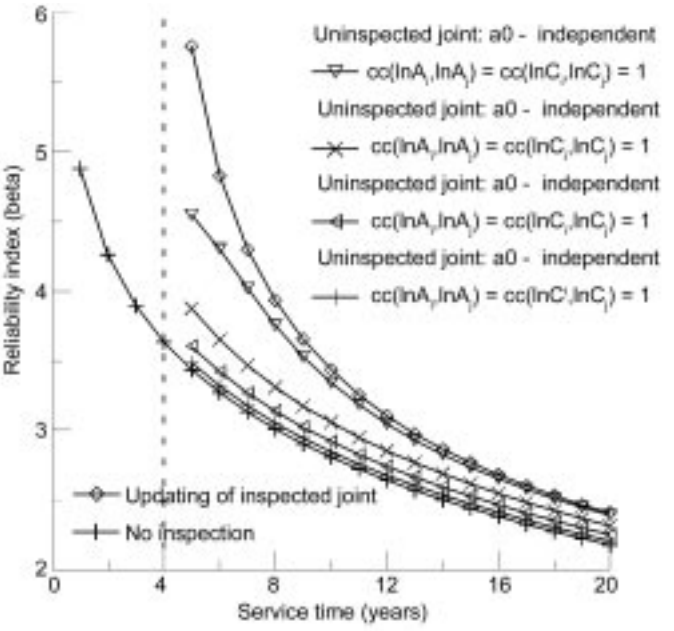


11.11 Updating of reliability based upon inspection with no crack detection after 15 years of a welded joint in a mobile structure with 10 years in harsh conditions, then in benign conditions. The relevant joint is designed for 20 years with an FDF equal to 1 in the harsh environment. The benign environment corresponds to an FDF of 3 in the harsh environment. The major uncertainties are $\sigma_{\ln C} = 0.514$ and $\sigma_{\ln A} = 0.198$. The mean detectable crack depth is varied (Moan *et al.*, 2004).

Offshore structures consist of various components. These joints can be grouped into different sets. It is assumed that all the structural components in the same set have the same or similar material properties and are subjected to the same or similar loading conditions. The information obtained for inspected joints can then be used for the uninspected joints.

Among the random variables in the safety margin, the initial crack size a_{0i} for the cracks in different joints i is regarded as independent. The Weibull scale parameter $\ln A_i$ and the material parameter $\ln C_i$ in different components are treated as partly correlated. The rest of the random variables entering the safety margin, M or inspection event, I are regarded as dependent. Then the correlation coefficient between linearized safety margins and inspection events can be obtained by normalizing the linearized safety margin $M_i(t)$ and inspection event I_j as $\rho = \alpha_M^{\mathrm{T}} \alpha_I$, where α_M and α_I are the linearized directional cosines of the M and I events. Figure 11.12 shows an example to illustrate the effect of correlation between variables involved in the failure and inspection events (Moan and Song, 2000).

© 2008 Woodhead Publishing Limited



11.12 Reliability of a single joint updated through no crack detection with different correlation between M_i and I_j (cc denotes correlation coefficient), based on uncertainty measures used by Moan and Song (2000). The major uncertainties are $\sigma_{\ln C} = 0.514$ and $\sigma_{\ln A} = 0.221$. Mean detectable crack depth is 1.0 mm.

11.11.8 Updating methods in general and reliability software

The updating procedures mentioned above provide updating, e.g., of mean value, standard deviation, etc., of the random variables associated with individual joints or groups of joints. In a given structure there may be different groups of joints, requiring different methods to determine loads and resistances with different uncertainty measures. The inspection results for one group may apply to different groups. The challenge then is to correlate predicted and observed crack occurrences and no occurrences and then adjust model parameters and even the model itself to fit better; see, e.g., Vårdal and Moan (1997).

Reliability software

Methods for reliability analysis of components, especially with time-invariant properties, have become mature, as borne out by the state-of-the-art regarding commercial software packages available (e.g. Schuëller, 2006). While time-variant problems associated with (the slow development of) corrosion are easy to deal with, caution is needed to deal with time-variant fatigue-induced fracture

© 2008 Woodhead Publishing Limited

(e.g. Ayala-Uraga and Moan, 2007b). Even if Monte Carlo simulation and response surface methods can be used to carry out systems reliability analysis, they are still limited because of the complexity of the mechanics as well as of the probabilistic model. In particular, realistic measures of correlation between the variables which describe the various component limit states are lacking.

11.12 Decision making during design of offshore structures and in service

11.12.1 Decisions during design or in service

Reliability methods may be used to support decisions with the purpose of maintaining an acceptable level of safety in an economical manner, during the life cycle of ageing offshore structures. At the design stage only generic data about the variability and uncertainty that affect the reliability are available. Hence, it is important to update the models on the basis of in-service experience. Partly, the theoretical models need to be updated based on service experience with classes of large structures, e.g. jackets, semi-submersibles and ships. However, it is most important to update the models on an individual basis for each structure, depending on its life cycle history (Moan, 2005). The decision making is based on ensuring that the implied reliability complies with the target reliability level.

11.12.2 In-service observations and predictions

Ageing of offshore structures is a complex process of corrosion and crack growth, which is influenced by many factors. In-service experiences are therefore crucial to support laboratory data and theoretical considerations. An overview of experiences with fatigue cracks in offshore structures operating in the North Sea is given by Moan (2005). Sucharski (1997) gives examples of fatigue crack experiences in ships. A brief account of some features of jackets, semi-submersibles and ship-type installations and the experiences with ageing of such structures is given here. A few remarks on corrosion are then made.

For jacket structures consisting of slender members, fatigue failures are confined to the tubular joints where significant bending stresses occur. Fatigue problems are normally confined to limited areas of the structure. Proper fatigue design practice for North Sea jackets emerged during the 1970s. Due to lack of access inside the underwater jacket structure, inspections have been carried out on the outside by divers or by remotely operated vehicles. This fact implies in general much higher inspection/repair costs per joint than for ships and semi-submersibles. Moreover, the geometrical configuration of jackets makes it possible to model system (global) failure as overload or fatigue failure of members or joints, followed by overload failure of one or more trusses/beams. A significant number of inspections have been devoted to North Sea fixed platforms since the

© 2008 Woodhead Publishing Limited

late 1970s, and especially after the fatigue failure of the Alexander Kielland platform in 1980. Vårdal and Moan (1997) compared cracks observed in about 4000 inspections of North Sea jackets with theoretical predictions. It was found that the number of propagating cracks was typically 3 to 10 times higher than predicted. On the other hand, it should be noted that 2–3% of the fatigue cracks detected occur in joints which are not predicted to be susceptible to fatigue. This fact is attributed to the occurrence of gross fabrication defects.

While the most critical joints in semi-submersibles are also tubular joints, they are normally designed to transfer loads by means of membrane stresses, with much less bending than in unstiffened tubular joints in jackets. Fatigue failures that occurred in semi-submersibles in the period 1965–70 led to design requirements. But the implementation of fatigue criteria varied, even for platforms built in the period 1970-80. The total loss of the Alexander Kielland platform was initiated by a fatigue failure. Emergency surveys carried out after this accident on platforms in the North Sea revealed many cracks, especially in brace–column connections (Potthurst *et al*, 1989). In special cases, such as in the case of Alexander Kielland, a detailed post-failure analysis was carried out (ALK, 1981; Moan, 1985). Actually, surveys conducted even up to today involve a significant number of platforms for which fatigue design checks were not explicitly carried out at the design stage. Initially several structural details had a design fatigue life of 2–6 years, or a mean fatigue life of 6–18 years. Even today the brace–column and column–pontoon connections for semi-submersibles with long pontoons present a challenge due to the complex geometry and high stress concentration involved (Vårdal *et al.*, to appear). However, the number of fatigue-prone areas in semi-submersibles is relatively small and the inspections can be focused. Moreover, inspections can to a large extent be carried out from the inside of the structure. This has a significant effect on the quality and costs of inspections.

Cracks have been known to occur in ships for decades. With some exceptions, such as hatch corners in container ships and LNG tanks, explicit fatigue requirements were not introduced before 1991–92. The new fatigue design rules were generally introduced as a response to the significant fatigue problems experienced for side longitudinals of 2–5-year-old VLCC tankers in the Alaska–California trade (e.g. Sucharski, 1997). Thousands of cracks occurred at the intersections between side longitudinals and primary members in tankers. Already when the first purpose-built ship for oil production in the North Sea came up in 1985, it became evident that fatigue of the hull girder was a governing strength criterion. However, this was realized too late to ensure that the vessel was built with adequate fatigue life. The required safety level was then achieved by a more extensive inspection programme, but with the economic penalty of more inspections and crack repairs (Bach-Gansmo *et al.*, 1987). Cracks in the main hull girder will grow continuously until global rupture of the hull occurs. Fatigue failure, as inferred for S-N curves, is normally taken

© 2008 Woodhead Publishing Limited

to be a crack through the plate thickness. For ship hulls, it is therefore necessary to have information about the crack propagation from a through-thickness crack until fracture, and especially the assessment of critical crack size.

The general corrosion rate for unprotected steel in seawater is about 0.1 mm/year. Corrosion rates fluctuate between 0.04 and 1.2 mm/year and in some cases up to 3 mm/year have been found in some ballast tanks (TSCF, 1997). Corrosion rates in ships exhibit a very large scatter depending upon location in the structure. Hence, follow-up of corrosion in service for individual ships becomes important. Normally offshore production platforms are protected with coating or by a cathodic protection. As soon as the corrosion protection system breaks down, free corrosion effects start to take place on the surface of the structural component, which implies a thickness reduction.

11.12.3 Abnormal defects

As mentioned above, the structural reliability methodology described above accounts for failure and crack detection due to normal uncertainties in wave-induced loads (stresses) and fatigue resistance. However, cracks may also occur for other reasons, for example:

- Abnormal initial defect size, e.g. due to wet electrodes
- Abnormal crack propagation, e.g. due to corrosion fatigue caused by overprotection or loss of protection
- Abnormal eccentricity, or other bad design fabrication detailing, causing bending stresses
- Error in load (stress) analysis (environmental conditions, method, stress concentration factor, etc.).

Evidence from in-service inspections and laboratory investigations of fatigue clearly show that 'abnormal' defects could occur. The effect of such an 'abnormal' defect is significant. It is noted, for instance, that more than 80% of the fatigue life is spent in crack propagation in a flat plate from an initial crack size of 0.11 mm to 0.9 mm. These issues are further discussed by Moan (2008). The possible occurrence of such defects could have implication on the design and inspection procedures. Hence, it may be considered whether such events should be taken as a damage condition for ALS criteria. The inspection strategy also needs to reflect the situation.

11.13 Target safety levels in reliability analysis

11.13.1 Analysis methodology

Reliability analysis is a decision tool. Hence, a calculated value of P_f is compared with an acceptable failure probability, P_{ft}, the target level for P_f. In

© 2008 Woodhead Publishing Limited

principle a target level which reflects all hazards (e.g. loads) and failure modes (collapse, fatigue, etc.), ultimate consequences such as fatalities, environmental damage and loss of assets, as well as the different phases (in-place operation and temporary phases associated with fabrication, installation and repair), could be defined with respect to each of the three ultimate consequences and the most severe of them would govern the decisions to be made. If all consequences were measured in economic terms, a single target safety level could be established.

The target safety level should depend upon the following factors (Moan, 2002):

- The method of SRA or QSRA analysis, especially which uncertainties are included
- The failure cause and mode
- The possible consequences of failure in terms of risk to life, injury, economic losses and the level of social inconvenience
- The expense and effort required to reduce the risk of failure.

As indicated above, SRA and QSRA account for different uncertainties, and SRA may in a sense be considered a special case of QSRA. In particular, QSRA accounts for human factors, which may lead to accidental loads and abnormal resistance. Even in SRA the various uncertainties may be assessed in different ways. Clearly, the corresponding target safety levels will differ. It is emphasized that consistent and state-of-the-art SRA methods should be applied in establishing target levels.

11.13.2 Failure cause and mode

The most important distinction between different failure causes is whether they are instantaneous or progressive, i.e. take time. Sometimes the notion *failures preceded and not preceded by a warning* is used. The most relevant practical examples would be a gradually developing failure due to fatigue or other deterioration versus an instantaneous overload failure, respectively. The failure development over time may influence the failure consequences, since a warning may initiate escape and evacuation of personnel, or even taking remedial action before the event progresses to total failure. The most important distinction of structural failure modes is between component and system modes. This fact also has implications on the consequences of failure.

For a statically determinant system under static loading it is observed that the component characteristics, i.e. whether the component behaviour is ideally elasto-plastic (ductile) or brittle, does not have any influence on such systems. For a redundant structure, however, the system strength will depend upon the component characteristics, as well as the system composition of components.

© 2008 Woodhead Publishing Limited

11.13.3 Failure consequences

In principle the target safety level is set with respect to consequences in terms of fatalities or human injury, environmental damage and economic losses. Three consequence classes may be established for offshore structures as shown in Table 11.5. However, besides these consequences the owner/operator of the structure may lose reputation, both from the public as well as from the government. This is a consequence that is hard to quantify, but it may affect the future business at large, and is therefore sometimes considered part of the economic consequences.

To obtain target levels for SRA and QSRA, the ultimate consequences mentioned above need to be related to structural failure modes, which are defined in terms of loss of strength as well as loss of containment. While, for instance, a ship hull girder apparently possesses significant residual strength after failure of individual stiffened deck panels, the loading in the deck panels is primarily due to vertical hull girder bending, and the loading in the different panels is hence fully correlated. This implies that an initial failure will be followed by failure of more panels. Yet, due to the nonlinear behaviour of the deck, some redistribution of loads occurs and yields a certain residual strength beyond first (gross) panel failure.

Fatalities induced by structural failure of offshore structures and ships occur primarily when they capsize or lose their global structural integrity, i.e. system failure occurs. The possible effect of (local) structural failure on flooding and hence capsizing should be noted. Failure of individual components (members, joints) commonly does not lead to fatalities. However, failure of primary transverse frames in a ship hull should be considered a global mode of failure. Failure of hatch covers in open ships could imply a significant risk of flooding and progressive failure. Clearly, the risk of fatalities would depend upon whether or not the structure could be evacuated before or during the accidental scenario. Extreme wave loads that could lead to hull failure are usually associated with severe storms, which make evacuation of the ship very dangerous, and maybe impossible.

Table 11.5 Assignment of overall consequence classes as a function of the consequences of fatalities, pollution and property losses

Consequence class	Description of potential consequences*		
	Fatalities	Pollution	Economic
High	H	S	VH
Medium	Me	Me	H
Low	Mi	Mi	Mi

* Mi – Minor, Me – Medium, H – High, S – Significant, VH – Very High.

© 2008 Woodhead Publishing Limited

The cost–benefit of increasing the safety would be judged differently depending upon the socio-economic system in the geographical region concerned. This is true not only in terms of human fatalities but especially in cases of oil pollution or loss of hazardous materials.

Fatigue criteria should be judged in light of the fact that a through-thickness crack can cause leaks that lead to a possible explosion, e.g. in ballast tanks. Fatigue cracks through the thickness of LNG containment may represent a significant hazard of brittle fracture of the primary hull structure, and/or fire/explosion and, hence, catastrophic consequences.

Ultimate and fatigue design criteria in current design codes are primarily based on *component failure modes* (limit states) and a linear global model of the structure to determine the load effects in the components. However, some codes, notably the NORSOK standards for offshore structures, contain progressive collapse and fatigue design criteria, which have implications for systems failure probability levels. Moreover, recently ULS criteria for the system have been introduced in connection with assessment of existing structures.

In the *systems approach* the relevant structure is assumed to be composed of different physical components (members, joints, etc.), each of which may have different failure modes, e.g. different collapse, fracture or fatigue modes. In general, global failure results after a sequence of failure modes for different components.

Another important feature of structural systems is that failure may occur in a large number of modes. For instance, system failure may be initiated by fatigue failure of a large number of joints. This feature is especially notable in a long member with n possible fatigue crack sites under the same load conditions, such as the deck of the ship. Depending upon the correlation of loads and resistances at the different sites, the failure probability will be bounded by 1 and n times the failure probability of a single site. This 'series system' issue is currently not explicitly addressed in design codes. This mode of failure is of particular concern because the individual failures are highly correlated. The system target level might be established by:

- using the implicit component reliability in the relevant design code for new structures as a reference failure probability, or
- requiring that the system reliability (failure probability) is higher (lower) than that for components.

Finally, it is again noted that target levels should be derived in a manner which is consistent with the calculation of the reliability levels that should be shown to comply with the target levels.

11.13.4 Reference period for the target level

The target failure probability should be referred to a given time period, i.e. a year or the service life. If the relevant consequence is fatalities, annual failure

© 2008 Woodhead Publishing Limited

probabilities are favoured to ensure the same fatality risk of individuals at any time. The ultimate consequence of this principle is that the target level should not depend upon the number of people at risk, i.e. not include risk aversion. However, often target levels are chosen to imply risk aversion. On the other hand, service life values are relevant if the emphasis is placed on cost–benefit considerations of the ship. By using the relationships expressed above, annual and service life values of P_f can easily be related to ultimate failure events relating to extreme loads. Fatigue failure probabilities naturally lend themselves for reference to service life. However, an alternative is to use the hazard rate, as discussed below.

11.13.5 Alternative approaches

Various methods may be applied to establish the target level, e.g.

- The implicit safety or risk level implied by existing codes, or in actual structures which are considered acceptable.
- The experienced likelihood of fatalities, environmental damage or property loss associated with operations which are considered acceptable.
- Cost–benefit criteria.

In code calibrations that have been conducted in civil and offshore engineering (e.g. Fjeld, 1977; Moses, 1987), the target level has been set by determining the implicit reliability level in acceptable structural designs. Sometimes, the target level can be reduced or increased compared to this implied level. Even if the decision is to maintain the same safety level of existing structures, it is subject to debate whether the target level should be the mean or any other measure of the implied level. Target levels for components will normally differ for different types depending upon the consequences of failure. The challenge is particularly large when structures with a novel type of function or novel layout are introduced in an industry. Consider for instance the introduction of FPSOs in the offshore industry. The way such vessels are operated compared, e.g., to tankers, implies differences in the still-water and wave-induced load effects.

The fact that P_f is sensitive to the assumption of distributions made for loads and resistance variables, especially the character of the distribution tail, shows that the target level needs to be determined based on the same reliability methodology that will be applied to demonstrate compliance with the target level. When assessing target levels for SRA, according to the second and third method above, it should be observed that the implicit risk associated with the accident potential handled by such methods only (should) represent a fraction of the true probability of fatalities, etc.

To set the target level it might be argued that explicit measures should be made for each type of consequence, namely fatalities, environmental damage and property loss. Alternatively, the target level may be based on a common

© 2008 Woodhead Publishing Limited

monetary measure that maximizes the expected utility, considering the costs of the initial construction, failures, inspection, maintenance and repair during the service life.

In particular, it is noted that failure consequences depend on component and system features. Hence, for a floating structure subdivision into compartments, as dictated by stability requirements, is crucial – also with respect to the consequences of structural damage. Compartment subdivision relates to damage stability (ALS) requirements and needs to be judged on the basis of a risk assessment considering various flooding scenarios. The strength of the compartment bulkheads needs to be determined to ensure an acceptable failure probability given relevant flooding scenarios.

The general picture is complex. Current practice is to establish target levels for component ULS and FLS criteria, depending upon immediate consequences. FLS criteria should also be a function of inspection plans.

11.14 Improving the reliability of offshore structures

11.14.1 Measures to ensure reliability

In general the safety philosophy for offshore structures is based on three measures to prevent degradation phenomena like cracks from developing into hazardous situations:

- Design criteria
- Inspections, including leak detection, wherever such monitoring is relevant
- Structural reserve capacity.

Decisions about actions to make ageing structures safe take place during design, fabrication and operation. During design the corrosion protection, possible corrosion allowance, structural scantlings and local geometry to achieve a desired fatigue life, inspection, maintenance and repair plan are decided. During fabrication it is ensured that the intended quality of possible coating for corrosion protection and geometrical tolerances is achieved. In-service corrections to all the safety features considered in design can be implemented depending upon the need. However, improving the fatigue strength by increasing plate thickness is very expensive, since it implies plate replacement or introducing doubler plates. Local grinding of welds would be more relevant. While the effect of toe grinding at the design stage corresponds to approximately a factor of 2 in terms of fatigue life, the effect is more significant if it is done at a later stage, when cracks of larger magnitude have appeared. Other improvement methods, such as hammer peening, may also be used. Larger-scale improvement techniques, such as grouting of tubular joints, are also relevant.

Reliability analyses to assess the need for actions to improve the reliability are of two main types, namely:

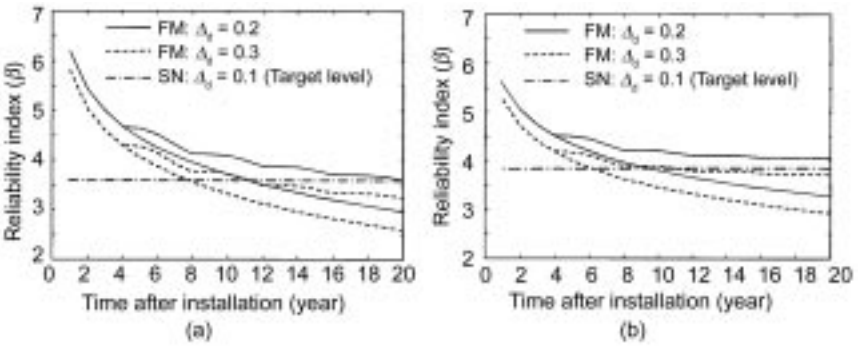
© 2008 Woodhead Publishing Limited

- during design: based only on generic information
- during fabrication and operation: with generic information updated by information about the quality of the as-fabricated structure as well as records of inspections and repairs during operation.

11.14.2 Decisions during design

The determination of scantlings, material qualities, fabrication procedures and inspection plans during design needs to be based on generic knowledge that reflects previous experiences with the relevant type of structure or related structures. Inspection plans are specified for a given type of inspection method by the frequency of inspections. A given fatigue reliability level may be achieved by the combined use of design and inspection criteria. As mentioned above, NORSOK N-001 specifies fatigue criteria as a function of failure consequences and (access for) inspection. Moan *et al.* (1993) show that the allowable cumulative damage (D) in design can be relaxed when inspection is carried out. Hence, Fig. 11.13 shows that the target level corresponding to that with a design criterion $\Delta_{\text{all}} = 0.1$ can be reached by $\Delta_{\text{all}} = 0.25$ and $\Delta_{\text{all}} = 0.2$ for a tubular joint in a jacket and a tether butt weld, respectively, when inspections are carried out every fourth year using NDE methods with a mean detectable crack depth of 1.5 mm.

Normally design and inspection criteria are based on generic information. However, even in design, life cycle costs may be assessed to establish a reasonable balance between the safety achieved by selecting scantlings and material qualities on the one hand and by inspection and repair on the other.



11.13 Reliability index for welded joints in offshore structures as a function of time, when inspections are carried out every fourth year: (a) in TLP tether, (b) in tubular joints of jackets. Updating of reliability is based on information available at the design stage. The major uncertainties for tethers are $\sigma_{\ln C} = 0.514$ and $\sigma_{\ln A} = 0.198$, and for tubular joints $\sigma_{\ln C} = 0.514$ and $\sigma_{\ln A} = 0.294$. Mean detectable crack depth is 1.5 mm.

© 2008 Woodhead Publishing Limited

11.14.3 Decisions during operation

The safety level is maintained during operation by inspection or monitoring, maintenance and repair or intentional structural modification. During operation the inspection plan, in terms of

- prioritizing which locations are to be inspected,
- selecting the inspection method (visual inspection, magnetic particle inspection, eddy current) depending upon the damage of concern,
- scheduling inspections, and
- repair strategy (size of damage to be repaired, repair method and time aspects of repair)

will normally have to be updated based on the particular experiences with a given structure, and, sometimes, also by using information from strongly related structures.

Condition assessment of the structure is crucial. There are often differences between 'as-designed' and 'as-is' conditions. Some discrepancies occur due to practical considerations during fabrication, such as the availability of space for welding. This can cause local changes of geometry that affect fatigue, which is sensitive to local details. Also, the structure may be operated differently from the intended operation. For instance semi-submersible drilling units may operate with a larger draft in transit than anticipated during design. The consequence may be more frequent slamming loads on horizontal braces than initially planned.

During operation, structural reassessment may be necessary due to:

- Novel use or increase of payload. For floating structures increased payload would imply larger displacement and hence larger hydrodynamic loads and shorter fatigue life. Moreover, it is noted that it is difficult to achieve high quality structural quality during modifications, especially undertaken at offshore sites
- Extension in service life
- Ageing or accidents.

Deviation from planned fabrication and operational procedures could increase ageing (crack growth).

While the calibration of fatigue design criteria is based on generic data, it is important that information obtained, e.g., by inspections during operation is used and the inspection plan is updated accordingly. For this reason structural reliability analysis of crack growth needs to be done for each individual structure, while ultimate strength criteria have been based on code calibration by code committees.

In particular it is noted that inspection planning for template, space frame structures is based on a simplified systems reliability approach, considering one

© 2008 Woodhead Publishing Limited

failure mode at a time (Moan *et al.*, 1999). The basic principle is to require that the system failure probability $P_{\mathrm{fSYS}(i)}$ associated with a fatigue failure of member i complies with a target level $P_{\mathrm{fSYS(T)}}$, i.e.

$$P_{\mathrm{fSYS}(i)} = P_{\mathrm{fSYS/FF}(i)} P_{\mathrm{FF}(i)} \leq P_{\mathrm{fSYS(T)}} \qquad 11.57$$

Sigurdsson *et al.* (2000) show how reliability analyses are applied to aid decisions regarding inspection planning during the operation of semi-submersible platforms.

11.14.4 Service life extension

Typically the service life for marine structures is 20 years. It is generally found to be more cost-effective to extend the service life of existing structures than to build new ones. If the component fatigue design criterion with due account of possible corrosion effects is not fulfilled, mitigation may be achieved by implementing one or more of the following measures:

- Carrying out inspections to detect cracks
- If no crack is detected, increased fatigue life is implied, i.e. by updating the reliability level
- Repair of possible cracks detected, by grinding, introducing additional brackets or strengthening, or by reducing loads by removing unnecessary equipment, marine growth, etc., reducing potential failure consequences by demanning
- Increase quality/frequency of inspections.

If the ultimate strength criteria are not fulfilled due to general corrosion effects, replacement of plates or stiffeners, or strengthening of stiffeners (e.g. by reducing the buckling length) needs to be done. The follow-up of ultimate limit state component criteria can primarily be transformed into a check of the following:

- Corrosion protection by coating or cathodic protection
- The average thickness reduction in view of the corrosion allowance.

Since the system safety is of main concern, there is an increasing focus on platforms modelled as systems, by considering the hull girder in bending to be represented by parallel components. A particular issue is concerned with documenting adequate safety against fatigue failure for an existing structure when the service life is to be extended beyond the initially planned value. A main issue is how much fatigue life remains and how much it may be increased by inspection (Vårdal *et al.*, 2000; Johannesen *et al.*, 2000). These authors assessed a semi-submersible platform that was initially built in 1985 and converted to a production unit and installed in the North Sea in 1989. The platform was dry-docked for modification in 1999, partly to increase payload

© 2008 Woodhead Publishing Limited

and partly for local reconstruction of the corner areas of pontoon/column connections. Additional payload capacity was achieved by adding extra buoyancy elements. Fatigue analysis using current methodology identified the most critical areas of the braces to have a 5–10 year fatigue life. Upon 10 years in-service and a requirement of an additional 15–20 years in operation, it was necessary to consider different structural modification alternatives and other measures to improve the fatigue endurance. One alternative to achieve acceptable extension of the service life was to add horizontal bracing between the four columns. However, this approach was very expensive. The alternative solution, which was selected, was to document adequate safety with respect to fatigue failure by utilizing the extensive inspection history of 'No Crack Growth Detection', application of weld improvement methods and more frequent in-service inspections (Vårdal *et al.*, 2000; Johannesen *et al.*, 2000). The effect on the safety level of this approach was demonstrated by applying the methodology outlined in this chapter.

11.15 Conclusions

In general, the safety of ageing structures is ensured by proper design and especially the provision of damage tolerance, as well as inspection, monitoring, maintenance and repair actions. This chapter outlines structural reliability modelling and analysis that can serve as a tool in decision making about safety of ageing offshore structures. The reliability should be estimated by properly validated FORM/SORM methods or Monte Carlo simulation methods. The results of the reliability analysis are crucially dependent upon the uncertainties applied. It is strongly recommended to use data that have been authorized through code committees or other expert panels. It is emphasized that the methodology needs to be consistent with the relevant accepted semi-probabilistic design methods. While in principle the same basic reliability methods are applied in all phases of the structural life cycle, there is a significant difference between the design and operation phases. In the design phase the uncertainties that affect the reliability are generic in nature while specific information about the particular structure is available during operation. It is crucial to properly account for all sources of uncertainty in connection with the updating of reliability based on additional information about the as-fabricated structure and in-service experiences.

Finally, in making decisions regarding safety, the actual, implied reliability of a certain structure, as documented based on a design and plan for operation, needs to be compared with the acceptable – or target – reliability level. The target value needs to be established by careful assessment of the implied safety level in structures that are considered to have acceptable safety, by using the same type of methodology that later will be used to demonstrate compliance with the target level.

© 2008 Woodhead Publishing Limited

11.16 References

ALK (1981), *Alexander L. Kielland ulykken* (English translation, 'The L. Kielland Aleksander Accident' by Translatørservice AS, Stavanger), NOU 11: 1981, Oslo, Universitetsforlaget.

Almar-Næss A (ed.) (1985), *Fatigue Handbook for Offshore Steel Structures*, Tapir Publishers, Trondheim, Norway.

Ang AHS and Tang WH (1984), *Probability Concepts in Engineering Planning and Design, Vol. II Decision, Risk and Reliability*, John Wiley & Sons, New York.

Ayala-Uraga E and Moan T (2002), 'System reliability issues of offshore structures considering fatigue failure and updating based on inspection', *Proc 1st Int ASRANet Colloquium*, Glasgow.

Ayala-Uraga E and Moan T (2007a), 'Fatigue reliability-based assessment of welded joints applying consistent fracture mechanics formulations', *Int J Fatigue*, 29(3), 444–456.

Ayala-Uraga E and Moan T (2007b), 'Time variant reliability assessment of FPSO hull girder with long cracks', *J OMAE*, 129, 81–89.

Bach-Gansmo O, Carlsen CA and Moan T (1987), 'Fatigue assessment of hull girder for ship type floating production vessels', *Proc Conf Mobile Offshore Units*, City University, London.

Beck AT and Melchers RE (2004), 'On the ensemble crossing rate approach to time variant reliability analysis of uncertain structures', *Probabilistic Eng Mech*, 19, 9–19.

Bin Z and Moan T (2005), 'Analysis of fatigue crack propagation in typical welded joints of FPSO', *Proc OMAE 24th Conf*, Halkidiki, Greece, ASME, paper no. OMAE2005-67058.

Bokalrud T and Karlsen A (1981), 'A probabilistic fracture mechanics evaluation of fatigue failure from weld defects in butt weld joints', *Proc Conf on Fitness for Purpose Validation of Welded Constructions*, London, paper 28.

BS 7910 (1999), 'Guidance on Methods for Assessing the Acceptability of Flaws in Fusion Welded Structures', BS 7910:1999, British Standards, London.

Celant MB *et al.* (1983), 'Fatigue characterization for probabilistic design of submarine pipelines', *Proc 1982 European Federation of Corrosion Meeting on Low Frequency Cyclic Loading Effects in Environment Sensitive Fracture*, Pergamon Press, Oxford.

Dalane JI (1993), 'System Reliability in Design and Maintenance of Fixed Offshore Structures', Dr. Ing. thesis, The Norwegian Institute of Technology, Trondheim.

De R *et al.* (1989), 'Study of redundancy in near-ideal parallel structural systems', *Proc 5th ICOSSAR*, 2, 975–982.

Dover WJ and Rudlin JR (1996), 'Defect characterisation and classification for the ICON inspection reliability trials', *Proc Conf Offshore Mechanics and Arctic Engineering*, ASME.

Dunlap WA and Ibbs CW (1994), *Proc Int Workshop on Assessment and Requalification of Offshore Production Structures*, New Orleans, 1993, Offshore Technology Research Center, Texas A&M University and University of California, Berkeley.

Faber MH, Sorensen JD and Kroon IB (1992), 'Optimal inspection strategies for offshore structural systems', *Proc OMAE*, Calgary, Alberta, 145–151.

Ferry Borges J and Castanheta M (1971), *Structural Safety*, 2nd edn, Laboratorio Nacional de Engenharia Civil, Lisbon.

Fjeld S (1977), 'Reliability of offshore structures', *Proc 9th OTC*, 4, 459–472, OTC 3027, Houston, TX.

© 2008 Woodhead Publishing Limited

Fujimoto Y *et al.* (1996), 'Study on fatigue reliability and inspection of ship structures based on enquete information', *J Soc Naval Arch Japan*, 180, 601–609.

Fujimoto Y *et al.* (1997), 'Inspection planning of fatigue deteriorating structures using genetic algorithm', *J Soc Naval Arch Japan*, 182, 729–739.

Hagen Ø and Tvedt L (1991), 'Vector process out-crossings as parallel system sensitivity measure', *J Eng Mech*, 117(10), 2201–2220.

Halkyard JE (2005), 'Floating offshore platform design', Chapter 7 in *Handbook of Offshore Engineering*, S Chakrabarti, ed., Elsevier, Vol. 1, pp 419–661.

Heideman J and Weaver T (1992), 'Static wave force procedure for platform design', *Proc Civil Engineering in the Oceans V*, College Station, TX, ASCE, 496–517.

Hovde GO and Moan T (1994), 'Fatigue reliability of TLP tether systems considering the effect of inspection and repair', *Proc 7th BOSS Conf*, MIT, Boston, MA, 3, 85–100.

Huang W and Moan T (2006), 'Fatigue under combined high and low frequency loads', *Proc 25th OMAE Conf*, paper no. OMAE2006-92247.

ISO 19900 (1994), 'Petroleum and Natural Gas Industries – Offshore Structures – Part 1: General Requirements', International Organization for Standardization, London.

ISO 2394 (1998), 'General Principles on Reliability for Structures', ISO/DIS 2394, Draft Revision.

Itagaki H, Akita Y and Nitta A (1983), 'Application of subjective reliability analysis to the evaluation of inspection procedures on ship structures', *The Role of Design, Inspection, and Redundancy in Marine Structural Reliability: Proc Int Symp*, 14–16 November 1983, National Academy Press.

Jiao G and Moan T (1990), 'Methods of reliability model updating through additional events', *Struct Safety*, 9, 139–153.

Johannesen MJ, Moan T and Vårdal OT (2000), 'Application of probabilistic fracture mechanics analysis for reassessment of fatigue life of a floating production unit – theory and validation', *Proc 19th OMAE Conf*, New Orleans, paper no. OMAE2000-2079.

Jordaan IJ and Maes MA (1991), 'Rationale for load specifications and load factors in the new CSA code for fixed offshore structures', *Canadian Inst Civil Engng,* 18(3), 454–464.

Karamchandani A (1990), 'New Methods in Systems Reliability', Ph.D. Thesis, Stanford, CA: Department of Civil Engineering, Stanford University.

Kam JCP and Dover WD (1989), 'Corrosion fatigue of welded tubular joints: fracture mechanics modelling and data interpretation', *Proc 8th OMAE Conf*, The Hague, The Netherlands.

Karsan DI (2005), 'Fixed offshore platform design', Chapter 6 in *Handbook of Offshore Engineering*, S Chakrabarti, ed., Elsevier, Vol. 1, pp. 279–417.

Kirkemo F (1989), *PIA Theory Manual*, Aker, Oslo.

Kountouris IS and Baker MJ (1989), 'Defect Assessment. Analysis of Defects Detected by MPI in an Offshore Structure', CESLIC Report No. OR6, Department of Civil Engineering, Imperial College, London.

Lloyd JR and Karsan DI (1988), 'Development of a reliability-based alternative to API RP2A', *Proc 20th OTC*, 4, 593–600, OTC 5882, Houston, TX.

Madsen HO and Sørensen SD (1990), 'Probability-based optimization of fatigue design inspection and maintenance', *Proc 4th Int Symp on Integrity of Offshore Structures*, Elsevier, London, 421–432.

Madsen HO, Krenk S and Lind NC (1986), *Methods of Structural Safety*, Prentice-Hall, Englewood Cliffs, NJ.

Madsen HO, Skjong RK, Tallin AG and Kirkemo A (1987), 'Probabilistic fatigue crack

© 2008 Woodhead Publishing Limited

growth analysis of offshore structures, with reliability updating through inspection', *Proc Marine Struct Symp*, Arlington, VA, 45–55.
Marley M and Moan T (1992), 'Time variant formulation for fatigue reliability', *Proc. OMAE*, Calgary, Alberta, Paper OMAE-92-1203.
Marshall PW (1969), 'Risk evaluations for offshore structures', *J Struct Div, ASCE*, 95(12), 2907–2929.
Marshall PW and Luyties WH (1982), 'Allowable stresses for fatigue design', *Proc BOSS '82*, McGraw-Hill, New York, 2, 2–25.
Melchers R (1999), *Structural Reliability. Analysis and Prediction*, Ellis Horwood, Chichester, UK.
Moan T (1985), 'The progressive structural failure of the Alexander L. Kielland platform', in *Case Histories in Offshore Engineering*, G Maier, ed., Springer-Verlag, Berlin.
Moan T (1988), 'The Inherent Safety of Structures Designed According to the NPD Regulations', SINTEF Report F8804.
Moan T (1994), 'Reliability and risk analysis for design and operations planning of offshore structures', keynote lecture, *Proc 6th ICOSSAR, Structural Safety and Reliability*, I, 21–43, Balkema, Rotterdam..
Moan T (1995), 'Safety Levels Across Different Types of Structural Forms and Materials, Implicit in Codes for Offshore Structures', SINTEF Report STF70A95210, Trondheim. Contributed to the ISO Offshore Code developments TC67/SC7.
Moan T (2000), 'Recent research and development relating to platform requalification', *J OMAE*, 122, 20–32.
Moan T (2002), 'Target Levels for Reliability-based Assessment of Offshore Structures during Design and Operation', Offshore Tech rept OTO 1999/060, Health and Safety Executive, London.
Moan T (2004), 'Safety of offshore structures', keynote lecture, *Proc 9th PRADS*, Lübeck-Travemünde, Germany, 1, 10–38.
Moan T (2005), 'Reliability-based management of inspection, maintenance and repair of offshore structures', *J Struct and Infrastruct Eng*, 1(1), 33–62.
Moan T (2007), 'Fatigue reliability of marine structures – from the Alexander Kielland accident to life cycle assessment', *J ISOPE*, 17(1), 1–21.
Moan T (2008), 'Development of accidental collapse limit state criteria for offshore structures', *J Structural Safety*, to appear.
Moan T and Ayala-Uraga E (2008), 'Reliability-based assessment of deteriorating ship structures operating in multiple sea loading climates', *Reliability Engineering and System Safety*, 93(3), 433–446.
Moan T and Song R (2000), 'Implications of inspection updating on system fatigue reliability of offshore structures', *J Offshore Mech & Arct Eng*, 122, 173–180.
Moan T, Hovde GO and Blanker AM (1993), 'Reliability-based fatigue design criteria for offshore structures considering the effect of inspection and repair', *Proc 25th Offshore Tech Conf*, Houston, TX, OTC 7189, 2, 591–599.
Moan T, Vårdal OT, Hellevig NC and Skjoldli K (1997), 'In-service observations of cracks in North Sea jackets – a study on initial crack depth and pod values', *Proc 16th Conf Offshore Mech & Arct Eng*, ASME, Yokohama, paper no. 1335.
Moan T, Vårdal OT and Johannesen JM (1999), 'Probabilistic inspection planning of fixed offshore structures', *Proc ICASP 8, Applications of Statistics and Probability*, 191–200, Balkema, Rotterdam.
Moan T, Wei Z and Vårdal OT (2002a), 'Initial crack depth and POD data based on underwater inspection of fixed steel platforms', *Structural Safety and Reliability,*

© 2008 Woodhead Publishing Limited

Proc 8th ICOSSAR'01, Balkema, Rotterdam.
Moan T, Amdahl J and Hellan Ø (2002b), 'Nonlinear analysis for ultimate and accidental limit state design and requalification of offshore platforms', *Proc Fifth World Congress on Computational Mechanics (WCCM V)*, Vienna, paper no. 81575.
Moan T, Ayala-Uraga E and Wang X (2004), 'Reliability-based assessment of FPSOs for service life extension', *SNAME Ann Mtg*, Washington, DC, 193–215.
Moan T *et al.* (2005), 'Uncertainty of wave-induced response of marine structures due to long term variation of extratropical wave conditions', *J Marine Struct*, 18(4), 359–382.
Moses F (1987), 'Load and Resistance Factor Design – Recalibration LRFD', Draft Report, API PRAC 87-22, API, Dallas, TX.
Moses F and Liu YW (1992), 'Methods of redundancy analysis for offshore platforms', *Proc 11th OMAE Conf*, II, 411–416, ASME, New York.
Newman JC and Raju JS (1981), 'An empirical stress-intensity factor equation for the surface crack', *Eng Fracture Mech*, 15(1–2), 185–192.
NORSOK N-004 (1998), *Steel Structures*, Norwegian Technology Standards, Oslo.
NORSOK N-001 (2002), *Structural Design*, Norwegian Technology Standards, Oslo.
NPD (1977), Regulations for Load Carrying Structures, Norwegian Petroleum Directorate, Stavanger, Norway.
Potthurst R, Coates AD and Nataraja R (1989), 'Fatigue Correlation Study – Semi-submersible Platforms', OTH88288, Report for the Department of Energy, London.
Rudlin JR and Austin J (1996), 'Topside inspection project: Phase I final report', Offshore Technology Report OTN 96 169, Health and Safety Executive, London.
Schuëller GI (ed.) (2006), 'Structural reliability software', *Structural Safety*, 28(1–2), 1–216.
Shetty NK (1992), 'System Reliability of Fixed Offshore Structures under Fatigue Deterioration', PhD thesis, Imperial College, London.
Shinozuka M and Deodatis O (1989), 'Reliability of Marine Structures under Bayesian Inspection', Report of Princeton University, Princeton, NJ, February.
Sigurdsson G, Lotsberg I, Myhre T and Ørbeck-Nilssen K (2000), 'Fatigue reliability of old semi-submersibles', OTC paper no 11950, *Proc Offshore Technology Conf*, Houston, TX.
Silk MG, Stoneham AM and Temple JAG (1987), *The Reliability of Non-destructive Inspection*, Adam Hilger, Bristol.
Sucharski D (1997), 'Crude oil tanker hull structure fracturing: an operator's perspective', in *Proc. Symposium and Workshop on the Prevention of Fracture in Ship Structure*, Ship Structure Committee, Washington, DC, 87–124.
Terada S and Takahashi T (1988), 'Failure-conditioned reliability index', *J Struct Eng Div, ASCE*, 114(4), 943–952.
Thoft-Christensen P and Baker M (1982), *Structural Reliability and its Applications*, Springer-Verlag, Berlin.
TSCF (1997), *Guidance Manual for Tanker Structures*, Tanker Structure Co-operative Forum & IACS, Witherby, London.
Turkstra CJ (1970), 'Theory of structural design decisions', *Solid Mechanics Study No. 2*, University of Waterloo, Ontario.
Vårdal OT and Moan T (1997), 'Predicted versus observed fatigue crack growth. Validation of probabilistic fracture mechanics analysis of fatigue in North Sea jackets', *Proc 16th OMAE Conf*, paper no. 1334, Yokohama, Japan.
Vårdal OT, Moan T and Bjørheim LG (2000), 'Applications of probabilistic fracture mechanics analysis for reassessment of fatigue life of a floating production unit –

© 2008 Woodhead Publishing Limited

philosophy and target levels', paper no. 00-2078, *Proc 19th OMAE Conf*, New Orleans.
Vårdal OT *et al.* (to appear), 'Comparison of observed and predicted crack occurrences in North Sea semi-submersibles'.
Videiro PM and Moan T (1999), 'Efficient evaluation of long-term distributions', *Proc 18th OMAE Conf*, paper no. OMAE99/S&R6014, St Johns, Newfoundland.
Vinnem JE (1999), *Offshore Risk Assessment*, Kluwer Academic Publishers, Dordrecht, The Netherlands.
Visser W (2002), 'POD/POS curves for non-destructive examination', Offshore Technology Report OTO 2000/018, Health and Safety Executive, London.
Wang X and Moan T (1996), 'Stochastic and deterministic of still water and wave bending moments in ships', *Marine Structures*, 9, 787–810.
Wen YK (1990), *Structural Load Modelling and Combination for Performance and Safety Evaluation*, Elsevier, Amsterdam.
Winterstein S, Ude T, Cornell CA, Bjerager P and Haver S (1993), 'Environmental parameters for extreme response: inverse FORM with omission factors', *Proc ICOSSAR'93*, Innsbruck, Austria; Balkema, Rotterdam.
Wirsching PH (1983), 'Probability-based fatigue design criteria for offshore structures', Report API-PRAC Project No. 81-15, Department of Aerospace and Mechanical Engineering, University of Arizona, Tucson, AZ.
Wu Y-L and Moan T (1989), 'A structural system reliability analysis of jacket using an improved truss model', *Proc 5th ICOSSAR*, San Francisco, 887–894.
Yang YN (1994), 'Application of reliability methods to fatigue, quality assurance and maintenance – the Freudenthal lecture', *Proc 6th ICOSSAR Conf, Structural Safety and Reliability*, 1, 3–18, Balkema, Rotterdam.

© 2008 Woodhead Publishing Limited

12

Reliability of aged land-based structures

R E MELCHERS, The University of Newcastle, Australia

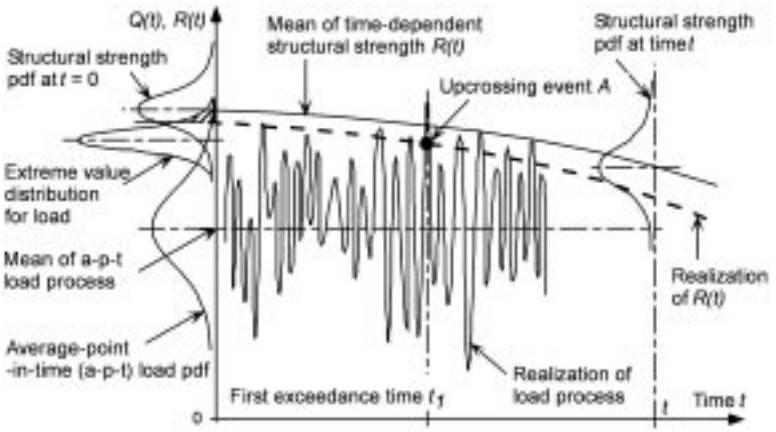
Abstract: This chapter outlines procedures for the estimation of the reliability of land-based structures as they deteriorate with time, such as resulting from fatigue and corrosion, including depth of pitting. Many forms of deterioration are influenced by environmental conditions. Materials of interest include structural steels, reinforced and pre-stressed concretes, masonry and stone, timber and, to a small extent, various fibre-reinforced plastics. Typically the likely 'design life' is of interest. As most structures consist of multiple components (or members) interaction between members must be considered, although many structures can be idealized as 'series' systems. The theory for this is outlined and solution techniques such as Monte Carlo analysis and importance sampling are also outlined. This includes situations with multiple loading systems, for which extreme value representations for loads are not appropriate since the occurrence of the maximum of one load is unlikely to coincide with the occurrence of the maximum of another load. The so-called Turkstra's rule is a convenient but simplified approach in this case. When the resistance of the structural system is time-dependent, and more than one stochastic load is applied, outcrossing theory must be applied and the 'outcrossing rate' $\nu(t)$ estimated. This may be a function of time and thus enable consideration of deteriorating structural systems. Some recent efforts for this in the literature are reviewed.

Key words: structures, land-based, deterioration, corrosion, fatigue, outcrossing, Monte Carlo.

12.1 Introduction

In this chapter an outline is given of the estimation of the reliability of land-based structures as they deteriorate with time. Deterioration for these structures may be caused by fatigue resulting from the repeated application of high-duty loadings, such as occurs, for example, for many highway bridges. Another form of deterioration in modern structures is that due to corrosion, such as from de-icing salts or seawater, erosion such as in scour of bridge piers, or wear of industrial components and chemical attack, such as in aggregate–alkaline reactions in reinforced concrete. Compared to fatigue, which depends entirely on the number and intensity of load applications, these latter forms of deterioration tend to be largely dependent on length of exposure and not much influenced by the number of load applications. This means that these forms of deterioration are best represented directly as functions of time. This function depends on the type of deterioration process being considered and will be different, for example, for

© 2008 Woodhead Publishing Limited



12.1 Typical loss of structural strength with time caused by material deterioration showing the outcrossing of the stochastic load process.

the loss of thickness of steel plates under immersion corrosion conditions and the pitting of aluminium plates such as in aircraft. Evidently, detailed information is required to model different types of deterioration.

Land-based infrastructure mainly consists of structural steels, reinforced and pre-stressed concretes, masonry and stone, as well as timber and, to a small extent, various fibre-reinforced plastics. All tend to exhibit generally similar deterioration behaviour (Fig. 12.1).

The other major characteristic feature of land-based structures as opposed to ocean or sea-based systems is the origin of the loads that act on the structure. Whereas wave loading often is the most significant for the latter, for land-based structures wind and snow loadings are the most significant environmental loads and these have high levels of uncertainty. Anthropological loading is mainly due to truck and crowd loadings. Industrial loads may be very high in absolute value but are often well defined and hence have low levels of uncertainty. Despite these differences, the basic concepts of structural reliability assessment for structures and structural systems, new or existing, are generally similar. This will now be outlined.

12.2 Components in structural reliability

12.2.1 Reliability of existing structures

Overall, there are two main areas for investigation in assessing structural reliability. The first is the assessment of the existing structure and the estimation of its reliability. This will rely on detailed investigation of the structure ‘as is’ rather than as it might have been designed. The distinction is important. The reliability analyses underpinning the conventional design rules used to design a structure are designed to take some account of variability in design,

© 2008 Woodhead Publishing Limited

documentation and construction, but these uncertainties will have been 'realized' or implemented during these processes. There is thus no need to consider them. There is no uncertainty about them since all variability due to them has been built into the structure. The problem that remains is to assess what has actually been constructed. If, in addition, the structure has already aged for some time, the outcome of the design and construction process becomes relatively less important in the face of the deterioration that will have occurred subsequently. To be sure, despite considerable investigative tools at the disposal of investigating engineers, the assessment of the state of an existing structure remains a challenge for the profession. Aspects are discussed elsewhere in this book.

12.2.2 Future reliability

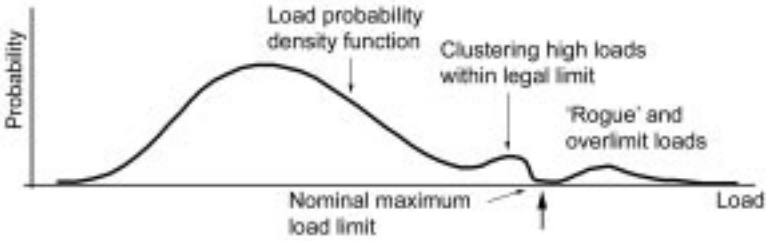
The second area for structural reliability is the prediction of the likely reliability at some time in the future. Evidently this requires estimation of the likely deterioration of materials involved, including the uncertainty related to that estimate. This is shown schematically in Fig. 12.1.

Estimates for the deterioration of structures due to corrosion depend very much on the materials involved. Corrosion wastage of steel is described in Chapter 4. But not all land-based structures are constructed from steel and many major structures including those close to the coast are executed in reinforced or pre-stressed concrete. Moreover, there is much domestic, low-rise commercial and institutional construction in masonry. All these materials have their characteristic deterioration modes. Space precludes a detailed review, but reference might be made to Monteiro *et al.* (2001).

One aspect of future reliability seldom considered by structural engineers is the effectiveness of protective measures such as protective coatings (paints) and, for steel and reinforced concrete structures in immersion zones or in waterlogged soils, of cathodic protection systems. While there is a considerable literature for these systems, quantitative assessment and prediction of their long-term reliability has not received much attention. This situation is exemplified by the estimation of the effective life of protective coatings (Melchers and Jiang 2006).

Estimation of future reliability also requires estimation of the likely changes in the load processes, including their mean values and their variability. Climate change may be instrumental in causing such changes. More typically they result from increased knowledge as the historical environmental data is analysed in more detail. Almost invariably the mean values of the loads increase! Unlike the models that are well-documented for standard load processes (e.g. Melchers 1999) there are few data or models for likely changes in environmental load processes. This situation is likely to improve as it becomes more evident that such information is necessary to make proper reliability assessments.

© 2008 Woodhead Publishing Limited



12.2 Probability density function for heavy vehicle load showing clustering around the nominal legal limit.

Similarly, changes in legal load limits and legal axle loads for lorries, trucks and heavy vehicles result in higher values of the mean for these load processes. There is increased realization that the legal limit has a profound effect on the extreme loads that occur for highway bridges (Melchers 2007). Moreover, enforcement is a critical issue in the form of the probability distribution, which is not, as often assumed, a standard extreme value distribution (see Fig. 12.2).

12.3 Outline of structural reliability theory

For illustrating the essential ideas it will be sufficient to concentrate on a simple structure subject to wind loading and live loading. Wind loading may be considered as a fluctuating force that can be modelled as a random process in time (usually known as a 'stochastic' process). Just one possible realization of such a process is shown in Fig. 12.1. Whenever the load exceeds the structural strength, failure is considered to have occurred. This is shown schematically at event A on Fig. 12.1. Of particular interest is the time t_1 to the first occurrence of such an event. This is known as the 'first exceedance event' t_1. For safe structures t_1 is very long, but deterioration of structural strength will reduce it. Since the loading is random, it follows that t_1 also will be a random variable. Its estimation is a central issue for structural reliability (although it is seldom explicitly determined).

Two probability density functions are shown at the left of Fig. 12.1. The main one (the 'average point in time' (a-p-t) distribution) refers to all possible wind loads described by the wind loading random process $Q(t)$. It cuts across the resistance realization and the small dark shaded area represents the probability that the load will be greater than this resistance. Obviously this shaded area will be smaller for higher values of resistance, that is, the probability of failure will be smaller and the time to the first up-crossing event (A), shown at the black circle, will take longer, on average. Thus the first exceedance t_1 will be longer.

The other probability density shown in Fig. 12.1 is the much narrower and 'spiky' extreme value distribution (EVD) for the loading. It represents the probability density function for the maxima of the loads in a given period, usually taken as one year. In this case only the maximum load in each year of

© 2008 Woodhead Publishing Limited

record is used as data and from this data set the 'extreme value' probability density is derived. Obviously it will be located higher up on the load axis. Failure is now associated with the probability that the maximum load in any one year will exceed the resistance of the structure (irrespective of the probability that some lower load level may also exceed the resistance). This is shown, at $t = 0$, by the cross-hatched area.

So far the structural resistance has been treated as a fixed quantity. More generally the resistance is not known precisely and typically it is modelled as a random variable, as indicated in Fig. 12.1. Therefore all possible realizations (values) of the structural resistance must be considered, allowing for the probability of occurrence of each of these values. This is expressed by the probability density function for structural resistance. Information about probability distributions for the strengths of a range of materials has been documented. Information about the variability of structural sizes also is available (Melchers 1999).

Usually the information about structural material strengths and member sizes needs to be combined to obtain the probabilistic description for structural members. This can be done by numerical integration (Stroud 1971) or Monte Carlo simulation (see below), or, more simply, by using 'second moment' analysis (Ditlevsen 1981). For example, if the strength of a cross-section consists of an uncertain material of strength M and an uncertain cross-sectional area A, the strength S of the member (in tension, say) is given by

$$S = M \cdot A \tag{12.1}$$

The probability density function $f_S(s)$ of S can be determined from the corresponding probability density functions for M and A through Eqn (12.1). Using 'second moment' analysis only the means and standard deviations are considered information about the actual distributions is ignored. Thus, the mean μ_S and the variance σ_S^2 are given by well-known rules for combining means and variances (Melchers 1999):

$$\mu_S = \mu_M + \mu_A \tag{12.2}$$

$$V_S^2 \approx V_M^2 + V_A^2 \tag{12.3}$$

where $V = \sigma/\mu$ is the coefficient of variation. The subscripts refer to the relevant variables in Eqn (12.1).

The probability of failure now may be stated as the probability that the load exceeds the resistance. For sufficiently rare extreme loads it is sufficient to assume that the failure event will occur only once in the lifetime of a structure (irrespective of whether it is rebuilt). The probability of failure will depend on (i) the value of the maximum load (a random variable), (ii) the probability of occurrence of different possible values of candidate maximum loads, and (iii) the actual strength of the structure as expressed by the probability density

© 2008 Woodhead Publishing Limited

function for strength. In the case of a single load only (i) and (iii) are relevant.

Consider now the simplest, one-load case. Since the structural resistance is probabilistic, it is necessary to consider the probability that the resistance $R(t)$ at time t is less than some given value of the load $x(t)$. This is given by $P(R(t) > x(t)) = F_R(x)|t$. However, since it makes only a small contribution to the total probability, it is necessary to weight it by the probability that the load $Q(t)$ is 'equal to' $x(t) = f_Q(x)|t$. Mathematically this can be stated as:

$$p_f|t = \int_{-\infty}^{+\infty} F_R(x)|t \cdot f_Q(x)|t \, \mathrm{d}x \tag{12.4}$$

where $F_R(\ )$ is the cumulative distribution function for R. It is given by

$$F_R(r) = \mathrm{Prob}(R < r) = \int_{-\infty}^{r} f_R(x) \, \mathrm{d}x \tag{12.5}$$

This is the so-called 'convolution' integral at time t. Combining Eqns (12.4) and (12.5) gives a more general version

$$p_f|t = \iint_{D_f} f_Q(x) \cdot f_R(x) \, \mathrm{d}x \tag{12.6}$$

where D_f represents the failure domain. Except for some special cases, Eqns (12.4) and (12.6) can only be solved numerically. This includes solution by Monte Carlo methods and the various refinements of it (Melchers 1999). Other methods such as the First Order Second Moment (FOSM) methods and their refinements also may be employed. FOSM requires very serious simplifications of the problem, including that all random variables are represented only by their means and variances and that the limit state function is linear. The refinements can remove one or both restrictions but in so doing add considerably to the computational requirements, in the limit approaching that of the refined Monte Carlo methods (Ditlevsen and Madsen 1996).

12.4 Structural systems reliability

12.4.1 Multi-member systems

Most structures consist of multiple components (or members). Usually it is not possible to predict which member will be critical to the reliability of the system. Moreover there will be interaction between them and dependence on common material strengths (for example). Many structural systems may be idealized as 'series' systems. For these, failure of some selection of members implies failure of the system. Let this selection be represented by the union $\cup_i[G_i(\mathbf{X}) < 0]$ of a number of individual performance functions $G_i(\mathbf{X}) < 0$ where i denotes failure of the ith member or in the ith failure mode. Here $\mathbf{X}$ collects all the random variables in the reliability problem. The generalization of Eqn (12.6) then becomes:

© 2008 Woodhead Publishing Limited

$$p_{\mathrm{f}} = \int \ldots \int_{\cup_i G_i(\mathbf{X})<0} f_{\mathbf{X}}(\mathbf{x})\ \mathrm{d}\mathbf{x} \tag{12.7}$$

where now $f_{\mathbf{X}}(\ )$ is the joint density function of the random variables $\mathbf{X}$. The solution of Eqn (12.7) in general is not a simple matter, particularly if the limit state functions describe a complex failure domain and/or $f_{\mathbf{X}}(\ )$ is not of simple form. In addition, the dimension of $\mathbf{X}$ for realistic structural systems is often quite high. More generally Eqn (12.7) may be written as

$$p_{\mathrm{f}} = \int \ldots \int_{D_{\mathrm{f}}} f_{\mathbf{X}}(\mathbf{x})\ \mathrm{d}\mathbf{x} \tag{12.8}$$

where, as before, D_{f} represents the failure domain.

The solution of Eqn (12.7) or (12.8) may be through numerical integration but this is usually not feasible for dimensions of $\mathbf{X}$ greater than about 5. A better option is to use Monte Carlo simulation for the integration. However, this can be a highly inefficient procedure unless some special techniques are employed.

12.4.2 Multiple loads and load combination

When there is more than one loading system applied to the structure it is not valid to represent each load by an extreme value distribution, such as was done above. This is because the occurrence of the maximum of one load is unlikely to coincide with the maximum of another load. A practical and simple approach to deal with this is to apply the so-called Turkstra's rule (Turkstra 1970). It states that the occurrence of the maximum of one load X_i should be associated with the 'average-point-in-time' values $\bar{X}_j$ of the other load(s). An 'average point in time' load $\bar{X}_j$ is one that would be expected to act on the structure at any arbitrary point in time. For most loads, this means rather low load levels. Of the various combinations, the maximum (or worst) combination will govern:

$$\max X \approx \max\left(\max X_i + \sum_{j=1}^{n} \bar{X}_j\right), \quad j \neq 1; i = 1, \ldots, n \tag{12.9}$$

12.4.3 Monte Carlo analysis

Expression (12.7) may be written also as

$$p_{\mathrm{f}} = J = \int \ldots \int I[G(\mathbf{x}) < 0]\, f_{\mathbf{X}}(\mathbf{x})\ \mathrm{d}\mathbf{x} \tag{12.10}$$

where $I[\ ]$ is an 'indicator' function by $I[\theta] = 1$ if the expression for θ is 'true' and zero otherwise. This formulation derives from the observation that there is a contribution to p_{f} only if the random vector $\mathbf{X}$ takes on values such that $I[\ ]$ is unity. Evidently the indicator function plays the same role as the limits of integration in Eqn (12.7). As before, $G(\mathbf{x})$ is the failure criterion (limit state or performance function) and here can be considered to include also the case of the

© 2008 Woodhead Publishing Limited

union $\cup_i[G_i(\mathbf{X}) < 0]$ of a number of individual performance functions $G_i(\mathbf{X}) < 0$.

The limits of integration in Eqn (12.10) are over the whole range of $\mathbf{X}$. It can be written in a discrete form:

$$p_f \approx J_1 = \frac{1}{N}\sum_{j=1}^{N} I[G(\hat{\mathbf{x}}_j) \leq 0] \tag{12.11}$$

where $\hat{\mathbf{x}}_j$ represents a (the jth) vector of random samples selected from $f_{\mathbf{x}}(\ )$. These are known also as 'random deviates' and can be obtained from computer subroutines.

To apply Eqn (12.11), a discrete set of values $\hat{\mathbf{x}}_j$ is developed using, say, a computer program, and the limit state function(s) is then evaluated. The sum in Eqn (12.11) is incremented by 1 if the limit state(s) is violated (i.e. the structure fails). This process is repeated N times and the number of failures is divided by the total number (N) of times the structure was checked for safety, thus producing the estimated probability of failure. Unfortunately, this process is very inefficient for high reliability structures since only a few limit state violations will be obtained in the total of N samples. The process can be improved by manipulating the way the samples are selected. The most well-known improvement is 'importance sampling' (see below). Latin hyper-cube sampling, antithetic variables and stratified sampling also have been applied (Rubinstein 1981).

12.4.4 Importance sampling

To carry out importance sampling the region where the samples are selected is restricted to an area that is known to be 'interesting' and corrections are made to allow for the biased choice of samples. Formally, Eqn (12.10) is rewritten as

$$p_f = J = \int \ldots \int I[G(\mathbf{x}) < 0] \frac{f_{\mathbf{x}}(\mathbf{x})}{h_{\mathbf{v}}(\mathbf{x})} h_{\mathbf{v}}(\mathbf{x}) \mathrm{d}\mathbf{x} \tag{12.12}$$

where $h_{\mathbf{v}}(\ )$ is an 'importance sampling' probability density function from which the sampling is done (instead of from $f_{\mathbf{x}}(\ )$ directly). As a result, Eqn (12.12) becomes:

$$p_f \approx J_2 = \frac{1}{N}\sum_{j=1}^{N} \left\{ I[G(\hat{\mathbf{x}}_j) \leq 0] \frac{f_{\mathbf{x}}(\hat{\mathbf{v}}_j)}{h_{\mathbf{v}}(\hat{\mathbf{v}}_j)} \right\} \tag{12.13}$$

This shows clearly that the indicator function $I[\ ]$ is weighted by the ratio $f_{\mathbf{x}}(\ )/h_{\mathbf{v}}(\ )$. Good choices of $h_{\mathbf{v}}(\ )$ can reduce considerably the number of sample vectors $\hat{\mathbf{v}}_j$ required to produce a good estimate of p_f. For general purposes a robust choice is to place the mean of $h_{\mathbf{v}}(\ )$ at or near the point of maximum likelihood in the failure domain (Melchers 1995). This usually

© 2008 Woodhead Publishing Limited

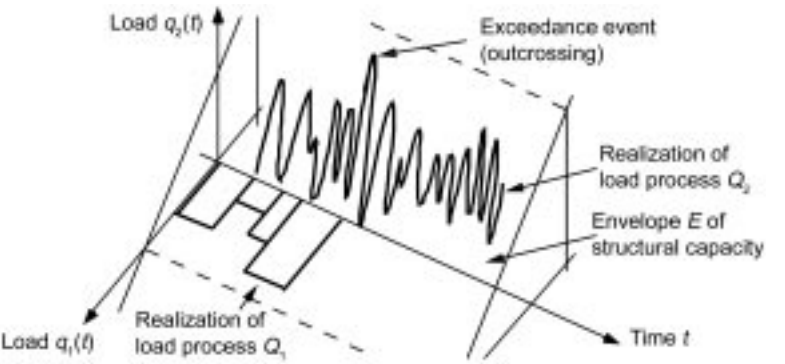
corresponds with the 'checking' or 'design' point in FOSM theory. As this point may not be known, a useful guide is to select the point in **x** space corresponding to the combination of random variables for which the structure is considered most likely to fail. Fortunately this point need not be identified precisely, since the estimate for p_f is not highly sensitive to the location of the importance sampling probability density function. It also is not highly sensitive to its precise form.

12.5 General approach

Strictly speaking it is not correct to assume that Eqn (12.4) or (12.6) can be evaluated separately for every value of time t since this assumes independence between such evaluations. Independence is clearly not the case as the magnitudes of the resistances at various points in time t are correlated. This becomes evident by considering what happens when the interval between such evaluations becomes smaller. The resistance values are not independently random at closely adjacent times, but are similar in value apart from a deterioration loss. Moreover, in practice there is often more than one load to consider. A somewhat more general formulation is described next.

With the resistance of the structural system being time-dependent, and more than one stochastic load, the more general scenario may be represented as in Fig. 12.1. Consider the example of two loads, one being a continuous process and the other a pulse process (Fig. 12.3). The probability of failure can now be defined as the probability that either or both the loads 'crosses-out' of the safe domain defined by the envelope E.

Typically the envelope must be constructed from knowledge of the resistance of the structure and how it is violated by the loads. The envelope is known also as the 'limit state function' (in general there may be several of these, and their union is then relevant). An example is column strength capacity under combined



12.3 Envelope of structural strength (resistance) showing a realization of the vector load process and an outcrossing by the floor loading component.

© 2008 Woodhead Publishing Limited

axial and bending action. The region under the envelope represents the so-called 'safe' domain and that outside the 'failure' domain.

The probability of structural failure in a given time period $[0, t_L]$ (e.g. the 'design life') can be stated as the sum of the probability that the structure will fail when it is first loaded, denoted $p_f(0)$, and the probability that it will fail subsequently (given that it has not failed earlier), denoted by the second term in the following expression:

$$p_f(t) \approx p_f(0) + [1 - p_f(0)] \cdot [1 - e^{-\nu t}] \qquad 12.14$$

where ν is the so-called 'outcrossing rate' (see below). The expression is approximate because the second [ ] term is based on the assumption that failure events are 'rare' and that such events therefore can be represented, as shown, by a Poisson distribution (the last term in Eqn (12.14)).

In Eqn (12.14) the estimation of $p_f(0)$ may be done using Eqn (12.6), (12.7) or (12.8) at time $t = 0$. The outcrossing rate at time t may be estimated as follows. Assume that the random load processes continue indefinitely and have a 'stationary' statistical nature (e.g. in the simplest case, their means and variances do not change with time). Then the rate at which the loads cross out of the safe domain at time t can be estimated from the 'outcrossing rate':

$$\nu = \int_{\text{safe domain}} E(\dot{X}_n | \mathbf{X} = \mathbf{x})^+ f_{\mathbf{X}}(\mathbf{x})\, d\mathbf{x} \qquad 12.15$$

Here $\mathbf{X} = \mathbf{X}(t)$ represents the vector process and $(\ )^+$ denotes its positive component, that is, the component that moves out of the safe domain (the other component moves back in and therefore is of no interest). The term $E(\dot{X}_n | \mathbf{X} = \mathbf{x}) = \dot{x}_n = \mathbf{n}(t).\dot{\mathbf{x}}(t) > 0$ represents the outward normal component of the vector process at the domain boundary. It is there for mathematical completeness. Finally the term $f_{\mathbf{X}}(\mathbf{x})$ represents the probability that the process is actually at the boundary (since if the process is not there it cannot cross-out from the safe domain). Expression (12.5) is valid in the form given for rare outcrossings such as are typically associated with structural failure. The result can be extended to allow for gradual deterioration or enhancement of the structural strength with time. In this case ν becomes time dependent.

Note that expressions (12.6)–(12.8) have ignored the initial failure probability $p_f(0)$ of Eqn (12.14). This is permissible for the way the problem was defined for Eqn (12.4). It assumed that the maximum load is applied only once during the lifetime of the structure. This assumes, reasonably for most structures, that the probability of failure is not affected by precisely when in the lifetime the failure event occurs. In Eqns (12.6)–(12.8) the actual load process is represented as a random variable of the extreme load applied at any time during the life of the structure, and the initial probability term of expression (12.14) is incorporated into the random variable representation.

© 2008 Woodhead Publishing Limited

12.6 Deteriorating structures

To consider deteriorating structural systems it is possible, in principle, to estimate the outcrossing rate $\nu(t)$ as a function of t and thereby develop an expression for the probability of failure as a function of time, $p_f(t)$. Some preliminary efforts in this direction have been described in the literature (Beck and Melchers 2004, Melchers and Beck 2005). From a practical viewpoint, however, there is at present no simple way to develop these expressions and hence to allow for the dependency of the failure probability between different points in time created by the common resistance deterioration of components. In most practical cases it will be necessary (and mostly sufficiently accurate) to estimate the probability of failure by an independent assessment using Eqn (12.7) or a simpler solution.

12.7 Conclusion

The estimation of the reliability of ageing land-based structures requires estimation of the probability of failure as the structure deteriorates with time. In principle the structural resistance of the components ensures that there often is a high degree of correlation between the structural capacities at different points in time. Unfortunately, this is not at present easily considered under the present state of development of theory. It requires estimation of the outcrossing rate as a function of time. For many practical applications it is usually sufficiently accurate to simply ignore correlation in time and simply estimate the failure probability independently at each time point.

12.8 References

Beck AT and Melchers RE (2004) On the ensembled upcrossing rate approach for time variant reliability analysis of uncertain structures, *Probabilistic Engineering Mechanics* 19(1–2) 9–19.

Ditlevsen O (1981) *Uncertainty Modeling*, McGraw-Hill, New York.

Ditlevsen O and Madsen HO (1996) *Structural Reliability Methods*, John Wiley & Sons, New York.

Melchers RE (1995) Load space reliability formulation for Poisson pulse processes, *J. Engineering Mechanics*, ASCE 121(7) 779–784.

Melchers RE (1999) *Structural Reliability Analysis and Prediction* (Second Edition), John Wiley & Sons, New York.

Melchers RE (2007) Structural reliability and existing infrastructure – Some research issues, Paper for Rackwitz Symposium 2007.

Melchers RE and Beck A (2005) Time-variant reliability, Chapter 18 in *Engineering Design Reliability Handbook*, ed. Nikolaidis E and Ghiocel D, CRC Press, Boca Raton, FL.

Melchers RE and Jiang X (2006) Estimation of models for durability of epoxy coatings in water ballast tanks, *J. Ships and Offshore Structures* 1(1) 61–70.

© 2008 Woodhead Publishing Limited

Monteiro PJM, Chong KP, Larsen-Basse J and Komvopoulos K (2001) *Long Term Durability of Structural Materials*, Elsevier, Amsterdam.
Rubinstein RY (1981) *Simulation and the Monte Carlo Method*, John Wiley & Sons, New York.
Stroud AH (1971) *Approximate Calculation of Multiple Integrals*, Prentice-Hall, Englewood Cliffs, NJ.
Turkstra CJ (1970) *Theory of Structural Design Decisions Study No. 2*, Solid Mechanics Division, University of Waterloo, Waterloo, Ontario.

© 2008 Woodhead Publishing Limited

Part V

Inspection and maintenance

© 2008 Woodhead Publishing Limited

13

Inspection of aged ships and offshore structures

C M RIZZO, University of Genova, Italy

Abstract: Reasons for inspection and inspection events are first described in this chapter, highlighting peculiarities that make ships and offshore structures among the most challenging to inspect. Actually, ships are the largest structures ever built, moving all around the world: this makes inspections different from those of land-based structures for a number of reasons.

Factors influencing inspection performances are then commented on in detail, recognising that it is not always possible to quantify the reliability of the complex process called 'detection and sizing of degradation', depending indeed on many parameters not always easy to be defined quantitatively. However, it would be enviable to attempt to do so rationally as far as possible. Current inspection practice is examined from the viewpoint of surveyors, who have to follow different instructions depending on their role but mainly relying on their experience. Methods for detection and sizing of degradation are discussed; traditional methods and future trends are presented for corrosion, fracture and mechanical damages.

Key words: surveys, inspection performances, inspection practices, detection methods, sizing methods, corrosion, fracture, mechanical damage.

13.1 Reasons for inspections

It is widely recognized that appropriate and planned maintenance of ships and offshore structures can save large amounts of money and can extend the design life. Actually, the so-called structural integrity management is becoming a stringent issue for both ongoing ships and offshore structures not only for safety reasons but also because of environmental and economic issues.

The designer is crucial in the initial definition and development of the structural integrity management system, accounting for structural response and design limits such as environmental restrictions, strength and service constraints, etc.

The owner (or the manager on his or her behalf) is responsible for ensuring that appropriate arrangements are in place for maintaining the integrity of a floating structure throughout its life cycle. Such arrangements include scheduled inspections of the structure taking account of actual conditions in relation to original design expectations, assessments of damage or suspected damage, and arrangements for maintenance and repair work.

Periodic inspections and assessments should reflect current good practice, advances in knowledge and changes in risk level, as appropriate; their frequency, scope and methods should be sufficient to assure, as far as reasonably

© 2008 Woodhead Publishing Limited

practicable, that the integrity of the structure is maintained and that adequate information is provided for maintenance and repair activities. Failure mechanisms, deterioration rates and likely consequences of failures should be considered in order to determine the methods, frequency and scope of inspections, and possible repairs. Planning of inspections should identify the procedures and techniques to be implemented to ensure that the objectives are realized.

So far, inspections should identify symptoms and tell-tales that originate from defects. In most cases, signs of damage are evident before the integrity of the structure is impaired; however, it should not be assumed that this is always the case. A 'walk-through survey' can often assist in the survey pre-planning stage. This helps in identifying deviations from the as-built drawings, evident damages or signs of deterioration and it indicates areas where inspections need to be tightened.

13.2 The inspection event

13.2.1 What, where, when and how to inspect

Inspections may be considered as events, scheduled or unscheduled, occurring during the ship's lifetime. They can be described as a minimum by the acronym '$3W + 1H$', being the fourth 'W' (why) already described in the previous paragraph. In fact each inspection needs to identify:

1. The object(s) of the inspection (what)
2. The location(s) of the inspection (where)
3. The time of the inspection (when) and, finally,
4. The manner(s) in which the inspection is performed (how).

All those specifications are necessary in a broad sense for ship and offshore structures. This means that all the above items should be as detailed as necessary considering the aims of the survey. What to inspect ranges from the description of the ship or offshore structure and its actual conditions to the type(s) of expected degradation; where to inspect indicates the geographical location, i.e. the port of call, as well as the specific areas of the structures covered during the specified survey; when to inspect includes either the scheduled time and date and the period of the operational life of the structure; and both the inspection methods and the situations during the inspection are covered by the 'how'. This latter item is the most challenging one, even if the others need to be properly considered as well.

Actually, all the above-mentioned four items influence the reliability of the results of the inspection, i.e. what, where, when and how to inspect may be seen as a categorization of the governing variables in the definition of the probability of detection (POD) and in the probability of sizing (POS) of the degradation of structures.

© 2008 Woodhead Publishing Limited

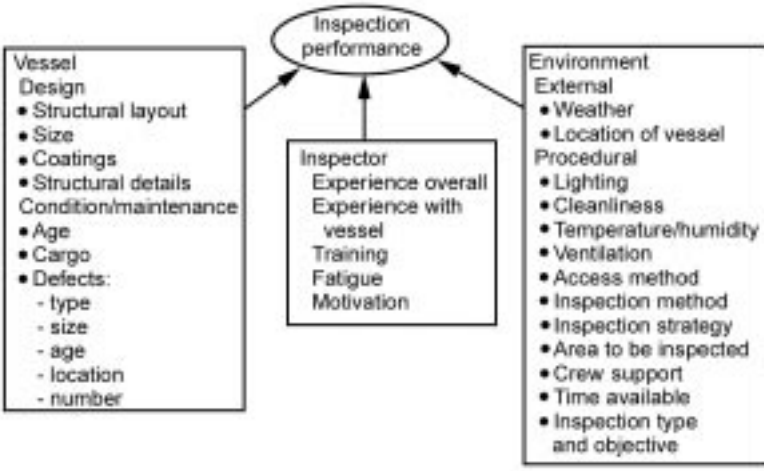
In general, the POD is defined depending only on what to detect (type of defect) and similarly the POS (size of defect). Sometimes the inspection methods and techniques are believed to influence the inspection outcomes and then the POD are corrected taking into account some parameters representing the influence of the inspection method (e.g. visual inspection vs. NDT – non-destructive tests). So far, how to inspect is accounted for in addition to what to inspect. Indeed, many other factors should be considered. Further details about inspection reliability evaluations are provided in Chapter 17 of this book but a more practical overview is offered in the following.

13.2.2 Factors influencing inspection performances

Inspection of ship and offshore structures, like any other diagnostic technique, is not perfect. Inspection will hopefully find degradation effects but they may often be ignored for a variety of reasons, including improper inspection technique, features of the structure and human errors. Only in the late 1980s did the reliability of the inspection process start to be quantified, even if answers to questions about the scatter of inspection data are not always satisfactory.

Inspection performance of ship structures is affected by several factors, which can be grouped according to Demsetz and Cabrera, 1999 [10] and Demsetz *et al.*, 1996 [11], as in Fig. 13.1.

Several practical difficulties are associated with the inspection process of ships and offshore structures, including the associated costs and the large dimensions of the structure being inspected.



13.1 Factors influencing inspections of ships and offshore structures, according to Refs [10] and [11].

© 2008 Woodhead Publishing Limited

In addition to the cost of labour and material, such surveys require the vessel to be out of service for some time. In cases where permanent access facilities are not installed, the inspection costs become even larger due to the high cost of providing temporary access facilities and safety devices for workers.

It should be admitted that, as a matter of fact, complex NDT methods involving instrumentation and/or structure preparation are seldom used, especially for ongoing ships, while visual inspections and close visual inspections are the techniques widely applied. The offshore field is far more advanced in this respect and more advanced measurements methods are used in the condition assessment of ageing platforms. On the other hand, platforms are generally fixed for long periods and this makes the structural monitoring easier, even adopting complex instrumentation permanently installed onboard.

The following technical documentation, although the list is not exhaustive, highlights the recent developments attempting to quantify the description of degradation phenomena from a very practical approach to a more scientific one:

- Guidance notes of the Tanker Structure Cooperative Forum, TSCF (1986, 1992, 1995, 1996) [50–53]
- International Association of Classification Societies (IACS) Recommendation No. 47, 'Shipbuilding and Repair Quality Standard' [23]
- IACS Unified Requirements [19], Group UR Z concerning survey and certification, especially the Enhanced Survey Program (ESP) set in UR Z.10 and UR Z.11
- A few Ship Structures Committee (SSC) projects: SSC-332, 1990 [5]; SSC-372, 1993 [6]; SSC-386, 1992 [41]; SSC-389, 1996 [11]; SSC-401, 1997 [48]; SSC-407, 1999 [40]; SSC-421, 2002 [3]; SSC-428, 2003 [54]
- IACS Recommendations Nos 74, 76, 84 and 96 concerning guidelines for surveys, assessment and repair of hull structures of specific types of vessels [28], [30], [32] and [56] up to the recently issued IACS Recommendation No. 87 relevant to coating maintenance in ballast tanks [20].

The ISSC (International Ship and Offshore Structures Congress) 2003 established the 'Inspection and Monitoring' Specialist Committee V.2 [37], aiming to review the state of the art of the subject with particular attention to structural degradation of steel ships. The Specialist Committee V.6 of the ISSC 2006 – Condition Assessment of Aged Ships was thereafter established and continued in ISSC 2009; they stated the basis of rational procedures for inspections, providing a useful overview of the papers available in the open literature.

Notwithstanding the above, it should be admitted that only in recent years has the condition assessment of ageing ships and offshore structures started to be considered in scientific literature linking the theoretical viewpoint with current practice, i.e. considering the improvement of inspection techniques and procedures as part of design optimization and structural management.

© 2008 Woodhead Publishing Limited

There is still considerable reluctance to quantify inspection performances in a quantitative way: often successes and shortfalls are both simply attributed to 'human factors' [11]. However, the human operator is only one ring of the chain and therefore the relevant effect on the inspection outcome should be quantified like those of the other rings. Of course, it should be admitted that quantification of the 'human factor' is much more difficult than the quantification of instrumentation performance, but it is not justifiable to simply attribute all uncertainties to it. Rather, it should be considered rationally as a complex process governed by several variables that are very difficult to quantify.

Table 13.1 attempts to summarize all the variables involved in the detection process and in the sizing process of corrosion, cracking and mechanical damage in ship and offshore structures, grouping them according to the four main items describing an inspection event (i.e. what, where, when and how), in more detail than in Fig. 13.1. Moreover, the variables were split in relation to their individual degradation effects on ship and offshore structures. Some variables are quantitative, e.g. size of defects or their location; others are qualitative, e.g. ranking or logic variables. As can be easily noted, the inspection process is a really complex one.

The upper part of Table 13.1 lists general variables affecting the inspection performance of ship and offshore structures: such variables are common to all the degradation effects and are not related to specific inspection methods and techniques. The second part of the table lists variables related to the main degradation effects of ship structures and the current practice of ship surveys.

In the following a brief examination of the main variables listed in the table is given, aiming to overview their quantification, as far as possible, and to better explain their meaning.

The ship type, the overall dimensions, the age and the ship conditions clearly influence inspection outcomes since degradation effects are different in different types of ships, being generally greater in older ships but lower for well-maintained ships. Ownership is also a parameter because collaboration from ship-owners and crews may dramatically improve the survey effectiveness.

The scope of the survey and the interpretation of outcomes are mainly related to the sizing of defects. Indeed, a special survey carried out every fifth year is far more extended than an annual survey. Therefore, during the annual survey relatively small defects may be neglected by surveyors if they do not impair the ship safety and may be left for the intermediate or the special survey, when repairs can be more easily carried out, the ship generally being out of service.

The location of the ship may have an impact, e.g. because facilities for inspections may or may not be available. The size of the ship and of her tanks/holds determines the extension of the area to be surveyed.

Tank and hold structures, underwater hull plating and the external shell are inspected in different environments. The structure type and the environment influence the inspection, e.g. if the surveyor needs to look for defects in a dirty

© 2008 Woodhead Publishing Limited

Table 13.1 Factors influencing inspections

(a) General variables affecting the performance of an inspection in ship and offshore structures

What (detection)	What (sizing)	Where	How	When
Ship type and dimensions Ship age Ship conditions Ship-owner/crews	Scope of survey Interpretation of outcomes Type of material	Location of ship Size of ship Structure type/area Cleanliness/environment Means of access Lighting	Skills of surveyor Fatigue and motivation of surveyors Manual or automatic Instrumentation portability Means of recording data Costs	Weather Ship in or out of service Time allowed for inspection

(b) Variables related to degradation effects affecting the POD and POS of inspection in ship structures

What (detection)	What (sizing)	Where	How (current practice)	When (classification survey) (current practice)
Corrosion				
General (uniform)	Thickness decrease (average)	Plate surface in general	Visual, close visual + NDT (UT)	Special + intermediate (or annual if required)
Localized (pitting)	Pit shape, depth and extension on surface	Plate surfaces	Visual, close visual (approx. % of affected area required)	Special + intermediate (or annual if required)
Grooving/necking	Extension and thickness decrease	Stiffener connections	Visual, close visual + NDT (UT)	Special
Protection systems (anodes, coating)	Wear and breakdown		Visual, close visual	Special

© 2008 Woodhead Publishing Limited

Cracking				
Brittle	Shape and sizes	Structural details	Visual, close visual (+ NDT)	Special
Fatigue	Shape and sizes	Structural details	Visual, close visual (+ NDT)	Special
Mechanical damage				
Dent (collision, impact)	Shape, depth, length, width	Shell	Visual, close visual	Special + intermediate + annual
Distortion	Misalignment	Stiffeners	Visual, close visual	Special + intermediate + annual

Notes: Current practice refers mainly to the surveys of classification societies.
Close visual inspections include measurements by means of, e.g., metre tape, callipers or similar instrumentation
UT means ultrasonic gauging by qualified/certified operators
The scope of annual surveys may be extended (up to the one of the intermediate survey) if in the previous surveys substantial corrosion (i.e. ›75% of allowed margins) was found.

© 2008 Woodhead Publishing Limited

environment or the geometry of the structure hides them. As a consequence, means of access are important too.

The skills of the surveyor are basic parameters for successful inspections, as it may easily be understood. The correct evaluation of the surveyors' skill is very difficult, even if classification societies rank the employees' skills according to a quality assurance scheme (see IACS Procedural Requirements nos 6, 7, 19 and 20 and documentation referenced therein [18]).

Typically, inspections are carried out according to survey procedures and checklists. Manual inspections are intended as inspections carried out by surveyors without any specific instrumentation other than simple equipment such as a tape and a calliper. Automatic inspections are carried out using NDT equipment; in some cases such equipment is not directly driven by surveyors who only analyse the measurements either in real time or after the inspection given by automatic sensors. For automatic inspections instrumentation portability corresponds to the means of access for surveyors.

In general, instrumentations give quite accurate measurements if correctly used and manufacturers provide quantification of the uncertainties related to the measurement systems. However, the scatter is often due to operators and practical difficulties rather than to the measurement system itself. These uncertainties are more difficult to define and quantify. The current practice to account for the uncertainties in NDT measurements is to statistically analyse actual inspection data, obtaining suitable statistical distributions of the probability of detection.

Means of recording data should also be considered: e.g., thickness measurements are sometimes inconsistent (e.g. measurement above the original plate size can be found in thickness measurement reports). This means that data were recorded wrongly; such an event is even worse than data missing.

Costs impose constraints on survey procedures and therefore on the relevant outcomes. It is noted that inspection costs need to be related to commercial revenues, i.e. the cost-effectiveness of inspections needs to be assured.

Although the weather would not seem to influence directly the inspection outcomes, consider an inspection carried out in extreme temperatures and/or humidity: surveyors would not spend so much time outside the ship examining the hull or inside a tank; similarly for a survey carried out ashore in a rough sea. Whether or not the ship is in service also influences the survey as, for example, commercial/operational activities prevent surveyors from carrying out some checks.

The time allowed for inspection may be considered as depending on other variables of those mentioned above, i.e. costs and operational constraints. However, classification societies might easily estimate the average time required for a given survey, thus quantifying an important parameter of inspection events.

© 2008 Woodhead Publishing Limited

13.2.3 Quality of inspections and certification

Even if classification societies and other inspection bodies set out their own regulations about qualification of surveyors and certification of devices, the basic requirements and criteria are practically the same.

According to the ISO 19904 standards [36] dealing specifically with offshore structures, all evaluations, inspections, maintenance and repair activities shall be performed by an appropriately qualified team who are:

1. Familiar with relevant information about the specific structures under consideration
2. Knowledgeable about degradation processes and prevention
3. Professionally competent in structural engineering
4. Experienced in offshore inspection tools and techniques.

Similar requirements are set out by classification societies for their surveyors (see IACS quality scheme and procedures [18]); in addition, exclusive surveyors appropriately skilled for the intended survey are generally required for classification surveys and are mandatory for surveys carried out on behalf of flag administrations.

Any equipment or measuring instruments used as part of a structural inspection and monitoring system shall be provided with current valid calibration certificates or ready means of confirming that they remain within acceptable calibration standards. The above requirements are sometimes difficult to apply for ships in service due to lack of support from shore-based firms in remote ports or because of time constraints.

These are the basic principles addressing the inspection quality, which are regulated in practice by a very large amount of rules, guidelines and instructions, whose applicability depends on the type of ship or offshore structure, location, type of inspection, inspection body, flag administration, etc.

In general, also a quality system, like the one of the ISO 9000 series, needs to be implemented for the inspection bodies. IACS members are subject to a dedicated quality scheme approved by IACS and subject to the control of the maritime administrations through bodies of international organizations such as, for example, the International Maritime Organization (IMO) or the European Maritime Safety Agency (EMSA).

13.3 Current inspection practices

13.3.1 International regulatory regime

Rules of classification societies and international conventions issued by IMO are the documents governing the inspection practice for ongoing ships while national and international standardization bodies like ISO, API and NORSOK dictate the inspection practice for offshore structures. However, classification

© 2008 Woodhead Publishing Limited

societies are involved in the safety network of offshore structures too and their services cover also platforms, FPSO, etc.

A brief overview of current inspection and maintenance practices for ongoing ships is given in the following. Further details can be found, e.g., in Basar and Jovino (1985 – SSC-332 [5]), Ma *et al.* (1999 – SSC-407 [40]), Ayyubb *et al.* (2002 – SSC-421 [3]), the report of ISSC 2006 Specialist Committee V.6 [38] and in Chapter 1 of this book.

Generally, the surveys of the structure of a ship can be divided into two main types:

- Those carried out on behalf of shipowners or insurers for management and economic purposes
- Those carried out by surveyors of an official body (e.g. a PSC officer, a flag state inspector or a surveyor of a classification society when acting on behalf of a flag administration) for safety purposes.

Both types are carried out either on a scheduled basis or upon request.

Owners' surveys include structural assessment prior to ship departure and at ship arrival. This includes close visual inspections looking for hull and cargo handling equipment, to ensure that the ship is capable of transporting the goods, and looking for potential damage occurring during the trip. Occasional surveys are generally carried out by owners after damages or accidents, involving third parties such as classification societies and insurers. Sale and purchase surveys are carried out at convenience. Surveys required by insurers are performed mainly during repairs, in order to assess the total costs of repairs to be born directly by insurers.

Most important for all ships and offshore structures are the routine inspections and planned maintenance activities for classifications and statutory needs. The frequencies of these inspections have been established based on in-service experience of various classes of ships, representing an equilibrium point between structure safety requirements and ship operational availability.

With the introduction of larger and larger ships, mainly for liquid or solid bulk transportation, the task of conducting structural inspection has become increasingly complex. Due to the large areas involved and the short time normally available to carry out inspections, it is necessary to focus on critical areas to optimize the effectiveness of the survey.

International conventions and national requirements impose the minimum survey schedule and requirements, but the description of the scope and the technical detail are generally less accurate than those set by classification societies' rules. As a matter of fact, international conventions list the parts to be surveyed relevant to safety at sea (SOLAS convention), environment and pollution (MARPOL convention), load line (ILL convention), etc., briefly referring to the substantial compliance with the applicable regulations.

However, for hull structures, the SOLAS convention requires that ships are designed, built and maintained according to the rules of a classification society

© 2008 Woodhead Publishing Limited

that is recognized by the flag administration of the ship or, alternatively, according to a national rule granting an equivalent level of safety (SOLAS Ch. II-1, Part A-1, Rule 3.1). This means that all vessels have routine inspections of hull structures and planned maintenance activities, for both classifications and statutory needs, as dictated by the practices of classification societies.

In recent discussions at IMO the development of goal-based standards has been proposed [34], [35]. One goal of these documents may be quoted here: 'the goals should aim to ensure that a properly operated and maintained ship remains safe for her whole life'. Then, the assessment of the ship safety (i.e. the assessment of her condition) will shortly became a global statutory requirement throughout all the ship's life according to specified rules aimed at demonstrating the ship's safety. It is now under debate at IMO how to verify that rules comply with the cited goal-based standards.

At present, surveyors largely depend on their own experience and knowledge to qualitatively prioritize structural areas for inspection, although the classification societies indicate the minimum requirements and record files of the ship are made available to class surveyors for survey planning in advance. In the following, some information about the practice of surveys of ship and offshore structures is provided.

13.3.2 Statutory surveys and other inspections by public bodies

As a matter of fact, flag state administrations are responsible for safety and environmental pollution of ships flying their flags under the legislative enactment of international conventions. Periodic surveys are required to check the compliance with the applicable international conventions. However, as foreseen by:

- SOLAS 74: Reg. I/6 (Surveys and inspections) and Reg. I/12(a)(vii) (Issue of certificates)
- Load Line Convention 1966: Art. 13 and Art. 16(3)
- MARPOL 73/78 Convention: Annex I Reg. 4(3) (Surveys and inspections) and Reg. 5(2) (Issue of certificates); Annex II Reg. 10(2) (Surveys) and Reg. 11(2) (Issue of certificates)
- International Tonnage Convention 1969: Art. 6,

the administration may entrust the inspection and survey activities to surveyors of recognized organizations. In 1993, wishing to develop a uniform procedure for the delegation of authority and to give standards for recognized organizations, which are authorized to act on behalf of flag administrations, the IMO Res. 739(18) was implemented (SOLAS Chapter XI, Reg. 1 refers to this Resolution).

As inspection activities are more and more delegated to classification societies by maritime administrations, schedules of class and statutory surveys

© 2008 Woodhead Publishing Limited

required by international conventions are generally aligned. The IMO Resolution states that any assignment of authority to recognized organizations should:

- determine that the organization has adequate resources in terms of technical, managerial and research capabilities to accomplish the task being assigned;
- sign a formal written agreement between the Administration and the organization being authorized;
- specify instructions to be followed in the event that a ship is found not fit to proceed to the sea;
- provide the organization with all appropriate instruments of national law giving effect to the provisions of the conventions.

It should be admitted that flag state inspections of structures are less deep than classification society ones, except in specific cases (accidents, damage). In fact, the main aim of such surveys is to have a spot check of activities delegated to inspection bodies and in particular on classification societies delegated to act on behalf of maritime administrations.

Port State Control (PSC) inspections are carried out by the national authorities of the ports of call, ensuring that ships meet international safety, security and environmental standards, and that crew members have adequate living and working conditions. International agreements among coastal states of a region, called memorandum of understanding (MoU), regulate these inspections. They are the only surveys carried out by public bodies, without direct financial support from other interested parties, since flag state inspections are supported by registration fees of ship owners.

The following MoU are currently active, covering in practice all coastal areas of economic interest:

- Paris MoU, Europe and Canada (www.parismou.org)
- Tokyo MoU, Asia Pacific Region (www.tokyo-mou.org)
- Carribean Memorandum of Understanding (www.caribbeanmou.org)
- Viña del Mar Agreement, Latin American Region (http://200.45.69.62/)
- Indian Ocean Memorandum of Understanding (www.iomou.org)
- Mediterranean Memorandum of Understanding (www.medmou.org)
- Black Sea MoU (www.bsmou.net).

The USCG started the PSC activity earlier (http://homeport.uscg.mil) and targets the ships calling at US ports for inspections. The other MoU follow similar criteria. The PSC officers firstly inspect the ship's certificates and record files of inspections of classification societies in order to check the overall compliance of the vessel with the documents. Since the PSC inspections are carried out with the ship in service, the survey is a general one, often limited to a look around superstructures, decks and accessible areas. In case of doubt, deeper inspections are required and carried out. If some structural deficiencies are found, the

© 2008 Woodhead Publishing Limited

classification society that issued the certificates is called by the PSC officer in order to deal with such deficiencies.

13.3.3 Classification societies' surveys

Mandatory inspections are detailed by rules of classification societies and described in the following [19].

Annual surveys are carried out each year to ensure that the hull structure and piping are maintained in satisfactory condition and typically take one or two days. Usually, the survey includes the visual inspection of external accessible hull and piping surfaces. Deeper inspections, including NDT, are only required when deemed necessary, e.g. thickness measurements, pressure/leakage tests, etc.

Intermediate surveys are carried out at the mid-point of the five-year special survey/certificate cycle, and include the same inspection of external hull and piping surfaces as the annual surveys plus an examination of some ballast tanks and some cargo tanks. The aim of the intermediate surveys is to verify that conditions have not deteriorated at a rate greater than that assumed during the preceding special survey. For vessels that are older than 10 years, the extent of survey is increased. Thickness measurements may be required (and they are actually required for ships subject to the Enhanced Survey Programme, ESP). Intermediate surveys take about three to four days to complete. Intermediate surveys for ESP ships older than 15 years were recently tightened further and made identical to the special surveys.

Special surveys are carried out each fifth year in order to provide an in-depth examination of the structural condition of the vessel. All compartments are subjected to survey, thickness measurements and close-up surveys of selected structures, whose extent increases with the ship's age. The vessel is dry-docked (for passenger ships dry-dock is required every 2½ years and underwater survey of the hull yearly). Special surveys take about one to two weeks and their extent and duration increase with the age and condition of the ship. These special surveys are generally very extensive and require the ship to be out of service. Part of the special survey items can be surveyed in advance, when the ship is in service, in order to shorten the survey time.

The special survey can be carried out with the ship in service, even at sea during voyages, to the greatest extent possible prior to dry-docking, so that survey data can be properly analysed and repair decisions made. This requires that the survey is started about 6 months in advance of the dry-docking, as allowed by the rules. Special surveys require an overall survey of all tanks and spaces and parts of structural elements within close visual inspection range, preferably within hand's reach. Required plate thickness measurements by an approved thickness measurement company require similar access to the structure.

© 2008 Woodhead Publishing Limited

Occasional surveys should be requested by ship managers when conditions of the ship altering the class certificate occur.

Although inspection requirements change among classification societies, a set of common minimum standards has been developed by the International Association of Classification Societies (IACS). Actually, there are many similarities among the rules of major classification societies as far as survey schedules, planning and minimum requirements are concerned. The classification societies that are members of IACS must include as a minimum the requirements of IACS Unified Requirements UR group Z [19], even if each member is free to require more frequent, more stringent or more detailed inspections.

Continuous survey plans have been introduced, mainly for machinery and equipment, but also for hull structures: each ship item is surveyed every fifth year but not necessarily all at the same time (IACS UR Z.6). Thus the survey schedules can be optimized taking into account the operational constraints.

Guidelines and checklists are provided by classification societies and by other regulatory bodies for specific problems, integrating and completing the inspection procedures and practice. Ongoing trends in this area include increased standardization of inspection and maintenance practices among organizations, a drive to decrease cost while improving reliability, and the increased use of information technology.

The widely adopted inspection practice of classification societies continues to be visual inspection by skilled personnel, integrated by ultrasonic thickness measurements. Other NDT methods are used for special cases on board ships but are more widely used in offshore structures.

The offshore field is far more advanced in this respect: complex measurement techniques are used in the condition assessment of ageing platforms, adopting sophisticated instrumentation, also permanently installed on board (see, e.g., H&SE 1988 [13]; H&SE 1998 [14]; H&SE 2000 [15]; NORSOK standards 1997 [43]).

13.3.4 Inspections of insurers, charterers and other involved parties

Insurance companies normally base their assessment on a number of issues such as past experience with the particular ship or ship owners and status of the class certificate. Generally such inspections, typically one-day inspections, are carried out with the ship in service and therefore can be assimilated to an annual survey of a classification society. Specifically, such inspections aim to verify that the ship is able to carry out the required service; they are therefore focused on operational plants and piping (e.g. pumps, ramps, hatches, hull outfitting, etc.) and cargo handling equipment, even if general conditions of the hull structures

© 2008 Woodhead Publishing Limited

are verified at the same time, looking for special critical areas and the general appearance of the ships to identify ships suspected to be substandard.

In cases of accident or damage, marine surveyors may be employed either exclusively or non-exclusively by a ship owner, underwriter, broker, ship builder, ship repairer, salvors, governmental agency and others for specific purposes, e.g. determining the nature, causes and extent of damage, agreeing and recording methods of required repairs and related costs and examining repairs carried out.

13.3.5 Crew inspections

The condition of the structure should be kept under constant surveillance by continuous and periodic inspections throughout its operating life by the crew while the vessel is in operation. However, the continuous trend of reducing the number of seafarers and their skills is preventing such practices from becoming the norm. It should be noted that some periodic inspections may be performed by crew, but others would require preparation beyond crew capabilities. Also, in some cases, parts of the ship's structure may not be inspected by crew while at sea since the area is inaccessible.

Crew inspections, when possible, can accomplish the following:

- detect and repair minor damage and deterioration (e.g. coating breakdown, scale formation on plates and shapes, localized wastage, etc.)
- obtain an early warning of major structural problems (e.g. dents in structural members, fractures, pitting)
- keep corrosion control systems under surveillance (e.g. wastage of zinc anodes)
- identify areas for detailed surveys and prepare planning and budgets for shipyard availability.

By doing all of the above, overall survey and repair costs can be noticeably reduced.

13.3.6 Reporting and information exchange

The outcomes of inspections need to be reported and exchanged among interested parties. This is a crucial point for ships and offshore structures, as a perfect inspection without adequate reporting is absolutely useless to many of the parties involved during the life of the structure.

Findings from inspection activities are recorded on appropriate forms and maintained in the ship's inspection file. Dedicated checklists and forms are developed by classification societies and inspection bodies for requesting, recording, reporting corrective action, analysing, and processing structural inspections and NDT examinations, etc. Each classification society provides checklists for the various types of survey, aiming to standardize the inspection

© 2008 Woodhead Publishing Limited

procedures; unfortunately, for the time being, such documentation is not unified among the inspection bodies and is considered confidential by classification societies. In general, checklists are supported by narrative reports of surveyors, completing the routine items of the survey with notes and comments as necessary. Appropriate wording is extremely important and therefore IACS has issued a surveyors' glossary [31].

All class provide scantling software able to check actual scantlings against applicable rules, if necessary even by FE models. BV and GL are focusing on the automation of thickness gauging and recording while ABS, DNV and NKK offer 3D-CAD databases useful to store inspection data, including measurments and photos, eventually linked to scantling sofware. Ship specific PC checklists/ reports are provided by LR. Classification societies have also developed computer-based schemes to implement the survey status. In general, access through the Internet is provided to surveyors of the society and to shipowners [18], [29]. Although classification societies are improving such systems assisting owners in planning maintenance schemes, current practice is still mainly dependent on manually recorded measured data, ship drawings and tables. It usually takes a long time for data reporting and analysis.

Some research projects have been funded that are achieving seamless electronic data exchange standards between information taken on board the ship and the use of structural assessment tools [39]. An international standard, the ISO 10303-STEP standard (Standard for the Exchange of Product Model Data), for representation and exchange of technical information about shipbuilding products has been proposed. Significant improvement in the overall efficiency of ship repairs and consequently in ship safety are expected from the integration of the process.

Specifically important is the feedback of inspection results to the structural designer. By being aware of the deficiencies found and the corrective actions accomplished on the structure he or she has designed, the designer can analyse the causes and consequences of the deficiency, decide whether the corrective action was sufficient, and determine if the original design should be modified to prevent recurrence of similar deficiencies in follow-on constructions. It is also desirable to have all inspection results statistically analysed.

An item of concern regards the confidentiality of exchanged data, as the condition of a ship or offshore structure involves large economic interests. Coordination and exchange of information among interested parties is therefore quite difficult, even though it is absolutely necessary.

13.4 Detection and sizing methods

13.4.1 General requirements for detection and sizing

Assessment of degradation of marine structures needs quantitative information, which can be processed in rational ways. Modern analytical methodologies, e.g.

© 2008 Woodhead Publishing Limited

reliability analyses, make full use of data acquired from Non Destructive Examination (NDE) and are able to gather, filter and process information about the actual condition of ageing structures, providing an estimate of the parameters defining the residual structural strength. However, further to problems related to NDE themselves, several practical difficulties are associated with the inspection of marine structures, as described in Section 13.2.2.

A huge amount of documentation is available in the literature dealing with NDE of structures from a general viewpoint, ranging from books and papers to national and international regulations. Among the others, Halmshaw (1997 [12]), Porter (1992 [44]) and Bøving (1989 [7]) provide comprehensive guides into the wider NDE world, covering some specific topics of marine structures. Halmshaw (1997 [12]) surveys the NDE European Standards (CEN) applicable to welded structures, also covering the introduction of computer technology and the digitization of data of the main techniques. Porter (1992 [44]) analyses NDE in shipbuilding. Bøving (1989 [7]) describes more than 85 methods and discusses their applications and limitations, ranging from simple visual inspections to the most advanced technologies, some not yet in use even in the industrial field. Very useful references to applicable rules and standards are also reported.

Until some decades ago, detection and measurement of structural deterioration of ships and offshore structures was qualitative to a large extent. More recently, sensors and quantitative measures have been more and more introduced. However, complex NDE methods, involving expensive instrumentation and/or time-consuming preparation, are still seldom used for ship structures; rather, visual inspections and close visual inspections are the techniques widely required, commonly associated with ultrasonic measurements of thickness. The main needs of structural degradation sensors in marine structures can be argued from what is reported in Section 13.2.2 and Table 13.1:

1. Capability of facing geometries and materials of ship structures
2. Usability in harsh environments
3. Capability of scanning large areas, possibly in a short time, and recording measured data
4. Ease of carrying and moving, even along difficult routes and in awkward positions
5. Capability of detecting and measuring main ship structural degradation phenomena
6. Ease of use by unskilled personnel, without preparation of surfaces potentially damaging the structure or its protection systems (i.e. coatings).

Non-destructive testing (NDT) techniques would probably be the best solution for the assessment of degradation of marine structures due to the size and complexity of the systems involved and, above all, because they provide quantitative information which can be processed in rational ways. It seems

© 2008 Woodhead Publishing Limited

therefore appropriate to better describe the main features of the sensors necessary for the survey of ship structures.

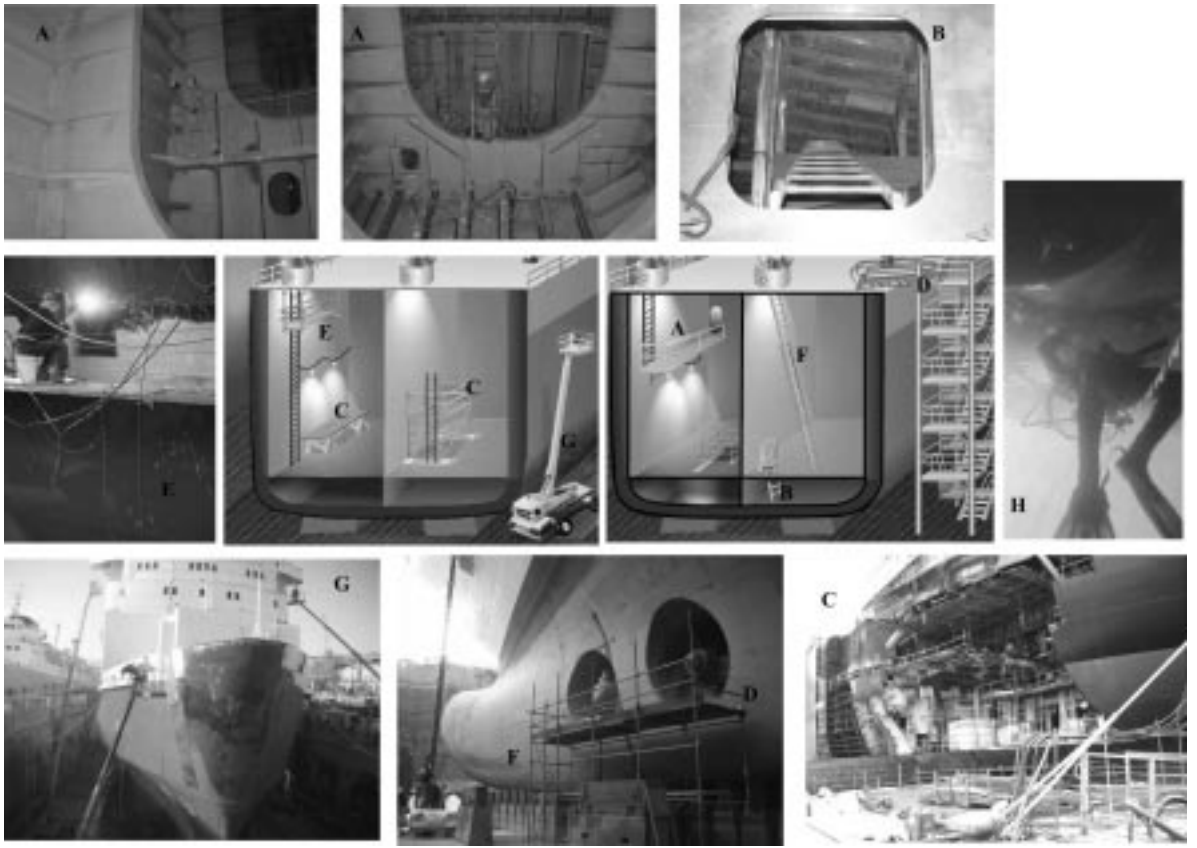
Weight and size of the equipment for detection of degradation are limited by the structure geometries. The size of systems must be smaller than the minimum standard manhole of ships (600 × 400 mm) and sensors must be able to access small areas, e.g. the corners of tanks or double bottom cells. The equipment should be light enough and easy to carry, even along difficult routes such as vertical ladders, and should be suitable for applications above the operator's head (e.g. gauging of deck stiffeners) or in other difficult positions. Table 13.2 compares different means of access during surveys, and Figs 13.2 and 13.3 show alternatives for access to structures.

Table 13.2 Means of access: advantages and disadvantages

Method	Advantages	Disadvantages
Walking through	Inexpensive	Poor accessibility, only line of sight view
Permanent means installed as built (ladders, bulwarks, etc.)	Safety increased, good accessibility	Cost, weight, maintenance, unwanted structural details
Climbing without safety devices	Increased accessibility, inexpensive	Unsafe and out of rules, impossible to climb some areas
Climbing with fall safety device	Increased accessibility, inexpensive	Initial rigging difficult, physically demanding
Wire lift platform	Increased accessibility, inexpensive	Initial rigging difficult, training required
Fixed staging	Access available to all members in party, repairs possible	Expensive and labour intensive, time consuming
Portable staging	Relatively safe, light repairs possible	Expensive, difficult initial rigging
Cherry picker	Increased accessibility	Expensive
Rafting	Applicable during service, inexpensive	Expensive, time consuming, unsafe
Binocular and other optical devices	Applicable during service	Hands-on inspection not possible, only line of sight view
Divers	Applicable during service, docking not required	Expensive, time consuming, unsafe, need divers experienced in ship inspections, only for outside shell
Remotely Operated Vehicles	Applicable during service, gas freeing not required (if equipment intrinsically safe)	Expensive, easy to be disoriented, skilled operators required

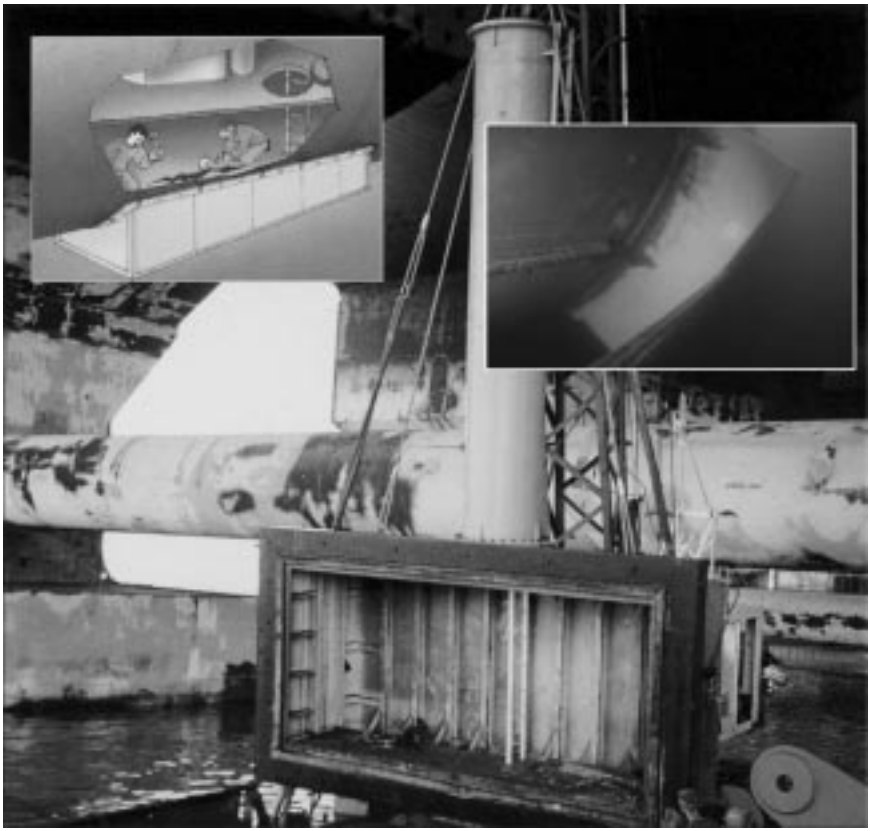
Note: as required by SOLAS Reg. II-1/3.6 for ships built on or after 1 January 2005.

© 2008 Woodhead Publishing Limited



13.2 Examples of means of access to ship and offshore structures. Key: **A** surveyor on permanent arrangements (ladders and bulkwarks, etc.); **B** permanent arrangements (ladders and manholes); **C** temporary staging (inside tanks/holds); **D** temporary staging (outside hull); **E** mobile platforms (wire lifting platform); **F** mobile vertical ladders; **G** cherry pickers; **H** diver with camera (courtesy of www.hydrex.be).

© 2008 Woodhead Publishing Limited

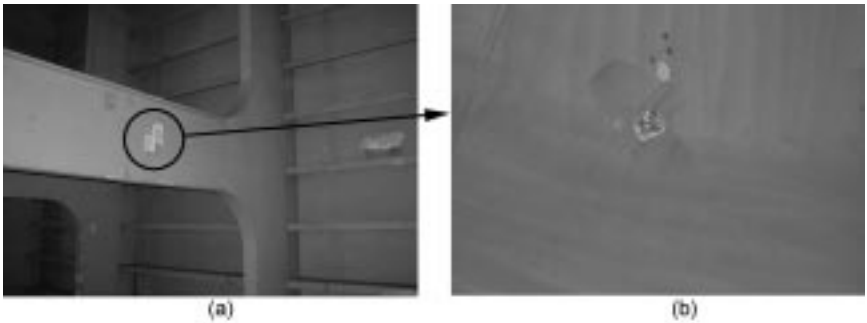


13.3 Mobile dock for dry repairs of underwater shell and structures (courtesy of www.hydrex.be).

Time is also of concern, as the length of time for which ships are out of service for inspection and maintenance should be limited as far as possible. Then, fast scanning of the structure is an advantage provided that the sensor is able to gather data at high frequencies. The assessment should take the shortest time possible, or in-service monitoring, by means of permanent systems able to record gathered data, will be preferred.

To reduce survey time, sensors able to collect average/overall information on plates and stiffeners rather than point by point are preferred, even if some degradation mechanisms, e.g. pitting corrosion or cracks, need local detection. The efficiency of detection varies depending upon the type, number, depth and size of defects. Failure modes like leakages can be caused even by a single corrosion pit or small crack, but general assessment can be carried out on the basis of overall information. It is worth noting that local information needs to be treated to obtain overall assessment while some techniques measure bulk conditions and implicitly provide an average status, informative for overall

© 2008 Woodhead Publishing Limited



13.4 (a) Coating damaged and recoated after thickness gaugings (the zoom on the pit (b) refers to an unrepaired surface).

assessments (e.g. hull girder corrosion) but not useful for local failure modes (e.g. fractures, dents).

The sensors should display information so that it is easy to read and should require minimum technical knowledge by operators in order to save costs of highly skilled NDT personnel. However, as already said, fewer crew are being employed and the man-hours necessary to operate detecting and monitoring instrumentation may not be available, nor even feasible in some cases.

As is well known, the environment of marine structures is generally not very clean. For most techniques accurate cleaning of the surface is necessary. The particular surface preparation or coupling medium needed for some techniques is a large disadvantage, particularly when damaging the coating protection (see Fig. 13.4).

Some emerging techniques (see Section 13.4.2) have the ability to detect corrosion on and under the coating without its preparation. These new technologies may reduce the time and cost of detection.

Durability and service lifetime of instruments are also important because of the use of these instruments in a harmful environment and, for continuous monitoring, because the long time span of ships' voyages requires reliable sensors and recording means.

Taking into account all the above, one of the most efficient sensors for structural degradation of marine structures remains the human body: weight and size are suitable for movement in ships, skill and experience integrate the relatively low accuracy of the human eye and can reduce the time for survey.

Moreover, it is noted that the scan rate of the human eye is quite fast, accounting for the large field of vision of the 'two coupled sensors'. Sense of hearing, smell and touch integrate the main sensors as well as small equipment such as a hammer for rust removal, a tape, an appropriate flashlight, a booklet, etc.

The recording rate and reliability may become a weak point for the human sensor, especially if it is limited to the 'buffer-memory' of the surveyor. Also the accuracy of the measurements may be not completely satisfactory for condition

© 2008 Woodhead Publishing Limited

assessments involving a review of the scantling. However, measurements of size of local defects are easy to obtain by a calliper or a meter with sufficient accuracy and overall data are efficiently stored, either in a booklet or recorded by a tape. New digital photography techniques are also really helpful and reference pictures have been recently introduced in surveyors' guidelines (e.g. IACS Rec. 87 [20]). Apart from the surveyor's costs (including training costs and personal safety equipment costs), the main disadvantage of human sensors is the subjectivity of the technical judgement.

Sometimes waterproof instrumentation is needed for underwater surveys. A widely accepted method is diving with a video-camera for visual underwater inspections: in such cases it is important to have a means of communication between the diver and the surveyor, who should drive the inspection and, where necessary, require the diver to carry out measurements or checks. ROV (Remotely Operated Vehicles) are being used more and more in place of divers, even though their work is generally limited to visual inspection and simple operations (H&SE 1988 [13]).

13.4.2 Corrosion detection and measurement

Current practice

Visual inspections are the first means of evaluating degradation of structures due to corrosion. Even a newly trained surveyor is able to evaluate whether the coating protection is still effective, since light-coloured painting is requested, aiming to highlight even small rust spots.

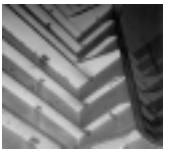
It is much more difficult to quantify the extent of the coating breakdown and to rank the coating condition according to, e.g., the IACS system described in all classification rules (see IACS UR Z.7 [19]):

1. Poor: condition with general breakdown of coating over 20% or more of areas or hard scale at 10% or more of areas under consideration.
2. Fair: condition with local breakdown at edges of stiffeners and weld connections and/or light rusting over 20% or more of areas under consideration, but less than as defined for poor condition.
3. Good: condition with only minor spot rusting.

Even if photos and templates are given in surveyors' guidelines (IACS Rec. 87 [20]), long training is needed to reach a sufficient level of confidence in the judgement. Similar qualitative guides are provided by other regulatory bodies (ISO, TSCF, commercial standards, etc.). The Tanker Structure Cooperative Forum (TSFC 1995 [52]) has tabulated the above definitions, comparing them to other references and descriptions. Table 13.3 merges TSCF and IACS definitions and compares them with ISO, ASTM and European rust scale: several photos and pictorial examples of coating conditions are reported in IACS Rec. 87 [20].

© 2008 Woodhead Publishing Limited

Table 13.3 Definitions of coating conditions

	IACS rating/condition		
	Good	Fair	Poor
Spot rust/light rust	Minor/Minor (<3%)	>20%	
Edge weld	<20%	>20%	
Hard rust scale	Minor (<3%)	<10%	>10%
General breakdown	Minor (<3%)	3–20%	>20%
Local breakdown of coating or rust on edges or weld lines	<20%	20–50%	>50%
Other references			
ISO	Ri3	Ri4	Ri5
European rust scale	Re3	Re5	Re7
ASTM D 610 rust scale	6	4	1–2
Photo reference (from IACS Rec. 87)			

Protective coating breakdown is generally estimated qualitatively and information on quantitative analysis is considered 'commercial in service' and rarely carried out by means of computer-aided imaging analysis, even though modern digital cameras are relatively inexpensive.

Few scientific papers about visual inspection are available. It can be concluded that only skill and experience govern the visual inspections of corrosion in ships and offshore structures, according to rules and standards provisions.

The distance of the element to be examined by the surveyor influences the inspection quality. Close-up visual inspections are accurately defined by IACS (IACS UR Z 7.1.2.4 [19]) as '... a survey where the details of structural components are within the close visual inspection range of the surveyor, i.e. normally within reach of hand'.

Some critical areas are requested to be closely surveyed by the rules, depending on the ship's age and type, as not all the ship's structures can be inspected close-up at every survey. This should grant that critical hidden areas are inspected but the general corrosion wastage level of the whole structure remains under the judgement of the surveyor. Table 13.4 shows the close-up survey requirement for general dry cargo ships. Similar requirements are set for other ship types.

The various means of access to structures such as permanent arrangements, temporary staging, mobile platforms or cherry pickers, rafting inside a tank/hold filled by water ballast, ROV, divers and cameras, mobile dry-docks, etc., allow

© 2008 Woodhead Publishing Limited

Table 13.4 Close-up survey areas at surveys (example from IACS UR Z 7.1 [19], general cargo ship)

Special Survey No. 1, age $\leq$ 5 years	Special Survey No. 2, 5 $<$ age $\leq$ 10 years	Special Survey No. 3, 10 $<$ age $\leq$ 15 years	Special Survey No. 4 and subsequent, age $>$ 15 years
(A) Selected shell frames in one forward and one aft cargo hold and associated tween deck spaces. **(B)** One selected cargo hold transverse bulkhead. **(D)** All cargo hold hatch covers and coamings (plating and stiffeners).	**(A)** Selected shell frames in all cargo holds and tween deck spaces. **(B)** One transverse bulkhead in each cargo hold. **(B)** Forward and aft transverse bulkhead in one side ballast tank, including stiffening system. **(C)** One transverse web with associated plating and framing in two representative water ballast tanks of each type (i.e. topside, hopper side, side tank or double bottom tank). **(D)** All cargo hold hatch covers and coamings (plating and stiffeners). **(E)** Selected areas of all deck plating and underdeck structure inside line of hatch openings between cargo hold hatches. **(F)** Selected areas of inner bottom plating.	**(A)** All shell frames in the forward lower cargo hold and 25% frames in each of the remaining cargo holds and tween deck spaces including upper and lower end attachments and adjacent shell plating. **(B)** All cargo hold transverse bulkheads. **(B)** All transverse bulkheads in ballast tanks, including stiffening system. **(C)** All transverse webs with associated plating and framing in each water ballast tank. **(D)** All cargo hold hatch covers and coamings (plating and stiffeners). **(E)** All deck plating and underdeck structure inside line of hatch openings between cargo hold hatches. **(F)** All areas of inner bottom plating.	**(A)** All shell frames in all cargo holds and tween deck spaces including upper and lower end attachments and adjacent shell plating. Areas **(B–F)** as for Special Survey No. 3.

(A) Cargo hold transverse frames.
(B) Cargo hold transverse bulkhead plating, stiffeners and girders.
(C) Transverse web frame or watertight transverse bulkhead in water ballast tanks.
(D) Cargo hold hatch covers and coamings.
(E) Deck plating and underdeck structure inside line of hatch openings between cargo hold hatches.
(F) Inner bottom plating.

Note: Close-up survey of cargo hold transverse bulkheads to be carried out at the following levels:

- Immediately above the inner bottom and immediately above the tween decks, as applicable.
- Mid-height of the bulkheads for holds without tween decks.
- Immediately below the main deck plating and tween deck plating.

© 2008 Woodhead Publishing Limited

Table 13.5 Thickness measurement requirements (example from IACS UR Z 7.1 [19], general cargo ship)

Special Survey No. 1, age $\leq$ 5 years	Special Survey No. 2, 5 $<$ age $\leq$ 10 years	Special Survey No. 3, 10 $<$ age $\leq$ 15 years	Special Survey No. 4 and subsequent, age $>$ 15 years
1. Suspect areas.	1. Suspect areas. 2. One transverse section of deck plating in way of a cargo space within the amidships 0.5L. 3. Measurement for general assessment and recording of corrosion pattern of those structural members subject to close-up survey according to Table 13.4.	1. Suspect areas. 2. Two transverse sections within the amidships 0.5L in way of two different cargo spaces. 3. Measurement for general assessment and recording of corrosion pattern of those structural members subject to close-up survey according to Table 13.4. 4. Within the cargo length area, each deck plate outside line of cargo hatch openings. 5. All wind and water strakes within the cargo length area. 6. Selected wind and water strakes outside the cargo length area.	1. Suspect areas. 2. Within the cargo length area: a) A minimum of three transverse sections within the amidships 0.5L. b) Each deck plate outside line of cargo hatch openings. c) Each bottom plate, including lower turn of bilge. d) Duct keel or pipe tunnel plating and internals. 3. Measurement for general assessment and recording of corrosion pattern of those structural members subject to close-up survey according to Table 13.4. 4. All wind and water strakes full length.

Notes:
1. Thickness measurement locations should be selected to provide the best representative sampling of areas likely to be most exposed to corrosion, considering cargo and ballast history and arrangement and condition of protective coatings.
2. For ships less than 100 metres in length, the number of transverse sections required at Special Survey No. 3 may be reduced to one and the number of transverse sections at Special Survey No. 4 and subsequent surveys may be reduced to two.

Guidance for additional thickness measurements in way of substantial corrosion

Structural member	Extent of measurement	Pattern of measurements
Plating	Suspect area and adjacent plates	Five-point pattern over 1 m^2
Stiffeners	Suspect area	Three measurements each in line across web and flange

© 2008 Woodhead Publishing Limited

different conditions for close-up surveys and then different accuracies of inspection. Several guidelines are provided by IACS [21], [22], [24]–[27] and other regulatory bodies [33]: such regulations involve also the International Labour Organization (ILO) and management problems. Table 13.2 shows the features of various means of access.

Nowadays, ultrasonic gauging is the widely applied method for thickness measurement rather than the 'drilling holes' method used several years ago. Time consumed to thoroughly test a large structure is the major disadvantage of ultrasonic measurement because of point-by-point examination. Furthermore, preparation of the surface (damaging the coating) and a coupling medium are required. Moreover, when many corrosion pits are generated, it is difficult to remove heavy rust and even if the rust is removed, correct thickness measurement is difficult due to unevenness of the surface. The problem is to determine which parameters (average thickness, minimum thickness, pit intensity and so on) are appropriate for the evaluation of the corrosion assessment.

Classification societies set out location and extension of thickness measurements depending on the ship's type and age, aiming to make inspection results objective and comparable, as shown, e.g., in Table 13.5. Generally, average thickness, pit maximum depth and pit intensity (as a percentage of the plate surface) is recorded. In some cases, only for quite limited areas, more specific inspections are required, reporting more accurate pit statistics.

Reference [2] reports very high localized corrosion rates with respect to the rules and interaction among corrosion, cracking and buckling, concluding that gauging, even if carried out according to the rules, does not represent reality in the captioned case.

The rules trend is therefore towards a more detailed quantitative definition of corrosion type and intensity (see e.g. Common Structural Rules for Tankers and Bulk Carriers issued by IACS [16], [17]): acceptance criteria for uniform and local corrosion are provided and also thickness measurement locations are more and more carefully described.

However, subjectivity of visual inspection and ultrasonic test remains a major fault: in the first case, the sensor being a human eye, it is clear that visual inspection is subjective; ultrasonic measurements are also subjective even if to a minor extent. Though classification society rules are more and more stringent on the gauging location (see IACS UR Z7 and Z10), in practice technicians are more or less free to take the measure in or outside a pit.

Several software programs used by classification societies cover ships' in-service assessment. Actual thickness can be assessed automatically according to the relevant classification rules. Such automatic methods could move onboard the condition assessment of ageing ships, now requiring time-consuming calculations in offices, and also settle the subjectivity of methods by fast and automatic analysis of large amounts of data.

© 2008 Woodhead Publishing Limited

Advanced methods

Advanced existing wastage assessment technologies are not common in ship structures but they are applied in the offshore field or to other steel structures, where in-situ monitoring techniques are more developed because of difficulties and costs in stopping production.

It has been noted that inspections can break or degrade coating. A brief summary of promising methods is reported below, mainly from References [1], [7], [12] and [47], having in mind emerging sensors and monitoring techniques applicable to marine structures but not damaging coatings and means of corrosion protection.

Acoustic emission methods, based on acoustic emissions of the structure excited by a known impulse, may be used to monitor overall corrosion by measuring the change of stiffness of the structure. They can be applied even to detect development of pitting corrosion. Such techniques are common in offshore platforms, because the structure is fixed and comparisons of structural response may be carried out during the structure's lifetime.

Radiographic methods are generally used to provide images of the variations in the thickness of metallic components for particular structural components (e.g. pressure tanks, thick butt welds, etc.): they need access from both sides of the plating. Furthermore, protection is necessary because such methods involve radiations dangerous to human life. Specialized technicians following the relevant safety standards are needed.

Thermal imaging (or time-resolved thermography), which claims to discover a defect by distinguishing thermal emissions from the surface of the structure in way of the defect itself, has been developed for the detection of hidden corrosion. It is a very complex technique, especially if used for metallic structures: its employment is really very limited. A high level of skill is necessary to interpret the images from the infrared camera.

The **weight-loss coupon method** is carried out by periodically monitoring a coupon exposed to field corrosion conditions. Measurement of weight loss is directly related to the corrosion rate. The coupons also provide direct measurement of the increasing electrical resistance of the conductor as the cross-sectional area of materials reduces. It is a simple but inaccurate and unreliable method.

Galvanic thin film micro sensors are used for in-situ corrosion monitoring: two different materials corrode at their corrosion rates if they are insulated. When they are short-circuited, they develop a current correlated with the corrosive nature of the environment. The coating performance and hidden corrosion are then measured.

Electrochemical techniques (**electrochemical sensors**, **electrochemical noise technique**) are complicated and difficult for ships and influenced by temperature and pH, as well as by reduction and re-oxidation behaviour.

© 2008 Woodhead Publishing Limited

Hydrogen measurement probe is sometimes used since the corrosion process often proceeds with the evolution of hydrogen. Such a method is rarely used in the dirty environment of ships, though it is sometimes used on board platforms.

Chemical sensors of various types (fluorescent, colour change) adopted in **dye penetrant** testing have not proven very practical for corrosion assessment because of the spreading corrosion of marine structures.

Strain gauges need calibration with the non-corroded element and sensors are generally affected by the corrosive environment as they need to be bonded to the structure, although it is possible to estimate the structural stiffness reduction as an indirect measure of corrosion.

Optical methods (optical fibres) are mainly used for non-metallic materials in place of strain gauges, where the sensor itself can be included in the structure matrix (e.g. FRP). High resolution and acquisition frequency are the main advantages of the method. Optical fibres on metallic structures can be bonded for monitoring applications, as they are safer than electrical sensors (i.e. strain gauges) in hazardous areas, e.g. of tankers.

Magnetic flux measurement was initially used for inspection of storage tank floors: a sensor is immersed to sense the current flow between anodic and cathodic areas, then the metal loss is measured. By using computer control and processing, a map of corrosion damage can be produced.

Ultrasonic guided waves have been used as passive sensors and give high penetration power; these waves have a long propagation distance through the complicated ship structure.

Natural frequency measurements (by accelerometers) are also used in offshore structures, monitoring them in a similar way to acoustic emission methods. This is a cheap and reliable method of detecting changes in structural responses (stiffness). The level of stiffness change is sufficient to detect the failure of main members or redundant configurations even if locating the damage needs other inspection methods.

Electrochemical impedance spectroscopy has been developed to measure the early stage degradation of coating and substrate corrosion underneath a paint coating. To monitor in-situ corrosion of surfaces and interfaces, implantable, permanently attached electrodes have been used. The corrosion of coated materials begins with the absorption of moisture into the coating, and then corrosion occurs after the water in the coating reaches the substrate. The resistance will be decreased as the coating degrades.

The **eddy current arrays method**, based on eddy currents generated in the structures by a fluctuating magnetic field, gives high resolution and easy-to-read outputs with fast response, but requires further development for application to large and geometrically complex ship structures, although it is common for offshore structural details.

© 2008 Woodhead Publishing Limited

13.4.3 Fracture detection and measurement

Current practice

Cracking is a localized problem but, as ship structural details are mainly typical, there may be repetition of cracking at geometrically similar locations: such behaviour generally points to design or fabrication deficiencies. Cracks occur typically at welded joints but may occur at other details that result in stress concentrations (also identified as hot spots). Therefore local detection is needed.

It is essential to know in advance the critical areas prone to fatigue cracks for correct survey performance. This is easier but not straightforward for standard details, and much more difficult in novel designs. Surveyors' skill is a key factor in this regard.

Cracks could be efficiently visually detected as too many locations would need to be monitored by individual sensors. A **visual examination** should determine the type of crack and assess whether it is likely to propagate.

Dye penetrant tests would also be used when carrying out a visual inspection, but they need a clean surface and provide an approximate measure of the surface crack length but not the crack depth. **Photographic records** of the tests may also be kept. Sometimes a **replica** of the crack surface is taken for further studies by a specialized laboratory: this consists of casting a mould of the cracked part. Such technique allows recording the crack path and surface to study its growth.

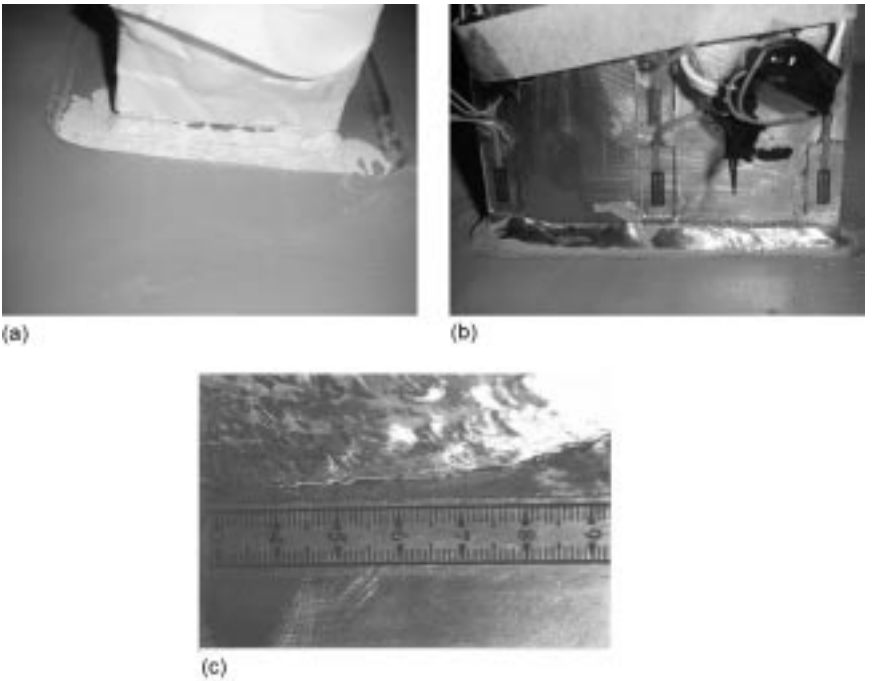
Another cheap and useful technique for crack detection is the **magnetic particle** test, which may be carried out even underwater as shown in Fig. 13.5.

When cracks are expected at structural hot spots, and also for monitoring purposes, strain gauges may be bonded in the way of the weld toes: deviation of gauge signals from their usual behaviour indicates a starting crack in the way of the gauge. Approximate sizing may be possible if some gauges are appropriately located in the area of crack growth.

Advanced methods

Tiku and Pussegoda (2003, SSC-428 [54]) compare several NDT methods for fatigue and fracture. An extensive literature review to seek out potential NDT techniques to estimate residual lives of ship structures was carried out, identifying suitable technologies that could provide crack detection and crack growth measurement. Conventional techniques have been ranked as per Table 13.6; advanced techniques are also described in detail (Acoustic Emission, Infrared Thermography, Laser Shearography, Direct Current Potential Drop (DCPD), Alternating Current Potential Drop (ACPD), Alternating Current Field Measurement (ACFM), Crack Propagation Gauges). Basically, all methods measure the increase (e.g. of acoustic or thermal emissions) or the drop (e.g. of

© 2008 Woodhead Publishing Limited



13.5 Example of crack sizing methods: (a) dye penetrant test; (b) strain gauges at hot spot; (c) underwater magnetic particle inspection on tubular joint weld toe.

electrical potential or of electric current) induced by the fracture with respect to an uncracked area of the structure.

Five additional potentially most efficient and accurate techniques were selected: the ABI (Automated Ball Indentation) technique, the acoustic emission technique and the crack propagation gauge technique were recommended for marine applications.

However, assessment methods other than visual inspection are generally seldom used in ship structures because a single crack does not impair structural safety due to redundancy until it is not clearly detectable even by a rough general inspection.

Different methods are used in the offshore field, especially **ultrasonic test**, **eddy current test**, **potential drop test** (using alternating or direct current: ACPD or DCPD) or other similar NDT techniques based on the electromagnetic field properties. Such techniques are generally able to characterize the crack dimensions and location with different accuracies, of course better than visual inspection, by examining an electromagnetic field generated in the structure that is supposed to be locally distorted by the presence of a defect.

It seems that ultrasonic and ACPD methods are the only two established NDTs used for measuring crack depth in welds. Unlike ultrasonic inspection,

© 2008 Woodhead Publishing Limited

Table 13.6 Comparison of NDE methods for fatigue fracture (adapted from ref. [54])

	Ultrasonics	X-ray	Eddy current	Magnetic particle	Liquid penetrant
Capital cost	Medium to high	High	Low to medium	Medium	Low
Consumable cost	Very low	High	Low	Medium	Medium
Time of results	Immediate	Delayed	Immediate	Short delay	Short delay
Effect of geometry	Important	Important	Important	Less important	Less important
Access problems	Important	Important	Important	Important	Important
Type of defect	Internal	Most	External	External	Surface breaking
Relative sensitivity	High	Medium	High	Low	Low
Formal record	Expensive	Standard	Expensive	Unusual	Unusual
Operator skill	High	High	Medium	Low	Low
Operator training	Important	Important	Important	Important	Important
Training needs	High	High	Medium	Low	Low
Portability of equipment	High	Low	High to medium	High to medium	High
Dependency on material composition	High	High	High	Magnetic only	Low
Ability to automate	Good	Fair	Good	Fair	Fair
Capabilities	Thickness gauging	Thickness gauging	Thickness gauging	Defects only	Defects only
Direct measure taken	Changes in acoustic impedance	Change in density of examined material	Change in electrical conductivity	Leakage of magnetic flux	Surface openings filling by liquid

© 2008 Woodhead Publishing Limited

which is used for both detection and sizing, ACPD is used almost exclusively for crack sizing. The ACPD method is only applicable to surface-breaking cracks and requires electrical contact with the specimen.

Generally, fatigue cracking detection needs off-service inspections. **Ultrasonic surface guided waves** are instead proposed by Vanlanduit *et al.* (2003 [55]) for in-service monitoring: one of the advantages noted by the authors is that loads should not be released and therefore open cracks can be detected, thus making the method much more sensitive.

13.4.4 Mechanical damage detection and measurement

Current practice

Deformation is the term applied to dents, buckling or general distortion found in plating or stiffeners. Deformation can occur as a result of poor design or from external forces arising from, e.g., collisions or wave action. Although deformation can occur anywhere, the compressive stressed areas of stiffened panels are more prone. Other critical areas are the side shell at berth level, the tank top and other areas exposed to loading/unloading operations in general. While early repair is not always needed, local stress raisers may lead to early fatigue cracking or cracking in case of compressive loads around the dent.

For the time being, no particular quantification seems to be needed by regulations, except approximate size measurements. It is generally left to the surveyor's skill and judgement to determine the acceptable limit of deformations within specified qualitative criteria relevant to extension and depth of dents (see IACS Rec. 47 [23] and Rec. 76 [30]). Then, only visual inspections or close visual inspections are required, as necessary. When the mechanical damage is believed to impair the ship's safety, it should be repaired generally by plate inserts or replacements, which can indeed introduce even worse structural degradation if not properly carried out.

However, it should be noted that mechanical damage due, e.g., to an impact locally modifies the material properties and even the stiffness of a stiffened panel because of the geometrical modifications.

Advanced methods

The measurement of dent geometry and stresses was studied by Babbar *et al.* (2005 [4]) using the magnetic flux leakage inspection method. Such a method, used for detecting corrosion and metal loss in pipelines, would also provide signals from both geometry and stress effects but is quite difficult to interpret. Magnetic finite element analysis and experimental tests are proposed to simulate the effects of a dent in a plate, then to be calibrated also for mechanical damage detection and measurement.

© 2008 Woodhead Publishing Limited

Table 13.7 Summary of methods for detecting and measuring age-related structural deterioration of ships

Technique	Degradation mechanism			Rank (1 – low to 5 – high)			Remarks and notes
	Wear/ corrosion	Fracture/ cracks	Mechanical damage	Skill needs	Results accuracy	Costs	
Visual inspection	X	X	X	5	4	2	Small equipment such as hammer, flashlight, calliper, measuring tape, weld-sizer, notebook, etc. are included. Surface defects only, no permanent records, applicable while work in progress with indication of incorrect procedures
Close-up inspection	X	X	X	4	4	3	
Digital imaging/endoscopy	X	X	X	3	2	2	Recently developed, need of regulations and automatic processing
Leak/pressure testing	X	X		1	5	4	Leaks of gases and liquid in tanks, pit and crack detection
Dye penetrants, chemical sensors		X		2	3	2	Affected by environmental factors (cleanliness and surface conditions), excellent in locating leaks in weldments, easy to use and low cost
Ultrasonic tests	X	X		5	3	4	Highly dependent on operator's skill for interpreting pulse echo patterns of defects (influence on time and costs), no permanent record (except for thickness gauging UT equipment)
Strain gauges	X	X		4	3	4	Reduction of stiffness, corrosion

© 2008 Woodhead Publishing Limited

Table 13.7 Continued

Technique	Degradation mechanism			Rank (1 – low to 5 – high)			Remarks and notes
	Wear/ corrosion	Fracture/ cracks	Mechanical damage	Skill needs	Results accuracy	Costs	
Electromagnetic field techniques*		X		5	4	5	Surface and subsurface cracks and seams, heat-treatment variations, wall thickness, coating thickness, crack depth
Magnetic particle		X		2	2	2	Only magnetic materials (sub)surface discontinuities, relatively low cost, difficult to use on rough surfaces
Radiometry (X-ray)		X		4	4	5	Danger of radiation; only by specialized firms. For interior large flaws but not suitable for fillet welds; costly. Permanent records
Acoustic-based techniques	X	X		5	4	5	Different techniques (acoustic emission, natural frequencies, noise, vibrations). Need of preliminary structural assessments (at commissioning) for measurement interpretation
Thermal imaging	X			5	4	5	Limited to specific materials/ situations
Replica		X		1	2	2	Simple and cost-effective, records surface defects
Test coupons	X			2	3	3	Needs preliminary calibration
Fibre optic		X		4	4	5	Emerging technique, safe even in oil tanker (no electric power)

* Alternating current field measurement (ACFM), alternating current potential drop (ACPD), eddy current, etc.

© 2008 Woodhead Publishing Limited

Development and application of guided wave techniques for damage testing in a ship hull is presented by Song *et al.* (2003 [49]). An approximate image of a damage is constructed using the reflected guided waves from the damage itself. A discontinuity locus map provides information on location and size.

13.4.5 Summary of methods and promising studies

Several engineering fields are interested in methods for detecting and measuring degradation of systems: in general the same theories are used and cooperation/exchange is desirable.

Innovative NDT techniques are available and inspection methods, especially of ships but also of offshore structures, can be further optimized. Particularly, their accuracy seems to be an interesting topic for further assessment, not only as regards the sensitivity of instrumentation but also considering the environmental conditions and other influencing factors [45].

In summary, Table 13.7 shows the methods for detecting and measuring age-related structural deterioration of ship and offshore structures, giving some brief advice in terms of needed skills, accuracy of results and costs.

13.5 Structural monitoring

Monitoring is different from inspection of structures as it implies that the structural check is continuously carried out by means of automatic or semi-automatic systems installed onboard. Results are displayed and recorded at convenience.

Continuous monitoring devices are required by rules for hull girder strength of bulk carriers, to be used during loading and unloading operations and throughout the voyage (i.e. loading instruments to be used in connection with loading manuals). Similar monitoring systems are typically installed on some naval and merchant ships, completed by stress monitoring of structural details prone to fatigue and sea condition measurement devices.

The classical HRMS (Hull Response Monitoring Systems) use long- and short-base strain gauges, accelerometers and pressure gauges to process and store results in a PC, providing real-time graphical output to assist decision making in heavy weather.

The monitoring system is intended as an aid to the judgement of the master and crew in operation rather than an inspection tool. Therefore, most sensors are dedicated to ship's motions and loads; structural response (strains, deformations) is measured for warning purposes in case a threshold is exceeded during accidental or occasional events, e.g. slamming and sloshing, or during loading and unloading operations.

Classification societies may issue voluntary class notations to ships installing a monitoring system according to their requirements. Different notations

© 2008 Woodhead Publishing Limited

correspond to different measured quantities and different processing of data leading to different objectives; requirements are quite similar among various classification rules and dictate general principles and criteria. Monitoring system requirements of classification rules include provisions concerning:

- Measured quantities
- Sensor specifications
- Locations of measurements
- Specifications of measurements (sampling, filtering, etc.)
- Real-time analysis, display and data recording specifications
- Post-processing specifications
- Power supply
- Operation
- Installation
- Set-up and calibration
- Maintenance.

Data recorded by such systems may be used for structural condition assessment, e.g. considering the time history of deflections, which are related to the stiffness degradation of the structure. Additional sensors, specific for measurement of degradation phenomena as described in Section 13.4, can be easily added to hull monitoring systems in order to complete the information set for structural condition assessment.

Further details of the requirements of classification societies and end-users (ship owners, operators) have been reviewed and summarized in [42]. Also a review of existing monitoring systems was carried out, including sea trial measurement systems. Moreover, Slaughter *et al.* (SSC-401, 1997 [48]) described the commercial state-of-the-art in HRMS with particular attention to ice transit.

In the offshore sector, the Norwegian Technology Standards Institution (NORSOK) has established a standard aiming to define safe and cost-effective inspection methods [43]. The NORSOK standard describes principles and functional requirements and guidelines for condition monitoring of load-bearing structures throughout their operating life until decommissioning. The standard is applicable to condition monitoring of complete structures of all kinds, including substructures, topside structures, vessel hulls, foundations and mooring systems, and covers all aspects related to condition monitoring, including in-service inspection and maintenance planning, implementation, structural integrity evaluation, and condition monitoring documentation.

The standard mainly considers conventional methods of in-service monitoring by means of inspection by operators. It is just mentioned that Instrumentation Based Condition Monitoring may be used as an alternative to the conventional inspection methods.

© 2008 Woodhead Publishing Limited

Reference [14] by H&SE (1998) is a review of structural monitoring of North Sea jackets from 1988 to 1998. It concerns the monitoring of the platform's structural response, by identifying the response modes and monitoring deviations in time of their frequencies to detect loss of stiffness. Then an analysis of the sensitivity of deviations of natural frequencies to the member severance, for various platform architectures, is presented. It is concluded that this monitoring method is usable for low redundant member configurations, i.e. not for ship-shaped structures.

Remote monitoring systems are used on platforms to monitor the structural conditions. These can incorporate permanently installed sensors to monitor steel potential, coating impedance or steel polarization inside the spaces to be periodically monitored by personnel or computer.

Conceivably, all remote monitoring could be accomplished via computer and trending or statistical analyses performed at a central location within the ship. This first line of inspection would offer the greatest opportunity for effecting a large scale inspection assessment with minimum personnel requirements.

As a potential future trend of ship monitoring techniques, it can be mentioned that a GPS RTK system for accurate ship motion measurements is currently used at the Department of Naval Architecture and Marine Technologies of the University of Genova (Italy), which is planned to be extended also to hull girder deflections and macro-deformations of ships. A brief description of this system and of the first results of validation tests performed are described, e.g., in Carrera (2003 [8]) and Carrera and Rizzo (2005 [9]). The purpose of this development is to provide a low-cost and accurate sensor which does not need calibration and shows no drift. These features are important for use in stand-alone condition monitoring systems.

13.6 Acknowledgements

The editors of this book, relying on a rather young professor for a very challenging task, are first acknowledged; I hope that my contribution will meet their expectations. Co-members of ISSC 2006 and ISSC 2009 Special Committee V.6 are also gratefully acknowledged, since working with them improved my skills about condition assessment of ageing ships and offshore structures.

I am indebted to several people who have supported my contribution to this book, including Ing. G. Damilano, Mr V. Vannucci and Mr G. Bolcano, former colleagues when I was a field surveyor, who indeed taught me the real practice of ship surveying.

Professor R. Tedeschi needs special acknowledgement: not only did he support my work but also he was, as ancient Romans used to say, the 'magister vitae' (teacher of life) since he became my PhD supervisor a few years ago. I also thank my parents and my wife, who actually became my wife while I was writing these chapters, for their endless patience and continuous encouragement.

© 2008 Woodhead Publishing Limited

13.7 References

[1] Agarwala V.S., Ahmad S. (2000), Corrosion detection and monitoring: a review, *CORROSION/2000 Congress*, Paper No. 271, NACE International.

[2] American Bureau of Shipping (2000), Investigation into the damage sustained by the M.V. Castor on 30 December 2000, www.eagle.org.

[3] Ayyubb B.M., Akpan U.O., Rushton P.A., Koko T.S., Ross J., Lua J. (2002), Risk Informed Inspection of Marine Vessels, Report SSC-421, August 2002, Ship Structures Committee, www.shipstructure.org.

[4] Babbar V., Bryne J., Clapham L. (2005), Mechanical damage detection using magnetic flux leakage tools: the effect of dent geometry and stress, *NDT&E International*, 38, 471–477.

[5] Basar N.S., Jovino V.W. (1990), Guide for Ship Structural Inspection, Report SSC-332, August 1990, Ship Structures Committee, www.shipstructure.org.

[6] Bea R.G., Hutchison S.C. (1993), Maintenance of Marine Structures; A State of the Art Summary, Ship Structures Committee SSC-372, May 1993, www.shipstructure.org.

[7] Bøving K. (editor) (1989), *NDE Handbook: Non-destructive Examination Methods for Condition Monitoring*, Woodhead, Cambridge, UK.

[8] Carrera G. (2003), Test of a GPS RTK system for ship motion measurements, *FAST 2003 Conference*, Ischia, Naples.

[9] Carrera G., Rizzo C.M. (2005), Measurements of motions, loads and structural response on a fast FRP pleasure craft, *FAST 2005 Conference*, St Petersburg.

[10] Demsetz L., Cabrera J. (1999), Detection Probability Assessment for Visual Inspection of Ships, Ship Structures Committee SSC-408, April 1999, www.shipstructure.org.

[11] Demsetz L., Carlo R., Schulte-Strathaus R. (1996), Inspection of Marine Structures, Ship Structures Committee SSC-389, August 1996, www.shipstructure.org.

[12] Halmshaw R. (1997), *Introduction to the Non-destructive Testing of Welded Joints* (2nd edition), Woodhead, Cambridge, UK.

[13] Health & Safety Executive, H&SE (1988), Handbook for Underwater Inspection, Report OTO 88-539, Offshore technology report.

[14] Health & Safety Executive, H&SE (1998), Review of Structural Monitoring, Report OTO 97-040, Offshore technology report.

[15] Health & Safety Executive, H&SE (2000), POD/POS Curves for Non-destructive Examination, Report OTO 2000-018, Offshore technology report.

[16] IACS (2006), Common Structural Rules for Bulk Carriers.

[17] IACS (2006), Common Structural Rules for Tankers.

[18] IACS (2007), IACS Procedural Requirements, IACS London, www.iacs.org.uk (continuously updated).

[19] IACS (2007), IACS Unified Requirements, IACS London, www.iacs.org.uk (continuously updated).

[20] IACS Rec. No. 87 (2004a), Guidelines for Coating Maintenance and Repairs for Ballast Tanks and Combined Cargo/ballast Tanks on Oil Tankers, IACS London, July 2004, www.iacs.org.uk.

[21] IACS Rec. No. 39 (2005), Safe Use of Rafts or Boats for Surveys, www.iacs.org.uk.

[22] IACS Rec. No. 42 (2004), Guidelines for Use of Remote Survey Techniques, www.iacs.org.uk.

[23] IACS Rec. No. 47 (1999), Shipbuilding and Repair Quality Standard, IACS London, www.iacs.org.uk.

© 2008 Woodhead Publishing Limited

[24] IACS Rec. No. 72 (2003), Confined Space Safe Practice, www.iacs.org.uk.
[25] IACS Rec. No. 78 (2002), Safe Use of Portable Ladders for Close-up Surveys, www.iacs.org.uk.
[26] IACS Rec. No. 90 (2005), Ship Structure Access Manual, www.iacs.org.uk.
[27] IACS Rec. No. 91 (2005), Guidelines for Approval/Acceptance of Alternative Means of Access, www.iacs.org.uk.
[28] IACS Rec. No. 74 (2001), A Guide to Managing Maintenance, IACS London, www.iacs.org.uk.
[29] IACS Rec. No. 75 (2001), Format for Electronic Exchange and Standard Reports, IACS London, www.iacs.org.uk.
[30] IACS Rec. No. 76 (2004), Guidelines for Surveys, Assessment and Repair of Hull Structure – Bulk Carriers, IACS London, www.iacs.org.uk.
[31] IACS Rec. No. 82 (2003), Surveyors' Glossary – Hull Terms and Hull Survey Terms, IACS London, www.iacs.org.uk.
[32] IACS Rec. No. 84 (2005), Guidelines for Surveys, Assessment and Repair of Hull Structure – Container Ships, IACS London, www.iacs.org.uk.
[33] International Maritime Organization, IMO (2003), Resolution MSC.134(76) and Resolution MSC.133(76) Technical Provisions for means of access for inspections (proposals for SOLAS amendments), www.imo.org.
[34] International Maritime Organization, IMO (2004), Goal-based New Ship Construction Standards, doc. MSC 78/6/2, February 2004, submitted by the Bahamas, Greece and IACS.
[35] International Maritime Organization, IMO (2006), Goal-based New Ship Construction Standards – Report of the Working Group (May 2006), doc. MSC 81/WP.7.
[36] International Organization for Standardization, ISO (2006), Final draft international standard, ISO/FDIS 19904-1 Petroleum and natural gas industries – Floating offshore structures – Part 1: Monohulls, semi-submersibles and spars.
[37] International Ship and Off-shore Structures Congress (2003), report of Specialist Committee V.2 Inspection and Monitoring, San Diego, CA.
[38] International Ship and Off-shore Structures Congress (2006), report of Specialist Committee V.6 Condition Assessment of Aged Ships, Southampton, UK.
[39] International Ship and Off-shore Structures Congress (2006), report of Technical Committee IV.2 Design Methods, Southampton, UK.
[40] Ma K., Orisamolu I.R., Bea R.G. (1999), Optimal strategies for inspections of ships for fatigue and corrosion damage, Report SSC-407, August 1999, Ship Structures Committee, www.shipstructure.org.
[41] Ma K., Holzman R.S., Demsetz L. (1992), Design and Maintenance Procedures and Advancements in Tankship Internal Structural Inspections Techniques, Report SSC-386-IV, September 1992, Ship Structures Committee, www.shipstructure.org.
[42] MARSTRUCT (2005), In service monitoring of structural strength, class requirements for hull monitoring notations, Report Task 2.7, European Network of Excellence, Project No. FP6-PLT-506141, Contract No. TNE3-CT-2003-506141, http://mar.ist.utl.pt/marstruct/.
[43] NORSOK standards (1997), Condition Monitoring of Load Bearing Structures, N-005 Rev. 1, December 1997.
[44] Porter R. (1992), Non-destructive examination in shipbuilding, *Welding Review*, 11, 1, 9–10, 12.
[45] Rizzo C.M., Paik J.K., Brennan F., Carlsen C.A., Daley C., Garbatov Y., Ivanov L., Simonsen B.C., Yamamoto N., Zhuang H.Z. (2007), Current practices and recent

© 2008 Woodhead Publishing Limited

advances in condition assessment of aged ships, *Ships and Offshore Structures*, 2, 2, 1–11.
[46] Rizzo C.M. *et al.* (2005), In service monitoring of structural strength, class requirements for hull monitoring notations, Report Task 2.7, MARSTRUCT Consortium (European Network of Excellence, Project no. FP6-PLT-506141, Contract no. TNE3-CT-2003-506141), http://mar.ist.utl.pt/marstruct/.
[47] Saidarasamoot S., Olson D.L., Mishra B., Spencer J.S., Wang G. (2003), Assessment of the emerging technologies for the detection and measurement of corrosion wastage of coated marine structures, *OMAE 2003-37371, Proc. International Offshore and Polar Engineering Conference*, 2003.
[48] Slaughter S.B., Cheung M.C., Sucharski D., Cowper B. (1997), State of the Art in Hull Monitoring Systems, Ship Structures Committee SSC-401, August 1997, www.shipstructure.org.
[49] Song W.J, Rose J.L. and Whitesel H. (2003), An ultrasonic guided wave technique for damage testing in a ship hull, *Material Evaluation*, 61, 1, 94–98.
[50] Tanker Structure Cooperative Forum (1986), *Guidance Manual for the Inspections and Condition Assessment of Tanker Structure*, International Chamber of Shipping Oil Companies, International Marine Forum.
[51] Tanker Structure Cooperative Forum (1992), *Condition, Evaluation and Maintenance of Tanker Structure*, TSCF Work Group report.
[52] Tanker Structure Cooperative Forum (1995), *Guidance Manual for the Inspection and Maintenance of Double Hull Tanker Structure*, TSCF and IACS.
[53] Tanker Structure Cooperative Forum (1996), *Guidance Manual for Tanker Structure*, TSCF and IACS.
[54] Tiku S., Pussegoda N. (2003), In Service Non Destructive Evaluation of Fatigue and Fracture Properties for Ship Structures, Ship Structures Committee SSC-428, August 2003, www.shipstructure.org.
[55] Vanlanduit S., Guillaume P., Van Der Linden G. (2003), On-line monitoring of fatigue cracks using ultrasonic surface waves, *NDT&E International*, 36, 601–607.
[56] IACS Rec. No. 96 (2007), Guidelines for Surveys, Assessment and Repair of Hull Structure – Double Hull Oil Tankers, IACS London, www.iacs.org.uk.

© 2008 Woodhead Publishing Limited

14

Inspection of aged land-based structures

A VAN GRIEKEN, Connell Wagner Pty Ltd, Australia

Abstract: There are six main reasons for the assessment of structures and three main groups of most common deficiencies. Assessment may be an incidental observation, part of a maintenance programme, in compliance with local regulations, in response to a deficiency, for a sale or purchase, or for refurbishment. This chapter discusses causes of deficiencies of construction materials and elements. Deficiencies in concrete structures broadly fall into three main groups. Group 1 includes chemical or physical degradation, group 2 mechanical due to external forces, and group 3 due to corroding reinforcement. These include amongst others the effects of acids, sulphates, saltwater, salts, alkalis and shrinkage and other physical forces. Furthermore, causes of reinforcement corrosion, including carbonation, chlorides and electrical currents, are detailed and relevant tests listed.

There are a range of tests to assess these deficiencies, including physical surface tests, chemical, electrochemical, non-destructive and laboratory tests. In addition, structures can be loaded or subjected to seismic impulses and bridges can be subjected to dynamic loads. Masonry structures mostly suffer from brick growth deficiencies and salt attack and thermal stresses. Deficiencies in steel structures are largely related to corrosion which can be categorised into eight main types. These include uniform, galvanic, crevice, pitting, intergranular and other forms of corrosion. Suitable non-destructive tests are listed.

Key words: concrete deficiencies and relevant tests, acids, sulphates, saltwater, salts, alkalis, shrinkage, carbonation, chlorides, electric currents, electrochemical tests, non-destructive tests, physical surface tests, masonry deficiencies, eight forms of steel corrosion and relevant non-destructive tests.

14.1 Introduction

From early childhood one will have experienced structural deterioration. Cracks are arguably the most commonly encountered manifestation that the structure or its main elements could not resist the forces imposed on it. Cracks may be simple and acceptable such as minor splitting of timber and the almost inevitable minor cracking of concrete. Most homes, whether new or aged, have cracks in their interior finishes due to either shrinkage movement, the settlement of foundations or the gradual uptake of loads as the building 'settles in', or a combination of these.

The human response to deficiencies varies greatly. Most persons would consider a fine crack in a slab or concrete wall a mere nuisance. An experienced professional may consider a fine crack in a particular element or material a

© 2008 Woodhead Publishing Limited

reason for concern and cause to investigate and monitor particular structures. A leaning wall or façade may be considered by some as adding charm and authenticity to a historic building and a streetscape and yet may be viewed by engineers as potentially dangerous. On the contrary, deflecting floors or bouncing walkways may cause alarm to the public and yet be considered quite acceptable to designers or constructors. Furthermore, significantly deflecting seesaws are a source of joy for children and even adults and yet similar elements suspended across waters such as a gangplank to a boat will cause alarm to many.

It is not uncommon for lightweight façade systems, in particular large glass panels which have been designed within acceptable design criteria, to deflect significantly under wind load. While significant deflections are likely to cause alarm to the tenants, particularly those sitting near windows, such deflections may be viewed by engineers as anticipated deformations. However, when a deficiency adversely affects the user or public and the element or structure does not appear to meet 'fitness for purpose', urgent investigations are required when deficiencies cause local failures, such as a dislodged piece of concrete or bricks, or a larger failure where elements are visibly dislodged or significantly cracked.

14.2 Six reasons for assessment

There are six general reasons to assess structures, namely:

- Incidental observation
- Part of maintenance programme
- Local regulations
- In response to deficiency
- For sale or purchase
- For refurbishment.

14.2.1 Incidental observation

Incidental inspections are those which occur without instruction or intent and include observations by the public or the users of the structure who 'happen to notice'. Furthermore, maintenance personnel frequently make important observations during maintenance works other than during intended inspection programmes.

14.2.2 Programmed maintenance

This category of inspections is carried out by experienced people who are professionals or tradespersons and who examine the structure. Typically these are carried out in accordance with a maintenance manual or inspection standards or guides. The previous condition and the repair and maintenance history will

© 2008 Woodhead Publishing Limited

need to be recorded and studied prior to undertaking the assessment. Findings and test results need to be included in reports and maintenance manuals. The scope of the assessment may vary such that the yearly scope is limited and, say, five-yearly assessments are more comprehensive.

14.2.3 Local regulations

There is a trend for councils or local authorities to require regular inspections. Previous incidents involving public safety have typically led to the across-the-board requirement to inspect and monitor structures similar to programmed maintenance.

14.2.4 Response to deficiency

Assessments in response to a deficiency which was noted incidentally or as part of a maintenance programme may be initiated by owners, managers or tenants and will need also to be carried out by professionals or tradespersons. The scope of the assessment needs to correspond to the noted deficiency but also needs to include the potential development of such or similar deficiencies in future at other locations and elements and to include the possibility of latent deficiencies. The urgency of this assessment varies with the risk associated with the observed deficiencies.

14.2.5 Due diligence (sale or purchase)

The purpose of this assessment category is to establish the condition and any deficiencies which may affect the sale or purchase price of the structure. These inspections may lead to the need for further exploratory or laboratory tests to assess non-visible conditions and find any latent conditions. Unless a thorough brief is prepared, the scope of such an assessment may be difficult to establish and the outcome needs to be carefully qualified and explained.

14.2.6 Refurbishment

As-built details and the capacity of an existing structure are required for refurbishments where this structure will be subjected to different proposed loading conditions. Furthermore, this assessment needs to include amongst others the condition and type of construction material as the proposed refurbishment may expose the existing structure and its material to different and more deleterious exposure conditions than those for which it was designed. This requires an adequate understanding of material properties and of the potentially deleterious effects of changed exposure conditions on the existing materials.

For example, most internal concrete elements are deeply or fully carbonated.

© 2008 Woodhead Publishing Limited

Whilst these elements remain dry they will not deteriorate. However, the introduction of moisture is likely to cause rapid corrosion of embedded reinforcement and concrete spalling. There are examples where this has occurred when saunas and kitchens were installed and where internal slabs became external balconies.

Similarly the installation of air-conditioning in a previously un-air-conditioned building will cool down a building and change moisture contents, both of which may lead to cracking. Thus moisture content measurements and dewpoint calculations are required as part of the assessment process.

As-built investigations are of paramount importance as designers must not make assumptions regarding matters of structural importance and contractors need to know what is expected of them and what they can expect.

14.3 Assessment outcome and sequence

In summary the assessment will need to achieve some or all of the following:

- Identify the location, size and extent of deficiencies.
- Identify the cause or causes of deficiencies.
- Establish if and where the deficiencies can be expected to develop at currently unaffected areas or elements.
- Establish the effects of deficiencies on the structural capacity, serviceability, durability and public safety.
- Identify actions which are required as a matter or priority for safety.
- Provide sufficient data from which to create prioritised remedial and maintenance works requirements.
- Provide sufficient data from which to prepare remedial documentation.

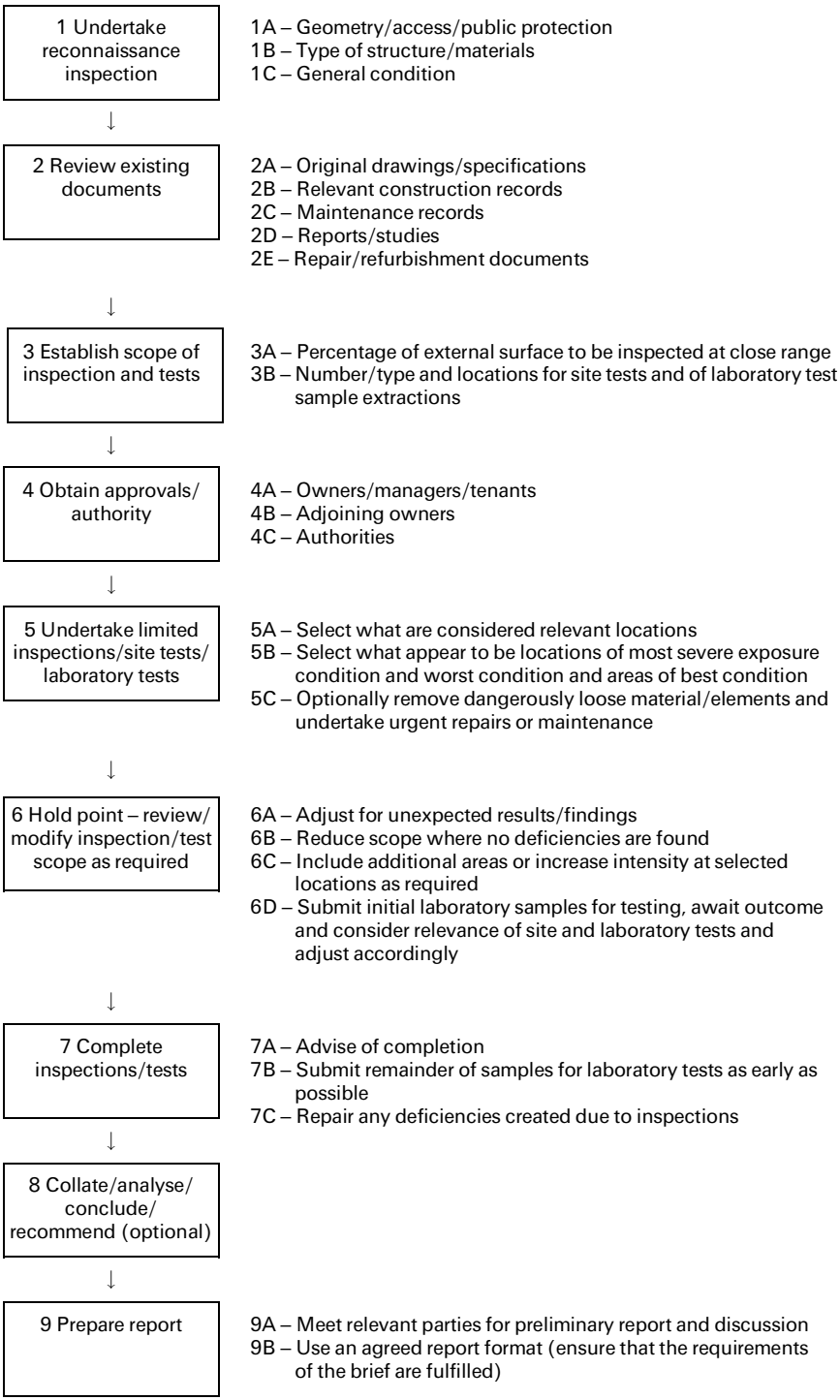
A vigorous and general conditional assessment will require all of the nine stages in Fig. 14.1. A more limited assessment needs to be targeted to suit the required outcome(s). It is important to identify critical path activities and related aspects, such as approvals, and to plan assessments around the needs of the 'users' of the structure.

14.4 Concrete structures

14.4.1 The evolution of concrete

When the ancient Egyptians used calcined impure gypsum as a cementing material more than 4000 years ago they could not have foreseen the evolution of concrete. This evolution involved the production of pozzolanic cement for structures by the Romans and the production of Portland cement by Joseph Aspin in 1824. Portland cement created many new opportunities and by the 1880s the first reinforced concrete buildings were being constructed in the USA. Reinforced concrete superstructures support some of the tallest buildings in the

© 2008 Woodhead Publishing Limited



14.1 Diagram showing how assessments need to be undertaken in a logical sequence and may involve some or all of the stages shown.

© 2008 Woodhead Publishing Limited

world. A large variety of concrete bridges span vast expanses of valleys and water, and concrete roads link communities and pave our cities. Concrete tunnels pass through inaccessible mountains and under vital waterways, and pipes transport important liquids above and below ground amongst many other applications of concrete. At present, concrete structures are arguably the most common artificial structures in the world. It is clear that concrete structures are an essential component of civilisation and play a vital part in the economy of a country. These structures are exposed to a significant range of different exposure and loading conditions and perform very different functions. As a result many of them have developed deficiencies which require assessment and most likely remediation.

14.4.2 The most common deficiencies

Deficiencies in concrete can be categorised in three main groups, as follows (Tuuti and Nilsson, 2005).

Group 1 – Chemical or physical degradation

- *Chemical* degradation of the concrete may occur due to or be accelerated by external exposure conditions, including the following.
  - *Acid* which dissolves the binder from the concrete matrix. This includes industrial acids such as vinegar, citric acid and even bird droppings.
  - Aggressive agents such as *sulphates* which can react with hardened cement paste in concrete, resulting in softening, cracking or exfoliation of the external layer.
  - *Soft water* attack causing alkalis and calcium oxide to leach and the dissolution of concrete constituents.
  - *Salt crystallisation* due to the ingress of soluble salt from the environment or from foundations or soil. Typically, this causes a subsurface build-up of hydratable salts inside the concrete capillaries near a given surface, which then crystallise, resulting in cracking or exfoliation due to the expansionary forces of the hydration pressure.
  - *Alkali aggregate reaction* whereby the aggregates swell due to the presence of sufficient alkaline species in concrete and moisture. This includes alkali–silica reaction (ASR), alkali–silicate reaction (reaction between fine-grained phyllosilicates such as chloride, vermiculite and mica to alkalis) and alkali–carbonate reaction (ACR). There are other types of alkali–aggregate reactions such as that which occurs between alkalis and organic complexes present on the aggregate surfaces. These are, however, very rare, particularly in comparison to alkali–silica reaction.
- *Physical* degradation is due to forces imposed on the concrete due to external exposure conditions or material properties, including the following.

© 2008 Woodhead Publishing Limited

- *Drying shrinkage*-induced cracking, which is the most common defect found in concrete elements caused by generated stresses resulting from outward movement of moisture from concrete to the environment and restraints. Drying shrinkage of concrete is different from other forms of concrete shrinkage, plastic shrinkage and autogenous shrinkage which occur in the plastic state and without net loss of concrete moisture respectively.
- Furthermore, movement due to shrinkage can cause damage at supports and interfaces with other materials or elements.
- *Thermal movement* may also cause cracking, but may also cause bowing and cracking.
- *Excessive heat* causing expansionary movement damage or explosive failure to surfaces when restrained.
- *Freeze/thaw* cycles causing water to solidify in concrete pore systems. When the pore system is of limited volume and there is inadequate spacing between pores, the freezing of pore water and its associated volume increase can lead to concrete surface deterioration and/or cracking.
- *Erosion and wear* resulting from interaction of a moving external medium (and materials carried by the medium) and the concrete surface. The interactions are mostly of a physical nature, though there are cases where the interaction can be a combination of physical and chemical effects such as erosion and wear of concrete hydraulic structures.

Group 2 – Mechanical degradation due to external forces

Mechanical defects include cracking, crushing and partial loss of surface concrete and may be caused by movement, overload, impact, vibrations and explosions.

Group 3 – Degradation due to corroding reinforcement

The two most common causes of defects in reinforced concrete structures are corrosion of embedded reinforcement or cast-in elements as a result of the carbonation of concrete and/or corrosive contaminants, mainly chloride ions, and stray currents which can also cause reinforcement to corrode.

Carbonation of concrete

Much has been written about the phenomenon of the carbonation of concrete. This is caused by reaction of carbon dioxide gas in the atmosphere with hardened hydrates, including calcium hydroxide, calcium silicate hydrates and calcium silicate hydrates in the concrete. The overall result of carbonation is lowering of concrete pH in the affected layer, termed neutralisation. In addition, neutralisation of concrete might occur due to acid rain which is the result of the

© 2008 Woodhead Publishing Limited

dissolution of carbon dioxide, oxides of nitrogen – nitrous oxide, nitric oxide and nitrogen oxide – and compounds of sulphur in water to form acid. In both cases the gases or liquids are diffused to the concrete pores and cause chemical changes. Following are some key characteristics which are relevant to assessments:

- Carbonation may 'harden' the concrete surface by reducing porosity (when there is no leaching involved). This is likely for sheltered or partially sheltered concrete surfaces. When this happens, the surface characteristics of the concrete may be affected, e.g. by increasing its resistivity.
- Carbonation progresses inwards from exposed surfaces.
- In a given exposure condition, carbonation occurs as a function of time approximately according to Fick's rule.
- Carbonated internal structures which are kept dry will not develop defects. However, when carbonated concrete is exposed to moisture and the carbonation front in the concrete has reached a distance close to the surface of the embedded reinforcement, steel corrosion will occur and result in concrete defects.
- The rate of carbonation is also non-linear and amongst others a function of the humidity of the external environment and moisture content in the cover concrete (Tuuti and Nilsson, 2005).
- The rate of carbonation drops to nearly zero as the relative humidity of the atmosphere exceeds 85%.
- Tests on samples extracted from buildings suggest that lightweight concrete carbonates at a greater rate than dense heavyweight concrete.

It is likely that carbonation will never be fully understood, as new additives create new concretes. Some consider new concretes 'chemical cocktails' which perform quite differently from the early concrete produced in the late nineteenth century in the USA.

As the concrete carbonates, the initial pH, which is in excess of 12.5, decreases to 9–10, at which the surrounding concrete will not provide a medium suitable for maintaining the passive film on steel reinforcement. Under adverse conditions, such as availability of moisture, the reinforcement will start to corrode and the concrete will burst when the expansive forces of the corrosion product exceed the tensile capacity of the concrete.

Corrosion contaminants

Corrosion of reinforcement due to corrosive contaminants is largely due to the presence of chloride ions. In the past, this phenomenon may be 'intrinsic' due to the practice of adding sodium chloride into fresh concrete mix to achieve early age strength. This practice was widely used until the mid-1970s. Intrinsic chlorides may also be present due to chloride-contaminated aggregates and sand.

© 2008 Woodhead Publishing Limited

Extrinsic chlorides may be present in the concrete near bodies of salt water due to external sources such as chloride-containing aerosols, or due to saltwater or other contaminants such as deicing salts.

The following are relevant to assessments of structures exposed to chlorides:

- Chloride penetrates into concrete approximately according to Fick's law which includes a coefficient of diffusion that is now considered to be a non-linear, time-dependent function.
- Much research is being carried out on the rate of external chloride ion ingress into different concretes under different exposure conditions.
- The chloride threshold for the initiation of corrosion of embedded steel varies with external conditions, concrete proportions and concrete cover.
- The corrosion current density may be in the order of 20 mA/m^2. If this current density is uniform over the whole metal surface, it would still take 50 years to lose 1 mm of metal over the whole surface. The passive Fe_2O_3 film on the surface of the embedded reinforcement corrodes at a rate in the order of 1 mm per 500 years (Cherry, 2006) while the concrete protects the film. However, as metal dissolution is localised, chloride ions can produce holes or 'pits' in the passive film and cause concrete to spall due to corrosion of the reinforcement within a few years of construction.
- Tests need to be conducted for soluble chloride rather than total chloride ion contents.

Stray current corrosion

Concrete defects due to stray current corrosion are less common but nevertheless no less important and may be due to a current source/supply well away from the concrete element. Typically, trains or tramlines are the source but industrial or other plants may also cause stray currents.

14.4.3 Tests to assess deficiencies

The following are the most commonly used tests for concrete deficiencies:

- Visual examination including crack survey
- Physical surface tests (impact/delamination tests)
- Chemical tests (chloride profile survey, carbonation depth survey)
- Electrochemical or electrical tests (resistivity, concrete cover survey, half-cell potential survey, linear polarisation resistance survey, surface moisture survey)
- Advanced NDT tests (including acoustic emission monitoring, magnetic field disturbance, radiography, computed tomography, surface penetrating radar, etc.)
- Laboratory and on-site chemical tests (depth of carbonation, chloride ion content, petrographic, other)

© 2008 Woodhead Publishing Limited

- Laboratory physical tests (material strength, element capacity)
- On-site load tests (progressing load, selected load)
- On-site seismic tests (length of piles, structural integrity)
- Dynamic bridge tests (load capacity, structural integrity).

Table 14.1 provides a guide to the most commonly used test methods for the above listed concrete deficiencies and includes comments regarding application, limitations and practical considerations.

14.5 Masonry structures

14.5.1 Changes in application

Structural load-bearing brickwork was arguably the most common exterior building material for more than a century. Depending on the height and the load carried, external walls may consist of multiple layers of brickwork with or without a cavity, and may reduce in thickness with the height of the building. Typically for buildings such as these, integrated brick piers support concrete-encased steel floor beams. There are many other applications of structural brickwork, including retaining walls, chimneys, industrial plants and pits and special structures such as church towers, etc.

By contrast, external non-loading brickwork is typically supported on exposed concrete slab perimeters or beams and more recently supported on steel shelf angles which have been bolted to the superstructure. There are a variety of brick sizes and bricks, with the main distinction being between solid and hollow bricks.

Load-bearing concrete blocks have found less application and are typically more commonly used as inner skins to an external brick wall. However, external load-bearing and non-load-bearing hollow and solid concrete blocks have been used on many buildings.

14.5.2 The four most common deficiencies

The four most common deficiencies in masonry structures are brick growth, axial shortening of the superstructure, physical attack, and mechanical deficiencies.

Brick growth

This is the phenomenon whereby the burnt clay brickwork expands volumetrically due to the absorption of moisture in the clay molecules. This process causes a volumetric swelling which is almost irreversible other than by placement in high-temperature ovens over a significant time.

© 2008 Woodhead Publishing Limited

Table 14.1 Concrete deficiencies assessment and tests

	Test	Equipment/application	Comments
1	Visual examination	• Clear vision • Clear mind • All structures and materials	Take time to study: • Structure as a whole • Individual elements • Materials • Unexpected/unusual aspects • Inconsistencies
2	Impact testing	• Metal ball at end of flexible rod • Hammer • Dragging chain For • Façade/slabs • Top surfaces of large areas of slabs	• Lightweight concrete sounds different from dense heavyweight concrete • Hollow/delaminated sounds at perimeter may not indicate a deficiency • There may be more than one interface of detachment. This will produce different tones
3	Compressive strength using rebound impact methods	• Schmidtor or Swiss hammer • Windsor probe For • Concrete surfaces	• Impact of pointed probe produces a rebound 'R' value for the compressive strength • Only measures property of surface concrete (sometimes referred to as 'surface crete') • Likely to give misleading results at top of slabs
4	Compressive core test	• Laboratory compressive testing equipment For • All concrete elements	• Need correct proportions of cone or cube • Not suitable for veneered concrete • Surface defects likely to yield incorrect results
5	Resistivity	• Werner Probe For • All concrete elements	• Four probes which are spring loaded and pushed into the surface • A current is applied between two outer probes and potential difference is measured between two inner probes • Need to measure beyond the surface laitance zone • Alternatively but less commonly a single probe can be used in conjunction with the reinforcement

© 2008 Woodhead Publishing Limited

Table 14.1 Continued

	Test	Equipment/application	Comments
			• Resistivity affected by concrete cement–water ratio, density of concrete, and type of concrete in terms of additives • In general poor quality, saturated concrete is likely to have a resistivity in the order of 100 ohm-m and high compressive strength; dry concrete is likely to have high resistivity $> 10^9$ ohm-m (Neville, 1981) • However, localised areas of very high resistivities adjacent to low resistivity areas can cause corrosion of reinforcement
			Likely corrosion rate based on resistivity (Mackechnie and Alexander, 2001)
			Resistivity (kohm-cm) — Likely corrosion rate given corrosive conditions
			<12 — High 12–20 — Moderate >20 — Low
6	Petrographic examination	• Binocular stereo microscope • Petrographic microscope • SEM (scanning election microscope) For • Concrete properties condition and cause of deficiency	• Thinly sliced samples are examined using a variety of light sources and filters (Quick, 2002) • Very useful in examining boundaries of aggregate for alkali aggregate to reactions • Provides visual insight, not density, distribution and type of aggregates • Shows void size and distribution and crack sizes and densities • Can be used to measure carbonation depth • Relatively expensive
7	X-ray diffraction, infrared spectroscopy	• X-ray tube For • Concrete properties and condition and cause of deficiency	• Provides, amongst others, cement contents, aggregate detail, pore size and distribution • Chemical composition, particularly the presence of deleterious elements such as chloride ions • Shows unusually high concentrations (or peaks) of particular elements

© 2008 Woodhead Publishing Limited

8	Chloride ion concentration	• Laboratory tests • In-situ tests To • Establish the concentration of free chloride ions	• Laboratory and site tests may be conducted on dust samples • Need to take care to obtain representative samples • Chloride aggregates may lead to misleading results • Typically measured at different depths to obtain a profile • Commonly used thresholds are subject to ongoing research. The probability of corrosion may be assessed from the following table for acid soluble chlorides:
9	Depth of carbonation	• On-site tests • Laboratory tests For • All concrete elements	• Mostly conducted on site by extracting dust samples and testing on site using a phenolphthalein indicator (typically 1% solution) • The phenolphthalein will colour the dust or concrete surface purple when the pH of the concrete is > 9.0 but will remain clear for carbonated concrete • Also conducted in laboratories on dust samples or freshly broken concrete surfaces • Need to ensure that the dust samples are not contaminated by the drilling process as carbonated surface dust is likely to be forced to the rear of a deep hole • The dust needs to be immediately tested on site or hermetically sealed in plastic bags for laboratory tests • Surface tests also need to be conducted as soon as the concrete is broken or split as carbonation will occur rapidly
10	Depth of concrete cover to reinforcement	• Magnetic cover meter For • Reinforced concrete	• Requires estimate of concrete compressive strength and size and type of reinforcement • Uses metal detector principles • Slow to use and interpolate • Heavily congested reinforcement and multiple layer reinforcement can yield incorrect or misleading results

Probability of corrosion (Mackechnie and Alexander, 2001)

Chloride content by mass of cement (%)	Probability of corrosion
<0.4	Low
0.4–1.0	Moderate
>1.0	High

© 2008 Woodhead Publishing Limited

Table 14.1 Continued

	Test	Equipment/application	Comments
			• Iron-containing aggregates can affect the magnetic field and yield incorrect or misleading results (Broomfield, 1997) • The presence of other metallic objects such as nearby windows, cast handrails, balustrades, formwork bolts, etc., is likely to render this test ineffective • Results not reliable when reinforced deeper than say 80 mm • Careful interpretation is required when measuring bars of a significantly different diameter which are in close proximity with each other • Should calibrate with local exploratory depth measurements
11	Hall cell potentials	• Voltmeter • Probe • Copper/copper sulphate or silver/silver chloride electrodes For • Reinforced concrete	• Measures the electrical potential difference between the two half-cells (e.g. copper in copper sulphate and iron in ferrous oxide) by linking a locally exposed section of the reinforcement to the surface of the concrete via a voltmeter • Choice of copper versus silver is subjective and may be subject to OH&S considerations • Need to pre-wet dry concrete surfaces with potable water • Should only be used as an indicator of corrosion risk of the reinforcement • Should be correlated with corrosion rate measurement • Results can be very misleading and need to be carefully interpreted • Very negative potentials can result in saturated concrete. However, corrosion cannot occur due to the lack of oxygen • The following provide a qualitative guide for the assessment of the probability of corrosion for copper/copper sulphate electrodes:

Probability of corrosion (Mackechnie and Alexander, 2001)

Rebar potential (mV)	Probable risk of corrosion
> -200	Low
-200 to -350	Uncertain
< -350	High

© 2008 Woodhead Publishing Limited

12 Corrosion rate

- Various systems

For

- On-site reinforced concrete elements

- Arguably the only test which indicates corrosion activity
- Based on linear polarisation principles
- Should be taken at lowest and highest electrical potential differences and at highest potential difference gradient densities
- Rates are subject to weather conditions and increase in warm conditions and as the concrete becomes wet
- Following is a general guidance for corrosion rates (Broomfield, 1997):

Corrosion rate (μA/cm^2)	Qualitative assessment of corrosion rate
>10	High corrosion expected in 2 years or less
1.0–10	Moderate corrosion expected in 2–10 years
0.2–1.0	Low – corrosion probable in 10–15 years
<0.2	Passive – no corrosion expected (under circumstances present at testing)

13 Ultrasonic pulse velocity

- Ultrasonic transducers
- Electrical reader

For

- Concrete quality
- Presence of internal cracks and voids
- Presence of discontinuities

- Measures the velocity of a pulse (up to 122 V for 1.5 ms) through concrete. Equipment detects first part of an ultrasonic signal to arrive at the transducer and delayed signals (Gibson, 2005)
- Presence of reinforcement can affect results
- Single point measurements are more difficult to interpret than those using scanning techniques (Grosse *et al.*, 2005)
- The presence of air in a crack or discontinuity will reduce the pulse velocity and increase the time to return
- Failure to achieve a good mechanical bond between the surface material and the transducers can result in completely erroneous results
- Need to prepare the surface with a gel

© 2008 Woodhead Publishing Limited

Table 14.1 Continued

	Test	Equipment/application	Comments
14	Infrared thermographic, infrared	• X-ray tube • Displayer • Infrared camera For • Surface delaminations • Building façades • Power plants • Chimneys • Airport pavements	• Infrared thermography enables surveys of surfaces which are not exposed to sunlight which is required to produce temperature variations for infrared surveys (Choo *et al.*, 2005) Infrared surveys: • Typically used for façades • Can give misleading results where for example internal walls have different temperatures • Local hot spots do not necessarily indicate delamination
15	'Seismic'	• Impact hammer • Transducer For • Length and structural integrity • Load capacity	• Wide range of applications including piles, foundations, retaining walls, rock anchors
16	Dynamic	• Applied load • Transducers For • Bridge deformation and integrity	• Concrete and steel bridges • Can establish load capacity and structural stiffness (Higgs and Tongue, 1999)

© 2008 Woodhead Publishing Limited

The performance of bricks and brick growth characteristics depend on a number of factors, including:

- Clay type
- Curing or grassing of the bricks
- Exposure conditions
- Permeability of the external surface
- Permeability of the water joints.

Brick growth can cause significant structural defects which most commonly occur as the following:

- Vertical cracks parallel to a corner of a wall and commonly in line with the heads of the bricks in the return wall
- Movement and cracking and dislodgement of parapets. In one case the parapets to the balcony of an old brick building had curved inwards in the order of 50 mm, due to the expansion of the outer brick skin
- Surface spalling, particularly at joints
- Crushing of enclosed elements such as window frames. In one instance a recessed window was framed with terracotta tiles which shattered and fell off the façade due to the in-plane compressive forces.

Axial shortening of concrete superstructure

Significant deficiencies can result due to the actual shortening of a superstructure which has been clad externally with brickwork. Typically, concrete superstructures shorten in the order of 1 mm per metre. This represents 3 to 4 mm per floor and a significant total dimension for medium- to high-rise buildings. In addition, if bricks grow, the brickwork will move in the opposite direction. As a result, significant in-plane forces develop which can:

- crush brickwork,
- cause brick walls to bulge,
- cause supporting shelf angles to rotate and/or shelf angle bolts to shear off the concrete superstructure,
- cause joints to close up and sealants to squeeze out of these joints.

Physical attack

Brickwork is susceptible to face fretting due to salt crystallisation, causing the outer 10 to 20 mm of brick to delaminate and spall. However, typically this happens in an erratic pattern as the quality and material properties of bricks vary.

Mechanical deficiencies

The most common deficiency in brickwork due to mechanical forces, as defined above, is due to excessive heat and/or cooling. This is particularly relevant at

© 2008 Woodhead Publishing Limited

burners and chimneys and can cause significant cracks and dislodgement of sections due to differential volumetric expansion. Furthermore, bricks are likely to spall under excessively hot conditions.

14.5.3 Blockwork structures

Shrinkage is the most common cause of deficiency in concrete blockwork. Typically this causes cracks at, for example, openings, and may cause the partial dislodgement of cavity ties.

Similar to brickwork, concrete blocks can suffer considerably due to salt crystallisation. As concrete blocks are typically more porous than brickwork they are more susceptible to salt penetration. Where the soil has a high salt content this will cause salts to be drawn up and crystallise at locations in the blockwork where equilibrium relative humidity relevant for the type of salt solution is reached, which is typically 10 to 20 mm inside the face of the block. The equilibrium relative humidities of some common saturated salt solutions occurring on walls are 97%, 87% and 75.3% for arcanite (K_2SO_4), mirabilite ($Na_2SO_4.10H_2O$) and halite (NaCl) respectively (Cao, 2007).

14.5.4 Assessment of deficiencies

The investigation of masonry defects requires an understanding of the exposure conditions, including for example humidity, airborne salts, atmospheric and other conditions such as soils which are in contact. Furthermore, construction details such as the means of vertical and horizontal supports, the brick ties in cavities, joints, flashings and concealed connections, all need to be established to decide on the scope and type of investigation and to derive correct conclusions regarding defects.

Table 14.2 lists typical investigation techniques.

14.6 Steel structures

14.6.1 Urban and iconic applications

Steel structures have always competed with concrete structures. Their use or preference in a given era is very much dependent on the economic considerations of the time. The application of steel in structures is widespread. Steel superstructures in older buildings consist of wrought iron elements, which may be riveted composite beams and columns. Some of the tallest buildings in the world have a steel superstructure. These typically support an external lightweight curtain-wall façade and internal concrete floors.

Steel bridges are typically elegant structures, some of which are iconic such as the Sydney Harbour Bridge and the Firth of Forth bridge in Scotland.

© 2008 Woodhead Publishing Limited

Table 14.2 Typical masonry deficiency investigation tests

	Deficiencies	Investigation/tests
1	• Brick growth • Axial shortening of superstructure	• Visual examination and recording of location and extent of cracks, spalls and movement related to defects • Boroscope examination of cavities to establish condition of cavity ties and damage due to movement and condition of shelf angles • Surface strain gauges to measure compressive stresses • Laboratory oven tests to establish brick growth characteristics • Electronic cover meters to locate brick ties
2	Salt attack	• Mapping of affected areas • Soil tests for salt content • Laboratory test to identify salts • Impact tests to establish extent and location of deterioration
3	Heat damage	• Physical examination and mapping of all deficiencies • Impact tests to check for surface dislodgement • Coring to measure depth of cracks and examine brick composition
4	Corroding mild steel support elements	• Electronic cover meter to locate the element • Boroscope examination above and below elements • Local exploratory investigation

Arguably, the most well-known steel structure is the Eiffel Tower in Paris, which was designed as a temporary structure. Furthermore, steel towers support vital electrical cables, steel tanks contain water and important fuel and liquids, and interlocking steel sections form retaining walls.

14.6.2 Most common deficiencies and means of assessment

The most common deficiency is due to corrosion. There are at least eight forms of corrosion (Fontana, 1986):

- Uniform (or general attack)
- Galvanic (or two-metal corrosion)
- Crevice corrosion
- Pitting
- Intergranular corrosion
- Selected leaching (or parting)
- Erosion corrosion
- Stress corrosion.

© 2008 Woodhead Publishing Limited

Uniform attack

This is the most common form of corrosion, and typically it occurs over an entire external surface. Due to the uniformly occurring electrochemical/chemical reaction, this type of corrosion is highly visible and requires no testing other than for the thickness of material, which may be carried out using an ultrasonic thickness gauge.

Galvanic or two-metal corrosion

Where two dissimilar metals are connected and are located in a corrosive or conductive solution or environment, an electrical potential difference will occur between these two metals and produce an electron flow between them. The less corrosion-resistant metal will corrode at an increasing rate and the more corrosion-resistant metal at a reduced rate. As a result of the contact the less resistant metal becomes more anodic and the more resistant metal more cathodic. While this is strictly an electrical chemical process, the term galvanic or dissimilar metal corrosion is more commonly used. The difference in the standard EMFs (electromotive forces) of the metals is often used as a means of predicting a galvanic corrosion tendency when the exposed environment is not known. The standard EMF of a metal can be obtained by measuring the potential differences between metals exposed to solutions containing approximately 1 gram atomic weight of their respective ions (unit activity), measured precisely at a constant temperature at 25 ºC versus a normal hydrogen electrode. Gold is the most noble or most cathodic metal, with an EMF potential versus a normal hydrogen electrode at 25 ºC of approximately 1.5 volts. Potassium is the most active or anodic metal with an equivalent potential in the order of −3 volts (Fontana, 1986).

An EMF series is useful in determining which of the two connecting metals will assume the role of anode and cathode. The EMF series, however, does not contain alloys. For this reason, a more practical tool in evaluating galvanic corrosion tendencies is the use of a galvanic series, which is a list of metals and alloys arranged according to their corrosion potentials as measured in a specific environment. While the galvanic series of metals and alloys in seawater is well known and commonly used for determining galvanic corrosion tendencies, evaluation of galvanic corrosion can be more accurately examined when the corrosion potentials of relevant metals in a solution similar to the exposure condition are used.

In seawater, the most noble or cathodic metal is platinum, which is just ahead of gold, and the most active anodic metal is magnesium and magnesium alloy, which are just below zinc, a slightly less active metal.

There are a number of effects which determine the extent and rate of corrosion. These include the area effect where a large cathode in a small anode will cause rapid corrosion of anodic metal, while the reverse may not cause accelerated corrosion at all. Furthermore the most severe corrosion will occur at

© 2008 Woodhead Publishing Limited

the point of contact and will diminish away from this point of contact, and the metal with a lower resistance to a given environment may become the anodic member of the couple. As an example, copper rivets in steel plates are unlikely to corrode, whereas steel rivets will corrode rapidly in copper plates. It should be noted that galvanic corrosion can occur when two metals are not physically in contact but are electrically in contact with each other in a suitable environment. Galvanic corrosion can also occur from run-off water and from metallic contamination incurred during fabrication or during service.

The assessment in cases of such corrosion is typically visual only. Where surfaces cannot be inspected, ultrasonic thickness measurements are relevant. However, it is frequently difficult to assess the condition of a concealed shaft of a rivet or bolt as these may be corroding while the heads and nuts may be in reasonably good condition. In this case ultrasonic tests may also be useful.

Crevice corrosion

Crevice corrosion is a form of localised corrosion which occurs when a small volume of stagnant liquid is trapped in crevices formed in or between components. Crevice corrosion starts with the formation of a differential aeration cell making the metal inside the crevice anodic relative to the metal outside. This subsequently results in an increase in the acidity and chloride content of the local solution in the crevice. Crevice corrosion propagates when a critical condition of the local solution is attained.

Pitting

Pitting is typically localised and results in small crater-like holes in the metal. These can easily be inspected visually unless they are inside containers such as water tanks, etc. However, pitting is one of the most destructive forms of corrosion and can cause tanks to leak and equipment to fail. It is often difficult to detect pits because of their small size. Pitting is more prevalent in welded parts for metals such as stainless steels which had been sensitised in the heat-affected zone due to chromium carbide precipitation.

Stress corrosion

Stress corrosion is considered to be quite relevant to structures and has caused, amongst others, riveted boilers to explode. Detection will involve the use of advanced NDT equipment.

14.6.3 Non-destructive tests

Table 14.3 summarises non-destructive tests which are relevant, and Table 14.4 gives a summary of which NDT method may be appropriate for various inspection tasks (Francis, 2007).

© 2008 Woodhead Publishing Limited

Table 14.3 Most commonly used non-destructive tests for metals

NDT visual	• Conducted according to AS 3978 • Success often depends on surface cleanliness and lighting arrangements • For restricted areas or for small defects, optical aids such as low power magnifiers, binocular microscopes, endoscopes, boroscopes and other fibre optic are useful • Inspect base metal, weld and fasteners
Ultrasonic inspection (UT)	• Piezo-electric transducer sends sound pulses. Reflected sounds are amplified and interpreted in a cathode ray tube • Accuracy of $\pm$0.02 mm possible with modern equipment (Francis 2007) • Locates flaws and measures wall thickness • Measures metal thickness • Accuracy diminishes with thickness
Magnetic particle test (MT)	• Not suitable for non-ferromagnetic materials • The best and most reliable test to defect surface and slightly subsurface cracks in ferromagnetic materials such as steel and cast iron • Tests can be done by placing strong permanent or electromagnetic field in the object using electromagnetic poles or a magnetic powder • Dry powder useful for rough or hot surfaces and wet powder for fine discontinuities, and fluorescent powder for increased visibility • Very few limitations to shape or size of element to be tested • May not be fully reliable for subsurface deficiencies • Generally requires expensive surface preparation
Liquid dye testing inspection (LDT) or dye penetration method (DPT)	• Identifies surface defects and uses a liquid penetrant and developer which reveals the presence of cracks • Fluorescent penetrants for use with UV light for greater visibility • Main advantage over magnetic particle test is that it can be used for non-ferrous, non-magnetic metals • Fast and cost-effective • Needs clean surfaces
Eddy current inspection (ET)	• Detects deficiencies such as local thinning, holes, pits and other defects in electrically conductive metals • Can test through coatings • Fast and immediate result • Expensive • Sensitive to slight material and temperature variations
Radiography (RT)	• Uses X-rays or gamma rays to create a visible image of the material • Expensive and time consuming for thick sections • Difficulty in detecting laminar defects unless parallel to beam • Needs sufficient safety precautions • Acoustic emissions • Thermal inspection, uses a variety of heat sensing devices

© 2008 Woodhead Publishing Limited

Table 14.4 Appropriate NDT methods (Francis, 2007)

Inspection task	Visual	Magnetic particle	Dye penetrant	Ultrasonic
Surface cracking – ferrous metals	✓✓	✓✓	✓	✓
Surface cracking – non-ferrous metals	✓✓	×	✓✓	✓
Pitting or grooving	✓✓	✓	✓	✓
Thinning	✓✓	×	×	✓✓

Key: ✓✓: ideal method, ✓: can be used in certain situations, ×: cannot be used.

14.7 References

Alexander M, Beushausen HD, Dehn F, Moyo P (eds) (2005), *Concrete Repair, Rehabilitation and Retrofitting*, London, Taylor & Francis.

Broomfield JP (1997), *Corrosion of Steel in Concrete*, London, E & FN Spon.

Cao T (2007), Internal Connell Wagner correspondence.

Cherry B (2006), How to make it last a little bit longer, *46th Annual Corrosion and Prevention Conference*, November 2006, Hobart, Tasmania.

Choo HM, Ryn HS, Ahn SR, Bac GS, Lee JY, Oh SG (2005), Study of the assessments of defects in tunnel testing using an infrared thermographic technique, *Concrete Repair Conference*, Hobart, Tasmania, Australasian Corrosion Association Inc.

Fontana MG (1986), *Corrosion Engineering*, Singapore, B & Jo Enterprise Pte Ltd.

Francis R (2007), IBC Engineering Steels and Alloys Course Notes, Kuala Lumpur.

Gibson N (2005), Ultrasonic testing of concrete, *Concrete Journal*, Concrete Institute of Australia, 32–33.

Grosse CU, Beutel R, Reinhard HW, Kruger M (2005), Impact-echo techniques for non-destructive inspection of concrete structures, in Alexander M *et al.* (eds), *Concrete Repair, Rehabilitation and Retrofitting*, London, Taylor & Francis.

Higgs JS, Tongue D (1999), Dynamic bridge testing systems (DBTS) for the evaluation of defects and load carrying capacity of in-service bridges, *International Conference on Current and Future Trends in Bridge Design, Construction and Maintenance*, Institute of Civil Engineers, Singapore.

Mackechnie JR, Alexander MG (2001), *Repair Principles for Corrosion-damaged Reinforced Concrete Structures*, Cape Town, University of Cape Town.

Neville AM (1981), *Properties of Concrete*, London, Pitman.

Quick GW (2002), *Australian Civil Engineers Transactions*, Vol CW43, 25–38, Institute of Engineers.

Tuuti K, Nilsson L-O (2005), Concrete durability – mechanisms in the deterioration of concrete, *Concrete in Australia*, Concrete Institute of Australia, 25–31.

© 2008 Woodhead Publishing Limited

15

Maintenance of aged ships and offshore structures

C M RIZZO, University of Genova, Italy

Abstract: This chapter overviews the maintenance of ship and offshore structures, introducing first preventive maintenance and protection methods. Especially as far as corrosion is concerned, protection is necessary since this degradation effect is unavoidable for materials used in shipbuilding and it is economically unfeasible to use corrosion-free materials.

Temporary repairs are then examined, mainly referring to current onboard practice: even if standards and regulations exist, harmonization and integration are still to be achieved and surveyors' skills and experience govern. As a matter of fact, for temporary repairs, decisions need to be taken on a case-by-case basis, considering not only technical issues but also operational and safety constraints.

Permanent repairs of degradation effects are presented, which are largely based on the same criteria as those used for new structures. Structures that have deteriorated beyond the acceptable limits are generally replaced by cropping and renewing. Attention should be paid to causes of degradation and fabrication of new parts in order to avoid even worse and more rapid damage. Finally, examination and tests of repairs are briefly summarized.

Key words: preventive maintenance, repair methods, temporary repairs, permanent repairs, examination of repairs.

15.1 Maintenance strategies

Two repair types may be considered in ship and offshore structures: mandatory repairs, in which shipowners carry out repairs to meet the requirements imposed by applicable international conventions, national regulations and classification societies' rules, and voluntary repairs carried out by shipowners to minimize the total maintenance cost for the intended remaining ship life.

In brief, the strategy of maintenance and repair is mainly based on the design life of the vessel and the future management plans of the shipowner. The optimum repair and maintenance strategy can be developed by combining various repair methods under the following constraints and considerations:

- Maintain the structural soundness and environmental protection within the intended remaining life or period of ownership.
- Maintain the effectiveness of the corrosion control system.
- Meet the flag administration's and classification society's requirements.
- Provide the most cost-effective repairs, minimizing out of service time.

Ideally, some months before the vessel is scheduled for the repair yard, an

© 2008 Woodhead Publishing Limited

initial visual and gauging survey should be carried out to check the corrosion protection systems and the degree and extent of steel wastage. This is the reason why class special surveys are allowed to start six months in advance (see Section 13.3.3 Chapter 13). Based on the results of this survey, a repair plan can be developed. Extensive visual and gauging surveys are then conducted with the structure out of service.

However, preventive and continuous maintenance of structures is also an option to be carefully considered for ship and offshore structures as, if it is correctly intended, it may minimize costs and time out of service.

15.1.1 Preventive maintenance and methods of protection from corrosion

For ship and offshore structures, corrosion and its prevention is a major concern. Corrosion prevention costs relate to exposure conditions, planned inspection and maintenance, design of structural details, protection specification, etc. The cost of initial corrosion protection is influenced by the steelwork details but more and more the maintenance costs and the corrosion protection system performances can be significantly affected. It is therefore easier and more cost-effective to design the structure to fit the protection method rather than to undertake late countermeasures against corrosion.

Before deciding how to protect any structure, the corrosion type needs to be defined considering the specific environment(s) during the ship's lifetime. The marine environment is a general wording as it needs to specify, e.g., whether the structure is always dry, wet or in a splash area, whether residual pools may exist, whether local pollution exists such as dregs and sludge, making the environment more aggressive, whether erosion may occur due to loading/unloading operations, grabbing, cavitations, etc., and whether the use of specific coatings or protection systems should be excluded in specific areas due to operational needs or other reasons.

Corrosion protection methods may be classified in several categories. These are only touched upon in the following, even though a general subdivision of corrosion protection systems is between:

- passive methods, i.e. systems preventing the chemical reaction, and
- active methods, i.e. systems altering the chemical reaction by modifying the reagents involved.

Indeed, the correct design of the structure and the selection of the building material is the first preventive maintenance method from corrosion, not strictly categorized as either an active or a passive method.

Good design of structures should account for eliminating corners and sharp notches, avoiding standing water and dirt or inaccessible areas, allowing drainage, providing safe and easy access to and around the structure so facilitating

© 2008 Woodhead Publishing Limited

inspections and coating applications, and providing adequate corrosion margins, etc. On the other hand, the choice of the corrosion protection system should match the features of the structure to be protected accounting for its effective and economical maintenance.

Any areas which are inaccessible require a protective system designed to last the required life of the structure, e.g. filling in such areas with inert material in order to avoid contact with the atmosphere.

In general, welded seams are more susceptible to corrosion. As can be easily noted, ship-like structures include several kilometres of welds. Current weld designs avoid intermittent or spot welding also because it is more prone to corrosion than continuous welding. Grinding of butt welds and of fillet welds may further improve the corrosion resistance of seams because of better coating application.

The choice of the correct material for the specific environment is a crucial point: as is widely known, the marine environment is very aggressive and some types of cargoes in tanks and holds are even worse. In general, periodic replacement of part of structures corroded above acceptable limits, according to the survey outcomes, is the cost-effective solution adopted by designers, since it is economically unfeasible to use corrosion-free material for the whole hull structure. Steel ships and offshore structures are built using carbon steel and corrosion margins are set by rules of classification societies. Such margins are derived from statistics of data from in-service ships and therefore derived corrosion rates are affected also by the effects of the protection systems usually applied, i.e. coatings and cathodic protection.

Stainless steel is too expensive and is therefore used for special cases only in ship and offshore structures, e.g. surfaces of cargo tanks of chemical tankers. Furthermore, building and welding procedures need higher accuracy and skills. Undoubtedly specialist advice from the steel industry is required before the type of stainless steel is specified.

Passive methods (coatings)

Coatings are a broad category including organic, inorganic, metallic and non-metallic coatings: they are a mixture of resins, pigments, fillers and solvents which form a liquid to be applied on the surface of a structure. Some books are specifically devoted to protective coatings and related topics, e.g. Ref. [1]; some notes are briefly recalled hereunder for the purposes of this chapter.

Resins are products of high molecular weight in which pigments and fillers are melted: the former are colouring agents or inhibitors, the latter increase the density and the abrasion resistance of the coating. Solvents are the dispersing medium and are very important in the drying and curing process.

Different types of coatings are categorized based on their main components: asphalts, oils, alkyds, acrylics, vinyl, epoxy, urethane, antifouling, zinc-rich, or metallic coatings.

© 2008 Woodhead Publishing Limited

Coatings are also divided into two basic categories, thermosets and thermoplastics. After drying, the thermoset chemical composition is different from that of the wet paint and can no longer be removed with a solvent. Wet and dry thermoplastics differ only in the lack of solvent in the dry coating and may be removed by simply reintroducing a solvent into the dry binder and pigment. Since thermoplastics can be removed by solvents, their use in tanks is limited because of the potential presence of hydrocarbon solvents.

Usually there are at least three coats in a coating system: primer, undercoat and finish [7]. Primers promote adhesion to the surface and protect from corrosion. Undercoats provide the right colour base for the finish, adhering to the primer and little else. They provide a second barrier should the steel be bared by damage or erosion. One important feature is to provide dry film thickness. Finishes supply the required colour and smoothness and resist weathering, abrasion and chemical attack, as appropriate.

Advantages of coatings, covering the requirements of ship and offshore structures, are as follows.

- They have a predictable life if the environment is accurately assessed.
- They do not affect the mechanical properties of structural materials.
- They can be applied to geometrically complex structures.
- They protect against most environments and conditions.
- Painting facilities are widely available.
- Most paints are easy to apply, repair and maintain.

The traditional, inexpensive and readily available coatings applied to marine structures are bitumen and coal-tar. Nowadays modified coal-tar epoxy coatings are the most common type of protection. Epoxy resin provides good resistance to water and other chemicals and has superior adhesion. Epoxy resin's material properties can be varied to suit the application based on how it is mixed, although controlling the chemical reactions is a very specialized matter.

The failure of epoxy coatings usually occurs gradually over time. However, under stress, the differences in cohesive strength and elongation between the steel and the coating film can cause cracking. Pitting and grooving will occur, sometimes at a very rapid rate, in the course of breakdown of the coating.

Anti-corrosive coatings work on three basic principles, the first being the separation effect which works simply by separating the chemical agents. The second principle is the inhibitor effect: primers applied to a surface sometimes contain a corrosion-inhibiting pigment such as zinc chromate, zinc phosphate, or inorganic zinc. The third principle is the sacrificial effect: sacrificial coatings use a metal (usually zinc) which is anodic to steel (or the building material). In the presence of an electrolyte, a galvanic cell is set up and the metallic coating corrodes instead of the metal. The concept of sacrificial coatings is similar in many ways to the inhibitive coating principle. However, in the case of zinc-rich

© 2008 Woodhead Publishing Limited

coatings, the zinc acts as an anode to the steel and in case there is a break in the coating film, the steel substrate tends to be still protected.

The surface of the steel must be cleaner when using a zinc-rich coating than when using other pigments because there must be good contact between the paint and the plate for galvanic action to occur. Consequently, the surface preparation costs are higher. Generally, sandblasting is adopted by shipyards but it may be not completely sufficient for these types of coating. The main disadvantage is that the zinc is rapidly consumed when breakdown of the coating occurs. Epoxy is the preferred choice also for recoating existing structures, because it is difficult to achieve the required surface preparation for zinc-rich coatings on corroded steel surfaces. Indeed, the Unified Requirement UR Z.9 of IACS [8], for cargo hold spaces, reports 'epoxy or equivalent' for use as a protective coating on all surfaces of shell and transverse bulkhead structures, including associated stiffening.

Procedures recommended by the coating manufacturer should be followed without compromise. One of the most important factors is the preparation prior to the application of a coating. The basic requirement for conventional coatings is that they are applied over a clean, dry surface, free from water-soluble materials like sodium chloride which can cause blistering, soluble ferrous salts which will initiate rusting of the steel, and oily residues which will reduce adhesion of the applied coatings. As defined by the coating manufacturer, the degree of surface roughness achieved by blasting, control of humidity and temperature of air and steel during application together with proper care of surface during curing can insure a long-lasting coating. So far, paint application is greatly influenced also by the weather conditions.

Surface preparation has a major influence in determining the effectiveness of a coating system. For metallic coatings it is usually an integral part of the manufacturing process and is included in the relevant standards. Further to standardization bodies, there are specific organizations involved in writing the standards for surface preparation, i.e. the Steel Structures Painting Council (SSPC) and the National Association of Corrosion Engineers (NACE). A comparison table of coating surface preparations, including a complete list of reference standards issued by the main standardization bodies, is obtained from IACS Rec. No. 87 [7] (see Table 15.1).

Moreover, commercial blast clean surface finish corresponds to SSPC SP-6, SSI Sa 2 and NACE No. 3. Brush-off blast clean surface corresponds to SSPC SP-7, SSI Sa 1 and NACE No. 4. Also, ISO standards (ISO-8501, ISO-8502, ISO-8503 and ISO-8504) address this subject in great detail. An item of considerable importance in the coating process is hand striping (Fig. 15.1), which is the process of having a painter with a brush manually coating all corners, details and edges. It has been found that coatings tend to be thinner on edges. Surface tension causes a drying coating to draw away from sharp edges. Hand striping applies additional coating to these areas.

© 2008 Woodhead Publishing Limited

Table 15.1 Comparison of sandblasting standards (from IACS Rec. No. 87 [7])

Standard	Highest degree = white metal	Good degree = near white metal
ISO 8501-1	Sa 3	Sa 2½
SIS 055900	Sa 3	Sa 2½
DIN 55928	Sa 3	Sa 2½
BS 4232	First quality	Second quality
NACE TM170-70	No. 1	No. 2
SSPC	SP 5	SP 10

Certain shapes, such as rolled sections and especially bulb flats, have advantages over fabricated sections when coating and corrosion are considered. The rolled shapes tend to have rounded edges, whereas fabricated shapes have cut edges which are sharper and require more attention with regard to grinding of edges and weld seams.

Active methods (cathodic protection and inhibitors)

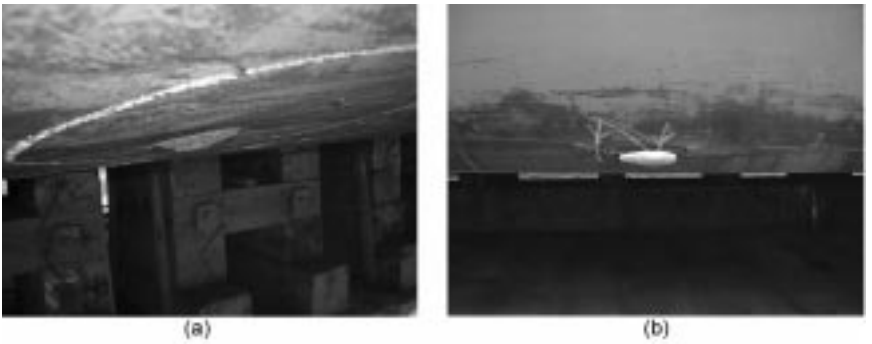
Painting costs are dependent on the area to be painted, whilst galvanizing costs are related to the weight of steel. Galvanizing therefore becomes a more attractive alternative for structures with a large surface area. In wet tanks and underwater body of the hull, the coating may be combined with active protection, which is then regarded as additional protection. Such protection must be designed not to damage the coating, i.e., the coating and active systems must be compatible.

The best-known active method for corrosion protection is cathodic protection but there are also other methods, i.e. impressed currents and electrical insulation. Cathodic protection relies upon the fact that, if the complete surface of a metal can be made cathodic by using an external electrode, then corrosion will not



15.1 (a) Hand striping coating of structures; (b) grinding necessary on worked edges before hand striping.

© 2008 Woodhead Publishing Limited



15.2 (a) Wasted zinc and (b) new zinc just welded on the bilge shell of a docked ship.

occur. The phenomenon of galvanic corrosion is the basis of cathodic protection from corrosion: the structure to be protected is made the cathode. For example, if iron and copper are connected in sea water, the iron corrodes; connecting a piece of zinc into the system the current flows from the zinc to the iron and copper and the iron turns into a cathode, i.e. the non-corroding pole in the electrochemical cell (see Fig. 15.2).

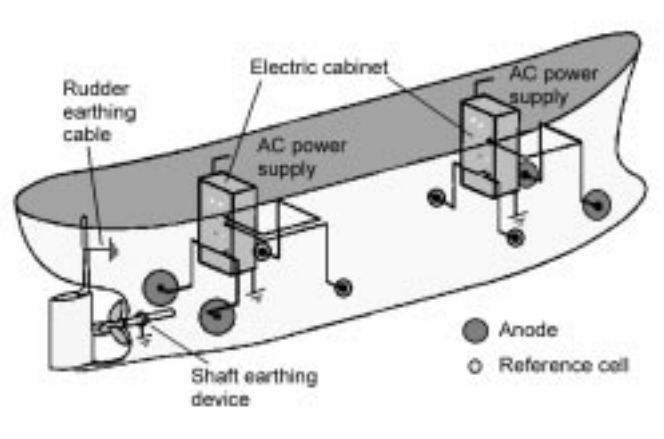
Cathodic protection using sacrificial anodes is a widely used method for the protection of steelwork under immersed conditions, but setting up a cathodic protection system on an immersed or semi-immersed structure requires expert advice.

Cathodic protection requires very little maintenance. The normal design basis for anode life is about five years, corresponding to replacement every special survey. Studies have shown anodes to be self-cleaning in most instances [19]. Anode wastage should be monitored when possible and anodes should be replaced on occasion before they are completely wasted. There are two disadvantages of sacrificial anodes. First, sacrificial anodes are restricted to environments of suitable conductivity. Only steel immersed in sea water is protected, i.e. side shell and ballast tanks. Second, the effectiveness of anodes is limited if the anodes are covered by wastage.

For large ships and offshore structures impressed current systems (see Fig. 15.3) are sometimes used. In these systems the anode is inert, e.g. graphite or titanium, and a DC supply provides the voltage. Such a method requires advanced specific skills as its mishandling may lead to accelerated corrosion instead of protection. The structure is usually coated because the current required to protect an uncoated structure would be too high to make the method economic. Thus, the coating is the prime defence with impressed current protection dealing with breaks in the coating.

Electrical insulation increases the resistance at some part of a corrosion cell, reducing the current flow and therefore the corrosion rate. This method has been

© 2008 Woodhead Publishing Limited



15.3 Impressed current protection system (courtesy of Sanitrade srl).

cited since in sea water, i.e. for ships and offshore structures, it is applied for specific cases only, e.g. insulating dissimilar metals from each other, such as aluminium from steel, eliminates the risks of galvanic corrosion. Rather, sea water is a good electrical conductor and galvanic corrosion occurs quite frequently in pipes and sea-chests where different metals may be used. There are, however, three points to remember when considering an active protection system.

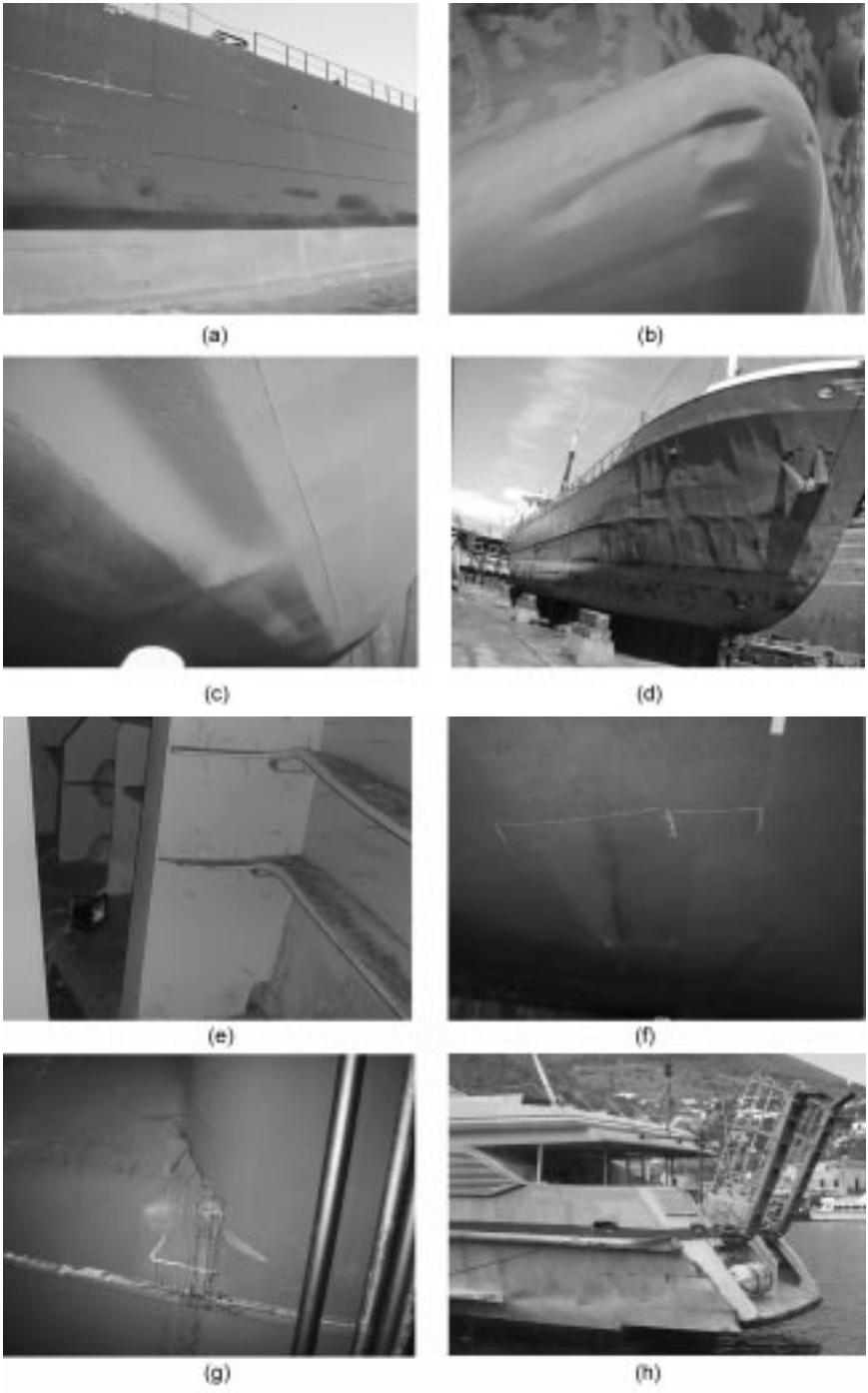
- To do their job, sacrificial anodes must corrode! They require regular inspection to ensure they are replaced before they disappear completely.
- There must be sufficient anodes to give the correct current density over the complete surface to be protected. Rough formulae for calculation of anode weight are reported in Ref. [19].
- In systems using an external DC supply the polarity of the electrical connection is vital. Reversed connections can cause extremely rapid corrosion of the item the system is supposed to protect.

15.1.2 Preventive maintenance and protection from fracture and mechanical damage

For the time being it seems that no specific preventive maintenance and protection methods from fracture and mechanical damage are applied to ship and offshore structures other than correct design, accurate construction, careful operation and management.

In order to prevent fractures and cracks, geometrical notches and discontinuities should be limited as far as practicable; however, it should be admitted that, though they could be minimized, they cannot be completely eliminated in plated stiffened structures.

© 2008 Woodhead Publishing Limited



15.4 Typical acceptable dents on (a) side shell, (b) bulbous bow and (c) bottom plate; typical unacceptable dents on (d) fore side shell, (e) side shell affecting internal stiffening (photo from inside), (f) bottom and (g) shell causing leakages; (h) damages and fractures caused during berthing.

© 2008 Woodhead Publishing Limited

Similarly, dents of plating whose dimensions are of the order of magnitude of the dimensional tolerances of shipyards' working practices are generally accepted, being practically and economically impossible to guarantee a smoothed surface of the ship's hull throughout the lifetime. Figure 15.4 shows dents and mechanical damage on hull shell due to normal welding or buckling deformations and impacts. Still acceptable dents due to impacts on a bulbous bow and an acceptable local buckling of the bottom plate are also illustrated.

Furthermore, dents and damages not acceptable because of large deformations also affecting internal stiffening, because of spreading corrosions or because of fractures, are shown.

Of course, berthing and loading operations may cause most of the damage due to impacts. In principle, cracks and excessive dents and distortions found during surveys should be appropriately repaired even if, due to redundancy in ship structures, fatigue cracks and relatively small buckling dents are typically not a threat to structural integrity. Therefore, the detection and (temporary) repair of occasional fatigue cracks and dents may be tolerated as a part of the routine maintenance. It is worth noting that interaction of fractures and mechanical damage with corrosion should be accounted for.

15.2 Current maintenance and repair practices

Maintenance and repair of ship and offshore structures is a challenging task involving engineering approaches as well as consolidated practices. When structural damages are found during inspections, in principle the structure should be restored to its initial condition or, alternatively, to a condition good enough to fulfil the service of the structure up to the end of its life. Temporary repairs are generally accepted if no means are available to carry out permanent repairs.

How to restore the structure depends on the type and extent of damage. In this section some general information is given. The following paragraphs are devoted to specific information about temporary repairs, permanent repairs and examination of repairs for the main damage modes of ship and offshore structures, i.e. corrosion, fracture and mechanical damages.

Rules and regulations provide only guidance for general cases but time, type and method of repair should be decided by surveyors in charge. In fact, an engineering judgement about the damage and its repair should consider at least the causes of defect, its entity and type, its position, the possibility of the damage growing/extending, the interaction of such damage with others and its influence on other adjacent structures and equipment. For instance,

- Relatively small accidental dents on hull shell, especially in the fore or in the aft areas, are considered more tolerable than buckling dents on main deck amidship or than a fatigue crack.

© 2008 Woodhead Publishing Limited

- A corroded welded seam is differently evaluated if the seam is longitudinal or transversal, depending on its location and function in the structure.
- Missing protection of the rudder system may be simply noted, while the same protection having the connection not properly fixed should be repaired in order to avoid possible rudder malfunction.

So far, when a structural failure in the form of either excessive corrosion, fractures or dents and distortions is discovered by inspection, a decision must be made as to the most effective repair. This decision is difficult due to the vast array of engineering, construction and repair knowledge that must be integrated to make a good repair decision.

The same technical issues as in the original design should basically be considered. However, many additional technical and non-technical factors must be considered in a much shorter time. As a result of the complexity and the short time allowed, the proper repair of marine structures currently relies heavily on the experience of repair engineers and repair yard personnel.

Even if the technically best repair is determined, logistic and economic factors may limit what type of repairs may be done. These factors include the future plans for the ship, the age of the ship, the total cost and time to complete repairs, cargo transport obligations, the money available, current steel costs, repair rates, wage rates, availability of yards and facilities, operational and environmental constraints, etc. Then, in any structural repair situation, there are three basic steps to determine the way to repair:

1. Determine modes and causes of structural failure: corrosion wastage, fractures and mechanical damage may originate from design problems, insufficient quality control, overloading, environmental factors, etc. In reality, structural failures usually result from combined effects.
2. Gather necessary data on structural failure: considering what was described in Section 13.2 in Chapter 13, inspection of ship structures is considered a 'heroic' task because all structural failures, even if discovered, are impossible to be properly and accurately identified and quantified in practice.
3. Once the mode and cause of failure have been determined with a degree of certainty, alternative repairs can be evaluated. The repair that best satisfies the technical, logistical, economic and other considerations is the one that should be chosen.

Furthermore, the expected life of the repair, the type of structure (primary, secondary or minor), the location of the structure, the trading route of the ship, the type of environment which may influence failure, and the corrosion protection systems involved (e.g. cathodic, coating, etc.) should be considered in the technical assessment. If the approximate time of significant damage is known, operational factors such as loading conditions, ship's speed and routes, etc. during the time of damage initiation and propagation, especially for

© 2008 Woodhead Publishing Limited

fractures, may be significant. Unfortunately, failures may go undetected for some time so that the conditions at the time of damage are often unknown.

The maintenance of ship structures is already mandatory for shipowners by virtue of the International Ship Management Code, whose provisions are recalled by the SOLAS convention. Recently the Goal Based Standards, under discussion within the IMO Maritime Safety Committee, recalled the need to properly maintain and operate ships (see www.imo.org).

However, the harmonization of current standards for hull repairs on existing vessels, including, e.g., TSCF and IACS documentation [2], [3], [5], [6], [9]–[12], and the integration of current yard practices still need to be achieved, better detailing technical procedures and standards for maintenance and repairs.

There are a few variations but the general guidance and views expressed by the classification societies that are the main regulatory bodies for ongoing ships and offshore structures follow IACS Recommendation No. 47, 'Shipbuilding and Repair Quality Standards' [2]. Part B of this document deals with permanent repairs of existing ships, while Part A deals with new builds. For offshore structures also national and international standards are applicable and widely recognized (e.g. standards by ISO, API, NORSOK, etc.).

Qualification of personnel and supervision by classification society surveyors is a prerequisite for repairing marine structures. Materials should be approved according to the rules and general requirements and standards in the same way as for new builds. The equivalence principle should be followed if materials and welding procedures are changed with respect to the original building drawings.

Repairs are to be carried out under working conditions that facilitate sound repairs with adequate provisions for proper accessibility, staging, lighting and ventilation (see Fig. 13.3 and Table 13.2 in Chapter 13). The following items, additional to the new build criteria, are moreover explicitly covered for repairs of existing ships by IACS Rec. 47 [2]:

- Correlation of welding consumables to hull structural steels
- General requirements for preheating and drying out
- Dry welding on hull plating below the waterline.

Standards provide several sketches and drawings of typical structural details addressing the repair recommendations, accounting for welding, renewal of plates and stiffeners, doublers, welding of pitting corrosion, and welding/grinding of cracks. Prescriptions about alignment, welding gaps, bevelling and sequences, fairness of plating with frames, discontinuities and tapering, preparations and pre-heating, etc. are also offered. Empirical and practical recommendations, presented as solutions for typical repair cases, are to be adapted to the captioned repair case according to the engineering judgement of the surveyor in charge.

It is unlikely that field surveyors carry out quantitative assessments and calculations in the selection of the repair works; rather, head offices are involved

© 2008 Woodhead Publishing Limited

in uncommon cases of repairs to obtain approved instructions and drawings of steel works to be done.

15.3 Temporary repairs

In the life of ships and offshore structures, maintenance and repair is mainly carried out every fifth year, during special surveys. Damages, deficiencies and defects found during annual and intermediate surveys, unless they do not impair the ship safety, are generally left for repair during dry-docking, and only monitored and/or temporarily repaired as deemed necessary.

Temporary repairs are considered when facilities do not exist for permanent repairs or if other good reasons exist for postponing permanent repairs. Surveyors should be satisfied that, in nature and extent, the temporary repairs maintain the strength and the watertight integrity of the ship for the time allowed until permanent repairs are carried out. It is always required that a deadline for permanent repair is stated by the surveyor in charge.

For both cracks and corrosion one option is to not repair and monitor the damage if this does not impair the ship safety. This option is usually only chosen for spot corrosion or minor cracks in non-critical structures. In worse cases, it needs to be specifically authorized by the head office of the involved society. On the contrary, no repair and monitor for limited fair dents and similar mechanical damage is a more frequent and allowed option, unless dents and distortions were generated by service-acting loads such as excessive buckling loads and/or fractures exist. If accidental loads, such as impact during loading/unloading operations, during berthing, etc., caused an acceptable fair dent in the plating, this is only noted for recording purposes in the ship status but no repairs are generally carried out until necessary [2], [5], [6].

15.3.1 Temporary repairs of corroded areas

Two types of corrosion wastage should be distinguished when considering temporary repairs: those impairing watertightness and those only decreasing the thickness of plates without threatening leakage.

Limited breakdown of the coating may only be monitored at time intervals depending on the coating condition according to the IACS definitions of poor, fair and good condition (see Section 13.4.2 in Chapter 13). However, hand striping or recoating should be considered to avoid faster degradation of wastage conditions. Regardless of the type of wastage, where thicknesses are lower than the permissible limits, the affected area is to be cropped and renewed. If replacement of defective parts must be postponed, in general the following temporary measures may be acceptable at the surveyor's discretion [2]:

- The affected area may be sandblasted and painted in order to reduce the corrosion rate.

© 2008 Woodhead Publishing Limited

- Doubler(s) may be applied over the affected area; special consideration should be given to areas buckled under compression.
- Stronger members may support weakened stiffeners by applying temporarily connecting elements.
- Cement may be applied over the affected area (sometimes formed in a box surrounded by stiffening structures): such repair is exceptionally accepted for a short time (a voyage or so) in order to avoid leakages in case of fractures or holes due to excessive wastage and in special circumstances where it is impossible to weld doublers (e.g. at oil tank boundaries because the tank is not gas free).

However, the last option has recently been replaced by composite repair, i.e. composite (fibre reinforced plastic) patches can be bonded or laminated over the structure to bridge and reinforce corroded areas. Generally, epoxy resins as matrix material and glass as reinforcing fibres are used.

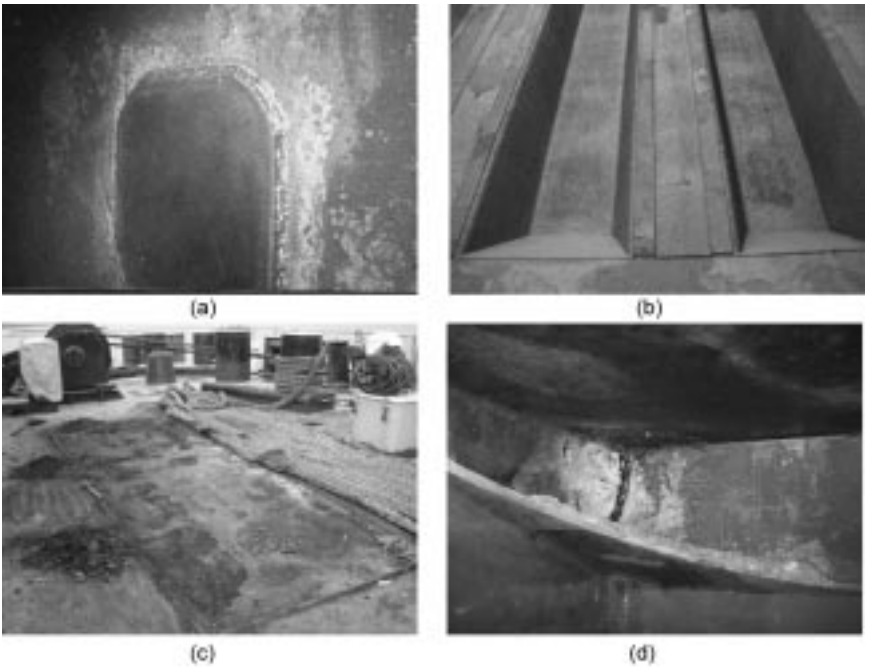
Since doublers should not be used to repair other than as a temporary measure, the regulations about the use of doublers are limited to basic welding schemes. In general, doubling is allowed for thickness greater than 5 mm and extending approximately 300 $\times$ 300 mm or more in order to avoid stress concentrations. Corners of doubler plates should be rounded as well. For doublers extending over large areas, slot welding is prescribed [2]. A more detailed study was carried out by SSC-443 [15], specifically dealing with plate repairs by doublers.

Decisions regarding size, location, thickness, material grade and welding are largely left to the discretion of the surveyor on site. In cases where the seriousness of the situation requires engineering in the development of the specific doublers, the surveyor will send information back to engineering offices of his or her society for evaluation and approval, but these cases are reviewed individually on a case-by-case basis. The classification surveyors always impose a recommendation to have the structure permanently repaired by means of welded inserts within a reasonable period of time, also specifying other limitations of the ship service and operation if any. The time frame of 'temporary' is somewhat undefined and is also left to a case-by-case interpretation.

Hull strips are also a form of doublers, which are mainly used to increase the strength and stiffness of the hull girder structure or of specific areas. This involves attachment of long plates (straps) to the plating, increasing the strength sectional modulus. Slot welding is required and regulated by IACS for large strips. Figure 15.5 shows the various temporary repair methods.

With their flexible properties, fibre reinforced plastics (FRP) improve the temporary repair techniques, providing durable repairs for both metallic and composite structures. For example, composite patches have proved highly cost-effective on Floating Production Storage and Offloading (FPSO) vessels and offshore structures. Traditional welded repairs can incur high costs because of out-

© 2008 Woodhead Publishing Limited



15.5 Temporary repairs of corrosion wastage: (a) underwater doubler, (b) strips on corrugated bulkhead, (c) cement on deck (removed before permanent repairs) and (d) cement in a corner of a structure.

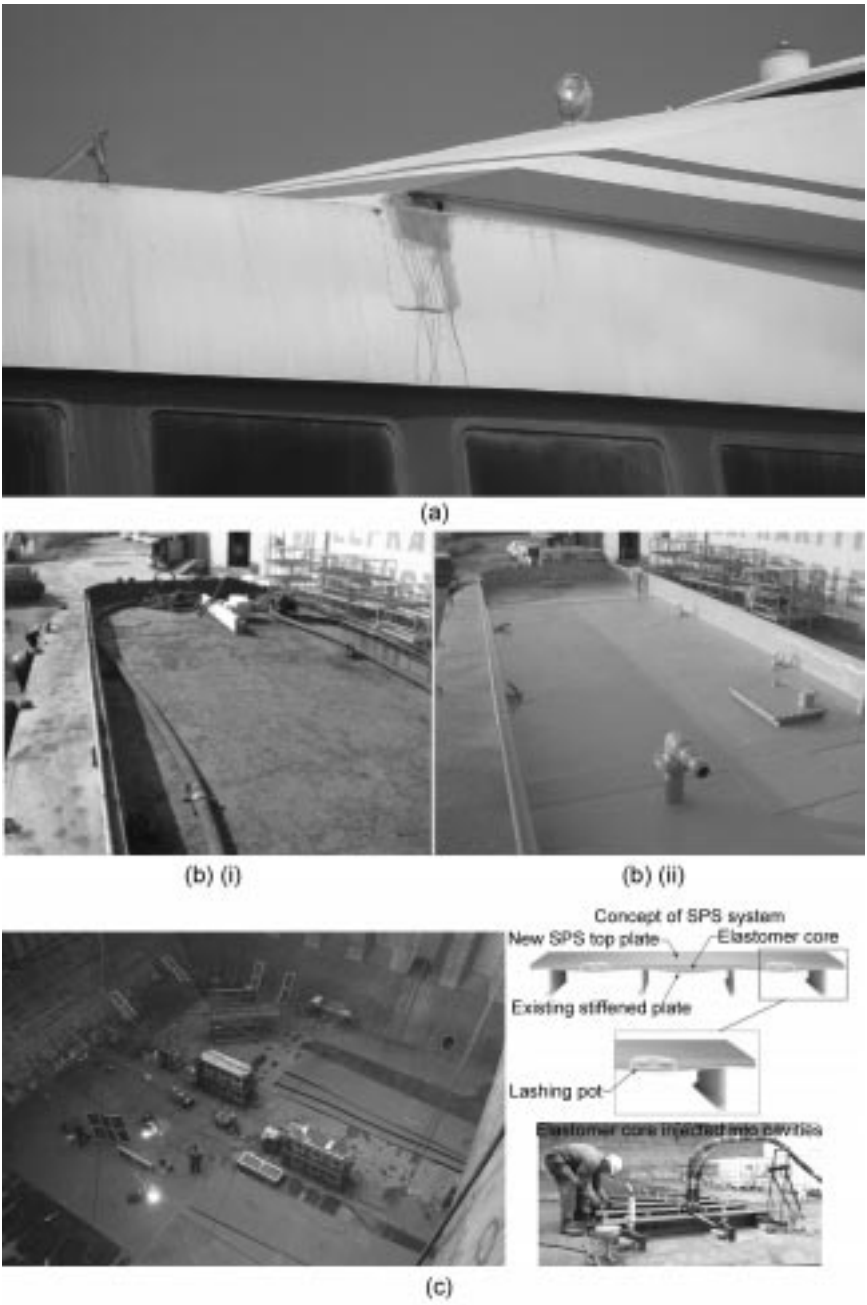
of-service time and hot works involving risk of fire and explosion. Composite patching mitigates these problems since, with carbon/epoxy patches curing at around 55 ºC, no hot work is involved. Repairs are quick to apply and can be carried out *in situ*, so limiting time spent out of service. However, excessively corroded, holed or cracked areas are not worth temporary repair by composite patches, as shown in Fig. 15.6a, as they are generally prone to crack again quickly.

A similar technology is the sandwich plate system (SPS) which consists of two metal plates bonded to a compact core. SPS bonds a new top plate to the existing structure, welding (or adhering) steel perimeter bars on it. This creates cavities into which polyurethane elastomer is injected to form the SPS overlay, i.e. a sandwich having the corroded plate as the lower skin and a new plate as the upper skin, being the core elastomer. Such repair may be considered permanent in some cases, effective for both corrosion and even large dents on plates (e.g. tank top of a cargo hold as in Fig. 15.6(c)). It is accepted by classification societies.

15.3.2 Temporary repairs of fractures

On plates, temporary repair of cracks by means of welded doublers is generally permitted provided that relief/arrestor holes are drilled at the ends of the crack.

© 2008 Woodhead Publishing Limited



15.6 Composite repairs: (a) a cracked detail (two different composite doublers fitted in this case at different times, both not successfully); (b) (i) wasted deck and (ii) successful composite repair of wasted deck; (c) SPS installation on a dented tank top plating of a bulk carrier (courtesy of www.ie-sps.com).

© 2008 Woodhead Publishing Limited

Sometimes, when watertightness is not necessary, only the arrestor hole is drilled, and permanent repairs are carried out by suitable insert as soon as practicable. A bolted patch may be a solution in some specific cases.

Underwater repairs are generally carried out by specialized firms securing a box on the underwater body so as to seal part of it off from the surrounding water. Water is pumped out from the box so work can be carried out within this protected 'dry' environment (see Fig. 13.3 in Chapter 13).

For through-thickness cracks that have propagated not only through the plate thickness but also away from the local stress concentration, hole drilling using either a drill bit or a hole saw has proven to be an effective retrofit (SSC-425 [13]). Holes essentially smooth the tip of the crack, reducing the stress concentration. The size of the hole must satisfy the relationship

$$D \geq \frac{\Delta\sigma \cdot a}{18\sigma_y}$$

where $\Delta\sigma$ is the stress range (MPa), a is the size of the crack (mm), and σ_y is the yield strength of the plate (MPa). If this relationship is not satisfied, the crack will most likely reinitiate from the edge of the hole. The validity of this retrofit has been studied in the laboratory on full-scale welded beams subjected to variable amplitude loading up to 90 million stress cycles (SSC-425 [13]).

Slightly better resistance to reinitiation can be obtained if bolts are inserted in the holes and tightened so as to introduce some local compression around the hole. Other methods attempt to cold-work the hole to introduce some beneficial residual stress state around the hole and crack tip. Hole drilling may also be used to isolate a fatigue crack so that it does not extend from a secondary component into the main girder. These methods are summarized in Fig. 15.7.

For distortion-induced cracks, stop holes are more effective than weld repairs, since cracking relieves the distortion-induced stresses, thereby reducing the driving force for subsequent crack extension. Weld repairs restore the distortion-induced stresses and will crack again, typically more quickly than the original cracking.

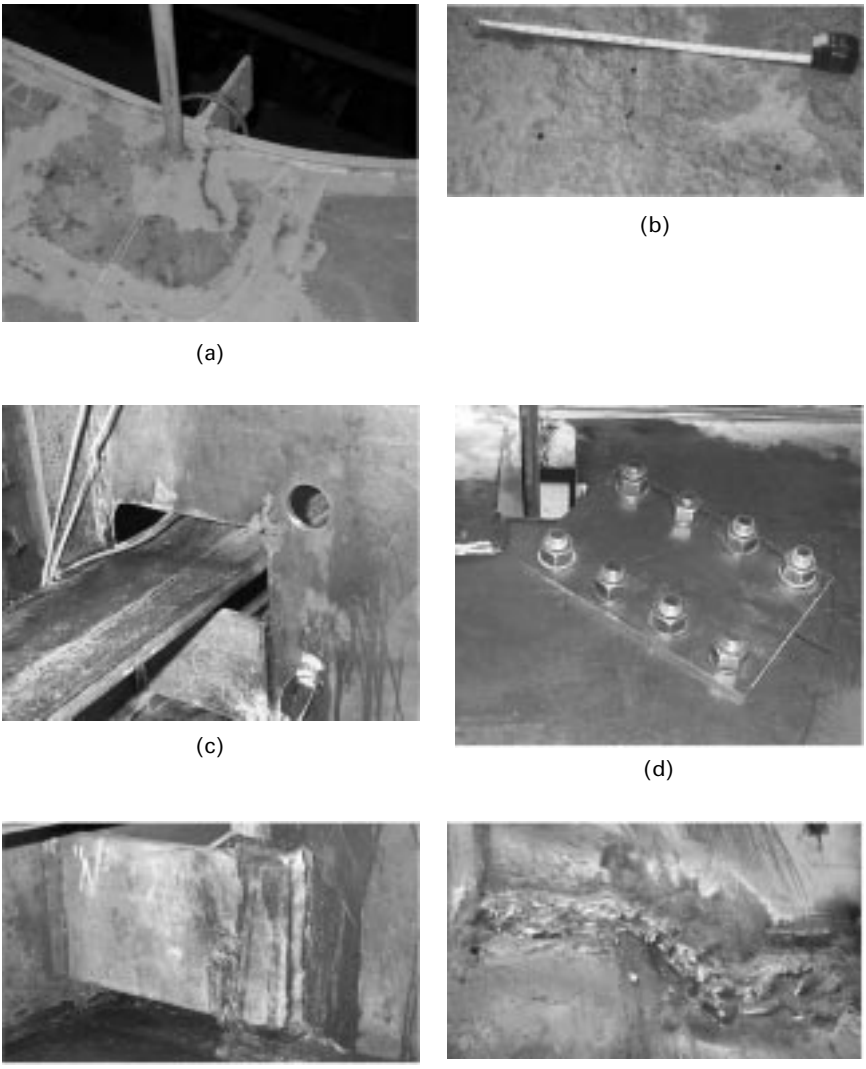
Rewelding a crack without drilling holes or without properly grinding the edges in order to remove the notches may be an ineffective repair as it will probably start to grow again in the same hot spot, where probably additional crack raisers have been shaped by the repair procedures.

A typical temporary repair of cracked fillet welds is toe grinding, provided that the grinding depth is not too large. The final fillet weld shape should be appropriate and residual strength section of the welding seam not excessively reduced; otherwise, after grinding, the fillet weld should be rewelded.

15.3.3 Temporary repairs of mechanical damages

Doubling and additional stiffening is generally carried out only when dents and damages are too deep and large. Otherwise no temporary repairs are required

© 2008 Woodhead Publishing Limited



(a) (b) (c) (d) (e) (f)

15.7 Temporary repairs of cracks: (a) crack in the web of a horizontal stringer (already repaired by an insert but crack raiser was not removed), (b) arrestor hole on a corroded plate, (c) arrestor hole on a crack, (d) bolted patch repair on the same crack, (e) rewelded crack in a lug plate, (f) rewelded crack without termination holes (not recommended).

unless watertightness is to be restored. In this case, steel or composite doublers are fitted in the same way as for corroded structures and temporary stiffeners added in the way of the dent, whose geometry and design should be studied on a case-by-case basis using the same criteria as for new builds and temporary repairs of corroded areas.

© 2008 Woodhead Publishing Limited

15.4 Permanent repairs

15.4.1 Permanent repair of corroded structures

When corrosion is discovered and wastage is above acceptable limits, there are few repair options to be selected other than to crop and renew. The replacement of complete panels of the structure may prove most cost-effective and ultimately more reliable than merely renewing individual members (see Fig. 15.8).

Restoration of the structure to the original standard may not constitute durable repairs of damage originating from insufficient strength or inadequate detail design. In such cases strengthening or improvements beyond the original design may be required.

Cutting, welding sequences, edge preparation and alignment should be done according to new-builds standards (IACS Rec. 47 Part A [2]). Minimum size of inserts (300 × 300 mm approx., with rounded corners) is the main additional recommendation. Sometimes, in order to improve the original design, thicker inserts are fitted. Where the difference in thickness between an insert and the adjacent plating is greater than 3 mm, the edge of the insert plate should be suitably tapered. In order to reduce the residual stress arising from this repair situation, the welding sequence and procedure are to be carefully monitored.

Corrosion in welded joints of plating may be eliminated by grinding and welding, after suitable preparation. Repairs of this type which are systematic and of considerable extent shall be clearly identified in the survey reports so that they can be easily located at subsequent surveys.

Repair of pitting corrosion by weld filling pits is a repair method which should account for the residual and localized stresses caused by the process. This method is generally accepted if no more than 2% of the plating surface is pitted. Table 15.2 summarizes the corrosion repair option currently adopted on ships and offshore structures.

15.4.2 Permanent repair of fractures

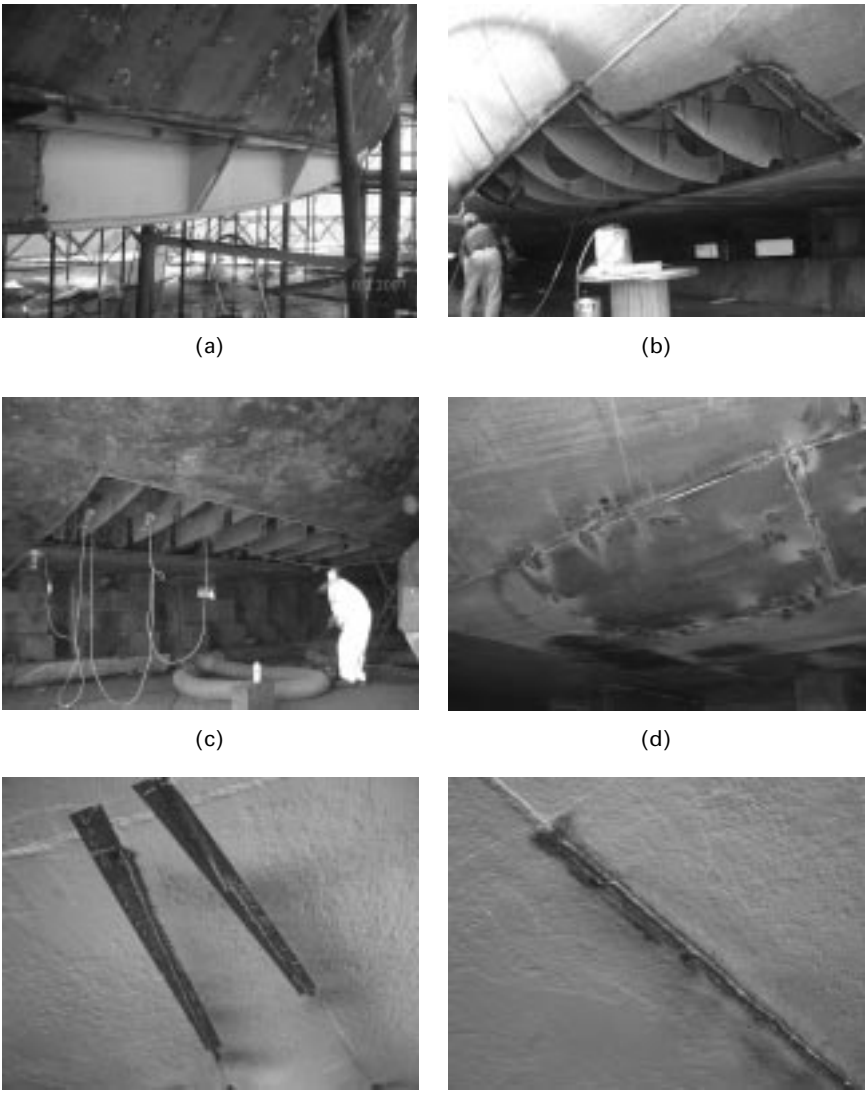
Three different repairs of fractures are distinguished:

- Repairs of surface cracks
- Repairs of through-thickness cracks
- Modification of the connection or structure to reduce the cause of cracking.

Strategies of repair include rewelding the cracks, replacing the cracked plate by suitable inserts either modifying the detail geometry or increasing the scantlings. The fatigue cracking that occurs at the boundary of weld connections as a result of latent defects should be veed-out (e.g. by grinding or arc gouging), appropriately prepared and rewelded.

As long as a crack is completely removed, a full-penetration weld completely restores the fatigue life of a cracked butt weld. Also, multiple cycles of repair

© 2008 Woodhead Publishing Limited



(a) (b)

(c) (d)

(e) (f)

15.8 Permanent repair of corrosion: (a) renewals of internal bottom fore structures, (b) renewals of floors in way of bilge, (c) bottom plating cropped, (d) insert fitted ready for welding, (e) corroded welded seams veed out and then (f) rewelded.

have no detrimental effect on the restored fatigue strength because fatigue is intrinsically a localized phenomenon. Vee-out and weld repairs are most effective when used to repair a previous weld that cracked, i.e. they will usually not crack again until at least the time it took to first crack the detail. A vee out-and-weld repair in a plate where there was no weld before is rarely effective, i.e.

© 2008 Woodhead Publishing Limited

Table 15.2 Corrosion repair methods

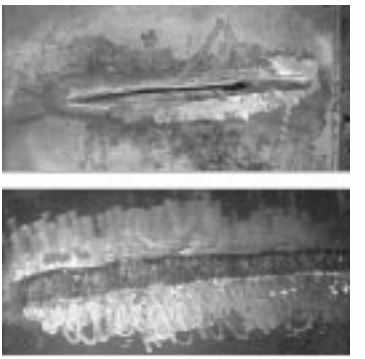
Severity/type of corrosion	Corrosion intensity/extent	Corrosion repair options
Minor coating breakdown and localized/limited corrosion	General corrosion	1. No repair and monitor (fix deadlines) 2. Spot blast and hand striping/patch coat 3. Add/maintain anodes
	Pitting corrosion: rare, small, shallow pits less than 50% in depth	1. No repair and monitor (fix deadlines) 2. Spot blast and hand striping/patch coat 3. Add/maintain anodes
Major coating breakdown and localized/limited corrosion	General corrosion	1. No repair and monitor (fix deadlines) 2. Reblast and recoat 3. Add/maintain anodes
	Pitting corrosion: large, deep pits greater than 50% plate thickness in depth, limited number	1. No repair and monitor (fix deadlines) 2. Spot blast, pit fill by weld and patch coat 3. Add/maintain anodes
Corrosion and wastage of plates and stiffeners	General corrosion	1. No repair and monitor (fix deadlines) 2. Spot blast, weld doubler plate, patch coat, fill in pits (temporary repair) 3. Cut out, weld insert plate, blast, coat (permanent repair) 4. Add/maintain anodes
	Pitting corrosion: large, deep pits greater than 50% plate thickness in depth, large number	
	Grooving of stiffeners edges and pitting	1. Welding only 2. Welding plus hard coating 3. Coating by pit filling compound of hard coating 4. Add/maintain anodes
	Heavy corrosion and wastage/pitting	1. Installation of doublers/intermediate stiffeners to restore to the equivalent original strength (temporary repair) 2. Replacement in kind with the original scantling 3. Replacement by less than original scantling plus additional reinforcement to restore structure to the equivalent original strength 4. Replacement by greater than original scantling/different geometries or design, if necessary 5. Add/maintain anodes

© 2008 Woodhead Publishing Limited

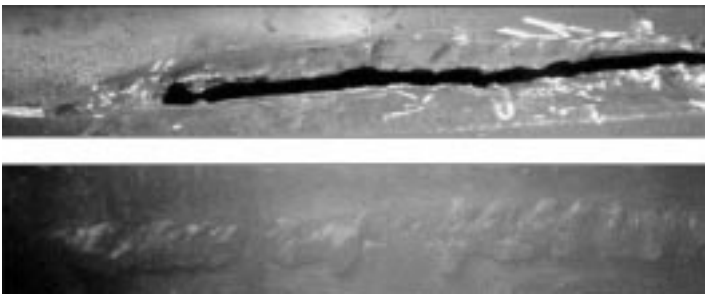
they will usually crack again in a time period less than the time it took to crack the detail in the first place. In this case it is necessary to modify the detail because of the thermal alteration of material properties [13], [14]. These methods are summarized in Fig. 15.9.



(a)



(b)



(c)



(d)

15.9 Permanent repair of cracks: (a) crack leaking from side shell, (b) repairs by veeing out and rewelding in air, and (c) similar repair carried out underwater; (d) erosion and cracks on a rudder shaft repaired by grinding and welding (still to be finished on the surface).

© 2008 Woodhead Publishing Limited

For fatigue cracking of some structures, renewal may not be a permanent solution and an attempt should be made to improve the design, e.g. by adding soft toes, brackets, thicker insert plates, etc.

Unfortunately, fatigue cracks are frequently repaired without sufficient consideration of the performance subsequent to the repair. Poorly designed or executed repairs can lead to quick reinitiation of fatigue cracks at the location of the repair. In some cases individual ships have been reported to have thousands of cracks. In these cases, the repair costs may be surprisingly high [13], [14].

In offshore structures with tubular joints, where the welds are very large, grinding is very effective at shaping the weld and enhancing fatigue strength by reducing the associated stress concentration factor.

Post-weld improvement techniques are always an option in the repair of cracks. Although they are usually quite expensive for ship structures, they are sometimes adopted for offshore ones. These methods serve to increase the fatigue life of a part at the weld and include both geometric and residual stress methods.

Geometric methods increase fatigue life primarily by reducing the geometric stress concentration at the weld location. Geometric methods include grinding (full profile burr grinding or disc grinding), weld toe remelting (TIG dressing or plasma dressing) and weld profiling. Grinding is always to be finished by a rotating burr and not a disc grinder [2].

Other methods increase fatigue life through the mechanical addition of residual compressive stresses on the surface of the weld to decrease the magnitude of the resultant tensile alternating stresses when the part is in service. These methods include shot peening and hammer peening.

Fractures are sometimes due to local shear stresses of stiffeners not being properly aligned along the shell. In such cases the repair should account for the cause, renewing the plating and modifying the end connections of stiffeners, e.g. by tapering the web of the stiffener and the bracket ends; see Fig. 15.10.



15.10 Instance of a crack due to misalignment of stiffeners, repaired by insert but cracked again.

© 2008 Woodhead Publishing Limited



15.11 Permanent repair of a fractured bilge keel by cropping and tapering.

Bilge keels are subject to fractures, often because of impact with submerged objects or berths. The typical repair method, other than renewal of the stiffener profile and of the connection plates, consists in cutting the damaged part of the bilge keel and tapering the end appropriately. The new bilge keel end should be in the way of an internal transverse stiffener. A small circular or elliptical doubler should also be fitted on the shell plate corresponding to the profile end in order to avoid sharp edges and notches. This is considered a permanent repair even if the repaired bilge keel is no longer of the same length as the original one (see Fig. 15.11). Table 15.3 summarizes the crack repair options.

Table 15.3 Crack repair methods

Crack repair method	Repair options and notes
No repair and monitor	Fix deadline and service limits, recommend monitoring procedures
Temporary fix and monitor	1. Drill hole at crack tip 2. Drill hole at crack tip, tighten bolts lug to impose compressive stresses at crack front 3. Add doubler plate 4. Cover crack with cold patch (e.g. composite)
Permanent fix, keep same design	1. Gouge out crack and reweld 2. Cut out section and butt weld inserts/replace cracked plate and stiffeners in way 3. Apply post-weld improvement techniques
Permanent fix, modify design	1. Gouge out crack and reweld, add/remove/modify/ design of scantlings, brackets, stiffeners, lugs or collar plates 2. Cut out sections, reweld, add/remove/modify scantlings, brackets, stiffeners, lugs or collar plates (soft toe, increasing radius, trimming face plate, enlarging drain holes, enhancing scantling in size or thickness, etc.) 3. Apply post-weld improvement techniques

© 2008 Woodhead Publishing Limited

Rules do not address fatigue life of ship repairs. Recommendations governing repair welds are provided, but none discuss resultant fatigue strength of repairs. Several books illustrating the types of cracks that commonly occur and the suggested repairs have been published (e.g. [9]–[12]). However, these books do not address the expected fatigue strength of the repairs.

Very few experimental fatigue test data exist for ship repairs. A Ship Structure Committee Project tested butt welds repairing through-thickness cracks multiple times (SSC-424 [13]). Other SSC reports (SSC-425 [14] and SSC-386-III [17]) discuss the analysis of repairs of cracked details in ship structures, but [13] includes testing while others were based on numerical calculations (FEM).

15.4.3 Permanent repair of mechanical damage

When scantlings have deteriorated to minimum levels permitted by the classification society, the wasted plating and stiffeners are to be cropped and renewed. Similarly, fractures are not generally allowed in ship and offshore structures and suitable repairs are required. On the contrary, dents and deformations of the shell plating may often be neglected, depending on their depth and extent. Every large plated structure, in fact, has some dents on the shell of the main body due to residual stresses and actions during construction. Contacts and impacts may also cause dents of limited dimensions, which may be disregarded or just noted in survey reports: see Fig. 15.4.

It is quite easy to identify them during surveys but much more difficult to decide whether or not to repair them. It should be noted that the dimensions of the dent are not the only criteria: causes, possibility of increase of the extension, shape of the dent and location also need to be considered. While examining the dent, it also needs to be established whether the internal structures in the vicinity have also been deformed. In such a case, the strength of the structure is generally impaired and renewals are required. Deformations on the hull bottom due to slamming, green seas, fatigue and buckling distortions need to be carefully considered.

The method of repair of fair intercostal dents consists of mechanical or thermal deformation of the plating by means of hammers, jacks, flame, hoist and other means adopted on a case-by-case basis by the practitioners of the shipyard. It is in general important that the procedure is appropriately slow and that thermal cycles of the steel do not change the material properties, e.g. by tempering the material. Sometimes small holes are drilled in the plating to release the stresses induced during the repair. These methods work well for plating of 15–20 mm thickness, even if the planarity of the shell will not be completely restored. For larger thicknesses, they should be applied with due diligence.

If the deformation is local and of a limited extent, it could generally be faired out. Deformed plating in association with a generalized reduction in thickness

© 2008 Woodhead Publishing Limited



15.12 Breakdown of coating due to dent.

should be partly or completely renewed because of corrosion wastage. Buckling can also occur in the local structure. In such cases, the damaged area is to be cropped and partly renewed.

If the deformations are extensive, replacement of the plating, partly or completely, may be necessary. If the deformation is due to excessive loading, additional strengthening should be considered.

During the repair of the mechanical damage and dents, particular attention should be paid to the breakdown of the coating (Fig. 15.12). In fact, some dents are not smoothed and the coating film is detached from the plating surface. In these cases, corrosion initiates rapidly under the coating.

15.5 Examination and testing of repairs

There is evidence that the quality of repair in shipyards is not always as good as new construction. Quality problems with repair welds in service should account for the suspected reduced strength. In such cases, the problem of repair quality must be solved through adequate quality control procedures. General advice is given below for the minimum examination and checking aimed at obtaining sound repairs. Reference is also made to Chapter 13 as appropriate.

15.5.1 Initial checks and checks during repairs

When starting repairs of a welded structure and in the course of these repairs, the following should be checked.

- The materials used are of the required type, have been duly tested and comply with the approved plans concerning the scantlings.

© 2008 Woodhead Publishing Limited

- The electrodes and the welding processes have been duly approved and are used in accordance with the relevant approvals; the welding materials are taken from original packages.
- The welders are qualified and employed in accordance with their qualification with satisfactory results.
- The welding equipment and plants are operating regularly and their measuring instruments have been calibrated.
- The joint preparations and back gouging are of the due shape and the prepared surfaces are satisfactory as to cutting and gouging.
- The assembling, alignment, tacking and cleanliness are satisfactory, or are rendered such by appropriate measures, special attention being given to the connection of prefabricated items.
- The welding sequences are correct and, where appropriate, in accordance with the approved plans.
- The welding and workmanship are in accordance with the applicable requirements and normal good practice.
- Any weld which is found to be defective or inadequate as far as soundness, shape or size is concerned is to be repaired.

15.5.2 Inspection after steelwork completion

Before paint is applied to the repairs to be examined, the fabricated parts shall be visually inspected and subjected to non-destructive tests as applicable. The visual examination is intended to ascertain in particular possible deformations, correct shape and required size of welds, any defects such as cracks, porosities, undercutting and lack of penetration in joints welded on one side only.

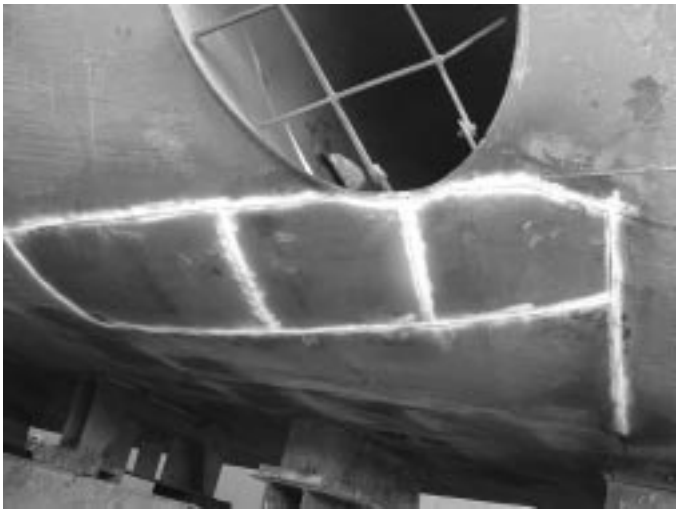
The following NDT may in general be performed at convenience after visual examination:

- Dye penetrant (normal or fluorescent) examinations (Fig. 15.13)
- Ultrasonic testing
- Magnetic particle examinations
- Radiographic or gamma-ray examinations.

Especially the following welded joints should be subjected to NDT after repair:

- Crossings of butt-joints of panels or strakes of strength deck, bottom and bilge, when welded simultaneously.
- Transverse butt-joints welded by special welding processes with one side only or with one single pass on both sides.
- Butts of round gunwale plates.
- Butt-joints of insert plates around openings in the shell and strength deck.
- Butt-joints of either flat bars or shapes used as longitudinals of the strength deck, bottom and bilge.

© 2008 Woodhead Publishing Limited



15.13 Dye penetrant of shell inserts.

15.6 Acknowledgements

The editors of this book, relying on a rather young professor for a very challenging task, are first acknowledged; I hope that my contribution will meet their expectations. Co-members of ISSC 2006 and ISSC 2009 Special Committee V.6 are also gratefully acknowledged, since working with them improved my skills about condition assessment of ageing ships and offshore structures.

I am indebted to several people who have supported my contribution to this book, including Ing. G. Damilano, Mr V. Vannucci and Mr G. Bolcano, former colleagues when I was a field surveyor, who indeed taught me the real practice of ship surveying.

Professor R. Tedeschi needs special acknowledgement: not only did he support my work but also he was, as ancient Romans used to say, the 'magister vitae' (teacher of life) since he became my PhD supervisor a few years ago. I also thank my parents and my wife, who actually became my wife while I was writing these chapters, for their endless patience and continuous encouragement.

15.7 References

[1] Munger C.G. (1984), *Corrosion Prevention by Protective Coatings*, NACE, Houston, TX.

[2] IACS Rec. No. 47 (1999), *Shipbuilding and Repair Quality Standards*, IACS, London, www.iacs.org.uk.

[3] IACS Rec. No. 74 (2001), *A Guide to Managing Maintenance*, IACS, London, www.iacs.org.uk.

© 2008 Woodhead Publishing Limited

[4] IACS Rec. No. 75 (2001), *Format for Electronic Exchange and Standard Reports*, IACS, London, www.iacs.org.uk.
[5] IACS Rec. No. 76 (2004), *Guidelines for Surveys, Assessment and Repair of Hull Structure – Bulk Carriers*, IACS, London, www.iacs.org.uk.
[6] IACS Rec. No. 84 (2005), *Guidelines for Surveys, Assessment and Repair of Hull Structure – Container Ships*, IACS, London, www.iacs.org.uk.
[7] IACS Rec. No. 87 (2004), *Guidelines for Coating Maintenance and Repairs for Ballast Tanks and Combined Cargo/ballast Tanks on Oil Tankers*, IACS, London, www.iacs.org.uk.
[8] IACS (2007), *IACS Unified Requirements*, IACS, London, www.iacs.org.uk (continuously updated).
[9] Tanker Structure Cooperative Forum (1986), *Guidance Manual for the Inspections and Condition Assessment of Tanker Structures*, International Chamber of Shipping Oil Companies, International Marine Forum.
[10] Tanker Structure Cooperative Forum (1992), *Condition, Evaluation and Maintenance of Tanker Structure*, TSCF Work Group report.
[11] Tanker Structure Cooperative Forum (1995), *Guidance Manual for the Inspection and Maintenance of Double Hull Tanker Structure*, TSCF and IACS.
[12] Tanker Structure Cooperative Forum (1996), *Guidance Manual for Tanker Structure*, TSCF and IACS.
[13] Kelly B.A., Dexter R.J. (2003), *Adequacy of Weld Repairs for Ships*, SSC-424, Ship Structure Committee, Washington, DC, www.shipstructure.org.
[14] Dexter R.J., FitzPatrick R.J., St Peter D.L. (2003), *Fatigue Strength and Adequacy of Weld Repairs*, SSC-425, Ship Structure Committee, Washington, DC, www.shipstructure.org.
[15] Sensharma P.K., Dinovitzer A., Traynham Y. (2003), *Design Guidelines for Doubler Plate Repairs of Ship Structures*, SSC-443, Ship Structure Committee, Washington, DC, www.shipstructure.org.
[16] Shield C.K., Swanson K.M., Dexter R.J. (2003), *In-service Non-destructive Estimation of the Remaining Fatigue Life of Welded Joints*, SSC-444, Ship Structure Committee, Washington, DC, www.shipstructure.org.
[17] Gallion K.A. (1992), *Repair Management System*, Report SSC-386-III, September 1992, Ship Structure Committee, Washington, DC, www.shipstructure.org.
[18] Bea R.G., Hutchison S.C. (1993), *Maintenance of Marine Structures: a state of the art summary*, Report SSC-372, May 1993, Ship Structure Committee, Washington, DC, www.shipstructure.org.
[19] Ma K., Holzman R.S., Demsetz L. (1992), *Design and Maintenance Procedures and Advancements in Tankship Internal Structural Inspection Techniques*, Report SSC-386-IV, September 1992, Ship Structure Committee, Washington, DC, www.shipstructure.org.

© 2008 Woodhead Publishing Limited

16

Maintenance of aged land-based structures

A VAN GRIEKEN, Connell Wagner Pty Ltd, Australia

Abstract: Maintenance, repair and protection of land-based concrete structures requires a structured approach and a full understanding of the relevant techniques and materials. This chapter addresses the selection of the most appropriate approach and critical aspects related to the design, documentation and execution. This involves a number of key considerations, including the function of the structure, the condition and exposure conditions, consequence of failure and cost of maintenance.

There are a wide range of concrete repair and protection options. This chapter examines the five main groups. Repair options include conventional concrete repairs, electrochemical treatment, structural modifications and modification of the exposure conditions. Surface treatments include anticarbonation coatings, coatings to protect against physical and chemical attack impregnation with silanes or silane-siloxane, and corrosion inhibitors. A range of repair mortars are available for conventional concrete repairs, including micro-concrete. Electrochemical repairs or treatment such as realkalisation and desalination modify the concrete, while cathodic protection halts corrosion. Structural modifications frequently involve carbon fibre strengthening techniques and overlays. Repair of masonry structures involves different techniques which are tailored to the construction details. The repair of metal structures is heavily dependent on the metal type and failure mode.

Key words: maintenance and repair of concrete, masonry and metal structures, chemical and physical concrete attack, anticarbonation coatings, concrete impregnation treatment, concrete crack treatment, concrete restoration, electrochemical treatment, structural strengthening, brick growth.

16.1 A structured approach

Regardless of the size of the structure, extent of deficiency or number of types of materials and deficiencies, a structured approach to the maintenance and repair of structures is required This needs to accommodate the increasing number of options which are available due to the increasing number of repair materials and techniques.

When deciding on an appropriate action to meet the future requirements of the life of the structures, the following options need to be considered as a minimum:

1. No remedial or protection action for a defined or indefinite time period.
2. Re-analysis of the structure for the present and intended or considered future use to establish acceptable load limits which do not require further actions.

© 2008 Woodhead Publishing Limited

3. Treatment, prevention or reduction of the deterioration without strengthening of the concrete structure, and acceptance of the current structural capacity.
4. Improvement, strengthening or refurbishment of selected elements of the concrete structure using methods which are the most suitable for the various structural elements.
5. Demolition.

16.2 Key considerations

The selection of the most appropriate approach and the design, documentation and execution of maintenance and repairs to structures involves a number of key considerations:

- Clear definition of maintenance target
- Functions and demands of the structure
- Relationship between structure and components
- Condition and ageing and deterioration mechanisms at component level
- Consequence of failure and cost of maintenance
- Maintenance strategies.

16.2.1 Maintenance targets

Maintenance targets for a structure can be one or a combination of the following:

- Reliability
- Availability
- Serviceability
- Durability
- Presentability.

16.2.2 Functions and demands of the structure

Both current functions and future demands of the structure will need to be taken into account in the formulation of maintenance and repair. The criticality of the structure in terms of its function and use will significantly effect the type and scope of the repairs. Clearly power stations and hospitals have a more critical and vital function than, for example, low-level concrete infill walls. Furthermore, the use of a building will affect the type and method of repairs as, for example, there are very limited opportunities to carry out noisy work at hospitals and hotels.

16.2.3 Relationship between structure and components

While maintenance and repair are usually carried out at component level, the type and nature of maintenance will depend not just on the component charac-

© 2008 Woodhead Publishing Limited

teristics but also on the consequences of the loss of function of this component at the structure level and in some cases even at the infrastructure level.

16.2.4 Adequate understanding of condition and cause

It is imperative that the cause and likely extent of the deficiencies is known. The assessment of structures is described in Chapter 14 in more detail. This will require investment by the owner and tolerance by the users of the structure during these investigations. It cannot be over emphasised that an inadequate understanding or investigation can lead to incorrect solutions and contractual problems. Furthermore, additional assessment costs are typically more than offset by reductions in contractors' bids due to greater certainty.

16.2.5 Consequences of failure

Consequences of failure can be complex. In general, all losses should be considered in the evaluation of the consequence of failure, including business-economic and social-economic losses. By clearly identifying and assessing consequences of failure, the cost of maintenance can be appropriately justified.

16.2.6 Maintenance strategies

Three basic maintenance strategies are:

- Failure-based maintenance: repair and maintenance actions taken when failure has been observed
- Use-based maintenance: maintenance actions taken after a certain use period or loading regime
- Condition-based maintenance: maintenance actions taken after a certain condition limit or criterion is exceeded.

Failure-based maintenance is usually considered acceptable for components with low risk of failure. Risk of failure consists of two components: failure consequences and failure probability. Use-based maintenance is acceptable for components whose failure mode and timing are predictable. Condition-based maintenance is acceptable when the extent of deterioration is measurable.

In addition to the above, the extent and type of maintenance and repair is a function of a number of factors, including the design life as required by the owner for commercial or functional reasons.

The required level of serviceability of the structure can also dictate the extent of repairs. For example, small cracks in concrete structures are tolerable in most cases and yet for water-retaining structures and those exposed to chlorides and aerosols they are not tolerable.

© 2008 Woodhead Publishing Limited

16.2.7 Access and public protection

A significant proportion of the cost to repair and remediate a structure is absorbed by access and public protection. For example, in the order of 20% of the cost to repair high-rise façades is used to create safe and adequate access to undertake the works and to construct and remove public safety measures such as gantries. This heavily influences the rate and location of work and the selected scope. Furthermore, when carrying out works which are dusty or involve high-pressure water, containment measures are required as, for example, cementitious contaminated water is likely to drift well away from the place of work and affect coatings, glass and the public.

16.2.8 Heritage listing

A heritage listed structure requires repairs which are sympathetic to the materials, geometry and aesthetics of the nominated era for which the structure is deemed to be most representative from a heritage perspective. It is often difficult to establish which era is the most representative as the original structure may not be considered to be the reference structure. Thus the materials need to be carefully considered and will need to be sympathetic and correspond to those which were used at the elected time which is deemed to be of greatest historical significance.

16.3 Documentation

Remediation documentation typically includes the following three components:

- Drawings
- Specifications
- Contractual documents.

16.3.1 Drawings

The drawings need to be representative of the as-built structure. Typically, existing or original as-designed drawings are found and used for repair purposes. However, it is likely that these drawings do not represent the façade or structure adequately due to alterations at the time of construction or subsequent modifications. Thus an accurate geometric survey is required. Furthermore, some contracts require that the drawings need to adequately show the location, type and extent of remedial works.

16.3.2 Specifications

Specifications may be prescriptive, proscriptive or performance type. Prescriptive specifications need to carefully describe the required products and

© 2008 Woodhead Publishing Limited

required outcomes. This approach may be used for unique structures with unique deficiencies where previous experience or prior research has identified materials which are suitable for this application.

Proscriptive specifications are not common and typically state what shall not be done and leave the decisions regarding materials and methods for the repairs open for the contractor. This is not a recommended approach and will make the evaluation of tender bids very difficult and may not adequately represent the owners' and users' requirements.

Performance-type specifications are common and should be carefully written such that they clearly describe the required outcomes and clearly define limits whilst enabling contractors and suppliers to propose their preferred methods and materials. This approach will produce the most competitive tenders and encourage the suppliers and builders to propose their most innovative or suitable materials and solutions. It is important that the specifications do not contradict or conflict with the drawings.

16.3.3 Contract documents

There are many forms of contracts for the repair and rehabilitation of structures, some of which are contained within national standards and codes. However, many owners have their own forms of contract. Regardless of the type of contract, the most challenging issue is that of quantities.

The most thorough approach is to fully survey and document the condition of the structure and to provide a full bill of quantities for the works. However, this approach is less favoured currently as it requires a very significant investment in time and money to prepare. This is typically not available to designers and specifiers. Furthermore, this approach can lead to contractual disputes.

The alternative contract is one where all types of deficiencies are identified and specified and scheduled in a list for the contractor to propose standard rates for works and variations. While this approach will not create disputes related to cost, it will nevertheless require intensive site control by the owner's representative to document the scope and type of work and to avoid overwork. Furthermore the owner will not know the final costs of works until the completion. Typically this is not an acceptable situation for owners.

As an alternative the contract can provide the results of the selected investigation and tests which are then deemed to be representative for the structure as a whole. The tenderer may then tender on this project on a lump sum basis with the inspection results as a basis.

16.3.4 Cost estimates

Typically cost estimates are required for projects such as these. These can be based on anticipated or known quantities of work and previous rates in

© 2008 Woodhead Publishing Limited

conjunction with specialist contractors. Standard rates need to be considered and may need to be modified based on project knowledge and relevant experience.

16.4 Site phase of the works

The new European code has nine parts, with EN1504-9 still in draft form. This code for the repair of concrete structures has identified six phases for repair projects:

1. Management of the structure
2. Process of assessment
3. General planning, including options, principles and methods
4. Design of the required works, including specifications, drawings and contract documents
5. Execution of the work and quality control tests
6. Acceptance of the work. This includes quality control testing, any remedial works as a result of inadequate work or test results which do not meet specified criteria and 'as-built' documentation of the repair work.

The successful execution of the works needs to include a significant number of, at times conflicting, requirements, including the following:

- Experienced subcontractors
- Cooperation, tolerance and acceptance by the user of the structure
- Consideration of the adjacent properties and owners in terms of noisy work periods, dust and of the effect of public protection and access on adjoining owners
- The effective implementation of the subcontractors' quality assurance programme and the effective implementation of the specified quality assurance testing regime.

16.5 Repair and protection of concrete structures

16.5.1 Repair and protection options

A number of models and codes have been developed including the new European standard EN1504 – Products and systems for the protection and repair of concrete structures. This code is the result of more than 10 years of intensive discussions within different working groups and is likely to become a model for countries outside Europe. This standard consists of 10 main standards and around 65 related standards for test methods.

Table 16.1 reflects a simplified overview of the repair principles and the various repair or protection options. These options can be grouped into five distinctly different groups, namely:

© 2008 Woodhead Publishing Limited

- Group 1
  - Surface coat
  - Impregnate
  - Treat crack/voids
- Group 2
  - Locally repair concrete
  - Local reinforcement
- Group 3
  - Treat electrochemically
- Group 4
  - Add extra mortar/concrete
  - Restore/strengthen structurally
- Group 5
  - Shelter
  - Replace

16.5.2 Surface coating

Prior to application of surface coating to concrete and masonry, it is worth noting that besides changing the appearance, coating may hamper subsequent inspection and monitoring of applied remedial measures, may obscure defects and will require regular maintenance.

Besides decorative purposes, the main reason for coating concrete and masonry structures is extending their durability performance. BS EN 1504-2 provides an excellent description of surface protection systems for concrete and relevant performance requirements.

Barrier coatings are the most commonly used coatings on concrete and masonry. The main objective of application of barrier coating is to provide a barrier between concrete and the environment or specific elements. The common function of the coating in this case is to prevent further ingress of harmful elements into concrete and to protect concrete from further damage. It also can be used to impart chemical resistance or physical resistance or a means of moisture control or a combination of these to the concrete/masonry substrate.

Sealers are another type of surface coating for repair and maintenance of concrete structures. The main difference between coatings and sealers is that sealer penetrates into concrete and does not leave a noticeable layer on the original concrete surface. There are two main types of sealer – non-film-forming and film-forming sealer.

Some of the commonly used surface coatings for maintenance of concrete structures are discussed below.

© 2008 Woodhead Publishing Limited

Table 16.1 Repair and protection principles and methods (courtesy of Connell Wagner)

Method	Group 1			Group 2		Group 3	Group 4		Group 5	
Principle	Surface coat	Impreg-nate	Treat cracks/ voids	Locally repair concrete	Coat reo	Treat electro-chemically	Add extra mortar/ concrete	Restore/ strengthen structurally	Shelter	Replace
Repair and protection of damaged concrete										
PI Protection against ingress	✓	✓	✓(a)							
MC Moisture control	✓	✓				✓				
CR Concrete restoration				✓						✓
SS Structural strengthening			✓(c)				✓	✓(d)		
PR Increase physical resistance	✓	✓					✓(e)			
RC Increase chemical resistance	✓	✓					✓(e)			

© 2008 Woodhead Publishing Limited

Protection of reinforcement against corrosion

RP Preserve/ restore passivity		✓(f)		✓(f)		✓(g)	✓	
IR Increase resistivity	✓	✓						✓
CC Cathodic control	✓	✓(h)						
CP Cathodic protection						✓		
CA Anodic control		✓(i)			✓(j)			

Notes:
(a) Various treatments/methods: bandage, fill, create joint
(b) Various treatments/methods: apply mortar by hand, recast with concrete, spray mortar or concrete
(c) Inject or fill cracks, voids or interstices
(d) Add/replace reinforcement, plate bond, post tension
(e) Overlay with thin concrete layer
(f) For carbonated concrete
(g) Realkalise carbonated concrete/extract chlorides
(h) By saturation
(i) Using inhibitors
(j) Coagulating active pigments/barrier coatings

The above approach distinguishes between treatments which protect or treat the concrete and those which protect the embedded reinforcement.

© 2008 Woodhead Publishing Limited

Anticarbonation coatings

There are many proprietary anticarbonation coatings which meet desired requirements. These are normally barrier-type coatings which must be applied completely over the surface of the concrete and must be defect-free. Generally anticarbonation coating on concrete will require multiple coats to eliminate or minimise the presence of defects and imperfections.

Requirements generally specified for anticarbonation coating on concrete include the following:

- A minimum carbon dioxide equivalent air layer thickness (e.g. >50 m using a test method such as DIN EN 1062-6)
- Water vapour diffusion equivalent air layer thickness (e.g. <4 m using a test method such as DIN EN ISO 7783-2)
- Bond strength, typically minimum 0.75 MPa
- Minimum dry film thickness (DFT) (e.g. 300 microns)
- Minimum effective period.

The most durable and effective anticarbonation coating is one which contains pigments. However, owners may object to the structure being 'painted'. Thus where the current image needs to be maintained, transparent anticarbonation coatings may be used. This is particularly applicable for pre-cast or *in situ* concrete surfaces with exposed aggravate and pigmented concretes.

The coating needs to be applied to a dry service and needs to breathe to allow vapour pressures which build up behind the coating to diffuse through the coating while blocking the ingress of external moisture. The dry film thickness of the coating and the adhesion to the base concrete need to be tested as part of the quality assurance programme.

Coatings to protect against deleterious chemicals

Other reasons for coating a concrete surface include the need to increase the physical resistance of the concrete and the resistance against exposure to chemicals. Such coatings will need to be specifically formulated and tested. Effective selection of a coating system for chemical resistance or physical resistance will require precise definition of the exposure and application.

Most acids and acid-producing substances (including organic) will 'attack' the concrete and cause degradation of the concrete. pH is not the only criterion determining the extent of attack on concrete. Concrete can also degrade in excessively highly alkaline environments, environments containing sufficient amounts of materials reactive to concrete's constituents, and environments where microbacterial-induced corrosion can operate. In these conditions, coating of concrete is critical for its durability.

© 2008 Woodhead Publishing Limited

However, the designer needs to know whether the coating is likely to deteriorate due to ultraviolet radiation (such as with epoxies) for the in-service life and cost evaluation process.

Table 16.2 lists the most commonly used protective coatings and their advantages and disadvantages.

Table 16.2 Most commonly used coatings to protect concrete against deleterious chemicals (Quick, 2007)

Coating type or family	General information	Advantages	Disadvantages
Epoxies	Two types of epoxy resin: • Bisphenol A (BisA) • Epoxy Novalac (EPN)	• EPN resistant to concentrated sulphuric, hydrochloric and phosphoric acids • EPN resistant to temperatures up to 150 °C, Bis A up to 100 °C • Excellent bond to concrete	• Bis A less resistant to these acids • EPN not resistant to concentrated nitric acid or concentrated organic acids • Limited ultraviolet resistance
Polyurethanes	Many types	• Good bond to concrete • Generally very good ultraviolet resistance • Excellent resistance to many solvents, alkalis and acids • Excellent water barrier • Now one of the most commonly used liquid applied membranes • Resistant to temperatures up to 130 °C • Thermal coefficient of expansion similar to concrete	• Limited vapour transmission • Low resistance to sulphuric or nitric acids • More easily damaged • Slippery when wet (may necessitate inclusion of sand or similar)

© 2008 Woodhead Publishing Limited

16.5.3 Impregnation – silanes/siloxanes

Silane

The amount of water absorbed into the surface of a material depends mainly on the radius of the pores. There are two categories of pores:

- Gel pores are interconnected interstitial spaces between the gel particles and range in size between 15 and 20 Å (Neville, 1981).
- Capillary pores are the spaces in the cement volume which have not been filled by products of hydration and range in size from 100 to 10 000 Å (Marconi *et al.*, 2002).

The water absorption coefficient (w) expresses the water uptake in kg/m^2 versus time (h$^{0.5}$). The following values provide an indication of the significant differences between, for example, brickwork and concrete (Wacker, 2002):

- Very dense concrete: 0.15 kg/(m^2 h$^{0.5}$)
- Highly absorbent brickwork: 11.5 kg/(m^2/h$^{0.5}$)

Thus it can be seen that concrete is relatively impervious. High-strength concrete or concretes with additives such as silicon fume or slag or fly ash may be too dense to be effectively treated with an impregnating silane.

Even though normal concrete is relatively impervious, the application of an impregnating silane which penetrates into the surface and repels moisture is a common form of protecting the concrete and embedded reinforcement against the ingress of moisture and dissolved aggressive and deleterious substances such as chlorides. The size of silane molecules is in the order of 10–20 Å, which is considerably smaller than that of concrete pores at 100–10 000 Å (Marconi *et al.*, 2002). Thus silanes will rapidly penetrate into the surface layer of the concrete and line the pores and create hydrophobic surface properties. Tests are required to establish the depth of impregnation prior to specification and during these works. A minimum of 5–10 mm impregnation is recommended to achieve the required durability.

Commercially available products based on iso-butyltriethoxysilane and iso-octyltriethylsilane with high concentrations of active components not less than 95% and 80% respectively have been used successfully for protection of above-ground concrete structures. In recent years, coatings based on fluorinated silane have also been available and can offer both hydrophobic and oleophobic characteristics to the concrete surface.

Silane–siloxane

A silane–siloxane blend is also used to provide a hydrophobic barrier but is different from silane, as it lines the pores but also reacts with the surface, leaving a ‘coating’ on the concrete. This surface material can degrade and may become

© 2008 Woodhead Publishing Limited

visible. However, as the vapour pressure of oligomeric siloxanes is negligible under typical conditions, they do not suffer from losses by evaporation. Siloxane molecules are larger than silane molecules and in the order of 25–75 Å. Table 16.3 provides a summary of silane and siloxane properties.

Other

Silicon resins are now not commonly used, as their relatively high molecular weight restricts penetration and some silicons such as standard methyl silicon resins are not very durable on alkaline substrates such as concrete.

16.5.4 Impregnation – corrosion inhibitors

Another form of impregnation is the application of an impregnating corrosion inhibitor, the use of which has been widely debated and studied. ISO8044–1999 defines a corrosion inhibitor as 'a chemical substance that decreases the corrosion rate when present in the corrosion system at a suitable concentration, without significantly changing the concentration of any other corrosion agent.' There are two types of inhibitors for concrete:

- Admixed corrosion inhibitors (ACI)
- Penetrating (or migrating) corrosion inhibitors (PCI).

Inhibitors such as calcium nitrite were introduced in the late 1970s but largely as admixtures. Other organic inhibitors such as amines and amino-alcohol based inhibitors have also been used. It is commonly accepted that inhibitors should only be used when concrete is relatively undamaged.

The use of penetrating corrosion inhibitors is more recent and has been widely promoted as a repair or prevention technique to delay corrosion of embedded reinforcement in reinforced concrete structures. However, as the limits of this relatively new technique are still not fully understood, it is the subject of ongoing research.

Surface-applied penetrating corrosion inhibitors (PCI) are based on organic and inorganic compounds which penetrate into the concrete and form thin protective films around the surface of the steel reinforcement. This restricts oxygen access to the steel and inhibits the corrosion.

PCIs are mostly used for carbonated but also for chloride-affected structures and contrast with admixed corrosion inhibitors (ACI) which are used with repair mortars or in new concrete mixes. Ingress via the pores of the concrete occurs by diffusion through the concrete as a vapour as well as a liquid.

The following is a general summary of the research findings and areas where consensus appears to have been achieved, as well as aspects which are currently under research, contentious or not fully understood.

© 2008 Woodhead Publishing Limited

Table 16.3 Silane and siloxane impregnation treatment comparison

Material	General information	Advantages	Disadvantages
Silane	• Liquid • Applied as solvent or water-based liquid or as a gel	• Reduces capillary water absorption and deleterious substances • Improves frost resistance • Relatively good penetration • Surfaces do not need to be air dry for application • Solvent/water-based silanes are volatile and evaporate easily • Gel or creme silanes have a thixotropic consistency which avoids loss due to evaporation • Almost total halt in chloride ion migration	• Not an effective water barrier against ingress of water under hydrostatic pressure • Methyl silanes not suitable for hydrophobic protection • Can cause differences in surface appearance due to different absorption rates • Does not halt carbonation
Silane/siloxane	• Liquid applied • Lines pores and leaves film on surface	• Can customise penetration, resistance to alkalis and water repellency	• Surface film degrades over time • Not an effective water barrier against ingress of water under hydrostatic pressure • Can cause differences in surface appearance due to different absorption rates
Siloxanes		• Not volatile, no losses due to evaporation • Forms active substance more rapidly than silane and therefore less prone to losses due to rain, etc.	• Remain in or on the surface to form active substances (silicone resin network) • Surface film degrades over time

© 2008 Woodhead Publishing Limited

- The rate and depth of diffusion vary with the porosity and humidity of the concrete.
- Porous low-grade concretes may allow a loss of the volatiles which carry the inhibitor.
- It appears that carbonated concrete will allow good penetration.
- Penetration through chloride-contaminated concrete varies with the percentage of 'blocking' chlorides.
- Inhibitor concentrations decrease sharply with depth. It appears that beyond 50 mm the concentrations are too low to have an effect.
- The use of PCIs should be limited to sound concrete where corrosion of reinforcement has not yet caused cracking and spalling.
- Good results have been obtained for cases of carbonation-induced corrosion.
- Tests have resulted in variable outcomes for cases of chloride-induced corrosion. Thus it is necessary to establish chloride ion concentrations before deciding on a PCI strategy. Research suggests the following:
  - Where chloride ion concentrations exceed 2% by weight of cement, the use of organic corrosion inhibitors is totally ineffective (Mackechnie *et al.*, 2004). At lower chloride levels some reduction in the corrosion rate is possible and the corrosion threshold may be almost doubled.
  - Some research suggests that if the chloride ion content at the level of the reinforcement exceeds the threshold, the use of PCIs is likely to be ineffective, but it is still effective up to this level.
- The duration of effectiveness of the PCI is subject to further investigation. When used in conjunction with a surface coating the effective lifespan is increased.
- Corrosion is considered passive at a rate of 0.1 μA/cm^2. This should become one of the performance criteria.
- Maeder *et al.* (2005) suggest the following alternative acceptance criteria:
  - Delay the onset of corrosion and maintaining corrosion rates at levels less than 5 μm per year.
  - Reduce existing corrosion rate at least 60% from base condition or less than 5 μm per year.
  - Control of incipient anodes following installation of a repair mortar.

It is critical that concrete will allow adequate penetration of the inhibitor to the depth of the reinforcement. Where, for example, the surfaces are contaminated or the concrete pores are saturated or partly saturated, the use of PCIs is likely to be largely ineffective. Wetting the surface after application of the PCI on a dry surface appears to drive the inhibitor into the substrate at a higher rate with less loss through evaporation.

16.5.5 Crack treatment

Repairs of cracks need to be based on the following:

© 2008 Woodhead Publishing Limited

- The cause(s) of the cracks
- The intended function of the cracked element (e.g. slab, water-retaining tank wall, cantilevering beam, etc.)
- The likely exposure conditions
- The design objective, including:
  - Restoring or improving structural capacity
  - Restoring or improving performance such as watertightness
  - Preventing the ingress of deleterious agents such as chlorides or carbon dioxide (as carbonation can progress from cracks)
  - Improving aesthetic appearance.

The traditional treatment of cracks involved surface routing and the installation of an elastomeric sealant. While this is typically effective, providing the sealant can accommodate dynamic movement, the result is very visible and often unacceptable to owners. As an alternative, cracks can be injected with a variety of materials including epoxy, polyurethane and others. Crack injection procedures are widely used and can be applied with a variety of proprietary equipment. It is important to ensure the following:

- That the cracks are not contaminated or blocked by debris or organic material.
- That the cracks are not saturated.
- The depth of penetration needs to be checked as part of the quality control system using small cores or local breakouts.
- Precautions need to be taken to ensure the substance which is injected into cracks externally does not exit at internal faces.
- That architecturally concrete surfaces are not contaminated at the exteriors as spillages are typically difficult to effectively remove.
- If the crack is dynamic a suitable flexible injection material such as polyurethane or similar is required. Typically epoxies are too rigid to accommodate dynamic movements of significance.
- Crack injection for structural strengthening or restoration purposes will require the use of epoxies.

It should be noted that fine cracks which are static may heal autogenously due to hardening of leached concrete constituents.

Cracks due to alkali aggregate reactions and due to aggregate containing sulphur (pyrite) are erratic and three-dimensional and typically require demolition. By injecting epoxy resins at high pressures some structures can be saved (Frala, 2005). In other developments research is underway to produce genetically engineered biosealants based on micro-organisms to fill cracks.

Table 16.4 provides a summary of crack repair options.

© 2008 Woodhead Publishing Limited

Table 16.4 Crack treatment

Repair	Method/material	Application	Unsuitable applications
Surface sealing	• Rout shallow groove of proportion to meet sealant manufacturers' geometric requirements • Prepare surfaces, apply elastomeric sealant suitable for the application (e.g. architectural wall or trafficable roof, etc.)	Most cases	• Where crack is subjected to high frequency of dynamic cycles • High hydrostatic pressure • Repair or restoration where aesthetic appearance is important
Injection	• Clean cracks • Face seal • Inject via ports	• Most cases • Structural repairs • Epoxy structural injection for cracks as narrow as 0.05 mm (ACI RAP-1)	• Epoxy not suitable for dynamic cracks • Where cracks are blocked • Flexible filler not suitable for structural cracks
Gravity fill/absorb	Gravity fill with or apply low viscosity polymers, monomers or resins including some epoxies and silanes	Cracks 0.03–2 mm (Goldie, 2004)	• For long term repair • Cracks wider than 2 mm • Silane where cracks exceed 0.3 mm • Where surface contamination will become visible and is not acceptable • Polymers not suitable for wet cracks • Resin not suitable for dynamic cracks
Grout fill	Fill with fine cementitious grout for wide cracks and chemical grouts	Cracks down to 0.5 mm wide	• Dynamic cracks • Water-retaining elements
Bandage/ coating/ overlays	• Chemically bond a flexible bandage to the surface (may include surface sealing) • Apply an elastomeric coating to entire surface • Install an overlay to entire surface for slabs/pavements	Mostly suitable for fine static cracks	• Not suitable where crack is subject to large number of dynamic cycles • Not suitable where subjected to heavy traffic

© 2008 Woodhead Publishing Limited

16.5.6 Restoration of concrete

There are a range of repair methods for defective concrete including, amongst others, the following:

- *Conventional patch repairs* involve the process of breakout, surface preparation of the concrete including the application of a bond coat, surface preparation of any exposed reinforcement through the application of a protective coat or bond coat, application of a repair mortar which is compacted and cured, and possibly the application of a finishing coat. The removal of defective concrete is destructive, dusty, expensive and slow using pneumatic equipment. A more effective means is the use of hydro demolition equipment which is less noisy, involves less dust, and is faster than conventional means. The high-pressure water lance readily cuts through the concrete and can even cut reinforcing bars. It produces a rough clean base surface which is ready for the application of the repair mortar. Furthermore it causes minimal damage to the base concrete in terms of micro-cracking. Hydro demolition robots are now being used on projects of significant size and are able to rapidly remove large volumes of concrete in controlled areas.
- *Large surface repairs* need the use of a suitable mortar which has very low shrinkage characteristics to avoid delamination. Where the restoration of the exposed area involves relatively large volumes, poured micro concrete may be a more suitable solution than the application of a proprietary and hand-placed mortar. As an alternative, sprayed mortar produces dense concrete and is suitable for a variety of applications.
- *Structural repairs* require carefully staged breakout and reapplication to ensure that the element has adequate structural capacity for the applied loads which are relevant during the works. Structural repairs differ from other repairs in that the structural capacity of the element needs to be restored to that of the original undamaged element or to a designed structural capacity. Thus the repair mortar in compression zones and columns needs to absorb compressive forces. This requires that the repair mortar is in full contact with the base concrete and does not shrink from the interfaces and that the repair mortar has adequate compressive capacity to take up the load. However, research is ongoing regarding the load path through or around structural repairs.

There are a number of repair mortars for patch repairs or larger restoration repairs:

- *Ordinary Portland cement concrete* is suitable for large volumes and non-aggressive exposure conditions. However, the concrete needs to have performance characteristics which are compatible with the base concrete. The placement sequence, vibration/compaction and curing need experienced contractors.

© 2008 Woodhead Publishing Limited

- *Polymer modified cement mortars* are now widely used and include a variety of polymers. These mortars are generally dense and have low carbon dioxide infusion properties and high chloride ingress/protection characteristics. The latest mortars have been designed to minimise linear shrinkage to around 500 micro strain. However it is important to ensure that this highly alkaline material does not create insipient anodes at the boundaries particularly in the case of chloride contaminated and wet structures.
- The fine aggregates in *micro concrete* produce a concrete which is suitable for heavily reinforced large repairs and for pouring into formed-up sections.
- *Calcium aluminate cements* (Scrivener, 2005) are special cements which:
  - harden rapidly
  - have high abrasion resistance
  - have high resistance to microbial acid attacks.

  These have been produced for more than 100 years but are costly, and have been used for, amongst others, dam spillways and sewerage structures.
- Special combinations are being trialled for special conditions such as in the Persian Gulf area where the addition of styrene butadiene latex (SBR) and silica fume resulted in increased durability and reduced crack formation and decreased chloride ingress rates.
- Research is being carried out into the feasibility of full or partial replacement of conventional polymer dispersions which are largely derived from petrochemicals, with renewable raw materials such as sugar-based dispersions and substituting conventional aggregates with waste fillers.

Table 16.5 provides a summary of restoration options.

16.5.7 Electrochemical treatment

Realkalisation

Electrochemical treatment can control moisture ingress, restore the pH of the concrete and thus reverse the carbonation. A number of methods have been commercially developed, including realkalisation and chloride extraction. Electrochemical realkalisation of concrete was developed in the late 1980s and is achieved by passing a small electric current, in the order of 1 A/m^2, between the embedded reinforcement and a temporary surface-mounted mesh anode which is surrounded by a sprayed celluloid fibre matrix which is kept wet with a highly alkaline electrolyte. The result is twofold, namely:

- The highly alkaline material is absorbed or drawn into the concrete.
- Hydroxyl ions form at the surface of the embedded reinforcement.

Thus carbonation is reversed. This appears to be a permanent process which reverses the effects of carbonation and protects the reinforcement.

However, realkalisation is not suitable for concrete which is susceptible to

© 2008 Woodhead Publishing Limited

Table 16.5 Restoration options

Method	Method/material/application	Unsuitable applications
Patch repair – polymer modified concrete	Polymer modified mortar suitable for most cases	• Where cathodic protection is applied • Structural repairs • Where adjacent incipient anodes may develop
Patch repair – cementitious	• Portland cement concrete: – Large volumes – To match existing – Non-aggressive exposure conditions	• For aggressive exposure conditions where the surface is not treated/coated
	• Portland cement mortar: – Smaller thin repair for non-aggressive exposure conditions	
	• Micro concrete: – Where access is difficult or geometrically complex – Larger volumes – Otherwise as for Portland cement concrete – Higher concentration of polymers where a degree of flexibility is achieved. This is applicable for repairs subject to dynamic forces	• Durability yet to be established
	• Styrene butadiene latex and silica fume modified mortars can reduce crack formation in hot climates and achieve improved durability	• Costly • Slightly lower strength than OPC
	• Calcium aluminate (Scrivener, 2005): – Rapid hardening – High microbial acid attack resistance – Used for special applications such as dam spillways, sewerage structures	• Durability yet to be established
	• With higher concentrations of polymers increased flexibility can be achieved	
Reconstruction	• Local replacement of element • Structural restoration	• Small repairs
Shotcrete	• High density mortar • Good for large surface area repairs	• Rebound mortar needs containment • Need heavy equipment which is difficult at heights

© 2008 Woodhead Publishing Limited

alkali aggregate (silica) reactions. While the impressed current is less than that for cathodic protection, it may still be high enough to cause hydrogen embrittlement to prestressed or post-tensioned cables and highly stressed steel reinforcement. Electrical continuity of the embedded reinforcement and a reasonable level and uniformity of conductivity of the concrete are required. Thus tests are required as part of the option evaluation process (Broomfield, 1997).

Desalination or chloride extraction

This is not a commonly used method for land-based structures and is more commonly applied to marine structures. The different exposure zones such as the splash zones are subjected to different cathodic protection solutions. However, buildings which are located near bodies of salt water and exposed to chloride-contaminated aerosols may benefit from this method.

Desalination or chloride extraction is deemed to be effective in the short term, but may not provide long-term protection. It involves a similar process to realkalisation and is achieved by the application of an impressed current at a typical density of 1–2 A/m^2. The chloride ions are repelled from the reinforcement surface and transported out of the concrete. It is believed that chlorides can re-migrate from external sources or internal areas into the concrete which has been treated. However, this may be mitigated by the application of an external coating system. Similar restrictions and precautions apply as for realkalisation of prestressed, post-tensioned concrete, highly stressed steel reinforcement, potential alkali aggregate reactions, lack of electrical continuity of embedded reinforcement, and high concrete densities and resistivity. Large variations in concrete properties can cause differential rates and quantities of chloride iron extraction.

Cathodic protection – to halt or prevent corrosion

Cathodic protection dates back more than 180 years but became more widely used in the 1920s (Ackland, 2006). Impressed current cathodic protection involves the following steps:

1. Installation of a permanently fixed anode. This may be:
   - A mesh anode system involving the application of a surface mounted mesh (usually titanium)
   - A grid anode system involving installation of strips of ribbons, usually titanium, based in a conductive overlay which is embedded into the surface of the concrete element into cut grooves
   - An internal anode system: mixed metal oxide-coated titanium rods are embedded at 90º to the surface into carbon or graphite paste-filled holes
   - A conductive surface coating, such as carbon or zinc. However, this coating needs to be gas permeable as hydrogen evolves at the anodes.

© 2008 Woodhead Publishing Limited

2. Installation of a transformer/rectifier power source.
3. Application of a direct current (DC) into the concrete via the anode.

There are three main criteria for selecting/designing the current density, namely (Broomfield, 1997):

- Sufficient to halt the anodic reaction at the reinforcement and/or significantly reduce the corrosion rate.
- Minimise the current density to as low a level as possible to minimise acidification around the anodes and/or attack of the anodes.
- Minimise hydrogen evolution and embrittlement of prestressed/post-tensioned cables and highly stressed embedded reinforcing steel.

The common current density is 20 mA/m^2 of steel surface area as per AS 2832.5. Preventative current densities may be as low as 1–3 mA/m^2 for alkaline structures where the reinforcement is not corroding and up to 30–50 mA/m^2 for structures with high chloride levels, wet fluctuating conditions, high oxygen levels, severe corrosion of steel, and low concrete covers (HB 84, 2006). The cathodic protection system needs to be designed by specialists and trialled as there are many variable and potential latent conditions. Ongoing monitoring and zoning will enable managers to modify outputs over the life of a system. Excessive current densities in early cathodic protection systems have resulted in failures. Typically, protection criteria include those from AS 2832.5 section J and others as follows:

- Negative instantaneous potential of −1100 mV Ag/AgCl
- Instantaneous off criteria
- Decay criteria
- Loop resistance
- 24-hour depolarisation > 100 mV potential shift
- 72-hour depolarisation.

Recent research (Bazler, 2005) on thermal sprayed pure zinc coating systems revealed that blisters are likely to form where chlorides exceed 1% by mass of concrete and that this method is not suitable where the structure is showing corrosion damage. Cathodic protection of building façades is not common, as it involves installation of external wiring systems which are visible and may traverse joints and as there are many isolated steel elements such as window fittings which are difficult to link into the system. Nevertheless it has been successfully applied to *in situ* concrete façades facing the sea.

Finally, it is important that the anodes do not touch the reinforcement or are not too close to the reinforcement to avoid short circuits (or leaks) which will negate the effectiveness of the systems and can cause accelerated local corrosion instead.

Recent developments include woven carbon mesh anodes in special cement slurries at current densities of 3–4 mA/m^2 (Vennesland, 2005).

© 2008 Woodhead Publishing Limited

Cathodic protection – electro-osmosis

Cathodic protection by means of electro-osmosis can also halt the corrosion of reinforcement and reverse the ingress of salts. This salt reversal technique has been successfully used for buildings where salts have been drawn up into the walls from salt-contaminated soils and have caused the deterioration of the wall and reinforcement corrosion. Electro-osmosis is an electrochemical treatment which involves the application of an external current which reverses the salt migration process and at the same time protects any reinforcement which was at risk of corrosion. Successful trials of a significant application at a large structure, which is found on heavily salt-contaminated clays, led to the installation of this innovative system.

Anodic protection

In reinforced concrete structures, anodic protection is a terminology used for the description of cathodic protection using a sacrificial anode. Anodic protection involves the installation of a metal which is more anodic than the embedded reinforcement, thereby reversing the corrosion process and protecting the reinforcement. This is more commonly used for marine applications. Commercial systems are now available involving anodes which are embedded into repair patches to halt the corrosion of reinforcement. However, the longevity is yet to be established. Systems such as these need to be designed and not installed 'off the shelf' as there are many variables to consider, including protective radius, electrical conductivity of the repair mortar and base concrete, reinforcement density and condition, chloride concentration and exposure conditions, amongst others.

Table 16.6 summarises the application of the various electrochemical methods and their advantages and disadvantages.

16.5.8 Structural strengthening

There are a significant number of methods to strengthen a structure or its elements, including the following.

- *Increasing the size of the element*. This is typically an unacceptable solution as it adds weight to the structure, alters the geometry and therefore the appearance, and in the case of buildings reduces the space for services and internal finishes.
- *Plate bonding.* This process, now discontinued, involved epoxy bonding or bolting steel plates to the structure. The disadvantage of this process was the weight of the steel, the potential for corrosion of this steel element, the potential for the plates to debond over time and the difficulty of applying the generally heavy plates in overhead repairs.

© 2008 Woodhead Publishing Limited

Table 16.6 Electrochemical treatment

Method	Application/advantages	Suitability/disadvantages
Realkalisation	• Carbonated structures to protect the reinforcement against corrosion • No breakout, noise, dust • Long-term, perhaps permanent solution • Maintains image of uncoated concrete structures	• May not be suitable for prestressed/post-tensioned structures • Risk of starting or accelerating alkali silica reaction in susceptible structures • May require one to two weeks to restore alkalinity
Desalination/ chloride extraction	• Extraction of chlorides from concrete to halt or significantly retard reinforcement corrosion • Long-term solution if re-migration of chlorides does not occur • No breakout, noise, dust • Does not alter image of structure	• As for realkalisation • Not suitable where concrete has cracked or spalled due to corroding reinforcement • Not suitable where structure is submerged or in splash zone • Risk of chloride re-migration • May require 4–12 weeks to achieve result
Cathodic protection – impressed current	• Chloride contaminated structures where the reinforcement is corroding or at risk of corrosion • Long-term protection • Remote monitoring and adjustment to changes to exposure conditions or corrosion rates • In some cases also applicable for corroding reinforcement in carbonated concrete • Many anode systems including surface mesh, embedded ribbons, embedded rods, conductive surface coatings	• As for realkalisation with reference to alkali aggregate reaction and post-tensioned, prestressed structures • External wiring/equipment • Need for ongoing monitoring • Limited life of the anodes • Not suitable where it is not possible to achieve electrical continuity of reinforcement and link in all isolated embedded steel elements
Cathodic protection – electro-osmosis	• To protect structures affected by salts from soils • Reverses salt ingress and reduces salt concentrations • Can protect embedded reinforcement against corrosion	• Needs anodes to be embedded into walls • Life expectancy not yet known
Anodic protection	• Protects embedded reinforcement against present and potential corrosion by means of anodes which are embedded in repair patches • No need for wiring or external equipment	• Unknown lifespan • Need to be designed to include the many variable conditions and as-built details • Monitoring is difficult and impractical

© 2008 Woodhead Publishing Limited

- By contrast, *external carbon wrapping or fibre reinforcement* is now a widely accepted procedure which can strengthen the underside of slabs to increase their structural capacity and stiffness, and strengthen beams to increase their structural capacity and shear capacity. Furthermore, wrapping columns, which increases the axial load-carrying capacity, is frequently used for damaged structures. There are a variety of bonding materials available, including carbon fibre. These are applied in strips to the structure using bonding agents. Furthermore, there are a number of other means of strengthening structures, including multiaxial warp-knitted fabrics to strengthen masts and increasing the shear resistance of wall frame structures using carbon fibre-reinforced polymer grids.
- Innovative research has led to the development of *textile reinforced* concrete for the repair and reinforcement of concrete elements.
- *External post-tensioning.* This involves the use of external tendons/cables which are post-tensioned and can result in a significant increase in flexural capacity. However, fire rating requirements may restrict the application of this effective method. A novel new approach involves the application of prestressed externally bonded carbon fibre-reinforced polymer (CFRP) strips (Meier, 2005).
- *Concrete overlays* involve the placement of a thin concrete layer. This is typically applicable for bridges and similar structures. However, debonding has occurred in a number of important cases and resulted in a number of studies which concluded, amongst others:
  - Debonding starts at and propagates from surface cracking.
  - Debonding of the overlay from the base concrete is a function of, amongst others, the method of removal of the existing concrete. It was found that crude methods such as hand percussion caused micro-cracking at the interface and a significant reduction in the bond strength. By contrast, removal with low impact methods such as hydro demolition creates very few surface defects and results in the highest possible bond strengths.
  - Research also found that a bond coat was not required when using very low disruption removal techniques (Garbacz *et al.*, 2005).

16.6 Brick growth repairs

The repair of brick growth-related defects is dependent on the extent of damage caused by brick growth and typically involves the following:

- Localised rebuilding of severely dislodged or bulging brickwork.
- Installation of remedial brick ties. There are a number of proprietary remedial brick ties which involve the drilling of holes though the outer and inner skin and the insertion of stainless steel pins which are epoxied into these walls. More recent techniques involve mechanically filled helical ties.

© 2008 Woodhead Publishing Limited

- Furthermore, helical ties can be installed into horizontal joints to act as stitches.
- Removal of existing sealants from joints, and saw cutting joints to a width which is suitable for the installation of the new elastomeric sealants to suit the suppliers' requirements for the cross-sectional proportions of these sealants. Old deteriorated sealants may be very difficult to remove, particularly if the sealant engages the blade and makes saw cutting difficult or impossible.
- Brick growth can cause a range of associated defects, including:
  - Failure of cavity ties
  - Failure of shelf angle bolts
  - Damage to windows
  - Curling of parapets and balustrades.

  These can occur singly or in combination and require engineered solutions.

16.7 Repair of metal structures

16.7.1 Corrosion damage

The most common deficiencies in steel structures are due to corrosion. Typically where structural elements have corroded to an extent where the structural capacity is inadequate, replacement or local strengthening is the most suitable means of repair. Repairs almost always involve some degree of strengthening.

16.7.2 Plating

Plating is a procedure where additional elements are spliced to the structural element to increase or replicate the original capacity. Before installation of the plates or additional elements, the contact surface between the new and existing members should be adequately cleaned and prepared and the joints cleaned as the interfaces need to be fully sealed. Metallurgical advice is needed to establish if the base elements can be welded, cut or drilled and structural analysis is required to model the existing and modified stresses.

16.7.3 Repair of connections

Connections could also be repaired using plating techniques. However, where only the fasteners are deficient, local replacement is the most common repair method. It is important to check the condition of the concealed shanks of rivets and bolts in order to establish the need or otherwise for replacement or strengthening. Furthermore, it is important to prevent the ingress of water at the fasteners. Such repairs need to be carefully staged to ensure that the connections remain structurally adequate during the repairs for the reduction of full loading conditions.

© 2008 Woodhead Publishing Limited

16.7.4 Wrought iron and cast iron material

The repair of wrought iron and cast iron metals requires great care as it is typically not possible to cut or weld these metals or to drill holes for additional fasteners. A metallurgical assessment is required to establish the metal type prior to designing the remedial solution.

16.7.5 Cracked welds

These also require great care and close examination and surface testing of the affected area. This needs skilled specialists, particularly in regard to the determination of the cause of weld cracking and implication. Repairs may involve grinding down the cracked weld until the crack is no longer visible, followed by inspection of the weld with dye penetrant (or other suitable NDT techniques) to ensure that the crack has been removed. The weld can then be replaced using appropriate procedures and filler techniques. Repairs may involve a variety of other techniques depending on the depth of crack, location, accessibility, metals involved and stresses.

16.8 References

ACI RAP-1 Committee E706, Structural Repair by Epoxy Injection.

Ackland B (2006), Cathodic protection – black box technology, *Corrosion and Materials*, 31(3) 20–25.

Bazler R (2005), Integrated protection system for chloride deteriorated concrete structures, in Alexander M, Beushausen HD, Dehn F, Moyo P (eds), *Concrete Repair, Rehabilitation and Retrofitting*, London, Taylor & Francis.

Broomfield JP (1997), *Corrosion of Steel in Concrete*, London, E & FN Spon.

Frala H (2005), Injection into cracks in concrete made with reactive aggregates, in Alexander M *et al.*, *op. cit.*

Garbacz A, Gorka M, Counard L (2005), Relationship between surface characteristics and superficial cohesion of concrete, in Alexander M *et al.*, *op. cit.*

Goldie B (2004), Guide to specifying concrete repair materials, *JPCL*, 18–31.

HB 84 (2006), Guide to Concrete Repair and Protection, Standards Australia, 55.

Mackechnie JR, Alexander MG, Heiyantudiduiwa R, Rylands T (2004), The effectiveness of organic corrosion inhibitors for reinforced concrete, Research Monograph No. 7, University of Cape Town and University of the Witwatersrand.

Maeder U, Wombacher F, Marazzani B (2005), Concrete repair strategies including surface applied corrosion inhibitors, in Alexander M *et al.*, *op. cit.*

Marconi G, Tittarell F, Corindaldesi V (2002), Review of silicone based hydrophobic treatment and mixtures for concrete, *Indian Concrete Journal*, 637–642.

Meier U (2005), A new novel carbon fiber reinforced polymer (CFRP) system for post-strengthening concrete repair and rehabilitation and retrofitting, in Alexander M *et al.*, *op. cit.*

Neville AM (1981), *Properties of Concrete*, London, Pitman.

Quick R (2007), Protection of concrete under extreme chemical conditions, *Corrosion and Materials*, 32(3) 11–14.

© 2008 Woodhead Publishing Limited

Scrivener KL (2005), Calcium aluminate cements for repair applications, in Alexander M *et al.*, *op. cit.*
Vennesland R (2005), Cathodic protection of reinforced concrete – a system with woven carbon mesh, in Alexander M *et al.*, *op. cit.*
Wacker BS (2002), *Protecting Façades with Silicones*, technical brochure.

© 2008 Woodhead Publishing Limited

17

Risk-based inspection and maintenance of aged structures

C SERRATELLA, G WANG and K TIKKA,
American Bureau of Shipping (ABS), USA

Abstract: The industry has seen an ever-increasing interest in applying risk-based approaches to better manage the integrity of structures in service. The next generation of inspection, maintenance and repair (IMR) takes the form of risk-based inspection (RBI), risk-based maintenance (RBM) and risk-based repairs (RBR).

Risk-based structural IMR includes risk assessment coupled with the understanding of degradation mechanisms and consequence of failures in order to develop an IMR program for the asset. The applied approaches vary from qualitative methods to quantitative methods. Structural analysis plays an important role in this process and is used to predict the likelihood of failure and accounts for the degradation that structures inevitably suffer. In some cases the structural analysis can be taken from the original design of the structure. The calculations that support IMR development are used to determine those areas that are critical to structural integrity and to estimate, given a degradation rate, when those areas could be predicted to fail. Combined with an assessment of consequence of failure, the structural components are risk ranked and then ultimately aggregated into an inspection plan in terms of priority, sequencing as well as scope and frequency.

RBI approaches allow a more optimized inspection program while maintaining the same level of safety. RBM uses a maintenance program to manage the risk of undesirable events associated with structural failures. RBR assesses the current and projected condition of an anomalous situation over time and projects the likelihood of a structural failure occurring. Future trends in risk-based approaches will include the increased use of quantitative methods, incorporation of historical data trends, and integration of risk and IMR into software.

Key words: risk-based inspection, risk-based maintenance, risk-based repairs, qualitative RBI, quantitative RBI, structural reliability analysis.

17.1 Introduction

Inspection, maintenance and repair are necessary aspects of the long-term structural integrity management (SIM) philosophy for marine and offshore structures. The goal of a SIM program is to identify and intercept anomalous conditions caused by various degradation mechanisms, such as fatigue and corrosion, prior to their development into significant issues that threaten the integrity of the structure. Inspection is the systematic review and oversight of the

© 2008 Woodhead Publishing Limited

structure via examination in search of deficient conditions or for signs of impending defects. Maintenance is work that is done regularly to keep the structure in good working order, for example the scheduled replacement of sacrificial anodes of cathodic protection systems. Repair is used to restore the structure to a good working order in the event that damage or defects are identified during inspection. Collectively, inspection, maintenance and repair are called IMR.

Historically, IMR has been applied via a prescriptive approach whereby the IMR activities are performed on a periodic basis, on most components, without regard for the degradation of the component with time (e.g. corrosion or fatigue) or the importance of the component in contributing to the structural integrity of the system. For example, ship hulls typically follow a cycle of survey and are drydocked and inspected on a five-year cyclic basis. Why five years? The five-year survey cycle has existed since the days of wooden ships. Ship structures and the associated machinery have evolved quite a bit since the days of the sailing ship, yet the industry still maintains a five-year drydock interval, not because steel corrodes or fatigues at the same rate as a wooden hull, but because this interval has served the industry well and is time tested.

So are there better ways to implement IMR? In the case of the five-year survey cycle for ships, past and present-day ship operators know the risk of longer intervals between IMR which include coating breakdown and subsequent steel degradation, etc. We can apply the same concepts today, utilizing risk-based tools that vary in complexity from the simplest approach to highly sophisticated reliability-based methods. We know the degradation mechanisms for marine and offshore steel structures, namely corrosion and fatigue. Modern structural strength and fatigue analysis approaches allow us to predict which regions of the structure are most vulnerable. We also know the areas and components of the structure that if degraded can lead to the most extensive escalating damage and downtime. We can focus IMR attention on areas most important to life safety, protecting the environment and protecting the asset. Such well-planned and engineered applications fall into the category of risk-based IMR.

IMR as applied to marine and offshore structures is a risk assessment and risk management process that is focused on failure modes initiated by material deterioration and degradation mechanisms that can be managed and controlled through structural inspection, maintenance and repair. The process combines risk techniques within all IMR activities, such as inspection and maintenance planning, inspection data gathering, analysis, repair strategies and documentation in order to develop inspection plans that are directed toward the areas of highest risk to prevent undesirable events. In short, it is a method which uses risk to determine the most appropriate IMR strategies for a particular asset to ensure it is fit-for-purpose.

This chapter describes risk-based IMR by first describing risk-based approaches in general terms in order to show benefits and limitations. The

© 2008 Woodhead Publishing Limited

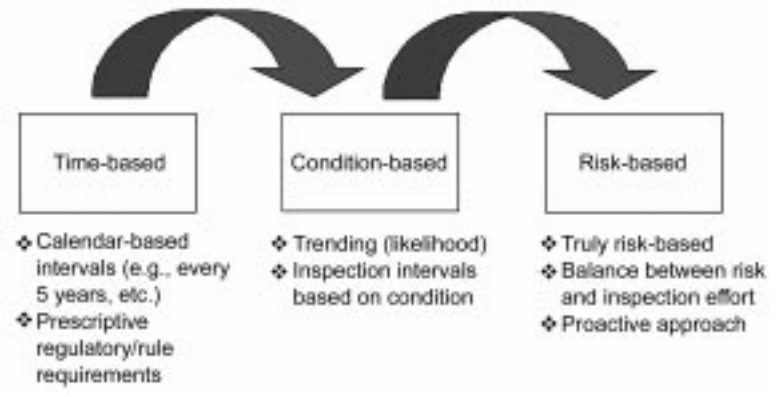
fundamentals of risk-based approaches are described in terms of how to determine risk and how to use it in a structural IMR program including acceptance criteria. Specific explanation is then provided for risk-based inspection (RBI), risk-based maintenance (RBM) and risk-based repairs (RBR). A risk-based IMR example using a specific Floating Production Storage and Offloading (FPSO) vessel is used throughout the chapter to assist in explaining the approaches. The chapter concludes with future trends and sources for further information.

17.2 Risk-based approaches

17.2.1 Evolution of inspection, maintenance and repair (IMR) strategies

Risk-based approaches to IMR originated in the nuclear industry in the 1970s [7, 8] and over the years have migrated into other industries, such as the downstream petrochemical and refining industries in the 1980s and 1990s [9, 10]. These approaches are now moving into the upstream offshore sector of the oil and gas industry and to a lesser extent the shipping industry [11–13].

Figure 17.1 provides a schematic of the progression and evolution of IMR strategies. The prescriptive time-based, also referred to as 'rule-based', methods are generally representative of the traditional requirements which in the case of marine and offshore structures were developed by regulators and by vessel classification societies. The plans derived from such an approach have generally been developed based on years of experience and tend to provide a comprehensive broad-brush set of inspection and survey requirements that have evolved over time. The ever-improving evolution of prescriptive requirements in this case is often the result of the reaction to a major event or loss or a series of recurring minor events which forces the entities in question to continually revisit



17.1 Evolution of IMR strategies.

© 2008 Woodhead Publishing Limited

and revise their requirements. In this way, the present-day standards, regulations and classification society requirements have been refined to cover aspects such as specific structural configurations and vessel types. However, even when considering the above, these requirements can only ever be a minimum baseline upon which to base one's IMR strategy. Additionally, since these requirements must by their nature cover all possible assets and structural configurations which fall under the remit of these regulations, they must be generic enough to be universally applied.

The condition-based method represents the next logical step in the evolution from traditional methods. In the case of offshore floating production installations that are ship-shaped or rely on stiffened plated steel design and compartmentation such as a Floating Production Facility (FPS) or non-ship shaped structures such as semisubmersibles and spars, these approaches are based on the experience obtained from inspections of unrestricted trading vessels (e.g., tankers) and the early generation of mobile offshore drilling units (MODUs). For offshore fixed-base steel jacket platforms that have been operating since the 1950s in the Gulf of Mexico, decades of experience have identified the common problem areas that are susceptible to corrosion and fatigue. For example, tubular members in the splash zone are prone to high corrosion, and conductor guide framing located at the first horizontal framing elevation below the waterline is prone to fatigue caused by wave-induced vertical hydrodynamic loading. Structural degradation models and input from subsequent inspections are used to forecast the condition of the structure. When the condition is predicted to reach a predefined minimum acceptable threshold, inspections are conducted. This method relies heavily on the likelihood of structural degradation but does not explicitly include the associated consequences if the component should fail, which is a key aspect of the next evolutionary step, the risk-based approach.

The risk-based method includes aspects of the condition-based methods using trending techniques to estimate likelihood of component failure, but it also factors in an estimation of the potential consequences of the structure's failure. Structural components whose failure can lead to significant consequences, particularly related to life safety and the environment, receive higher inspection priority. Examples include structural supports for quarters buildings on offshore fixed facilities, or supports for safety-critical and process-critical facilities for onshore industrial facilities. Of course the consequence of failure must be balanced against the likelihood that the structural member or members may be actually damaged or degraded. It is this challenge that complicates risk-based approaches.

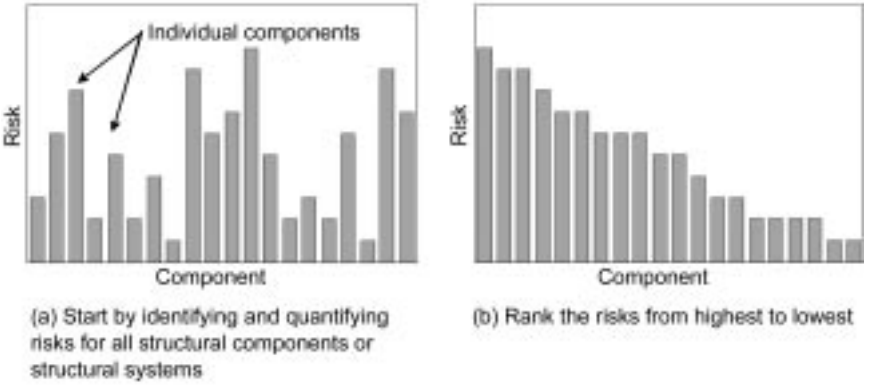
17.2.2 The risk-based approach

Risk-based structural IMR includes risk assessment coupled with the understanding of degradation mechanisms and consequence of failures in order

© 2008 Woodhead Publishing Limited

to develop an IMR program for the asset. The risk process can be simple or complex. A simple approach involves 'qualitative' methods whereby experience and expert judgment are predominately used to establish risk. A complex approach involves 'quantitative' methods whereby structural analysis and formal numerical risk and reliability methods are used to establish risk. Structural analysis plays an important role in this process and is used to predict the likelihood of failure and accounts for the degradation that structures inevitably suffer. In some cases the structural analysis can be taken from the original design of the structure. In other cases, a new formal strength and fatigue structural analysis can be conducted using the present condition of the structure. Also, such analyses can be either deterministic or probabilistic in nature. However, in either case, the calculations that support IMR development are used to determine those areas that are critical to structural integrity and to estimate, give a degredation rate, when those areas could be predicted to fail. Combined with an assessment of the consequences of failure, the structure components are risk ranked and then ultimately aggregated into an inspection plan in terms of priority sequencing as well as scope and frequency. This represents a significant improvement in structural integrity management (SIM) approach over traditional methods where there is little, if any, asset specificity or interaction between the design and in-service phases for the life of the asset. Further, targeted IMR and associated data collection of asset health for critical areas within the hull leads to risk reduction overall.

How does risk get incorporated into the IMR process? There are two key parts to the process. The first part is to identify, quantify and rank the risks as shown in Fig. 17.2. This part of the risk-based IMR process deals specifically with risks and is the most challenging. The specific risks are first identified for each structural component (or structural system) in terms of what can go wrong. Each of the vertical bars on Fig. 17.2(a) is the aggregate of risk for a specific structural component that makes up the structural system. For example, the storage

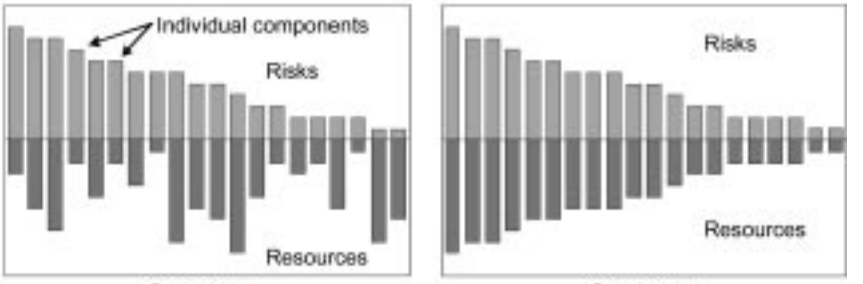


17.2 Identify, quantify and rank risks.

© 2008 Woodhead Publishing Limited

compartment of an FPSO may develop a crack at a bulkhead, or a corrosion-related hole through the hull plate. In terms of the consequence of this problem, what would happen if the crack grows or corrosion spreads such that it becomes a more serious problem? Would the oil leak into the environment, causing a high consequence situation, or just into another compartment, creating a lower consequence situation? Recall that risk is a combination of consequence and likelihood. So, given the site-specific loading on the vessel, what is the likelihood of the crack growing – low or high? If the likelihood of the crack or corrosion getting worse is low, then the conclusion may be to allow the condition to remain for a period. If the likelihood is moderate or high then this may be a high-risk situation and an immediate repair may be warranted. Similarly, if an owner has a 'fleet' of 20 fixed offshore platforms, some being manned drilling and production platforms and others being unmanned satellite platforms with only a single well, which ones should receive the most IMR attention? Figure 17.2(a) shows a set of structural components where the vertical height of each of the bars represents the quantity of risk, measured as the combined likelihood and consequence, for each of the structural components. For the examples above, the each of the structural components would represent one of the FPSO tanks or one of the fixed platforms. Quantifying risks is a more complex process with many options, both qualitative and quantitative, as described later. After the risks are quantified, the risks are *ranked* from highest to lowest, as in Fig. 17.2(b), providing a clear picture of risks and the structural components requiring the most attention.

The second part of the IMR process as shown in Fig. 17.3 is to allocate the appropriate IMR resources to each risk. IMR resources may be manpower, time, cost, equipment, enhanced inspection techniques, etc. Figure 17.3(a) shows the prior, prescriptive IMR plan for the individual structural components, for example the compartments of the FPSO or each of the platforms in the fixed platform fleet. The upper part of the figure shows the quantified risks, as



17.3 Allocate IMR resources based upon risk.

© 2008 Woodhead Publishing Limited

previously described, associated with various structural components that make up the structure. The lower part of the figure shows the resources presently assigned according to a long-standing prescriptive IMR approach for the facility (or fleet of platforms). In this case, the resources related to IMR for each of the tanker compartments are not necessarily assigned according to its risk. Typically, even for a prescriptive IMR program, there is some form of resource prioritization based upon prior experience and known problem areas of a structure. However, a much better prioritization is possible with risk-based IMR, particularly through approaches now available for the quantification of risks (even if it is a qualitative risk approach). With the existing prescriptive IMR program, some of the high-risk structural components receive too little IMR, while some of the low-risk structural components receive too much IMR. Figure 17.3(b) shows the same facility after a risk-based IMR program has been implemented. The risks have been identified and risk-ranked with a more thorough understanding of the likelihood and consequence of failure (i.e., risk) of each of the structural components. The IMR resources have been reallocated to apply the necessary effort depending upon risk. The result is a risk-based IMR approach for the facility that is balanced and focuses IMR resources on the structural components and systems where it is most needed.

17.2.3 Benefits of a risk-based approach

Prescriptive structural IMR programs are typically based on industry standards, classification society or regulatory requirements. These are generally prescriptive in format with pre-established intervals, regardless of a component's contribution to the facility's risk profile. The general belief in prescriptive approaches is that a decrease in the level of IMR activities would bring an associated increase in failures and hence a risk increase. Conversely, an increase in activities is thought to result in a safer installation, amid an increase in IMR cost. As demonstrated in Figs 17.2 and 17.3, this belief is not always accurate, as indicated in the following:

- If failure of a component does not result in significant risk, then any inspection activity for that component will result in additional costs without any risk reduction and the IMR is ineffective and unnecessary.
- Excessive IMR (i.e., inspecting too frequently) may not bring any additional risk reduction. The extra activities could even cause a risk increase due to issues such as human error during maintenance and damage to protective coatings during inspection.
- Activities that do not focus on the inspection detection, or repair of the specific degradation mechanisms to which the component is subjected, will result in cost without benefit.

In contrast, risk-based approaches provide the tools and processes to determine

© 2008 Woodhead Publishing Limited

the optimum combination of IMR methods and frequencies. These approaches ensure that maximum effectiveness and improved efficiency are gained by:

- Prioritizing the components based on risk to differentiate criticality.
- Ensuring that the correct items within the system are selected for IMR (the most 'at risk' components).
- Ensuring that the optimal IMR frequency is determined and met.
- Ensuring that the correct resources are selected for the job (skills set, competence).
- Selecting the correct IMR methods, since there is a thorough understanding of the potential failure modes.
- Planning IMR to minimize business interruptions.
- Providing greater focus for future IMR programs since results are used to update the program.

It is important to recognize that seeking ways to relax or reduce IMR is not the primary goal of a risk-based process. Modifications to inspection plans are not achievable in all circumstances and sometimes the existing prescriptive plan is adequate. The process of developing a risk-based IMR plan may uncover the fact that the facility has actually been operating, maintaining and inspecting some components in a manner which did not provide the most efficient use of resources. Risk-based approaches are specifically useful at matching the correct activities to the level of risk posed by the structural component.

When risk-based IMR is implemented, it is common to observe improvement in both the technical and economic performance of the equipment and installation. This improved performance is delivered through the following:

- Reduced downtimes due to unexpected failure of systems or components (reduction in the number of reactive repairs)
- Safer operation due to higher level of integrity and reduction in failures
- Greater focus to planned maintenance activities through providing predictive replacement times from derived inspection data for critical components or structures
- Improved budgetary control and forecasting of forward IMR planning and execution
- Reallocated IMR effort and resources to the items that provide the biggest impact on risk reduction.

Risk-based inspection (RBI) programs in particular address risks due to structural deterioration from a safety, environment and economic perspective. Implementation of RBI plans can provide and document the overall reduction in risk for the facilities assessed. RBI programs may identify risks of such low level that they require little or no inspection as a means of mitigation, consequently improving management of inspection activities by directing resources to higher-risk areas.

© 2008 Woodhead Publishing Limited

17.3 Fundamentals of risk-based approaches

17.3.1 Risk assessment

Risk assessment is the process of identifying the sources of an event, estimating the risk as a function of the likelihood and consequence of the event, and evaluating the results. Fundamentally, this process answers the following three questions to determine risk:

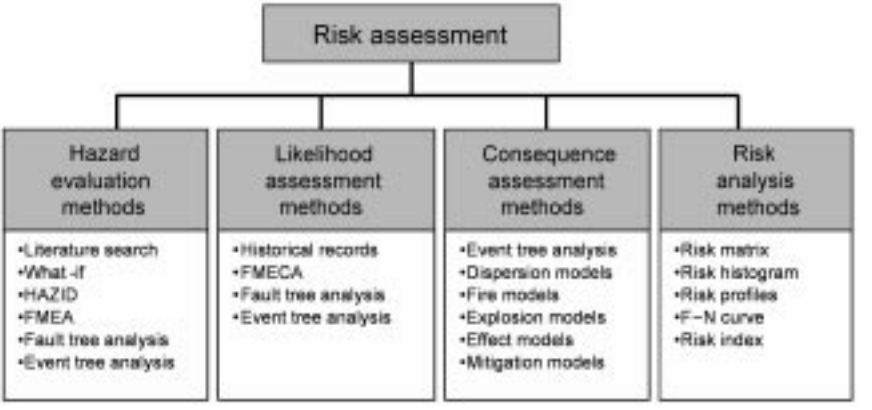
- What can go wrong?
- How likely is it?
- What are the consequences?

Risk is defined as the product of the likelihood that an event may occur and the consequence of the event's outcome. In mathematical terms, risk is calculated by:

$$\text{Risk} = \text{likelihood} \times \text{consequence}$$

Figure 17.4 shows the overall process used to determine risk and consists of *hazard evaluation*, *likelihood assessment*, *consequence assessment* and the *risk analysis*.

A *hazard evaluation* uses a team approach to postulate the things that can go wrong. For example, will the structural component fail and lead to life safety or environmental hazards such as an oil spill? A variety of common techniques are typically used when evaluating structural systems, including hazard analyses such as What-If or a checklist of common hazards typical of such systems; formal HAZID (HAZard IDentification analysis) to identify hazards; FMEA (Failure Modes and Effects Analysis) to identify failures and the ensuing effects; and Fault and Event tree analysis to determine the path of failure and the resulting events leading to failure. Table 17.1 provides further definitions of the



17.4 Overall risk assessment process.

© 2008 Woodhead Publishing Limited

Table 17.1 Summary of commonly used risk techniques

Risk assessment tool	Summary of method	More common uses
What-if and HAZID analysis	What-if analysis is a problem-solving approach that uses loosely structured questioning to (1) suggest structural issues that may result in problems and (2) make sure the proper safeguards against those problems are in place. Hazard identification (HAZID) analysis is a similar approach that uses pre-planned questioning via checklists to help identify issues, safeguards and solutions.	• Useful for any type of structural system. • Most often used when the use of other, more precise, methods (e.g., FMEA) is not possible or practical. • These are frequently combined with checklist analysis to add structure to the analysis.
Failure Modes and Effects Analysis (FMEA)	FMEA is a reasoning approach usually suited for mechanical and electrical systems, but which can also be used for structures. The FMEA technique (1) considers how the failure modes of each system component can result in problems and (2) makes sure the proper safeguards are in place. A quantitative version of FMEA is known as Failure Modes Effects and Criticality Analysis (FMECA).	• Used for reviews of mechanical and electrical systems (e.g., fire suppression systems, vessel steering and propulsion systems). • Often used to make planned maintenance and inspection plans more effective. • Sometimes used to gather information to help find trouble areas in structural systems.
Fault Tree Analysis (FTA)	FTA is a technique that graphically models how logical relationships between structural failures, external events and human errors can combine to cause specific accidents of interest. Probabilities and frequencies can be added to the analysis to estimate risks numerically.	• Suited to almost every type of risk assessment, but best used to focus on the basic causes of specific system failures of relatively complex combinations of high-consequence failures.
Event Tree Analysis (ETA)	ETA is an analysis technique that uses decision trees to model the possible outcomes of an event that can produce an incident of interest. Probabilities and frequencies can be added to the analysis to estimate risks numerically.	• Suited to almost every type of risk assessment, but best used to focus on possible results of events for which many safeguards are in place as protective features. • Often used for analysis of vessel movement incidents, the spread of fires or explosions or toxic releases.

© 2008 Woodhead Publishing Limited

more commonly used methods for structural systems. Detailed discussions of these methods can be found in Reference 3.

Likelihood assessment determines how often a failure can be expected. Likelihood is often also referred to as the frequency of failure. Historical records for similar systems or some of the more formal risk assessment techniques shown in Table 17.2 can be used to determine likelihood. Likelihood can often be defined in a qualitative ranking manner, such as seldom, common, or frequent. Where supporting data is available, likelihood can also be defined in a quantitative manner, typically in terms of failure rate per cycle, annual probability of failure or lifetime probability of failure.

Consequence assessment determines the impact of a failure. Consequences are typically divided into three types – life safety, environmental and financial. 'Life safety' includes potential for injuries and deaths. 'Environmental' is used to define quantities of hazardous materials that can be released or other detrimental actions to the environment. 'Financial' includes cost impact of the failure, including repair or replacement of the directly damaged structure as well as repair to collateral damage. 'Financial' also covers consequences such as

Table 17.2 Comparison of qualitative and quantitative risk methods

Qualitative		Quantitative	
Pros	Cons	Pros	Cons
Captures expertise of persons most familiar with facility	Needs time commitment from qualified persons	Can generate results based on existing data	Need to determine which models to use and how they will be integrated with each other
Can quickly screen out equipment or structures with no damage mechanisms or with low consequence of failure	May fail to consider all failure mechanisms in all modes of operation, especially combination of failures	Requires less time on part of experts during the analysis	Expensive to build and maintain, may require software support
Can be less costly than quantitative analysis	Results may be difficult to defend to third party	Becomes less costly with experience in use of models	May be high cost on initial studies
Can be faster than quantitative study	Inconsistent results, care must be taken to provide audit trail	Consistent results, auditable, perception of accuracy	Accuracy depends on data availability and accuracy

© 2008 Woodhead Publishing Limited

schedule delays and business interruption. In some cases social and political consequences can also be considered, including damage to reputation. Figure 17.4 shows some of the analytical methods used to determine consequences including dispersion, fire, explosion and consequence effects modeling that use complex physical modeling to determine the effects of hazardous material releases and explosions in air and water.

Risk analysis combines the likelihood and consequence results to determine risk. Different types of risk methods are identified in Fig. 17.4, including the qualitative approaches such as the risk matrix and quantitative approaches such as F-N curves which express frequency versus number of associated consequence outcomes (e.g. lives lost) and target risk indexes. Section 17.3.4 provides additional discussion of risk analysis methods.

17.3.2 Likelihood of failure

The frequency of a failure or occurrence of an undesirable event is called its likelihood. Likelihood is considered to be the most important factor in the risk equation since it most directly affects the selection of inspection or maintenance frequency. Figure 17.4 and Table 17.1 list some of the more common methods used to determine likelihood of structural failure.

Degradation mechanisms and likelihood are intrinsically linked, thus determining degradation mechanisms and degradation rates are essential requirements for inspection and maintenance planning. Personnel performing failure mode assessments must be knowledgeable of the potential modes of failure, degradation mechanisms that can cause them and deterioration rates that may be prevalent for each component type or service duty. They must also be knowledgeable on the types of inspection techniques that can be used to locate and define the degradation modes in question.

Degradation models and data are available and are often utilized in a failure analysis study. Specific analysis of the data using industry-recognized methods, formulas or algorithms must be applied to provide an accurate threat value for each given degradation mechanism. Generic or specific degradation models may also be adopted to predict the remaining safe working life for components.

An important consideration is that the initiating event for the failure should be inspection-preventable. If a structural steel component is subject to corrosion which may ultimately cause failure of the component if the corrosion goes undetected by inspection or unmaintained, then a risk-based program is warranted. However, if the component is instead subject to failure, say by a dropped object from a crane, then IMR will have no effect on that failure. In this case, a better method of risk management of the crane operations is to develop operational procedures to prevent the dropped object. This is an important concept for risk-based inspection and maintenance activity in that the activity must be able to influence the likelihood of failure of the component.

© 2008 Woodhead Publishing Limited

17.3.3 Consequence of failure

Consequence is the outcome of the failure of a structural component or system. This activity is geared towards assessing and differentiating the relative ranking of components in relationship to each other and to their relative consequence, should failure occur. The consequence of failure can be assessed qualitatively or quantitatively. Qualitatively, consequences can be assessed by performing hazard analysis activities such as HAZID/HAZOP type studies, FMEAs (Failure Mode and Effects Analysis) and functional failure analysis. Within quantitative assessment methods, calculation of consequence estimates is possible, often utilizing tools such as fire, blast and dispersion modeling or any other accident-modeling tool. Figure 17.3 lists some of the methods used to determine the consequence of failure.

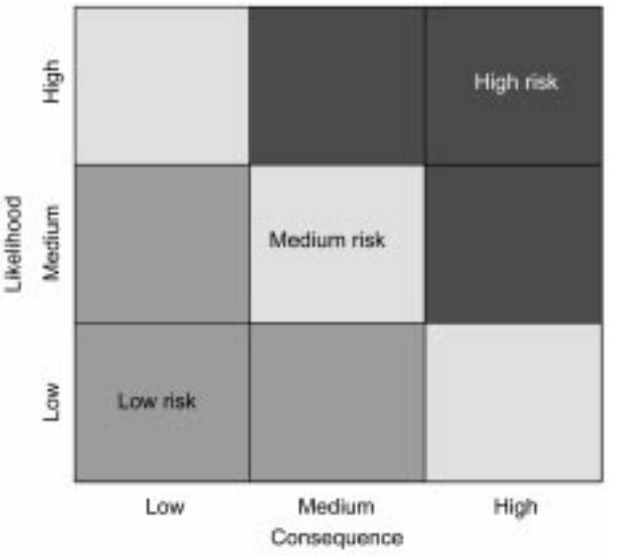
17.3.4 Risk analysis methods

Risk analysis can be qualitative or quantitative or some combination (semi-quantitative). For the qualitative method, competent personnel may make expert judgments to determine the consequence and likelihood of failure of each structural component or system under review. The associated risk is derived by placing the derived likelihood and consequence within a risk matrix, defined below, for each component or system assessed, thus delivering a final risk score or rank.

Qualitative assessment normally uses descriptive ranges for inputs and outputs that are intended to be broad enough to cover the ranges of uncertainty involved. The most typical use of this technique is for the purpose of screening out low-risk items for which the time and cost of a quantitative study cannot be justified. As an aid to solicitation of input, it is common to establish predefined categories or ranges for likelihood and consequences. This process has one unique advantage in that all of the strategic personnel who are involved with the daily management of the installation are directly involved in the evaluation process. In fact, best practice is to ensure that such individuals drive the outcome of the risk evaluation, as their knowledge of the installation and potential scenarios that may occur is crucial.

Presenting risk qualitatively is an effective means of illustrating and understanding risk, specifically when considering applications to structures. A simple 3×3 (likelihood $\times$ consequence) qualitative risk matrix is shown in Fig. 17.5 and illustrates how risk is related to the likelihood and consequence. This matrix is simply a plot with likelihood on one axis and consequence on the other axis. The matrix shows the basic principles behind all evaluations of risk. A low likelihood combined with a low consequence results in a low risk, located in the lower left-hand corner of the figure (shaded light gray). Modern risk matrices often portray this as a green color, indicating that it is safe to proceed (similar to

© 2008 Woodhead Publishing Limited



17.5 A simple risk matrix.

a traffic light). A high likelihood combined with a high consequence results in a high risk, located in the upper right-hand corner of the figure (shaded dark gray). This would usually be shown as a red color, indicating that it may not be safe to proceed due to concern and action is necessary.

A low-risk or high-risk situation usually does not present a difficult decision for the persons conducting the risk assessment. If the risk is low, then the situation is tolerable and no changes need to be made. If the risk is high, then the situation is not acceptable and changes must be made to lower the risk. For IMR planning purposes, this can mean it is time to inspect, increase maintenance or repair. The challenge lies in addressing risks in the central area of the matrix between low and high, shown typically in shaded light gray, indicating caution. In this medium-risk range, the question arises as to how much risk is acceptable. An important concept to understand is that high consequence may not mean high risk, and similarly, high likelihood may not mean high risk. The level of risk can only be determined once both of these variables are known or estimated.

A key feature of risk matrices is that they can be structured to suit just about any operation, likelihood or consequence situation. Figure 17.5 is just one example. Risk matrices also come in all forms and sizes. Some are a simple 3×3 matrix with likelihood and consequence defined as low, medium or high. Others are complex 5×7 or 7×7 matrices with complex definitions for the rows and columns. The more rows and columns, the finer the user is able to differentiate between actions as high or low risk. The tradeoff is that larger matrices require more detailed definition of likelihood and risks and sometimes this information is not available. Recall that risk matrices are intended to be

© 2008 Woodhead Publishing Limited

qualitative and if such information is available, then a quantitative approach may be more appropriate.

Figure 17.6 shows a more complex risk matrix. In this case the matrix has been expanded to a 4×4 grid. The larger grid allows for a more refined definition of likelihood or consequence. In this case the matrix also provides additional information to provide guidance for likelihood and consequence. The likelihood axis has brief descriptions of the meaning of each row. Similarly, the consequence axis has descriptions of consequence of failure in terms of the impact on life, environment, and economics.

		LIKELIHOOD				
Frequent Incident is likely to occur at this facility within the next 5 years	4				High Risk	
Occasional Incident is likely to occur at this facility within the next 15 years	3					
Seldom Incident has occurred at a similar facility and may reasonably occur at this facility within the next 30 years	2			Medium Risk		
Unlikely Given current practices and procedures, incident is not likely to occur at this facility	1	Low Risk				
		CONSEQUENCE				
		1	2	3	4	
		Incidental	**Minor**	**Serious**	**Major**	
Personnel		Minor or no injury, or lost time	Single injury, not severe, possible lost time	One or more severe injuries	Fatality or permanently disabling injury	
Community		No injury, hazard or annoyance to the public	Odor or noise complaint from the public	One or more minor injuries	One or more severe injuries	
Environmental		Environmentally recordable event with no Agency notification or permit violation	Release which results in Agency notification or permit violation	Significant release with serious offsite impact	Significant release with serious offsite impact and likely to cause immediate or long term health effects	
Facility		Minimal equipment damage at an estimated cost less than US$100K, negligible down time	Some equipment or structural damage at an estimated cost greater than US$100K, 1 to 10 days of downtime	Major damage to installation at an estimated cost more than US$1m but less than US$10m, 10 to 90 days downtime	Major or total destruction to installation estimated at a cost greater than US$10m, downtime exceeds 90 days	

17.6 A complex risk matrix.

© 2008 Woodhead Publishing Limited

Reference 3 provides examples of risk matrices used by several regulatory and governmental agencies worldwide, including the US Coast Guard, UK Health and Safety Executive, US Department of Energy (DOE), International Maritime Organization (IMO) and others.

For the quantitative method, rather than making use of experience or subjective decision making to enumerate risk, quantitative methods use formulas, algorithms, engineering analysis or event modeling to provide a direct numerical value for each factor of consequence and likelihood. While this method has greater substance (i.e., mathematically calculating risk rather than subjectively evaluating it), it often overlooks the value that is gained from the input offered by experienced operations personnel.

In practice, it is doubtful that any RBI approach could be termed wholly qualitative (without use of any analytical tools) or wholly quantitative (without use of judgment). Almost all approaches are 'semi-quantitative', although some are on the qualitative side of the spectrum while others are on the quantitative analytical side. Thus the qualitative and quantitative approaches do not compete with each other, but complement each other.

There are certain limitations with both quantitative and qualitative methods. For qualitative methods, the main issue that may undermine the results is that this method is largely an expert scoring process. As a result, the outcomes of such a study could be considered to be overly judgmental. Qualitative analysis can still be fairly labor-intensive, but simpler to complete. In certain cases, the qualitative method may not be adequate to accurately evaluate the worst-case as certain key factors, e.g., failure degradation/propagation rates, may have critical importance.

By comparison, quantitative analysis in support of IMR programs requires considerable quantities of detailed data and can be exceptionally labor-intensive and technologically demanding. As a result of these factors, choices or compromises are often made, given the realistic economics within which risk-based IMR must be achieved. For this reason, it is usual to perform a first-pass qualitative analysis in advance of the quantitative in order to pre-screen for components where use of quantitative methods would be neither technically appropriate nor cost-effective due to low risk. Table 17.2 provides various pros and cons associated with the two approaches. Reference 3 provides detailed descriptions of qualitative and quantitative risk assessment techniques as applied to marine and offshore structures.

17.4 Risk-based inspection (RBI)

The use of RBI approaches for developing inspection plans for offshore structures is becoming a prevalent trend in the oil and gas industry. Operators feel there are significant benefits in developing RBI plans that are tailored to their asset in regards to both design and operation. By taking this approach, the

© 2008 Woodhead Publishing Limited

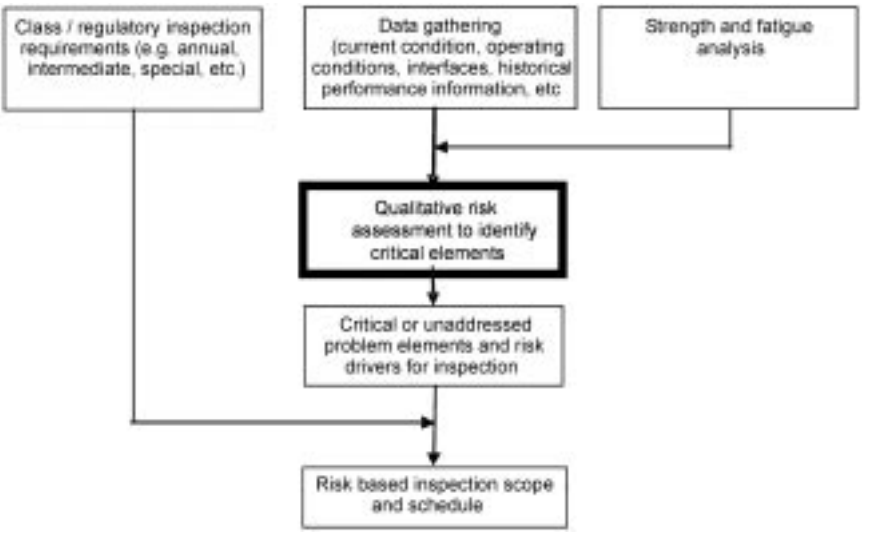
inspections are more targeted and the operational constraints better managed, resulting in a more optimized inspection program while maintaining the same level of safety. The following sections describe the key steps in the approach using a ship-shaped Floating Production Storage and Offloading (FPSO) vessel as an example.

17.4.1 Qualitative risk-based inspection (RBI) method

The qualitative method provides a first-pass assessment of the facility to develop an initial understanding of risks and development of the RBI plan. Figure 17.7 shows a flowchart for a typical qualitative RBI.

The process begins with gathering of the relevant data for the facility including its current condition, operating conditions, interfaces with other facilities or operations, historical performance of the facility, etc. This type of information is used to understand the overall risk of the facility. In traditional prescriptive IMR programs the focus is typically on the structural component itself with little or no concern for the impact of the failure of this component on the rest of the facility. The data set used in developing the IMR program may only be a few structural drawings in the vicinity of the component. With risk-based IMR, the concern goes beyond the local area of the component.

Also required are the regulatory or classification IMR requirements for the facility. These are required for later comparison against the IMR program developed. It is best to understand these at the very beginning of the program development since in some cases there may be restrictions that prevent the use



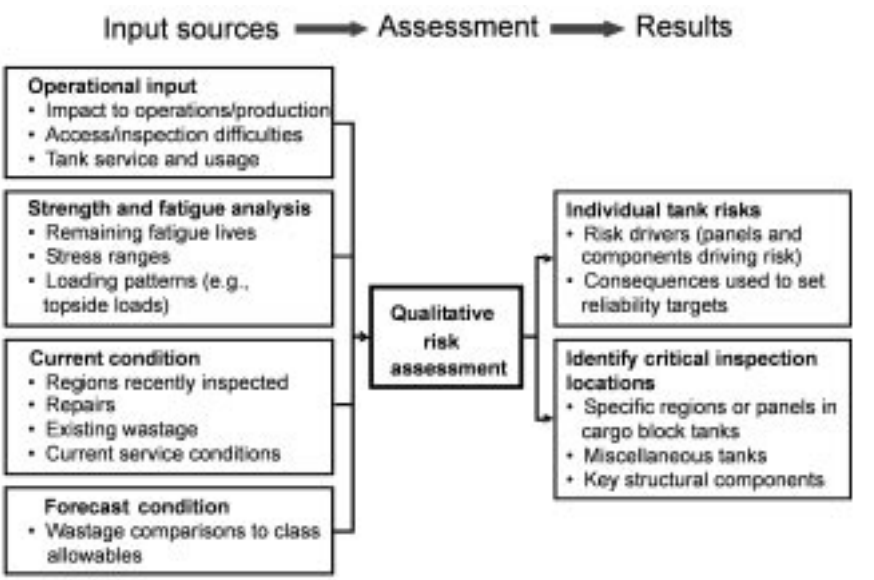
17.7 Qualitative structural RBI program.

© 2008 Woodhead Publishing Limited

of RBI on some parts of the facility and instead the prescriptive rules must be used. Regulatory and classification requirements also provide an initial first estimate for the IMR plan, based upon prescriptive approaches. This initial plan can then be adjusted to best fit the risk-based approach, such as increasing inspection intervals on low-risk components.

Strength and fatigue information about the facility is also required, for example identification of structural components that are the most heavily loaded and those that are the most prone to fatigue. For qualitative RBI this may be limited to anecdotal information about susceptibility of a particular component to strength or fatigue failure. As seen later for quantitative RBI, specific analysis results are required, although this type of detailed quantitative information can also be used in qualitative RBI.

A qualitative risk study is then performed as shown by the box with the bold outline in Fig. 17.7. Generally this will involve a structured workshop similar to a hazard identification (HAZID) study where risks associated with the system are systematically identified and assessed. Figure 17.8 shows some of the typical issues considered in a qualitative risk assessment, in this case using an FPSO as an example. Other methods can also be used but simplifications ultimately result in limitations in the plan (i.e., not all of the key aspects are covered in detail). The risk assessment is used to highlight and account for other factors that may impact hull integrity not necessarily covered by the strength and fatigue analyses or the reliability analysis. The results from this assessment are used to adjust the individual component target reliabilities up or down on a risk basis which in turn



17.8 Typical issues considered in qualitative RBI of an FPSO.

© 2008 Woodhead Publishing Limited

influences the required inspection intervals. Furthermore, the input from the operations personnel and risk results generated during the exercise provides a forum to identify key or critical inspection locations as well as to understand potential consequences (i.e., impact on operations) related to structural integrity.

Figure 17.9 shows results of a qualitative RBI that risk-ranked the compartments of an FPSO based upon fatigue and strength. The risk level for each compartment is shown by the different shading/hatching, with dark gray being the highest risk. Risk is defined as a combination of likelihood of failure and consequence. The shading/hatching matches a risk matrix, similar to Fig. 17.5, which was used in the process to determine the risk of the compartment to failure. The likelihood of failure for this case is based upon existing fatigue and strength analysis of the facility that was 'qualitatively' reviewed to determine areas that may be prone to damage such as cracking. Structural analysis is often used like this in qualitative RBI as an input to the likelihood component for the risk. A quantitative RBI would use strength and fatigue results in a more explicit manner, for example as a basis for structural reliability or as a basis for fatigue degradation to determine inspection intervals, as discussed later in this section.

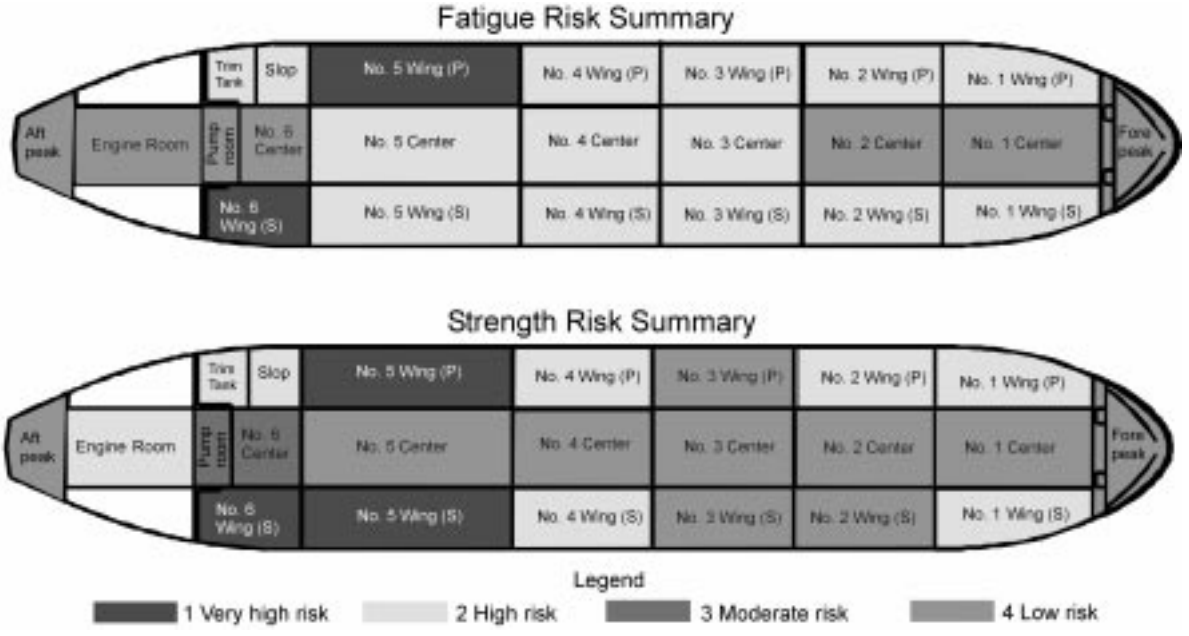
The fact that risk is a combination of likelihood and consequence is clearly seen by comparing the fatigue risk and strength risk in Fig. 17.9. The compartments have the same consequence of failure for fatigue or strength since the same consequence of failure, such as oil spill, would occur if the cause was fatigue or strength related failure. However, the risk is different for the tanks due to the likelihood component. For example, compartment no. 5 starboard has a low risk (shown as light gray) for fatigue but has a very high risk (shown as dark gray) for strength.

Once the risks of the structural components are known, an inspection plan can be developed that emphasizes the higher-risk items. For qualitative methods, the inspection plan may follow prescriptive rules, whereas the higher-risk compartments would receive additional inspection attention, if possible supplemented with specific areas to inspect based upon the strength and fatigue analysis. Section 17.4.7 discusses the typical RBI plan that would be developed based upon this type of information.

17.4.2 Quantitative risk-based inspection (RBI) method

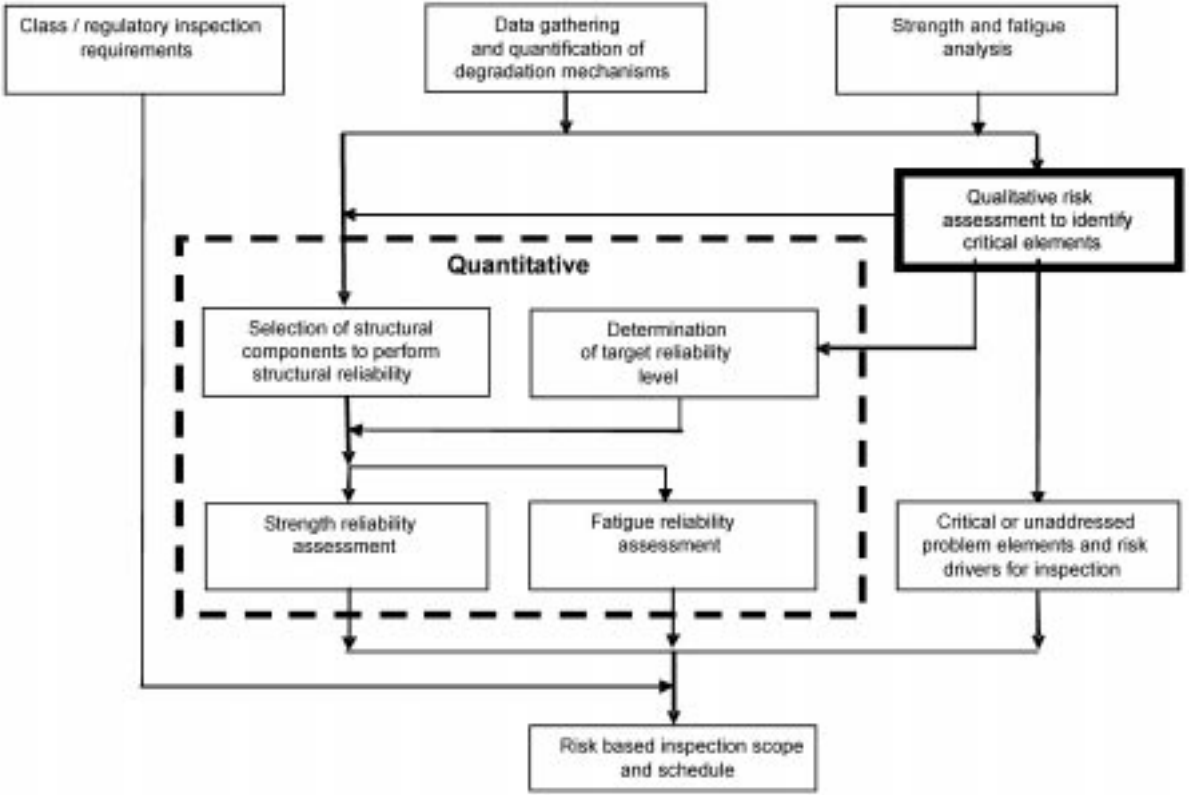
Quantitative RBI extends the qualitative method by using analytical approaches to explicitly consider reliability based upon degradation mechanisms, especially fatigue and corrosion. Figure 17.10 shows a flowchart for a typical quantitative RBI. The approach is similar to the qualitative RBI shown in Fig. 17.7, except that the qualitative risk assessment shown by the bold box is extended to use quantitative techniques to determine structural reliability. The results of the structural reliability are used to establish the specific IMR program. Note that the qualitative risk assessment is still performed for the quantitative approach as

© 2008 Woodhead Publishing Limited



17.9 Qualitative approach for tanker RBI – risk ranking of compartments for inspection.

© 2008 Woodhead Publishing Limited



17.10 Quantitative structural RBI program.

© 2008 Woodhead Publishing Limited

it helps establish the key risk issues that is then used to focus the specific quantitative work.

The remaining sections describe the various parts of the quantitative RBI in more detail.

17.4.3 Data gathering and baselining

The data collected as part of the plan development includes structural drawings, design and analysis report and operational data. Although described here for quantitative RBI, the same data is typically needed for qualitative RBI, although not as much data needs to be gathered. The structural drawings generally include both as-built as well as current information. These documents provide information on how the facility is laid out and what systems and components make up the structural systems. Operational data may include manuals or other documents indicating how certain systems or components are intended to perform and have performed during its service life. Operational personnel can provide anecdotal and historical input into how the operating company approaches integrity management from a company-wide as well as asset-specific perspective.

The most important information is related to the current condition of the structure. Risk is increased when there is a lack of, or uncertainty in, the key information required to assess integrity. In consideration of this fact, typically some form of 'baseline' data collection effort will be conducted prior to beginning the development of the RBI program. This effort is typically conducted either prior to the vessel coming into operation (i.e. at a shipyard during construction) or, in cases where the vessel is already operating, there may be a need for enhanced inspection to confirm the condition and eliminate any unknowns. This information is used to determine if there are any holes in the data, understand how the service life has affected the structural integrity, and identify critical or problem regions which may warrant attention and provide initial guidance for the RBI program.

17.4.4 Structural analysis

Strength and fatigue analysis results are used in both the qualitative risk assessment and the reliability analysis. For the qualitative risk assessment, stress and fatigue results are captured as one of the contributing factors influencing the likelihood of a structural failure and as such it is accounted for in the risk-ranking exercise.

For the structural reliability calculations of quantitative RBI, the results are used first to identify the most critical components and connections. For these components, structural reliability analysis will be conducted. Once these locations are selected, stress/loading details (e.g. stresses due to various loadings

© 2008 Woodhead Publishing Limited

on the component in question) must be extracted from the structural analysis results to conduct the reliability calculations.

17.4.5 Risk assessment

The risk assessment is developed using the strength and fatigue analysis as well as all other data gathered on the asset. The risk assessment is typically qualitative and serves three purposes:

- To identify the potential consequences related to hull structural damage which are used to set the structural reliability targets
- To identify conditions or factors that will influence the likelihood of structural damage (e.g., loading conditions, tank service conditions, condition of corrosion protection systems, past experiences of similar vessels or service conditions, etc.)
- To identify other factors that may impact hull integrity not necessarily covered by the fatigue and strength analysis or the reliability analysis.

The qualitative risk assessment captures information related to features of the individual tank component (stiffened or unstiffened panel, weld detail, etc.) or overall tank, the deterioration scenario, potential consequences, factors that should be considered in assigning the likelihood, safeguards, and risk ranking. Again, the focus of the assessment is only on inspection-preventable hazards.

The identified hazards are risk-ranked using an appropriate risk matrix as discussed previously. Since the consequences are used to set the structural reliability targets for the individual components and connections, the consequence categories on the risk matrix must be directly related to the reliability target levels. The consequence categories are related to the reliability values used in the degradation modeling for both strength and fatigue. For example, the highest consequence category on a risk matrix may represent a financial loss of greater than $100 million, equivalent to the loss of the entire asset. Similarly, the reliability target associated with this consequence category would need to be related to the hull girder reliability, since loss of strength could result in loss of the asset. Other consequence categories will have similar relationships depending on the structures impacted.

17.4.6 Structural reliability analysis

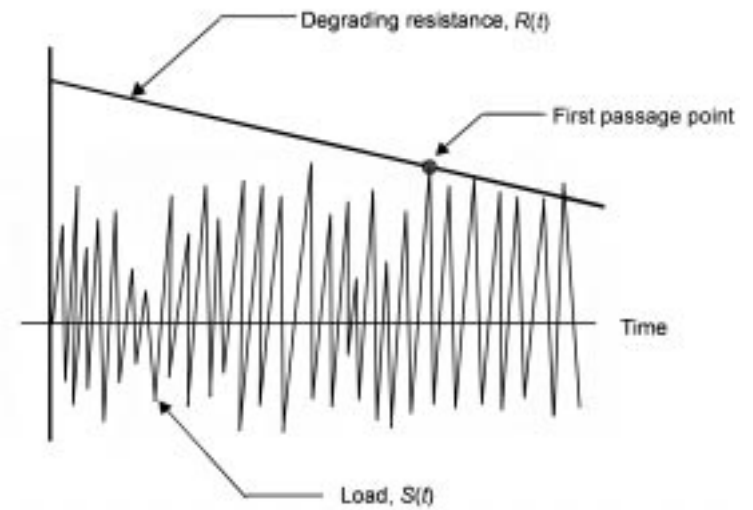
Structural reliability analysis is part of quantitative RBI and takes deterministic stress/fatigue analysis results, coupled with degradation mechanisms (e.g. corrosion rate, crack propagation parameters, etc.), and calculates the time-varying structural reliability index of selected structural components or connections. The results are used to identify how often the components should be inspected.

© 2008 Woodhead Publishing Limited

The reliability target level is an acceptance criterion used to judge the adequacy of the calculated structural reliability index (or equivalently, the failure probability). These targets are effectively used to determine what the appropriate inspection frequency should be, knowing that degradation of the structure is occurring with time (i.e., strength loss is occurring due to corrosion as well as fatigue damage accumulation) and, if a particular failure occurs, the specific consequences that may result.

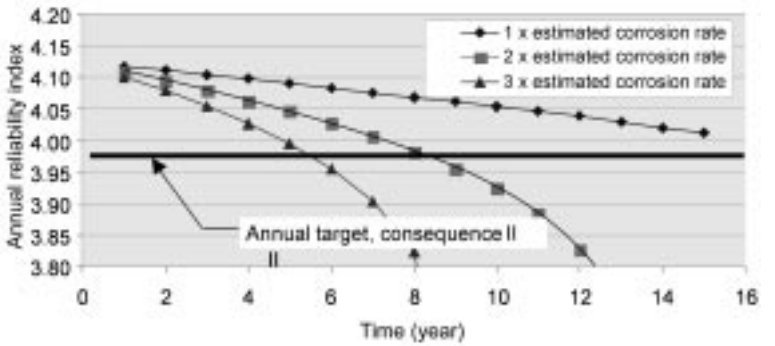
Strength reliability analysis considers changes in both loading and strength with time. An illustration of the time-variant reliability problem is shown in Fig. 17.11. $S(t)$ represents the loading with time and $R(t)$ represents the strength resistance which is degrading with time due to corrosion. The figure shows a deterministic representation of the problem. In the reliability analysis, whether the resistance will cross the load process (i.e. first-passage) is a probabilistic quantity (i.e. probability of failure). The acceptance of this probability of failure needs to be set from the criticality (i.e., consequence) of the component. The consequence of the component is identified in the qualitative risk assessment.

Generally, the annual target reliabilities vary depending on the component or structure's criticality to the integrity of the asset. Figure 17.12 shows an example of an annual reliability of a component. The component falls below the assigned target reliability at differing years depending on the predicted corrosion rate (three are specified). The component should be inspected before the component crosses this threshold. Note that if the reliability fails below this target it does not represent failure. It simply implies that the reliability is too low (or inversely the probability of failure is too high) for that particular component given that its



17.11 Time-variant reliability caused by corrosion.

© 2008 Woodhead Publishing Limited



17.12 Example of component annual reliability index.

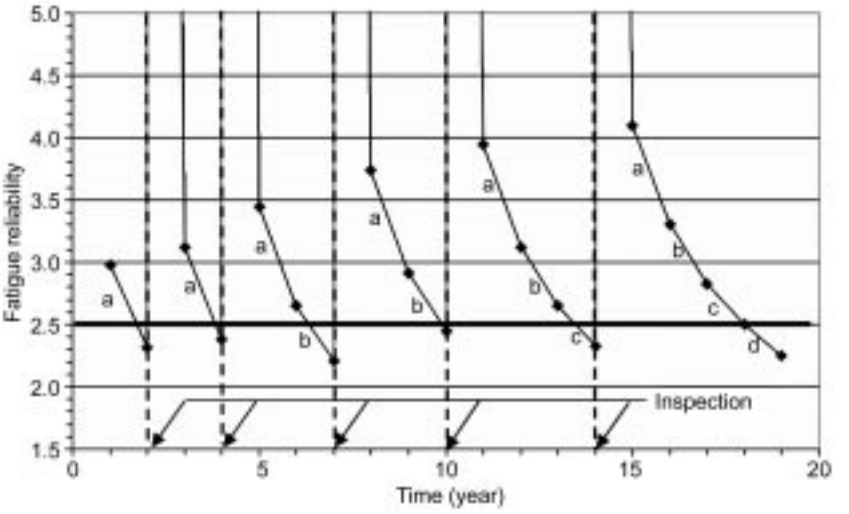
assigned risk tolerability and inspection activity prior to reaching this threshold will increase the reliability back to an acceptable level.

Fatigue reliability calculations are conducted in a similar fashion. The information from the structural analysis such as the fatigue life, stress range, etc. is extracted. Fracture mechanics methods are typically used since they relate defect sizes (i.e., crack size) to fatigue life. The use of this fracture mechanics-based reliability formulation enables the inspection effect on fatigue reliability to be included, based on the various methods of inspection. For example, close visual inspection (CVI) will have a lower probability of detection (POD) than a non-destructive method such as magnetic particle inspection (MPI). As a result, the reliability increase to be obtained from a successful inspection (i.e., no crack detected) will be higher for a method such as MPI than for CVI.

Figure 17.13 shows an example of the reliability increase obtained from successful inspections of a connection. In this example the inspections were carried out immediately after the time when the fatigue reliability is predicted to fall below the acceptable level, which is a reliability index of 2.5 in this case. In the example, inspections were carried out in the 2nd, 4th, 7th, 10th, 14th and 18th year. It is shown in the figure that once inspections are carried out without finding any cracks, the fatigue reliability index increases dramatically (since no crack was found), and then decreases as time elapses. The experience gained at each inspection interval is used to establish the next inspection interval. This is seen in Fig. 17.13 by the additional experience (based upon prior inspections) used to adjust the prediction for the next interval (shown as the segmented lines a, b, c and d). The result is a growing confidence at each inspection interval about the lack of crack growth. Note that in this example it is assumed that the inspection technique used, such as MPI, has done an adequate job to demonstrate that there is no crack present at each inspection.

Another feature of the fatigue reliability is the ability to account for correlation between similar connections. This enables one to calculate the increased reliability of certain connections for given successful inspection on similar

© 2008 Woodhead Publishing Limited



17.13 Example of component annual reliability index with periodic inspections.

connections in another location which can be shown to be correlated to the initial set of connections. This correlation aspect is also useful in determining how many more similar connections must be inspected in order to raise the reliability to the set target when one connection is found to have a crack.

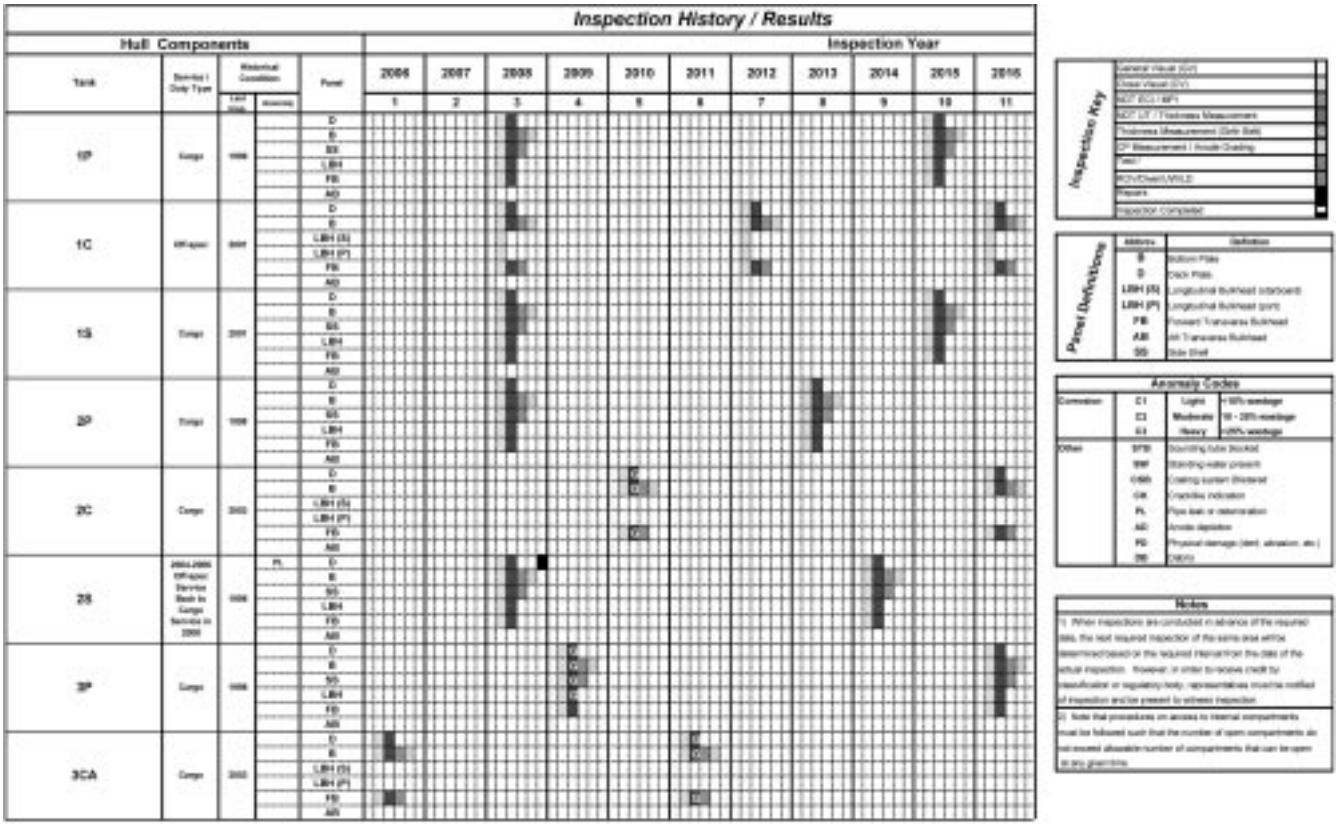
17.4.7 The risk-based inspection (RBI) plan

The final step in the RBI development process requires the organization and aggregation of this information to define the initial inspection frequencies and scopes. The RBI plan at this point is the initial starting point and most likely will change as inspections are conducted and information is collected to confirm, validate and update the degradation models.

The less complex methods may allow automated risk scoring, but the limitation is that they are not as comprehensive. To process this information, typically a systematic approach is adopted which uses the strength and fatigue reliability as the primary basis (i.e., starting point) for setting the intervals and then draws upon other information such as critical inspection points or other issues to adjust the intervals and related work scopes. The approach incorporates general rule sets to combine each of the relevant sources such that it is objective and repeatable. The end result is an approach that couples both the reliability analysis results with engineering judgment to set inspection ranges and work scopes.

Although the RBI plan development provides the primary framework for the structural inspection scopes and intervals, regulatory requirements are referenced to ensure the overall RBI scope conforms to statutory requirements as well. The end result of this initial plan aggregation work is an upper level

© 2008 Woodhead Publishing Limited



17.14 Typical RBI plan.

© 2008 Woodhead Publishing Limited

'initial' inspection plan framework or 'Master Inspection Plan' laid out for the asset's entire planned operational life. Figure 17.14 shows the top-level lifetime plan for the RBI plan developed for the example FPSO. The plan is focused on when to inspect the specific FPSO tanks along with a basic understanding of the scope to be utilized during that inspection.

Since a RBI plan is a dynamic document that changes with time and the results of findings, there is a formal approach to collecting and assessing inspection information and managing the plan. The RBI management team is typically a combination of operations personnel and engineers consisting of staff from the operator, regulator or classification society and engineering contractors. The make-up of this team and their oversight of the plan can have a significant influence on the quality of the hull inspections.

17.5 Risk-based maintenance (RBM)

Risk-based maintenance (RBM) of structural systems is a part of overall risk management so that the risk of undesirable end events associated with structural failures can be effectively managed by the maintenance program. This failure management is achieved by allocating maintenance resources to maintenance tasks based on a risk or criticality assessment. For example, reliability-centered maintenance (RCM) analysis can be employed to:

- Identify functional failures with the highest risk, which will then be focused on for further analyses
- Identify equipment items and their failure modes that will cause high-risk functional failures
- Determine a maintenance strategy that will reduce risk to acceptable levels.

For process systems, RCM has been prevalent in the industry for over 25 years, primarily for machinery and rotating equipment. A brief overview of the RCM process is provided in the *Guide for Survey Based on Reliability-centered Maintenance* (RCM Guide) by the American Bureau of Shipping (ABS, 2003 [14]). One of the key concepts of RCM is that all equipment failure patterns are not the same; therefore, the maintenance tasks necessary to prevent failures may require different strategies in order to successfully manage them. In fact, depending on the dominant system failure mechanisms, system operation, system operating environment, and system maintenance, specific equipment failure modes exhibit a variety of failure rates and patterns.

One of the primary objectives of the RBM analysis is to define a set of proactive maintenance tasks needed to manage potential structural failures or degradation. These tasks can manage these potential failures by:

- Detecting onset of failure with sufficient time to allow corrective action before the failure occurs, e.g. condition monitoring tasks

© 2008 Woodhead Publishing Limited

- Preventing the failures before they occur, which are referred to in the RBM program as planned maintenance tasks
- Discovering and correcting hidden failures before they impact system performance, e.g. failure finding tasks
- Applying operational restrictions or some other action, e.g. any applicable and effective task.

In addition, the RBM analysis might indicate that the failure does not warrant any proactive maintenance and continued degradation is acceptable. Also, RBM analyses should include routine servicing tasks to ensure the assumed failure rate and failure pattern are valid.

17.6 Risk-based repairs (RBR)

Typically, an inspection program will provide at least some results that are anomalous, that is inspection results that do not meet specific criteria in the inspection plan (for example, thickness values below a preselected threshold). These criteria are set slightly below the threshold where failure would be anticipated, attempting to identify anomalies before they become structural integrity problems.

When anomalies occur, they must be assessed. To use an RBR approach for anomaly assessment, two factors are considered:

- What are the current and projected conditions of the anomaly over time and, given this, what is the likelihood that a structural failure will occur?
- What are the consequences if the anomaly causes a structural failure?

Using the risk matrix, it is then possible to determine the current and projected risk (high, medium, or low) due to the observed anomaly (corrosion, cracks, dents, holes, etc.). If the current risk condition of the structure due to the anomaly is above the acceptable risk level (typically high risk), repair is required. Otherwise, depending on the level of projected damage over the anticipated service life, three outcomes are possible:

- *No action*. The projected degradation over the period of interest will not exceed threshold criteria. These outcomes can occur, for example, when service changes result in a lower structural demand than the original design assumptions. Low risk.
- *Monitor*. The projected degradation will be at (or slightly above) the tolerable degradation at the end of the anticipated service life. The required monitoring frequency will then typically depend primarily on consequence. Monitoring frequency may also increase as the component nears the design life. Medium risk.
- *Repair*. The projected degradation will be above the acceptability threshold at the some point before the anticipated service life is reached. High risk.

© 2008 Woodhead Publishing Limited

Note that the acceptable level of degradation may be either prescriptive (rules based) or determined by engineering analysis. Prescriptive thresholds are based on permissible levels of degradation on an element (typically a plate) level. Engineered thresholds are determined by calculating actual structural demand and determining at what point in the degradation process the capacity will be insufficient to meet that demand. These calculations are usually done on a component (set of connected elements) level.

When repairs are indicated, it is then possible to use the anomaly risk-ranking determined above to prioritize the repair program. The primary benefits of using risk to prioritize repairs is that the overall facility risk is more quickly reduced and limited resources can be allocated to those areas of highest risk. In practice, for multiple anomalies that have high risk levels, further differentiation of anomalies is based on consequence.

17.7 Future trends

Risk-based approaches for IMR have been applied in the aircraft, nuclear and process industry for the past few decades. However, their use for structural systems, especially in marine and offshore applications, is still at a comparatively early stage, with applications starting only in the past decade. Hence, risk-based structural approaches have a lot of catching up to do, but can also learn from the more advanced programs of these other industries. Some areas for future trends are described below.

17.7.1 Increased use of quantitative methods

Qualitative approaches such as risk matrices are the easiest to employ in the early stages of implementing risk-based approaches. This indeed has been the case with structures where the traditional prescriptive approaches have been modified using simple rules and risk matrices to help focus IMR on high-risk areas and to adjust IMR intervals. As experience is gained with these programs, engineers are using progressively more complex risk-ranking rules and quantitative techniques such as structural reliability to help implement IMR programs.

17.7.2 Incorporation of historical data trends

The early stages of risk-based IMR must rely on experience and engineering judgment to develop forward-looking programs and in particular establish IMR intervals. As experience is gained, and data trends begin to develop such as corrosion and fatigue degradation rates, these can be fed back into the program to plan future IMR, particularly to determine areas of repeat anomalies and to best fit IMR intervals. One of the problems with structural IMR is the limited data available since there are few facilities from which to gather information. In

© 2008 Woodhead Publishing Limited

the aircraft and process industry there are hundreds and even thousands of components, and trends become obvious quickly. But in offshore FPSOs, for example, there are only a few dozen facilities. In these cases, data sharing and joint industry projects whereby owners cooperate to pool and share structural performance data can assist all involved.

17.7.3 Integration of risk and IMR into software

Risk-based approaches have been incorporated into software for aircraft and process systems. For structures this is more difficult since most structures are very different with few common designs, and more importantly, environmental conditions that determine structural strength, fatigue and corrosion may be different from site to site, even if the structure is the same. This makes it difficult to develop software that can be applied repeatedly on multiple assets. However, several software packages, often web-based, are emerging, including long-term collection of IMR data for a facility in order to assist with trending calculations (e.g., corrosion rates), direct links to structural analysis programs for automated structural strength and fatigue checks based upon the latest inspection results, and future IMR planning including development of inspection and maintenance work packs that can be implemented in the field. In the longer term, these software packages will integrate with structural reliability codes to assist in developing risk profiles for the facility which can then be used to establish the IMR programs.

17.7.4 Increased acceptance by regulators and classification societies

Traditionally IMR has relied upon prescriptive approaches that have developed over a long period of time. As previously discussed, these approaches are time tested and are a 'safe' and defensible approach for regulators. But risk-based approaches offer the promise of even better long term performance of facilities with fewer failures and downtime which is in the best interest of all parties. Regulators and classification societies are working with owners to help develop risk-based IMR programs as well as the verification programs that are needed to ensure proper implementation. Within the next few decades, as these programs are more fully developed and implemented successfully, risk-based IMR is expected to be the leading approach for owners, regulators and classification societies alike.

17.8 References and bibliography

1. Ku, A., Serratella, C., Spong, R., Basu, R., Wang, G., Angevine, D., 'Structural reliability applications in developing risk-based inspection plans for a floating production installation', *Proceedings of the Offshore Mechanics and Arctic Engineering Conference*, OMAE2004-51119, Vancouver, 2004.

© 2008 Woodhead Publishing Limited

2. Wang, G., Spong, R., 'Experience based data for FPSO's structural design', *Proceedings of the Offshore Technology Conference*, OTC 15068, 2003.
3. *Guide for Risk Evaluation for the Classification of Marine-Related Facilities*, American Bureau of Shipping (ABS), June 2003.
4. *Guide for Survey Using Risk-Based Inspection for the Offshore Industry*, American Bureau of Shipping (ABS), December 2003.
5. *Guide for Risk Based Inspection of Hull Structures*, American Bureau of Shipping (ABS), June 2007.
6. Ku, A., Spong, R., Serratella, C., Wu, S., Basu, R., Wang, G., 'Structural reliability applications in risk-based inspection plans and their sensitivities to different environmental conditions', *Proceedings of the Offshore Technology Conference*, OTC 17535, 2005.
7. NRC (Nuclear Regulatory Commission), Reactor Safety Study: *An Assessment of Accident Risks in U.S. Commercial Nuclear Power Plants*. Report No. WASH-1400 (NUREG-75/014), Washington, DC, 1975.
8. ANS (American Nuclear Society) and Institute of Electrical and Electronics Engineers (IEEE), *A Guide to the Performance of Probabilistic Risk Assessment for Nuclear Power Plants*. NUREG/CR-2300, 1983.
9. API-581, *Base Resource Document – Risk-Based Inspection*, Version 1.0, 2000.
10. NORSOK Standard Z-013, *Risk and Emergency Preparedness Analysis*, Rev. 2, 2001-09-01.
11. Ship Structure Committee, *Risk Based Life Cycle Management of Ship Structure*, SSC-416, 2001.
12. Ship Structure Committee, *Risk Informed Inspection of Marine Vessels*, SSC-421, 2001.
13. Ship Structure Committee, *Life Expectancy Assessment of Ship Structures*, SSC-427, 2003.
14. *Guide for Survey Based on Reliability-Centered Maintenance*, American Bureau of Shipping (ABS), 2003.

© 2008 Woodhead Publishing Limited